Mechanisms of Tenascin-C dependent tumor angiogenesis

Tristan Rupp

UNIVERSITÉ DE STRASBOURG

ÉCOLE DOCTORALE 414

UMR_S INSERM 1109 – MN3T

THÈSE présentée par :

Tristan RUPP

Né le 22 juillet 1984 (Thionville)

soutenue le : **18 septembre 2015**

pour obtenir le grade de : **Docteur de l'université de Strasbourg**

Discipline : Sciences de la Vie et de la Santé

Spécialité : Pharmacologie

Mechanisms of Tenascin-C dependent tumor angiogenesis

THÈSE dirigée par :

Dr. Gertraud Orend	Université de Strasbourg

PRESIDENT DU JURY :

Prof. Maxime Lehmann	Univeristé de Strasbourg, France

RAPPORTEURS :

Prof. Anna-Karin Olsson	Univeristé de Upsalla, Suède
Dr. Martin Hagedorn	Univeristé de Bordeaux, France

Acknowledgements (in French)

Ce travail, ce titre et cette future carrière, je la dois d'abord à mes parents Patricia et Jean-Claude qui m'ont soutenu depuis le début de ma formation universitaire. Je suis fier du parcours que j'ai suivi, des rencontres que j'ai faites (en particulier avec ma femme Claire) et de pouvoir devenir le premier scientifique de la famille. Sans l'éducation que j'ai reçue et sans les valeurs qu'ils m'ont transmises, rien n'aurait pu être possible, et pour cela je tiens à leur exprimer mes plus grands remerciements et mon amour. MERCI LES RUPP !

Comme je l'écrivais au dessus le parcours qu'a été le mien m'a permis de rencontrer la femme de ma vie, Claire Duquesnoy. Claire, tu m'as toujours soutenu, tout donné et si j'en suis là aujourd'hui c'est aussi grâce à toi. Maintenant grâce à mes connaissances et ma pratique expérimentale, on va pouvoir se lancer dans un projet de longue date ! Obtenir un mini-nous et en faire le meilleur des biologistes/artiste du monde. Merci pour tout et le meilleur est encore à venir là où nous allons continuer notre chemin.

Je tiens bien sûr à remercier ma directrice de doctorat Gertraud Orend pour m'avoir confié ce travail. Nos relations n'ont pas toujours été simples mais l'expérience de cette thèse m'aura été profitable. J'ai appris à développer mon indépendance, le travail d'équipe, mon esprit critique, j'ai progressé en tant que scientifique et maintenant je vais avancer vers autre chose.

Malgré les hauts et les bas que m'a fait traverser ce métier, je vais garder un souvenir éternel de la collaboration que j'ai eu avec toi et les autres « big chiefs » de l'équipe. En effet, je suis satisfait de la façon dont le sujet a évolué, des résultats obtenus, et de l'histoire que j'ai réussi à construire avec toute l'équipe. Néanmoins il reste encore beaucoup à faire, de nombreuses questions à résoudre et certains « dogmes » sur la TNC sont à clarifier. Je ne pense pas continuer dans le domaine de la matrice mais j'aurai toujours en mémoire, peu importe mon futur domaine, que le microenvironnement et surtout les matrices sont des éléments cruciaux à intégrer partout ! vraiment partout ! D'ailleurs comme dirait un « grand penseur » de notre époque : « Si à 50 ans on n'a pas » bossé sur les matrices, « c'est qu'on a quand même raté sa vie ». Ou le contraire … l'avenir nous le dira.

Ensuite quelques mots sur les binômes. Benoit et Thomas, on a globalement commencé ensemble au labo, on a bien galéré mais vous m'avez beaucoup appris et soutenu. J'ai vraiment apprécié travailler et délirer avec vous. Les soirées « terrasses » avec de la science ou non, de la pétanque et les autres bonnes grosses soirées ont vraiment été géniales.

Spéciale cassedédi (comme on disait dans les années 90) à tous mes collègues et surtout potes adorés. La taré, tabasseuse, campagnarde, en talons qui a commencé avec moi sa thèse, Mathilde, et qui va beaucoup me manquer. Lionelu qui m'a prouvé qu'on pouvait être d'alsacien et être un mec (à moitié sourd) génial. Just1, te laisse pas faire par le blondinet dégarni, ce n'est pas un neuro qui va la ramener devant une pharmaco quand même !

Mes potes (Niko, Ju, Jon, Guillaume, Eugénie, Anne-So, clairette, Djoule et Ulux) qui maintenant que je suis docteur vont encore plus être soulés par mes réponses « scientifiques » (« Tristan, arrête avec ta science !» mais qui au fond adorent ça !)

J'ai eu aussi la chance d'accumuler de super collègues durant ses années au labo. L'U682, U1109, U1113, Uchoucroute etc … et l'ensemble des personnes qui y travaillent ou y ont travaillées me manqueront. Surtout pendant les soirées de Noël et autres.

La série des petites et grosses pensées :

-Les nouveaux de la GO team : Sun, Constance, Anna et Selven, ben bon courage tout d'abord, et vous inquiétez pas … je m'en suis sorti … vous aussi peut être …

-Grosses pensées pour mes anciens collègues forçats de la TNC, Anja, Falk Inès et Isabelle qui fous qu'ils sont pour au moins deux d'entre eux travaillent toujours sur les matrices.

-pour le monument de la salle de culture, Elisabeth, avec qui forcément je passais beaucoup de temps (ben oui j'ai du passer autant voir plus de temps que toi sous ma PSM …)

-les éternels du labo, Christiane, Annick, Olivier, Patricia et Caro (eh oui fais gaffe ils te laisseront plus partir à force), ne vous laissez pas faire par Gertraud, lâchez pas les laminines !

-Mikette (ou maman), ninja qui a toujours mal quelque part, qui construit une maison (oui à ce niveau c'est plus de la rénovation), qui aime se plaindre, jouer à Forge (ce n'est pas le seul) et aime être le vieux du groupe et bien sûr auusi à la famille Ambre et Nath (ou papa).

-la Goetz team (horrible en être réduit au nom de son chef ! Luc Goetz, Guillaume Goetz, Ninette Goetz, Vincent Goetz…). Lulu merci d'être un pyromane ! et merci pour les pétanques maintenant je sais comment que les gens du sud jouent... je m'inquiète moins pour

mon niveau … ; Guillaume (notre Breton) merci d'apporter un peu de « tenue » (et autre chose que la bio !) à ce labo, mon gars « à 100% » (merci pour ce souvenir aussi, Claire s'en souviendra toute sa vie en plus ! Elle me le ressortira de temps en temps)

-grosses bises aux mamans (il y en a partout !) Marie-Elodie et Camille …

-grosses pensées pour les déjà partis de la DB team : Alexia, Nadège, Laurent et Aurore (maman fernandouille pour toi c'est une grosse pensée ma collègue, **amie**, binôme même ! gros bisous !, et une grosse pensée au poulet papa sauce Mulhouse et à Gnocchi !), Elmina (mini-jupe woman, si on te met un masque t'es une super héroïne à l'accent slave et aux clopes de « distingués »), Manon (rousse préférée, copine de bibine, un grand bonheur !), Isabelle (ma lulu préférée du monde entier), mes stagiaires toutes mignonnes Elise et Mary, Caro (et son neurone de blonde, phrase que tu répètes encore et encore et encore et encore…), vonGette (Yannick), la princesse mexicaine Cynthia, Shankette (notre petit indien grand amoureux de pétanque avec son lancé unique), Sofiette (« ça va ») et les autres.

-grosses bises à Isa Gross (qui comme moi aime les pots de thèse, soirées, et fêtes du labo) et à Isa Gillot (fini les commandes pour moi en tout cas), Léo, Isa D, Claire, JNF (l'homme fan de jazz), Christian et sa moto, Georg et sa plus petite moto, Véro, Paula, Christophe, les jeunes, les voisins de bureau : Dominique G, Audrey, Radhia, Marie, Christelle, Damien, Pierre, Cyril et tous les autres !!!

Merci !

Tristan

Abstract (in French)

INTRODUCTION

Pendant des années le cancer a été considéré comme une maladie initiée uniquement par des mutations aux sein des futures cellules tumorales (Sonnenschein and Soto, 2000). Cependant si l'initiation de la tumeur est caractérisée par une prolifération anarchique des cellules cancéreuses, le développement du cancer nécessite la mise en place d'un microenvironnement tumoral (MET). Le point de départ d'un cancer est devenu non plus seulement une cellule "renégate", mais plutôt un ensemble de cellules mutées dans un microenvironnement dynamique et permissif en remodelage constant. Ainsi le travail de ces dernières années sur le MET a montré qu'il assure un rôle prépondérant dans la progression tumorale et la formation de métastases (Bissell and Hines, 2011). En effet, la première hypothèse sur le rôle de MET a d'abord été énoncée par Paget, qui en 1889 a proposé son hypothèse du « seed and soil » pour expliquer la sélectivité des métastases au sein d'organes spécifiques lors d'un cancer. Paget a suggéré que le développement de métastases n'est pas une question de « chance », mais est plutôt associé à une affinité spécifique des cellules tumorales (« seed ») pour un organe (« soil ») qui peut alors fournir un environnement de croissance favorable. Depuis, plusieurs modèles expérimentaux soutiennent cette hypothèse. Le rôle clé du microenvironnement dans la régulation de la progression du cancer a été démontré pare exemple, dans des expériences où le phénotype néoplasique de cellules tumorales est réprimé lorsque ces cellules sont gréffées dans un micro-environnement "normal" (McCullough et al., 1998; Sonnenschein and Soto, 2000). En effet, McCullough et ses collègues ont montré que des cellules épithéliales tumorigéniques de foie de rat génèrent une tumeur uniquement lorsqu'elles sont dans leur propre micro-environnement, le foie, mais pas lorsqu'elles sont greffées dans un autre organe comme la rate (McCullough et al., 1998). De façon convaincante, le travail de Illmensee et Mintz a montré que greffer des cellules de tératocarcinome murin dans un blastocyste d'embryon de souris ne conduit pas à la formation d'une tumeur, mais plutôt au développement d'une souris normale, présentant une incorporation de cellules tumorales dans les différents tissus, y compris au sein de la lignée germinale (Illmensee, 1978; Stewart and Mintz, 1981). Le travail de Bissell et Dolberg a aussi montré que le potentiel oncogénique des cellules transformées par le virus du sarcome de

Rous est inhibé lorsque les cellules sont injectées dans un embryon de poulet. Ce résultat indique que les propriétés de ces cellules tumorales peuvent être réprimées par un micro-environnement non permissif (Dolberg and Bissell, 1984). En outre l'injection de fibroblastes activés avec des cellules non-cancéreuses est suffisante pour déclencher la formation d'une tumeur tandis que ces cellules seules sont incapables de le faire par elles-mêmes (Camps et al., 1990; Olumi et al., 1998, 1999).

Si le micro-environnement "normal" peut réprimer la tumorigenèse, alors un microenvironnement anormal pourrait être, à l'opposé, capable de promouvoir ou même de déclencher l'initiation de la tumeur. Il existe des résultats soutenant cette hypothèse. Le travail de Maffini et ses collègues a montré que l'exposition du stroma à un agent cancérogène tel que la N-nitrosométhylurée (NMU) permet le développement de tumeurs. Cependant, le traitement *in vitro* de cellules épithéliales mammaires par ce carcinogène conduit à la formation d'une tumeur uniquement si leur greffe se fait dans un tissu préalablement exposé à ce même agent cancérigène (Maffini et al., 2004). Des conclusions similaires ont été tirées des expériences effectuées avec un autre agent cancérigène, un 4-nitroquinoléine N-oxyde (4-NQO) qui est utilisé pour induire expérimentalement par voie orale un carcinome des cellules squameuses chez la souris (Hawkins et al., 1994; Schoop et al., 2009). De même, la greffe de cellules épithéliales prénéoplasiques dans un micro-environnement mammaire préalablement irradié (facteur connu pour induire des mutations dans les cellules affectées) donne lieu à la formation de tumeurs mammaires (Barcellos-Hoff, 1998). Ces études soutiennent fortement que le microenvironnement est un puissant régulateur capable d'initier la formation de tumeurs à partir de cellules présentant des mutations oncogéniques.

Schématiquement, le MET comprend une composante cellulaire avec des cellules tumorales, des fibroblastes associés au cancer (CAF) ou des cellules vasculaires, ainsi que des composants moléculaires comme les protéines de la matrice extracellulaire (MEC) (Bissell and Hines, 2011; Lorusso and Rüegg, 2008). Initialement considérées pour leur rôle structural et passif, les molécules de la MEC sont maintenant bien connues pour réguler l'homéostasie tissulaire et d'autres phénomènes physiopathologiques (Frantz et al., 2010). Les protéines de la MEC jouent un rôle actif en modulant le comportement cellulaire. Elles agissent en activant des récepteurs d'adhésion et des cascades de signalisation, en régulant les contraintes biomécaniques du tissu ou en jouant un rôle potentiel de réservoir de facteurs de croissance (Erler and Weaver, 2009; Hynes, 2009). Dans le MET, certaines molécules sont surexprimées

par rapport au tissu normal. A titre d'exemple, des membre de la famille des collagènes (Chen et al., 2013), des laminines (Simon-Assmann et al., 2011) et des ténascines (Midwood et al., 2011) sont des protéines fortement surexprimées dans la plupart des tumeurs solides, en particulier dans le stroma tumoral. Les molécules de la MEC et les facteurs de croissance coopèrent dans le MET pour fournir des signaux biochimiques (par exemple, cytokines, chimiokines, matrikines) et les contraintes structurelles (molécules d'adhésion, forces biomécaniques) qui dictent leur comportement aux cellules afin de favoriser le développement du cancer (Schmeichel et al., 1998). En effet, les molécules de la MEC ne sont plus considérées comme de simples fibres d'ancrage pour les cellules (Frantz et al., 2010). Comme Richard Hynes l'a souligné dans l'une de ses revues, les molécules de la MEC ne sont pas « seulement des jolies fibres ». La MEC peut stimuler directement des signalisations cellulaires par l'activation de récepteurs d'adhésion cellulaire telles que les intégrines et moduler l'accès aux facteurs de croissance présents dans le micro-environnement (Hynes, 2009).

Toutes les cellules dans un tissu donné interagissent avec la MEC de façon dynamique. Les molécules de la MEC sont des agonistes puissants de multiples voies de signalisation qui modulent le comportement des cellules. Les intégrines sont un exemple de famille de récepteurs qui interagissent avec de nombreuses protéines de la MEC et qui sont impliqués dans la régulation du comportement cellulaire (Harburger and Calderwood, 2009). Les intégrines sont des hétérodimères composés de deux sous-unités β et α. Ils constituent une superfamille de récepteurs d'adhésion à la surface des cellules (comprenant trente membres fonctionnels connus). Les intégrines sont liées à la régulation du cytosquelette et jouent un rôle essentiel dans la régulation du comportement des cellules tel que leur ancrage, leur forme, leur polarité, leur prolifération, leur migration, leur survie ou leur différenciation. Les intégrines régulent plusieurs processus physiologiques tels que la cicatrisation ou l'organogenèse, mais sont également impliquées dans des pathologies telles que le cancer (Giancotti and Ruoslahti, 1999; Harburger and Calderwood, 2009). Les protéines de la MEC sont généralement de longues molécules possédant différents domaines. Ces domaines présentent des motifs qui ont le potentiel de se lier directement aux récepteurs d'adhésion. Cette interaction directe induit des réponses cellulaires à travers les voies de signalisation comme c'est le cas par exemple avec la fibronectine (FN). La FN est une glycoprotéine impliquée dans l'adhérence cellulaire et est retrouvée dans une grande variété de tissus (Hynes and Yamada, 1982). La FN se lie directement aux intégrines comme la α5β1, α4β1 or αvβ3 à travers son motif Arg-Gly-Asp (RGD), et détermine la polarité et la morphologie des cellules

ce qui affecte, par exemple, leur survie (Astrof and Hynes, 2009). Un rôle important des protéines de la MEC est aussi de servir de supports de signalisation pour les vaisseaux sanguins (Dejana and Orsenigo, 2013; Simon-Assmann et al., 2011). En effet, l'interaction entre les cellules qui composent les vaisseaux sanguins et les récepteurs aux intégrines comme $\alpha v\beta 3$ and $\alpha v\beta 5$ par l'intermédiaire des molécules de la MEC, a montré un rôle essentiel dans le développement et la stabilisation de ces vaisseaux (Oliveira-Ferrer et al., 2008). En outre, les intégrines sont des modulateurs indispensables de la polymérisation de l'actine et donc de l'organisation du cytosquelette. L'actine est l'une des protéines intracellulaires les plus abondantes dans les cellules eucaryotes. La propriété fondamentale de l'actine est sa capacité à polymériser et donc de passer de manière réversible d'une forme monomérique, l'actine globulaire appelée G-actine, en une actine polymérisée filamenteuse ou F-actine. Les monomères de G-actine sont capables de s'associer dans un agencement hélicoïdal pour former des filaments ou des structures de F-actine capables elles-mêmes de former des fibres de stress dans les cellules. Cette réorganisation du cytosquelette couplée à des protéines contractiles joue un rôle prépondérant dans la survie et la mobilité cellulaire. En effet la liaison des myosines et d'autres molécules avec ces fibres de stress ou câbles d'actine forme des prolongements cellulaires de type lamellipodes ou filopodes, qui régulent directement des processus tels que l'adhésion cellulaire, la migration et la morphogenèse (Ridley et al., 2003). La polymérisation de l'actine est régie essentiellement par trois membres de la famille des Rho GTPases, Rho, Rac et Cdc42, par le biais de facteurs spécifiques, les guanine-nucleotide-exchange factors (GEF) et les GTPase-activating proteins (GAP) (Allen et al., 1997).

Les cellules détectent les stimuli extracellulaires comme par exemple ceux de la MEC. Une question importante est de savoir comment est intégré ce signal et comment il est traduit et transduit menant à une voie de signalisation intracellulaire. La liaison des protéines de la MEC aux intégrines et la réorganisation induite du cytosquelette d'actine jouent un rôle crucial dans ce phénomène (Schwartz, 2004). En effet, l'activation des intégrines génère des complexes focaux qui modulent et orientent la polymérisation d'actine dans la cellule. Cela conduit à une activation de voie de transcription qui induit à partir du cytoplasme la translocation de facteurs de transcription vers le noyau. Grâce à la liaison de ces facteurs à des motifs spécifiques sur l'ADN, la polymérisation de l'actine a un impact sur l'expression de nombreux gènes (Allen et al., 1997; Ridley et al., 2003; Schwartz, 2004). Récemment à titre d'exemple, la polymérisation de l'actine cellulaire a montré qu'elle modulait deux effecteurs importants dans le développement, l'homéostasie mais aussi dans le cancer, YAP (Yes

associated protein) et un son co-activateur transcriptionnel TAZ (Tafazzin) (Halder et al., 2012). Des études récentes indiquent que YAP et TAZ sont des facteurs cruciaux pour relayer les signaux mécaniques provenant du micro-environnement (Halder et al., 2012; Tschumperlin, 2015; Tschumperlin et al., 2014). La signalisation YAP et TAZ influe sur la prolifération cellulaire, la migration ou la différenciation et est sensible aux molécules de la MEC et à l'état du cytosquelette (Calvo et al., 2013a; Dupont et al., 2011). En effet, YAP et TAZ sont régulés par la polymérisation de l'actine en F-actine qui permet ainsi leur translocation dans le noyau. Le complexe YAP/TAZ interagit alors dans le noyau avec les membres de la famille des TEAD 1 à 4 et active l'expression de gènes cibles pouvant par exemple moduler l'angiogenèse. En l'absence d'actine polymérisée, YAP subit une phosphorylation et est soit séquestré dans le cytoplasme, soit dégradé par le protéasome inhibant cette voie de signalisation (Halder et al, 2012;. Lapi et al., 2008).

Ensemble, ces données mettent en évidence l'importance d'étudier l'impact des molécules de la MEC dans l'homéostasie et la physiopathologie. Dans le laboratoire, nous nous intéressons principalement à un des membres de la famille des ténascines, la ténascine-C (TNC). La TNC est une glycoprotéine importante de la MEC qui est fortement induite lors de la cicatrisation, de l'inflammation ou dans le MET. Successivement nommée glial-mesenchymal extracellular matrix antigen, hexabrachion, cytotactin, J1 220/200, neuronectin et tenascin, la TNC appartient à une famille contenant quatre membres connus, les ténascines C, R, X et W (Midwood et al., 2011; Chiquet-Erishman et al., 2014). La TNC forme un hexamère résultant de la liaison de six monomères par des ponts disulfure dans la partie N-terminale de chaque protéine (Jones et Jones, 2000). Les monomères de TNC ont un poids moléculaire qui fluctue entre 180 et 320 kDa chez l'homme avec des rôles potentiellement indépendants (Jones et Jones, 2000). La TNC peut se lier à d'autres protéines telles que des facteurs de croissance, des récepteurs de surface cellulaire ou d'autres protéines de la MEC (Martino et al., 2014; Midwood et al., 2011; Saupe et al., 2013). La TNC est une molécule virtuellement absente ou très faiblement exprimée dans le tissu normal, mais est fortement surexprimée en conditions pathologiques comme dans le cancer. De plus, son expression est corrélée avec un mauvais pronostic pour la survie des patients (Herold-Mende et al., 2002; Ishihara et al., 1995; Midwood et al., 2011; Mitselou et al., 2012; Ohtsuka et al., 2013). La TNC favorise la progression du cancer en soutenant l'invasion des cellules tumorales et la formation de métastases (Hirata et al., 2009, Saupe et al., 2013). En effet la TNC jouerait un

rôle de niche pro-métastatique assurant un MET permissif au développement de la tumeur secondaire ou métastase (Lowy and Oskarsson, 2015).

De façon intéressante, l'expression de la TNC n'est pas limitée aux cellules cancéreuses mais est fortement présente dans le stroma (Castellani et al., 1995; Herold-Mende et al., 2002; Martina et al., 2010). En effet, malgré son absence au niveau des vaisseaux sanguins normaux, la TNC peut être fortement exprimée autour des vaisseaux sanguins tumoraux, en particulier dans les hauts stades de gliomes (Herold-Mende et al., 2002; Martina et al., 2010; Mustafa et al., 2012). L'expression périvasculaire de la TNC augmente avec le grade tumoral et est corrélée avec la malignité du cancer (Herold-Mende et al., 2002). Ces données et d'autres mentionnées dans différents types de tumeurs (Galler et al., 2011; Renkonen et al., 2013) indiquent que la TNC modulerait à l'angiogenèse tumorale.

L'angiogenèse correspond à la formation de nouveaux vaisseaux sanguins à partir de vaisseaux pré-existants (Folkman et al., 1989). La vascularisation de la tumeur est indispensable pour fournir les nutriments et l'oxygène requis à la progression tumorale. L'angiogenèse est contrôlée par un déséquilibre entre les facteurs pro- et anti-angiogéniques qui régulent la prolifération, la migration et l'organisation des cellules endothéliales (CE) et périvasculaires ainsi que le remodelage de la MEC et plus spécifiquement de la membrane basale vasculaire (Carmeliet and Jain, 2000). L'angiogenèse normale est un processus très structuré qui maintient l'homéostasie tissulaire, à contrario de l'angiogenèse pathologique qui est peu efficace et conduit à la progression de la maladie. L'angiogenèse tumorale est une caractéristique essentielle du développement des cancers (Hanahan and Weinberg, 2000, 2011). La formation du système vasculaire assure la progression de la tumeur, l'entretien et favorise la dissémination des cellules tumorales (Carmeliet and Jain, 2000). Grâce au travail de Judah Folkman nous savons qu'en l'absence d'une vascularisation suffisante la plupart des tumeurs ne peut pas dépasser 2 mm^3 et reste cliniquement inactive (Folkman, 1996; Hanahan and Folkman, 1996). En effet beaucoup de lésions cancéreuses ne progressent jamais à un stade invasif, probablement en raison d'une répression par le micro-environnement, ce phénomène est appelé « cancer sans maladie » (Folkman and Kalluri, 2004) ou dormance tumorale (Aguirre-Ghiso et al., 2007; Ghajar et al., 2013). De ce point de vue, les cellules tumorales ont besoin pour quitter leur état de dormance d'initier la formation de nouveaux vaisseaux pour ainsi proliférer, migrer et reprogrammer le microenvironnement. L'angiogenèse tumorale commence tôt au cours de la progression tumorale. L'initiation de l'angiogenèse tumorale résulte du déséquilibre entre facteurs pro- et anti-angiogéniques et est

appelée le « switch angiogénique » (Folkman et al., 1989). Ce déséquilibre de la balance vers une accumulation de facteurs pro-angiogéniques est responsable de la formation de néo-vaisseaux (Bergers and Benjamin, 2003). Ceci représente une série d'événements tels que la sécrétion de facteurs pro-angiogéniques, la survie accrue, l'activation, la migration des CE et la sécrétion d'enzymes protéolytiques (suivie par le remodelage de la membrane basale et la MEC alentour). Tout ceci qui conduit finalement à la formation d'un nouveau réseau vasculaire anarchique dans les tumeurs. Dans les cancers, l'angiogenèse est aberrante et conduit souvent à la formation de réseaux vasculaires désorganisés, chaotiques et peu fonctionnels (Carmeliet and Jain, 2011). Ceci conduit, en association avec une faible couverture péricytaire, à la déstabilisation des vaisseaux sanguins augmentant la perméabilité et l'hypoxie tumorale. Ainsi une angiogenèse incontrôlée dans les tumeurs solides entraîne un réseau vasculaire peu fonctionnel favorisant la formation de métastases (McDonald and Choyke, 2003).

Malgré son absence au niveau des artères ou des veines normales non endommagées ou en condition angiogénique physiologique comme dans l'endomètre ou le placenta (Martina et al., 2010; Mustafa et al., 2012; Trescher et al., 2013; Wallner et al., 1999; Zagzag et al., 1996), la TNC est exprimée autour des vaisseaux sanguins dans le MET (Brösicke et al., 2013; Galler et al., 2011; Herold-Mende et al., 2002; Martina et al., 2010; Renkonen et al., 2013). Ces informations suggèrent un rôle de la TNC dans l'angiogenèse tumorale. Cependant, les mécanismes sous-jacents du rôle de la TNC dans l'angiogenèse tumorale sont encore très mal compris voire contradictoires (Alves et al., 2011; Ballard et al., 2006; Besser et al., 2012; Castellon et al., 2002; Chung et al., 1996; Martina et al., 2010; Pezzolo et al., 2011; Saito et al., 2008; Schenk et al., 1999; Sumioka et al., 2011; Tanaka et al., 2003; Zagzag and Capo, 2002; Zagzag et al., 1995, 1996).

Notre hypothèse est que la TNC peut moduler l'angiogenèse de différentes manières dans le MET en agissant sur différents types de cellules. En effet, la TNC pourrait favoriser un microenvironnement pro-angiogénique et dans le même temps altérer l'endothélium qui pourrait conduire à une vascularisation importante mais inefficace et donc promouvoir l'agressivité de la maladie, comme il est classiquement décrit (Hanahan and Weinberg, 2011),. **Dès lors, le but de ce travail de thèse a été de déterminer comment la TNC affecte l'angiogenèse tumorale en établissant différents modèles d'étude de l'angiogenèse.**

RÉSULTATS

La TNC joue de multiples rôles dans l'angiogenèse tumorale avec des effets opposés encore mal compris. Dans ma thèse, j'ai abordé ses rôles aux niveaux cellulaire et moléculaire utilisant des modèles *in vitro, ex vivo* et *in vivo*.

But 1 & 2 : Établir des modèles *in vivo*, *ex vivo* et *in vitro* pour élucider les rôles de la TNC dans l'angiogenèse normale et tumorale & Identifier les mécanismes moléculaires en aval de la TNC pertinents pour l'angiogenèse tumorale

Nous avons voulu tout d'abord caractériser la distribution spatiale de la TNC *in vivo*. Pour ce faire nous nous sommes focalisés sur un modèle de tumeur cérébrale, les gliomes, décrits comme présentant chez l'homme une expression importante et hétérogène de TNC mais aussi une forte expression au niveau périvasculaire (Hirata et al., 2009; Martina et al., 2010). Nous avons alors vérifié que la TNC était exprimée dans un modèle de xénogreffes de biopsie humaine de glioblastome (GBM). Ainsi nous avons montré que la TNC présente dans le tissu provenait des cellules tumorales et des cellules du stroma (en utilisant respectivement des anticorps espèce spécifique pour la TNC humaine et de souris). De plus la TNC se retrouve fortement exprimée autour des vaisseaux sanguins et est co-localisée avec des cellules stromales périvasculaires et des cellules tumorales. Ces cellules tumorales participeraient donc à l'organisation des vaisseaux tumoraux probablement par un processus de « vasculogenic mimicry », déjà décrit dans d'autres travaux (Pezzolo et al., 2011). De plus nous avons observé *in vitro* que, contrairement aux péricytes et fibroblastes, les CE n'exprimaient pas la TNC. Ces éléments suggèrent que **l'expression de la TNC autour des vaisseaux tumoraux proviendrait des cellules périvasculaires comme les péricytes ou les fibroblastes ainsi que des cellules cancéreuses.**

Afin de comprendre comment la TNC agit sur l'angiogenèse, nous avons analysé l'impact direct de la TNC sur les CE. Nous avons dans un premier temps établi et utilisé un modèle de formation de protrusions endothéliales multicellulaires appelé « aortic ring assay ». Nous avons utilisé des anneaux d'aortes thoraciques de souris invalidées pour la TNC (knock out, KO) ou non (wt). Ces anneaux ont alors été incorporés dans une matrice 3D afin de quantifier les structures endothéliales formées. Nous avons pu mettre en évidence que la **TNC**

exprimée dans les anneaux de souris wt réduisait le nombre et la longueur des protrusions angiogéniques par rapport aux anneaux de souris invalidées pour la TNC. Afin de se rapprocher du contexte du MET, nous avons établi un modèle de co-culture microvasculaire qui utilise des CAF exprimant différents niveaux de TNC ensemencés avec des CE ; modèle qui permet la formation d'un réseau de type vasculaire *in vitro* (Ghajar et al., 2013). Grâce à ce système nous avons montré que **le réseau angiogénique formé par les CE était réduit en présence d'un fort niveau d'expression de la TNC**. Enfin en analysant la tubulogenèse des CE induite par du matrigel, nous avons démontré que la capacité des CE à former des pseudo-tubes était réduite de façon dose dépendante par l'ajout de TNC purifiée. Ces différents résultats nous ont montré que la **TNC réprime les protrusions angiogéniques et la tubulogenèse.**

Afin de comprendre par quels mécanismes cellulaires la TNC module le comportement des cellules vasculaires, nous avons tout d'abord analysé l'effet de la TNC sur la survie et la migration des CE et des péricytes (qui stabilisent les vaisseaux sanguin). Pour ce faire nous avons établi un modèle de MEC sécrétées par des fibroblastes exprimant différents niveaux de TNC et appelé matrices dérivées de cellules (MDC). Ce modèle présente l'avantage de fournir un feuillet 3D complexe de protéines contenant un assemblage de molécules de la MEC organisées de façon comparable à un tissu normal *in vivo* (Goetz et al., 2011). Grâce à ce système nous avons montré que **la TNC réduisait la croissance d'une population de CE en augmentant l'apoptose cellulaire.** En utilisant des molécules purifiées pour produire un substrat contrôlé de MEC, nous avons pu aussi montrer que **la prolifération des CE était diminuée sur un substrat réalisé avec de la TNC purifiée** et que celui-ci augmentait aussi l'apoptose cellulaire. Cependant à la différence des CE, **la croissance d'une population de péricytes sur une MDC exprimant ou non la TNC ou un substrat de TNC purifiée n'était pas affectée**.

Pour analyser l'impact de la TNC sur la migration cellulaire nous avons utilisé le modèle de blessure sur feuillet confluant avec des CE et péricytes. Nous avons montré que **la TNC réduisait la migration des différents modèles de CE mais aussi des péricytes**. De plus en utilisant une méthode de traçage des CE sur substrat de protéine purifiée nous avons montré que la directionalité et la mobilité des CE étaient diminuées sur TNC. Nous avons aussi pu constater que la **TNC réduisait fortement l'adhésion des CE et des péricytes.** Tous ces résultats combinés nous ont indiqué qu'**un réseau matriciel contenant de la TNC en**

contact avec les cellules vasculaires réprimait plusieurs caractéristiques de l'angiogenèse que sont la tubulogenèse, la migration et la survie des cellules du compartiment vasculaire.

D'un point de vue moléculaire, la voie de signalisation YAP/TAZ a été récemment décrite comme facteur clé de la mécano-transduction dans le contexte tumoral. YAP et TAZ sont des facteurs de transcription capables de réagir et d'intégrer des signaux extracellulaires émanant de la MEC qui aboutissent à l'expression de gènes dont la plupart sont reliés à l'angiogenèse. YAP est régulé par la polymérisation de l'actine et la morphologie des cellules qui permettent sa translocation dans le noyau et donc l'activation de la voie de signalisation et l'expression de gènes cibles (Halder et al., 2012). Dans un test de contraction de collagène par des fibroblastes nous avons démontré que des fibroblastes exprimant un niveau élevé de TNC augmentaient la contraction du gel. Ces éléments indiquent que la **TNC pourrait modifier les propriétés mécaniques d'un tissu et donc réguler la signalisation YAP**. Nous avons montré qu'un substrat contenant de la TNC réduisait drastiquement l'étalement des CE et la formation de fibres de stress, deux éléments régulant YAP. De plus nous avons observé que la TNC réprimait la translocation de YAP dans le noyau et l'expression de gènes cibles spécifiques comme les protéines CTGF et Cyr61. Ces éléments proposent que la **TNC réprime l'activité de YAP qui participerait à l'effet direct anti-angiogénique de la TNC sur les cellules vasculaires.**

Enfin nous avons étudié l'effet indirect ou paracrine de la TNC sur l'angiogenèse lorsqu'elle interagit avec des cellules tumorales. Pour cela nous avons utilisé une MDC exprimant ou non la TNC afin d'étudier son impact sur le sécrétome de cellules de glioblastome mais aussi des CAF. Nous avons ainsi pu montrer qu'une matrice de TNC favorisait de manière paracrine la survie des CE et la tubulogenèse *in vitro*. De façon intéressante, en développant des cellules de glioblastome sous-exprimant la TNC par stratégie knock down, nous avons observé de façon similaire que le sécrétome des cellules exprimant fortement la TNC favorisait l'angiogenèse *in vitro*. Au final, ces résultats suggèrent qu'**un MET riche en TNC promeut une modification de sécrétome des cellules de glioblastome et des CAF en faveur d'un sécrétome pro-angiogénique.** Enfin, d'un point de vue moléculaire, nous avons pu identifier par spectrométrie de masse différentes molécules candidates du sécrétome, soit **réprimées par la TNC**, comme la **lipocaline-1 (LCN1)** décrite comme répresseur potentiel de la migration cellulaire (Zhang et al., 2006) et dont nous avons montré la capacité de réprimer l'angiogenèse des CE dans une expérience de tubulogenèse sur

matrigel ; soit **induites par la TNC**, comme la cytokine pro-angiogénique **CXCL12 (ou SDF1)** (Ho et al., 2010), participant au phénotype pro-angiogénique du sécrétome induit par la TNC, confirmer par l'utilisation d'un inhibiteur pharmacologique. Ainsi la modulation du sécrétome par la TNC favoriserait indirectement l'angiogenèse tumorale.

But 3 : Description du rôle de la TNC dans l'angiogenèse tumorale en utilisant un modèle de tumorigenèse spontanée chez la souris.

Mes expériences ont aussi contribué à deux publications où nous avons pu montré que la TNC promeut le switch angiogénique et l'angiogenèse tumorale dans un modèle stochastique de tumeur pancréatique chez la souris (Langlois et al., 2014; Saupe et al., 2013). Nous avons utilisé le modèle Rip1-Tag2 (RT2) dans lequel sont induites de façon spontanée des tumeurs neuroendocrines du pancréas (PNET) et qui nous a permit de disséquer les mécanismes de la progression tumorale et de l'angiogenèse (Hanahan, 1985). En effet dans ce modèle les cellules pancréatiques β des îlots de Langerhans expriment de façon ectopique l'antigène T de l'oncogène SV40 (Tag) sous le contrôle du promoteur de l'insuline du rat (Rip). Ceci entraîne la transformation séquentielle d'une fraction des îlots normaux en tumeurs hyperplasiques, suivies de tumeurs angiogéniques et finalement pour une fraction d'entre elles de tumeurs macroscopiques. Le modèle RT2 présente plusieurs avantages par rapport à des modèles de xénogreffe de souris car il reproduit une tumorigenèse spontanée en plusieurs étapes successives dans un environnement immunitaire intact, comme c'est le cas dans un cancer humain. Le modèle RT2 a été fortement utilisé pour étudier le switch angiogénique qui se produit entre 5 et 10 semaines dans ce modèle (Hanahan and Folkman, 1996).

Ainsi nous avons pu analyser le rôle de la TNC dans la progression et l'angiogenèse tumorale *in vivo* dans le modèle RT2. Nous avons d'abord utilisé une analyse transcriptomique afin d'analyser les gènes impliqués dans le switch angiogénique. En comparant des tumeurs non-angiogéniques versus des tumeurs angiogéniques sur des souris âgées de 8 semaines nous avons démontré que le profil d'expression des gènes révélait l'expression différentielle de 298 gènes lors du switch angiogénique avec une part importante de ceux-ci appartenant au matrisome (Naba et al., 2012). De façon intéressante, **la TNC a été identifiée comme l'une des molécules de la MEC les plus fortement surexprimées lors du switch angiogénique**. Ces données de transcriptomique ont ensuite été validées par RT-qPCR

et immunohistochimie et ont montré une forte expression de la TNC dans les tumeurs angiogéniques, absente des tumeurs non-angiogéniques (Langlois et al., 2014).

Afin d'analyser en détail le rôle de la TNC dans l'angiogenèse tumorale, nous avons développé deux modèles de gain et de perte de fonction pour la TNC dans le modèle RT2 en croisant des souris RT2 avec des souris TNC knock out (KO) ou RipTNC (expression ectopique de TNC dans cellules pancréatiques β sous la répression du Rip). Tout d'abord, nous avons montré que **l'expression de la TNC était associée à la progression tumorale et favorisait la formation des métastases**. Nous avons aussi prouvé que la TNC promeut le switch angiogénique avec une diminution des tumeurs angiogéniques dans le modèle TNC KO (RT2/TNCKO) et une augmentation dans le modèle RT2 surexprimant la TNC (RT2/TNC) par rapport à leur contrôle respectif. Ainsi ces résultats ont montré que la **TNC n'est pas nécessaire pour induire le switch angiogénique, mais joue un rôle important dans sa promotion**.

Dans une analyse détaillée de l'impact de la TNC sur l'angiogenèse tumorale, nous avons observé que la TNC favorise la formation de vaisseaux sanguins peu-fonctionnels dans les tumeurs RT2 (Saupe et al., 2013). En effet, nous avons analysé l'ultrastructure de la vascularisation tumorale dans nos modèles par une méthode de « vascular cast corrosion » suivant d'une analyse par microscopie électronique à balayage. Ainsi nous avons pu observer avec le modèle RT2/TNC que **lorsque la TNC est surexprimée l'anatomie des vaisseaux semble fortement aberrante avec des vaisseaux de forme irrégulière, très ramifiés et agglomérés**. Lorsque la TNC n'est pas exprimée (RT2/TNCKO), les vaisseaux sont également différents avec des diamètres très hétérogènes qui suggèrent que le flux sanguin est perturbé. En outre, nous avons montré par immunofluorescence que **la densité des vaisseaux sanguins dans la tumeur est plus importante dans le modèle RT2/TNC et diminuée dans le modèle RT2/TNCKO**. Nous avons également évalué l'impact de la surexpression de la TNC sur le recouvrement des vaisseaux par les péricytes, et nous avons montré que celui-ci était réduit, **indiquant un défaut dans la maturation/stabilisation des vaisseaux sanguins**. Nous avons également déterminé qu'en absence de TNC la perfusion de la tumeur était réduite et aussi que **la perméabilité des vaisseaux était inversement corrélée avec le niveau d'expression de la TNC**. En conclusion, nous avons pu montrer en utilisant le modèle RT2 que la TNC **régule l'angiogenèse tumorale en favorisant une forte vascularisation peu fonctionnelle, qui est corrélée avec la formation de métastases** (Saupe et al., 2013).

DISCUSSION

Dans ce travail, j'ai analysé le rôle de TNC dans l'angiogenèse physiologique et tumorale. La TNC est une molécule de la MEC virtuellement absente du tissu normal et fortement exprimée dans des situations pathologiques, et en particulier dans les tumeurs solides (Abdou et al., 2012; Adams et al., 2002; Arican Ozluk et al., 2015; Midwood and Orend, 2009; Mitamura et al., 2002; Mustafa et al., 2012; Oskarsson et al., 2011; Trescher et al., 2013). La TNC a été clairement impliquée dans l'invasion tumorale et la formation de métastases (Hirata et al., 2009; O'Connell et al., 2011; Oskarsson et al., 2011; Saupe et al., 2013; Tang et al., 2015). Elle est également corrélée au pronostic des patients dans plusieurs types de tumeurs (Emoto et al., 2001; Herold-Mende et al., 2002; Leins et al., 2003; Mitselou et al., 2012; Nong et al., 2015; Ohtsuka et al., 2013; Tang et al., 2015). Il est intéressant d'observer que la TNC est exprimée uniquement autour des vaisseaux sanguins en condition pathologique comme c'est le cas dans le cancer, suggérant un rôle dans l'angiogenèse tumorale, mais que sa fonction n'a pas été correctement caractérisée (Alves et al., 2011; Chung et al., 1996; Galler et al., 2011; Herold-Mende et al., 2002; Martina et al., 2010; Pezzolo et al., 2011; Saito et al., 2008; Tanaka et al., 2003; Zagzag and Capo, 2002; Zagzag et al., 1995, 1996).

Nous avons montré que la TNC favorise la progression tumorale *in vivo* en utilisant le modèle de tumorigenèse spontané RT2. J'ai contribué dans cette étude à révéler que la TNC joue de multiples rôles en améliorant la survie, la prolifération et l'invasion des cellules tumorales. La TNC améliore également l'angiogenèse tumorale et la formation de métastases pulmonaires dans ce modèle (Saupe et al., 2013). Alors que la TNC promeut le switch angiogénique et augmente la densité des vaisseaux sanguins, le niveau d'expression de la TNC semble également favoriser une vascularisation altérée avec une faible couverture péricytaire et une forte perméabilité des vaisseaux sanguins (Langlois et al., 2014; Saupe et al., 2013). Au total, ces résultats suggèrent que la TNC peut avoir des fonctions multiples et potentiellement opposées dans l'angiogenèse tumorale.

Au cours de ma thèse, j'ai utilisé plusieurs méthodes afin d'analyser l'angiogenèse en laboratoire. J'ai utilisé de façon complémentaire des méthodes *in vivo*, *ex vivo* et *in vitro* qui m'ont permis de caractériser les rôles de la TNC dans le MET pendant l'angiogenèse

physiopathologique et tumorale ainsi que d'apporter un nouvel aperçu sur les mécanismes sous-jacents de la TNC. Les résultats de mon travail de doctorat ont montré qu'une interaction directe des cellules vasculaires (CE ou péricytes) avec la TNC altérait les critères de l'angiogenèse tels que la survie, la migration et la tubulogenèse. Inversement, l'utilisation de milieux conditionnés provenant des cellules tumorales de glioblastome ou de CAF cultivées sur une matrice contenant de la TNC promeut l'angiogenèse. Ainsi mes résultats suggèrent que TNC régule de façon différentielle l'angiogenèse par deux effets, anti-angiogénique direct par contact de la TNC avec des cellules endothéliales et péricytaires, et par un effet paracrine pro-angiogénique du à la capacité de la TNC de favoriser un sécrétome pro-angiogénique. J'ai également identifié des mécanismes moléculaires intervenant dans les rôles pro- et anti-angiogéniques de la TNC (Rupp et al., en préparation).

1. La TNC est un marqueur des vaisseaux sanguins pathologiques y compris dans le cancer

La TNC est très abondante dans le MET, des cellules tumorales ainsi que des cellules stromales interagissent avec elle. Dans ce travail nous avons analysé l'expression et la localisation de la TNC dans un modèle de xénogreffe de cellules de glioblastome humaines par immunofluorescence. Nous avons montré que la TNC est exprimée par les cellules tumorales par un marquage spécifique de la TNC humaine. Nous avons également observé l'expression de la TNC au niveau du compartiment périvasculaire provenant des cellules stromales (cellules périvasculaires de type péricytaires ou fibroblastiques) et tumorales. En effet, les cellules tumorales peuvent se transdifférencier en CE, comme déjà décrit dans la littérature, par exemple, par les observations de Pezzolo et ses collègues qui ont montré que les cellules tumorales pouvaient exprimer des marqueurs endothéliaux et participaient fortement à l'expression de la TNC au niveau de l'endothélium dans un modèle de médulloblastome (Pezzolo et al., 2011). De plus nous avons montré en utilisant quatre modèles de CE *in vitro* dans différentes conditions que la TNC n'était pas exprimée par ces cellules. Cette observation est cohérente avec celle de Alves et collaborateurs qui n'ont pas détecté de TNC provenant d'HUVEC (Alves et al., 2011). En outre nous n'avons pas observé d'expression de la TNC dans notre modèle physiologique d'angiogenèse rétinienne. Différentes autres équipes ont également noté l'absence d'expression de la TNC au niveau de structures vasculaires normales telles qu'autour de vaisseaux cardiaques, pulmonaires,

hépatiques, mammaires, dans les néo-vaisseaux du placenta ou dans le cerveau en condition physiologique (Ballard et al., 2006; Kimura et al., 2014; Kuriyama et al., 2011; Martina et al., 2010; Mustafa et al., 2012; Natali et al., 1991; Shimojo et al., 2015; Zagzag et al., 1996). Cependant la TNC absente au niveau de l'aorte ou d'artères de la glande mammaire, se retrouve ré-exprimée dans les tissus de patients présentant une dissection aortique ou des plaques d'athérome (Trescher et al., 2013; Wallner et al., 1999). Au total, ces travaux et d'autres suggèrent fortement que la TNC est probablement absente de vaisseaux sanguins normaux et pendant l'angiogenèse normale. Toutefois, dans un contexte pathologique comme dans les tumeurs la TNC est ré-exprimée principalement par les cellules tumorales et périvasculaires mais non par les CE. Ainsi l'expression de la TNC autour des vaisseaux sanguins pourrait être classée comme un marqueur de stress vasculaire qui participerait à déstabiliser les vaisseaux sanguins favorisant l'avancée de la maladie, puisque notre étude et la littérature suggèrent que la TNC est associée à une vascularisation aberrante.

2. Le contact direct de la TNC avec les CE altère l'angiogenèse et implique la répression de la voie de signalisation YAP

Nous avons démontré que l'interaction de la TNC avec les CE perturbait l'angiogenèse. Grâce à nos modèles *in vivo* d'angiogenèse physiologique rétinienne et *ex vivo* de sprouting angiogénique à partir d'anneaux d'aorte thoracique, nous avons montré que l'expression de la TNC réduisait la capacité des CE à former de nouveaux vaisseaux. Nous avons observé des résultats similaires en utilisant un modèle de co-culture 3D avec des CAF ou en utilisant de la TNC purifiée dans un modèle de tubulogenèse sur matrigel. Enfin en utilisant des modèles 2D et 3D de substrat matriciel nous avons montré que la TNC réprimait la prolifération, la survie, l'adhésion et la migration des CE. Nous avons également observé que la TNC réduisait l'adhésion et la migration des péricytes. Ainsi l'expression de la TNC pourrait altérer l'organisation des vaisseaux sanguins à l'intérieur de la tumeur. Cette hypothèse est appuyée par nos résultats dans notre modèle d'insulinome spontané RT2 où les souris exprimant fortement la TNC présentent une perméabilité vasculaire plus forte (Saupe et al., 2013). De plus plusieurs équipes ont pu montrer que la TNC affectait négativement l'angiogenèse dans d'autres modèles physiopathologiques ou *in vitro*. Alves et collaborateurs ont décrit une réduction de la tubulogenèse d'HUVEC pré-éduqués par un substrat contenant de la TNC dans un essai de tubulogenèse sur matrigel (Alves et al., 2011). Ballard et ses

collègues ont utilisé un modèle où les CE sont étalées sur un substrat de TNC qui est recouvert par un gel de collagène I. Ils ont montré que les CE s'échappent d'avantage du substrat de TNC et envahissent le gel de collagène, ce qui suggère que la TNC pourrait agir en molécule répulsive pour les CE (Ballard et al., 2006) et donc orienter un guidage des cellules. Cette idée se retrouve dans le travail d'Andreas Faissner qui a montré des effets répulsifs similaires de la TNC sur les neurones et les cellules gliales (Faissner and Kruse, 1990; Scholze et al., 1996). D'autres travaux montrent que l'expression de la TNC perturbe la stabilité des vaisseaux sanguins dans un contexte de pathologie vasculaire comme dans la dissection aortique (Trescher et al., 2013). Il est intéressant de voir que la TNC a été également décrite pour augmenter la perméabilité des vaisseaux du tronc céphalique lors de la régénération des tissus après lésions chez la souris (Peter et al., 2012). En outre Bicer et ses collègues ont suggéré que la TNC serait associée à un défaut de la maturation des vaisseaux sanguins en analysant une forte expression de la TNC au niveau des malformations artério-veineuses cérébrales (Bicer et al., 2010). Kuriyama et ses collègues ont aussi montré que la TNC non détectée dans le foie normal se retrouve ré-exprimée après une ischémie induite, en particulier autour des vaisseaux sanguins ce qui conduit à une faible re-vascularisation et plus de nécrose (Kuriyama et al., 2011). Ces résultats et les notre suggèrent fortement que la TNC altère l'angiogenèse. Ainsi la TNC participerait à une vascularisation inefficace dans les tumeurs augmentant l'hypoxie, facteur crucial relié à l'agressivité de la tumeur (Jain, 2005).

J'ai pu montrer que la TNC réduisait fortement l'adhésion, l'étalement et polymérisation de l'actine en fibres de stress dans les CE, résultats déjà connus dans d'autres modèles cellulaires (Huang et al., 2001b; Saupe et al., 2013). Cependant l'impact en termes de signalisation est peu connu. Récemment, la voie Hippo comprenant YAP/TAZ a été liée à la régulation de la survie et la prolifération en réponse à l'adhésion cellulaire (Halder et al., 2012). Cette voie de signalisation est régulée par la polymérisation de l'actine et mène à l'expression de gènes impliqués dans l'angiogenèse. En effet la voie de signalisation YAP/TAZ est importante pour la survie et la migration des CE et est régulée par la géométrie de la cellule (Dupont et al., 2011). Dans ce travail, j'ai montré qu'un substrat de TNC était capable de réprimer l'activité de YAP/TAZ dans les CE ce qui abouti à la régulation négative de gènes cibles tels que CTGF et Cyr61. Ces gènes sont connus pour favoriser l'angiogenèse physiologique et tumorale *in vitro* et *in vivo* (Brigstock, 2002; Leu et al., 2002; Maity et al., 2014) et donc participeraient aux effets délétères de la TNC sur les CE. L'inhibition de RhoA (induisant la polymérisation de l'actine) (Lange et al., 200; Wenk et al., 2000) ou la

surexpression par la TNC de l'inhibiteur de la voie YAP/TAZ, la protéine 14-3-3 Tau (Lapi et al., 2008 ; Martin et al., 2003) pourraient aussi participer à expliquer comment la TNC réprime cette voie.

3. La TNC favorise de façon paracrine l'angiogenèse tumorale en orientant le sécrétome des cellules tumorales et des CAF vers un sécrétome pro-angiogénique

Nous avons montré que le contact direct entre la TNC et les CE induisait une répression des mécanismes de l'angiogenèse. Cependant ces résultats n'expliquent pas les observations *in vivo* montrant que la TNC favorise la formation de vaisseaux sanguins dans les tumeurs (Saupe et al., 2013). De façon intéressante, le niveau d'expression de la TNC est corrélé avec le grade tumoral (Herold-Mende et al., 2002; Orend et al., 2005; Saupe et al., 2013). En effet plus la tumeur est agressive plus l'expression de la TNC est importante. De façon intéressante on retrouve ce pattern d'expression au niveau périvasculaire avec dans les premiers stades de développement de la tumeur une absence d'expression, suivie dans les hauts grades d'une forte expression. Cette caractéristique est particulièrement évidente dans les gliomes ce qui est corrélé avec un pronostic de survie aggravé pour les patients (Herold-Mende et al., 2002; Midwood et al., 2011). Ainsi notre hypothèse est que la TNC, qui pour induire un phénotype d'une cellule doit directement interagir avec elle, ne peut affecter négativement les vaisseaux que dans les stades les plus agressifs, c'est-à-dire quand la TNC est exprimée et peut interférer avec les cellules périvasculaires et les CE. Cependant nous avons montré que la TNC influençait l'angiogenèse dès les premiers stades du développement tumoral par interaction avec de nombreuses autres types cellulaires comme les cellules tumorales ou les CAF (Hanahan and Weinberg, 2011; Kalluri and Zeisberg, 2006). Ici, nous avons mis l'accent sur les cellules de GBM puisque celles-ci expriment de façon importante la TNC et dont on retrouve sa forte expression dans ce type de tumeurs, en particulier autour des vaisseaux sanguins (Herold-Mende et al., 2002; Midwood et al., 2011). Nous avons observé que trois différentes lignées de cellules de glioblastome humain peuvent être « éduquées » par contact avec la TNC et déclencher la sécrétion de facteurs qui favorisent la survie, la prolifération et la tubulogenèse des CE. En effet nous avons montré que la TNC induit chez des cellules de GBM un sécrétome qui stimule l'angiogenèse, ceci a été observé en utilisant une stratégie knock down pour la TNC dans ces mêmes cellules ou en les mettant en contact avec une matrice exprimant fortement la TNC. Les fibroblastes sont aussi connus pour être

une source importante de TNC dans les cancers (Kalluri et Zeisberg., 2006; O'Connell et al, 2011) et donc pourraient également être « éduqués » par la TNC. Ainsi nous avons observé que tout comme pour les cellules de GBM, le contact de fibroblastes avec de la TNC conduisait un sécrétome pro-angiogénique.

Ainsi au contraire de son effet par contact direct avec les CE, la TNC induit de manière indirecte/paracrine un effet pro-angiogénique à travers la modulation du sécrétome des cellules tumorales et des CAF. Un effet indirect potentiel de la TNC sur l'angiogenèse avait également été suggéré mais jamais caractérisé. En effet, Martina et ses collaborateurs ont montré une augmentation des prolongements endothéliaux provenant de sphéroïdes formées à partir d'HUVEC cultivées dans un gel de collagène, lorsqu'elles étaient en co-culture avec des cellules sur-exprimant la TNC ensemencées au dessus du gel (Martina et al., 2010). Sumioka et collaborateurs ont utilisé le test de néo-vascularisation cornéenne après blessure avec des souris TNC KO ou sauvages afin d'analyser l'effet de la TNC sur la régénération vasculaire et tissulaire. Ils ont montré que l'absence de TNC chez les souris déficientes réduisait la formation de vaisseaux sanguins vers le site de la cicatrice. En effet, ils ont démontré que la TNC favoriserait l'expression de cytokines pro-angiogéniques telles que le VEGFA et le TGFβ1 par les fibroblastes présents au-dessous de l'épithélium cornéen mais non en contact avec les vaisseaux sanguins (Sumioka et al., 2011). Ces résultats suggèrent que les fibroblastes ou plus généralement d'autres types cellulaires peuvent être éduqués par la TNC afin qu'ils sécrètent des facteurs pro-angiogéniques et puissent promouvoir l'angiogenèse. Tanaka et ses collègues ont utilisé un modèle de xénogreffe de mélanome où les cellules tumorales ont été greffées en sous-cutané dans des souris sauvages ou KO pour la TNC. Ils ont pu montrer que l'expression de la TNC par le stroma tumoral augmentait la croissance tumorale et ont suggéré que la densité et la perfusion des vaisseaux sanguins tumoraux étaient plus importantes (Tanaka et al., 2003). Cette observation est en accord avec nos résultats montrant, pour la première fois et de façon significative, que la perfusion des vaisseaux tumoraux est réduite chez les souris RT2 n'exprimant pas la TNC tout comme leur densité (Saupe et al., 2013; ce travail). Ces résultats suggèrent que les cellules du stroma peuvent, sous l'influence de la TNC, promouvoir l'angiogenèse physiologique dans le cas d'un phénomène de cicatrisation, de régénération tissulaire ou lors de l'angiogenèse tumorale. L'expression de la TNC par des cellules cancéreuses peut également jouer un rôle important lors de la progression tumorale. Dans un modèle de xénogreffe de neuroblastome, Pezzolo et collaborateurs ont observé une augmentation de la densité vasculaire et de la croissance

tumorale lorsque les cellules tumorales exprimaient la TNC en comparaison à des cellules knock down pour la TNC (Pezzolo et al., 2011). Ces expériences et les notres démontrent que la TNC qui dérive du stroma ou des cellules tumorales (au moins dans contexte de neuroblastome, de gliome, de mélanome ou d'insulinome) régule l'angiogenèse tumorale.

Dans ce travail, nous avons utilisé de nombreux de modèles afin d'aborder les différents versants qui caractérisent l'angiogenèse. Au final, nous avons apporté de nouveaux éléments démontrant que le rôle de la TNC dans l'angiogenèse esr multiples voire contradictoires. La TNC par contact direct avec les cellules composant les vaisseaux sanguins affecteraient négativement leur organisation et leur survie alors que l'interaction de la TNC avec d'autres types cellulaires dans la tumeur comme les cellules tumorales et les fibroblastes induirait un sécrétome pro-angiogénique qui favoriserait l'angiogenèse. C'est pourquoi, nous avons cherché à déterminer la composition moléculaire de ce sécrétome induit par la TNC et à caractériser les effecteurs moléculaires. Pour ce faire, nous avons utilisé une approche de protéomique qui nous a révélé une forte abondance de molécules angio-modulatrices dans ce sécrétome. En effet, par une technique de spectrométrie de masse (LC-MS/MS), nous avons identifié près de 685 molécules sécrétées significativement dérégulées en présence de TNC ou non. Plus important encore, nous avons observé que les molécules ayant une fonction anti-angiogénique étaient principalement retrouvées dans le sécrétome des cellules de GBM cultivées dans un environnent pauvre en TNC. En effet nous avons identifié plusieurs puissants inhibiteurs de l'angiogenèse dont l'angiotensinogène (Corvol et al., 2003; Vincent et al., 2009), l'activateur tissulaire du plasminogène (Shim et al., 2005), la cytokine CXCL14 (Shellenberger et al., 2004) ou la molécule de la MEC, thrombospondine-1 (Lawler, 2002). En outre, nous avons identifié une autre protéine LCN1 qui de façon intéressante, est complètement réprimée par la TNC. De plus nous avons montré, pour la première fois, que cette molécule était capable de réduire l'angiogenèse *in vitro*. La LNC1 est surexprimée dans certaines pathologies comme la rétinopathie diabétique (Csősz et al., 2012), la dégénérescence maculaire liée à l'âge (Yao et al., 2013), la fibrose kystique (Redl et al., 1998) ou dans la maladie pulmonaire obstructive chronique (Wang et al., 2014). Néanmoins la LCN1 jouerait un rôle anti-inflammatoire en particulier dans certaines pathologies pulmonaires (Nicolas et al., 2010; Wang et al., 2014). Ainsi la TNC, connue pour promouvoir l'inflammation (Chockalingam et al., 2013; Mancuso et al., 2006; Midwood et al., 2009;. Page et al, 2012; Patel et al., 2011), pourrait réprimer l'expression de molécules anti-inflammatoires comme la

LCN1 afin de favoriser la maintien d'un micro-environnement pro-inflammatoire propice au développement du cancer.

A contrario les molécules ayant une fonction pro-angiogénique ont été principalement retrouvées dans les sécrétome des cellules « éduquées » par un environnement riche en TNC. Ces résultats suggèrent que la TNC est un puissant inducteur d'une signature pro-angiogénique en particulier dans les cellules de GBM. Parmi les molécules présentes dans cette signature, nous avons identifié la transglutaminase-2 (Haroon et al., 1999; Wang et al., 2013b), la pléiotrophine (Papadimitriou et al., 2009;. Perez-Pinera et al., 2008) ou les agonistes de la voie Wnt, Wnt7b (Mongiat et al., 2010) et Wnt5a/b (Masckauchán et al., 2006), tous décrits comme inducteurs de l'angiogenèse. De façon intéressante, nous avons également montré qu'un autre membre de la famille des lipocalines, la lipocaline-7 (LCN7 ou tubulointerstitial nephritis antigen-like 1, TINAGL1) était la protéine la plus surexprimée par la TNC et que celle-ci était une protéine récemment décrite comme nouveau angio-modulateur. En effet, la LCN7 est exprimée dans les vaisseaux sanguins (Li et al., 2007) et le groupe de Allan Albig a montré que sa surexpression promeut la tubulogenèse, le sprouting angiogénique, l'invasion et la survie des CE. Ils ont aussi démontré que la LCN7 favorisait l'angiogenèse physiologique *in vivo* dans le modèle zebrafish (Brown et al., 2010). Ces données et les nôtres concernant en particulier la LCN1 soulignent un rôle intéressant des membres de la famille des lipocalines dans l'angiogenèse avec des propriétés pro-angiogéniques pour la LCN7 et potentiellement anti-angiogéniques pour LCN1, toutes les deux régulées par la TNC.

Enfin, nous avons identifié un autre puissant facteur pro-angiogénique CXCL12 (Ho et al., 2010; Kryczek et al., 2005; Orimo et al., 2005) qui est surexprimé par la TNC. Par inhibition pharmacologique de son récepteur CXCR4 (AMD3100 ou Plerixafor de Sanofi Aventis) nous avons validé que la TNC favorise de manière paracrine l'angiogenèse par cette voie de signalisation. Dans l'avenir, il serait intéressant de déterminer si le ciblage de CXCR4 (ou d'une autre voie pro-angiogénique modulée par la TNC) et donc la neutralisation partielle de l'effet pro-angiogénique de la TNC se confirme dans une étude pré-clinique chez la souris. Ceci pourrait donc ouvrir la voie à une thérapie ciblant les effets délétères de la TNC. De façon intéressante une étude clinique en cours pour les gliomes de haut grade (numéro de l'étude : NCT01339039) associe à la fois, le ciblage de la voie CXCL12/CXCR4 avec l'inhibiteur que nous avons utilisé l'AMD3100 (approuvé par la FDA, Lanza et al., 2015) et le bloqueur de la voie du VEGFA, le bevacizumab (Vredenburgh et al., 2007) en plus des

premières lignes de traitement. Cette approche, après analyse rétrospective, pourrait nous apporter des éléments probant quant à l'effet de la TNC dans ces tumeurs et s'avérer supérieure au seul ciblage du VEGF, en particulier dans les MET riches en TNC.

CONCLUSION

Les résultats que j'ai pu obtenir lors de mon doctorat montrent que l'interaction directe des cellules vasculaires avec la TNC altère l'angiogenèse par une répression de la signalisation YAP. A l'inverse, le sécrétome des cellules tumorales cultivées sur une matrice contenant de la TNC favorise l'angiogenèse faisant intervenir des acteurs comme certaines lipocalines ou la cytokine CXCL12. Ce travail propose donc que la TNC régule de façon différentielle l'angiogenèse à la fois par un effet anti-angiogénique direct par contact de la TNC avec le compartiment vasculaire et par un effet pro-angiogénique indirect en modulant le sécrétome de cellules tumorales et de fibroblastes associés au cancer. La TNC favoriserait dès lors deux mécanismes indépendants pro- et anti-angiogéniques en fonction du type cellulaire avec lequel elle interagirait. Ces effets sembleraient donc coexister au cours de la progression tumorale afin de contribuer à la formation d'un réseau vasculaire dense mais peu fonctionnel favorisant l'agressivité du cancer. Ainsi cibler des molécules du sécrétome identifiées dans ce travail dans les tumeurs présentant un MET riche en TNC se révélerait potentiellement intéressant du point de vue d'une thérapie personnalisée mêlant anti-angiogénique et médicament(s) ciblé(s) contre le micro-environnement induit par la TNC, tout ceci afin d'améliorer la prise en charge des patients.

Biobliographie disponible à partir de la page 151

Contribution to manuscripts

This thesis has provided results that have already been published in two manuscripts. In addition my work contributed to four additional manuscripts that are in preparation.

- **Manuscripts in preparation or submitted:**

1.- Tristan Rupp[1-4]+, Benoit Langlois[1-4]+, Maria M Koczorowska[5-7], Agata Radwanska[8], Thomas Hussenet[1-4], Christiane Arnold[1-4], Elise Naudin[1], Oliver Schilling[5-7], Ellen Van Obberghen-Schilling[8] and Gertraud Orend[1-4] *. **Tenascin-C promotes tumor angiogenesis through pro-angiogenic and anti-angiogenic effects involving CXCR4 and YAP signaling.** + equal contribution, * corresponding author

I organized, planed and did most of the experiments. In addition, the following people contributed as indicated:
- Agata Radwanska (University Nice, ANR funded project Angiomatrix, G. Orend coordinator) provided results from a HUVEC-bead sprouting assay
- Maria Koczorowska (University Freiburg, Germany) did the proteomic analysis of the conditioned medium from U87MG cells
- Benoit Langlois did the retinal and aortic ring assays with me.

2.- **Rupp T.**, Murdamoothoo D.M., Saupe F., Lefebvre O., Tannoo R.M., Langlois B., Hussenet T. and Orend G. **Cerberus 1, a novel anti-angiogenic molecule, is regulated by tenascin-C and modulates tumor progression.** *In preparation*

In this study I organized planned and did most of the ongoing experiments. This work derived from a gene expression profiling that was done on pancreatic islets derived from RT2 TNC wt and TNC KO mice. A former PhD student, Falk Saupe and former postdoc Thomas Hussenet identified that TNC upregulated Cerberus-1 (Cer1) in this model. TNC induced upregulation of Cer1 was validated by RT-qPCR. Cer1 plays a role during embryogenic development presumably by modulating activities of morphogens such as BMP, nodal and Wnt that Cer1

inhibits. Cer1 has not been described so far to play a role in angiogenesis. I addressed this possibility. First, I showed that TNC regulates expression of Cer1 in other tumor and stromal cells. Moreover, by using recombinant Cer1 protein I showed that Cer1 interferes with HUVEC matrigel tubulogenesis. A potential role of Cer1 in tumor angiogenesis and a link to TNC is currently further addressed by my colleagues in the laboratory, Selven Murdamoothoo under my supervision.

3.- Zhen S.*, Schwenzer A.*, **Rupp T.** *, Ahowesso C., Klein A., Hussenet T., Lefebvre O., and Orend G. **Tenascin-C downregulates Dickkopf-1 expression through impairment of YAP/TAZ** * co-authors, *In preparation*

This work is based on the results published in Saupe et al. (2013) (see below) where we observed that TNC downregulates Dickkopf-1 (DKK1) expression through impairment of actin stress fiber formation by TNC in tumor and endothelial cells. Since DKK1 is a direct target of YAP signaling and YAP signaling depends on actin polymerization that is blocked by TNC we wanted to know whether TNC potentially downregulates DKK1 through YAP. Indeed, YAP translocation and transcriptional activity were blocked in tumor cells on a TNC substratum. This correlated with downregulation of several YAP target genes including DKK1. By using expression constructs with dominant negative and constitutive active YAP molecules, respectively we are currently addressing a potential functional link. I contributed to this analysis by demonstrating that the subcellular localization of YAP is affected by TNC, that TNC repress F actin formation and supervised in vitro experiments done by my colleague Sun Zhen.

4.- Mammadova-Bach E., **Rupp T.**, Hussenet T., Jivkov I., M. Edwards, Klein A., Pisarsky L., Méchine-Neuville A., Cremel G., Kedinger M., De Wever O., Ambartsumian N., Robine S., Pencreach E., Guenot D., Goetz J., Simon-Assmann P., Orend G. and Lefebvre O. **Laminin α1 orchestrates VEGFA signaling in the tumor ecosystem to promote colon cancer**. *In press*

Abstract: In human colorectal tumors LMα1 is the most highly expressed laminin isoform suggestive of a role of LMα1 in tumorigenesis. We describe the laminin α1 chain (LMα1) as driver of cross talk between tumor and stromal cells promoting tumorigenesis. LMα1 overexpression leads to increased colon tumor incidence, growth and angiogenesis. LMα1 attracts carcinoma-associated-fibroblasts (CAF) and promotes CXCR4-dependent VEGFA secretion, which in turn stimulates tumor cell survival, proliferation and angiogenesis.

I analyzed the effect of the conditioned medium that was derived from carcinoma associated fibroblasts upon growth on laminin-111 on HUVEC tubulogenesis. Moreover, I used a VEGF inhibitor to prove that the laminin-111 triggered pro-angiogenic effect was mediated by VEGFA.

- **Published articles**

1.- Langlois B.[*], Saupe F.[*], **Rupp T.,** Arnold C., van der Heyden M., Orend G.[$] and Hussenet T.[$] **AngioMatrix, a signature of extracellular matrix components specific to the tumor angiogenic switch, correlates with poor prognosis for human cancer patients.** *Oncotarget,* 2014, 5: 10529-45. [*] co-authors, [$] co-corresponding authors.

This work was mainly performed by the postdocs Benoit Langlois and Thomas Hussenet. I contributed by sampling tumor material, immunostaining and reviewing of the manuscript text. I was also in charge of in vitro experiments expected for the review.

2.- Saupe F.[*], Schwenzer A.[*], Jia Y.[*], Gasser I., Spenlé C., Langlois B., Kammerer M., Lefebvre O., Hlushchuk R., **Rupp T.**, Marko M., van der Heyden M., Cremel G., Arnold C., Klein A., Simon-Assmann P., Djonov V., Neuville-Méchine A., Esposito I., Slotta-Huspenina J., Janssen K.P., de Wever O., Christofori G., Hussenet T.[$] and Orend G.[$] **Tenascin-C promotes tumor angiogenesis and progression in a neuroendocrine tumor model by downregulation of Wnt inhibitor Dickkopf.** *Cell Reports*, 2013, 5: 482-92**.** [*] co-authors, [$] co-corresponding authors.

I was implicated in this study at the beginning of my thesis. I analyzed the tumor islets isolated from wt mice, and mice lacking or overexpressing TNC by electron microscopy in collaboration with Ruslan Hlushchuk. I participated with Isabelle Gasser to the injection and analysis of DKK1 overexpressing cells into nude mice. I did the matrigel tubulogenesis assay upon DKK1 addition and participated in the discussion.

Table of contents

List of figures and tables

Abbreviations

%: percentage

3D: three dimensional

AMD: Age-related Macular Degeneration

Ang1: angiopoietin 1

AO: Acridine Orange

BBB: blood–brain barrier

bFGF: basic fibroblast growth factor

BMP: Bone morphogenetic protein

CAF: carcinoma associated fibroblasts

CDM: cell derived matrix

CEC: circulating endothelial cells

CM: conditioned medium

CNS: central nervous system

Col I: type I collagen

Col IV: type IV collagen

CTGF: Connective-tissue growth factor

CTRL: control

CXCR4: chemokine (C-X-C motif) receptor 4

Cyr61: Cysteine rich protein 61

Da: Dalton

DAPI: 4',6'-diamidino-2-phenylindole

DKK1: Dickkopf-1

EAE: experimental allergic encephalomyelitis

EB: Ethidium Bromide

EC: endothelial cells

ECM: extracellular matrix

EDTA: ethylenediaminetetraacetic acid

EGF: epidermal growth factor

EM: Electron microscopy

EPC: endothelial progenitor cells

FAK: focal adhesion kinase

FAP: fibroblast activation protein

FGF: fibroblast growth factor

FN: fibronectin

FSP1: fibroblast specific protein 1

GBM: glioblastoma

GM7373: immortalized BAEC-derived cells

HDMEC: human dermal microvascular endothelial cell

HEK293: human embryonic kidney 293

HIF-1α: Hypoxia Inducible Factors-1α

HUAEC: human umbilical aortic endothelial cells

HUVEC: human umbilical vein endothelial cells

IF: immunofluorescence

IGFBP: insulin-like growth factor-binding proteins

IL: interleukin

KD: knockdown

KO: knock out

LATS: large tumor suppressor kinase

LC-MS/MS: liquid chromatography–tandem mass spectrometry

LCN: Lipocalin

LGR5: Leucine-rich repeat-containing G-protein coupled receptor 5

LPA: lysophosphatidic acid

MGP : matrix Gla protein

MMP: matrix metalloproteases

MRI: Magnetic resonance imaging

MS: Multiple sclerosis

NDS: normal donkey serum

NG2: Chondroitin Sulfate Proteoglycan

NGS: normal goat serum

PBS: phosphate buffered saline

PDGF: platelet-derived growth factor

PDGFR: platelet-derived growth factor receptor

PlGF: placenta growth factor

PMSF: phenylmethanesulfonyl fluoride

PNET: pancreatic neuroendocrine tumorigenesis

POSTN: periostin

RA: rheumatoid arthritis

Rip: Rat insulin promoter

ROCK: Rho-associated protein kinase

RT2: Rip1-Tag2

S4: syndecan-4

SDF1: stromal cell-derived factor-1

SEM: Scanning electron microscopic

Tag: SV40 T-antigen

TAM: tumor-associated macrophages

TAZ: Tafazzin

TCA: trichloracetic acid

TEAD: TEA domain family member

TME: tumor microenvironment

TG2: transglutaminase-2

TGFb: transforming growth factor b

TGFbR: transforming growth factor b receptor

TIF: telomerase immortalized fibroblasts

TINAGL1: tubulointerstitial nephritis antigen-like

TNC: tenascin-C

tPA: tissue-type plasminogen activator

TSP1: thrombospondin-1

VEGF: vascular endothelial growth factor

VEGFR: vascular endothelial growth factor receptor

VSGP: Vascular smooth muscle cell growth-promoting factor

WB: western blot

YAP: yes-associated protein

A. INTRODUCTION

1. Importance of the tumor microenvironment in cancer initiation and progression

For many decades understanding of cancer was focused on the tumor cells. Cancer was considered as a merely genetic disease (Sonnenschein and Soto, 2000). Indeed, re-expression of oncogenes or repression of tumor suppressors, due to accumulation of mutations or epigenetic phenomena, is associated with the intrinsic properties of cancer initiation and progression (Balmain, 2001). However the concept of cancer as a disease of tissue homeostasis has emerged that is not only based on mutated epithelial cells. Cancer development is characterized by anarchic cancer cell proliferation, yet manifestation of cancer requires more than that, in particular a permissive microenvironment that allows tumor cells to thrive and form metastasis (Bissell and Hines, 2011). The starting point of cancer becomes no longer only a "renegade" cell but is considered as a complex interplay of tumor cells with tumor stroma which has been coined by the term "tumor microenvironment" (TME) (Bissell and Hines, 2011; Lorusso and Rüegg, 2008) (**Fig. 1**).

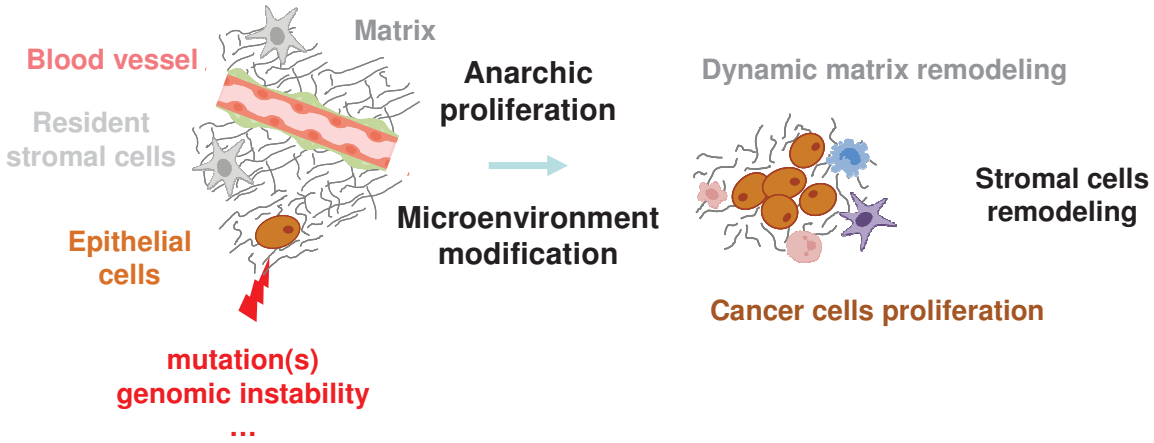

Figure 1. Cancer initiation in a "permissive" microenvironment

Transformed cell(s) in an "adapted" microenvironment switches to an aggressive phenotype and starts to proliferate uncontrolled. This dynamic change modulates the tissue in terms of stromal cells and matrix content which leads to cancer initiation.

Cancer is not a singular disease but cancer turned out to be multiple highly complex diseases and their underlying mechanisms are still not yet fully understood. This lack of knowledge

largely contributes to recurrent failures of antitumor treatment (Hanahan and Weinberg, 2000).

1.1. Role of the TME in cancer

The role of the TME was first recognized by Paget, who in 1889 proposed the "seed and soil" hypothesis to explain the selectivity of breast cancer metastasis to specific distant organs. Paget suggested that metastasis development is not a matter of "luck" but rather due to a specific affinity of tumor cells ("seed") for an organ ("soil") that can provide an advantageous growth environment. Meanwhile multiple experimental evidences support this hypothesis. The key role of the microenvironment in regulating cancer progression has been nicely demonstrated. The neoplastic phenotype could be repressed when tumor cells were placed in a "normal" tissue microenvironment (McCullough et al., 1998; Sonnenschein and Soto, 2000). McCullough and colleagues showed that tumorigenic rat liver epithelial cells did not raise tumor formation when grafted into the spleen but did when implanted into the liver. Even more convincing was the work of Illmensee and Mintz who had grafted tumorigenic murine teratocarcinoma cells into the blastocyst of a mouse embryo. This grafting did not lead to tumor formation but rather to the development of a normal mouse, exhibiting incorporation of tumor cells into the various tissues including the germ line (Illmensee, 1978; Stewart and Mintz, 1981). The work of Dolberg and Bissell showed that the oncogenic potential of cells transformed by the Rous sarcoma virus is inhibited when cells were injected into a chicken embryo. This result indicate that tumorigenic properties of these cells could be repressed by a non-permissive microenvironment (Dolberg and Bissell, 1984). Moreover activated fibroblasts co-injected with non-tumorigenic cancer cells triggered cells to form a tumor whereas cancer cells were unable to trigger tumor formation on their own (Camps et al., 1990; Olumi et al., 1998).

If the "normal" microenvironment can repress tumorigenesis, one wonders if an abnormal microenvironment would promote or even trigger tumor initiation. There is supporting evidence for this hypothesis. The work of Maffini and colleagues showed that the exposure of the stroma to a carcinogen such as *N*-nitrosomethylurea (NMU) allowed the development of tumors. However in vitro carcinogen-induced mammary epithelial cells did not lead to tumor formation after re-implantation into tissue that had not been exposed to the carcinogen prior to cell grafting (Maffini et al., 2004). Similar conclusions were drawn from experiments that had

been done with another carcinogen, 4-Nitroquinoline N-oxide (4-NQO) that is used to induce experimentally oral squamous cell carcinoma in mice (Hawkins et al., 1994; Schoop et al., 2009). The authors observed tumor formation only in the presence of the carcinogen. Similarly, irradiating the stroma of the mammary gland resulted in a microenvironment that initiated tumor formation from engrafted pre-neoplastic mammary epithelial cells (Barcellos-Hoff, 1998).

These studies strongly argue that the microenvironment is a powerful regulator of initiating tumor formation of cells with oncogenic mutations.

1.2 The composition of the TME

In normal tissues, the microenvironment plays instrumental roles to regulate tissue homeostasis. Similarly in cancer, the TME is critical all along tumor initiation and progression (Bissell and LaBarge, 2005). Tumor cells are not simply single cell islets residing in a particular organ but rather a complex structure embedded in a specific TME. Schematically, the TME comprises cellular and molecular components. Stromal cells include in particular, carcinoma associated fibroblasts (CAF), immune cells such as tumor-associated macrophages (TAM), endothelial cells (EC), pericytes and others (**Fig. 2**).

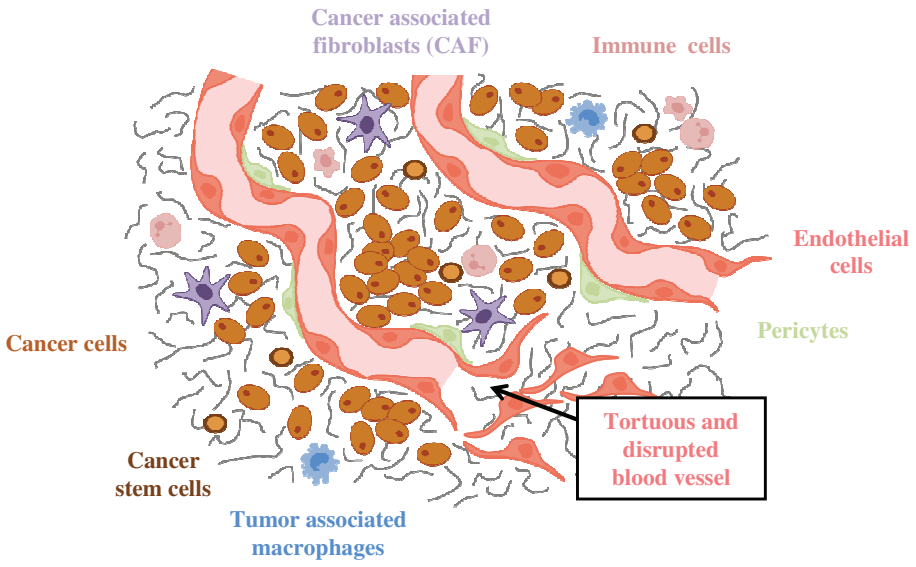

Figure 2. The composition of the TME

The TME is a complex tissue that is composed of tumor and stromal cells such as immune cells, TAM, CAF and vascular cells (EC and pericytes), embedded into a network of ECM molecules.

1.3. Role of ECM molecules

Cells of the TME promote tumor development by secreting cytokines, growth factors and extracellular matrix (ECM) proteins (Lorusso and Rüegg, 2008). ECM molecules and growth factors cooperate in the TME to provide biochemical signals (e.g. cytokines, chemokines, matrikines) and structural constraints (adhesion molecules, biomechanical forces) that dictate cell behavior in order to promote cancer (Schmeichel et al., 1998). Initially considered as passive scaffold that serves as architectural support for organs, ECM molecules are not considered any longer as anchoring fibrils for cells (Frantz et al., 2010). As Richard Hynes pointed out ECM molecules are "not just pretty fibrils" (Hynes, 2009). It is now well acknowledged that ECM proteins play an active role in regulating tissue homeostasis. ECM can trigger cell signaling through activation of specific cell adhesion receptors such as integrins and modulate the access to soluble signaling molecules by binding these factors (Hynes, 2009) thus altogether determining cell behavior.

1.3.1. Integrin adhesion receptors are crucial for ECM-inducing cell signaling

All cells in a given tissue interact with their ECM in a dynamic process. ECM molecules are localized and potent activators of multiple signaling pathways that modulate cell behavior. Integrins are one of the important receptors involved in homeostasis and disease (Harburger and Calderwood, 2009). Integrins are heterodimers composed of two subunits, α and β. They constitute a superfamily of cell surface adhesion receptors (including thirty functional members known) for various ECM molecules. Integrins are linked to the cytoskeleton and integrin mediated signaling is one of the major pathways that transduce signals from the ECM into the cell. Integrins play an essential role in regulating cell behavior such as cell anchorage, shape, polarity, proliferation, migration, survival or differentiation. Integrins regulate several physiological processes such as wound healing or organogenesis but are also involved in pathologies such as cancer (Giancotti and Ruoslahti, 1999; Harburger and Calderwood, 2009).

Several domains and motifs in ECM proteins have the potential to bind directly to cell surface expressed adhesion receptors. This direct interaction induces cell responses through signaling pathways as is here exemplified for fibronectin (FN) (**Fig. 3**). FN is a glycoprotein involved in cell adhesion and found in a variety of tissues (Hynes and Yamada, 1982), binds directly to

α5β1, α4β1 or αvβ3 integrin through its Arg-Gly-Asp (RGD) motifs and by that determines polarity and morphology of cells affecting on cell survival (Astrof and Hynes, 2009).
As an example of their role, the ECM serves as a scaffold and signaling device for blood vessels (Dejana and Orsenigo, 2013; Simon-Assmann et al., 2011). In particular, adhesion to ECM through integrins such as αvβ3 and αvβ5 had been demonstrated to be important in tumor angiogenesis. Drug targeting integrin signaling has been designed such as cilengitide (Merck). Cilengitide showed inhibitory effects in preclinical and clinical studies. Despite anti-tumoral and anti-angiogenic effects in vitro (Oliveira-Ferrer et al., 2008) and in vivo (Burke et al., 2002; Yamada et al., 2006), cilengitide has been discarded due to its poor clinical efficacy (Stupp et al., European Organisation for Research and Treatment of Cancer (EORTC) et al., 2014).

One of the crucial effects of ECM and integrin interaction is the modulation of the cytoskeleton organization in the cells. Integrins are important modulators of actin polymerization. Actin is one of the most abundant intracellular proteins in all eukaryotic cells. The fundamental property of actin is its ability to polymerize and thus to transform in reversible manner, a monomeric form, that is termed globular actin (G-actin), into a polymerized filamentous actin (F-actin) form. G-actin monomers are able to associate in a helical arrangement to form filaments or F actin structures. F-actin then polymerizes further to form actin cables. Upon binding of myosins and other contractility providing molecules these actin cables form actin stress fibers, lamellipodia or filopodia that regulate processes such as cell adhesion, migration and morphogenesis (Ridley et al., 2003).

Actin polymerization is regulated basically by three Rho GTPase members, Rho, Rac and Cdc42, through specific guanine-nucleotide-exchange factors (GEF) and GTPase-activating proteins (GAP) (Allen et al., 1997). When small GTPases are activated, they bind to variety of effectors to stimulate downstream signaling pathways affecting cell behavior. Rho activation for example stimulates Rho kinase 1 (also known as ROCK1) and ROCK2 and downstream cofilin or myosin light chain (MLC) proteins. Rac and CDC42 are involved in PAK, Raf/MEK/ERK or PI3K activation. Integration of these events leads to the regulation of actin polymerization thus modulating cell adhesion and migration.

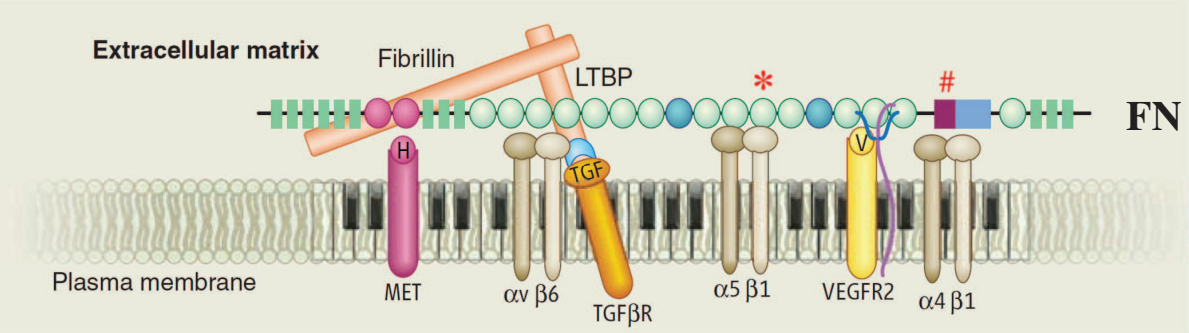

Figure 3. Multidomain interactions of ECM proteins with cells as exemplified for fibronectin (Adapted from Hynes, 2009).

Cells bind to FN through integrin receptors and to FN-bound growth factors through the respective receptors. This model suggests that FN and its associated ECM proteins orchestrate signaling in cells.

1.3.2. ECM modulates biomechanical properties of the tissue and influences cancer progression

The influence of the ECM is not restricted to ligand activity and thus receptor modulation. ECM molecules are flexible and extendable and can modulate the biomechanical properties of a tissue. The deformability of the ECM also affects the responses of cells (Discher et al., 2009; Engler et al., 2006). ECM-induced mechanical tension can modulate directly cell behavior and aggressiveness of diseases such as cancer (Erler and Weaver, 2009; Frantz et al., 2010). It is well exemplified that during tumor progression rigidity of the tissue increases from the premalignant into the malignant state of the cancer disease. Indeed stiffness induced by the transformation of the microenvironment is a classical example of how breast cancer is first diagnosed by palpation. This phenomenon is generally correlated to collagen crosslinking involving LOX proteins (Baker et al., 2013) and tissue fibrosis (Kalluri and Zeisberg, 2006). Valerie Weaver and colleagues showed that the matrix rigidity or stiffness increases mammary epithelial cell growth and alters their polarity and morphology. They demonstrated that stiff tissue increases cell tensions, cytoskeleton reorganization and focal adhesion points through β1 integrins. Thus β1 integrin activation enhanced activation of PI3K, ERK and Rho signaling that altogether promoted the tumor phenotype of mammary epithelial cells (Levental et al., 2009; Paszek et al., 2005). Fibroblasts, as a major producer of ECM, also react to changes in mechanical properties of the ECM (Kalluri and Zeisberg, 2006). Matrix stiffening appears to have a positive feedback on ECM deposition in these cells thus

enhancing tissue stiffening (Frantz et al., 2010; Tschumperlin, 2015; Tschumperlin et al., 2014). Interestingly the analysis of adjacent tissue close to the tumor showed an increase in tissue stiffness related to paracrine mechanisms inducing ECM secretion (Levental et al., 2009).

1.3.3. ECM-generated extracellular stimuli influence cell cytoskeleton organization and signaling activity

Cell senses extracellular stimuli as e.g. a rigid matrix or ECM content through activation of integrins that initiate cellular signaling. This involves modification of the cell cytoskeleton. An important question is how is an integrin mediated signal transduced and translated into intracellular signaling. For this signal conversion from outside-the-cell into inside-the-cell, the integrin link to the actin cytoskeleton is pivotal (Schwartz, 2004). Upon integrin ligation focal complexes are formed, which represent signaling "organelles" where actin polymerization is initiated. Here monomeric G-actin is polymerized into fibrillar F-actin that then forms actin stress fibers. This leads to signaling pathway activation through translocation of transcriptional coactivators from the cytoplasm into the nucleus. Through binding to transcription factors that themselves bind to specific DNA motifs, polymerized actin has an impact on genes expression (Allen et al., 1997; Ridley et al., 2003; Schwartz, 2004). As an example, recently, the actin polymerization state has been shown to modulate two important effectors in development, homeostasis and disease, YAP (yes-associated protein) and one of its co-transcriptional activators TAZ (Tafazzin) (Halder et al., 2012).

Recent studies indicate that YAP and TAZ are crucial factors in relaying mechano-responsiveness to cells (Halder et al., 2012; Tschumperlin, 2015; Tschumperlin et al., 2014). YAP and TAZ support a central role in matrix stiffness-dependent activation of cells. They influence cell proliferation, migration or differentiation and are sensible to matrix deposition and to the cytoskeleton status (Calvo et al., 2013a; Dupont et al., 2011). Importantly, YAP and TAZ are regulated by F-actin formation that leads to repression of their inhibitor, the large tumor suppressor kinase (LATS) 1 and 2, and thus allows their translocation into the nucleus. In the nucleus YAP/TAZ complexes interact with the TEA domain family member (TEAD) 1 to 4 and activate target gene expression. In the absence of polymerized actin LATS 1/2 inhibit YAP/TAZ translocation by phosphorylation, YAP/TAZ are sequestered in the cytoplasm or are degraded by the proteasome (Halder et al., 2012; Lapi et al., 2008).

1.3.4 ECM molecules serve as a reservoir for growth factors

Matrix remodeling is dynamic and involves progressive modulation of ECM content and fibrillar organization in a tissue. Matrix remodeling appears in a physiological context to maintain tissue homeostasis. In a pathological context matrix remodeling either promotes or represses disease progression (Mueller and Fusenig, 2004). Remodeling of the interstitial ECM and of the basement membrane by enzymes such as matrix metalloproteases (MMP) is more than just remodeling. Indeed, MMP-dependent cleavage of ECM within the basement membrane challenges its function as barrier such as to physically separating epithelial cells from other components around them. ECM degradation may generate signals by the release of sequestered molecules thus affecting cell behavior (Hynes, 2009; Kalluri, 2003; Martino et al., 2014). A variety of soluble factors are bound to the ECM such as collagen and FN (**Fig. 3**) and are potentially released during matrix remodeling (Hynes, 2009). These factors include vascular endothelial growth factor (VEGF) (Wijelath et al., 2002, 2006), transforming growth factor β (TGFβ) (Martino et al., 2013), Wnt (Martino et al., 2014), epidermal growth factor (EGF) and fibroblast growth factor (FGF) (Simian et al., 2001) amongst others. As example Martino and colleagues showed that fibrinogen binds through its heparin-binding site several growth factors such as platelet-derived growth factor-BB (PDGF-BB), placenta growth factor 2 (PlGF2), VEGF-B or FGF2. These fibrinogen bound-growth factors promoted wound healing through a better re-vascularization in murine models (Martino et al., 2013).

1.3.5. Importance of ECM molecules in cancer progression

In the TME, ECM molecules surround tumor and stromal cells where they exert both scaffolding and signaling roles. A characteristic of the TME is the high expression of ECM such as collagens (Chen et al., 2013; Öhlund et al., 2009), laminins (Simon-Assmann et al., 2011), FN (Galler et al., 2011) and tenascins (Midwood et al., 2011). There is evidence that some of these ECM molecules promote tumor progression. Often their high expression correlates with worsened clinical outcome and resistance to therapy. As example, Aguilera and colleagues demonstrated that myofibroblasts contributed to decreased sensitivity of tumors to anti-angiogenic agents by secretion of type I collagen (Col I) (Aguilera et al., 2014). Moreover the importance of ECM expression in a tumor context suggests that these molecules could be targeted and thus improve disease outcome. This knowledge has recently been

exploited by the group of Anna-Karin Olsson. Indeed they showed that immunization of mice with the ED-A domain of FN repressed metastasis formation in a spontaneous breast cancer model and thus extend life expectancy of the treated mice (Femel et al., 2014).

Altogether these data highlight the importance of ECM molecules in normal tissue homeostasis as well as in pathological conditions. It is clear that we need more knowledge about the dynamics of ECM expression and remodeling in normal and diseased tissues to develop strategies to improve cancer diagnosis and therapy.

1.4. Structure and role of tenascin-C

1.4.1. Structure of tenascin-C

The ECM molecule tenascin-C (TNC) is one important glycoprotein that is recurrently strongly induced during wound healing, inflammation of many tissues and in the TME. Successively named glial-mesenchymal extracellular matrix antigen, hexabrachion, cytotactin, J1 220/200, neuronectin and tenascin, TNC belongs to a family of oligomeric glycoproteins containing four known members, the tenascins C, R, X and W (Midwood et al., 2011, Choquet-Erishman et al. 2014). TNC is a glycoprotein that forms a hexamer resulting from the binding of six monomers by disulfide bridges through the N-terminal part of each protein (Jones and Jones, 2000). Each monomer of TNC is composed of 14.5 EGF-like repeats, 8 constants and 9 variables fibronectin type III repeats and a fibrinogen globe. TNC is thus composed of a minimum of nine modules of fibronectin type III repeats which can be added between the fifth and sixth repeats of alternatively spliced modules. The presence or absence of alternatively spliced in modules is largely tissue specific (Lowy and Oskarsson, 2015) (**Fig. 4**).

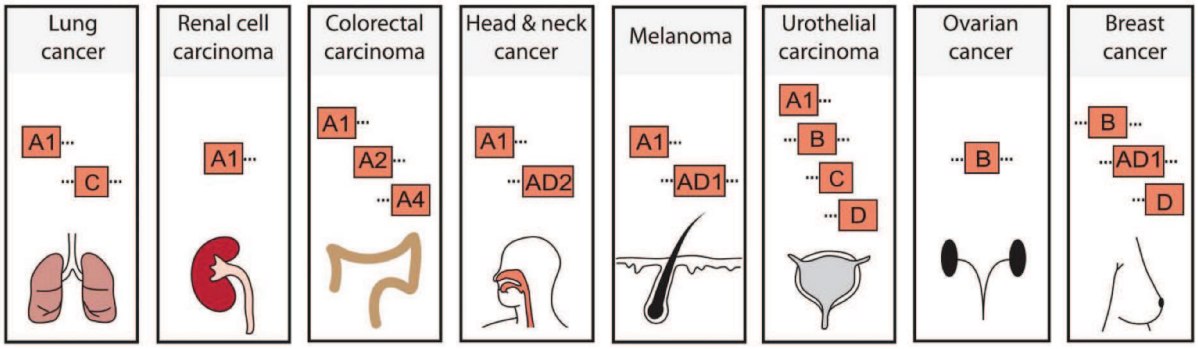

Figure 4. Tissue specific expression of TNC spliced variants. (Adapted from Lowy and Oskarsson, 2015)

Alternatively spliced variant of TNC revealed specific cancer type expression with mainly TNC A1 isoform.

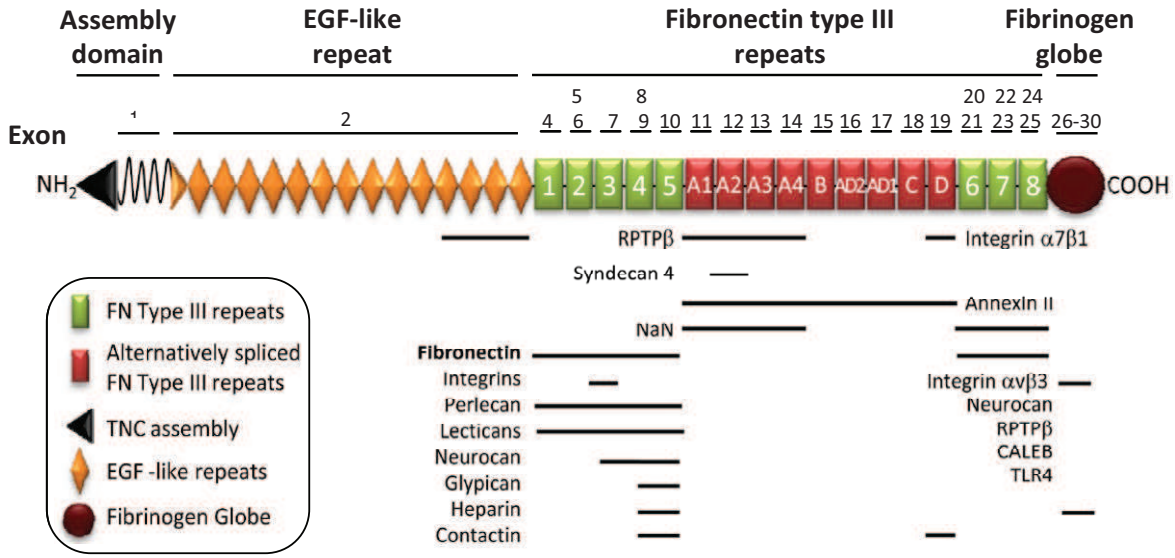

Figure 5. Domain structure of tenascin-C and potential binding partners. (Adapted from Midwood et al., 2011 & Van Obberghen-Schilling et al., 2011)

Monomeric TNC structure presents an assembly domain in the N-term part allowing hexamer formation of TNC. TNC is formed by three other domains containing an EGF-like repeats, fibronectin type II repast and a fibrinogen globe. Each domain is encoded by specific exons. TNC interacts with several ECM molecules and receptors through defined modules.

TNC presenting fibronectin type III repeat A1 is for example one isoform highly expressed in solid tumors or atherosclerotic plaques (Berndt et al., 2010; Brack et al., 2006; Pedretti et al.,

2010a). Adding to the complexity of these isoforms, a great heterogeneity of glycosylation exists. TNC monomers have a molecular weight that fluctuates between 180 and 320 kDa in humans with potential independent roles (Jones and Jones, 2000). TNC can be cleaved by MMP at different sites and cleaved TNC molecules may have distinct functions involving release of growth factors (Jones and Jones, 2000). Moreover TNC was shown to bind others proteins such as growth factors, cell surface receptors or others ECM proteins (Martino et al., 2014; Midwood et al., 2011; Saupe et al., 2013) (**Fig. 5**).

1.4.2. TNC-dependent described molecular signaling

From a molecular point of view, TNC was shown to interact with multiple receptors and extracellular molecules (Midwood et al., 2011; Orend and Chiquet-Ehrismann, 2006). TGFβ1, Bone morphogenetic protein 4 (BMP4), FGF2, angiotensin II, TNFα, Notch-2 or PDGF-BB have been described to promote TNC expression in neural stem cells, fibroblasts and tumor cells (Hau et al., 2006; Mackie et al., 1992; Nong et al., 2015; Sailer et al., 2013; Sivasankaran et al., 2009). TNC is a target and is regulated by Notch signaling (Oskarsson et al., 2011; Sivasankaran et al., 2009). Interestingly TNC was shown to be overexpressed in hypoxic regions of GBM and might be induced by Hypoxia Inducible Factors-1α (HIF-1α) (Lal et al., 2001)

TNC can also inhibit the activity of focal adhesion kinase (FAK) and RhoA, two molecules able to influence the actin organization of the cytoskeleton (Huang et al., 2001a; Midwood et al., 2011; Ruiz, 2004). In tumor cells, TNC regulates Wnt signaling, through the repression of the Wnt inhibitor Dicckopf-1, and enhances Leucine-rich repeat-containing G-protein coupled receptor 5 (LGR5) expression and Notch signaling that promote tumor progression (Oskarsson et al., 2011; Saupe et al., 2013). Moreover TNC has the ability to upregulate and activate indirectly c-met in mammary epithelial cells that promotes tumor phenotype (Taraseviciute et al., 2010). Interestingly TNC has been described to be a activator of EGF receptors through the direct interaction by its EGF-like repeat domain (Grahovac et al., 2013; Swindle et al., 2001).

1.4.3. Role of tenascin-C in embryogenesis and tissue homeostasis

Present during gastrulation and during somite formation, TNC is expressed very early in embryonic development (Chiquet-Ehrismann et al., 2014; Van Obberghen-Schilling et al., 2011). TNC is present in different organs of the embryo as thymus, brain, heart and lung (Saga et al., 1992). TNC is for example transiently expressed in the heart between E7.5 to 13 and afterwards is repressed (Imanaka-Yoshida et al., 2003). The spatiotemporal distribution of TNC is restricted and its expression is especially associated with particular structures as cortex or striatum during brain ontogenesis (Crossin et al., 1986; Faissner and Kruse, 1990). Nevertheless TNC knock out (KO) mice develop normally and are fertile suggesting compensatory mechanisms, making TNC a dispensable molecule during embryogenesis (Forsberg et al., 1996; Saga et al., 1992). Only minor differences in the behavior of adult TNC KO mice were observed with lowered anxiety, poor swimming ability and increased locomotor activity, but normal coordination and cognitive skills (Fukamauchi et al., 1996; Kiernan et al., 1999; Morellini and Schachner, 2006). In adult tissue TNC distribution is restricted to specific compartments associated with stemness niche in the thymus, spleen, brain or bone marrow (Chiquet-Ehrismann et al., 2014).

1.4.4. Role of TNC in disease progression

Conversely in pathological conditions TNC is re-expressed at the site of inflammation, close to damaged blood vessels or within many types tumors (Berndt et al., 2010; Brack et al., 2006; Herold-Mende et al., 2002; Midwood et al., 2011; Stegemann et al., 2013).

1.4.4.1. Role of TNC in cardiovascular diseases

TNC is absent from non the normal vasculature (Mustafa et al., 2012; Trescher et al., 2013; Wallner et al., 1999; Zagzag et al., 1996), but is expressed in cardiovascular diseases (Golledge et al., 2011) such as atherosclerosis (Schaff et al., 2011; Wang et al., 2012, 2013a), hypertension (Mackie et al., 1992), acute myocardial infarction (Arican Ozluk et al., 2015) or aortic acute dissection (Kimura et al., 2014; Trescher et al., 2013).

Although not detectable in the normal adult heart, TNC is expressed at very early stages of embryonic development as potential inducer of cardiomyocyte differentiation (Imanaka-

Yoshida et al., 2003) and TNC is re-expressed in cardiomyopathy such as myocardial infarction (Tamaoki et al., 2005). TNC is accumulated in atherosclerotic plaques and participate in their destabilization (Pedretti et al., 2010a; Wallner et al., 1999). TNC modulates arterial stiffness and thus mechanotransduction and flow in blood vessels, this promotes hypertension and other vascular diseases (Fujimoto et al., 2013; Imanaka-Yoshida and Aoki, 2014). In patient with high TNC levels myocardial reperfusion was hampered and TNC is thus a potential prognosis marker of left ventricular deficiency (Arican Ozluk et al., 2015). TNC expression is increased in proliferative diabetic retinopathy and participate to disease progression (Mitamura et al., 2002).

1.4.4.2. Role of TNC in inflammation, tissue regeneration and central nervous system associated diseases

TNC has been implicated in tissue regeneration (Kuriyama et al., 2011) since its inhibition impairs locomotor recovery, axon regrowth or synapse activity in a model of spinal cord regeneration in zebrafish (Yu et al., 2011). TNC deficiency in mice impairs recovery after nerve lesion (Guntinas-Lichius et al., 2005). Lack of TNC delayed brain regeneration after lesion (Ikeshima-Kataoka et al., 2008).

Moreover TNC expression is increased and promotes inflammation and fibrosis (Brissett et al., 2012; Carey et al., 2010; El-Karef et al., 2007; Islam et al., 2014). Other evidence implicates an immunosuppressive role of TNC on T cells (Hauzenberger et al., 1999; Jachetti et al., 2015; Rüegg et al., 1989).

TNC seems to contribute to central nervous system (CNS) diseases such as multiple sclerosis progression through modulation of inflammation, lymphocyte circulation, astrocyte-derived myelination or CNS repair (Harada et al., 2015; Jakovcevski et al., 2013; Kwok et al., 2011; Nash et al., 2011). Moreover TNC deposition is increased in the CNS upon injury and is expressed by astrocytes or glial cells and modulates their behavior (Nishio et al., 2005; Wiese et al., 2012). In vitro studies also suggested specific actions of TNC in the CNS, notably in neural precursor cell migration as well as in neuron guidance and outgrowth (Faissner and Reinhard, 2015; Van Obberghen-Schilling et al., 2011).

1.4.4.3. Role of TNC in tumor progression

TNC is highly expressed in most solid tumors where its high expression correlates with bad

prognosis for patients including lung, colorectal, brain, breast, hepatocellular carcinoma or head and neck tumor (Emoto et al., 2001; Herold-Mende et al., 2002; Ishihara et al., 1995; Leins et al., 2003; Midwood et al., 2011; Mitselou et al., 2012; Nong et al., 2015; Ohtsuka et al., 2013; Orend and Chiquet-Ehrismann, 2006; Renkonen et al., 2013; Rolle et al., 2010; Tang et al., 2015). TNC has been described to be highly expressed into tumor-specific fibrillar networks or tracks (Spenlé et al., 2015) (**Fig. 6**).

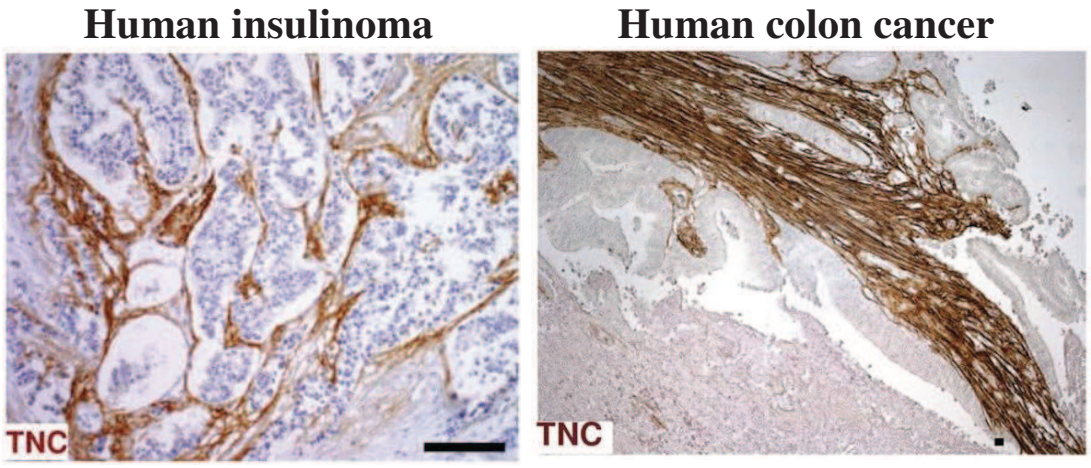

Figure 6. Spatial organization of the TNC microenvironment in human cancer. (Pictures taken from Spenlé et al., 2015)

TNC distribution and organization as tracks in particular in stromal compartment of human insulinoma and colon cancer.

TNC promotes cancer progression by supporting tumor cell invasion and metastasis formation. TNC protein expression increases with tumor grading in mouse models (Saupe et al., 2013) and in human breast cancer, brain cancers, insulinoma and pheochromocytomas (Goepel et al., 2000; Herold-Mende et al., 2002; Salmenkivi et al., 2001; Saupe et al., 2013). TNC promotes migration/invasion of glioblastoma (GBM), melanoma and pancreatic cancer cell lines (Grahovac et al., 2013; Herold-Mende et al., 2002; Hirata et al., 2009; Li, 2009; Tanaka et al., 2003), tumor growth of melanoma and a highly invasive phenotype in GBM, and metastasis formation of breast, lung and pancreatic cancer (Li, 2009; O'Connell et al., 2011a; Oskarsson et al., 2011; Tang et al., 2015). TNC has distinct effects on tumor cells, CAF, TAM and EC within the TME which are as yet not fully understood. The strong expression of TNC in cancer tissue suggests that TNC is involved in providing a permissive "tumor-bed" together with other ECM molecules that are coexpressed in the TNC rich niches. This TNC-derived tumor bed promotes the survival and expansion of tumor and tumor-

associated cells and thus may support tumor progression (Gilbertson and Rich, 2007; Orend et al., 2014).

The origin of TNC in tumor tissue is still not fully elucidated. Nevertheless different cell types have been shown to express TNC. A well characterized TNC provider are myofibroblasts, CAF and the cancer cells themselves that secrete and deposit TNC in a fibrillar matrix together with other ECM molecules (Chou et al., 2013; Gravina et al., 2013; Kharaishvili et al., 2014; Tamaoki et al., 2005). In vitro and in xenograft mouse models it was shown that TNC can be expressed by both the tumor and the stromal cells (Brack et al., 2006; Herold-Mende et al., 2002; Hicke et al., 2006; Hirata et al., 2009; Huang et al., 2010). In vitro fibroblasts and epithelial tumor cells (derived form brain colon and breast cancer) were shown to secrete TNC (Dandachi et al., 2001; Degen et al., 2007, 2008; Spenlé et al., 2015; De Wever et al., 2004). In addition some factors as TGFβ could stimulate TNC secretion in specific cell types as myofibroblasts by inducing αSMA and thus TNC expression (Islam et al., 2014; Untergasser et al., 2005). In human cancers such as melanoma or GBM, mainly tumor cells appear to abundantly secrete TNC (Carnemolla et al., 1999; Castellani et al., 1995; Herlyn et al., 1991; Herold-Mende et al., 2002; Mahesparan et al., 2003; Martina et al., 2010; Natali et al., 1990).

Thus tumor cells and activated fibroblasts express TNC, but several studies suggested or demonstrated that TNC is also secreted by other stromal cells. Immunohistological analysis in particular in high grade glioma revealed that TNC is present around blood vessels (Herold-Mende et al., 2002; Mustafa et al., 2012). Interestingly Martina and colleagues observed a perivascular localization of TNC in human GBM biopsies. They showed that desmin positive perivascular cells, a classical marker of vascular smooth muscle cells and activated fibroblasts (Beamish et al., 2010; Kalluri and Zeisberg, 2006), are surrounded by TNC which suggest vascular smooth muscle cells as one of the providers of TNC around tumor vessels (Martina et al., 2010). Immune cells might also express TNC in cancer. Indeed, monocytes or TAM could potentially be a source of TNC in tumor and damaged tissue (Chanmee et al., 2014; Kulla et al., 2000; Wallner et al., 1999). Finally, also astrocytes express TNC which is triggered by TGFβ1 together with basic fibroblast growth factor (bFGF) (Smith and Hale, 1997).

Altogether these data highlight the role of TNC in multiple processes of disease progression that may deliver a particular signaling to the cells through direct and indirect mechanisms.

1.5. TNC and CAF as close partners in the TME

Fibroblasts are highly abundant in the TME and play an active role in tumor angiogenesis and progression. During wound healing, fibroblasts change their phenotype to become active. Activated fibroblasts or myofibroblasts share properties with both fibroblasts and smooth muscle cells. Activated fibroblasts are found in tumors and are called CAF (Haviv et al., 2009; Kalluri and Zeisberg, 2006). CAF alter cancer cell behavior and promote tumor progression (Jia et al., 2013; Tyan et al., 2011). An important early role of CAF in promoting tumorigenesis had been shown by several laboratories (Camps et al., 1990; Hwang et al., 2008; Olumi et al., 1998, 1999). In further support a high expression of CAF markers such as αSMA and fibroblast activation protein (FAP) are associated with bad clinical prognosis (Cohen et al., 2008; Henry et al., 2007; Tsujino et al., 2007). It is now well accepted that the tumor stroma contains a heterogeneous population of CAF that express various markers such as αSMA, FAP, fibroblast specific protein 1 (FSP1), desmin or vimentin which are not exclusive for this cell type (Kalluri and Zeisberg, 2006; Kharaishvili et al., 2014). CAF may originate from resident fibroblasts but appear also to derive from pericytes, adipocytes, stem cells or bone marrow derived cells (Haviv et al., 2009). In addition to expressing multiple soluble factors such as cytokines and growth factors CAF are significant providers of ECM proteins (Kalluri and Zeisberg, 2006) amongst them TNC, collagens, FN and others (Adams et al., 2002; Mertens et al., 2013; O'Connell et al., 2011; Yoshimura et al., 2011). Moreover it was shown that CAF-derived TNC has a particular impact on breast cancer cells by promoting their invasiveness (Hancox et al., 2009) and by contributing to a metastasis permissive "soil" in the lung (O'Connell et al., 2011; Oskarsson et al., 2011). Thus these data suggest that fibroblast-derived TNC in cancer is a strong actor of disease severity.

2. Crucial role of tumor angiogenesis in the TME

The vascular network in the body is a hierarchical and highly organized system of blood and lymphatic vessels. Whereas lymphatic vessels play a role in body fluid homeostasis and immunity, blood vessels ensure an optimal supply of oxygen and nutrients to cells within tissues, export toxic metabolites to the liver and eliminate waste through the kidneys. The vessels are also used as a highway by immune cells, which monitor pathogens in order to protect the body (Pugsley and Tabrizchi, 2000). The vascular wall is composed of endothelial

cells, vascular smooth muscle cells and fibroblasts which are surrounded by a vascular basement membrane composed of a complex structured network of ECM proteins such as laminins, collagens or perlecan (Simon-Assmann et al., 2011). The mutual interactions between the ECM and the cells are necessary for growth, development and remodeling. However, various pathological situations disturb these homeostatic interactions and lead to various diseases.

2.1. Mechanisms of blood vessel formation

The formation of new blood vessels is a highly regulated mechanism implicating different independent processes such as **vasculogenesis**, **arteriogenesis** and **angiogenesis.** These processes initiate, maintain and recycle the vascular network and are described in the following cartoon (**Fig. 7**).

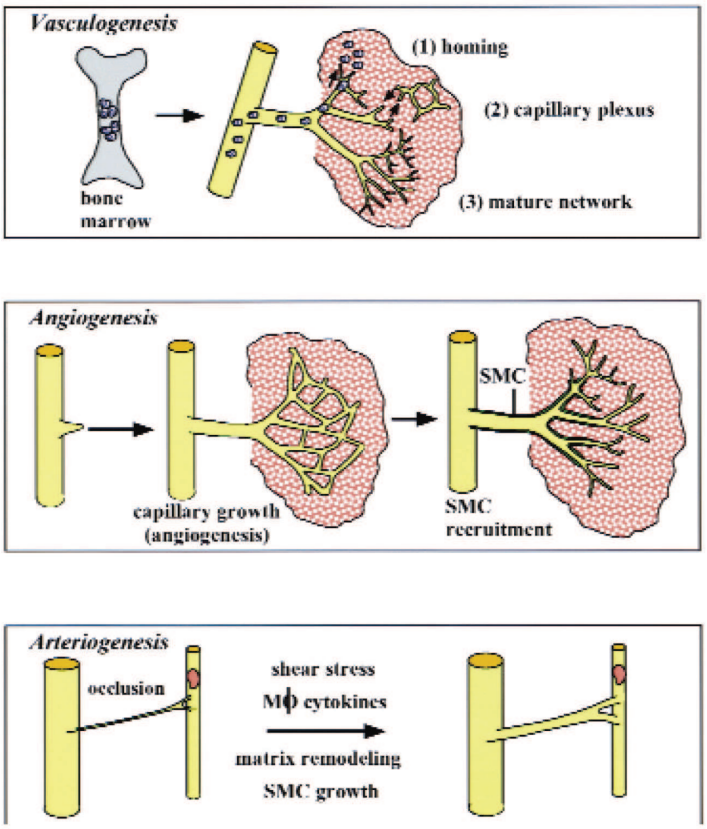

Figure 7. Different mechanisms of blood vessel formation. (Adapted from Carmeliet, 2000). Vasculogenesis starts in non-irrigated tissue by homing of bone marrow-derived cells that form a capillary plexus. Then a mature network is constructed by growth of new capillary from the

preexisting plexus (angiogenesis) which are stabilized by smooth muscle cells (SMC). These SMC as perivascular cells allow the maturation of the vessels that could differentiate into veins or arteries. In addition the arteriogenesis process allows the formation of bigger contractile vessels through signals such as mechanical shear stress, cytokine, matrix remodeling or SMC recruitment.

Vasculogenesis

Vasculogenesis involves the formation of a vascular network resulting from the differentiation and proliferation of endothelial progenitor cells (EPC) or angioblasts. This process is essential for the formation of a primitive vascular network. Angioblasts migrate extensively before in situ differentiation and plexus formation (Hur et al., 2004). Vasculogenesis is regulated by VEGF, VEGF receptor 2 (VEGFR2) and bFGF that influence EPC differentiation. Vasculogenesis only leads to immature vessels and needs to be consolidated by a vascular wall through the recruitment of mural cell progenitors which involves PDGF amongst other factors. Then vessels are stabilized by mural cell, generating a vascular basement membrane with EC where TGFβ signaling and ECM deposition are instrumental (Carmeliet, 2000) (**Fig. 8**). It is now established that EPC contribute to revascularization in adults in the context of ischemia or inflammation. The use of EPC represents a considerable hope for treating ischemic pathologies (Silvestre, 2012).

Arteriogenesis

Arteriogenesis is a mechanism contributing to vessel remodeling by maturation of preexisting vessels into larger ones giving rise to arterioles with up to 50 nm in diameter. Under physiological conditions arteriogenesis occurs during embryonic development. In pathological contexts such as ischemia arteriogenesis is induced by changes in blood flow or inflammation (Carmeliet, 2000). During arteriogenesis vascular myogenesis occurs where pericytes and smooth muscle cells are recruited. These mural cells proliferate and thus participate in the formation of the arterial vessel. The proliferative mural cells induce matrix and tissue remodeling leading to arterial vessel enlargement and formed different layers, the media and the adventitia that participate to vessel contractibility. These vessels are highly contractile due to differentiation of mural cells into pericytes. FGF, monocyte chemotactic protein 1, renin-angiotensin system or shear stress are described factors that regulate arteriogenesis (Carmeliet, 2000; Deindl et al., 2003; Murakami et al., 2008; Pipp et al., 2004; Schirmer et al., 2009).

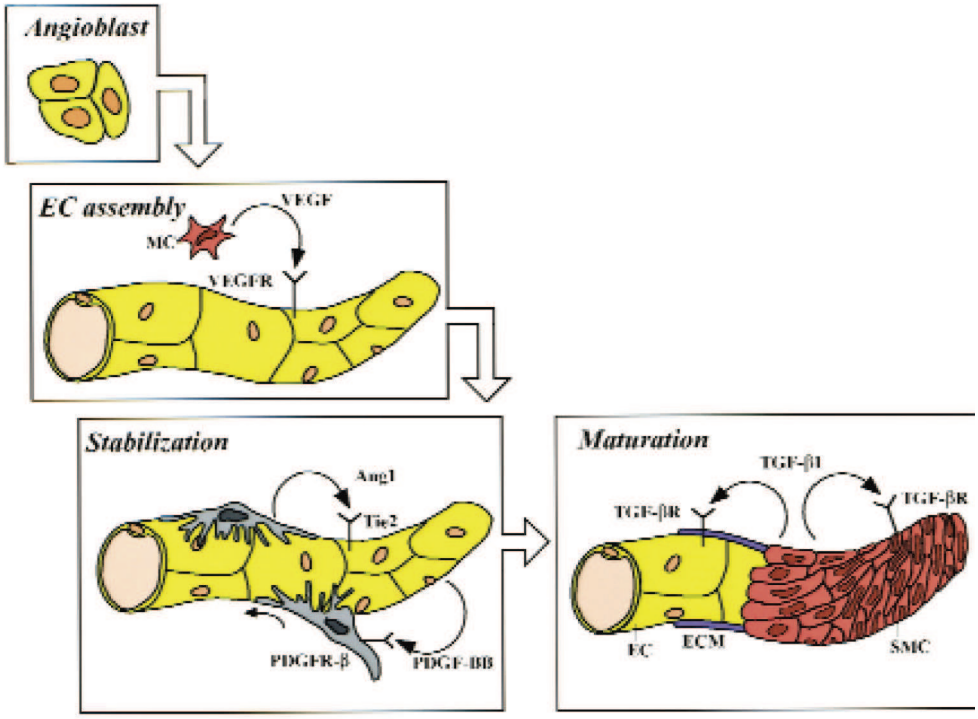

Figure 8. Mechanism of vasculogenesis and vessel maturation. (Adapted from Carmeliet, 2000) Vasculogenesis involves endothelial progenitor cells (red cells) or angioblasts that contribute to blood vessel assembly through VEGF/VEGFR signaling. Then perivascular cells are recruited (grey cells) through PDGF-BB/PDGFRβ signaling. The perivascular cells secrete angiopoietin 1 (Ang1) and TGFβ which interact with their respective receptors Tie-2 and TGFβR which stabilizes the nascent vessel by ECM deposition and cell differentiation.

Angiogenesis

The term angiogenesis describes the formation of new blood vessels from already existing vessels (Folkman et al., 1989). Vascularization is indispensable to provide nutrients and oxygen to tissues. Angiogenesis is controlled by a balance between pro and anti-angiogenic factors that regulate proliferation and migration of EC and contribute to ECM remodeling (Carmeliet, 2000; Carmeliet and Jain, 2000). Angiogenesis co-exists with other processes of vascular remodeling such as vasculogenesis and arteriogenesis (**Fig. 7**).

2.2. Angiogenesis related mechanisms

In physiological conditions angiogenesis takes places not only during embryonic development but also in the adult organism. Angiogenesis is a key process of pregnancy as well as in the

body's protective response to ensure wound healing, tissue regeneration and inflammatory responses. Angiogenesis is a highly regulated process leading to structured, hierarchically organized and well-functioning vascular networks (Carmeliet and Jain, 2000). Different types of angiogenic processes have been described and contribute to the development of a new vascular network (Adams and Alitalo, 2007a; Carmeliet, 2003). These include sprouting and intussusceptive angiogenesis, attraction of endothelial precursor and circulating endothelial cells or vascular co-option.

Sprouting angiogenesis

Sprouting angiogenesis starts with a change in EC polarity, the induction of a motile and invasive phenotype, modulation of cell–cell contacts and local matrix degradation. The growing EC sprouts are guided by cytokine gradients including attractive or repulsive cues that guide cells in the tissue environment under the influence of blood flow (Carmeliet and Jain, 2000; Herwig et al., 2011). This process involves several successive stages that mimic developmental events of angiogenesis. Activation of endothelial cells by various growth factors is followed by dilation of the pre-existing vessels. In this process an EC at the front (the so called "tip cell") is selected to guide the formation of the new vessel involving Notch and VEGFR signaling (Adams and Alitalo, 2007a) (**Fig. 9**).

In consequence, the ECM and the basal membrane surrounding the EC are degraded by locally activated proteases, such as MMPs. This allows EC to invade the surrounding matrix and stimulates their proliferation. The migrating cells polarize and form an immature blood vessel composed of the tip cell at the front and stalk cells that altogether build the new vessel (Geudens and Gerhardt, 2011) (**Fig. 9**). In normal angiogenesis, junctions between EC need to be maintained after lumen formation to prevent leakage. In order to stabilize the vessel, EC release growth factors such as PDGF-BB that promote the recruitment of perivascular cells and in particular pericytes to new sprouts. Pericytes, which adhere to the vascular basement membrane, surround the new vessels. Perfusion promotes maturation processes such as the stabilization of cell junctions, matrix deposition and tight pericyte attachment. Blood flow improves oxygen delivery and thereby reduces pro-angiogenic signals that are hypoxia-induced (Adams and Alitalo, 2007a; Carmeliet, 2000, 2003).

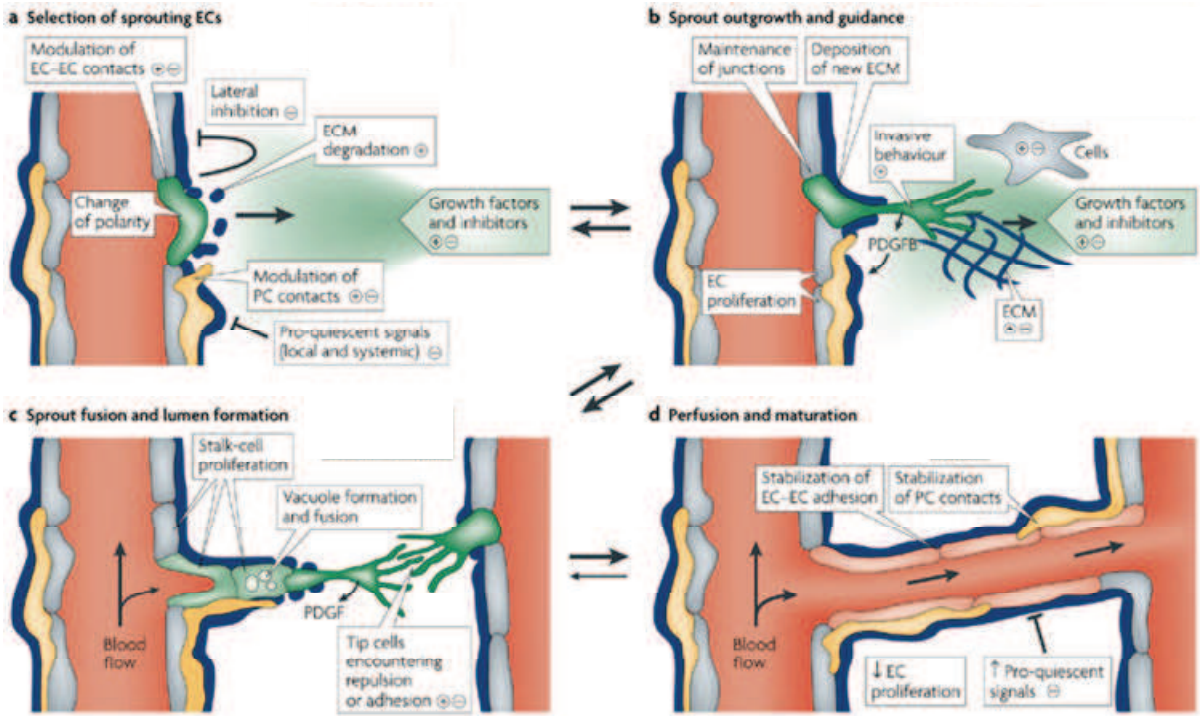

Figure 9. Mechanisms of sprouting angiogenesis. (Adapted from Adams and Alitalo, 2007) Activation of pro-angiogenic signaling favors EC activation by flipping of apical–basal polarity, the induction of motile and invasive activity, the modulation of cell–cell contacts and local matrix degradation. b. The growing EC initiates sprouting guided by pro-angiogenic gradients or repulsive molecule. Release of PDGFB by the tip cells promotes the recruitment of perivascular cells to nascent sprouts. c. EC–EC junctions lead the fusion of adjacent sprouts and vessels and are maintained after lumen formation to allow vessel functionality and perfusion. Lumen formation induces differentiation of EC in stalk or tip cells. Stalk cells proliferate to elongate the vessels. Fusion processes at the EC–EC interfaces establish a continuous lumen. Blood flow finishes to functionalize the vessels which lead to stabilization of EC-EC adhesions, perivascular coverage and inhibition of EC proliferation. Oxygen delivery reduces pro-angiogenic signals that are hypoxia-induced which induces also quiescent signaling.

Intussusception

Intussusceptive angiogenesis describes a mechanism whereby the splitting of a vessel occurs through the insertion of tissue pillars. This leads to the formation of two or more new blood vessels from a single existing one (Adams and Alitalo, 2007a). Despite strong morphological evidence that supports a role for intussusceptive processes in physiological and pathological angiogenesis, little is known about physiological functions or molecular regulation of intussusception. Nevertheless the process should involve EC proliferation, migration, basement membrane degradation, ECM deposition and perivascular cell recruitment (De

Spiegelaere et al., 2012). This mechanism of new blood vessel formation could be highly important in embryonic development to create a rich microvascular network from an existing vessel network (**Fig. 10**).

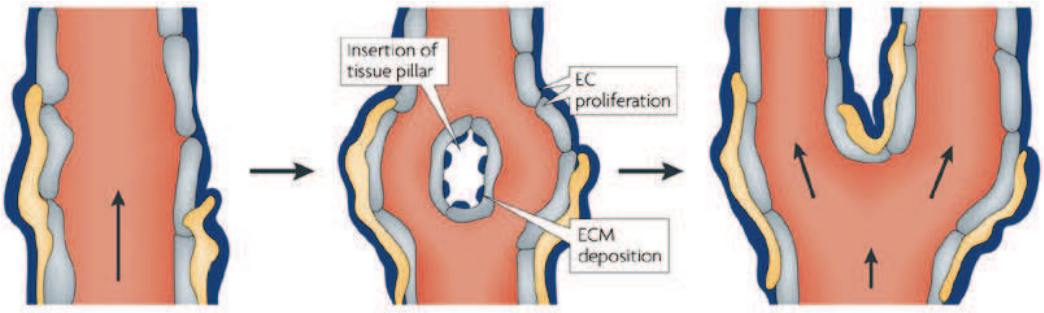

Figure 10. Intussusceptive angiogenesis model. (Adapted from Adams and Alitalo, 2007)

Intussusceptive angiogenesis comprises vessel splitting through an insertion of a tissue pillar. Observations suggest that this process involves EC proliferation and ECM remodeling.

Attraction of endothelial precursor and circulating endothelial cells

In addition to sprouting and intussusceptive angiogenesis other mechanisms contribute to the formation of new vessels and vessel growth which involve circulating endothelial cells (CEC) and EPC. Both cell types have been described to play a role in vasculogenesis and angiogenesis. Circulating cells are described to incorporate into the vessels and thus contribute to angiogenesis (**Fig. 11**). Both cell types are circulating cells that have been found in blood and that have a distinct origin. CEC are differentiated and mature EC that detach from an endothelial lining of a blood vessel. Whereas very rare in healthy patients, CEC are found in a relative high abundance in patients with vessel damage (Blann et al., 2005) or various cancers (Bertolini et al., 2006). EPC derive from bone marrow and are mobilized during repair of damaged vessel walls or during angiogenesis (Asahara et al., 2011; Bertolini et al., 2006). Given their importance in vascular pathologies, these cells have been approached as interesting candidate biomarkers in vascular diseases and cancers. In vivo analysis in mouse models it was shown that EPC contribute to a relative degree in the tumor vasculature (Rafii and Lyden, 2008; Sieveking et al., 2008). More recently, data also suggest a role of EPC in resistance to anti-angiogenic treatment and possibly in resistance to cytotoxic agents which could promote metastasis through re-vascularization (Rafii and Lyden, 2008; Rafii et al., 2002). However, in humans, the importance of EPC in these processes remains unclear. Several studies suggest that the role of EPC might be less important in humans than in mice (Hilbe et al., 2004; Peters et al., 2005). These endothelial cell populations likely contribute at

certain stages of the angiogenesis process and having structural and paracrine functions in some cancer types to ensure an efficient tumor vasculature.

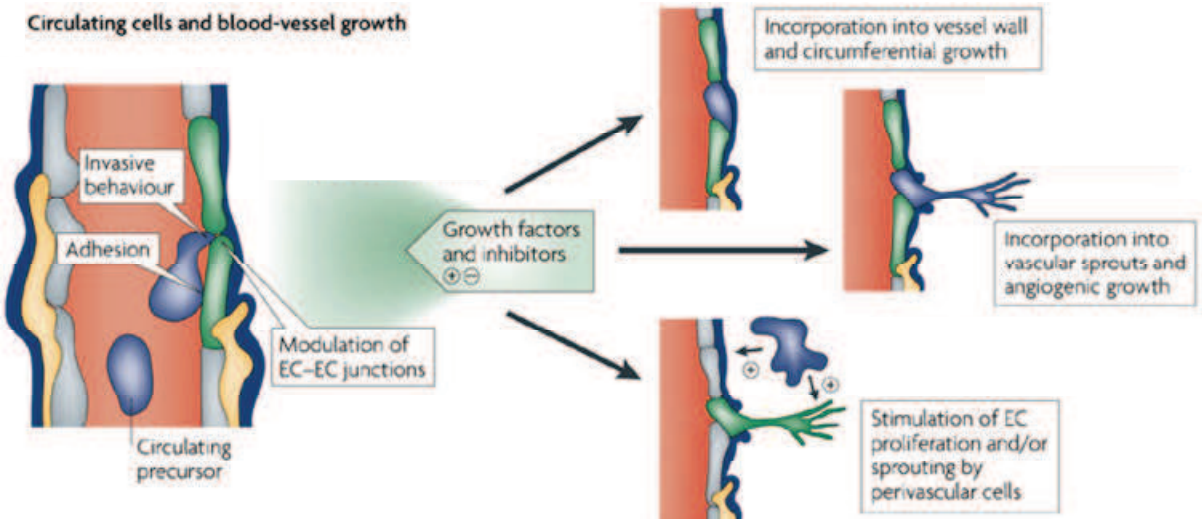

Figure 11. Role of CEC and EPC in angiogenesis. (Adapted from Adams and Alitalo, 2007)

Circulating cells in blood through chemotactic signals could adhere to the endothelium and could be incorporate in vessels. Thus these cells may be activated and generates vascular sprouts or may indirectly stimulate EC sprout from a perivascular location.

Vascular co-option

In vascular co-option seen in cancer, tumor cells can integrate into existing vessels or cancer cells mimicking endothelial cells and by that forming vessels. This phenomenon, that involves transdifferentiation of tumor cells, also called vascular mimicry, was reported for the first time in melanomas and thereafter also in others cancers such as GBM (El Hallani et al., 2010; Maniotis et al., 1999). The tumor cells acquire a phenotype to form pseudoendothelial tubular covering structures. This plasticity process in cells or transdifferentiation allows tumor cells to participate to the circulation system, regardless of angiogenesis. In particular neuroblastoma or GBM cells have been described to actively contribute to tumor vascularization by transdifferentiation (Golebiewska et al., 2013; Ricci-Vitiani et al., 2010; Pezzolo et al. 2011) and express EC marker as CD31.

2.2. Angiogenesis in pathological context

Since normal angiogenesis is a highly structured process that maintains homeostasis, pathological angiogenesis is poorly efficient and often leads to disease progression. Multiple diseases are characterized or caused by abnormal vessel formation with lack or excess of angiogenesis (Carmeliet, 2003).

Multiple sclerosis (MS) is a chronic inflammatory disease of the CNS. This pathology is characterized by a blood–brain barrier (BBB) breakdown, inflammatory infiltration of the CNS by lymphocytes, demyelination and eventual axonal destruction. Magnetic resonance imaging (MRI) analysis in patients showed that blood flow, blood volume, blood vessel density and vessel permeability are significantly increased and correlated with disease progression, which strongly suggests a role of blood vessel remodeling in this pathology (Girolamo et al., 2014; Lengfeld et al., 2014). The production of several other angiogenic molecules such as VEGF is associated with MS. In the classical experimental allergic encephalomyelitis (EAE) mouse model that recapitulates hallmarks of human MS, BBB disruption and vascular remodeling appeared before demyelinating lesions occur where VEGFA is released mostly by astrocytes or neurons (Macmillan et al., 2011; Seabrook et al., 2010). Thus the role of angiogenesis in MS remains unclear since angiogenesis promotes neural progenitor differentiation and myelination through VEGFA but also impairs endothelial barrier function which is associated with more infiltrating immune cells (Kirk et al., 2004). Interestingly, abnormal angiogenesis is a common feature of several neurological diseases such as Alzheimer (Vagnucci and Li, 2003) or Parkinson disease (Desai Bradaric et al., 2012).

Angiogenesis is a key phenomenon in the development of **psoriasis** (Heidenreich et al., 2009) and in **rheumatoid arthritis (RA),** chronic inflammatory disease of the joints, where angiogenesis allows the growth and maintenance of the inflammatory status by enhancing the flow of nutrients, cytokines and inflammatory cells into the synovium (Szekanecz et al., 2009). Moreover the prototypical factor of angiogenesis VEGFA is overexpressed in the synovial fluid and has been correlated with disease severity (Lee et al., 2001; Sone et al., 2001). Clinical trials of recent angiogenic inhibitors have not been done yet in patients with RA. However targeting interleukin-6 (IL-6), a potent pro-inflammatory cytokine (Nilsson et al., 2005), with tocilizumab, an anti-IL-6 receptor antibody, that is already used in the clinic

for rheumatoid arthritis patients (Kremer et al., 2011), showed strong anti-angiogenic effects (Nagasaki et al., 2014; Yoo and Chung, 2014). Consequently recent strategic approaches to treat RA suggests a potential interest for anti-angiogenic therapy, with VEGFA blockade as potent candidate (Paleolog, 2009).

Age-related Macular Degeneration (AMD) is a chronic degenerative disease of the retina where one form is driven by abnormal angiogenesis. Degeneration selectively reaches the central part of the retina called the macula and causes the loss of retinal visual cells. The formation of new vessels promotes vascular permeability and destroys the normal architecture of the retina and therefore its function. Photoreceptors suffer and ultimately scar tissues are generated which permanently destroy the macula (Kent, 2014; Ng and Adamis, 2005). Thus, dissecting the roles of angiogenesis in the progression of neovascular AMD has led to the development of anti-VEGFA therapy. The main drug used is ranibizumab (Lucentis) which is a recombinant humanized monoclonal antibody. It binds with high affinity to different isoforms of VEGF-A, preventing activation of the VEGFR signaling platform. Therefore ranibizumab inhibits the growth and permeability of new blood vessels and prevents disease progression (Gibson and Gibson, 2014; Kent, 2014; Schmid et al., 2015).

Atherosclerosis is a chronic inflammatory disease of the arterial wall that is induced by physical, chemical, biological or infectious agents. The inflammatory response involves development of lipid-rich plaques followed by monocyte recruitment. Unhealthy lifestyles (alcohol, smoking, high fat diet), diabetes, obesity and hypertension are promoting factors of the pathology but the atherosclerotic process is often initiated before adulthood with accumulation of cholesterol-containing low-density lipoproteins in the intima. Inflammation leads to the formation of an atherosclerotic plaque that can become unstable and results in its breakage or acute occlusion of the vessel (Jaipersad et al., 2014; Slevin et al., 2009). Several lines of evidence propose angiogenesis as a crucial event for atherosclerosis initiation, growth and plaque destabilization. Atherosclerotic lesions present local high vessel density and high hemorrhaging (Celletti et al., 2001; Kolodgie et al., 2003). PIGF, a member of the VEGF family, is a mediator of inflammation highly expressed in atherosclerosis and correlates with levels of plaque inflammation and stability (Pilarczyk et al., 2008). In vivo the prototypical angio-modulatory molecule, VEGFA, promotes monocyte/macrophage infiltration into the plaque, local angiogenesis and atherosclerotic lesion progression (Celletti et al., 2001; Heinonen et al., 2013).

In contrast to atherosclerosis, AMD or RA with abnormal excessive vessel formation, **ischemia** in the brain, himblimb or heart is characterized by insufficient angiogenesis that lead to hypoxia and tissue necrosis. When an artery is occluded, its vascular territory becomes ischemic due to impaired blood flow (Carmeliet, 2003). In order to restore the vascularization in the tissue, angiogenesis is activated and new vessels are generated from collateral vessels. However aging (Rivard et al., 1999) or hypertension (Belle et al., 1997) impair the angiogenic response to ischemia and lead to severe health problems as e.g. organ loss.

2.3. Tumor angiogenesis

In sharp contrast to physiological conditions, in cancer, angiogenesis is aberrant and leads to the formation of disorganized, chaotic and poorly functional vascular networks. In normal tissues, blood vessels interact with the sub-endothelial basement membrane composed of several ECM proteins in particular type IV collagen (Col IV) and laminins. This vascular basement and the recruitment of pericytes stabilize and contribute to vessel function (Simon-Assmann et al., 2011). In the TME**,** the vasculature is structurally and functionally abnormal. Compared to normal blood vessels, tumor blood vessels are permeable, tortuous, highly variable in diameter size and form patterns of anarchic interconnections (McDonald and Choyke, 2003) (**Fig. 12**).

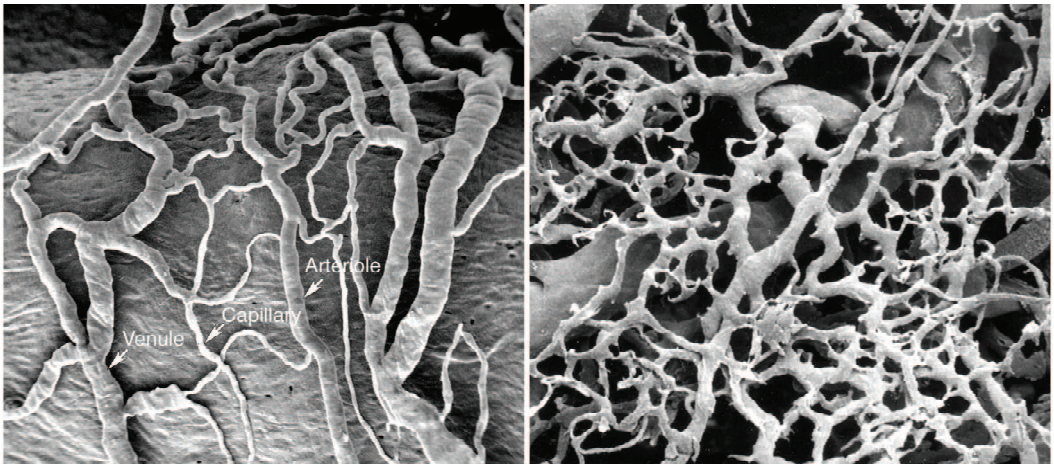

Figure 12. Microscopic imaging of normal and angiogenic blood vessels. (Pictures taken from McDonald and Choyke, 2003) (Left) Scanning electron microscopic (SEM) imaging of polymer cast of normal microvasculature of rat carotid sinus with simple organized arrangement of

arterioles, capillaries, and venules. (Right) SEM image of cast of tumor microvasculature, showing disorganized and anarchic blood vessels. Arterioles, capillaries, and venules are not identifiable.

Tumor vessels have defects such as a fragmented basement membrane, low pericyte coverage (or completely absent) and increasing permeability/leakage (Dejana and Orsenigo, 2013; Kalluri, 2003). An abnormal basement membrane seems to be instrumental in causing an aberrant vasculature in the tumor (Jain, 2005). An uncontrolled high angiogenesis process seen in solid tumors could result in an anarchic vascular network presenting high leakiness due to maturation failure (**Fig. 13**).

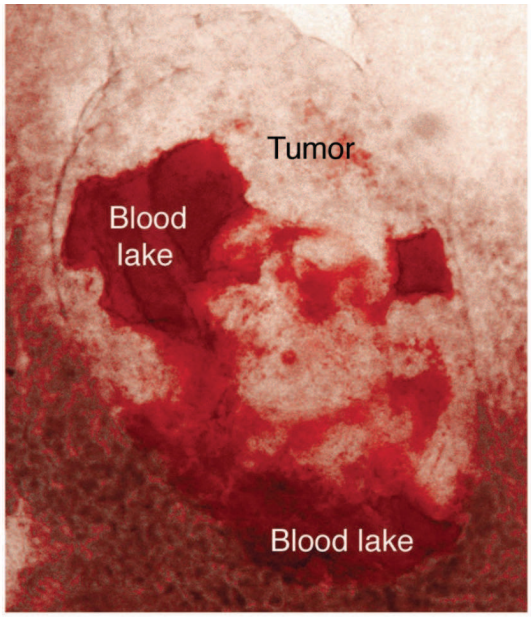

Figure 13. Massive blood leakage in tumors. (Taken from Adams and Alitalo, 2007) Bright-field microscopic image of a huge hemorrhage in a whole tumor from an insulinoma mouse model as an example of tumor vessel leakage.

Tumor angiogenesis is one of a critical hallmark of cancer (Hanahan and Weinberg, 2000, 2011). The formation of the vasculature is essential for tumor progression, maintenance and tumor cell dissemination (Carmeliet and Jain, 2000). Thanks to the pioneer work of Judah Folkman we know that in the absence of sufficient vascularization most tumors cannot exceed 2 mm^3 in volume, and remain clinically silent (Folkman, 1996). Tumor-associated vessels promote tumor growth and maintenance by providing oxygen and nutrients, and also favor metastasis formation by facilitating tumor cell entry into the systemic circulation. Many in situ cancers never progress to an invasive stage, most likely due to host factors that prevent this development, a phenomenon termed “cancer without disease” (Folkman and Kalluri,

2004) or tumor dormancy (Aguirre-Ghiso, 2007; Ghajar et al., 2013). In this conceptual view, tumor cells need to initiate new vessel formation to exit dormancy, proliferate, migrate and reprogram the microenvironment.

Tumor angiogenesis starts early during tumor progression. The initiation of tumor angiogenesis results from the imbalance between pro- and anti-angiogenic factors and is called the "angiogenic switch" (Folkman et al., 1989). An imbalance towards more pro-angiogenic factors is thought to be responsible for neo-vessel formation (Bergers and Benjamin, 2003). This switch represents a series of events such as secretion of pro-angiogenic factors, enhanced survival, activation and migration of endothelial cells, secretion of proteolytic enzymes (followed by the degradation of the basement membrane and ECM), which ultimately leads to the formation of a new blood vessel (**Fig. 14**).

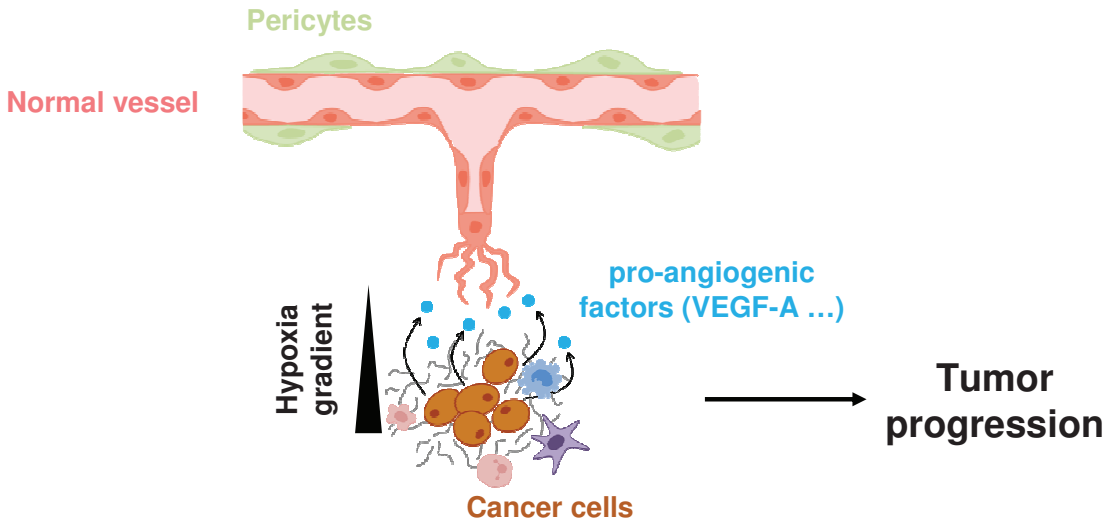

Figure 14. Simplistic representation of mechanisms of angiogenic switch.
Secretion of pro-angiogenic factors from an avascular hypoxic tumor that triggers angiogenesis and facilitates blood supply in the developing tumor.

The expression of pro-angiogenic factors is often induced by a hypoxic local microenvironment (**Fig. 14**). One crucial molecular mechanism that comes into play during tumor angiogenesis involves the HIF-1α transcription factor. In response to hypoxic stress as is the case in early stages of development of tumors, HIF-1α stimulates the expression of target genes such as VEGF-A, erythropoietin, and glycolytic enzymes such as the carrier Glut-1 for glucose transport (Adams and Alitalo, 2007a). VEGF-A is the prototypical pro-angiogenic factor recurrently involved in tumor angiogenesis. VEGF-A expression is known

to be strongly induced in the TME through HIF-1α stabilization (Forsythe et al., 1996; Lin et al., 2004).

This neo-angiogenesis decreases the rate of necrotic cells and increases the concentration of GF resulting in an increase of tumor size. Next to its effects on tumor growth, angiogenesis also provides an escape route for tumor cells (Quail and Joyce, 2013). Moreover this structural weakness contributes to abnormal blood flow in tumors. A leaky vessel and irregular blood flow as seen in the newly formed vessels facilitate entry of tumor cells into the bloodstream, thus promoting metastasis formation (Hashizume et al., 2000).

2.4. Anti-angiogenic strategies in cancer

Given the importance of the vascular network, anti-angiogenic therapies promised to be a good cure for cancer towards starving tumors to death and blocking their growth (Folkman, 1972). Therefore, drugs have been developed to target pro-angiogenic factors as a means to eradicate tumors.

Bevacizumab also known as Avastin (from Genentech) is a humanized monoclonal antibody directed against VEGFA, which is currently extensively used in the clinics. Bevacizumab traps VEGFA and prevents the interaction with its receptors (VEGFR2) and thereby blocks the VEGF signaling pathways that are crucial for angiogenesis (Midgley and Kerr, 2005). This prevents EC proliferation and migration which are required for angiogenesis (Bergers and Hanahan, 2008). Bevacizumab has recently shown promising results in phase II/III clinical trials on recurrent GBM, in combination or not with chemotherapy (Kreisl et al., 2009; Vredenburgh et al., 2007). But importantly, Bevacizumab failed to produce enduring clinical responses in 46% of treated patients (while 54% of patients responded) for which no clinical benefits are observed and were referred as “non-responders” (Kreisl et al., 2009). Overall patients tolerated Bev treatment well: thromboembolic events were the most frequently observed severe side effects in 12.5% of treated patients (Kreisl et al., 2009). When compared to temozolomide (the chemotherapeutic agent classically used in GBM), Bev relatively increased both median progression-free survival (=percentage of individuals where disease has remained stable, indicate treatment efficiency) and overall survival (percentage of alive individuals) after 6 months (Kreisl et al., 2009; Vredenburgh et al., 2007). For these

reasons, Avastin was approved in the US and in France for the treatment of high grade GBM alone or in combination with irinotecan in adult patients where prior treatment had not impacted on cancer progression. Other anti-angiogenic agents such as sunitinib (Sutent, Pfizer) are also used in anti-cancer therapy (Lee and Motzer, 2015; Roskoski Jr., 2007).

Angiogenesis inhibitors targeting the VEGF signaling pathways afford therapeutic efficacy on human tumors but not as the anti-angiogenic theory foreshadowed. Phenomena of "resistance" to treatment have been observed as well as upon classical chemotherapy (Bergers and Hanahan, 2008). For these reasons, benefits of these therapeutics are transitory and are followed by a restoration of tumor growth and progression after the treatment, as for example in treated patients with late-stage colon cancers (Hurwitz et al., 2004). On the other side VEGFA inhibition also resulted in blood vessel "normalization" where pericytes improve functionality/maturation of the blood vessels (Bergers and Hanahan, 2008; Mancuso et al., 2006; Stallcup and Huang, 2008). Significant improvements in chemotherapy response rates and mouse survival was also found when VEGFA inhibition is administrated in combination with chemotherapeutic drugs (Jain, 2014). Several mechanisms have already been evoked to explain this regrowth of the microvasculature which include abundant pericytes (that were not targeted by the treatment) and the so called "sleeves" of ECM (mostly representing the left over of the endothelial basement membrane). In particular, the ECM appears to serve as guiding track for the regrowth of new vessels (Mancuso et al., 2006). Moreover depletion of VEGFA may increase hypoxia in the tumor which would induce HIF-1α that improves VEGFA expression that could counterbalance the VEGFA trapping. Other pro-angiogenic factors and receptors such as VEGF-C and -D (Grau et al., 2011), PlGF and FGFs were found to be induced upon an anti-angiogenic targeting VEGF/VEGFR pathways (Bergers and Hanahan, 2008). Another possibility of resistance could be the recruitment of vascular progenitors and/or immune cells from the bone marrow that would trigger blood vessel regrowth through secretion of pro-angiogenic factors (Bergers and Hanahan, 2008).

3. TNC and tumor angiogenesis

Despite its absence in non-damaged arteries or veins (Martina et al., 2010; Mustafa et al., 2012; Trescher et al., 2013; Wallner et al., 1999; Zagzag et al., 1996) or in normal angiogenic tissue as endometrium or placenta (Mustafa et al., 2012), TNC is locally expressed in the

tumor blood vessel microenvironment (Brösicke et al., 2013; Galler et al., 2011; Herold-Mende et al., 2002; Martina et al., 2010; Renkonen et al., 2013). The TNC molecule is localized close to others ECM proteins such as FN, laminins and collagens that are found to be expressed around tumor blood vessels (Midwood and Orend, 2009; Spenlé et al., 2015). These informations propose a role of TNC in tumor angiogenesis. However the underlying mechanisms behind TNC in tumor angiogenesis are poorly understood and previous reports for its role are contradictory (Alves et al., 2011; Ballard et al., 2006; Castellon et al., 2002; Chung et al., 1996; Martina et al., 2010; Pezzolo et al., 2011; Saito et al., 2008b; Schenk et al., 1999; Sumioka et al., 2011; Tanaka et al., 2003; Zagzag et al., 1995, 1996, 2002). These data will be dissected in the discussion part of the manuscript. Nevertheless until 2013, no in vivo model had been used to address the angio-modulatory effects of TNC in tumor angiogenesis and to decipher the underlying molecular mechanisms. The publication by Saupe and collaborator where I am co-author provided significant important insight into the roles of TNC in tumor angiogenesis (Saupe et al., 2013). This will be addressed in the discussion part.

4. A particular role of TNC and angiogenesis in glioblastoma

GBM is the most common primary tumor of the CNS. Gliomas are brain tumors and are classified in 4 grades by the World Health Organization depending on histological status and patient prognosis: astrocytoma grade I and II, anaplastic astrocytoma grade III, and GBM multiform grade IV (Louis et al., 2007). High-grade (III and IV) tumors are considered as malignant gliomas and are associated with an adverse patient prognosis. Despite intensive treatment including surgical resection, chemotherapy and radiotherapy, this treatment only enhances patient median survival to 10-12 months and therefore GBM still represents a true clinical challenge with no real perspectives for the patient (Wen and Kesari, 2008). GBM are highly vascularized tumors and therefore represent attractive targets for anti-angiogenic drug-based therapies (Keunen et al., 2011).

Since its discovery, TNC reveals as a critical disease promoter in glioma. TNC has been associated with poor patient survival in glioma and particularly in GBM (Herold-Mende et al., 2002; Leins et al., 2003; Maris et al., 2008; Rolle et al., 2010; Sarkar et al., 2006, 2015; Varga et al., 2012; Midwood et al. 2011). TNC levels increase with glioma grading from no

detectable or weak expression in normal brain to low or modest expression in astrocytoma and to high expression in GBM (Herold-Mende et al., 2002; Higuchi et al., 1993; Leins et al., 2003; Nie et al., 2015; Rolle et al., 2010; Zagzag and Capo, 2002; Zagzag et al., 1995). Similar results for TNC staining in mouse normal brain compared to xenografted GBM were obtained (Brösicke et al., 2013; Pedretti et al., 2010b). TNC promotes GBM invasion in vitro and in vivo through matrix degradation involving MMP-12 or ADAM-9 proteases (Hirata et al., 2009; Sarkar et al., 2006, 2015). TNC expression in GBM overlaps with CD133 positive cells (Nie et al., 2015), marker of cell stemness (Brescia et al., 2013). GBM-derived TNC represses migration of T cells in vitro and perivascular TNC serves as reservoir for CD3 positive cell in vivo, suggesting an immune suppressive role of TNC (Huang et al., 2010). A role of TNC in angiogenesis and immune suppression as well as promoting tumor cell invasion could explain its disease promoting role in GBM.

The description of TNC as a clinical marker of glioma aggressiveness drove different strategies in order to fight this cancer. Thus targeting TNC-rich tumor with TNC antibody coupled with anti-tumoral factor as IL-2 in adjuvant strategymay reduce tumor progression, already strongly suggested by promising results of patient outcome with acute myeloid leukemia (Brack et al., 2006; Pedretti et al., 2010b) through transient destruction of metastasis (Gutbrodt et al., 2013; Schliemann et al., 2015). Moreover in GBM patients, RNA interference technology specific for TNC partially repressed tumor recurrence on the site of injection in the brain and thus patient well being and prolonged survival (Zukiel et al., 2006).

Interestingly, TNC expression is not restricted to the cancer cells or diffusely expressed in the stroma (Carnemolla et al., 1999; Castellani et al., 1995; Herold-Mende et al., 2002; Martina et al., 2010; McLendon et al., 2000) but TNC is highly expressed around tumor blood vessels (Herold-Mende et al., 2002; Huang et al., 2010; Martina et al., 2010; Mustafa et al., 2012; Rascher et al., 2002) in most malignant GBM (Higuchi et al., 1993). The perivascular expression of TNC increases with glioma grade and is particularly present in hyperplasic vessels. Strong perivascular staining of TNC was found to correlate with brain tumor malignancy suggesting it as a prognostic marker (Herold-Mende et al., 2002). Moreover this perivascular pattern has been correlated with glioma recurrence in patients (Herold-Mende et al., 2002). These data and other reports in different tumor types (Galler et al., 2011; Renkonen et al., 2013) indicate that TNC might modulate tumor angiogenesis.

B. AIMS

There are multiple published evidences that TNC is involved in tumor angiogenesis. In particular, while TNC is absent from the normal vasculature, TNC is highly expressed around tumor blood vessels. TNC deposition is increasing with tumor grade suggesting not only a role in angiogenesis but also in disease progression. Yet it is largely unclear how TNC impacts on vascular cell behavior and what molecular pathways are involved.

Here I addressed the question of how tumor and stromal cells respond to TNC thus impacting on vessel formation by employing in vivo, ex vivo and in vitro assays.

The specific aims were:

Major aims:

1. To establish and employ in vivo, ex vivo and in vitro methods to elucidate the roles of tenascin-C in normal and tumor angiogenesis.

2. To identify molecular mechanisms downstream of TNC relevant for TNC-related tumor angiogenesis.

Additional aim:

3. Contribute to the understanding of the impact of TNC on tumor angiogenesis in an in vivo mouse model of cancer.

C. MATERIELS & METHODS

1. Cells and regeants

1.1. Antibodies

Antibodies against the following molecules were used: mouse anti human TNC (B28.13, home made, FN type III repeat 6-8, 0.4-1 µg/ml final concentration), rat anti mouse TNC (mTN12, home made, FN type III repeats 7-8, 1-2 µg/ml final concentration), rabbit anti human & mouse FN (Sigma F3648, 1/200), rabbit anti human and mouse periostin (POSTN) (gift J. Huelsken, Lausanne, 1/1000), mouse anti mouse and human type I collagen (sigma C2456, 1/1000) mouse anti human and mouse α-tubulin (Oncogene CP06, Boston, MA, USA, 1/1000), mouse anti αSMA (clone 1A4, Sigma A2547, 1/200 for immunofluorescence and 1/500 for western blot (WB)), rabbit anti mouse and human NG2 (Millipore AB5320, 1/200), mouse anti human CD31 (Invitrogen clone MEM-5, 1/400), rat anti mouse CD31 (clone MEC 13.3, Pharmigen, 1/50), rabbit anti mouse and human von Willebrand factor (vWF, Abcam ab6994, 1/200) and rabbit anti mouse and human Cleaved caspase 3 (Cell signaling 9661, 1/200). Secondary antibodies used were ECL horseradish peroxidase linked whole anti-rabbit (NA934V) Anti-rat (NA935) and anti-mouse (NXA931) (GE Healthcare, Buckinghamshire, UK) and donkey anti-goat IgG (sc-2020, Santa Cruz, Biotechnology) or fluorescently coupled secondary antibodies goat anti-mouse, -rabbit, -goat or –rat IgG (Jackson laboratory 1/2000).

1.2. Cell culture and drugs

Primary human brain vasculature pericytes (HBVP, ScienCell, 1200) were cultured in pericyte medium (PM, ScienCell, 1201). U87MG (ATCC ® HTB-14™), U118MG (ATCC ® HTB-15™) and U373MG (previously ATCC® HTB-17™ described recently to have potential common origin with U251MG, (Torsvik et al., 2014)) glioblastoma tumor cell lines, human colorectal CAF CT5.1 (O. deWever, Ghent, Belgium, (De Boeck et al., 2013; De Wever et al., 2004) were maintained in DMEM 4.5g/l glucose, and 10% FBS. Primary bovine aortic endothelial cells (BAEC) were cultured in DMEM/1g/l glucose/10% FBS. Primary human umbilical vein endothelial cells (HUVEC, Promo cell, C-12203), primary VeraVec HUVEC (hVeraVec 101, Angiocrine) or primary VeraVec human umbilical aortic endothelial cells (HUAEC, hVeraVec 105, Angiocrine) were maintained in Endothelial cell growth medium (ECGM, PromoCell, C-22010). U87MG knock down for TNC were cultured DMEM

4.5g/l glucose/10%FCS with 3 µg/ml puromycin (Invitrogen). CAF knock down for TNC were cultured DMEM 4.5g/l glucose/10%FCS with 1000 µg/ml G418 (Invitrogen). Cells were starved in DMEM, 1% FCS (tumor cells, pericytes, CAF, BAEC) or M199, 1% FCS, 1µg/ml hydrocortisone, and 90µg/ml heparin (HUVEC). Pericytes experiments were used passages 2-10. HUVEC, VeraVec HUVEC and BAEC experiments were used at passages 2-6. All cell media were supplemented with 100 U/ml penicillin and 100 µg/ml streptomycin. All cells were cultured at 37°C and 5% CO_2. A Trypsin (0.05g/l) and EDTA (0.2g/l) solution was used to split cells and the medium was changed every 2-3 days.

Reagent used, see **Table 1**, ELISA kit for stromal cell-derived factor-1 (SDF1 or CXCL12) and VEGFA, purified lipocalin 1 were purchased from R&D system.

Table 1. Conditions used for drug and growth factor treatment.

Drug/Growth Factor	Solvent	Concentration used	Company
VEGFA $_{165}$	H_2O	10 - 100 ng/ml	Sigma
Lipocalin 1	PBS	1 - 25 µg/ml	R&D system
AMD3100	H_2O	10 - 1000 µg/ml	Sigma

1.3. Lentiviral transduction of cells

The silencing of TNC was done by use of short hairpin (sh) mediated gene expression knockdown (KD). For sequences and clone IDs used in this study, see **Table 2**. For generation of shTNC cells, U87MG and CAF cells were transduced with MISSION lentiviral transduction particles (TRC2, Sigma‑Aldrich, containing neomycin or puromycin box) or MISSION non-target shRNA control transduction particles (pLKO.1 vector, Sigma–Aldrich) with a MOI=2, transduced cells were selected with 3 µg/ml puromycin or 1000 µg/ml of G418 for U87MG and CAF respectively. Validation of effective knock down was checked to be effective at protein level after 20 passages post infection.

Table 2. TRC numbers and si/shRNA sequence.

Gene	Name	Clone ID	Sequence (5'-3')
non-coding (control)	TRC2 sh1	Mission Non-Target shRNA Control Vector	CCGGCAACAAGATGAAGAGCACCAACTC-GAGTTGGTGCTCTTCATCTTGTTGTTTTTT

TNC	TRC2 sh1	TRCN0000230785	CCGGGGAGTACTTTATCCGTGTATTCTCGA GAATACACGGATAAAGTACTCCTTTTTG
	TRC2 sh2	TRCN0000230787	CCGGCAGGCGCAAACGGGCATAAATCTCG AGATTTATGCCCGTTTGCGCCTGTTTTTG
	TRC2 sh3	TRCN0000230788	CCGGCCAGTGACAACATCGCAATAGCTCG AGCTATTGCGATGTTGTCACTGGTTTTTG

2. In vivo experiments

2.1. Animal experiments

C57Bl6, nude (Charles Rivers) or TNC KO (Forsberg et al., 1996) mice that had been backcrossed for at least 10 generations into C57Bl6 (Saupe et al., 2013) were used. Experiments comprising animals were performed according to the guidelines of INSERM and the ethical committee of Alsace, France (CREMEAS).

2.2. Retinal physiological angiogenesis assay

Retinal angiogenesis was analyzed on tissue from wt mice and TNC KO mice (C57BL6) seven days after birth (P7). Briefly mice were euthanized using CO2 asphyxia and process was validated by ethical committee (CREMEAS, France). Eyes were isolated and fixed in 4% PFA-PBS at 4°C one hour with agitation and washed twice in PBS. Retinas were dissected, permeabilized in PBS, NDS 5% and 0.1% Triton X-100 at 4°C 2h30 under agitation. Retinas were washed twice in PBS, and incubated with NG2 (1/200, Millipore, marker of pericytes) and mTNC12 (home made) in PBlec (PBS, pH 6.8, 1% Triton-X100, 0.1 mM $CaCl_2$, 0.1 mM $MgCl_2$, 0.1 mM $MnCl_2$) at 4°C overnight with agitation. After two washes in PBlec, samples were incubated with secondary conjugated antibodies (1/2000, Cy3 and Cy5; Jackson laboratories) and isolectin B4 (1/50, Sigma-Aldrich, marker for endothelial vessels) diluted in PBlec for two hours. Finally retinas were washed two times and Vectashield Antifadding (Invitrogen) served for nuclear staining and whole mounting. Flat mounted retinas were analyzed by fluorescence microscopy using a Zeiss Imager Z2 inverted microscope equipped with a digital camera. Images were acquired and processed using AxioVision software (Carl Zeiss).

2.3. Tumor material and animals

A heterotopic xenograft model had been generated in the *Laboratoire de Biochimie et Biologie Moléculaire Plateforme Hospitalière de Génétique Moléculaire des Cancers CHU Strasbourg-Hautepierre* by using human GBM material (all analyzed tumors derived from the same original material "TC7 patient") to implant subcutaneously tumors in immune-compromised nude mice. A mechanically prepared tumor mixture was injected subcutaneously in both flanks of three nude mice. The tumors grew for approximately 6 weeks. Mice were sacrificed and tumors were put in Tissue-Tek® O.C.T. Compound. Samples were frozen on dry ice and conserved at -80°C until use.

3. Ex vivo experiment: Aortic ring sprouting assay

Aortic rings were prepared adapted from previously described method (Baker et al., 2012). Briefly, C57BL6 mice (wt or TNCKO) were euthanized with CO2 asphyxia. The animal surface was sterilized with 70% ethanol. The thoracic aorta following the vertebral spine was carefully dissected and cut at the posterior mediastinum and the anterior occipital parts, placed in serum-free Opti-MEM (Gibco) with antibiotics and cleaned of blood and fibroadipose tissue under a stereoscope, using fine microdissecting forceps and microscissors. Aorta extremities were trashed and the remaining was cut in pieces of 500 µm using Tissue Chopper (McIlwain Technology Engineering, UK). Fifteen to twenty rings were obtained per mice and were starved overnight in Opti-MEM with antibiotics. The aortic rings were embedded in 1 mg/ml collagen gels (BD Bioscience rat tail collagen I), one per gel and let polymerized 1 hour at 37°C. Then Opti-MEM 2.5% FBS 30 ng/ml $VEGF_{165}$ (Invitrogen) with antibiotics medium was added and cultured during 6 days. The growth medium was changed every 2 days. Then the living cultures were fixed with PFA 4% and stained for Isolectin B4 (recognizing EC structures) and αSMA (fibroblasts and perivascular cells). Immunofluorescence images were acquired under Macroscope AXIOZoom V16 (Zeiss) using Z-stack and number and length of angiogenic sprouting structures were measurement with ZEN software tools (Zeiss). Aortic rings negative for αSMA positive migrative cells were excluded from the analysis.

4. In vitro experiments

4.1. Adhesion assay

Ninety six well plates (BD Bioscience) were coated with 1 or 2 µg/cm2 of purified FN, Col I or TNC (6 replicates). 40,000 pre-starved human umbilical vein endothelial cells (HUVEC), bovine aortic endothelial cells (BAEC) or human brain vascular pericytes (HBVP) were plated for 1h at 37°C and then wash extensively (5 times) with phosphate buffered saline (PBS) to remove non-adherent cells. Cells were fixed with methanol 30 minutes at room temperature then washed. Cells were stained with Cristal Violet 0.1% (in H_2O) then wash 5 times 5 minutes. Pictures were taken at 100X magnification in the center of the well and then cells were solubilized in 50 µl DMSO and the OD at 595 nm was measured using multiplate reader EV L800 (BIO-TEK INSTRUMENTS, INC).

4.2. Assessment of apoptosis by cleaved caspase 3

Serum starved HUVEC were seeded on CDM deposited by wt or TNC KO MEF or on FN and TNC precoated plastic surfaces (labtek permanox) in full medium at a concentration of 25.000 cells in 200 µl. After 72 hours cells were fixed and stained for cleaved caspase 3 and 4',6'-diamidino-2-phenylindole (DAPI). Three independent assays were done with 4 replicates with 6 pictures taken per well at 100X magnification. The apoptotic index was determined as the percentage of cleaved caspase 3 positive cells per all DAPI positive cells.

4.3. Assessment of cell death by Ethidium Bromide / Acridine Orange (EB/AO) uptake

Following of alive, apoptotic and necrotic cells were done by the EB/AO uptake method adapted from (Ribble et al., 2005) and classification of cells status from (Baskić et al., 2006). Briefly 5,000 HUVEC or BAEC are seeded on pre-coated wells with FN, Col I or TNC at 1 µg/cm^2 or 2 µg/cm^2 respectively for HUVEC and BAEC for 48h in their culture medium or mixed with conditioned medium (CM) from cells on cell derived matrix (CDM). After 48h EB and AO solutions in PBS at 5 µg/ml was added to the culture medium followed by precipitation (400g, 5 minutes). Up to two pictures per well were acquired with at least 100 cells counted per well using Zeiss AXIOZoom V16 stereoscope with 112X magnification. Totally green (AO) cells were considered as alive cells, green and red (EB) costain and /or nucleus accumulation are considered as apoptotic cells and red cells were considered as dead cells. In addition cells morphology was considered during the analysis (fragmentized nuclei

were considered as apoptotic cells). Three independent experiments were done with 3 replicates per experiment, and measures were averaged.

4.4. BrdU incorporation, cell proliferation assay

Determination of HUVEC proliferation was done using Cell Proliferation ELISA, BrdU (chemiluminescent) Kit (Roche Applied Science). Briefly serum starved HUVEC were cultured in 96-well plates at a density of 5000 cells/well (6 replicates) in 100 µl in complete growth media on pre-coated wells (Col I – FN – TNC). Wells surrounding were filled with 200 µl of water to limit medium evaporation. After 48 hours, the cells were labeled using 10 µl of BrdU labeling solution at 100µM per well and incubated 3 hours at 37°C in a humidified atmosphere. Then, the culture media was removed, the cells were fixed, and the DNA was denatured in one step by adding FixDenat solution. Next, the cells were incubated with the anti-BrdU-POD antibody for 90 minutes at room temperature. After the removal of the antibody conjugate solution, the cells were washed and 100 µl of pre-warmed substrate solution was added for 10 minutes at dark. The measure of chemiluminescence was directly quantified in adapted plate using a with a TriStar2 Multimode Read LB 942 (Berthold Technology) multiplate reader. To normalized to the relative cell number the luminescence signal the cells were labeled with DAPI and fluorescence was measured with a TriStar2 Multimode Read LB 942 (Berthold Technology) fluorescence multiplate reader using 345/455 nm filters. A minimum of 3 independent experiments were done with 6 replicates per experiment, and measures were averaged.

4.5. Cell derived matrix production

Cell derived matrix (CDM) were prepared adapted from previously described method (Beacham et al., 2007; Castello-Cros et al., 2009). Briefly, 33,000 cells/cm^2 for MEF wt and 50,000 cells/cm^2 for MEF TNC KO and CAF control or knock down for TNC were plated on chemically cross-linked gelatin on tissue culture dishes to achieve confluent dishes Cells were maintained in confluent conditions for up to 8 days supplemented every 24 hours with 50 µg/ml fresh medium plus L-ascorbic acid (L-AA) that allowed collagen production and thus stabilized ECM components. The resulting CDM were checked for quality by phase contrast and cells were removed with cell extraction buffer (20mM NH_4OH, 0.5% Triton-X-100 in PBS, 30 minutes at 37°C and overnight at 4°C). The cell-free 3D matrix were treated with DNAse 100 U/ml (Invitrogen) for 1 hour at 37°C to remove remaining genomic DNA and

was conserved at 4°C for maximum one month for further analysis.

4.6. Cell multiplicity assay

Serum starved cells (HUVEC, BAEC and HBVP) were plated into 96-well plates (2`000 or 6`000 cells/well with 6 replicates for each time point) on ECM coated surfaces (Col I, FN or TNC) or CDM. Well surrounding were fill with 200 µl of water to avoid medium evaporation. MTS incorporation assay were done according to the manufacturer's instructions (CellTiter 96 aqueous non-radioactive cell proliferation assay, Promega) after 8h, 24h, 48h and 72h. Measured values (490nm) were normalized to the relative cell number at 8h.

4.7. Collagen contraction assay

The measure of collagen contraction was done as previously described (Goetz et al., 2011). Briefly, 100,000 CAF control of KD for TNC were mixed with Col I mixture (BD Bioscience, with DPBS 10X, DMEM and NaOH 1M following the manufacturer's protocol) to a final collagen I concentration of 1 mg/ml. The mixture was rapidly transferred to a 24-well plate and gels were allowed to solidify for 1h at 37°C. Then CAF knock-down culture medium was added to each well and gels were manually detached by circular movements using a P200 sterile pipette tip and plate swirling. Gels were placed at 37°C and contraction was documented. Three to four fibroblast-containing gels were used for each condition. Gel contraction index was calculated with ImageJ software from the gel surface area measured on acquired images, and reported as the percentage of contraction of the initial surface area.

4.8. Collection and preparation of the conditioned medium

U87MG, U118MG and CAF as well as U87MGshCTRL, shTNC1 and shTNC3 cells were grown in DMEM 4.5 g/l glucose, 10% FCS, but without selection antibiotic for U87MG knock down cells. Cells were seeded at 2 millions cells per 10 cm dish. Conditioned medium (CM) was collected from after 48h of culture filtrated (0.22 µm), aliquoted and store at -80°C until use. Boiled CM was prepared as previously described (Vjetrovic et al., 2014) by heat-inactivated protein activity at 100°C for 10 minutes followed by cooling at room temperature. The boiled CM was then filtrated (0.22µm) and used directly.

4.9. HUVEC spheroid sprouting assay

The fibrin gel bead assay was done according to Nakatsu et al., 2007 (Nakatsu et al., 2007). The culture media of HUVEC and fibroblasts (TIF = telomerase immortalized fibroblasts, routinely cultured in DMEM 20% FBS), were changed for EGM2 (Promocell) one day before coating on beads and embedding, respectively. HUVEC were trypsinized and coated on Cytodex beads at a ratio of 10^6 cells for 1mg of beads during 4 hours at 37°C with occasional agitation, and then cultured overnight in 6 cm dish. Next day, HUVEC-coated beads were combined at a concentration of 500 beads/ml in the 2 mg/ml fibrinogen pre-gel solution supplemented with 0.15 U/ml of aprotinin. Fibrin gel formation was initiated by adding 0.625 U/ml of thrombin and then the gels were allowed to stand for 5 minutes at room temperature, followed by 15 minutes incubation at 37°C for. Meanwhile, TIFs were trypsinized and plated on top of a fibrin gels at 40,000 cells in EGM-2 medium per well in 12-well plate. The cells were cultured for up to 12 days with the media change every other day. Phase micrographs of growing tubes were captured every day using 10x objective and/or video microscopy were done (Zeiss inverted microscope Axiovert 200M with Coolsnap HQ). Quantification of number and length of sprouts was done in ImageJ software. Sprout length was calculated by measuring the distance from the bead to the end of the sprout. 10-20 beads were analyzed per well condition and each condition was done in triplicate, three independent experiments were done.

4.10. In vitro endothelium-like permeability assay

400.000 HUVEC were grown to confluence for three days in the top well of a transwell filter (0.4 µm, 6.5 mm diameter, Corning) pre-coated with Col I, FN or TN at 1 µg/cm^2. 40-kDa FITC-dextran (Sigma) was added to the top chamber of the transwell for a final concentration of 1 mg/ml. At 30, 60 and 120 minutes, 100 µl sample was removed form the bottom compartment and read in a fluorometer (TriStar2 Multimode Read LB 942 Berthold Technology), excitation 485 nm, emission 520 nm). Then cells were fixed with PFA 4% 15 minutes and stained for their nuclei (DAPI) and F-actin (phalloidin-FITC, Sigma) to visualized the endothelium-like layer in each condition

4.11. Matrix tubulogenesis assay

Matrix was prepared by adding 10 µl of Matrigel (Corning) into 15 well dishes (µ-Slide Angiogenesis, Ibidi LLC) followed by solidification at 37°C in a humidified incubator for

1hour. HUVEC (140`000 cells/ml) and BAEC (200`000 cell/ml) were trypsinized and resuspended in low FBS-containing medium (M199, 1% FBS, 1 µg/ml heparin, 200 ng/ml hydrocortisone with 10 ng/ml VEGF165 or DMEM low glucose, 1% FBS with 10 ng/ml VEGF165) with 0,01 % PBS-Tween (control for TNC), 2.5 µg/ml, 5 µg/ml or 10 µg/ml TNC or with CM from U87MG, U118MG or CAF. After incubation for 8h at 37°C, bright field mosaic pictures were taken (Zeiss Imager Z2 inverted microscope and AxioVision software (Carl Zeiss) at 50X magnification, a total of 9 pictures per condition) and tube-like structures or tube length were assessed by using the AxioVision or ZEN Blue software (Carl Zeiss). A minimum of 3 independent experiments were done with 5 replicates per experiment.

Tube-like structures (defined by the numbers of closed loops) and/or total capillary lengths were counted using the AxioVision or ZEN Blue software (Carl Zeiss). A minimum of 3 independent experiments were done with 5 replicates per experiment, and measures were averaged.

4.12. Mobility cell tracking assay

Cell mobility of isolated cells in 2D culture conditions was analyzed in MatLab (The MathWorks) after manual tracking of non-dividing cells. Phase contrast and video microscopy were done with Zeiss inverted microscope (Axiovert 200M) equipped with a CoolSnap HQ cooled charge-coupled-device camera (Roper Scientifique). Image acquisition and cell tracking was done using the LSM image brower software (Zeiss).

4.13. Vascular co-culture assay

The protocol from (Ghajar et al., 2013) was adapted. Briefly, the microvascular niche was generated with fibroblasts (MEF wt or TNCKO) or CAF (shTNC) seeded at a density of 50,000 cells per well in 96-well culture plates with 20,000 HUVEC or VeraHUVEC (ratio 5:2). Cells were suspended in ECGM at a concentration of 70,000 cells per 100µl (fibroblasts+ EC).Plates were left on a flat surface for 20 minutes to allow even cell seeding before incubation. During the 7 days of co-culture in ECGM the medium was replenished every 2 days. Then cells were stained with CD31 antibody (Invitrogen) and DAPI. Tube-like structures (defined by the numbers of closed loops) were counted using the ZEN Blue software (Carl Zeiss). A minimum of 3 independent experiments were done with 6 replicates per experiment, and measures were averaged.

4.14. Wound closure assay

Equal quantity of cells was grown to confluence in 24-well plates during 24 hours. The confluent monolayer of HUVEC, BAEC or HBVP was starved for 24 hours and then cells were treated with mitomycin C at 2µg/ml (2 hours) to inhibit their proliferation (data not shown). Cells were mechanically scratched using a P200 tip. Cell debris was removed by washing with PBS before adding low serum media plus or minus purified recombinant human TNC at (0, 2.5, 5, 10 or 20 µg/ml in PBS-Tween 0.01%) to the cells. Two images of the wounding area were acquired immediately after scratch and then at the same locations after 12 hours for BAEC, 18 hours for HBVP and 24 hours for HUVEC. The relative wound closure was quantified by measuring the width of the cell-free area at the time of injury and the end point of the experiment. Values were presented as a percentage of migration from four replicates and three independent experimental conditions.

5. Histology, molecular biology and proteomic analysis

5.1. Immunofluorescence staining of tissue, cells and CDM

For immunochemical tissue analysis, 7 µm sections were obtained with a cryostat (LEICA CM3050S). Cells or CDM were fixed in 4% PFA for 15 minutes, then wash 3 times in PBS and permeabilized in PBS-Triton 0.25% for 10 minutes. Tissue was fixed in PFA 4% for 10 minutes at room temperature, washed 3 times for 5 minutes with PBS and permeabilized in PBS-Triton 0.25% for 10 minutes. Then tissue, cells or CDM are incubated in blocking buffer containing PBS 1X solution and 10% normal donkey serum (NDS) or normal goat serum (NGS) for 2 hour at room temperature for blocking unspecific antibody binding. Tissue was incubated at 4°C overnight and cells or CDM at room temperature 2 hours with the primary antibodies (**Antibodies** section) diluted in blocking buffer. Sections were washed with PBS 3 times for 5 minutes, then incubated for 1-2 hours at room temperature with species-specific secondary antibodies donkey or goat antibody(ies) conjugated with fluorochrome emitting at 488, 555 or 647 nm (Jackson ImmunoResearch; 1/2000) in blocking buffer. Sections were washed again with PBS 3 times for 5 minutes, then nuclei were stained with 4',6-diamidino-2-phenylindole (DAPI) (Sigma D9542, 1/50,000) for 10 minutes at room temperature. Finally after 3 washes with PBS, the slides were mounted with non polymerized aqueous medium (Swartz and Santi, 1996) or a polymerization medium (FluorSave^{TM}Reagent,

CALBIOCHEM) and stored at 4°C until analysis. For phalloidin staining cells were incubated for 45 minutes with phalloidin-tetramethylrhodamine B isothiocyanate (Sigma P1951, methanol, 20 µg/ml) or -fluorescein Isothiocyanate (Sigma P5282, methanol, 20 µg/ml) with secondary antibody(ies).

5.2. Protein purification and purified ECM coating

Protein purification was carried out with the ÄKTA Prime Plus (GE Healthcare) with the Prime view 5.0 Software.

FN protein purification

FN was purified from filter‐sterilized horse serum (Amimed, Bioconcept). A gelatine-agarose (Sigma) column was equilibrated with PBS. The serum was loaded on the column and the column was washed with PBS until the OD280 reached again the baseline. Triton-buffer (1 M NaCl/0.01 M Tris-HCl pH 8.3/0.05% Triton X‐100) was applied on the column. The column was washed with PBS before applying Elution buffer (PBS/4M Urea). The protein concentration of the collected samples was determined by measurement of the OD280. Fractions with an OD280 higher than 0.3 were pooled. Pooled fractions were dialyzed (Cellu Sep T3 cellulose tubular membrane, nominal MWCO: 12,000 – 14,000) 2x for 2 hours and 1x overnight against PBS at 4°C. Aliquots were frozen in liquid nitrogen and stored at ‐80°C.

TNC protein purification

Conditioned medium containing human TNC with a C-terminal His tag (Lange et al., 2007) was collected from HEK293 c18:TNC grown for 2 days in DMEM without supplements. Conditioned medium was filtered over a bottle top filter (0.22 µM, Stericup, Millipore) and protein was precipitated by adding 291 g Ammonium sulphate per one liter of conditioned medium (CM) and stirring for 2 hours at 4°C. Precipitated protein was enriched by centrifugation at 12000 x g for 20 minutes. The precipitate was resuspended in PBS/T (0.01% Tween‐20) and dialyzed 2 X for 2 hours and one time overnight at 4°C against PBS/T. Dialyzed protein was centrifuged at 12000 x g for 10 minutes. In order to remove FN from the sample, the supernatant was passed over a gelatine-agarose column equilibrated with PBS/T. The flow through was collected and adjusted to the same concentrations as the equilibration buffer (250 mM Sodium Phosphate/450 mM NaCl/20 mM Imidazol/500 mM Urea). Ni2+ resin (Nalgene, Jena Bioscience) equilibrated with Equilibration buffer was incubated with the protein sample on an overhead-rotator at 4°C overnight. The Ni2+ beads were packed in a column. The flow through was again passed over the column. The column was washed with

the equilibration buffer until optical density was back to baseline. The column was washed with 250 mM Sodium Phosphate/450 mM NaCl/20 mM Imidazol and protein was eluted with 250 mM Sodium Phosphate/450 mM NaCl/300 mM Imidazol. Fractions with an OD280 higher than 0.3 were pooled. Pooled fractions were dialyzed 2x for 2 hours and 1x overnight against PBS/T at 4°C. Aliquots were frozen in liquid nitrogen and stored at ‑80°C. Protein fractions were analyzed by Western Blotting or on an 8% SDS gel, which was stained with a 45% Ethanol/15% Acetic Acid/0.025% (w/v) Coomassie Blue solution and destained with a 5% Ethanol /7.5% Acetic Acid solution.

5.3. Coating with fibronectin, collagen type I and TNC

Coating of cell-culture dishes with FN, Col I and TNC was done using standard protocols as described earlier (Huang et al., 2001b; Lange et al., 2007). Briefly, FN, Collagen type I (Col I, Corning CB-40236) and TNC were sequentially coated in PBS/0.01% Tween-20 at 0.001-100 µg/cm2 before saturation of the non-coated surface with 10 mg/ml BSA/PBS. Cells were seeded on the coated surfaces and analyzed using standard protocols described underneath.

5.4. Protein silver staining

Protein determination of CM content was analyzed using SilverXpress Kit (Invitrogen) according to manufacturer. Briefly CM from U87MG educated by MEF wt or TNC KO CDM were separated by PAGE in pre-casted 4-20% gradient gel (Invitrogen) (20 µg of proteins, determined by Bradford assay). After migration at 140V, the gel was fixed and stained. Image of the gel was acquired using a scanner (2560x1920 pixels).

5.5. Quantitative Secretome Profiling

U87MG cells were plated on the cell derived matrix generated by TNC KO or TNC wt MEF and cultivated in DMEM containing 10 % FCS until 90 % confluence, washed three times with phosphate buffered saline (PBS), and incubated for 24 h (37 °C, 5% CO2) in serum-free DMEM without phenol red. After 24 h, cell-conditioned medium (CM) was collected, supplemented with protease inhibitors (5 mM ethylenediaminetetraacetic acid (EDTA), 0.01 mM trans-epoxysuccinyl-L-leucylamido(4-guanidino)butane (E64), 1 mM phenylmethanesulfonyl fluoride (PMSF), centrifuged (5min, 1000 x g, 4°C), and filtered using a 0.2 µm filter to remove debris. Samples were stored in -80°C until processing.

Samples for comparative proteomic analysis were prepared as described previously (Tholen et al., 2013) and Koczorowska et al. in preparation). Briefly, proteins were precipitated with

trichloracetic acid (TCA), solubilized, trypsinized, reduced, and alkylated. Samples were then labeled with 20 mM either “light” 12CH2O formaldehyde, (U87MG/CDM TNC wt) or “heavy” 13CD2O formaldehyde (U87MG/CDM-TNC KO) in the presence of 20 mM sodium cyanoborohydride. After quenching the reaction with glycine, both samples were combined in 1:1 ratio. Following desalting by C18 solid phase extraction (Sep-Pak C18 Plus Light Cartridge, Waters, Frankfurt, Germany), samples (ca. 300 µg) were fractionated by strong cation exchange chromatography as described previously (Biniossek and Schilling, 2012; Shahinian et al., 2014; Tholen et al., 2013) and analyzed by liquid chromatography–tandem mass spectrometry (LC-MS/MS).

5.6. LC-MS/MS analysis

For nanoflow-LC-MS/MS analysis, a Q-Exactive plus (Thermo Scientific GmbH) mass spectrometer coupled to an Easy nanoLC 1000 (Thermo Scientific) with a flow rate of 300 nl / min each was used. Buffer A was 0.5 % formic acid, and buffer B was 0.5 % formic acid in 100 % acetonitrile (water and acetonitrile were at least HPLC gradient grade quality). A gradient of increasing organic proportion was used for peptide separation. As the analytical column served an Acclaim PepMap column (Thermo Scientific), 2 µm particle sizes, 100 Å pore sizes, length 150 mm, I.D. 50 µM. The mass spectrometer operated in data dependent mode with a top 10 method.

5.7. LC-MS/MS Data Analysis

LC-MS/MS data in raw format was converted to the mzXML (Pedrioli et al., 2004) format, using msconvert (Kessner et al., 2008) with centroiding of MS1 and MS2 data, and deisotoping of MS2 data. For spectrum to sequence assignment X! Tandem (Version 2013.09.01) (Craig and Beavis, 2004) was used. The proteome database consisted of human reviewed canonical uniprot sequences (without isoforms) downloaded from UniProt on November 26, 2013. It consists of 20,240 real protein entries. It was appended with an equal number of shuffled decoy entries derived from the original human protein sequences. The decoy sequences were generated with the software DB toolkit (Martens et al., 2005). X! Tandem parameters included: pre-cursor mass error of ± 10 ppm, fragment ion mass tolerance of 20 ppm, tryptic specificity with up to one missed cleavage, static residue modifications: cysteine carboxyamidomethylation (+57.02 Da), variable modifications were isotope-labeled (+6.02 Da) arginine and lysine. X!Tandem results were further validated by PeptideProphet at a confidence level of >95 % (MPT = 0.05). Corresponding protein identifications are based on

the ProteinProphet algorithm (Nesvizhskii et al., 2003) with a false discovery rate <1.0 %. The relative quantitation for each protein was calculated from the relative areas of the extracted ion chromatograms of the precursor ions and their isotopically distinct equivalents using the XPRESS algorithm (Han et al., 2001) as described previously (Biniossek and Schilling, 2012; Shahinian et al., 2014; Tholen et al., 2013).

5.8. RT-qPCR analysis

RNA isolation was done with TRIZOL according to the manufacturer's instructions (Invitrogen). Specific primers for YAP target genes: CTGF, Cyr61, LCN1 and LCN7 were used and listed in **Table 3**. For normalization of gene expression GAPDH was used as housekeeper gene. For SYBR Green real-time RT-PCR, a total of 1 µg of RNA was reverse transcribed into cDNA using the High capacity cDNA Reverse transcription kit (Apllied Biosystem©) following the manufacturer's protocol. The conditions for PCR were as follows for each samples: 10 ng of cDNA with 2 µl SYBR specific polymerase, 0.8 nM dNTP, 2 µl DNAse I reaction buffer, and 2 µM of the particular sense and antisense primers under standard conditions (at 95°C for 3 minutes followed by 40 cycles at 95°C for 30 s, 60°C for 45 s, and 72°C for 30 s and an extension at 72°C for 8 min). All products were from Invitrogen©. Five biological replicates were analyzed.

Table 3. Human primers used for RT-qPCR analysis.

Gene	Forward primer (5'-3')	Reverse Primer (5'-3')
CTGF	AGGAGTGGGTGTGTGACGA	CCAGGCAGTTGGCTCTAATC
Cyr61	AGCCTCGCATCCTATACAACC	TTCTTTCACAAGGCGGCACTC
LCN1	CAAGAACAACCTGGAAGC	CAAGGTGTCCCCCTAATC
LCN7	AAACAGCAGTTGGATGTATG	GATGGCTTTGATCATGTCTG

5.9. Western Blotting

Cells were washed with cold PBS and lyzed in 100 µl of lysis buffer (25 mM Tris-HCl pH 7.6, 150 mM NaCl, 1% NP-40, 1% sodium deoxycholate, 0.1% SDS). Cells were scraped. The cell lysates were vortexed and incubated 10 minutes on ice. Then samples were centrifuged at 13.000 rpm (centrifuge 5415D, Eppendorf), 4°C for 15 minutes. The supernatant containing the protein lysate was stored at −20°C until use. For aortic rings protein extraction, three aortic rings after 6 days in culture in collagen I gel from two mice from wt or TNC KO

genotype were pooled in eppendorf tube and treated with collagenase I (Sigma) 100 U/ml 30 minutes at 37°C. Then collagenase I was stopped with 3X volume of serum solution activity and samples were centrifuged at 13.000 rpm at 4°C. The pellet was washed in PBS and centrifuged again. Finally pellet was lysated in RIPA buffer and sonicated. The supernatant containing the protein lysate was stored at −20°C until use. Protein concentration was determined by Bradford Assay using the Protein Assay reagent (500 - 006, Bio - Rad) with a BSA standard curve. 40 µg of protein were diluted 1:1 in 2x Laemmli buffer (125 mM Tris pH 6.8, 4% SDS, 20% Glycerol, 5% Mercaptoethanol and 0.01% Bromphenolblue) and loaded on SDS−Polyacrylamide gels (10% with a 4% stacking gel) or pre-casted 4-15% gradient gel (Invitrogen). Gels were run during 1h30 at 160V with the following running buffer: 1X Tris/Glycine with 0.2% SDS. Proteins were transferred onto PVDF or nitrocellulose membranes with a pore size of 0.45 µm (IPVH00010, Immobilon) for 2h minutes with 260 mA with cold 1X Tris/Glycine/20% Ethanol blotting buffer, or using Transblot™ machine (Biorad). Successful blotting was verified by incubating the membrane with the Ponceau-S dye (81462, Sigma). The membrane was blocked with 5% Blocking−Grade Blocker (170−6404, Biorad) in PBS/0.1% Tween for 2 hours. The membrane was incubated with the primary antibody in 1.5% Blocking−Grade Blocker in PBS/0.1% Tween overnight at 4°C. After washing (3x 10 minutes) with PBS/0.1% Tween, the secondary antibody in 1.5% Blocking - Grade Blocker in PBS/0.1% Tween (Horseradish Peroxidase linked) was applied for 1h at RT. Concentrations of the primary and secondary antibody can be found in **Antibodies** section. Immunocomplexes were revealed by addition of detection reagents Amersham ECL Western Blotting detection reagent (RPN2106, GE Healthcare) or Amersham ECL Plus Western Blotting Detection System (RPN2132, GE Healthcare) and the emitted signal was captured in with a PXi touch imager (Ozyme). Images were acquired and processed using GeneSys software (Ozyme). Protein Ladder (10-250 kDa) (Biorad, Precision Plus Protein™ Dual Color Standards #161-0374) was used. Purified recombinant human TNC are used as positive control (0.1 µg).

5.10. G- and F-actin fractionation

Actin fractionation was prepared adapted from previously described method (Posern, 2002). Briefly, one million HUVEC were seeded in 6 well plate precoated with Col I, FN or TNC. After 5 hours HUVEC were washed with PBS and then buffer (20 mM HEPES pH 7.7, 50 mM NaCl, 1 mM EDTA and 0.5% (v/v) Triton X-100) was added. Cells were scraped and

centrifuged at 100.000 g at 4°C, 1 hour. Supernatant is considered as G-actin fraction and pellet resuspended in buffer by sonication is considered as F-actin fraction. The G- and F-fractions were quantified using the Bradford method, and 20 μg of each fraction was analyzed by PAGE and actin staining.

6. Statistical analysis and graphical representation

Statistical analysis was done using GraphPad Prism or R. Statistical differences were analyzed by unpaired t-test or ANOVA one-way with Tukey post test (Gaussian distribution), non-parametric Mann-Whitney test or Kruskal-Wallis and Dunn post-test (no Gaussian distribution). Gaussian data sets with different variances were analyzed by Permutation ANOVA one-way and Permutation Tukey post-test. Gaussian distribution was tested with a minimum population ($n = 18$) by the d'Agostino-Pearson normality test, p-values < 0.05 were considered as statistically significant. All experiments were repeated at least 3 times.

C. RESULTS

TNC plays multiple roles in tumor angiogenesis with presumably opposing effects that are poorly understood. In my thesis I have addressed these roles at cellular and molecular level. Following **Aim 1** I had established multiple state-of-the-art angiogenesis assays in the laboratory including the retinal angiogenesis assay, aortic ring sprouting angiogenesis assay, fibroblast stimulated EC tubulogenesis assay or matrigel EC tubulogenesis assay. Moreover, I determined how TNC affects EC adhesion, survival, proliferation, migration, tube formation, sprouting and vessel functionality.

Following **Aim 2** I have addressed molecular mechanisms by which TNC exerts its anti- and pro-angiogenic activities.

Finally, in **Aim 3** I had contributed to two studies in the laboratory that addressed the impact of TNC on tumor angiogenesis by using a spontaneous tumor mouse model with defined TNC levels.

Aim 1. Establish and employ in vivo, ex vivo and in vitro methods to elucidate the roles of TNC in normal and tumor angiogenesis.

Since my in vitro study focused on EC and GBM derived cellular models I started my thesis with an in vivo GBM xenograft experiment that supported results from other studies (Herold-Mende et al., 2002; Martina et al., 2010; Mustafa et al., 2012) showing high TNC expression in close association with vessels. My experiments provided evidence that tumor and stromal cells express TNC in this GBM model setting the stage to address how autocrine and paracrine interactions with TNC impact on EC behavior.

1.1. TNC is expressed around tumor vessels by tumor and perivascular stromal cells in a GBM xenograft model

Several reports (Berndt et al., 2010; Herold-Mende et al., 2002; Martina et al., 2010) describe a perivascular pattern of TNC expression but the cellular origin of TNC remained elusive. By using a xenograft nude mouse model with a subcutaneous tumor derived from grafted human GBM cells I had addressed the question whether the host and/or the tumor cells expressed TNC. By using the mTNC12 (rat anti-murine TNC) and B28.13 (mouse anti-human TNC) it was possible to determine the source of TNC. I observed that both the host and the tumor cells expressed TNC in this model (**Fig. 15A, B**). Interestingly I detected that TNC co-localized with perivascular αSMA cells (**Fig. 15A**) and that TNC is expressed by tumor cells close to the vasculature (**Fig. 15B**). To further address which perivascular cells express TNC, I determined TNC expression by WB in cultured pericytes. Pericytes expressed low amounts of TNC which was enhanced upon stimulation with TGFβ1 (important modulator of tumor progression and angiogenesis (Cunha and Pietras, 2011) yet not upon treatment with $VEGFA_{165}$ (important mediator of angiogenesis overexpressed in tumors (Carmeliet, 2003; Roskoski, 2007) (**Fig. 15C**). These results suggested that perivascular TNC observed in human tumors including GBM (Berndt et al., 2010; Herold-Mende et al., 2002; Martina et al., 2010) is most likely expressed by pericytes, tumor cells and other not identified stromal cells. Similar observations had been made in another colorectal xenograft model using SW480 cells (Spenlé et al., 2015).

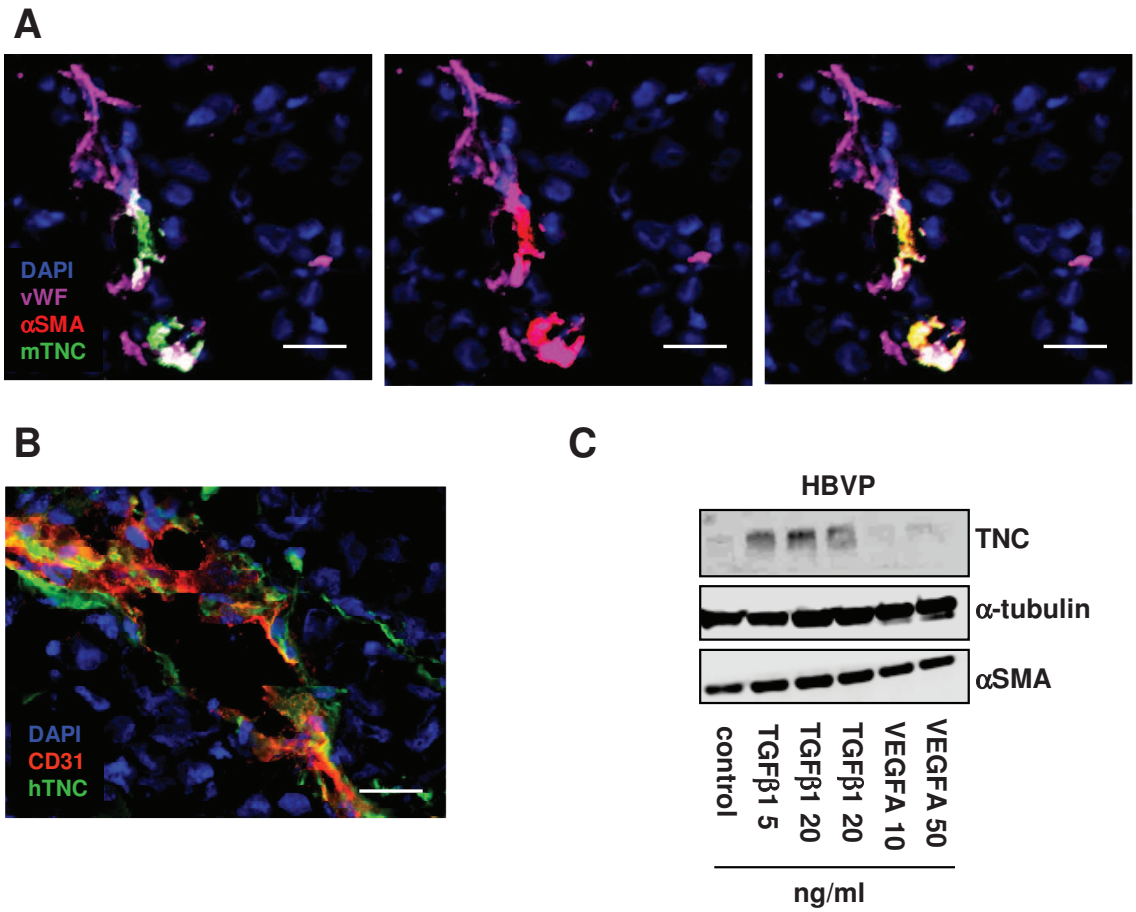

Figure 15. Perivascular expression of TNC in glioblastoma xenograft model

(**A**) Expression of murine TNC (mTN12, green) close to EC labeled with vWF (von Willebrand Factor, purple) in a heterotopic xenograft tumor of a human biopsy in a nude mouse. TNC colocalized with smooth muscle cells (αSMA, red) (scale bar, 10 µm). (**B**) Perivascular expression of human TNC (B28.13, green) indicating tumor cells secreted TNC around vessels (CD31, red) (scale bar, 10 µm). (**C**) Immunoblot of human TNC, αSMA and α-tubulin in HBVP stimulated or not with TGFβ1 or VEGFA.

1.2. Impact of TNC on vessel sprouting assessed in an aortic ring assay

Then we analyzed the role of TNC on nagiogeneis. First, we used tissue from TNC wt and TNC KO mice (**Fig. 16A**), respectively in an aortic ring assay, to determine sprouting angiogenesis in dependence of TNC. Aortic rings from TNC KO and wt mice were embedded into collagen gels for 7 days and sprout formation was assessed by immunostaining and quantification. The sprouts were composed of EC and mural cells as determined by staining for isolectin B4 and αSMA, respectively and expressed TNC (**Fig. 16B**). Interestingly we

detected TNC expression around the endothelial sprouting structures (**Fig. 16C**). We observed that the number and length of endothelial sprouts was higher in the absence of TNC suggesting a negative impact of TNC on vessel formation in this assay (**Fig. 16D - F**).

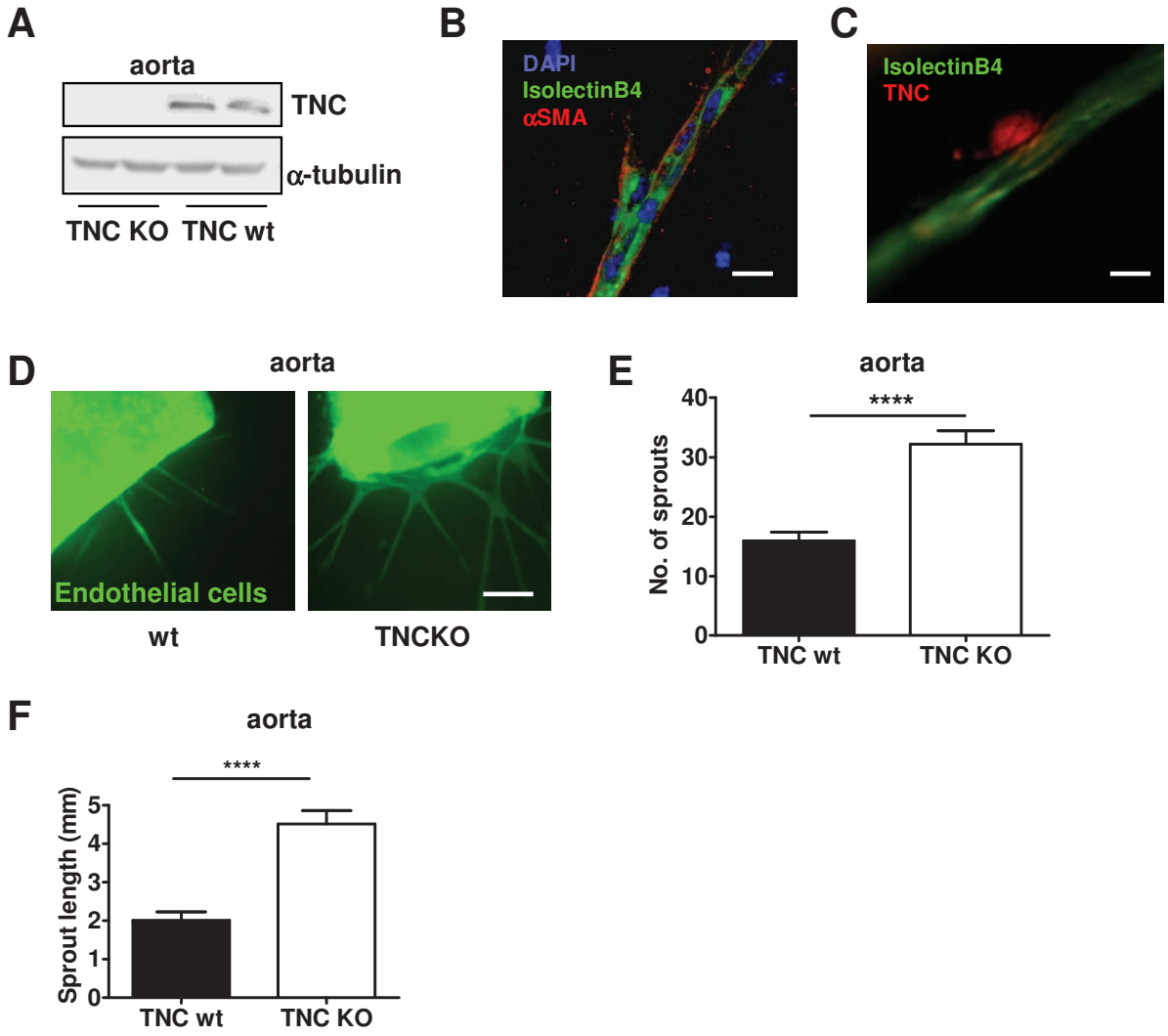

Figure 16. TNC is expressed in wt aorta and reduces angiogenic sprouting

(**A**) Expression of TNC in aorta of TNC KO and wt mice upon growth for 6 days in Col I gels assessed by immunoblotting for TNC with a-tubulin as control. (**B, C**) Co-staining of endothelial cell spouts for EC (isolectin B4, green), perivascular cells (αSMA, red) (**B**) or TNC (mTN12, red) (**C**) and EC (isolectin B4, green) (DAPI) (scale bar = 10 µm). **(D)**, Representative images of vessel sprouts from TNC KO and wt aortic rings upon staining with Isolectin B4 (scale bar, 150 µm). (**E**, **F**) Quantification of number (**E**) and length (**F**) of aortic sprouts. Mean with SEM (3 independent experiments, 9 mice per genotype, wt aortic rings, n = 105, TNC KO aortic rings, n = 123, $p < 0.001$).

1.3. Impact of TNC on retinal angiogenesis

We also used a retinal angiogenesis assay with tissue from TNC KO and wt mice and determined sprouting angiogenesis in dependence of TNC. Therefore, retina (P5.5) stained with isolectin B4 and the outgrowth of vessels was determined. Whereas absence of TNC expression in wt retina (**Fig. 17A**). the outgrowth of the vascular network was slightly reduced (<5%) but the number of branching points and endothelial filopodia density was similar in the TNC KO context suggesting that TNC does not play a major role in this angiogenic process (**Fig. 17B-H**).

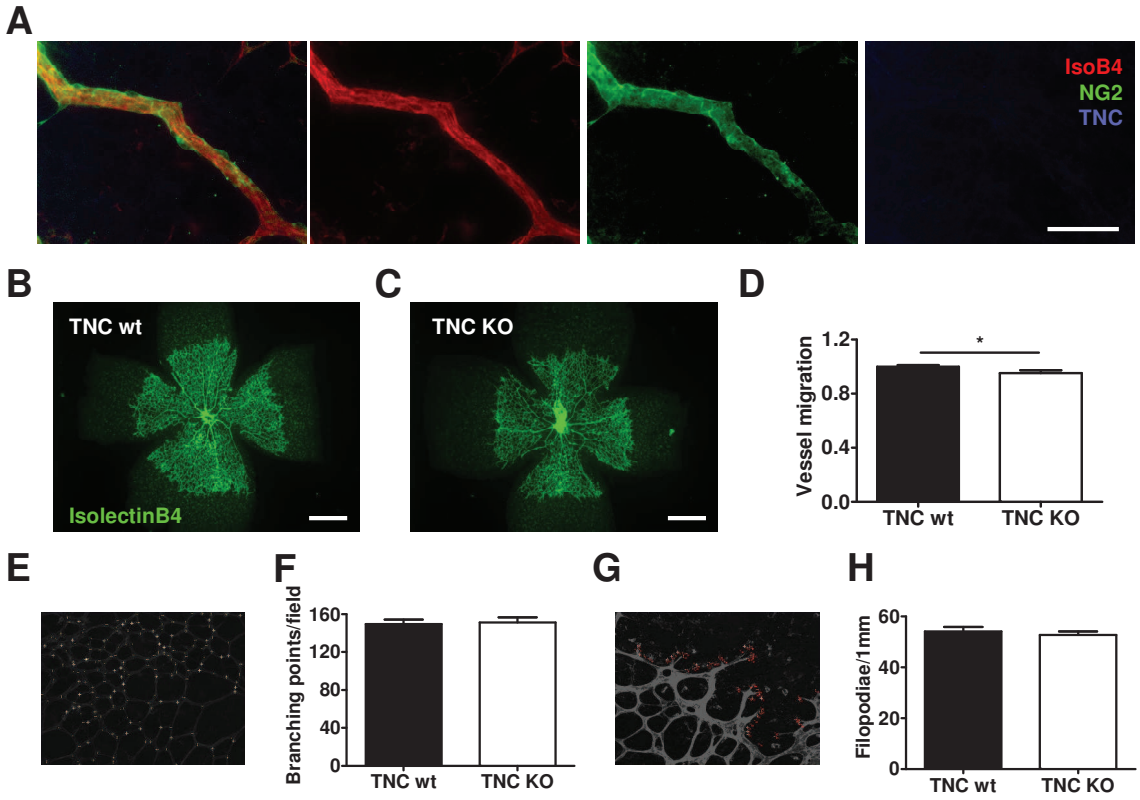

Figure 17. TNC does not regulated physiological retinal angiogenesis

(**A**) Immunofluorescence staining of P5.5 wt mouse retina for EC (Isolectin B4, green), pericytes (NG2, red) and TNC (blue). Note no expression of TNC in the retinal tissue (scale bar, 10 µm). (**B**, **C**) representative pictures of vessel outgrowth in culture upon labeling with isolectin B4 (green) (scale bar, 500 µm). (**D**) Quantification of the migration front of the vascular network. Bars represent mean with SEM (wt, n = 33 retinas and TNC KO, n = 27 retina, $p < 0.05$). (**E**, **F**) Representative picture (**E**) and quantification (**F**) of vessel branching in retinas from wt and TNC KO mice. Mean with SEM (wt, n = 38 retinas, TNC KO, n = 42 retinas, no statistical difference). (**G**, **H**) Representative images of

retinal filopodia at the migration front upon staining with isolectin B4 and quantification (**H**). Mean with SEM (wt, n = 38 retinas, TNC KO, n = 48, no statistical difference).

1.4. Impact of TNC on endothelial cell tubulogenesis determined in a coculture assay of endothelial cells with carcinoma associated fibroblasts

Fibroblasts had been described as a major source of TNC in a breast cancer model (O'Connell et al., 2011a) and were shown to play an important role in promoting tumor angiogenesis (Kalluri and Zeisberg, 2006). Therefore, we had used CAF as provider of TNC and cocultured them with EC, to create a 3D vascular network using published innovative model (Ghajar et al., 2013) and mimic their spatial vicinity seen in a tumor context (**Fig. 18A**). This system allowed the formation of a vascular-like network where EC are lined by a vascular basement membrane as exemplified by Col IV staining (Adams and Alitalo, 2007b) (**Fig. 18B**). Importantly the EC can sprout (**Fig. 18C**) with multiple filopodia (**Fig. 18C, arrow**) extending in the 3D microenvironment. Upon staining with an anti-CD31 antibody we visualized tube-like structures and quantified them as read out for network complexity. We observed that veraHUVEC had formed EC network after 7 days.

Since CAF expressed TNC in culture, we generated cells with reduced TNC levels by shRNA knockdown (KD) (**Fig. 18D**) and determined whether TNC secreted by these cells had an impact on tubulogenesis. We observed more tube-like structures when veraHUVEC were grown together with CAF harboring a TNC KD. In comparison to CAF with TNC wt levels this number was 2.7-fold higher in the TNC KD. This result suggests that TNC expressed by CAF represses endothelial tubulogenesis (**Fig. 18E, F**).

Cells sense their microenvironment not only through soluble signals or cell-cell contact but also through biophysical and mechanical cues. ECM molecules serve as tissue scaffold and modulate cell behavior as adhesiveness that could modulate tissue contraction and stiffness (Dupont et al., 2011). Here, using a collagen contraction assay we demonstrated that CAF expressing high levels of TNC increased the contractibility of a Col I gel (**Fig. 18G**). This observation suggests that TNC may impair angiogenesis by modulating tissue stiffness which is described to affect negatively vessel organization and lumen formation in vitro (Forget et al., 2013; Ghajar et al., 2008; Urech et al., 2005). This hypothesis needs to be confirmed but suggests that TNC may impact on tissue stiffness (Roduit et al., 2009).

In addition to CAF coculture, we also observed an important delay of vessel-like formation with MEF expressing TNC compared to TNC KO cells (**Fig. 18H**) when they were cocultured with veraHUVEC after 4 days (**Fig. 18I**).

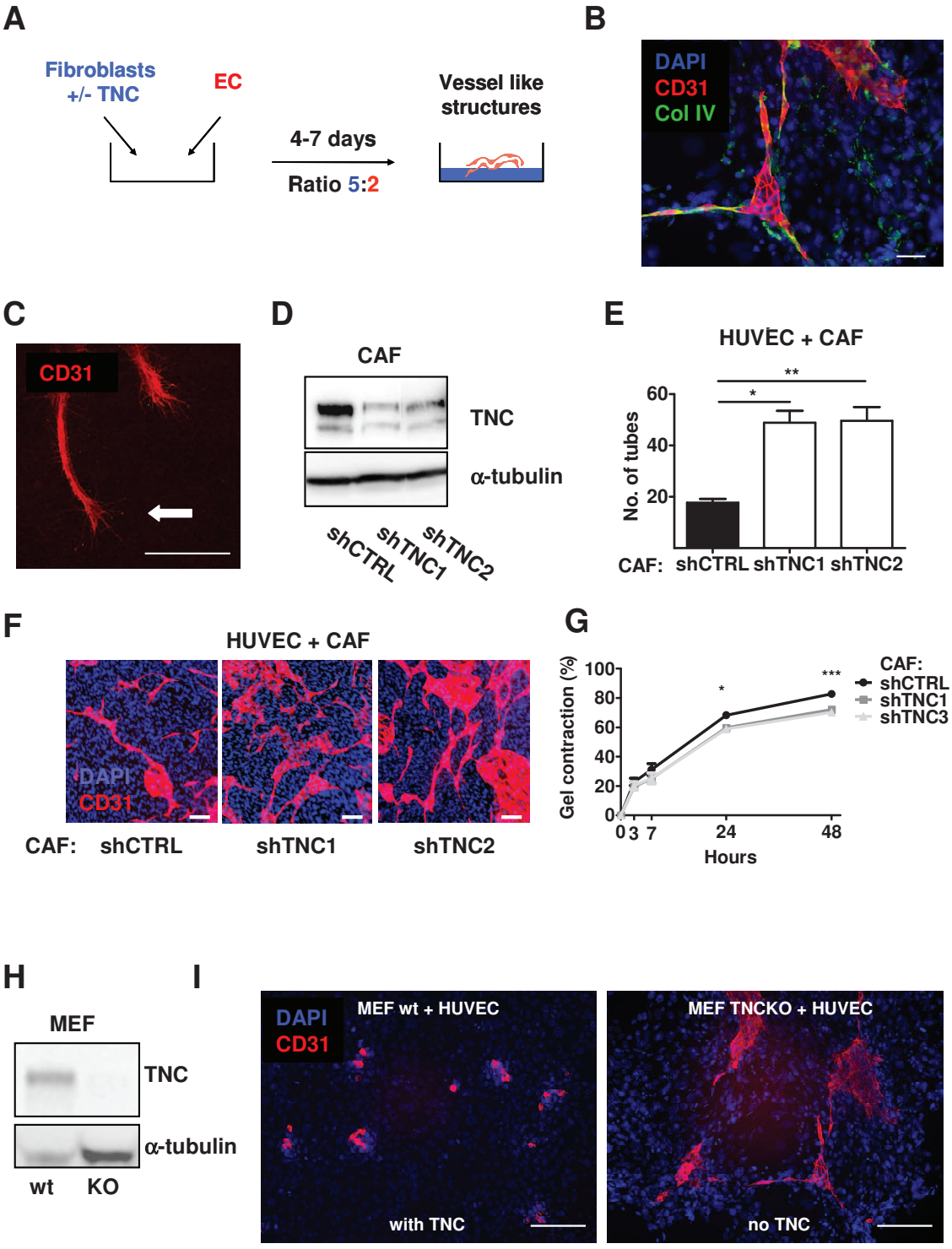

Figure 18. TNC represses tubulogenesis in a 3D coculture assay

(**A**) Vascular coculture model. (**B**) Staining showing that type IV collagen (Col IV, green) lines the EC structures (CD31, red) in the coculture model (scale bar, 10 µm). (**C**) Confocal acquisition of

sprouting EC like structures (CD31, red) showing multiple filopodia (white arrow) (scale bar, 10 µm). (**D**) Immunoblot of CAF with shCTRL and shTNC for TNC and α-tubulin. (**E**, **F**) Tubulogenesis in a coculture assay of VeraHUVEC with CAFshCTRL, shTNC1 or shTNC2; quantification of the number of tubes (**E**) and representative images (scale bar, 20µm) (**F**) of a 7 days culture, staining the vessel network with an anti-CD31 antibody (red). Nuclei are visualized upon staining with DAPI (blue). Mean with SEM (n = 9 wells, 3 independent experiments, 3 replicates, * $p < 0.05$ and ** $p < 0.01$). (**G**) Collagen gel contraction with CAFshCTRL, CAFshTNC1 and CAFshTNC2 cells over 48 hours. Curve represent mean + SEM (n = 9, 3 experiments, 3 replicates, * $P<0.05$, *** $P<0.001$). (**H**) Immunoblot of MEF TNC wt and TNC KO for TNC and α-tubulin. (**I**) Representative images of the tubulogenesis in a coculture assay of HUVEC (CD31, red) with MEF TNC wt and TNC KO after 4 days (scale bar, 100 µm). Note the absence of vessel sprouts with TNC.

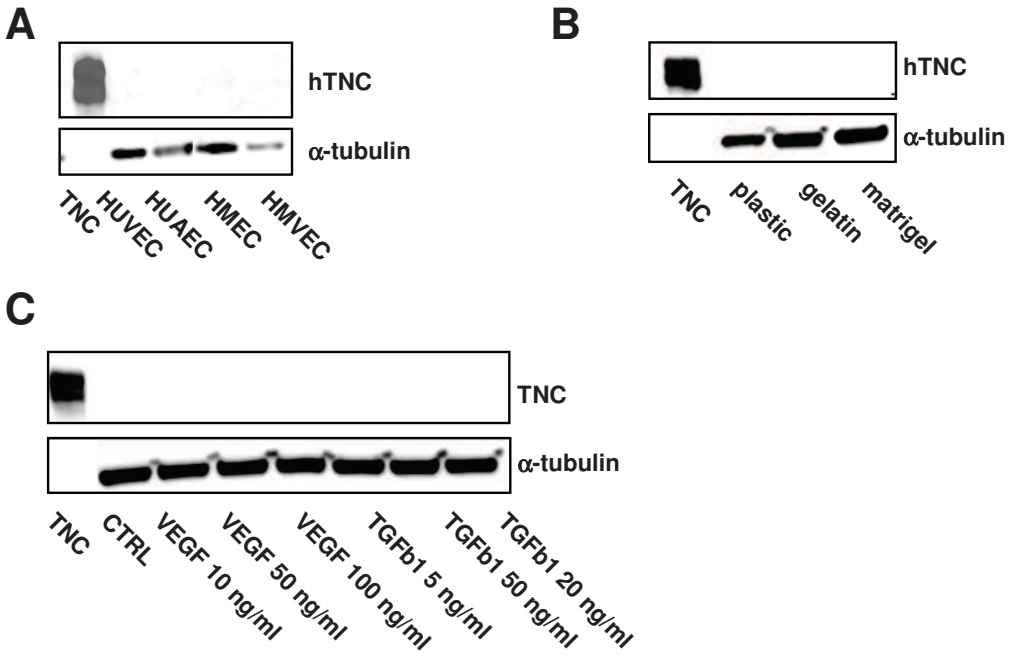

Figure 19. TNC is not expressed by EC in vitro

(**A-C**) Assessment of TNC expression in EC (VeraHUVEC, VeraHUAEC, HMEC-SV40 and HMVEC-hTERT) (**A**) by immunoblotting for TNC (α-tubulin as control) upon growth of cells on different substrata (24h) (**B**), or upon stimulation with VEGF or TGFβ (24h) (**C**).

To address whether HUVEC also expressed TNC we determined TNC expression in HUVEC by western blot. We did not detect TNC expression in HUVEC under any conditions tested that would trigger tubulogenesis such as upon plating cells on gelatin, matrigel nor upon

stimulation with growth factors that had been shown to promote angiogenesis (VEGFA and TGFβ) or TNC expression (TGFβ (Scharenberg et al., 2014)), respectively (**Fig. 19A, B**). Similarly, also other human EC (HUAEC, HMEC, HMVEC) (**Fig. 19C**) or BAEC (Radwanska et al., in preparation) did not express TNC in culture. Thus we conclude that TNC provided by CAF represses tubulogenesis of HUVEC in the coculture assay.

1.5. TNC impairs in vitro permeability of an endothelial monolayer

Until now we demonstrated that TNC interferes with survival and proliferation of EC as well as tubulogenesis which could explain a negative impact of TNC on tumor angiogenesis. To address the possibility that TNC potentially impairs vessel stability we used a dye permeability assay. In a Boyden chamber setting we generated a confluent monolayer of HUVEC (**Fig. 20A**) and determined diffusion of fluorescently labeled dextran through this monolayer in dependence of TNC. Therefore we coated the surface underneath the EC with Col I or TNC. By IF for DAPI and phalloidin we saw that both monolayers were confluent (**Fig. 20A**). We observed that a TNC substratum increased diffusion of a fluorescent dye through this layer over 120 minutes (**Fig. 20B**). This experiment suggested that TNC disturbed endothelium organization potentially leading to vessel abnormalities and leakiness.

1.6. Contact with TNC represses endothelial tubulogenesis, adhesion and migration

So far our results suggested that TNC negatively impacts on endothelial sprouting and tubulogenesis which could be a result of a direct interaction with TNC. Therefore, we addressed whether contact of EC with purified recombinant TNC has an impact on their tubulogenic behavior. We added purified recombinant TNC to HUVEC and BAEC in a matrigel tubulogenesis assay. Whereas the length and the number of HUVEC tube-like structures were the highest in the control condition, both numbers were reduced in a dose-dependent manner upon addition of TNC (**Fig. 21A - C**). TNC also reduced the number of tube-like formed by BAEC (**Fig. 21D, E**). This result suggests that contact of EC with TNC has a negative impact on EC tubulogenesis.

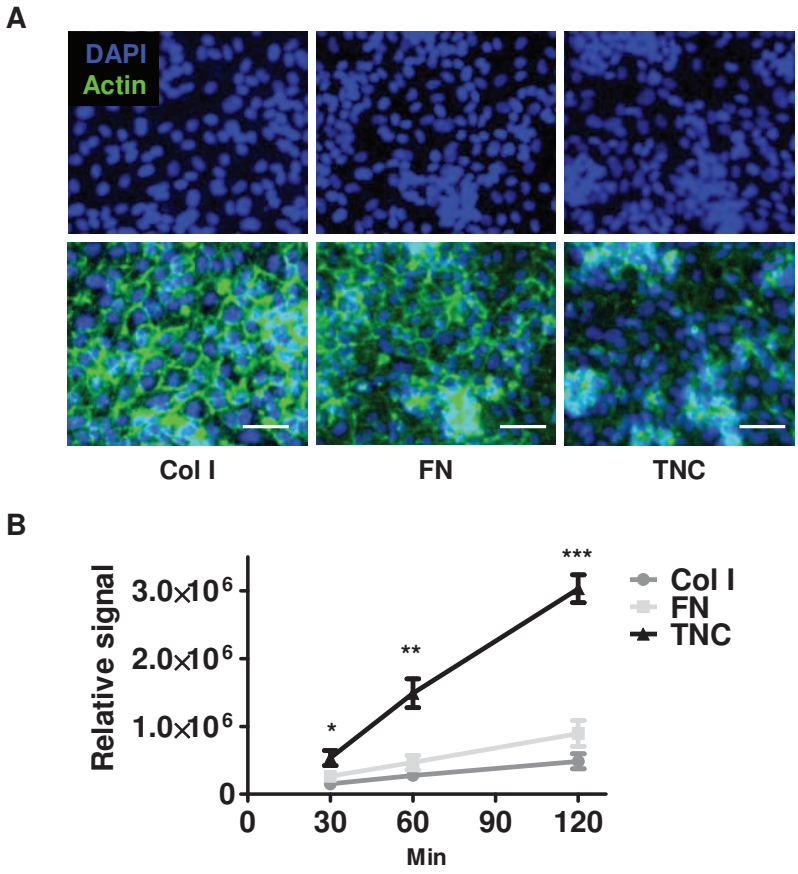

Figure 20. TNC increases endothelium-like permeability in vitro.

A, Nuclei (Blue, DAPI) and actin staining (green, phalloidin) of a dense monolayer of HUVEC after 48h, seeded in the upper part at 400,000 cells per boyden chamber insert (0.4 µm pore size) (scale bar = 10 µm). B, In vitro permeability assay by measuring diffusion through the membrane of a fluorescent dye (40 kDa dextran-FITC) over 120 minutes. Curve represents mean with SEM (n = 13, * $p<0.05$, ** $p<0.01$, ***$p<0.001$).

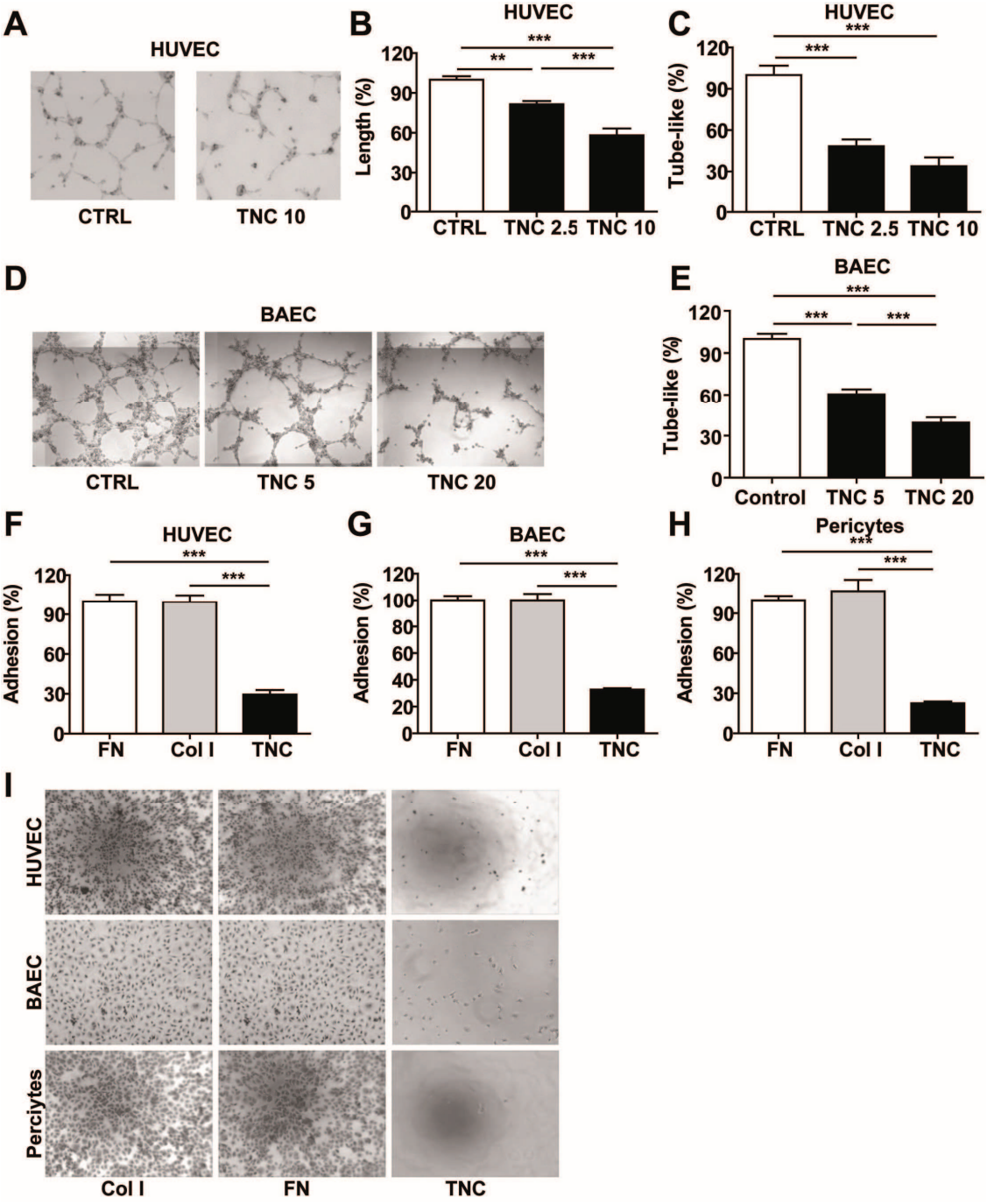

Figure 21. TNC impairs EC tubulogenesis and adhesion

(**A-C**) Tube formation of HUVEC in dependence of TNC. (**A**) Representative images of tubes formed by HUVEC upon plating on matrigel together with 10 µg/ml of TNC or 0.01% PBS-Tween 20 as control (CTRL) followed by quantification of tube length (**B**) and tube numbers (**C**) per condition. Mean with SEM (n = 15 wells, 3 independent experiments with 5 replicates, ** $p < 0.01$, *** $p < 0.001$). (**D, E**) Tube formation of BAEC in dependence of TNC. Representative images of tubes formed by BAEC upon plating on matrigel together with 5 or 20 µg/ml TNC or 0.01% PBS-Tween 20 as control (CTRL) (**D**) with quantification of number of tubes (**E**) per condition. Mean with SEM (n = 15 wells, 3 experiments with 5 replicates, $p < 0.001$). (**F-H**) quantification of adherent cells, HUVEC

(**F**), BAEC (**G**) and HBVP (**H**) upon plating for 1h on wells coated with Col I, FN and TNC at 1 µg/cm2 for HUVEC and HBVP and 2 µg/cm^2 for BAEC. Mean with SEM (n = 18 wells, 3 independent experiments with 6 replicates, *** $p < 0.001$). (**I**) Phase contrast images of crystal violet stained HUVEC, BAEC and HBVP upon adhesion on the indicated substrata for 1h.

Since tubulogenesis is largely dependent on cell adhesion and migration (Adams and Alitalo, 2007a) and TNC is an adhesion modulatory ECM molecule (Chiquet-Ehrismann et al., 1988), the observed effect may be due to TNC affecting cell adhesion and/or migration of EC. Therefore, we determined cell numbers upon plating HUVEC and BAEC for one hour on TNC, FN and Col I, respectively. We saw that whereas all cells attached and spread on FN and Col I they poorly adhered and did not spread on the TNC substratum (**Fig. 21F, G, I**).

Pericytes play an important role in maturation of blood vessels (Armulik et al., 2005) and were seen to poorly cover tumor blood vessels in tumors expressing highly abundant TNC (Saupe et al., 2013). To address whether TNC potentially had an impact on pericyte adhesion, we plated human brain vascular pericytes (HBVP) on the different substrata. We observed again that whereas all cells adhered and spread on FN and Col I, only a few cells adhered (and remained rounded) on TNC at 1h after plating (**Fig. 21H, I**).

We addressed cell migration by a scratch assay and observed that migration of HUVEC, BAEC and pericytes was reduced by TNC in a dose dependent manner down to 40% (HUVEC), 60% (BAEC) and 40% (pericytes) in comparison to control treatment, with the highest dose of TNC (10 and 20 µg/ml, respectively) (**Fig. 22A-F**).

By video time lapse microscopy we also addressed the role of TNC on cell migration in more detail. We observed that in comparison to a FN substratum, TNC delayed HUVEC spreading (**Fig. 22G**) and reduced mobility (**Fig. 22H**).

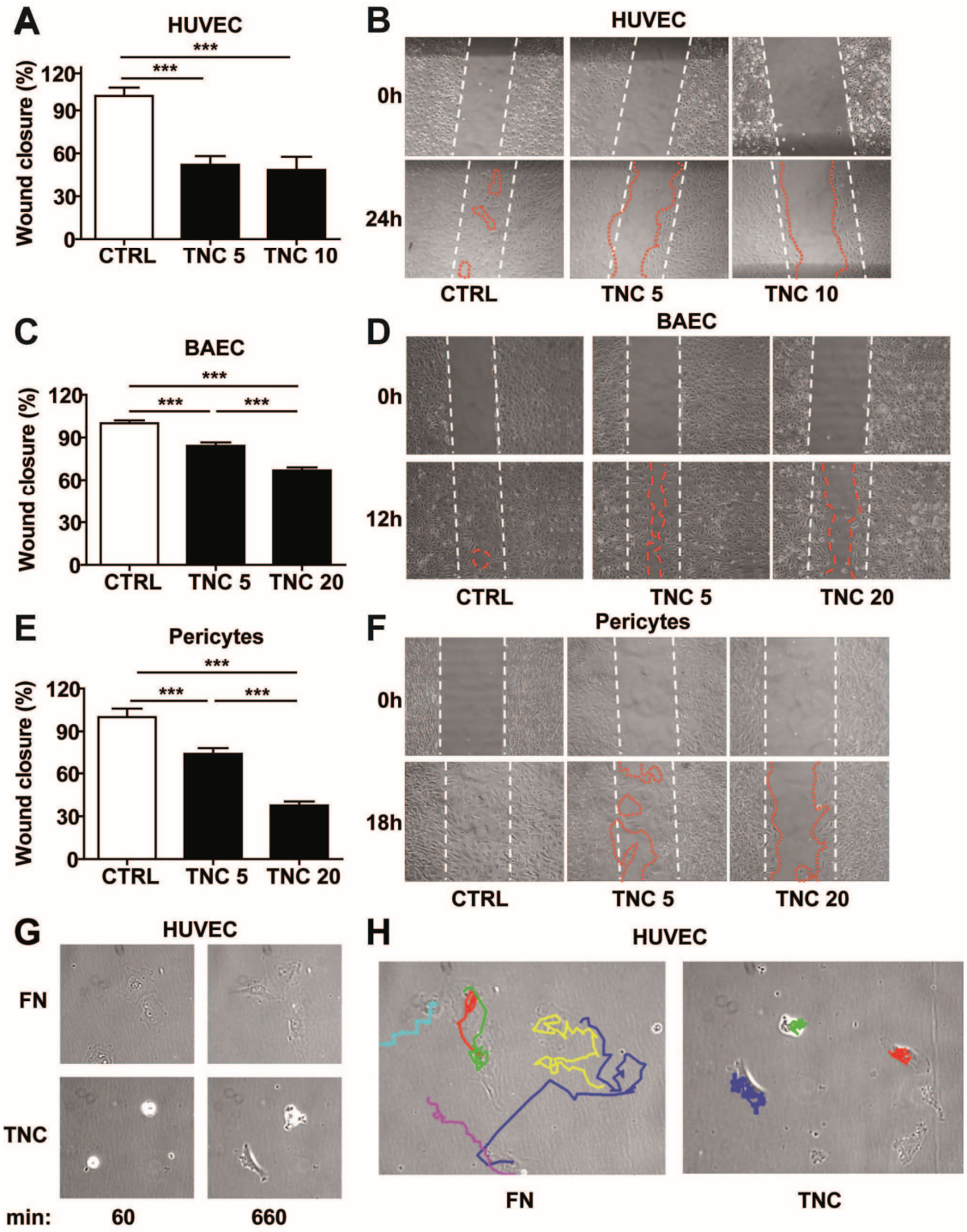

Figure 22. TNC disturbs EC migration in vitro

Scratch wound closure assay**.** (**A-F**), Scratch wound closure of HUVEC (24h) (**A**), BAEC (12h) (**C**) and HBVP (18h) (**E**) and their respective representatives phase contrast images of confluent monolayers of HUVEC (**B**), BAEC (**D**) and HBVP (**F**) was quantified upon addition of TNC (5, 10 and 20 µg/ml) or 0.01% Tween 20 (CTRL). Mean with SEM (n = 12 wells, 3 independent experiments with 4 replicates, ** $p < 0.01$, *** $p < 0.001$). (**G**, **H**), Representative phase contrast images (**G**) of HUVEC on a FN or TNC substratum (lime lapse acquisition) after 1 hour and 11 hours and manual cell tracking of six cells on FN and three cells on TNC over the 11 hour time period (**H**).

1.7. Impact of TNC on survival and proliferation of endothelial cells and pericytes

Until now we had shown that cell contact with TNC impairs cell adhesion and migration which could explain repression of tubulogenesis by TNC. We wanted to know whether impaired cell adhesion affected survival and/or proliferation of EC. We used MTS incorporation to determine cell multiplicity and compared cell numbers on TNC with that on FN and Col I substrata, respectively after 24h, 48h and 72h. Whereas HUVEC and BAEC expanded on FN and Col I over the 3 days time course, cell numbers only slightly increased on TNC in the same time frame suggesting an inhibitory effect of TNC on cell multiplicity (**Fig. 23A, B**). Importantly, this inhibitory effect was dose dependent (**Fig. 23C**, IC50 = 3.665 +/- 0.652 $\mu g/cm^2$). As another read out of survival we used the fluorescence ethidium bromide / acridine orange (EB/AO) uptake assay that allows the stratification into alive, apoptotic and necrotic cells through their peculiar morphology of the nucleus as apoptotic (fragmented nuclei) and dye uptake indicative for alive cells (green nuclei) and apoptotic cells (green with red points in the nuclei) or as dead cells (red nuclei) (Baskić et al., 2006; Ribble et al., 2005). Similarly, by using HUVEC and BAEC we showed that a 2D TNC substratum increased the number of apoptotic and necrotic/dead cells (**Fig. 23D, E**). In contrast to EC, despite of reduced cell adhesion on TNC, multiplicity of pericytes was unaffected by TNC and was similar to that seen on the FN and Col I substrata suggesting a cell type specific effect of TNC (**Fig. 23F**).

A lowered cell number by TNC could be explained by reduced survival and/or less proliferation. We investigated both possibilities by plating HUVEC on FN or TNC substrata. We found that TNC containing substrata reduced survival through an increase of EC apoptosis (**Fig. 23G**). Moreover, by measuring BrdU incorporation we assessed proliferation and observed a reduction on TNC by around 45% in comparison to FN and Col I, respectively (**Fig. 23H**).

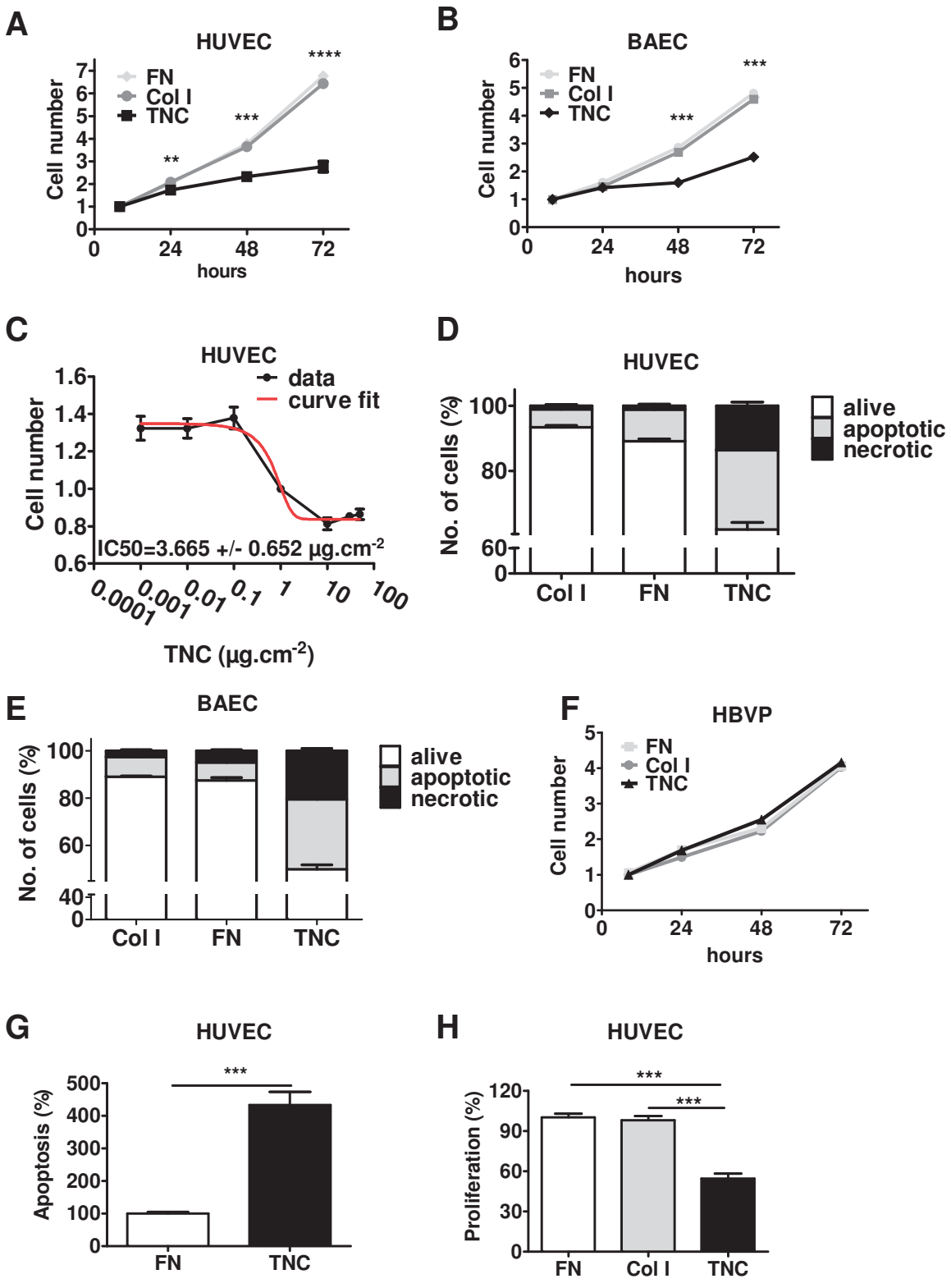

Figure 23. TNC reduces EC survival and proliferation when offered as 2D substratum

(A, B) MTS multiplicity assay for HUVEC (**A**) and BAEC (**B**) upon plating on the indicated ECM molecules (1 or 2 µg/cm^2 respectively) for up to 72h. Mean with SEM (n = 18 wells, 3 independent experiments with 6 replicates, **** $p < 0.0001$, TNC vs. FN or Col I). **(C)** Assessment of cell

numbers with an MTS assay in HUVEC that were grown for 24 hours on substrata with different amounts of TNC. The IC50 was extrapolated upon non-linear curve fit (red) as 3.665 +/- 0.652 µg/cm2. Mean with SEM (n = 9 wells, 3 experiments with 3 replicates). (**D**, **E**) HUVEC (**D**) and BAEC (**E**) viability was determined by an EB/AO uptake assay allowing stratification of between alive, apoptotic and necrotic cells on Col I, FN and TNC substrata. **(F)** MTS multiplicity assay for pericytes (HBVP) upon plating on the indicated ECM molecules (1 µg/cm^2) for up to 72h. Mean with SEM (n = 18 wells, 3 independent experiments with 6 replicates, no significant difference). (**G, H)** Assessment of apoptotic (number of cleaved caspase 3 positive cells on the whole population in percentage) (72h) (**G**) and proliferating HUVEC (BrdU uptake) (48h) (**I**) upon growth or on FN, Col I or TNC coated wells (**H, I**). (**G, H**) Four random fields were quantified. Mean with SEM (n = 12 wells, 3 independent experiments with 4 replicates, * p <0.05, *** p < 0.001, **** p < 0.0001) (**G).** Mean with SEM n = 18 wells (3 independent experiments with 6 replicates, *** p <0.001, **** p < 0.0001) (**H**).

To mimic the three dimensional (3D) matrix environment we used cell derived matrix (CDM) (**Fig. 24A**) with abundant and no TNC. CDM had been generated and deposited by mouse embryo fibroblasts (MEF) derived from TNC wt or TNC KO mice or CAF. Pictures taken after seven days of culture showed dense layers of fibroblasts for both MEF and CAF. The layer was treated with a detergent to remove the cells, thus leaving a decellularized CDM containing some cell debris that was removed by washing (**Fig. 24B**). We wanted to know whether the organization of ECM molecules was similar in the two CDM which we addressed by immunofluorescence staining. We observed that both CDM presented a fibrillar network of Col I, (POSTN), FN and thrombospondin-1 (TSP1) (**Fig. 24C-E**) and that CDM from TNC KO MEF indeed was devoid of TNC (**Fig. 24D**).

Next we tested whether growth of EC on these substrata had an impact on cell multiplicity. Upon growth on these CDM we observed that multiplicity of both EC types (HUVEC, BAEC) was very poor on CDM that contained TNC whereas multiplicity was high when the CDM lacked the TNC protein (**Fig. 25A, B**). A similar result was also obtained when CDM was generated by CAF with abundant (shCTRL) and lowered (shTNC) TNC levels. The number of BAEC was significantly lowered when cells had grown on the control TNC containing CDM (**Fig. 25C**).

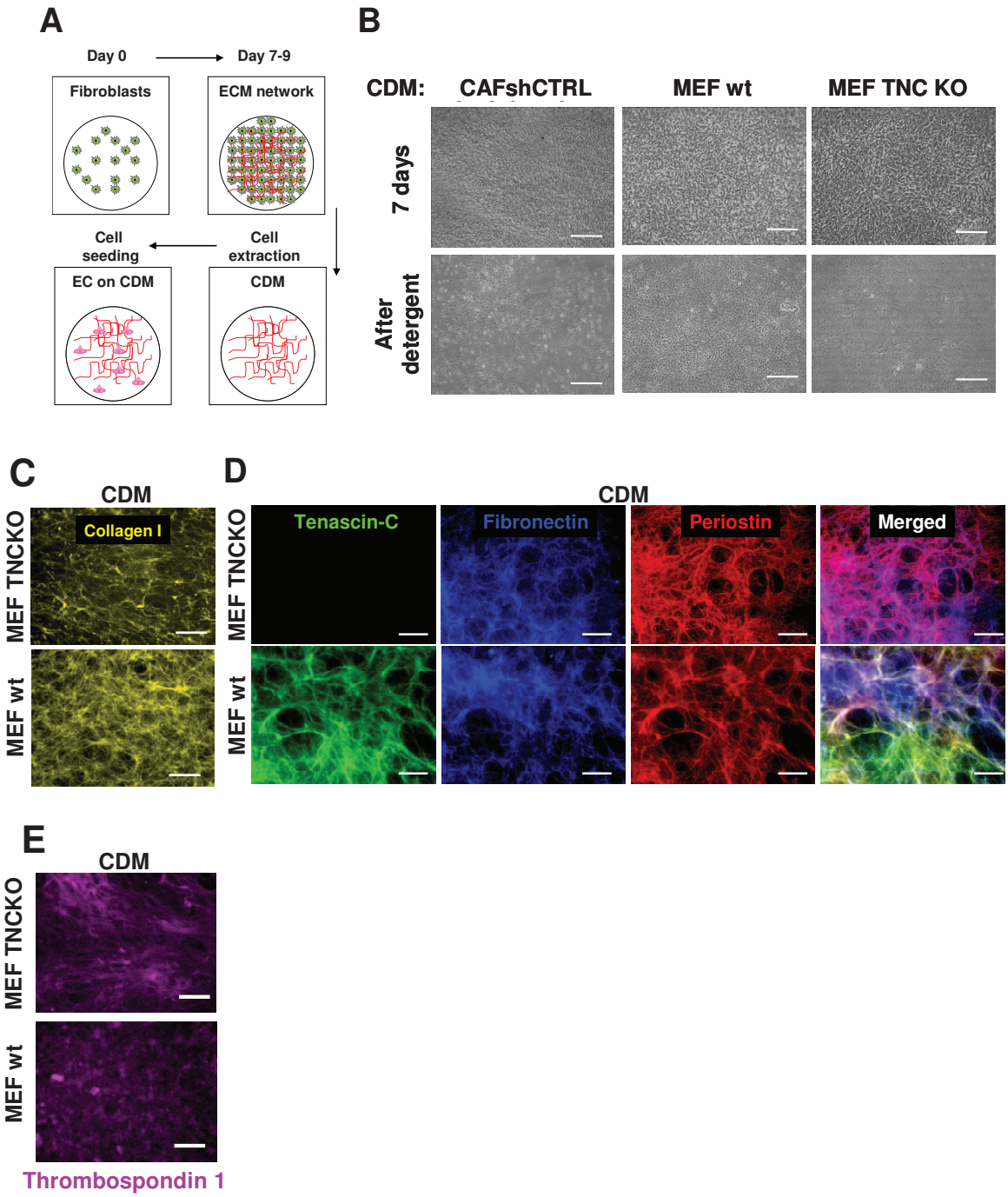

Figure 24. Establishment of CDM to address the role of TNC on survival of EC

(**A**) Schematic showing the protocol to obtain CDM. (**B**) Phase contrast acquisition of over-confluent layer of CAFshCTRL (Note that appearance of CAFshTNC1 and CAFshTNC2 are identical), MEF wt and MEF TNCKO CDM after 7 days and after decellularization by overnight treatment with detergent followed by several washes (scale bar, 50 µm). (**C**-**E**) Representative immunofluorescence images of CDM laid down by TNC KO or TNC wt MEF for Col I (**C**) and TNC, POSTN and FN (**D**) and thrombospondin-1 (**E**). Pictures displayed in (**D**) have been merged to demonstrate partial overlap of the ECM networks (scale bar, 40 µm). CDM was up to 15 µm of thick (extrapolated from z-stack image acquisition).

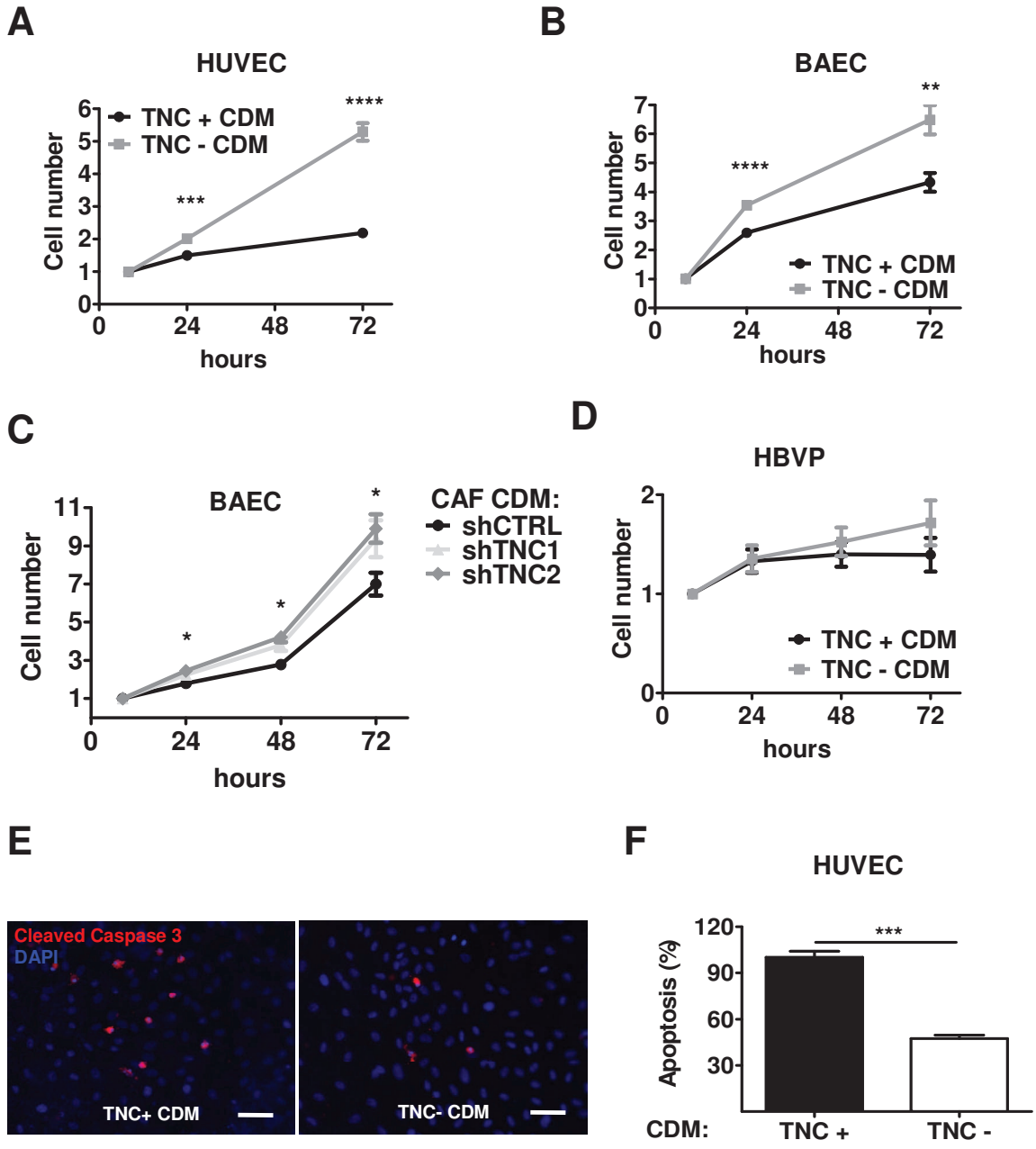

Figure 25. EC survival and multiplicity on 3D CDM

(A-C) MTS multiplicity assay for HUVEC (**A**) and BAEC (**B**) upon plating on the CDM derived from TNC KO (TNC -) or TNC wt MEF (TNC +) (**D-F**) for up to 72h. Mean with SEM, n = 29 (4 independent experiments with 4-6 replicates) for HUVEC and n = 9 (3 independent experiments with 3 replicates) for BAEC, ** p <0.01, *** p < 0.001, **** p < 0.0001). (**F**) Cell multiplicity assessed by a MTS assay of BAEC plated on CDM laid down by CAF shCTRL, shTNC1 and shTNC2. Mean with SEM (n = 20-24 wells, 4 independent experiments with at least 5 replicates, shCTRL vs. shTNC1, p < 0.05 and shCTRL vs. shTN2, * p < 0.05). (**D**) MTS multiplicity assay HBVP upon plating on the

CDM derived from TNC KO (TNC -) or TNC wt MEF (TNC +) for up to 72h. Mean with SEM, n = 24 (4 independent experiments with 6 replicates) no significant difference. (**E, F)** Assessment of HUVEC apoptotic (72h). Representative images of immunofluorescence staining for cleaved caspase 3 (Cl. caspase 3) in HUVEC upon growth on CDM containing (TNC +) or lacking TNC (TNC -) (scale bar, 20 µm) (**E**) and quantification of the number of apoptotic cells in the whole population in percentage (**F**). Four random fields were quantified. Mean with SEM (n = 12 wells, 3 independent experiments with 4 replicates, *** $p < 0.001$).

This result phenocopied the result of plating cells on a substratum of purified TNC. We concluded that CDM with abundant TNC does not only recapitulate features of 2D TNC substrata but also add the 3D aspect seen in vivo and therefore are a useful tool (Beacham et al., 2007; Goetz et al., 2011). In contrast to EC, pericyte multiplicity was not significantly different whether TNC was present or absent from the CDM (**Fig. 25D**) suggesting that TNC had no impact on the expansion of pericytes under the tested conditions and thus corroborated a cell specific effect.

Again we investigated possibilitiy that plating HUVEC on TNC 3D matrix might alos promote apoptosis and found that TNC containing CDM reduced survival through an increase of EC apoptosis (**Fig. 25E, F**).

Altogether these results strongly suggest that TNC impairs angiogenesis by direct contact with vascular cells (e.g. EC and pericytes). Nevertheless several reports suggested that TNC may also promote angiogenesis (Martina et al., 2010; Saupe et al., 2013; Tanaka et al., 2003). This suggests that TNC may also affect angiogenesis by other mechanisms.

1.8. Induction of an angio-modulatory secretome in GBM cells and CAF by TNC

In search for a mechanism that could explain the pro-angiogenic activity of TNC in cancer tissue we considered a paracrine mechanism that potentially involves tumor and stromal cells. First, we determined whether TNC had an impact on the secretome of GBM cells. We used GBM cells since GBM cells highly express TNC mostly around blood vessels (Herold-Mende et al., 2002; Leins et al., 2003; Martina et al., 2010) and high TNC expression correlates with worsened survival of GBM patients (reviewed in Orend et al., iConcept Press). Therefore, we

plated U87MG on MEF-derived CDM containing or lacking TNC, collected the conditioned medium (CM) after 48h, added the CM to HUVEC and determined survival, tubulogenesis and sprouting (**Fig. 26A**). Similar analysis was also done using knock down cells for TNC (**Fig. 26A**). We observed that CM of U87MG cells grown on CDM containing TNC ("educated" by TNC) promoted HUVEC survival (**Fig. 27A**). Also cell multiplicity was increased by 1.5-fold (48h) and 1.9-fold (72h) in comparison to CM derived from cells educated by a CDM lacking TNC (**Fig. 27B**). Similarly, TNC-educated CM enhanced BAEC numbers by 1.5-fold (48h) and 1.7-fold (72h), respectively (**Fig. 28A**).

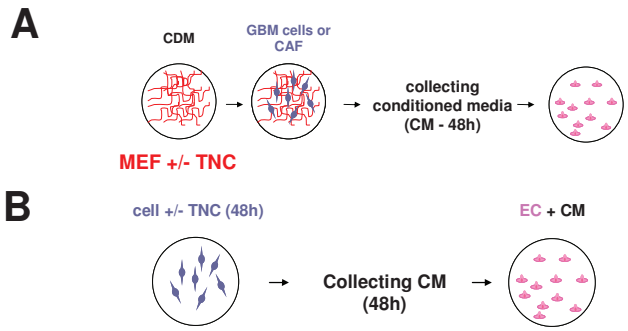

Figure 26. Preparation of TNC-educated conditioned medium

(**A**, **B**) Schematic representation of the protocol used to collect conditioned medium (CM) from GBM cells and CAF grown on MEF CDM (**A**) and U87MG control or knock down cells for TNC (**B**).

Next, we addressed whether a TNC-educated CM had an impact on tubulogenesis. We observed that CM from U87MG cells grown on CDM containing TNC enhanced matrigel tubulogenesis by 2.4-fold in comparison to control CM derived from tumor cells educated by a CDM lacking TNC (**Fig. 27C**). A similar TNC promoting effect on tubulogenesis was seen when CM from two other GBM cell lines (U118MG and U373MG) was added to HUVEC or when CM from U87MG cells was added to BAEC suggesting a general effect (**Fig. 28B**). To rule out that the observed effect potentially was due to a difference of cell numbers we did a cell multiplicity assay. We observed that the cell numbers were identical for all tested cell lines (U87MG, U118MG, U373MG) with CM from TNC-educated and non-educated cells (**Fig. 28A**).

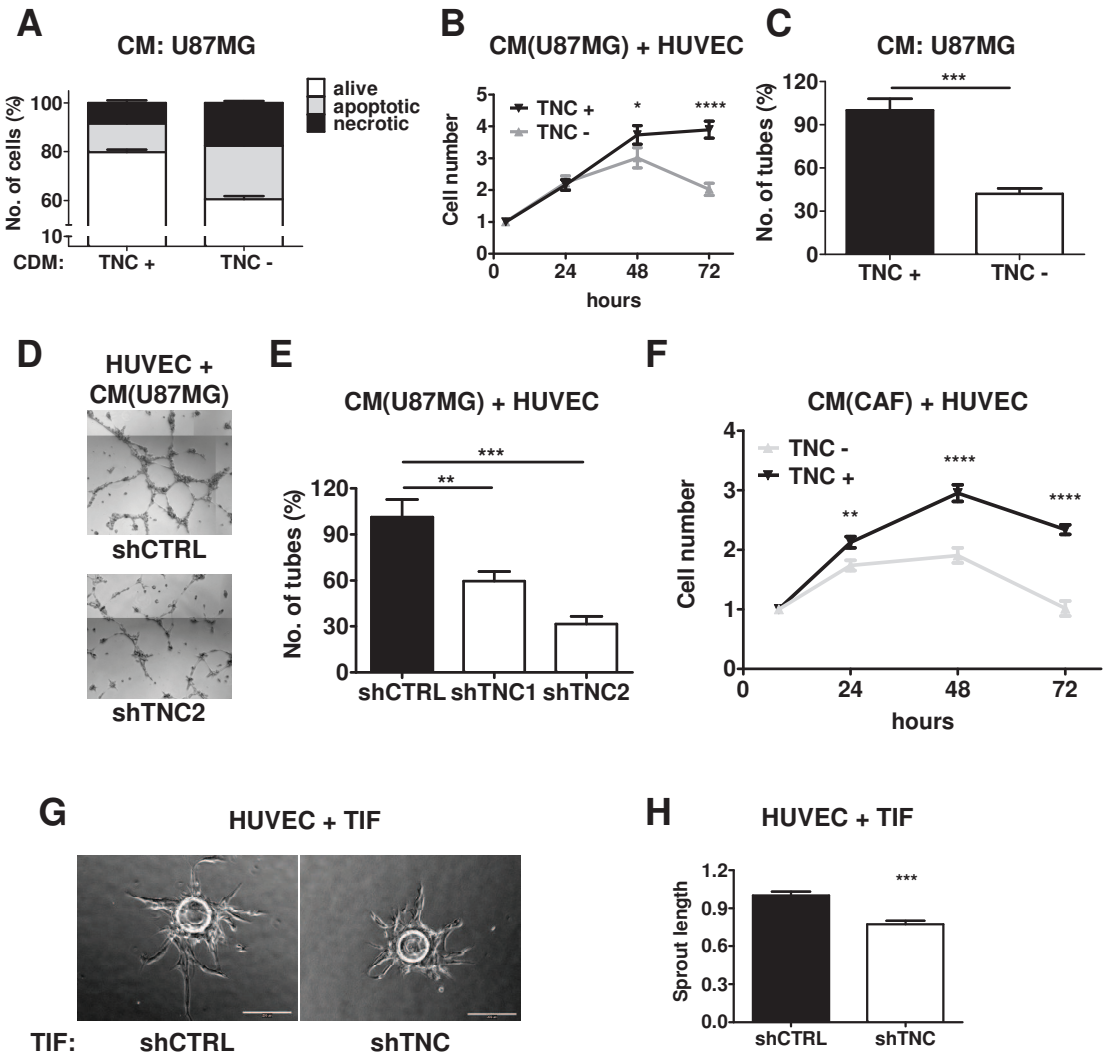

Figure 27. TNC-educated CM from GBM cells or transformed fibroblasts promotes angiogenesis in vitro

(A), Assessment of HUVEC viability by EB/AO staining upon addition of CM derived from U87MG cells that had been grown on CDM laid down by TNC KO (TNC -) and wt MEF (TNC +). Bars represent the percentage of viable, apoptotic and dead cells with SEM (n = 9 wells, 3 independent experiments, 3 replicates). (**B**) Assessment of HUVEC multiplicity (MTS assay) upon treatment with CM derived from TNC educated U87MG cells. Mean with SEM (n = 18 wells, 3 independent experiments, 6 replicates, * $p < 0.05$, **** $p < 0.0001$). (**C**) Number of tubes upon growth of HUVEC (7h) on matrigel and treatment with CM from TNC educated U87MG cells (grown on CDM from MEF expressing or lacking TNC). Mean with SEM (wt, n = 13 wells, TNC KO, n = 15 wells, 3 independent experiments with at least 4 replicates, *** $p < 0.001$). (**D, E**) Tube formation with CM of TNC educated U87MG cells. (**D**) Representative phase contrast images of HUVEC upon growth on matrigel for 7h with CM derived from U87MG shCTRL, shTNC1 and shTNC2 cells. (**E**) Quantification of tubes. Mean with SEM (n = 15 wells, 3 independent experiments with 5 wells, ** $p < 0.01$, *** $p < 0.001$). (**F**) Cell multiplicity (MTS assay) for HUVEC treated with CM derived from

TNC educated U87MG cells. Mean with SEM (n = 18 wells, 3 experiments with 6 replicates, ** $p < 0.01$, **** $p < 0.0001$). (**G**, **H**) Sprouting upon coculture with TIF. (**G**) Representative images of HUVEC sprouting from cytodex bead in co-culture with TIFshCTRL and TIFshTNC after 3 days of embedding into fibrin gels (scale bar, 200 µm). (**H**) Quantification of sprout length. Mean with SEM (TIF shCTRL, n = 47 beads, 3 independent experiments, 3 replicates, TIFshTNC, n = 46 beads, 3 independent experiments, 3 replicates, *** $p < 0.001$).

To further address secretion of pro-angiogenic factors by TNC, we determined whether CM from U87MG with lowered TNC levels (shRNA mediated KD) (**Fig. 28D**) also had an impact on tube-like formation. We observed that CM from cells with wt levels of TNC triggered 40-70% more tube-like in comparison to CM from cells with TNC KD levels (**Fig. 27D, E**). Again abundance of cells lacking TNC was not different to that from cells expressing TNC since multiplicity of U87MG cells was equal (**Fig. 28E**).

Next we wanted to know whether TNC potentially also induced a pro-angiogenic secretome in fibroblasts. Therefore, we prepared CM from CAF that were grown on CDM derived from wt and TNC KO MEF, respectively. First we observed again no variation of CAF cell numbers in dependence of TNC in the CDM (**Fig. 28F**). We measured HUVEC cell multiplicity and HUVEC matrigel tubulogenesis upon addition of this CM. Whereas no effect was seen on tubulogenesis (**Fig. 28G**), we noticed 1.2-fold (24h), 1.7-fold (48h) and 2.2-fold (72h) more HUVEC when the CM was derived from TNC-educated CAF in comparison to CM from CAF grown on TNC-negative CDM (**Fig. 27F**).

Finally, we used a co-culture assay in a fibrin gel where HUVEC and telomerase immortalized fibroblasts (TIF) were physically separated from TIF that served as source of TNC (**Fig. 28H**). In contrast to HUVEC that did not express TNC (**Fig. 19A-C**) TIF expressed TNC. Therefore we lowered TNC expression in TIF by shRNA (**Fig. 28I**). We observed that whereas the number of sprouts was not different, the sprout length was significantly reduced upon coculture with shTNC TIF (**Fig. 27G, H and Fig. 28 J**).

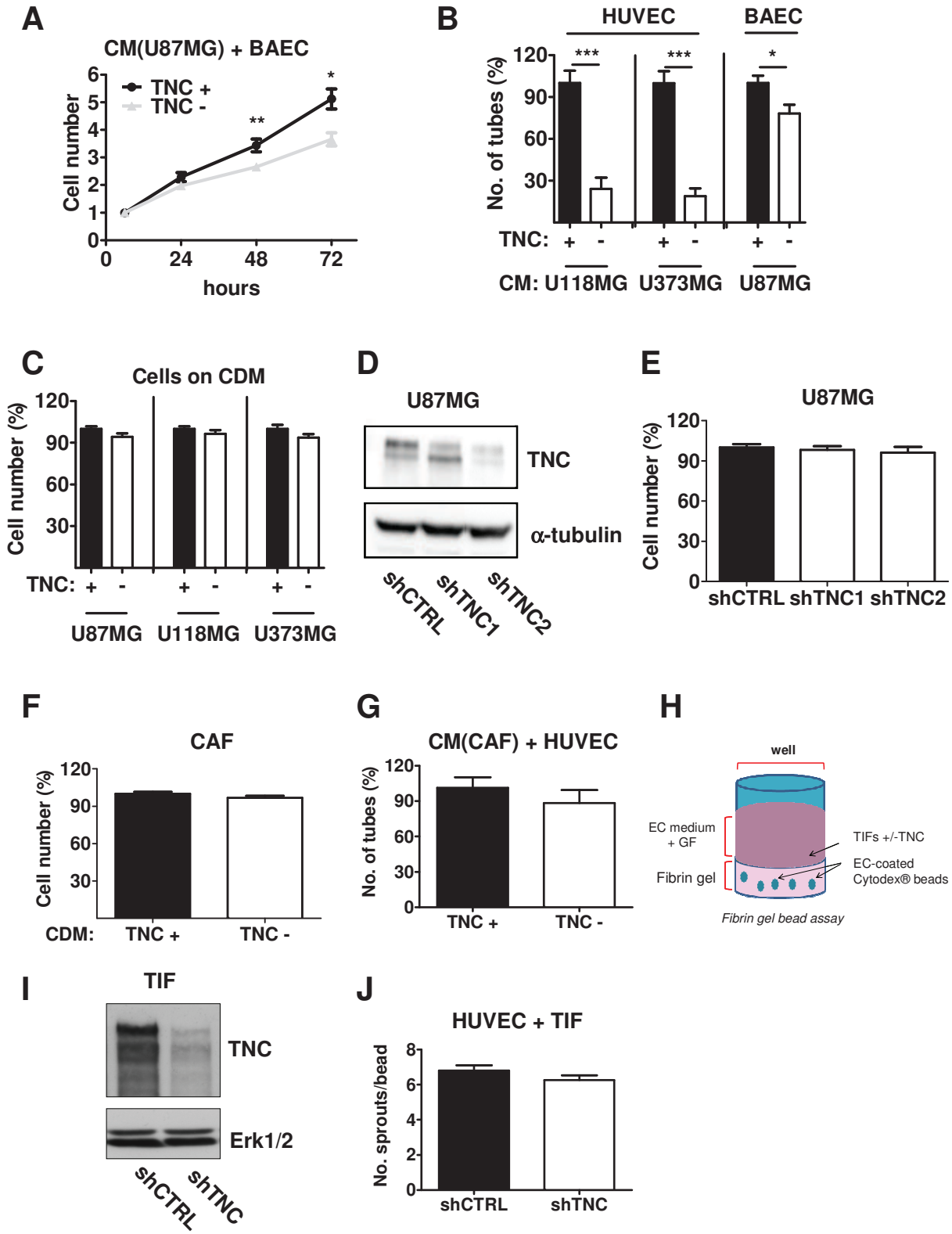

Figure 28. TNC-educated CM from GBM cells and from transformed fibroblasts promotes EC multiplicity, tubulogenesis and sprouting

(**A**) Cell numbers of BAEC assessed by an MTS assay upon growth on CDM lay down by MEF expressing (TNC +) or lacking TNC (TNC -). Mean with SEM (n = 18 wells, 3 experiments with 6

replicates, * $p < 0.05$, ** $p < 0.01$). (**B**) Number of tubes of HUVEC grown on matrigel (7h) upon treatment with CM from TNC-educated U118MG or U373MG that had been grown on CDM laid down by MEF expressing (TNC +) or lacking TNC (TNC -). Mean with SEM (n = 15 wells, 3 experiments with 5 replicates, * $p < 0.05$, **** $p < 0.001$). (**C**) Comparison of cell numbers of U87MG, U118MG and U373MG upon growth (24h) and treatment with TNC-educated CM (described in B). Mean with SEM (n = 18 wells, 3 experiments with 6 replicates, no statistical difference). (**D**) Expression of TNC in U87MG shCTRL and shTNC by immunoblotting with α-tubulin as control 48h after plating. (**E**) Assessment of HUVEC cell numbers by MTS assay (48h) upon addition of CM from U87MG shCTRL, shTNC1 and shTNC2 cells. Mean with SEM (n = 18 wells, 3 experiments, 6 replicates, no statistical difference). (**F, G**) Assessment of cell numbers (**F**) and number of tubes on matrigel (**G**) in HUVEC upon treatment with CM from CAF that had been grown on CDM of MEF expressing (TNC +) or lacking TNC (TNC -). (F) Mean with SEM (n = 12 wells, 3 experiments, 4 replicates, no statistical difference). (**G**) Mean with SEM (n = 15 wells, 3 experiments, 5 replicates, no statistical difference). (**H**) Schematic representation of the HUVEC sprouting assay in fibrin gel co-culture with TIF control or knock down for TNC. (**I**) Expression of TNC in 24h cultures of TIF shCTRL and TIF shTNC as determined by immunoblotting for TNC and ERK as control. (**J**) Quantification of the number of HUVEC sprouts per bead. Mean with SEM (TIFshCTRL, n = 47 beads, TIF shTNC, n = 46 beads, 3 independent experiments, no statistical difference).

In summary, we had shown that TNC triggered the secretion of pro-angiogenic factors in fibroblasts (CAF, TIF) and tumor cells that enhanced EC survival, growth and tubulogenesis. The composition of the angiogenesis promoting CM was further investigated in collaboration with O. Schilling (Freiburg University) by mass spectrometry and two candidates were functionally validated (see below, **Aim 2**).

AIM 2. Identify molecular mechanisms downstream of TNC relevant for TNC-associated tumor angiogenesis

We identified two independent roles of TNC on EC behavior. Direct contact negatively affects EC survival, tubulogenesis and sprouting but TNC also activates paracrine mechanisms that promote EC survival and tubulogenesis indirectly. Nevertheless the molecular mechanisms were unknown.

2.1. TNC represses YAP transcriptional activity through inhibition of actin polymerization

We showed that TNC impairs angiogenesis when EC directly interacted with TNC. However the underlying molecular mechanism is unknown. Importantly TNC was shown to impair cell adhesion (Chiquet-Ehrismann et al., 1988; Orend et al., 2014) and actin cytoskeleton dependent signaling pathways in tumor cells and fibroblasts (Huang et al., 2001a; Midwood and Schwarzbauer, 2002; Orend et al., 2003; Saupe et al., 2013). We showed that TNC delays EC adhesion (**Fig. 21F, G, I**) and impairs stress fiber formation (Saupe et al., 2013). Thus we wanted to understand whether and how TNC impacts on actin polymerization-dependent gene expression and cell survival. Therefore, we followed the at 2, 5 and 24 hours actin stress fiber formation in HUVEC upon adhesion on FN, Col I and TNC substrata, or upon plating of cells on CDM from TNC wt and TNC KO MEF at 24h. Upon staining with FITC-phalloidin we observed that whereas HUVEC formed actin stress fibers on FN and Col I, they poorly did on TNC (**Fig. 29A and Fig. 30A**). Also on CDM containing TNC few actin stress fibers were seen which was in contrast to CDM lacking TNC where actin stress fibers have formed (**Fig. 30B**). By fractionation followed by immunoblotting we quantified the relative abundance of filamentous/polymerized (F) versus globular/non-polymerized (G) actin (Posern, 2002). We found that after 5h F-actin formation is reduced by 8.5-fold on TNC in comparison to Col I and FN substrata, respectively (**Fig. 29B, C**).

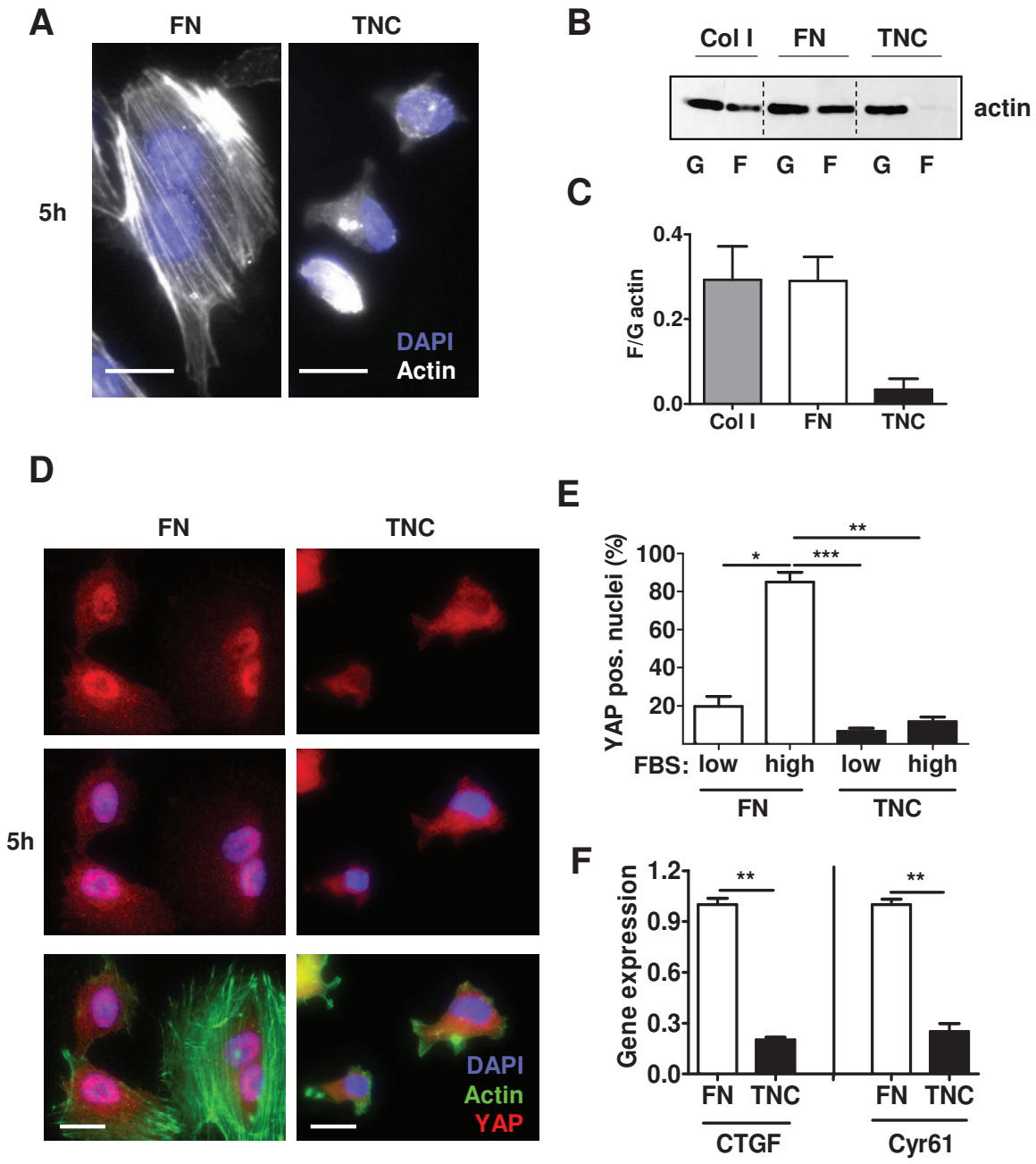

Figure 29. TNC represses actin polymerization and YAP activation in EC

(**A**) Representative images of actin polymerization (phalloidin, white) and nuclei (DAPI, blue) of HUVEC upon growth on FN or TNC for 5 hours (scale bar, 5 µm). (**B, C**) Analysis of G and F actin in HUVEC by immunoblotting upon plating on the indicated substrata for 5 hours. (**C**) Quantification of the immunoblotting signal represented as ratio of F/G actin. (n = 3 wells). (**D**) Representative images of YAP (red), polymerized actin (phalloidin, green) and nuclei (DAPI, blue) of HUVEC upon growth on FN or TNC for 5h (scale bar, 5 µm). (**E**) Quantification of YAP positive nuclei normalized to DAPI positive nuclei. 30-40 cells were counted in the triplicates (3 experiments) of 4-6 randomly chosen fields per condition. Mean with SEM as a percentage of nuclei positive for YAP (n = 9 wells, 3 independent experiments with 3 replicates, * $p < 0.05$, ** $p < 0.01$, *** $p < 0.001$). (**F**) RT-qPCR

analysis of YAP target genes CTGF and Cyr61 in HUVEC upon growth on FN or TNC for 24 hours (n = 5, ** p < 0.01).

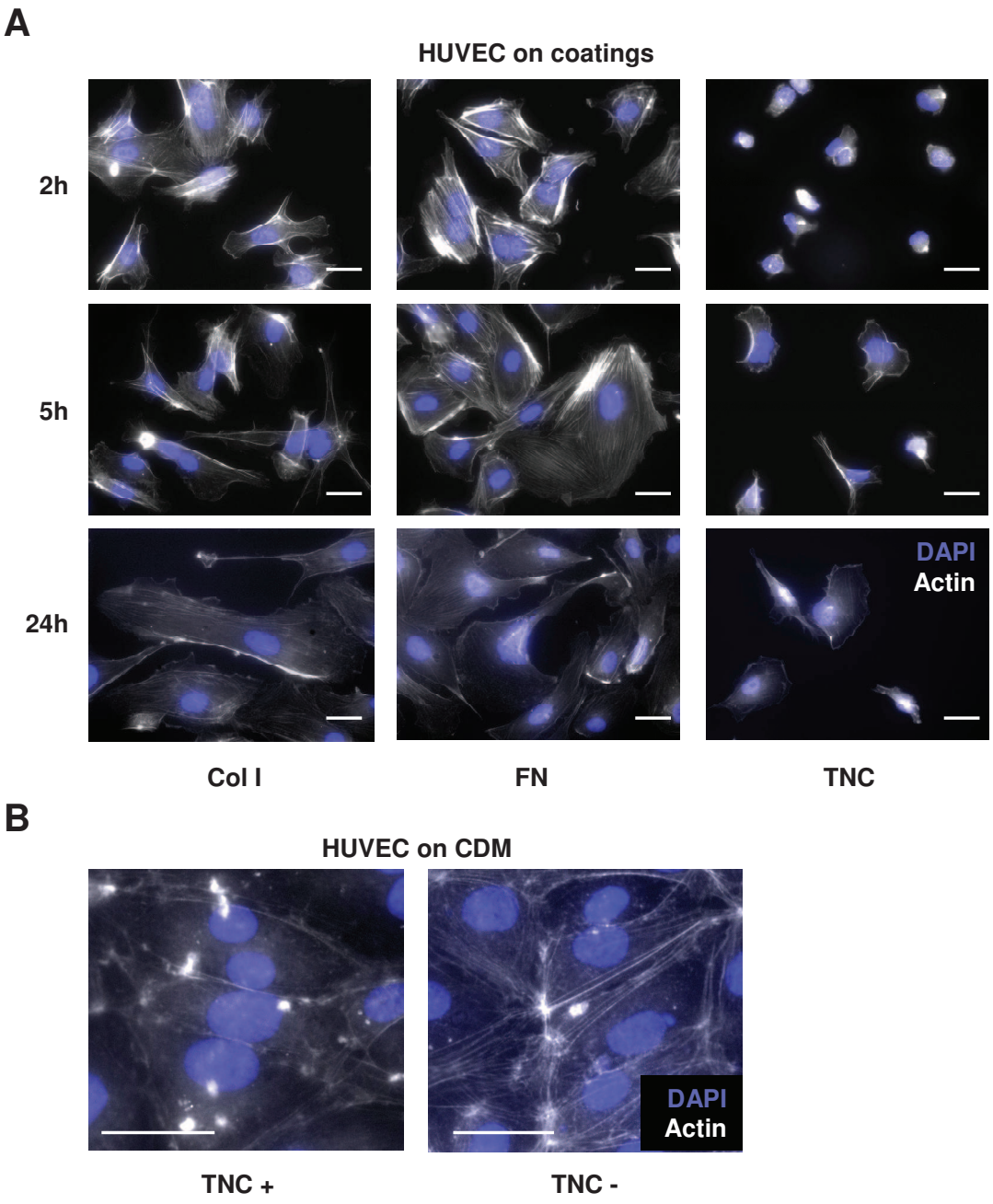

Figure 30. TNC represses cell spreading and actin stress fiber formation

(**A, B**) Representative images of HUVEC grown for 2h, 5h and 24h on the indicated 2D substrata (**A**) or upon growth (24h) on CDM lay down by MEF expressing or lacking TNC (**B**) upon staining for polymerized actin with phalloidin. Note that TNC inhibited actin stress fiber formation (scale bar, 5 µm).

The transcriptional integrator of extracellular stimuli, YAP, is one of the molecules that senses the status of actin cytoskeleton (Halder et al., 2012). Upon actin polymerization YAP is translocated into the nucleus where it binds to the TEAD transcription factor and induces gene expression (Calvo et al., 2013b; Halder et al., 2012). By immunofluorescence analysis we determined localization of YAP and observed that whereas 85% of HUVEC plated on FN had nuclear YAP this number was reduced to 12 % in cells plated on TNC which was in the range of FN in low serum representing a condition that prevents nuclear localization of YAP (Calvo et al., 2013b) (**Fig. 29D, E**).

Connective-tissue growth factor, CTGF (CCN2) and Cysteine rich protein 61, Cyr61 (CCN1), two pro-angiogenic molecules (Brigstock, 2002; Maity et al., 2014), have been described as YAP target genes (Calvo et al., 2013b; Xie et al., 2013). By RT-qPCR we determined their expression and observed that in HUVEC on the TNC substratum expression of CTGF and Cyr61 was downregulated by 80% and 75%, respectively in comparison to cells grown on FN (**Fig. 29F**). These results suggested that adhesion to a TNC substratum prevents actin polymerization, nuclear localization of YAP and expression of pro-angiogenic factors, most likely triggering apoptosis of endothelial cells.

Altogether we demonstrated that interaction of endothelial cells or pericytes with TNC interferes with multiple hallmarks of angiogenesis such as endothelial adhesion, survival, migration, tubulogenesis, sprouting and endothelial monolayer integrity. Lowered cell adhesion had a profound effect on YAP-dependent gene expression that was largely downregulated by TNC in EC leading to repression of pro-angiogenic factors.

2.2. Proteomic analysis of the angio-modulatory secretome induced by TNC and functional validation of candidates LCN1 and SDF1

2.2.1. Characterization of the TNC-regulated secretome

During this work, we also identified that TNC promotes a pro-angiogenic secretome by educating GBM cells and CAF. To determine the molecular identity of the pro-angiogenic secretome, we collected CM from U87MG cells that had been grown on CDM derived from

TNC KO and wt MEF, respectively. We analyzed this CM by quantitative shotgun proteomics, employing chemical stable isotope tagging as described previously (Koczorowska et al., in preparation; Shahinian et al., 2014). We identified a total of 1955 proteins. The ratio "proteins from U87MG cells educated by a CDM from MEF wt versus proteins from U87MG educated by a CDM from MEF TNC KO" was log-transformed and followed a near normal distribution with most proteins displaying none or very little quantitative alterations. To distinguish proteins with altered abundance, we chose a cutoff of 0.58 (-0.58 for decreased abundance), representing an increase or decrease in abundance by more than 50 %. According to this cutoff, 685 proteins were differentially abundant when comparing TNC-educated and non-educated CM (**Fig. 31A**). We further focused on proteins annotated as secreted or as localized at the cell surface. These criteria yielded more than 350 proteins with affected abundance in U87MG cells educated by TNC containing CDM (**Fig. 31B, Table 4**). Such first-line criteria have been successfully applied previously (Tholen et al., 2013).

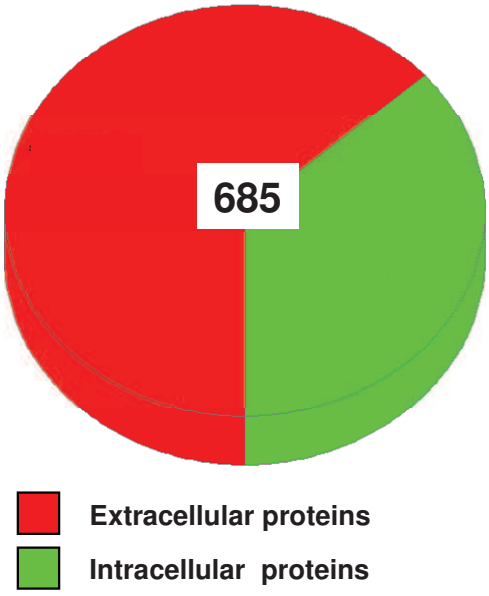

Figure 31. Proteomic analysis of the U87MG-derived CM

(**A**) Pie chart representing all proteins deregulated in U87MG educated by CDM laid down by MEF expressing or lacking TNC.

(**B**) Heat-map of proteomic profiling

2.2.2. TNC triggers an angio-modulatory secretome

A clear pro- or anti-angiogenic fingerprint of secreted proteins with increased or decreased abundance was not noted. However, for many secreted proteins, contrasting findings are reported with regard to their involvement in angiogenesis, leading to blurred functional profiles. Given the clear pro-angiogenic functionality of the TNC-educated CM, we specifically searched our proteomic data for proteins with increased abundance in TNC-educated CM and for which there is a clear pro-angiogenic functional profile. Several proteins are of note, including Cyr61 and CTGF (Brigstock, 2002; Leu et al., 2002; Maity et al., 2014), which are both members of the CCN family of growth factors, pleiotrophin (Papadimitriou et al., 2009; Perez-Pinera et al., 2008), lipocalin 7 (LCN7, synonym is tubulointerstitial nephritis antigen-like TINAGL1) (Brown et al., 2010; Li et al., 2007) and Wnt family members, Wnt5a, Wnt5b and Wnt7b (Masckauchán and Kitajewski, 2006; Yeo et al., 2014). An upregulation of pro-angiogenic Wnt ligands by TNC and downregulation of the Wnt inhibitor DKK1 by TNC (Saupe et al., 2013) supports the possibility that TNC might also promote angiogenesis through this pathway. We also noted an increased abundance of CXCL12/SDF1 (Stromal cell-derived factor-1) (Ho et al., 2010; Kryczek et al., 2005; Orimo et al., 2005), a chemokine with an important link to angiogenesis. We also searched for proteins with clear anti-angiogenic functionality that present decreased abundance in the TNC-educated CM. These included angiotensinogen (Vincent et al., 2009), tissue factor pathway inhibitor 2 (Sierko et al., 2007), CXCL14 (Shellenberger et al., 2004) and several members of the insulin growth factor binding protein family (IGFBP3, 5, 6 and 7) (Chen et al., 2011; Kim et al., 2011; Rho et al., 2008; Zhang et al., 2012) and thrombospondin-1 (TSP1) (Lawler and Lawler, 2012) (**Fig. 31B, Table 4**).

Table 4. Expression of selected TNC-regulated angio-modulatory factors

	Molecule	Fc (Log2)	Function in angiogenesis	Reference
Up	LCN7 (TINAGL1)	5.158	promote angiogenesis in vivo, ex vivo and in vitro	(Brown et al., 2010)
	TG2	3.308	promote angiogenesis through VEGF signaling and ECM remodeling	(Haroon et al., 1999)
	Pleiotrophin	2	stimulate normal and pathological angiogenesis	(Perez-Pinera et al., 2008)
	Wnt 7b	1.434	promote the angiogenic switch	(Yeo et al., 2014)

	CXCL12 (SDF1)	1.336	promote angiogenesis in vitro and tumor angiogenesis	(Orimo et al., 2005)
	Cyr61	1.279	promote angiogenesis in vitro and tumor angiogenesis	(Maity et al., 2014)
	Semaphorin-3A	1.111	modulate tumor angiogenesis	(Casazza et al., 2011; Maione et al., 2009)
	Wnt 5a/b	0.548 / 0.798	induce tumor angiogenesis	(Masckauchán et al., 2006)
	CTGF	0.644	promote angiogenesis in vitro and tumor angiogenesis	(Brigstock, 2002)
Down	LCN1	na	no described role	(Dartt, 2011)
	Angiotensinogen	3.737	inhibit tumor angiogenesis and growth	(Vincent et al., 2009)
	tPA	2.077	decrease VEGFA expression and angiogenesis	(Shim et al., 2005)
	Vitamin D-binding protein	1.932	impair angiogenesis in vitro and in vivo	(Kisker et al., 2003)
	Semaphorin-5A	1.932	promote tumor vessel density and metastasis formation	(Sadanandam et al., 2012)
	Neprilysin	1.515	inhibit angiogenesis via proteolysis of FGF2	(Goodman et al., 2006)
	IGFBP5	1.37	act as tumor suppressor by inhibiting angiogenesis	(Rho et al., 2008)
	CXCL14	1.235	inhibit angiogenesis	(Shellenberger et al., 2004)
	Gremlin-1	1.235	act as agonist of VEGFR2	(Mitola et al., 2010)
	IGFBP6	1.114	reduce angiogenesis in vitro, in zebrafish and in tumors	(Zhang et al., 2012)
	IGFBP3	0.966	repress tumor angiogenesis and progression	(Kim et al., 2011)
	IGFBP7	0.737	inhibit tumor angiogenesis	(Chen et al., 2011)
	TSP1	0.678	inhibits angiogenesis	(Lawler and Lawler, 2012)

Candidate list of angio-modulatory molecules identified by LC-MS/MS that were differentially abundant in CM of U87MG cells that had been grown on CDM laid down by MEF TNC KO or TNC wt. Expression in presence of TNC is compared to its absence. Fc, fold change, na, not applicable.
Abbreviations: Cysteine-rich angiogenic protein 61 (Cyr61), Connective tissue growth factor (CTGF), Chemokine (C-X-C motif) ligand 14 (CXCL14), Chemokine (C-X-C motif) ligand 12 (CXCL12) or Stromal cell-derived factor 1 (SDF1), Insulin-like growth factor-binding protein (IGFBP), Tubulointerstitial nephritis antigen-like 1 (TINAGL1)/Lipocalin-7 (LCN7), Thrombospondin-1 (TSP1), Tissue plasminogen activator (tPA), Transglutaminase-2 (TG2).

2.2.3. TNC differentially regulates two members of the lipocalin family and promotes SDF1 expression

Upon analysis of the CM by one-dimensional SDS-PAGE, we noticed a protein band at approximately 18 kDa, which was missing in TNC-educated CM and was only present in the CM of U87MG cells that were educated by a CDM lacking TNC (**Fig. 32A**). Mass spectrometric analysis of this gel band highlighted the presence of lipocalin-1 (LCN1) (**Table 5**). At the opposite we identified LCN7 as the highest upregulated protein by TNC in our profiling (**Fig. 31B**) and by RT-qPCR we confirmed transcriptional downregulation of LCN1 as well as upregulation of LCN7 by the TNC education of U87MG cells (**Fig. 32C**). Opposing regulation of related proteins has been previously observed in other systems; for example, increased kallikrein activity in ovarian cancer cells yields augmented levels of semaphorin-3A and reduced levels of semaphorin-6C (Shahinian et al., 2014). Since LCN7 is a described angiogenesis promoting factor (Brown et al., 2010) we examined how LCN1 affects angiogenesis. We addressed this by a matrigel tubulogenesis assay. We observed that addition of purified recombinant human LCN1 downregulated tube formation in a dose dependent manner suggesting an opposite role of LCN1 to that of LCN7 on angiogenesis (**Fig. 32D**). Thus through downregulation of LCN1 TNC may relieve its anti-angiogenic activity and promote angiogenesis. Despite binding to its cell surface receptor (Dartt, 2011) LCN1 has been described to elicit its functions through binding to not well known factors of protein or lipid origin (Dartt, 2011). By heating the CM we aimed to discriminate between these two possibilities and found that boiling completely blocked the pro-angiogenic activity of the TNC-educated CM on tube formation suggesting a proteinacious nature of responsible factors (**Fig. 32D**). Future studies need to determine through which mechanism LCN1 may affect angiogenesis.

Table 5. Identification of protein expression of the gel band, related to Fig. 32A

Name	MW (Da)	gene name	GO compartment	Uniprot localization
Proline-rich protein 4	15097	PRR4	extracellular space	Secreted
Lipocalin-1	19250	LCN1	extracellular region; extracellular space; extracellular vesicular exosome	Secreted

Candidate list of secreted (Uniprot localization) protein identified by LC-MS/MS that were identified from the gel band (15-20 kDa) in CM of U87MG cells that had been grown on CDM laid down by MEF TNC KO or TNC wt. Note that no secreted molecules have been detected in CM from U87MG educated by TNC.

SDF1 is an important mediator of tumor progression and angiogenesis (Ho et al., 2010; Kryczek et al., 2005; Orimo et al., 2005). We identified increased levels of SDF1 in TNC-educated CM (**Fig. 31B, Table 4**), which was corroborated by ELISA (**Fig. 32F**). We further addressed whether the impact of TNC-education on angiogenesis is mediated by SDF1/CXCR4 signaling. We determined tube formation upon addition of CM from U87MG cells (that had been grown on TNC containing or lacking CDM) in the presence or absence of the CXCR4 inhibitor AMD3100. We observed that the inhibitor repressed tube formation in a dose dependent manner. This effect was not seen upon addition of CM from U87MG cells that were grown on CDM lacking TNC where both numbers were very low (**Fig. 32F**). Thus SDF1 is one factor of the TNC-educated secretome that is important to convey the angiogenesis-promoting activity of TNC.

VEGFA, one of the major pro-angiogenic molecule (Adams and Alitalo, 2007a; Carmeliet, 2003; Carmeliet and Jain, 2011b; Roskoski, 2007) detected in the 1955 identified proteins of the whole proteomic analysis, is not modulated by TNC in our study which was confirmed by ELISA (**Fig. 33**).

Altogether this study had shown that TNC modulates the proteome composition and angiogenic properties of the tumor cell secretome. Amongst some 150 secreted angio-modulatory molecules that are regulated by TNC we identified LCN1 is a novel anti-angiogenic factor that is downregulated by TNC. On the contrary the pro-angiogenic factor SDF1 is upregulated by TNC and largely conveys the TNC pro-angiogenic activity. These combined activities of TNC could explain the TNC pro-angiogenic function in tumors. In contrast to this paracrine effect, a direct interaction of TNC with cells triggers EC death and represses migration of pericytes which provides insight into angiogenesis counteracting activities of TNC. We had described YAP as a novel downstream target of TNC whose impaired function is linked to the anti-adhesive activity of TNC resulting in repression of autocrine pro-angiogenic signaling in EC.

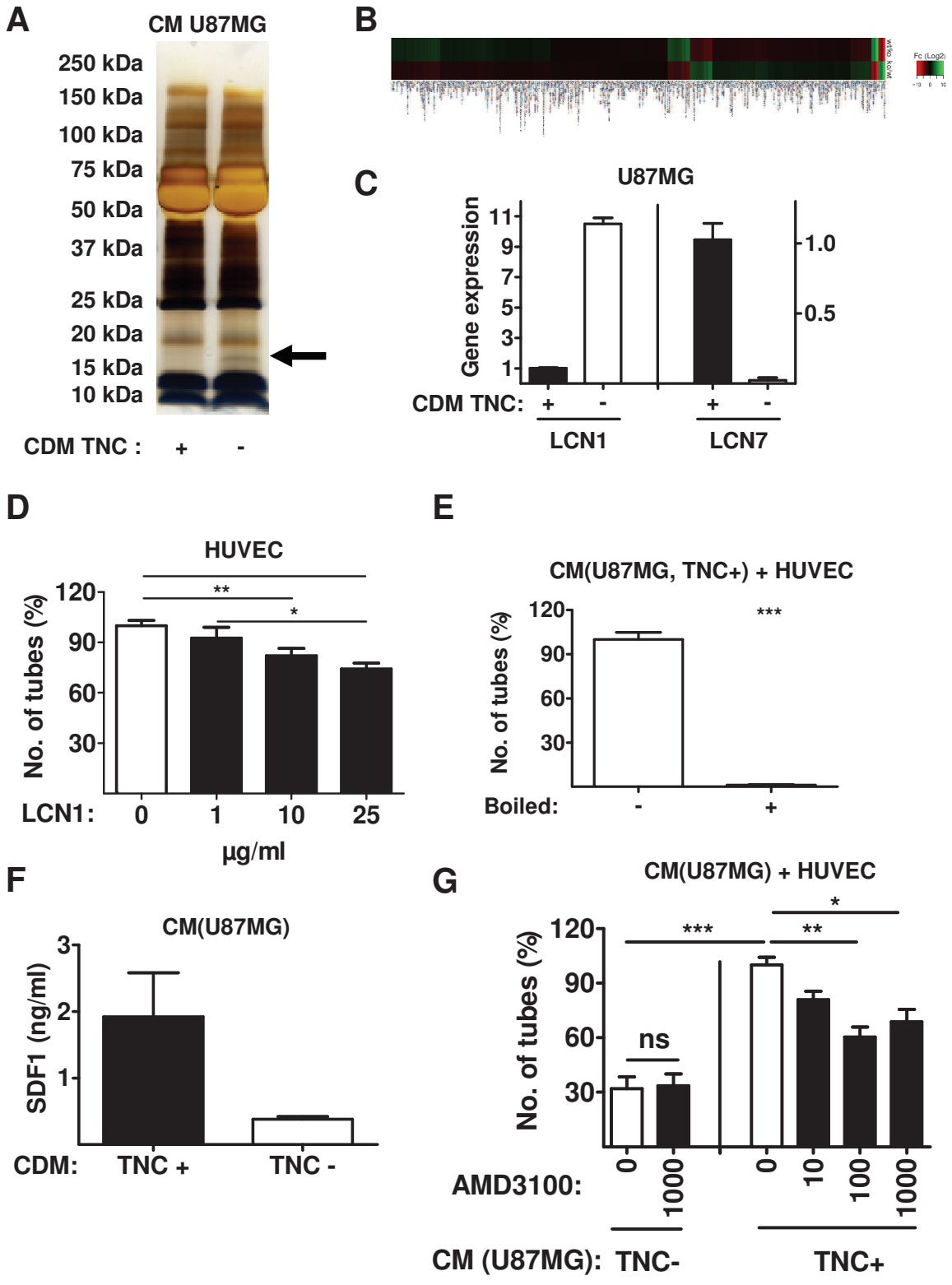

Figure 32. TNC regulates LCN1, LCN7 and SDF1 expression in U87MG

(**A**) Representative image of a silver stained polyacrylamide gel. CM from U87MG grown on CDM lay down by TNC KO or wt MEF was separated by PAGE before staining. The experiment was repeated four times with four independently prepared batches of CM. Arrow points at the LCN1 containing band around 18 kDa. (**B**) Heat map representing selected secreted molecules from U87MG-

educated cells involved regulated by TNC. Color coding red and green showed respectively upregulated and downregulated proteins (Log_2 values). Magnification in Fig. 31B (**C**) Validation of differential expression of LCN1 (lipocalin-1) and LCN7 (lipocalin-7) in TNC educated CM of U87MG cells that had been grown on CDM laid down by MEF expressing or lacking TNC. (**D**) Number of tubes upon growth of HUVEC (7h) on matrigel together with recombinant LCN1. Normalization towards CTRL (no LCN1). Mean with SEM (n = 15-20 wells, 3 independent experiments with at least 5 replicates, * $p < 0.05$, ** $p < 0.01$). (**E**) Number of tubes upon growth of HUVEC (7h) on matrigel together with boiled CM of TNC educated U87MG cells. Mean with SEM (n = 15 wells, 3 experiments with 5 replicates, **** $p < 0.0001$). (**F**) Quantification (ELISA) of the human SDF1 (CXCL12) in TNC educated CM from U87MG cultivated for 48h on CDM of MEF expressing or lacking TNC. Mean with SEM (n = 2-5). (**G**) Assessment of tubes (7h) upon growth of HUVEC on matrigel together with TNC-educated CM derived from U87MG cells and AMD3100 (10 - 1000 ng/ml). Mean with SEM (n = 15 wells, 3 independent experiments with 5 replicates, * $p < 0.05$, ** $p < 0.01$, *** $p < 0.001$).

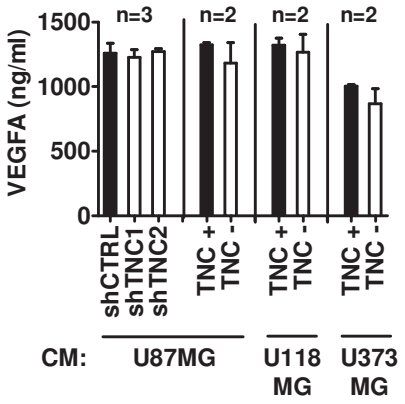

Figure 33. TNC does not regulate VEGFA expression in U87MG cells

Quantification of the human VEGFA concentration in CM from U87MG grown for 48h on CDM lay down by MEF expressing or lacking TNC. Mean with SEM (n = 2-3 independent batches of CM).

Aim 3. - Contribution to the description of the roles of TNC in tumor angiogenesis by using an in vivo mouse model of cancer.

My experiments had contributed to two publications where we had shown that TNC promotes the angiogenic switch and enhances tumor angiogenesis in a stochastic murine tumor model (Langlois et al., 2014; Saupe et al., 2013). We used the murine Rip1-Tag2 (RT2) model of pancreatic neuroendocrine tumorigenesis (PNET) which allows to dissect molecular and cellular mechanisms of tumor progression and angiogenesis (Hanahan, 1985). In this multistep model of tumorigenesis, pancreatic β-cells of the Langerhans islets ectopically express the oncogene SV40 T antigen (Tag) under the control of the rat insulin promoter (Rip). SV40 T antigen expression drives the sequential transformation of a fraction of normal islets into hyperplastic, angiogenic and macroscopic tumor islets. The RT2 model has several advantages compared to mouse xenograft models. Most importantly, RT2 mice are immune-competent which allows to study tumorigenesis in a context of an intact immune system. Moreover, tumorigenesis occurs spontaneously in multiple consecutive steps as it happens in human cancer and occurs over a time frame of up to 12 - 16 weeks. The RT2 model had been heavily used to study the angiogenic switch that occurs between 5 - 10 weeks of age in this model (Hanahan and Folkman, 1996). Depending on the genetic background RT2 mice can form macrometastasis (Sennino et al., 2012), yet in the C57Bl6 background that we had used only micrometastasis formation was observed because mice die due to hypoglycemia (even upon glucose addition in the drinking water).

3.1. TNC is an important molecule driving the angiogenic switch

We had used the RT2 model to address whether TNC plays a role in the angiogenic switch. By using RNA profiling we had addressed the gene expression profile at the angiogenic switch. Therefore, pancreatic islets of 8 week old mice had been sampled and were classified into non angiogenic white and angiogenic red islets. This profiling revealed the differential expression of 298 genes. TNC has been identified as one of the most highly up-regulated ECM molecules during the angiogenic switch (**Fig. 34A**). Therefore, by tissue staining I had determined when TNC is expressed and found that TNC was absent from non-angiogenic islets but was expressed in angiogenic islets (**Fig. 34B**).

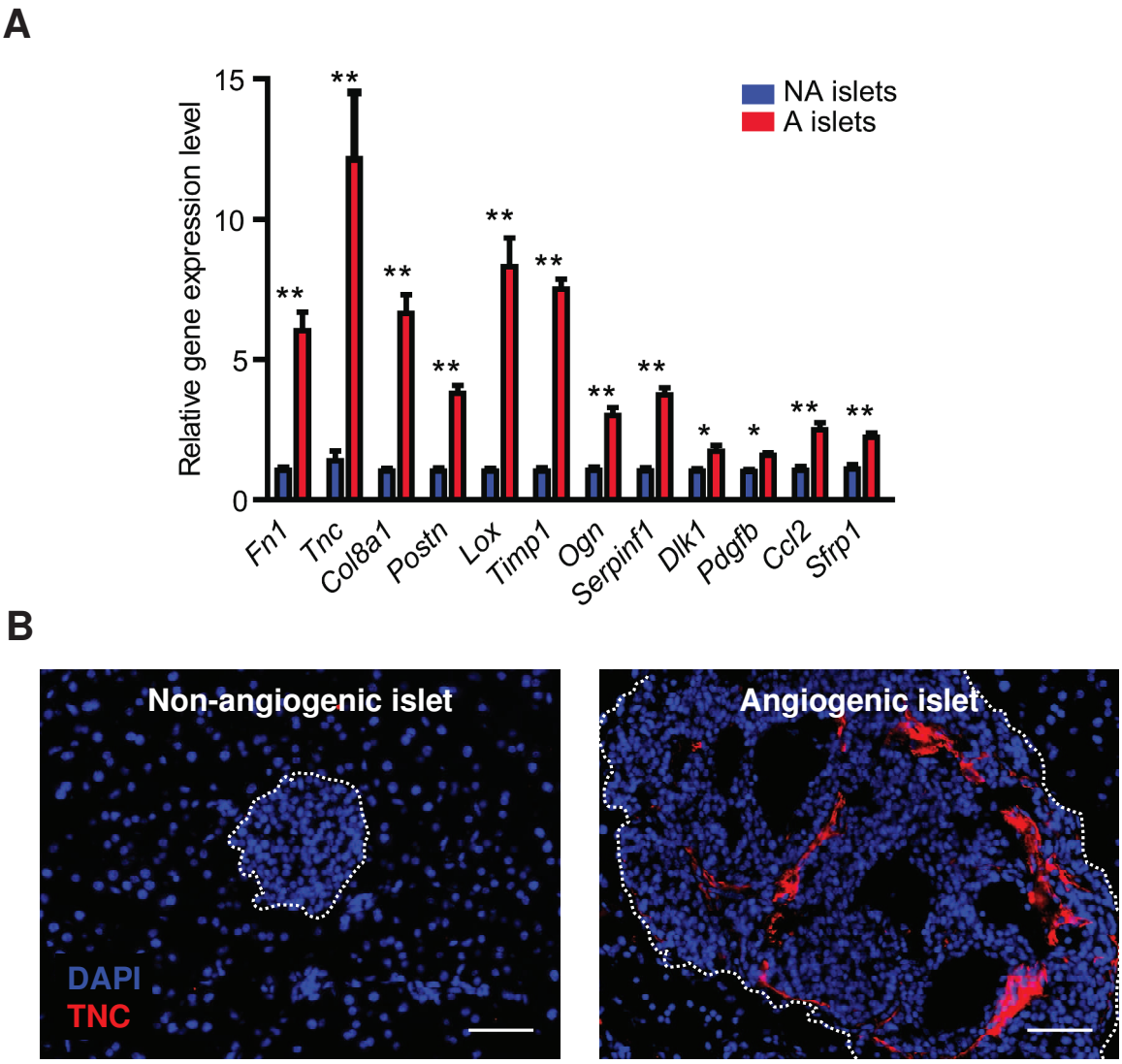

Figure 34. In the RT2 model TNC is one of the most overexpressed genes during the angiogenic switch (**A**) RT-qPCR validation of increased expression for 12 candidate genes that are up-regulated in angiogenic islets. Data (blue, non-angiogenic; red, angiogenic islets) represent mean and error bars the SEM from two independent experiments. **, $p < 5x10^{-3}$; *, $p < 10^{-2}$. (**B**) Immunofluorescence staining of murine TNC (red) in non-angiogenic islets compared to angiogenic islets in RT2 wt mice (scale bar, 50 µm). Notice that angiogenic vs. non-angiogenic islets was distinguished by size exclusion with less than 500 µm of diameter for non-angiogenic islets.

To address the impact of TNC on the angiogenic switch and on tumor angiogenesis in general we had developed two models with a TNC lack and gain of function of TNC in the RT2 model by crossing RT2 mice with TNCKO or RipTNC mice (ectopic expression of TNC in pancreatic β-cells under the repression of the rat insulin promoter). First we showed that TNC expression increased with progression from hyperplasic to macroscopic tumors (**Fig. 35A**)

and confirmed the absence of the TNC protein from RT2/TNCKO pancreatic islet tissue (**Fig. 35B, C**). In this model we had further proven that TNC plays an important role in the angiogenic switch by counting the number of angiogenic islets in RT2 mice lacking the TNC protein (TNCKO mouse) or overexpressing TNC (RipTNC). We observed that in RT2/TNCKO mice the number and the ratio of angiogenic versus non-angiogenic islets were lowered in comparison to RT2 mice (**Fig. 35D**). On the contrary, RT2/TNC mice with ectopic expression of TNC, had a higher angiogenic versus non angiogenic islet index (Saupe et al., 2013). Whereas these results showed that TNC is not required to induce the angiogenic switch they revealed that TNC plays a role in promoting the angiogenic switch.

3.2. TNC promotes tumor angiogenesis leading to poorly functional vessels

In depth analysis of TNC expression after angiogenic staging showed that TNC regulates tumor angiogenesis by promoting non-functional blood vessel formation in RT2 tumors (Saupe et al., 2013). To learn more whether TNC has an impact on the function of blood vessels we analyzed vessel morphology using the vascular cast corrosion model and scanning electron microscopy. When TNC is overexpressed the vessel anatomy appears highly aberrant with irregularly shaped, highly branched and collapsed vessels (**Fig. 35E, F**). When TNC was not expressed, vessels were also not normal but had a heterogeneous vessel diameter that suggests that blood flow is disturbed in these tumor vessels (**Fig. 35G**). Moreover we showed that tumor vessel density, as quantified by an EC specific CD31signal, was higher upon TNC overexpression and lower in the TNC KO condition (**Fig. 35H, I**). We also assessed the impact of TNC overexpression on vessel lining by pericytes, and we showed that colocalization of NG2 pericyte signal with C31 EC signal is reduced compared to control mice (**Fig. 35J**), indicating a defect in vessel maturation and stabilization. We also determined that in the absence of TNC tumor perfusion was reduced using the ratio of perfused lectin-FITC vessel normalized to total CD31 EC signal (**Fig. 35K**). This reduced vessel perfusion in TNC KO mice is associated with a reduce vessel permeability, measured by fibrinogen that has leaked into the surrounding tissue (**Fig. 35L**). Non significant but close to significance ($P = 0.064$) increase of vessel leakage was observed upon TNC overexpression compared to controls (**Fig. 35M**).

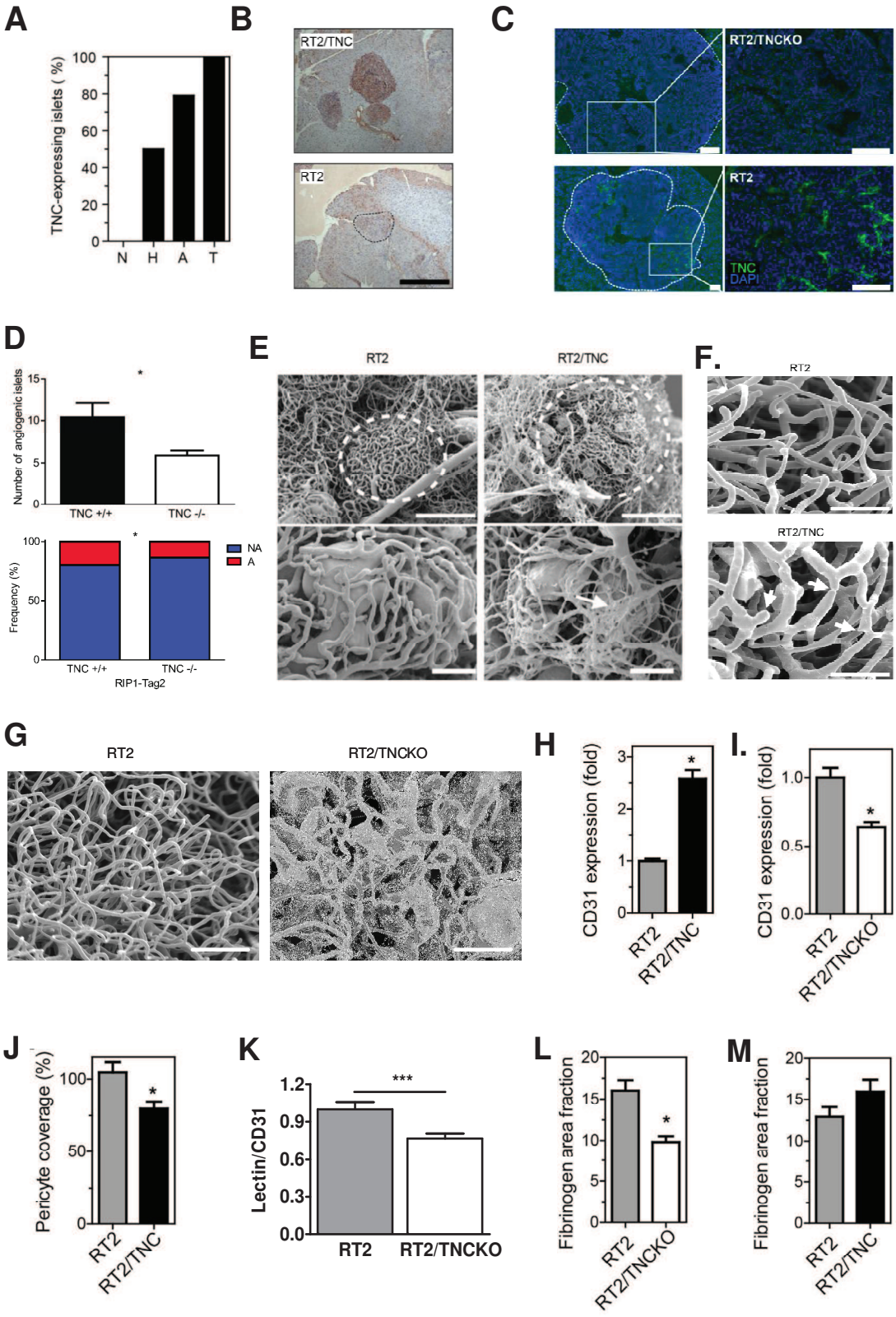

Figure 35. TNC is an important molecule for the angiogenic switch and promotes a dense but poorly functional tumor vasculature in vivo

(**A**) TNC expression in RT2 islets determined by IF analysis (MTn12 antibody) in tissue sections of 12

week old RT2 mice. In contrast to the absence of TNC from normal islets (N < 0.2 mm diameter), TNC is expressed in 50%, 80% and 100% of hyperplastic (H, 0.2 – 0.5 mm diameter), angiogenic (A, > 0.5 – 1 mm diameter) and tumorigenic islets (T, diameter above 1 mm), respectively. Right panels, dotted lines delineate the islet circumferences. 82 islets (N = 26, H = 34, A = 14, T = 8) of 3 RT2 mice were analyzed. Scale bar, 100 µm. (**B**) TNC expression analysis in RT2/TNC tumor pancreatic tissue by IHC, C, and in RT2/TNCKO by IF. Scale bar 100 µm. (**D**) Functional validation of tenascin-C contribution to the angiogenic switch. The number (**F**) and relative proportion (**G**) of angiogenic islets are significantly decreased in RIP1-Tag2 TNC KO mice (n = 8 mice) as compared to TNC wt controls (n = 5 mice). A: angiogenic islets, NA: non angiogenic islets. * $p < 5x10^{-2}$. (**E**) Representative SEM pictures from RT2 (n = 5 mice) and RT2/TNC tumors (n = 3). Arrow points at small collapsed vessels. Scale bars: top panels 200 µm, bottom panels 100 µm. (**F**), morphology of the tumor vasculature in Mercox perfusion casts from 12-week-old RT2 and RT2/TNC mice. Arrows point at break point, branching, and constriction. Scale bars, 50 µm. (**G**), representative SEM pictures from RT2 (n = 5 mice) and RT2/TNCKO tumors (n = 2). Arrow points at small collapsed vessels. Scale bars: top panels 200 µm, bottom panels 100 µm. (**H**, **I**), tumor blood vessel quantification upon CD31 staining of tumor sections from 12-week-old mice as CD31-positive area fraction per tumor normalized to RT2 controls. (**H**) RT2 (n = 6 mice, n = 34 tumors) and RT2/TNC (n = 4, n = 17) and (**I**) RT2 (n = 3, n = 71) and RT2/TNCKO (n = 3, n = 111). (**J**) Pericyte coverage of tumor blood vessels upon quantification of the ratio of NG2 over CD31 staining signals. RT2 (n = 6 mice, n = 155 tumors) and RT2/TNC (n = 8, n = 204). (**K**) Quantification of perfused lectin-FITC signal normalized to CD31 EC signal in RT2 mice with wild-type or no TNC expression. (**L**, **M**) Quantification of tumor blood vessel leakage upon fibrinogen staining of tumor sections from 12-week-old mice as fibrinogen-positive area fraction per tumor. (**L**) RT2 (n = 5 mice, n = 62 tumors) and RT2/TNC (n = 3, n = 50). (**M**) RT2 (n = 4, n = 60) and RT2/TNCKO (n = 5, n = 125). Error bars represent SEM. *p < 0.05.

Altogether, these results suggested that TNC impacts on the function of tumor vessels by promoting the formation of new vessels that are poorly functional. Interestingly this angiogenic phenotype is correlated with a higher tumor invasive phenotype (**Fig. 36A**) and lung micro-metastasis formation in RT2 mice (**Fig. 36B-D**).

In conclusion we established a working hypothesis that integrates the multiple effects of TNC on the TME thus promoting tumor angiogenesis. This is schematically depicted in **figure 37**.

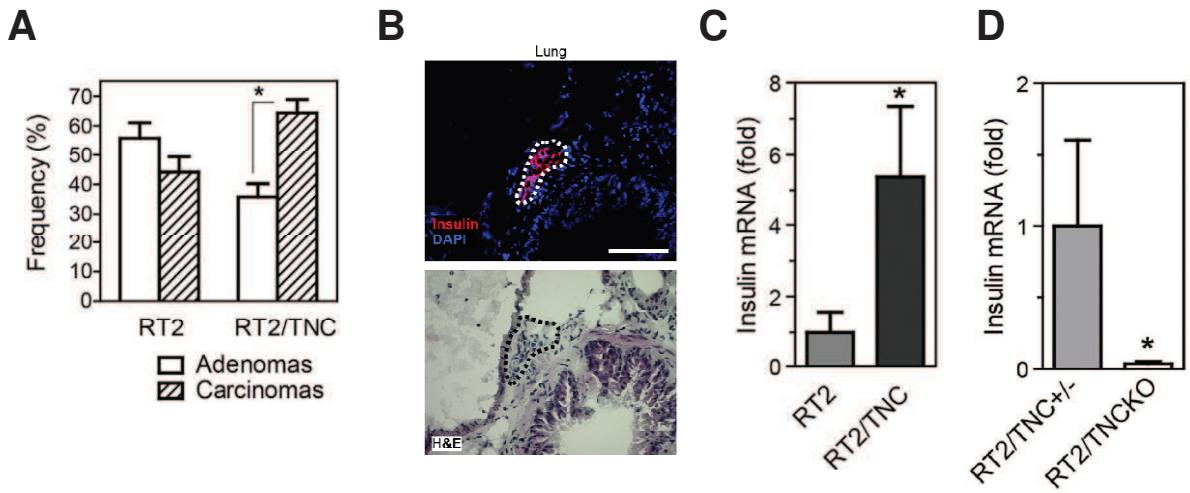

Figure 36. TNC promotes lung micro-metastasis formation in RT2

(**A**) Tumor grading into adenoma or invasive carcinoma (H&E-stained tumor sections) of RT2 tumors (n = 26 mice, 78 adenomas, 79 carcinomas) and RT2/TNC (n = 22, 44 adenomas, 76 carcinomas). (**B**) Detection of metastasized insulin-positive tumor cells in lung parenchyma (RT2 mouse) by immuno-staining (upper panel) and H&E staining (adjacent section, lower panel). (scale bar, 50 µm). (**C**, **D**) Quantification by RT-qPCR of insulin expression (C) in RT2 (n = 9) and RT2/TNC mice (n = 11) and (D) in RT2/TNC+/-(n = 8) and RT2/TNCKO (n = 4). Error bars represent SEM. *p <0.05.

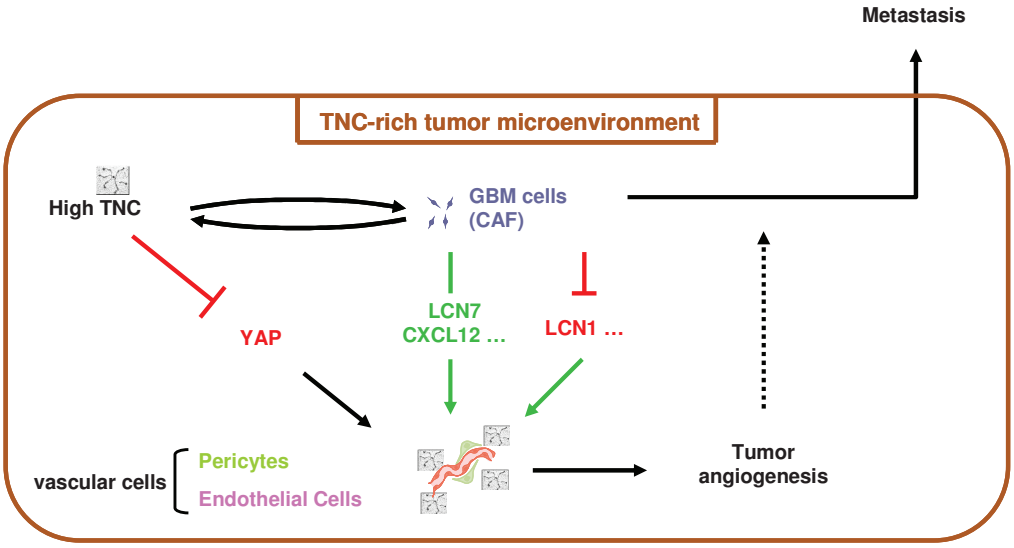

Figure 37. Working model of the role of TNC in the tumor microenvironment

Cartoon representing new working model about the role of TNC on angiogenesis in tumor microenvironment. TNC inhibits YAP signaling in EC and impair vessel maturation by direct contact. However TNC, secreted by GBM cells and CAF, promotes a pro-angiogenic secretome by upregulated LCN7 and SDF1 and downregulated LCN1. This lead to more but poorly functionalized angiogenesis by TNC that increases tumor progression and metastasis formation.

D. DISCUSSION & PERSPECTIVES

In this work, I provided results from a comprehensive analysis addressing the roles of TNC in physiological and tumor angiogenesis. As it was already described in the introduction part, TNC is a well known ECM molecule mainly absent from normal tissues and highly expressed in pathological situations, in particular in solid tumors (Abdou et al., 2012; Adams et al., 2002; Arican Ozluk et al., 2015; Midwood et al., 2009, 2011; Mitamura et al., 2002; Mustafa et al., 2012; Oskarsson et al., 2011; Trescher et al., 2013). In cancer, TNC has been clearly involved in tumor invasion and metastasis formation (Hirata et al., 2009; O'Connell et al., 2011a; Oskarsson et al., 2011; Saupe et al., 2013; Tang et al., 2015). TNC is also related to worse patient prognosis in several tumor types (Emoto et al., 2001; Herold-Mende et al., 2002; Leins et al., 2003; Mitselou et al., 2012; Nong et al., 2015; Ohtsuka et al., 2013; Tang et al., 2015). Interestingly TNC is expressed around tumor blood vessels suggesting a role in tumor angiogenesis but its function was not well characterized (Alves et al., 2011; Chung et al., 1996; Galler et al., 2011; Herold-Mende et al., 2002; Martina et al., 2010; Pezzolo et al., 2011; Saito et al., 2008a; Tanaka et al., 2003; Zagzag et al., 1996, 1996, 2002).

How TNC promotes tumor progression was recently addressed in a comprehensive approach by using the bona fide multistage immune competent Rip1Tag2 tumorigenesis model with spontaneous tumorigenesis in the context of no and abundant endogenous or ectopically overexpressed TNC. I had contributed to this study that revealed that TNC plays multiple roles by enhancing survival, proliferation and invasion of tumor cells. TNC also enhanced tumor angiogenesis and lung metastasis in this model (Saupe et al., 2013). While TNC promoted the angiogenic switch and increased blood vessel density, high TNC levels also triggered a corrupt vasculature as seen by electron microscopy, poor pericyte coverage and enhanced vessel leakiness (Langlois et al., 2014; Saupe et al., 2013). Altogether, these results suggested that TNC may have multiple and potentially opposing functions in tumor angiogenesis.

During my thesis I had introduced several state-of-the-art methods to analyze angiogenesis to the laboratory. Complementary in vivo, ex vivo and in vitro models allowed me to determine the roles of TNC in the TME during tumor angiogenesis and to gain novel insight into the

underlying mechanisms. The results of my thesis showed that a direct interaction of vascular cells with TNC impaired classical hallmarks of angiogenesis such as survival, migration and tubulogenesis. Conversely, media conditioned by tumor cells or CAF cultivated on a TNC-containing CDM increased these hallmarks of angiogenesis. Thus my results suggest that TNC differentially regulates angiogenesis through both direct anti-angiogenic effects by contact of TNC with endothelial cells and pericytes and by an indirect paracrine pro-angiogenic effect that triggered a pro-angiogenic secretome in GBM cells and CAF. I also identified molecular mechanisms responsible for the pro- and anti-angiogenic activities (**Rupp et al., in preparation**). This mechanistic information could be useful to develop novel strategies to target TNC activities during tumor progression. Pro- and anti-angiogenic activities of TNC probably coexist simultaneously during tumor progression and contribute to the expansion of vessels with poor functionality. Several lines of evidence support this conclusion that will be discussed below taking into account what already had been known about the roles of TNC in tumor angiogenesis from published literature.

1. TNC is a marker of pathological blood vessels including cancer

Direct contact of cells with the surrounding ECM in the TME triggers cellular signaling that shapes cell behavior. Since TNC is highly abundant in the TME, tumors as well as stromal cells interact with TNC. What impact that has on the different cell types is incompletely understood and my work had contributed to an improved understanding of the consequences of cell adhesion to TNC. To determine whether cells can directly interact with TNC, because they express TNC, we analyzed the expression of TNC in a xenograft model with grafted human GBM cells by IF analysis with species specific antibodies. We showed that TNC is expressed by tumor cells and by stromal cells. We also observed a close vicinity of TNC to the perivascular compartment. Indeed we detected that murine TNC co-localized with perivascular stromal cells (αSMA cells). We also observed that tumor cell derived TNC is close to blood vessels raising the possibility that tumor cells are part of the tumor vasculature. A potential transdifferentiation of tumor cells into endothelial like cells needs to be addressed in the future. Such a possibility is supported by observations from Pezzolo and colleagues who observed that transdifferentiated CD31 positive tumor cells that were part of the vasculature secreted TNC (Pezzolo et al., 2011).

A few studies on primary non-tumor derived EC have described expression of TNC when the EC were cultured in vitro: EC from normal human brain (derived from an autopsy) expressed TNC at protein level (Zagzag et al., 1996); rat cardiac-derived EC were shown to express TNC at RNA level (Ballard et al., 2006); EC derived from retinas of patients with diabetes expressed the TNC protein (Castellon et al., 2002). Moreover, Schenk and colleagues showed that TNC is expressed in a specific immortalized clonal population of BAEC. Nevertheless this expression was only detected in an assay where sprouting-like dells formed on a pre-established full confluent layer of cells (Schenk et al., 1999). These results suggest that in some particular in vitro culture conditions TNC can be re-expressed by EC.

However, our revealed showed that expression analysis of TNC in four different EC in culture that these cells do not express TNC in culture even after stimulation with TGFβ which is a known inducer of TNC (Islam et al., 2014). This observation is consistent with that from Alves and colleagues who also did not observe a TNC protein in HUVEC (Alves et al., 2011). As we had seen in postnatal retinas, several studies confirm that TNC is not expressed around the vasculature of normal tissues. Mustafa and collaborators noted the absence of TNC from the vasculature of heart, lung, liver, breast, placenta and others tissues (Ballard et al., 2006; Kimura et al., 2014; Kuriyama et al., 2011; Mustafa et al., 2012; Natali et al., 1991; Shimojo et al., 2015). Also in normal brain TNC expression is not detected around blood vessels at RNA or protein level (Martina et al., 2010; Mustafa et al., 2012; Zagzag et al., 1996). TNC is also absent from human aortae or arteries of mammary gland tissue. Yet a strong TNC expression was observed in tissue from patients with injured arteries inflicted by dissection or upon chronic dilation, or upon artheriosclerosis (Trescher et al., 2013; Wallner et al., 1999). In mouse models, the group of Andreas Faissner, Saika Shizuya or Marlene Rabinovitch showed that TNC is not expressed in blood vessels of the retina during embryogenesis, nor in blood vessels of the cornea or the arteries of adult mice (Besser et al., 2012; Jones and Rabinovitch, 1996; Sumioka et al., 2011). Altogether these results suggest that TNC is presumably absent from normal blood vessels and during normal angiogenesis. However in a pathological context such as in tumors TNC is re-expressed mostly likely by tumor cells and perivascular cells such as pericytes (Martina et al., 2010) yet not by EC. Thus TNC expression around blood vessels may be classified as a potential marker of vascular stress, since our study and the litterautre strongly suggest a role of TNC in vascular defect.

2. Direct contact of TNC with EC impairs hallmarks of angiogenesis

We demonstrated that TNC interaction with EC disturbed classical hallmarks of angiogenesis such as sprouting, tubulogenesis, migration, survival and cohesion. Using in vivo and ex vivo models with tissue from TNC KO and wt mice, we addressed the impact of TNC loss on retinal angiogenesis and aorta sprouting. We observed no effect and an inhibitory angiogenic property of TNC, respectively corraleted with TNC expression. In an assay with purified TNC or with TNC provided by co-cultured CAF we showed that TNC repressed endothelial tubulogenesis. This effect could be due to impaired cell adhesion since TNC is an adhesion modulatory ECM molecule (Chiquet-Ehrismann et al., 1988; Huang et al., 2001a; Saupe et al., 2013). Indeed we observed that a 2D substratum of purified TNC prevented cell adhesion and spreading of EC. This had substantial consequences on EC survival and migration that was reduced by TNC. We determined also that TNC impaired EC and pericyte migration and adhesion which may affect vessel stability and functionality. Perivascular cells were shown to be colocalized with TNC in human GBM (Martina et al., 2010) and we observed that mural cells (most likely pericytes) and tumor cells expressed TNC around vessels in the used GBM xenograft model.

Our observation that TNC triggers death and impairs proliferation and migration of EC could be relevant in a tumor context. As it is written above, TNC is not expressed in non-damaged arteries or veins (Martina et al., 2010; Mustafa et al., 2012; Wallner et al., 1999) or in normal highly angiogenic tissue such as the endometrium or placenta (Mustafa et al., 2012). Although TNC is highly expressed around tumor blood vessels (Galler et al., 2011; Herold-Mende et al., 2002; Martina et al., 2010; Mustafa et al., 2012), we rarely could detect EC in close contact with TNC in human and murine insulinoma and colon cancer tissue (Spenlé et al., 2015). Also in other studies TNC was found abundantly expressed around mural cells covering blood vessels yet not in direct vicinity to the EC (Martina et al., 2010). Cancer cells have been shown to physically contribute to the formation of tumor blood vessels through a mechanism called vasculogenic mimicry (El Hallani et al., 2010). In a neuroblastoma xenograft model cancer cells seem to have transdifferentiated into EC identified by expressing both tumor and EC antigens on the surface. More importantly, these cells expressed TNC which is incorporated in the vasculature suggesting a role of TNC in this process (Pezzolo et al., 2011). In cancer tissue we had described that TNC is forming ECM rich niches that seem to attract highly abundant lymphocytes and fibroblasts. Yet, EC were rarely found inside these

TNC tracks (Spenlé et al., 2015). It is tempting to speculate that TNC matrix tracks are devoid of EC because a direct contact of EC with TNC would trigger their death. Along this line, since TNC is continuously expressed in a tumor, TNC will contact EC at one point. This contact may cause EC death and potentially holes in the vessel and thus subsequent leakage.

In support of this hypothesis we showed that high TNC levels increased vessel leakage in the Rip1Tag2 model (Saupe et al., 2013). Similar data from the literature corroborates this conclusion. Alves and collaborators already described a reduction of tubulogenesis with HUVEC educated by a TNC-containing substratum, in a matrigel assay (Alves et al., 2011). Ballard and colleagues used a model where EC are plated on a TNC substratum that is covered by collagen I gel. They showed that EC escaped from the TNC substratum and invaded the collagen gel, suggesting TNC to be repulsive for EC (Ballard et al., 2006). Thus TNC may serve as a guiding molecule. This interpretation is corroborated with the work of Andreas Faissner that showed similar repulsive effects of TNC on neurons and glial cells (Faissner and Kruse, 1990; Scholze et al., 1996). A possible scenario is that TNC causes EC cell death and blocks migration in those cells that survive thus destabilizing the endothelium which would lead to increased blood vessel permeability (Saupe et al., 2013). This hypothesis is also supported by the TNC-dependent reduction of pericyte coverage in vivo (Saupe et al., 2013), crucial for vessel stability (Armulik et al., 2005), and the increase of vessel leakiness in the TNC expressing tumors (Saupe et al., 2013). Moreover we showed that a TNC substratum destabilized EC cohesion that promotes permeability in vitro. In previous reports, TNC expression has shown to disturb stability of the blood vessels in a vascular disease context as aortic dissection (Trescher et al., 2013). Interestingly TNC has been also described to impair blood-spinal cord barrier repair after lesion and thus increased blood vessel permeability in vivo (Peter et al., 2012). Moreover Bicer and colleagues suggested that TNC is associated with a defect in blood vessel maturation by analyzing TNC expression at immunohistological level in cerebral carvenous and arteriovenous malformations (Bicer et al., 2010). Kuriyama and colleagues showed that TNC is not detectable in normal liver but that TNC is upregulated upon ischemia in particular around blood vessels. They observed that TNC promoted pro-inflammatory cytokine expression associated with more necrotic tissue that was associated with an impaired re-vascularization (Kuriyama et al., 2011). This result is in agreement with our observation of a direct role of TNC in impairing angiogenesis. Thus TNC may participate to vessel disruption and increase hypoxia, well-known factors of tumor aggressiveness (Jain, 2005). Indeed TNC was already shown to be induced by hypoxia (Lal et al., 2001) and its

expression correlated with hypoxic areas in medullary thyroid carcinomas supporting induction of TNC by hypoxia in tumor tissue (Koperek et al., 2011).

TNC is a large protein presenting different domains (Van Obberghen-Schilling et al., 2011). The interaction of cells with these different domains of TNC most likely will occur through different receptors eliciting distinct signaling pathways (Lowy and Oskarsson, 2015; Midwood et al., 2011). Thus specific domains or fragments of TNC (e.g. generated by proteolysis) could have particular angio-modulatory effects. In support of this possibility Saito and collaborators showed that peptide TNCIIIA2 (covering the FNIIIA2 domain, comprising 22 amino acids) repressed human dermal microvascular endothelial cell (HDMEC) migration, proliferation and in vivo angiogenesis in a chicken chorio-allantoic membrane assay through modulation of β1 integrins (Saito et al., 2008a).

Despite some reports about anti-angiogenic activities of TNC several studies describe a pro-angiogenic activity to TNC (Castellon et al., 2002; Chung et al., 1996; Zagzag et al., 1996, 2002). Yet until our study (Saupe et al., 2013) this had not been proven in vivo and was not supported by contradictory in vitro results (Alves et al., 2011; Ballard et al., 2006; Saito et al., 2008a). However the role of TNC was mainly based on speculations due to its high expression around tumor vessels. Two reports suggest that TNC promotes EC migration in a wound healing assay with immortalized BAEC-derived cells (GM7373, after 48h of migration) (Chung et al., 1996) or with mouse retinal EC (after 7 days of migration) (Castellon et al., 2002). Importantly in both studies, the authors did not stop replication of EC which largely compromises the conclusions from these experiments. Thus the difference observed might be at least partially explained by a difference in proliferation of the EC. Indeed in the first paper, Chung and colleagues showed that addition of purified human TNC to a full layer of bovine aortic EC (BAEC & GM7373) promoted their proliferation (thymidine incorporation assay) (Chung et al., 1996). In addition in the second paper, Castellon and collaborators showed that a TNC substratum promotes EC survival of bovine retinal EC in a dose dependent manner (Castellon et al., 2002) which is the opposite to results from this work which showed a dose-dependent reduction of HUVEC survival. Moreover a recent report even described a direct pro-angiogenic effect of TNC. Martina and colleagues described an increase of in vitro sprouting angiogenesis. They used collagen I gels as matrix to mix in purified TNC (or BSA as control) and added beads that where pre-coated with HUVEC. They demonstrated that a mixed substratum of Col I and TNC promotes HUVEC

migratory speed compared to a mixed substratum of Col I and FN (Martina et al., 2010). Strikingly in this study the authors used the same source of recombinant TNC protein that was used in this thesis work. Yet, we cannot reproduce their data and even obtained an opposite result. More work is needed to dissect the impact of experimental differences on EC behavior. It cannot be ruled out that addition of purified TNC (solubilized in 0.01% Tween-20) or purified FN (not containing 0.01% Tween-20) does not have an impact on the organization of the collagen fibrils and thus indirectly impacts on EC migration. Moreover addition of PBS-Tween-20 in Col I gel impaired its normal polymerization leading to a reduce gel density (Agata Radowska, personnal observation). Zagzag and colleagues showed that TNC does not repress bovine retinal EC (BREC) adhesion on TNC (versus a FN substratum) and found instead that TNC increased adhesion in a TNC dose dependent manner. The author further claimed that migration of bovine retinal EC (forming aggregates) on the TNC substratum was reduced in a dose dependent manner. Without any quantification the authors also suggested a similar result for HUVEC (Zagzag et al., 2002). However TNC has been well described for its anti-adhesive properties in multiple cell types (Orend, 2005) including EC (Alves et al., 2011; Ballard et al., 2006; Chung et al., 1996; Schenk et al., 1999; this work). Since this classical hallmark of TNC was not shown in the study by Zagzag et al., (2002), the quality of the applied TNC may be questioned, in particular since no source or any validation of purity of TNC was provided.

By using multiple complementary models and different EC lines I throughly had addressed the impact of TNC on cell adhesion, survival and migration and provided significant valid evidence that TNC is counteracting these properties. We had used recombinant TNC that we had purified by chromatography with a gelatin sepharose column to deplete FN and subsequent affinity chromatography for the his-tagged TNC protein (with nickel beads). We had proven a high purity by commassie staining and immunoblotting for TNC. We also excluded contamination by FN by immunoblotting (data not shown). In addition, to rule out a bias due to potential peculiarities of the recombinant TNC protein, I had established and used CDM that contained or lacked TNC. I obtained similar results with both substrata supporting the validity of the results with both substrata.

3. The TNC anti-angiogenic activity may be linked to repression of YAP signaling

I had confirmed that adherence to TNC impaired cell adhesion signaling thus blocking actin polymerization into actin stress fibers in EC as had previously been shown also for other cell types (Huang et al., 2001b; Saupe et al., 2013). How cells interpret this particular adhesion is not completely understood. Recently, the Hippo pathway comprising YAP/TAZ has been linked to regulating survival and proliferation in response to cell adhesion (Halder et al., 2012). Importantly, YAP/TAZ is translocated into the nucleus when actin gets polymerized. In the nucleus YAP/TAZ bind to the DNA binding coreceptor TEAD triggering gene transcription (Halder et al., 2012). Here, we identified that YAP signaling is modulated by TNC in EC. YAP and its transcriptional coactivator TAZ are intracellular sensors of extracellular mechanical signals exerted by ECM rigidity and cell shape. This regulation involves actin cytoskeleton dependent, Rho activion and is further dependent on integrin signaling. Matrix stiffness is crucial for EC behavior (Levental et al., 2009). Barbolina and collaborators have shown that a stiffened collagen substratum, represses YAP/TAZ activity and DKK1 target gene expression in several cell types including EC (Barbolina et al., 2013). YAP activation is related to cell spreading in EC and poorly stretched cells have no or few nuclear YAP and poor YAP activity (Halder et al., 2012). We showed that TNC level in CAF increased collagen contraction that is as an indicator of modulation of the tissue mechanical properties which might be considered as stiffness modulation. Interestingly a correlation between stiffness and TNC was already suggested in vascular diseases. A potential link of TNC to tissue stiffness has been seen upon injury. TNC was shown to be overexpressed in arteries upon injury. Moreover high TNC levels triggered vessel stiffening in response to shear stress (Kimura et al., 2014).

YAP/TAZ activity is required for survival and migration of EC and is regulated by cell geometry (Dupont et al., 2011). Here I showed that a TNC substratum was able to repress YAP/TAZ activity in EC which resulted in downregulation of target genes such as CTGF, Cyr61. Recently, we had shown that TNC downregulates DKK1 (another angio-modulatory molecule (Reis et al., 2012; Saupe et al., 2013) in an actin stress fiber dependent manner (Saupe et al., 2013) presumably through regulation of YAP by TNC since constitutive active YAP restored DKK1 expression (Zhen, Schwenzer, Rupp et al., manuscript in preparation). Moreover, most of the described YAP/TAZ target genes have been correlated with vasculogenesis or angiogenesis. As examples, Cyr61 and CTGF promoted EC adhesion,

survival, migration and tubulogenesis in vitro and in vivo and these factors are important in tumor angiogenesis (Brigstock, 2002; Leu et al., 2002; Maity et al., 2014). Given that CTGF and Cyr61 are promoting angiogenesis and are downregulated by TNC in EC it remains to be seen whether reduced expression of these molecules has an impact on their survival.

One way of regulation of YAP signaling by TNC may involve Rho inhibition. Indeed we showed that TNC repressed cell spreading and F-actin polymerization in EC and thus stress fiber formation. Moreover TNC was shown to repress Rho expression and activation in cells such as murine fibroblasts (Wenk et al., 2000) and GBM cells (Lange et al., 2007). A TNC substratum also repressed actin stress fiber formation in several tumor cells and human fibroblasts (Huang et al., 2001b; Orend et al., 2003; Wenk et al., 2000). Thus, my results suggest that TNC may be an important regulator of YAP/TAZ signaling.

Another mechanism by which TNC may impact on YAP activity is through 14-3-3 tau (Lapi et al., 2008). 14-3-3 tau proteins belong to a family of phospho-serine/threonine phosphorylated proteins known to bind several proteins. One described binding partner of 14-3-3 tau is YAP (Zhao et al., 2010). 14-3-3 tau acts by retaining YAP in the cytoplasm. It was shown that plating MCF-7 breast cancer cells on a TNC substratum impaired cell spreading which promoted 14-3-3 tau protein expression (Martin et al., 2003). Thus TNC may block YAP transcriptional activity by two independent mechanisms, by upregulation of the 14-3-3 tau protein that would sequester YAP in the cytoplasm and by impairing actin polymerization also preventing translocation to the nucleus.

One possibility to challenge the role of TNC in YAP signaling could be to rescue actin polymerization in EC on a TNC substratum. Indeed we already showed that lysophosphatidic acid (LPA) restored spreading in tumor cells seeded on a TNC substratum (Saupe et al., 2013). Moreover LPA treatment is known to enhance YAP translocation to the nucleus in epithelial cells. In addition, LPA promotes Rho signaling and thus represses LATS 1/2 that would phosphorylate YAP (targeting YAP for proteasomal degradation). Recently it was shown that LPA increases CTGF and Cyr61 expression through YAP (Hwang et al., 2014). Thus we suggest that LPA restored EC cell spreading and actin stress fiber formation may rescue survival on the TNC substratum through activation of YAP. This hypothesis will soon be tested.

These hypotheses are compiled in a cartoon describing how TNC may affect YAP activity in EC (**Fig. 38**).

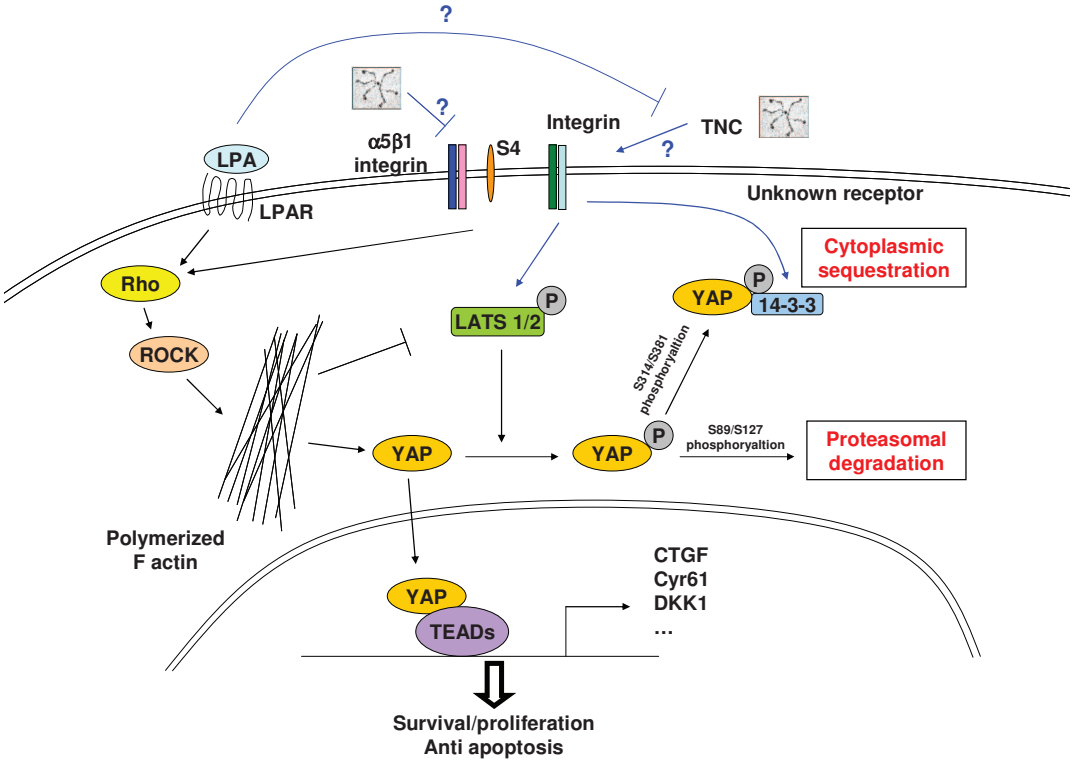

Figure 38. Working model of TNC inhibition of YAP pro-survival pathway in EC

Blue arrows represent expected role of TNC on Yap signaling. ROCK: Rho-associated protein kinase; LATS: large tumor suppressor; YAP: Yes-associated protein; TEAD: transcriptional enhancer associate domain; CTGF: connective tissue growth factor; Cyr61: cysteine-rich, angiogenic inducer, 61; DKK1: Dickkopf-1 (for more informations see: Chan et al., 2011; Halder et al., 2012; Huang et al., 2001b; Hwang et al., 2014; Julian Downward, 2009; Rhee and Grinnell, 2006; Wenk et al., 2000)

4. TNC promotes tumor angiogenesis through paracrine signaling in tumor cells and CAF

Since a direct contact of EC with TNC promotes their cell death we searched for a paracrine mechanism that could explain the angiogio-modulatory properties of TNC seen in cancer tissue. Here we had focused on GBM since these cells express copious amounts of TNC and high TNC expression especially around blood vessels correlates with worsened survival prognosis in patients with glioma (Herold-Mende et al., 2002; Midwood et al., 2011). We observed that growth of three different human GBM cells triggered the secretion of soluble

factors that promoted survival, proliferation and tubulogenesis of EC (HUVEC, BAEC) in a TNC context. A context with different TNC levels was either accomplished by plating cells on CDM containing or lacking TNC or by downregulating TNC expression in U87MG through shRNA. Fibroblasts have been shown to be a source of TNC in cancer models (Kalluri and Zeisberg, 2006; O'Connell et al., 2011) and thus might also be instructed by TNC to secrete a pro-angiogenic secretome. We addressed this possibility in CAF by plating cells on CDM containing or lacking TNC and in TIF by downregulating TNC expression (shRNA technology). Again, we observed that TNC-instructed cells secreted factors that promoted HUVEC multiplicity (CAF) and HUVEC sprout length (TIF).

Thus in contrast to a direct negative effect of TNC on angiogenesis, we showed that TNC induces a paracrine pro-angiogenic effect through modulating the secretome of tumor cells and CAF. A potential indirect effect of TNC on angiogenesis had also been identified by others. In particular, Martina and collaborators showed an increase of sprouting structures from HUVEC-coated beads upon co-culture with TNC-overexpressing HEK293 cells (compared to control HEK293 not expressing TNC) embedded into collagen gels (Martina et al., 2010).

Sumioka and collaborators used the physiological corneal neovascularization assay on tissue from TNC KO and wt mice to generate scars to determine what impact TNC has on tissue repair. They showed that lack of TNC in mice impaired blood vessel extension into the scar site. They demonstrated that TNC promotes the expression of important angiogenic cytokines such as VEGF and TGFβ1 in fibroblasts that were present underneath the corneal epithelium yet not in contact with the blood vessels (Sumioka et al., 2011). These results suggested that fibroblasts or other cells are potentially induced by TNC to secrete pro-angiogenic factors such as VEGFA and TGFβ. Whether these growth factors indeed were responsible for the TNC associated angiogenesis effect was not shown.

Ballard and collaborators using a model of cardiac allograft transplantation in TNC KO and wt mice showed that TNC is expressed in the microenvironment of the allografted ear. Moreover, TNC KO mice failed to vascularize cardiac allografts upon grafting of the tissue into the ear (Ballard et al., 2006). Again, this experiment suggests that factors secreted by the host are essential for angiogenesis and that expression of these factors is dependent on TNC. The identity of these factors remained elusive.

Tanaka and colleagues used a melanoma xenograft model where melanoma cells (highly expressing TNC) were grafted subcutaneously into an immune compromised host lacking TNC (TNC KO). Despite expression of TNC by the tumor cells vessel density was somewhat reduced in TNC KO mice. Most importantly, perfusion of the tumor vasculature seemed to be impaired in the absence of TNC. What that exactly means in terms of vessel functionality and which stromal cells contributed to tumor vessel formation was not addressed. Nevertheless, these results demonstrated that factors secreted by the host in a TNC dependent manner were important for vessel perfusion (Tanaka et al., 2003). This observation is in agreement with our results showing that vessel perfusion is reduced in Rip1Tag2 mice lacking TNC (TNC KO). That tumor cells are also important to provide pro-angiogenic factors was shown in a neuroblastoma xenograft model where Oct-4 positive/TNC positive tumor cells were grafted. The authors observed a higher vessel density and increased tumor growth when the tumor cells expressed TNC (in comparison to a TNC KD) (Pezzolo et al., 2011). These experiments indicated that TNC-derived from stromal and from tumor cells (at least in neuroblastoma and melanoma tumor context) regulate tumor angiogenesis which is consistent with what we observed for the first time in an immunocompetent mouse model (Saupe et al., 2013).

Here, we had used a plethora of state-of-the art angiogenesis models to address the multiple roles of TNC in tumor angiogenesis. Altogether, our studies provide convincing evidence for multiple and potentially opposing roles of TNC in blood vessel formation and function in tissue homeostasis and pathologies which also had been seen by others. What is novel is that we demonstrated that TNC induces a pro-angiogenic secretome in CAF and tumor cells that promoted EC survival and tubulogenesis. Moreover, we determined the molecular composition of this TNC-induced secretome and validated candidate effector targets (see below).

5. TNC induces an angio-modulatory secretome in GBM cells involving the lipocalin family and CXCL12/SDF1

In order to analyze the secretome of cells educated by TNC, we used a proteomic approach that revealed a selective high abundance of angio-modulatory molecules in this secretome. We identified a differential effect of TNC on the CAF and GBM secretome. We proved that

TNC promoted a pro-angiogenic signature in particular in GBM cells in vitro. By mass spectrometric (LC-MS/MS) analysis we observed that the secretome of U87MG cells that had been educated by TNC was very different to that of cells not being educated by TNC. In particular, we observed that around 685 secreted molecules were significantly different between the two conditions. Most importantly, whereas molecules with an anti-angiogenic function were predominantly found in CM from U87MG cells grown on a CDM lacking TNC, molecules with a pro-angiogenic function were mainly found in CM of cells that grew on a TNC containing CDM, suggesting that TNC is a potent inducer of a pro-angiogenic secretome in GBM cells.

We observed several pro-angiogenic molecules to be upregulated by TNC and other anti-angiogenic proteins that are repressed. We identified several human secreted proteins with pro- and anti-angiogenic properties which are repressed by TNC. Angiotensinogen was shown to be the most downregulated protein by TNC. Angiotensinogen is a potent inhibitor of angiogenesis that delays tumor angiogenesis and growth (Corvol et al., 2003; Vincent et al., 2009). The tissue-type plasminogen activator (tPA) was also downregulated by TNC and its kringle domain was shown to suppress growth factor-induced angiogenesis (mainly VEGF) that decreases vessel density in a lung cancer xenograft model (Shim et al., 2005). Nevertheless tPA was also shown to correlate with tumor progression and angiogenesis in a transgenic pancreatic tumor model (Díaz et al., 2002). Semaphorin-5A is repressed by TNC and is known to promote EC survival and migration as well as vessel density in a xenograft pancreatic tumor mouse model (Sadanandam et al., 2010, 2012). Calreticulin which is the precursor of the potent angiogenic and tumor growth inhibitor, vasostatin, is downregulated by TNC (Pike et al., 1998). TNC repressed also the metalloprotease Neprilysin which is known to inhibit angiogenesis via proteolysis of FGF2 (Goodman et al., 2006). CXCL14, described to be a potent inhibitor of tumor angiogenesis (Shellenberger et al., 2004), is also repressed by TNC. Gremlin-1 which is an agonist of the major pro-angiogenic receptor VEGFR2 (Mitola et al., 2010). Moreover the expression of the potent anti-angiogenic ECM molecule thrombospondin-1 and two agonists of the transforming growth factor family, TGFβ1 and TGFβ2 were also slightly reduced in the TNC conditions. Several anti-angiogenic insulin-like growth factor-binding proteins (IGFBP) were also downregulated (Chen et al., 2011; Kim et al., 2011; Rho et al., 2008; Zhang et al., 2012). Other interesting already described angio-related ECM proteins also belong to this TNC-repressed list of molecules

such as lumican which inhibits angiogenesis (Niewiarowska et al., 2011; Sharma et al., 2013) or the protein NOV homolog (or IGFBP9) which promotes angiogenesis (Lin et al., 2003).

In addition we identified LCN1 as a novel candidate downregulated by TNC and showed for the first time that LCN1 represses EC tubulogenesis. LCN1 or Von Ebner gland protein is a protein with a predicted molecular mass of 18 kDa part of the lipocalin super-family. This family is composed of small secretory proteins that play a role as carriers of lipophilic substances or play a role as protein transporters (Dartt, 2011). LCN1 may play a role in taste reception, inflammatory response and cell motility (Bratt, 2000; Flower, 1994). LCN1 was shown to impair cancer cell motility and invasion (Zhang et al., 2006) and to repress cysteine proteinase activity (Hof et al., 1997; Wojnar et al., 2001). Moreover LCN1 exhibits antimicrobial and endonuclease activity (Fluckinger et al., 2004; Yusifov et al., 2000). Interestingly LCN1 was described as potential marker of severity of inflammatory diseases (Wang et al., 2014; Xu and Venge, 2000). LNC1 is overexpressed in some pathological situation as diabetic retinopathy (Csősz et al., 2012), age-related macular degeneration (Yao et al., 2013), in cystic fibrosis (Redl et al., 1998) or in chronic obstructive pulmonary disease (Wang et al., 2014). Nevertheless LCN1 expression is anti-correlated with chronic obstructive pulmonary disease (Nicholas et al., 2010; Wang et al., 2014). Thus one hypothesis of the function of LCN1 in pathology is that it might act as a protective factor against inflammation (Dartt, 2011; Xu and Venge, 2000). Since TNC exerts pro-inflammatory activities (Chockalingam et al., 2013; Mancuso et al., 2006; Midwood et al., 2009; Page et al., 2012; Patel et al., 2011), the potential protective role of LCN1 in inflammation (Dartt, 2011; Xu and Venge, 2000) is potentially alleviated by TNC and thus repression of LCN1 may contribute to the pro-inflammatory effect of TNC. Although inflammation is promoting cancer and in particular tumor angiogenesis it is not well established whether and how TNC plays a role in this scenario (Albini et al., 2005; Colotta et al., 2009; Hanahan and Weinberg, 2011; Ono, 2008).

At the opposite TNC promoted the expression of several secreted pro-angiogenic molecules such as transglutaminase-2 (TG2) (Haroon et al., 1999; Wang et al., 2013b), pleiotrophin (Papadimitriou et al., 2009; Perez-Pinera et al., 2008), Wnt7b (Mongiat et al., 2010) and Wnt5a/b (Masckauchán et al., 2006 and thesis work from Shengda Lin from Diane Slusarski's lab). Together with previous observations that TNC promoted Wnt signaling, enhanced expression of Wnt ligands could be important for promoting angiogenesis by TNC through

this pathway (Saupe et al., 2013). Interestingly we also isolated the two pro-angiogenic YAP target genes, Cyr61 and CTGF (Brigstock, 2002; Leu et al., 2002; Maity et al., 2014) which were upregulated by TNC. This finding suggests that a differential regulation of YAP by TNC applies in GBM and in EC.

We showed that another member of the lipocalin family, lipocalin-7 (LCN7) also named tubulointerstitial nephritis antigen-like (TINAGL1), is the most upregulated protein by TNC (5.16 fold, log2 value). LCN7 is expressed in normal vessels (Li et al., 2007). The group of Allan Albig has shown that overexpression of LCN7, expressed in normal vessels (Li et al., 2007), promoted EC tubulogenesis, invasion and survival. They showed that recombinant LCN7 increased EC invasion in vitro and sprouting angiogenesis in the aortic ring assay. Finally they demonstrated that knock down of LCN7 using the morpholino strategy in zebrafish repressed vessel formation (Brown et al., 2010). Another member of the lipocalin family, lipocalin-2 (LCN2) has been already described to modulate angiogenesis. The group of Marsha Moses showed that LCN2 expression promoted $VEGF_{165}$ expression at protein level and thus enhanced EC migration. They demonstrated that recombinant LCN2 also increased VGEF-induced angiogenesis in a mouse corneal pocket assay (Yang et al., 2013). These data and ours highlight an interesting role of lipocalin family members in angiogenesis with pro-angiogenic properties of LCN7 and potential anti-angiogenic effects of LCN1. Finally, expression of LCN1 and LCN7 is oppositely regulated that may result in a pro-angiogenic or anti-angiogenic net balance depending on other unknown factors.

So far we observed a clear shift towards a pro-angiogenic signature by TNC. Nevertheless some described angiostatic or anti-angiogenic molecules are upregulated by TNC such as semphorin-3A (Casazza et al., 2011; Maione et al., 2009), matrix Gla protein (MGP) (Sharma and Albig, 2013; Yao et al., 2011), spondin-1 (F-spondin or Vascular smooth muscle cell growth-promoting factor VSGP) (Terai et al., 2001) and potentially matrilin-2 and -3. Although matrilin-2 and -3 have not been analyzed in an angiogenesis context family member matrilin-1 (not express in the profiling) is a known anti-angiogenic molecule (Foradori et al., 2014).

Finally, we identified the potent pro-angiogenic factor SDF1 or CXCL12/SDF1 (Ho et al., 2010; Kryczek et al., 2005; Orimo et al., 2005) to be induced by TNC. By pharmacological inhibition of its receptor CXCR4 (AMD3100) we revealed that TNC largely promotes

angiogenesis through this pathway. In a U87MG grafting model it was recently shown that blocking CXCR4 was highly efficient in reducing tumor angiogenesis and growth (Ping et al., 2011). This reveals that in this model CXCR4 signaling is crucial to drive tumor angiogenesis. Our results show that TNC enhances signaling through this pathway and thus enhances tumor angiogenesis.
Interestingly VEGFA, a potentially TNC-modulated factor , did not belong to the list of regulated TNC-educated molecules in our study which was confirmed by ELISA.

Several matrisomal core-proteins such as Col (COL14A1, COL15A1, and COL18A1), CTGF, SRPX2 and SLIT3 as well as the Loxl1 matrisome-associated molecule were upregulated by TNC in our study. Several of these molecules belong to the AngioMatrix, a gene expression signature that characterizes the angiogenic switch and has predictive value in glioma and colon cancer malignancy (Langlois et al., 2014). Several other members of the AngioMatrix were in the list of molecules that were downregulated by TNC which suggests that there are potentially two groups of AngioMatrix molecules, one group that is downregulated by TNC and another that is upregulated by TNC. Both groups are potentially interesting for a further stratification of patient survival. Future work needs to address whether a list of genes with TNC-upregulated AngioMatrix molecules is potentially of worse prognostic value for cancer patients than the whole AngioMatrix signature.

In conclusion, our study revealed cellular and molecular insight into the multiple effects of TNC on tumor angiogenesis showing that TNC exerts direct anti-angiogenic activities towards EC and paracrine pro-angiogenic activities through tumor cells and CAF. These opposing effects could explain that TNC promotes more but poorly functional tumor blood vessels. Identification and detailed insight into molecules responsible for the pro- and anti-angiogenic activities of TNC might provide for the first time opportunities to counteract TNC activities at the molecular level in cancer.

Despite these interesting results, we still do not know if the observed mechanisms are relevant in a tumor context. Therefore, two important experiments are ongoing in the laboratory. We are addressing whether the pro-angiogenic secretome induced by TNC drives angiogenesis in U87MG tumor grafts and whether the candidate list of pro-angiogenic molecules correlates with angiogenesis and worsened patient survival in glioma and other cancer patients.

6. CDM with abundant and no TNC as valid model to determine the roles of TNC in cancer

In tumor tissue TNC acts in concert with other ECM molecules. This cannot be recapitulated by a 2D TNC substratum. To mimic the 3D context we established CDM with abundant and no or low TNC expression in CAF and MEF. We had characterized the CDM of these fibroblasts in some detail by IF analysis and proteomic approach (Koczorowska, Rupp, Radwanska, et al., in preparation) and observed that the ECM networks were fibrillar in the presence and absence of TNC. In the MEF derived CDM we did not see an obvious difference in the organization of the collagen and FN networks in the absence of TNC in comparison to its presence. Yet the molecular composition was different (Koczorowska, Rupp, Radwanska et al., in preparation) suggesting that eliminating expression of one ECM molecule from a fibroblast has a profound impact on the ECM that this cell produces. In the tumor context a TNC-dependent ECM could have a significant impact on the microenvironment affecting mechanical properties and abundance of ECM-sequestered or ECM-presented soluble factors. Most importantly, CDM from TNC KO MEF was devoid of TNC. By comparing cell behavior on CDM with abundant and no TNC we recapitulated properties of 2D substrata containing or lacking TNC such as repressed EC survival and proliferation by TNC. This result suggests that the observed biological effects seen in cells plated on CDM can be linked to the abundance of TNC and thus CDM with abundant and no TNC, respectively is a good substratum to address the functions of TNC.

7. What upstream signaling is triggered by TNC to promote or inhibit tumor angiogenesis?

By which mechanism TNC induces a pro-angiogenic secretome in GBM cells or CAF is unknown. TNC could directly bind to integrins and by that induce a pro-angiogenic secretome. These integrins would comprise αvβ3 (Jones et al., 1997; Sriramarao et al., 1993), αvβ6 (Yokosaki et al., 1996), α2β1 (Sriramarao et al., 1993), α8β1 (Schnapp et al., 1995) or α9β1 (Yokosaki et al., 1994) or the α5β1/syndecan-4 complex (Huang et al., 2001). Our understanding is largely based on the fact that we had compared conditions with abundant and no/low TNC levels. Taking TNC away seems to have a global impact on the abundance of

molecules in the ECM, and potentially also impacts on their crosslinking, matrix stiffness and abundance of soluble factors. Altogether this will have a huge impact on how a cell is responding and thus could be indirect not following TNC-receptor mediated signaling.

As future outlooks to determine how TNC induces an angio-modulatory secretome the following questions should be address:

i) Which cell adhesion receptors for TNC are involved? Does receptor mediated binding to TNC induce expression of the angio-modulatory secretome? Would this involve any of the known TNC binding integrins or syndecan-4? These possibilities can be tested with specific integrin inhibitors or the syndecan-4 activating peptide.

ii) Does the presence or absence of TNC have an impact on stiffness of the CDM? This should be addressed by AFM microscopy. Does matrix stiffness per se have an impact on the angio-modulatory secretome? This could be addressed by lowering the stiffness of the CDM by using matrix (collagen) crosslinking inhibitors such as LOX inhibitors or a TG2 KD amongst others. Also substratum stiffness could be designed by using polyacrylamid gels with different concentrations (Barbolina et al., 2013).

iii) Does any / how many of the molecules that are differentially expressed in the CDM in the presence or absence of TNC (Rupp, Koczorowska, Radwanska et al., in preparation) have an impact on the angio-modulatory secretome?

8. Hypothesis how TNC potentially impacts on tumor angiogenesis

TNC is already expressed early in tumorigenesis and is continued to be expressed at all stages during tumor progression (Saupe et al., 2013). Thus TNC may play multiple roles during these events. Indeed our study confirms this possibility. During tumorigenesis the following scenario may apply:

1.- Tumor cells divide and generate a tumor mass that gets hypoxic. Hypoxia will induce TNC (Lal et al., 2001). Hypoxia as well as TNC may recruit fibroblasts that convert into CAF.

There is evidence that TNC plays a role in the conversion of fibroblasts into CAF (De Wever et al., 2004).

2.- Tumor cells and CAF get in contact with TNC which triggers the expression of an angio-modulatory secretome (Rupp et al., in preparation). This angio-modulatory secretome is part of a larger signature, the AngioMatrix, that drives the angiogenic switch where TNC is one of the most highly induced matrisomal molecules (Langlois et al., 2014). There is evidence that TNC plays a functional role in the angiogenic switch since this is reduced in the absence of TNC and increased upon ectopic overexpression of TNC in the Rip1Tag2 model (Saupe et al., 2013; Langlois et al., 2014).

3.- TNC by modulating balance of GF in the TME could attract CAF (De Wever et al., 2004), EC and other cells that form the new vessels. TNC is expressed by tumor and stromal mural cells yet not by EC thus generating a TNC rich TME around the newly formed vessels (Rupp et al., in preparation; Martina et al., 2010: Herold-Mende et al., 2002). A better understanding of how TNC is repressed in EC may provide opportunities to develop novel strategies to counteract TNC expression in the TME.

4.- TNC is continuously expressed and forms tracks that serve as local niches for CAF, immune cells and potentially cancer stem cells (Spenlé et al., 2015).

5.- Due to its high abundance TNC may also get into close vicinity to EC. A direct contact with TNC challenges survival of EC presumably by a mechanism that involves impairment of YAP signaling. This impaired YAP signaling potentially promotes cell death due to downregulation of pro-angiogenic factors such as Cyr61 and CTGF that would maintain EC survival (Rupp et al., in preparation).

6.- Those EC that do not die upon contact with TNC proliferate and migrate less which would impair their tubulogenic properties (Rupp et al., in preparation). TNC also appears to reduce EC cohesion and pericyte migration (Rupp et al., in preparation) that would lead to reduced coverage by pericytes (which we had seen in the Rip1Tag2 model (Saupe et al., 2013). Altogether these events may culminate in destabilized poorly functional vessels that would offer a poor barrier for cancer cells thus promoting metastasis. Indeed we saw increased

vessel leakage and enhanced lung micrometastasis in dependence of TNC in the Rip1Tag2 model (Saupe et al., 2013).

7.- Finally contact of tumor cells with TNC may contribute to their transdifferentiation into cells that integrate into the tumor vasculature. A potential role of TNC in vasculogenic mimicry had already been suggested by us and others (Kääriäinen et al., 2006; Pezzolo et al., 2011; Spenlé et al., 2015).

E. CONCLUSION

In conclusion, I had used several in vitro, ex vivo and in vivo models to study the roles of TNC in angiogenesis. These approaches were used to determine how TNC impacts on tumor angiogenesis at cellular and molecular level. Our results support that TNC has multiple and opposing roles in tumor angiogenesis. TNC promotes the angiogenic switch, and increases the formation of new vessels, yet these vessels are badly shaped and leaky, thus poorly functional. We have shown that TNC disturbs directly EC functions such as survival, proliferation, migration and tubulogenesis. Due to its adhesion inhibitory effect TNC impaired YAP signaling. Altogether this could explain how TNC contributes to vessel malformation. Moreover, we demonstrated that contact of tumor cells and CAF with TNC induces an angio-modulatory secretome in these cells that promotes hallmarks of angiogenesis such as survival and tubulogenesis. This paracrine mechanism appears to be linked to LCN1 downregulation and LCN7 upregulation. In addition induction of CXCL12/SDF1 is largely responsible for TNC-induced EC tubulogenesis. In the future it will be important to determine whether targeting CXCR4 (or other identified TNC regulated pro-angiogenic molecules) is neutralizing the TNC promoting effect on tumor angiogenesis in vivo. Importantly, targeting CXCR4 signaling with the FDA-approved SDF1 inhibitor AMD3100 (also known as Plerixafor, Sanofi Aventis) (Lanza et al., 2015) together with Bevacizumab (blocking VEGFA signaling (Vredenburgh et al., 2007) is currently applied in a clinical study for recurrent high-grade glioma (study number: NCT01339039). This approach could be superior over targeting VEGFA alone because additional targeting of CXCR4 may also counteract an important pro-angiogenic activity of TNC. Thus targeting the inherently TNC-rich TME in GBM with anti-angiogenic drugs in combination with drugs that block the TNC-related pro-angiogenic activities may lead to significantly reduced tumor angiogenesis and retarded tumor growth. Tumor vessels may also regress or normalize when the vessel corrupting activity of TNC is blocked (Jain, 2005) thus enhancing the delivery of adjuvant chemo-therapeutics such as temozolomide (Pedretti et al., 2010b) into the tumor tissue. Targeting TNC activities may also have an impact on the tumor bed promoting tumor relapse and malignancy but remains largely unaffected by any of the currently applied therapeutic approaches.

F. BIBLIOGRAPHY

Abdou, A.G., Maraee, A.H., Shoeib, M.A.E.-M., and Elbana, R. (2012). Immunolocalization of tenascin-C in vitiligo. Appl. Immunohistochem. Mol. Morphol. AIMM Off. Publ. Soc. Appl. Immunohistochem. *20*, 501–511.

Adams, R.H., and Alitalo, K. (2007a). Molecular regulation of angiogenesis and lymphangiogenesis. Nat. Rev. Mol. Cell Biol. *8*, 464–478.

Adams, R.H., and Alitalo, K. (2007b). Molecular regulation of angiogenesis and lymphangiogenesis. Nat. Rev. Mol. Cell Biol. *8*, 464–478.

Adams, M., Jones, J.L., Walker, R.A., Pringle, J.H., and Bell, S.C. (2002). Changes in tenascin-C isoform expression in invasive and preinvasive breast disease. Cancer Res. *62*, 3289–3297.

Aguilera, K.Y., Rivera, L.B., Hur, H., Carbon, J.G., Toombs, J.E., Goldstein, C.D., Dellinger, M.T., Castrillon, D.H., and Brekken, R.A. (2014). Collagen Signaling Enhances Tumor Progression after Anti-VEGF Therapy in a Murine Model of Pancreatic Ductal Adenocarcinoma. Cancer Res. *74*, 1032–1044.

Aguirre-Ghiso, J.A. (2007). Models, mechanisms and clinical evidence for cancer dormancy. Nat. Rev. Cancer *7*, 834–846.

Albini, A., Tosetti, F., Benelli, R., and Noonan, D.M. (2005). Tumor inflammatory angiogenesis and its chemoprevention. Cancer Res. *65*, 10637–10641.

Allen, W.E., Jones, G.E., Pollard, J.W., and Ridley, A.J. (1997). Rho, Rac and Cdc42 regulate actin organization and cell adhesion in macrophages. J. Cell Sci. *110 (Pt 6)*, 707–720.

Alves, T.R., da Fonseca, A.C.C., Nunes, S.S., da Silva, A.O., Dubois, L.G.F., Faria, J., Kahn, S.A., Viana, N.B., Marcondes, J., Legrand, C., et al. (2011). Tenascin-C in the extracellular matrix promotes the selection of highly proliferative and tubulogenesis-defective endothelial cells. Exp. Cell Res. *317*, 2073–2085.

Arican Ozluk, O., Topal, D., Tenekecioglu, E., Peker, T., Yilmaz, M., Karaagac, K., Vatansever, F., Boyraz, B., and Aydın, O. (2015). High tenascin-C levels cause inadequate myocardial blush grade in patients with acute myocardial infarction. Int. J. Clin. Exp. Med. *8*, 2554–2561.

Armulik, A., Abramsson, A., and Betsholtz, C. (2005). Endothelial/Pericyte Interactions. Circ. Res. *97*, 512–523.

Asahara, T., Kawamoto, A., and Masuda, H. (2011). Concise review: Circulating endothelial progenitor cells for vascular medicine. Stem Cells Dayt. Ohio *29*, 1650–1655.

Astrof, S., and Hynes, R.O. (2009). Fibronectins in Vascular Morphogenesis. Angiogenesis *12*, 165–175.

Augsten, M. (2014). Cancer-associated fibroblasts as another polarized cell type of the tumor microenvironment. Mol. Cell. Oncol. *4*, 62.

Baker, A.-M., Bird, D., Lang, G., Cox, T.R., and Erler, J.T. (2013). Lysyl oxidase enzymatic function increases stiffness to drive colorectal cancer progression through FAK. Oncogene *32*, 1863–1868.

Baker, M., Robinson, S.D., Lechertier, T., Barber, P.R., Tavora, B., D'Amico, G., Jones, D.T., Vojnovic, B., and Hodivala-Dilke, K. (2012). Use of the mouse aortic ring assay to study angiogenesis. Nat Protoc. *7*, 89–104.

Ballard, V.L.T., Sharma, A., Duignan, I., Holm, J.M., Chin, A., Choi, R., Hajjar, K.A., Wong, S.-C., and Edelberg, J.M. (2006). Vascular Tenascin-C Regulates Cardiac Endothelial Phenotype and Neovascularization. FASEB J. *20*, 717–719.

Balmain, A. (2001). Cancer genetics: from Boveri and Mendel to microarrays. Nat. Rev. Cancer *1*, 77–82.

Barbolina, M.V., Liu, Y., Gurler, H., Kim, M., Kajdacsy-Balla, A.A., Rooper, L., Shepard, J., Weiss, M., Shea, L.D., Penzes, P., et al. (2013). Matrix Rigidity Activates Wnt Signaling through Down-regulation of Dickkopf-1 Protein. J. Biol. Chem. *288*, 141–151.

Barcellos-Hoff, M.H. (1998). The potential influence of radiation-induced microenvironments in neoplastic progression. J. Mammary Gland Biol. Neoplasia *3*, 165–175.

Baskić, D., Popović, S., Ristić, P., and Arsenijević, N.N. (2006). Analysis of cycloheximide-induced apoptosis in human leukocytes: fluorescence microscopy using annexin V/propidium iodide versus acridin orange/ethidium bromide. Cell Biol. Int. *30*, 924–932.

Beacham, D.A., Amatangelo, M.D., and Cukierman, E. (2007). Preparation of extracellular matrices produced by cultured and primary fibroblasts. Curr. Protoc. Cell Biol. Editor. Board Juan Bonifacino Al *Chapter 10*, Unit 10.9.

Beamish, J.A., He, P., Kottke-Marchant, K., and Marchant, R.E. (2010). Molecular Regulation of Contractile Smooth Muscle Cell Phenotype: Implications for Vascular Tissue Engineering. Tissue Eng. Part B Rev. *16*, 467–491.

Belle, E.V., Rivard, A., Chen, D., Silver, M., Bunting, S., Ferrara, N., Symes, J.F., Bauters, C., and Isner, J.M. (1997). Hypercholesterolemia Attenuates Angiogenesis but Does Not Preclude Augmentation by Angiogenic Cytokines. Circulation *96*, 2667–2674.

Bergers, G., and Benjamin, L.E. (2003). Tumorigenesis and the angiogenic switch. Nat Rev Cancer *3*, 401–410.

Bergers, G., and Hanahan, D. (2008). Modes of resistance to anti-angiogenic therapy. Nat Rev Cancer *8*, 592–603.

Berndt, A., Köllner, R., Richter, P., Franz, M., Voigt, A., Berndt, A., Borsi, L., Giavazzi, R., Neri, D., and Kosmehl, H. (2010). A comparative analysis of oncofetal fibronectin and tenascin-C incorporation in tumour vessels using human recombinant SIP format antibodies. Histochem. Cell Biol. *133*, 467–475.

Bertolini, F., Shaked, Y., Mancuso, P., and Kerbel, R.S. (2006). The multifaceted circulating endothelial cell in cancer: towards marker and target identification. Nat. Rev. Cancer *6*, 835–845.

Besser, M., Jagatheaswaran, M., Reinhard, J., Schaffelke, P., and Faissner, A. (2012). Tenascin C regulates proliferation and differentiation processes during embryonic retinogenesis and modulates the de-differentiation capacity of Müller glia by influencing growth factor responsiveness and the extracellular matrix compartment. Dev. Biol. *369*, 163–176.

Bicer, A., Guclu, B., Ozkan, A., Kurtkaya, O., Koc, D.Y., Necmettin Pamir, M., and Kilic, T. (2010). Expressions of angiogenesis associated matrix metalloproteinases and extracellular matrix proteins in cerebral vascular malformations. J. Clin. Neurosci. *17*, 232–236.

Biniossek, M.L., and Schilling, O. (2012). Enhanced identification of peptides lacking basic residues by LC-ESI-MS/MS analysis of singly charged peptides. Proteomics *12*, 1303–1309.

Bissell, M.J., and Hines, W.C. (2011). Why don't we get more cancer? A proposed role of the microenvironment in restraining cancer progression. Nat. Med. *17*, 320–329.

Bissell, M.J., and LaBarge, M.A. (2005). Context, tissue plasticity, and cancer: Are tumor stem cells also regulated by the microenvironment? Cancer Cell *7*, 17–23.

Blann, A.D., Woywodt, A., Bertolini, F., Bull, T.M., Buyon, J.P., Clancy, R.M., Haubitz, M., Hebbel, R.P., Lip, G.Y.H., Mancuso, P., et al. (2005). Circulating endothelial cells. Biomarker of vascular disease. Thromb. Haemost. *93*, 228–235.

De Boeck, A., Hendrix, A., Maynard, D., Van Bockstal, M., Daniëls, A., Pauwels, P., Gespach, C., Bracke, M., and De Wever, O. (2013). Differential secretome analysis of cancer-associated fibroblasts and bone marrow-derived precursors to identify microenvironmental regulators of colon cancer progression. Proteomics *13*, 379–388.

Brack, S.S., Silacci, M., Birchler, M., and Neri, D. (2006). Tumor-Targeting Properties of Novel Antibodies Specific to the Large Isoform of Tenascin-C. Clin. Cancer Res. *12*, 3200–3208.

Bratt, T. (2000). Lipocalins and cancer. Biochim. Biophys. Acta BBA - Protein Struct. Mol. Enzymol. *1482*, 318–326.

Brescia, P., Ortensi, B., Fornasari, L., Levi, D., Broggi, G., and Pelicci, G. (2013). CD133 Is Essential for Glioblastoma Stem Cell Maintenance. STEM CELLS *31*, 857–869.

Brigstock, D.R. (2002). Regulation of angiogenesis and endothelial cell function by connective tissue growth factor (CTGF) and cysteine-rich 61 (CYR61). Angiogenesis *5*, 153–165.

Brissett, M., Veraldi, K.L., Pilewski, J.M., Medsger, T.A., and Feghali-Bostwick, C.A. (2012). Localized expression of tenascin in systemic sclerosis-associated pulmonary fibrosis and its regulation by insulin-like growth factor binding protein 3. Arthritis Rheum. *64*, 272–280.

Brösicke, N., Landeghem, F.K.H. van, Scheffler, B., and Faissner, A. (2013). Tenascin-C is expressed by human glioma in vivo and shows a strong association with tumor blood vessels. Cell Tissue Res. *354*, 409–430.

Brown, L.J., Alawoki, M., Crawford, M.E., Reida, T., Sears, A., Torma, T., and Albig, A.R. (2010). Lipocalin-7 Is a Matricellular Regulator of Angiogenesis. PLoS ONE *5*, e13905.

Burke, P.A., DeNardo, S.J., Miers, L.A., Lamborn, K.R., Matzku, S., and DeNardo, G.L. (2002). Cilengitide Targeting of αvβ3 Integrin Receptor Synergizes with Radioimmunotherapy to Increase Efficacy and Apoptosis in Breast Cancer Xenografts. Cancer Res. *62*, 4263–4272.

Calvo, F., Ege, N., Grande-Garcia, A., Hooper, S., Jenkins, R.P., Chaudhry, S.I., Harrington, K., Williamson, P., Moeendarbary, E., Charras, G., et al. (2013a). Mechanotransduction and YAP-dependent matrix remodelling is required for the generation and maintenance of cancer-associated fibroblasts. Nat. Cell Biol. *15*, 637–646.

Calvo, F., Ege, N., Grande-Garcia, A., Hooper, S., Jenkins, R.P., Chaudhry, S.I., Harrington, K., Williamson, P., Moeendarbary, E., Charras, G., et al. (2013b). Mechanotransduction and YAP-dependent matrix remodelling is required for the generation and maintenance of cancer-associated fibroblasts. Nat. Cell Biol. *15*, 637–646.

Camps, J.L., Chang, S.M., Hsu, T.C., Freeman, M.R., Hong, S.J., Zhau, H.E., von Eschenbach, A.C., and Chung, L.W. (1990). Fibroblast-mediated acceleration of human epithelial tumor growth in vivo. Proc. Natl. Acad. Sci. U. S. A. *87*, 75–79.

Carey, W.A., Taylor, G.D., Dean, W.B., and Bristow, J.D. (2010). Tenascin-C deficiency attenuates TGF-ß-mediated fibrosis following murine lung injury. Am. J. Physiol. Lung Cell. Mol. Physiol. *299*, L785–L793.

Carmeliet, P. (2000). Mechanisms of angiogenesis and arteriogenesis. Nat. Med. *6*, 389–395.

Carmeliet, P. (2003). Angiogenesis in health and disease. Nat Med *9*, 653–660.

Carmeliet, P., and Jain, R.K. (2000). Angiogenesis in cancer and other diseases. Nature *407*, 249–257.

Carmeliet, P., and Jain, R.K. (2011a). Principles and mechanisms of vessel normalization for cancer and other angiogenic diseases. Nat Rev Drug Discov *10*, 417–427.

Carmeliet, P., and Jain, R.K. (2011b). Molecular mechanisms and clinical applications of angiogenesis. Nature *473*, 298–307.

Carnemolla, B., Castellani, P., Ponassi, M., Borsi, L., Urbini, S., Nicolo, G., Dorcaratto, A., Viale, G., Winter, G., Neri, D., et al. (1999). Identification of a glioblastoma-associated tenascin-C isoform by a high affinity recombinant antibody. Am. J. Pathol. *154*, 1345–1352.

Casazza, A., Fu, X., Johansson, I., Capparuccia, L., Andersson, F., Giustacchini, A., Squadrito, M.L., Venneri, M.A., Mazzone, M., Larsson, E., et al. (2011). Systemic and targeted delivery of semaphorin 3A inhibits tumor angiogenesis and progression in mouse tumor models. Arterioscler. Thromb. Vasc. Biol. *31*, 741–749.

Castellani, P., Dorcaratto, A., Siri, A., Zardi, L., and Viale, G.L. (1995). Tenascin distribution in human brain tumours. Acta Neurochir. (Wien) *136*, 44–50.

Castello-Cros, R., Khan, D., Simons, J., Valianou, M., and Cukierman, E. (2009). Staged stromal extracellular 3D matrices differentially regulate breast cancer cell responses through PI3K and beta1-integrins. BMC Cancer *9*, 94.

Castellon, R., Caballero, S., Hamdi, H.K., Atilano, S.R., Aoki, A.M., Tarnuzzer, R.W., Kenney, M.C., Grant, M.B., and Ljubimov, A.V. (2002). Effects of tenascin-C on normal and diabetic retinal endothelial cells in culture. Invest. Ophthalmol. Vis. Sci. *43*, 2758–2766.

Celletti, F.L., Waugh, J.M., Amabile, P.G., Brendolan, A., Hilfiker, P.R., and Dake, M.D. (2001). Vascular endothelial growth factor enhances atherosclerotic plaque progression. Nat. Med. *7*, 425–429.

Chan, S.W., Lim, C.J., Chong, Y.F., Pobbati, A.V., Huang, C., and Hong, W. (2011). Hippo Pathway-independent Restriction of TAZ and YAP by Angiomotin. J. Biol. Chem. *286*, 7018–7026.

Chanmee, T., Ontong, P., Konno, K., and Itano, N. (2014). Tumor-associated macrophages as major players in the tumor microenvironment. Cancers *6*, 1670–1690.

Chen, D., Yoo, B.K., Santhekadur, P.K., Gredler, R., Bhutia, S. k, Das, S.K., Fuller, C., Su, Z., Fisher, P.B., and Sarkar, D. (2011). Insulin-like growth factor binding protein-7 (IGFBP7) functions as a potential tumor suppressor in hepatocellular carcinoma (HCC). Clin. Cancer Res. clincanres.2774.2010.

Chen, P., Cescon, M., and Bonaldo, P. (2013). Collagen VI in cancer and its biological mechanisms. Trends Mol. Med. *19*, 410–417.

Chiquet-Ehrismann, R., Kalla, P., Pearson, C.A., Beck, K., and Chiquet, M. (1988). Tenascin interferes with fibronectin action. Cell *53*, 383–390.

Chiquet-Ehrismann, R., Orend, G., Chiquet, M., Tucker, R.P., and Midwood, K.S. (2014). Tenascins in stem cell niches. Matrix Biol. J. Int. Soc. Matrix Biol. *37*, 112–123.

Chockalingam, P.S., Glasson, S.S., and Lohmander, L.S. (2013). Tenascin-C levels in synovial fluid are elevated after injury to the human and canine joint and correlate with markers of inflammation and matrix degradation. Osteoarthritis Cartilage *21*, 339–345.

Chou, J., Shahi, P., and Werb, Z. (2013). microRNA-mediated regulation of the tumor microenvironment. Cell Cycle *12*, 3262–3271.

Chung, C.Y., Murphy-Ullrich, J.E., and Erickson, H.P. (1996). Mitogenesis, cell migration, and loss of focal adhesions induced by tenascin-C interacting with its cell surface receptor, annexin II. Mol. Biol. Cell *7*, 883.

Cohen, S.J., Alpaugh, R.K., Palazzo, I., Meropol, N.J., Rogatko, A., Xu, Z., Hoffman, J.P., Weiner, L.M., and Cheng, J.D. (2008). Fibroblast Activation Protein and Its Relationship to Clinical Outcome in Pancreatic Adenocarcinoma: Pancreas *37*, 154–158.

Colotta, F., Allavena, P., Sica, A., Garlanda, C., and Mantovani, A. (2009). Cancer-related inflammation, the seventh hallmark of cancer: links to genetic instability. Carcinogenesis *30*, 1073–1081.

Corvol, P., Lamandé, N., Cruz, A., Celerier, J., and Gasc, J.-M. (2003). Inhibition of angiogenesis: a new function for angiotensinogen and des(angiotensin I)angiotensinogen. Curr. Hypertens. Rep. *5*, 149–154.

Craig, R., and Beavis, R.C. (2004). TANDEM: matching proteins with tandem mass spectra. Bioinforma. Oxf. Engl. *20*, 1466–1467.

Crossin, K.L., Hoffman, S., Grumet, M., Thiery, J.P., and Edelman, G.M. (1986). Site-restricted expression of cytotactin during development of the chicken embryo. J. Cell Biol. *102*, 1917–1930.

Csősz, É., Boross, P., Csutak, A., Berta, A., Tóth, F., Póliska, S., Török, Z., and Tőzsér, J. (2012). Quantitative analysis of proteins in the tear fluid of patients with diabetic retinopathy. J. Proteomics *75*, 2196–2204.

Cunha, S.I., and Pietras, K. (2011). ALK1 as an emerging target for antiangiogenic therapy of cancer. Blood *117*, 6999–7006.

Dandachi, N., Hauser-Kronberger, C., Moré, E., Wiesener, B., Hacker, G.W., Dietze, O., and Wirl, G. (2001). Co-expression of tenascin-C and vimentin in human breast cancer cells indicates phenotypic transdifferentiation during tumour progression: correlation with histopathological parameters, hormone receptors, and oncoproteins. J. Pathol. *193*, 181–189.

Dartt, D.A. (2011). Tear Lipocalin: Structure and Function. Ocul. Surf. *9*, 126–138.

Degen, M., Brellier, F., Kain, R., Ruiz, C., Terracciano, L., Orend, G., and Chiquet-Ehrismann, R. (2007). Tenascin-W Is a Novel Marker for Activated Tumor Stroma in Low-grade Human Breast Cancer and Influences Cell Behavior. Cancer Res. *67*, 9169–9179.

Degen, M., Brellier, F., Schenk, S., Driscoll, R., Zaman, K., Stupp, R., Tornillo, L., Terracciano, L., Chiquet-Ehrismann, R., Rüegg, C., et al. (2008). Tenascin-W, a new marker of cancer stroma, is elevated in sera of colon and breast cancer patients. Int. J. Cancer *122*, 2454–2461.

Deindl, E., Hoefer, I.E., Fernandez, B., Barancik, M., Heil, M., Strniskova, M., and Schaper, W. (2003). Involvement of the fibroblast growth factor system in adaptive and chemokine-induced arteriogenesis. Circ. Res. *92*, 561–568.

Dejana, E., and Orsenigo, F. (2013). Endothelial adherens junctions at a glance. J. Cell Sci. *126*, 2545–2549.

Desai Bradaric, B., Patel, A., Schneider, J.A., Carvey, P.M., and Hendey, B. (2012). Evidence for angiogenesis in Parkinson's disease, incidental Lewy body disease, and progressive supranuclear palsy. J. Neural Transm. Vienna Austria 1996 *119*, 59–71.

Díaz, V.M., Planagumà, J., Thomson, T.M., Reventós, J., and Paciucci, R. (2002). Tissue plasminogen activator is required for the growth, invasion, and angiogenesis of pancreatic tumor cells. Gastroenterology *122*, 806–819.

Discher, D.E., Mooney, D.J., and Zandstra, P.W. (2009). Growth factors, matrices, and forces combine and control stem cells. Science *324*, 1673–1677.

Dolberg, D.S., and Bissell, M.J. (1984). Inability of Rous sarcoma virus to cause sarcomas in the avian embryo. Nature *309*, 552–556.

Dupont, S., Morsut, L., Aragona, M., Enzo, E., Giulitti, S., Cordenonsi, M., Zanconato, F., Le Digabel, J., Forcato, M., Bicciato, S., et al. (2011). Role of YAP/TAZ in mechanotransduction. Nature *474*, 179–183.

El Hallani, S., Boisselier, B., Peglion, F., Rousseau, A., Colin, C., Idbaih, A., Marie, Y., Mokhtari, K., Thomas, J.-L., Eichmann, A., et al. (2010). A new alternative mechanism in glioblastoma vascularization: tubular vasculogenic mimicry. Brain *133*, 973–982.

El-Karef, A., Yoshida, T., Gabazza, E.C., Nishioka, T., Inada, H., Sakakura, T., and Imanaka-Yoshida, K. (2007). Deficiency of tenascin-C attenuates liver fibrosis in immune-mediated chronic hepatitis in mice. J. Pathol. *211*, 86–94.

Emoto, K., Yamada, Y., Sawada, H., Fujimoto, H., Ueno, M., Takayama, T., Kamada, K., Naito, A., Hirao, S., and Nakajima, Y. (2001). Annexin II overexpression correlates with stromal tenascin-C overexpression. Cancer *92*, 1419–1426.

Engler, A.J., Sen, S., Sweeney, H.L., and Discher, D.E. (2006). Matrix elasticity directs stem cell lineage specification. Cell *126*, 677–689.

Erler, J.T., and Weaver, V.M. (2009). Three-dimensional context regulation of metastasis. Clin. Exp. Metastasis *26*, 35–49.

Faissner, A., and Kruse, J. (1990). J1/tenascin is a repulsive substrate for central nervous system neurons. Neuron *5*, 627–637.

Faissner, A., and Reinhard, J. (2015). The extracellular matrix compartment of neural stem and glial progenitor cells. Glia *63*, 1330–1349.

Femel, J., Huijbers, E.J.M., Saupe, F., Cedervall, J., Zhang, L., Roswall, P., Larsson, E., Olofsson, H., Pietras, K., Dimberg, A., et al. (2014). Therapeutic vaccination against fibronectin ED-A attenuates progression of metastatic breast cancer. Oncotarget *5*, 12418–12427.

Flower, D.R. (1994). The lipocalin protein family: a role in cell regulation. FEBS Lett. *354*, 7–11.

Fluckinger, M., Haas, H., Merschak, P., Glasgow, B.J., and Redl, B. (2004). Human Tear Lipocalin Exhibits Antimicrobial Activity by Scavenging Microbial Siderophores. Antimicrob. Agents Chemother. *48*, 3367–3372.

Folkman, J. (1972). Anti-angiogenesis: new concept for therapy of solid tumors. Ann. Surg. *175*, 409–416.

Folkman, J. (1996). New perspectives in clinical oncology from angiogenesis research. Eur. J. Cancer Oxf. Engl. 1990 *32A*, 2534–2539.

Folkman, J., and Kalluri, R. (2004). Cancer without disease. Nature *427*, 787.

Folkman, J., Watson, K., Ingber, D., and Hanahan, D. (1989). Induction of angiogenesis during the transition from hyperplasia to neoplasia. Nature *339*, 58–61.

Foradori, M.J., Chen, Q., Fernandez, C.A., Harper, J., Li, X., Tsang, P.C.W., Langer, R., and Moses, M.A. (2014). Matrilin-1 Is an Inhibitor of Neovascularization. J. Biol. Chem. *289*, 14301–14309.

Forget, A., Christensen, J., Lüdeke, S., Kohler, E., Tobias, S., Matloubi, M., Thomann, R., and Shastri, V.P. (2013). Polysaccharide hydrogels with tunable stiffness and provasculogenic properties via α-helix to β-sheet switch in secondary structure. Proc. Natl. Acad. Sci. U. S. A. *110*, 12887–12892.

Forsberg, E., Hirsch, E., Fröhlich, L., Meyer, M., Ekblom, P., Aszodi, A., Werner, S., and Fässler, R. (1996). Skin wounds and severed nerves heal normally in mice lacking tenascin-C. Proc. Natl. Acad. Sci. U. S. A. *93*, 6594–6599.

Forsythe, J.A., Jiang, B.H., Iyer, N.V., Agani, F., Leung, S.W., Koos, R.D., and Semenza, G.L. (1996). Activation of vascular endothelial growth factor gene transcription by hypoxia-inducible factor 1. Mol. Cell. Biol. *16*, 4604–4613.

Frantz, C., Stewart, K.M., and Weaver, V.M. (2010). The extracellular matrix at a glance. J. Cell Sci. *123*, 4195–4200.

Fujimoto, M., Suzuki, H., Shiba, M., Shimojo, N., Imanaka-Yoshida, K., Yoshida, T., Kanamaru, K., Matsushima, S., and Taki, W. (2013). Tenascin-C induces prolonged constriction of cerebral arteries in rats. Neurobiol. Dis. *55*, 104–109.

Fukamauchi, F., Mataga, N., Wang, Y.-J., Sato, S., Yoshiki, A., and Kusakabe, M. (1996). Abnormal Behavior and Neurotransmissions of Tenascin Gene Knockout Mouse. Biochem. Biophys. Res. Commun. *221*, 151–156.

Galler, K., Junker, K., Franz, M., Hentschel, J., Richter, P., Gajda, M., Göhlert, A., Eggeling, F. von, Heller, R., Giavazzi, R., et al. (2011). Differential vascular expression and regulation of oncofetal tenascin-C and fibronectin variants in renal cell carcinoma (RCC): implications for an individualized angiogenesis-related targeted drug delivery. Histochem. Cell Biol. *137*, 195–204.

Geudens, I., and Gerhardt, H. (2011). Coordinating cell behaviour during blood vessel formation. Development *138*, 4569–4583.

Ghajar, C.M., Chen, X., Harris, J.W., Suresh, V., Hughes, C.C.W., Jeon, N.L., Putnam, A.J., and George, S.C. (2008). The Effect of Matrix Density on the Regulation of 3-D Capillary Morphogenesis. Biophys. J. *94*, 1930–1941.

Ghajar, C.M., Peinado, H., Mori, H., Matei, I.R., Evason, K.J., Brazier, H., Almeida, D., Koller, A., Hajjar, K.A., Stainier, D.Y.R., et al. (2013). The perivascular niche regulates breast tumour dormancy. Nat. Cell Biol. *15*, 807–817.

Giancotti, F.G., and Ruoslahti, E. (1999). Integrin signaling. Science *285*, 1028–1032.

Gibson, J.M., and Gibson, S.J. (2014). A safety evaluation of ranibizumab in the treatment of age-related macular degeneration. Expert Opin. Drug Saf. *13*, 1259–1270.

Gilbertson, R.J., and Rich, J.N. (2007). Making a tumour's bed: glioblastoma stem cells and the vascular niche. Nat Rev Cancer *7*, 733–736.

Girolamo, F., Coppola, C., Ribatti, D., and Trojano, M. (2014). Angiogenesis in multiple sclerosis and experimental autoimmune encephalomyelitis. Acta Neuropathol. Commun. *2*, 84.

Goepel, C., Buchmann, J., Schultka, R., and Koelbl, H. (2000). Tenascin—A Marker for the Malignant Potential of Preinvasive Breast Cancers. Gynecol. Oncol. *79*, 372–378.

Goetz, J.G., Minguet, S., Navarro-Lérida, I., Lazcano, J.J., Samaniego, R., Calvo, E., Tello, M., Osteso-Ibáñez, T., Pellinen, T., Echarri, A., et al. (2011). Biomechanical remodeling of the microenvironment by stromal caveolin-1 favors tumor invasion and metastasis. Cell *146*, 148–163.

Golebiewska, A., Bougnaud, S., Stieber, D., Brons, N.H.C., Vallar, L., Hertel, F., Klink, B., Schröck, E., Bjerkvig, R., and Niclou, S.P. (2013). Side population in human glioblastoma is non-tumorigenic and characterizes brain endothelial cells. Brain *136*, 1462–1475.

Golledge, J., Clancy, P., Maguire, J., Lincz, L., and Koblar, S. (2011). The role of tenascin C in cardiovascular disease. Cardiovasc. Res. *92*, 19–28.

Goodman, O.B., Febbraio, M., Simantov, R., Zheng, R., Shen, R., Silverstein, R.L., and Nanus, D.M. (2006). Neprilysin inhibits angiogenesis via proteolysis of fibroblast growth factor-2. J. Biol. Chem. *281*, 33597–33605.

Grahovac, J., Becker, D., and Wells, A. (2013). Melanoma cell invasiveness is promoted at least in part by the epidermal growth factor-like repeats of tenascin-C. J. Invest. Dermatol. *133*, 210–220.

Gravina, G.L., Mancini, A., Ranieri, G., Di Pasquale, B., Marampon, F., Di Clemente, L., Ricevuto, E., and Festuccia, C. (2013). Phenotypic characterization of human prostatic stromal cells in primary cultures derived from human tissue samples. Int. J. Oncol. *42*, 2116–2122.

Guntinas-Lichius, O., Angelov, D.N., Morellini, F., Lenzen, M., Skouras, E., Schachner, M., and Irintchev, A. (2005). Opposite impacts of tenascin-C and tenascin-R deficiency in mice on the functional outcome of facial nerve repair. Eur. J. Neurosci. *22*, 2171–2179.

Gutbrodt, K.L., Schliemann, C., Giovannoni, L., Frey, K., Pabst, T., Klapper, W., Berdel, W.E., and Neri, D. (2013). Antibody-Based Delivery of Interleukin-2 to Neovasculature Has Potent Activity Against Acute Myeloid Leukemia. Sci. Transl. Med. *5*, 201ra118–ra201ra118.

Halder, G., Dupont, S., and Piccolo, S. (2012). Transduction of mechanical and cytoskeletal cues by YAP and TAZ. Nat. Rev. Mol. Cell Biol. *13*, 591–600.

Han, D.K., Eng, J., Zhou, H., and Aebersold, R. (2001). Quantitative profiling of differentiation-induced microsomal proteins using isotope-coded affinity tags and mass spectrometry. Nat. Biotechnol. *19*, 946–951.

Hanahan, D. (1985). Heritable formation of pancreatic beta-cell tumours in transgenic mice expressing recombinant insulin/simian virus 40 oncogenes. Nature *315*, 115–122.

Hanahan, D., and Folkman, J. (1996). Patterns and emerging mechanisms of the angiogenic switch during tumorigenesis. Cell *86*, 353–364.

Hanahan, D., and Weinberg, R.A. (2000). The Hallmarks of Cancer. Cell *100*, 57–70.

Hanahan, D., and Weinberg, R.A. (2011). Hallmarks of Cancer: The Next Generation. Cell *144*, 646–674.

Hancox, R.A., Allen, M.D., Holliday, D.L., Edwards, D.R., Pennington, C.J., Guttery, D.S., Shaw, J.A., Walker, R.A., Pringle, J.H., and Jones, J.L. (2009). Tumour-associated tenascin-C isoforms promote breast cancer cell invasion and growth by matrix metalloproteinase-dependent and independent mechanisms. Breast Cancer Res. *11*, R24.

Harada, M., Kamimura, D., Arima, Y., Kohsaka, H., Nakatsuji, Y., Nishida, M., Atsumi, T., Meng, J., Bando, H., Singh, R., et al. (2015). Temporal Expression of Growth Factors Triggered by Epiregulin Regulates Inflammation Development. J. Immunol. 1400562.

Harburger, D.S., and Calderwood, D.A. (2009). Integrin signalling at a glance. J. Cell Sci. *122*, 159–163.

Haroon, Z.A., Hettasch, J.M., Lai, T.S., Dewhirst, M.W., and Greenberg, C.S. (1999). Tissue transglutaminase is expressed, active, and directly involved in rat dermal wound healing and angiogenesis. FASEB J. Off. Publ. Fed. Am. Soc. Exp. Biol. *13*, 1787–1795.

Hashizume, H., Baluk, P., Morikawa, S., McLean, J.W., Thurston, G., Roberge, S., Jain, R.K., and McDonald, D.M. (2000). Openings between Defective Endothelial Cells Explain Tumor Vessel Leakiness. Am. J. Pathol. *156*, 1363–1380.

Hau, P., Kunz-Schughart, L.A., Rümmele, P., Arslan, F., Dörfelt, A., Koch, H., Lohmeier, A., Hirschmann, B., Müller, A., Bogdahn, U., et al. (2006). Tenascin-C protein is induced by transforming growth factor-beta1 but does not correlate with time to tumor progression in high-grade gliomas. J. Neurooncol. *77*, 1–7.

Hauzenberger, D., Olivier, P., Gundersen, D., and Rüegg, C. (1999). Tenascin-C inhibits beta1 integrin-dependent T lymphocyte adhesion to fibronectin through the binding of its fnIII 1-5 repeats to fibronectin. Eur. J. Immunol. *29*, 1435–1447.

Haviv, I., Polyak, K., Qiu, W., Hu, M., and Campbell, I. (2009). Origin of carcinoma associated fibroblasts. Cell Cycle *8*, 589–595.

Hawkins, B.L., Heniford, B.W., Ackermann, D.M., Leonberger, M., Martinez, S.A., and Hendler, F.J. (1994). 4NQO carcinogenesis: a mouse model of oral cavity squamous cell carcinoma. Head Neck *16*, 424–432.

Heidenreich, R., Röcken, M., and Ghoreschi, K. (2009). Angiogenesis drives psoriasis pathogenesis. Int. J. Exp. Pathol. *90*, 232–248.

Heinonen, S.E., Kivelä, A.M., Huusko, J., Dijkstra, M.H., Gurzeler, E., Mäkinen, P.I., Leppänen, P., Olkkonen, V.M., Eriksson, U., Jauhiainen, M., et al. (2013). The effects of

VEGF-A on atherosclerosis, lipoprotein profile, and lipoprotein lipase in hyperlipidaemic mouse models. Cardiovasc. Res. *99*, 716–723.

Henry, L.R., Lee, H.-O., Lee, J.S., Klein-Szanto, A., Watts, P., Ross, E.A., Chen, W.-T., and Cheng, J.D. (2007). Clinical Implications of Fibroblast Activation Protein in Patients with Colon Cancer. Clin. Cancer Res. *13*, 1736–1741.

Herlyn, M., Graeven, U., Speicher, D., Sela, B.-A., Bennicelli, J.L., Kath, R., and Guerry, D. (1991). Characterization of Tenascin Secreted by Human Melanoma Cells. Cancer Res. *51*, 4853–4858.

Herold-Mende, C., Mueller, M.M., Bonsanto, M.M., Schmitt, H.P., Kunze, S., and Steiner, H.-H. (2002). Clinical impact and functional aspects of tenascin-C expression during glioma progression. Int. J. Cancer *98*, 362–369.

Herwig, L., Blum, Y., Krudewig, A., Ellertsdottir, E., Lenard, A., Belting, H.-G., and Affolter, M. (2011). Distinct cellular mechanisms of blood vessel fusion in the zebrafish embryo. Curr. Biol. CB *21*, 1942–1948.

Hicke, B.J., Stephens, A.W., Gould, T., Chang, Y.-F., Lynott, C.K., Heil, J., Borkowski, S., Hilger, C.-S., Cook, G., Warren, S., et al. (2006). Tumor targeting by an aptamer. J. Nucl. Med. Off. Publ. Soc. Nucl. Med. *47*, 668–678.

Higuchi, M., Ohnishi, T., Arita, N., Hiraga, S., and Hayakawa, T. (1993). Expression of tenascin in human gliomas: its relation to histological malignancy, tumor dedifferentiation and angiogenesis. Acta Neuropathol. (Berl.) *85*, 481–487.

Hilbe, W., Dirnhofer, S., Oberwasserlechner, F., Schmid, T., Gunsilius, E., Hilbe, G., Wöll, E., and Kähler, C.M. (2004). CD133 positive endothelial progenitor cells contribute to the tumour vasculature in non-small cell lung cancer. J. Clin. Pathol. *57*, 965–969.

Hirata, E., Arakawa, Y., Shirahata, M., Yamaguchi, M., Kishi, Y., Okada, T., Takahashi, J.A., Matsuda, M., and Hashimoto, N. (2009). Endogenous tenascin-C enhances glioblastoma invasion with reactive change of surrounding brain tissue. Cancer Sci. *100*, 1451–1459.

Ho, T.K., Tsui, J., Xu, S., Leoni, P., Abraham, D.J., and Baker, D.M. (2010). Angiogenic effects of stromal cell-derived factor-1 (SDF-1/CXCL12) variants in vitro and the in vivo expressions of CXCL12 variants and CXCR4 in human critical leg ischemia. J. Vasc. Surg. *51*, 689–699.

Hof, W. van't, Blankenvoorde, M.F.J., Veerman, E.C.I., and Amerongen, A.V.N. (1997). The Salivary Lipocalin Von Ebner's Gland Protein Is a Cysteine Proteinase Inhibitor. J. Biol. Chem. *272*, 1837–1841.

Huang, J.-Y., Cheng, Y.-J., Lin, Y.-P., Lin, H.-C., Su, C.-C., Juliano, R., and Yang, B.-C. (2010). Extracellular matrix of glioblastoma inhibits polarization and transmigration of T cells: the role of tenascin-C in immune suppression. J. Immunol. Baltim. Md 1950 *185*, 1450–1459.

Huang, W., Chiquet-Ehrismann, R., Moyano, J.V., Garcia-Pardo, A., and Orend, G. (2001a). Interference of tenascin-C with syndecan-4 binding to fibronectin blocks cell adhesion and stimulates tumor cell proliferation. Cancer Res. *61*, 8586–8594.

Huang, W., Chiquet-Ehrismann, R., Moyano, J.V., Garcia-Pardo, A., and Orend, G. (2001b). Interference of tenascin-C with syndecan-4 binding to fibronectin blocks cell adhesion and stimulates tumor cell proliferation. Cancer Res. *61*, 8586–8594.

Hur, J., Yoon, C.-H., Kim, H.-S., Choi, J.-H., Kang, H.-J., Hwang, K.-K., Oh, B.-H., Lee, M.-M., and Park, Y.-B. (2004). Characterization of Two Types of Endothelial Progenitor Cells and Their Different Contributions to Neovasculogenesis. Arterioscler. Thromb. Vasc. Biol. *24*, 288–293.

Hurwitz, H., Fehrenbacher, L., Novotny, W., Cartwright, T., Hainsworth, J., Heim, W., Berlin, J., Baron, A., Griffing, S., Holmgren, E., et al. (2004). Bevacizumab plus irinotecan, fluorouracil, and leucovorin for metastatic colorectal cancer. N. Engl. J. Med. *350*, 2335–2342.

Hwang, R.F., Moore, T., Arumugam, T., Ramachandran, V., Amos, K.D., Rivera, A., Ji, B., Evans, D.B., and Logsdon, C.D. (2008). Cancer-Associated Stromal Fibroblasts Promote Pancreatic Tumor Progression. Cancer Res. *68*, 918–926.

Hwang, S.-M., Jin, M., Shin, Y.H., Ki Choi, S., Namkoong, E., Kim, M., Park, M.-Y., and Park, K. (2014). Role of LPA and the Hippo pathway on apoptosis in salivary gland epithelial cells. Exp. Mol. Med. *46*, e125.

Hynes, R.O. (2009). The Extracellular Matrix: Not Just Pretty Fibrils. Science *326*, 1216–1219.

Hynes, R.O., and Yamada, K.M. (1982). Fibronectins: multifunctional modular glycoproteins. J. Cell Biol. *95*, 369–377.

Ikeshima-Kataoka, H., Shen, J.-S., Eto, Y., Saito, S., and Yuasa, S. (2008). Alteration of inflammatory cytokine production in the injured central nervous system of tenascin-deficient mice. Vivo Athens Greece *22*, 409–413.

Illmensee, K. (1978). Reversion of Malignancy and Normalized Differentiation of Teratocarcinoma Cells in Chimeric Mice. In Genetic Mosaics and Chimeras in Mammals, L.B. Russell, ed. (Springer US), pp. 3–25.

Imanaka-Yoshida, K., and Aoki, H. (2014). Tenascin-C and mechanotransduction in the development and diseases of cardiovascular system. Front. Physiol. *5*, 283.

Imanaka-Yoshida, K., Matsumoto, K., Hara, M., Sakakura, T., and Yoshida, T. (2003). The dynamic expression of tenascin-C and tenascin-X during early heart development in the mouse. Differ. Res. Biol. Divers. *71*, 291–298.

Ishihara, A., Yoshida, T., Tamaki, H., and Sakakura, T. (1995). Tenascin expression in cancer cells and stroma of human breast cancer and its prognostic significance. Clin. Cancer Res. *1*, 1035–1041.

Islam, M.S., Kusakabe, M., Horiguchi, K., Iino, S., Nakamura, T., Iwanaga, K., Hashimoto, H., Matsumoto, S., Murata, T., Hori, M., et al. (2014). PDGF and TGF-β promote tenascin-C expression in subepithelial myofibroblasts and contribute to intestinal mucosal protection in mice. Br. J. Pharmacol. *171*, 375–388.

Jachetti, E., Caputo, S., Mazzoleni, S., Brambillasca, C.S., Parigi, S.M., Grioni, M., Piras, I.S., Restuccia, U., Calcinotto, A., Freschi, M., et al. (2015). Tenascin-C Protects Cancer Stem-like Cells from Immune Surveillance by Arresting T-cell Activation. Cancer Res. *75*, 2095–2108.

Jain, R.K. (2005). Normalization of Tumor Vasculature: An Emerging Concept in Antiangiogenic Therapy. Science *307*, 58–62.

Jain, R.K. (2014). Antiangiogenesis Strategies Revisited: From Starving Tumors to Alleviating Hypoxia. Cancer Cell *26*, 605–622.

Jaipersad, A.S., Lip, G.Y.H., Silverman, S., and Shantsila, E. (2014). The Role of Monocytes in Angiogenesis and Atherosclerosis. J. Am. Coll. Cardiol. *63*, 1–11.

Jakovcevski, I., Miljkovic, D., Schachner, M., and Andjus, P.R. (2013). Tenascins and inflammation in disorders of the nervous system. Amino Acids *44*, 1115–1127.

Jia, C.-C., Wang, T.-T., Liu, W., Fu, B.-S., Hua, X., Wang, G.-Y., Li, T.-J., Li, X., Wu, X.-Y., Tai, Y., et al. (2013). Cancer-Associated Fibroblasts from Hepatocellular Carcinoma Promote Malignant Cell Proliferation by HGF Secretion. PLoS ONE *8*, e63243.

Jones, F.S., and Jones, P.L. (2000). The tenascin family of ECM glycoproteins: Structure, function, and regulation during embryonic development and tissue remodeling. Dev. Dyn. *218*, 235–259.

Jones, P.L., and Rabinovitch, M. (1996). Tenascin-C Is Induced With Progressive Pulmonary Vascular Disease in Rats and Is Functionally Related to Increased Smooth Muscle Cell Proliferation. Circ. Res. *79*, 1131–1142.

Jones, P.L., Crack, J., and Rabinovitch, M. (1997). Regulation of tenascin-C, a vascular smooth muscle cell survival factor that interacts with the alpha v beta 3 integrin to promote epidermal growth factor receptor phosphorylation and growth. J. Cell Biol. *139*, 279–293.

Julian Downward, S.B. (2009). YAP and p73: a complex affair. Mol. Cell *32*, 749–750.

Kääriäinen, E., Nummela, P., Soikkeli, J., Yin, M., Lukk, M., Jahkola, T., Virolainen, S., Ora, A., Ukkonen, E., Saksela, O., et al. (2006). Switch to an invasive growth phase in melanoma is associated with tenascin□C, fibronectin, and procollagen□I forming specific channel structures for invasion. J. Pathol. *210*, 181–191.

Kalluri, R. (2003). Basement membranes: structure, assembly and role in tumour angiogenesis. Nat. Rev. Cancer *3*, 422–433.

Kalluri, R., and Zeisberg, M. (2006). Fibroblasts in cancer. Nat. Rev. Cancer *6*, 392–401.

Kent, D.L. (2014). Age-related macular degeneration: beyond anti-angiogenesis. Mol. Vis. *20*, 46–55.

Kessner, D., Chambers, M., Burke, R., Agus, D., and Mallick, P. (2008). ProteoWizard: open source software for rapid proteomics tools development. Bioinformatics *24*, 2534–2536.

Keunen, O., Johansson, M., Oudin, A., Sanzey, M., Rahim, S.A.A., Fack, F., Thorsen, F., Taxt, T., Bartos, M., Jirik, R., et al. (2011). Anti-VEGF treatment reduces blood supply and increases tumor cell invasion in glioblastoma. Proc. Natl. Acad. Sci. *108*, 3749–3754.

Kharaishvili, G., Simkova, D., Bouchalova, K., Gachechiladze, M., Narsia, N., and Bouchal, J. (2014). The role of cancer-associated fibroblasts, solid stress and other microenvironmental factors in tumor progression and therapy resistance. Cancer Cell Int. *14*, 41.

Kiernan, B.W., Garcion, E., Ferguson, J., Frost, E.E., Torres, E.M., Dunnett, S.B., Saga, Y., Aizawa, S., Faissner, A., Kaur, R., et al. (1999). Myelination and behaviour of tenascin-C null transgenic mice. Eur. J. Neurosci. *11*, 3082–3092.

Kim, J.-H., Choi, D.S., Lee, O.-H., Oh, S.-H., Lippman, S.M., and Lee, H.-Y. (2011). Antiangiogenic antitumor activities of IGFBP-3 are mediated by IGF-independent suppression of Erk1/2 activation and Egr-1–mediated transcriptional events. Blood *118*, 2622–2631.

Kimura, T., Shiraishi, K., Furusho, A., Ito, S., Hirakata, S., Nishida, N., Yoshimura, K., Imanaka-Yoshida, K., Yoshida, T., Ikeda, Y., et al. (2014). Tenascin C protects aorta from acute dissection in mice. Sci. Rep. *4*, 4051.

Kirk, S., Frank, J.A., and Karlik, S. (2004). Angiogenesis in multiple sclerosis: is it good, bad or an epiphenomenon? J. Neurol. Sci. *217*, 125–130.

Kisker, O., Onizuka, S., Becker, C.M., Fannon, M., Flynn, E., D'Amato, R., Zetter, B., Folkman, J., Ray, R., Swamy, N., et al. (2003). Vitamin D binding protein-macrophage activating factor (DBP-maf) inhibits angiogenesis and tumor growth in mice. Neoplasia N. Y. N *5*, 32–40.

Kolodgie, F.D., Gold, H.K., Burke, A.P., Fowler, D.R., Kruth, H.S., Weber, D.K., Farb, A., Guerrero, L.J., Hayase, M., Kutys, R., et al. (2003). Intraplaque hemorrhage and progression of coronary atheroma. N. Engl. J. Med. *349*, 2316–2325.

Koperek, O., Bergner, O., Pichlhöfer, B., Oberndorfer, F., Hainfellner, J.A., Kaserer, K., Horvat, R., Harris, A.L., Niederle, B., and Birner, P. (2011). Expression of hypoxia-associated proteins in sporadic medullary thyroid cancer is associated with desmoplastic stroma reaction and lymph node metastasis and may indicate somatic mutations in the VHL gene. J. Pathol. *225*, 63–72.

Kreisl, T.N., Kim, L., Moore, K., Duic, P., Royce, C., Stroud, I., Garren, N., Mackey, M., Butman, J.A., Camphausen, K., et al. (2009). Phase II Trial of Single-Agent Bevacizumab Followed by Bevacizumab Plus Irinotecan at Tumor Progression in Recurrent Glioblastoma. J. Clin. Oncol. *27*, 740–745.

Kremer, J.M., Blanco, R., Brzosko, M., Burgos-Vargas, R., Halland, A.-M., Vernon, E., Ambs, P., and Fleischmann, R. (2011). Tocilizumab inhibits structural joint damage in rheumatoid arthritis patients with inadequate responses to methotrexate: results from the double-blind treatment phase of a randomized placebo-controlled trial of tocilizumab safety and prevention of structural joint damage at one year. Arthritis Rheum. *63*, 609–621.

Kryczek, I., Lange, A., Mottram, P., Alvarez, X., Cheng, P., Hogan, M., Moons, L., Wei, S., Zou, L., Machelon, V., et al. (2005). CXCL12 and Vascular Endothelial Growth Factor Synergistically Induce Neoangiogenesis in Human Ovarian Cancers. Cancer Res. *65*, 465–472.

Kulla, A., Liigant, A., Piirsoo, A., Rippin, G., and Asser, T. (2000). Tenascin Expression Patterns and Cells of Monocyte Lineage: Relationship in Human Gliomas. Mod. Pathol. *13*, 56–67.

Kuriyama, N., Duarte, S., Hamada, T., Busuttil, R.W., and Coito, A.J. (2011). Tenascin-C: a novel mediator of hepatic ischemia and reperfusion injury. Hepatol. Baltim. Md *54*, 2125–2136.

Kwok, J.C.F., Dick, G., Wang, D., and Fawcett, J.W. (2011). Extracellular matrix and perineuronal nets in CNS repair. Dev. Neurobiol. *71*, 1073–1089.

Lal, A., Peters, H., St Croix, B., Haroon, Z.A., Dewhirst, M.W., Strausberg, R.L., Kaanders, J.H., van der Kogel, A.J., and Riggins, G.J. (2001). Transcriptional response to hypoxia in human tumors. J. Natl. Cancer Inst. *93*, 1337–1343.

Lange, K., Kammerer, M., Hegi, M.E., Grotegut, S., Dittmann, A., Huang, W., Fluri, E., Yip, G.W., Götte, M., Ruiz, C., et al. (2007). Endothelin receptor type B counteracts tenascin-C-induced endothelin receptor type A-dependent focal adhesion and actin stress fiber disorganization. Cancer Res. *67*, 6163–6173.

Langlois, B., Saupe, F., Rupp, T., Arnold, C., Heyden, M.V. der, Orend, G., and Hussenet, T. (2014). AngioMatrix, a signature of the tumor angiogenic switch-specific matrisome, correlates with poor prognosis for glioma and colorectal cancer patients. Oncotarget *5*, 10529–10545.

Lanza, F., Gardellini, A., Laszlo, D., and Martino, M. (2015). Plerixafor: what we still have to learn. Expert Opin. Biol. Ther. *15*, 143–147.

Lapi, E., Di Agostino, S., Donzelli, S., Gal, H., Domany, E., Rechavi, G., Pandolfi, P.P., Givol, D., Strano, S., Lu, X., et al. (2008). PML, YAP, and p73 Are Components of a Proapoptotic Autoregulatory Feedback Loop. Mol. Cell *32*, 803–814.

Lawler, P.R., and Lawler, J. (2012). Molecular Basis for the Regulation of Angiogenesis by Thrombospondin-1 and -2. Cold Spring Harb. Perspect. Med. *2*.

Lee, C.-H., and Motzer, R.J. (2015). Sunitinib as a paradigm for tyrosine kinase inhibitor development for renal cell carcinoma. Urol. Oncol. *33*, 275–279.

Lee, S.S., Joo, Y.S., Kim, W.U., Min, D.J., Min, J.K., Park, S.H., Cho, C.S., and Kim, H.Y. (2001). Vascular endothelial growth factor levels in the serum and synovial fluid of patients with rheumatoid arthritis. Clin. Exp. Rheumatol. *19*, 321–324.

Leins, A., Riva, P., Lindstedt, R., Davidoff, M.S., Mehraein, P., and Weis, S. (2003). Expression of tenascin-C in various human brain tumors and its relevance for survival in patients with astrocytoma. Cancer *98*, 2430–2439.

Lengfeld, J., Cutforth, T., and Agalliu, D. (2014). The role of angiogenesis in the pathology of multiple sclerosis. Vasc. Cell *6*, 23.

Leu, S.-J., Lam, S.C.-T., and Lau, L.F. (2002). Pro-angiogenic Activities of CYR61 (CCN1) Mediated through Integrins αvβ3 and α6β1 in Human Umbilical Vein Endothelial Cells. J. Biol. Chem. *277*, 46248–46255.

Levental, K.R., Yu, H., Kass, L., Lakins, J.N., Egeblad, M., Erler, J.T., Fong, S.F.T., Csiszar, K., Giaccia, A., Weninger, W., et al. (2009). Matrix Crosslinking Forces Tumor Progression by Enhancing Integrin signaling. Cell *139*, 891–906.

Li (2009). Role of fibrillar Tenascin-C in metastatic pancreatic cancer. Int. J. Oncol. *34*.

Li, D., Mukai, K., Suzuki, T., Suzuki, R., Yamashita, S., Mitani, F., and Suematsu, M. (2007). Adrenocortical zonation factor 1 is a novel matricellular protein promoting integrin-mediated adhesion of adrenocortical and vascular smooth muscle cells. FEBS J. *274*, 2506–2522.

Lin, C., McGough, R., Aswad, B., Block, J.A., and Terek, R. (2004). Hypoxia induces HIF-1alpha and VEGF expression in chondrosarcoma cells and chondrocytes. J. Orthop. Res. Off. Publ. Orthop. Res. Soc. *22*, 1175–1181.

Lin, C.G., Leu, S.-J., Chen, N., Tebeau, C.M., Lin, S.-X., Yeung, C.-Y., and Lau, L.F. (2003). CCN3 (NOV) is a novel angiogenic regulator of the CCN protein family. J. Biol. Chem. *278*, 24200–24208.

Lorusso, G., and Rüegg, C. (2008). The tumor microenvironment and its contribution to tumor evolution toward metastasis. Histochem. Cell Biol. *130*, 1091–1103.

Louis, D.N., Ohgaki, H., Wiestler, O.D., Cavenee, W.K., Burger, P.C., Jouvet, A., Scheithauer, B.W., and Kleihues, P. (2007). The 2007 WHO Classification of Tumours of the Central Nervous System. Acta Neuropathol. (Berl.) *114*, 97–109.

Lowy, C.M., and Oskarsson, T. (2015). Tenascin C in metastasis: A view from the invasive front. Cell Adhes. Migr. *9*, 112–124.

Mackie, E.J., Scott-Burden, T., Hahn, A.W., Kern, F., Bernhardt, J., Regenass, S., Weller, A., and Bühler, F.R. (1992). Expression of tenascin by vascular smooth muscle cells. Alterations in hypertensive rats and stimulation by angiotensin II. Am. J. Pathol. *141*, 377–388.

Macmillan, C.J., Starkey, R.J., and Easton, A.S. (2011). Angiogenesis is regulated by angiopoietins during experimental autoimmune encephalomyelitis and is indirectly related to vascular permeability. J. Neuropathol. Exp. Neurol. *70*, 1107–1123.

Maffini, M.V., Soto, A.M., Calabro, J.M., Ucci, A.A., and Sonnenschein, C. (2004). The stroma as a crucial target in rat mammary gland carcinogenesis. J. Cell Sci. *117*, 1495–1502.

Mahesparan, R., Read, T.-A., Lund-Johansen, M., Skaftnesmo, K.O., Bjerkvig, R., and Engebraaten, O. (2003). Expression of extracellular matrix components in a highly infiltrative in vivo glioma model. Acta Neuropathol. (Berl.) *105*, 49–57.

Maione, F., Molla, F., Meda, C., Latini, R., Zentilin, L., Giacca, M., Seano, G., Serini, G., Bussolino, F., and Giraudo, E. (2009). Semaphorin 3A is an endogenous angiogenesis inhibitor that blocks tumor growth and normalizes tumor vasculature in transgenic mouse models. J. Clin. Invest. *119*, 3356–3372.

Maity, G., Mehta, S., Haque, I., Dhar, K., Sarkar, S., Banerjee, S.K., and Banerjee, S. (2014). Pancreatic tumor cell secreted CCN1/Cyr61 promotes endothelial cell migration and aberrant neovascularization. Sci. Rep. *4*, 4995.

Mancuso, M.R., Davis, R., Norberg, S.M., O'Brien, S., Sennino, B., Nakahara, T., Yao, V.J., Inai, T., Brooks, P., Freimark, B., et al. (2006). Rapid vascular regrowth in tumors after reversal of VEGF inhibition. J. Clin. Invest. *116*, 2610–2621.

Maniotis, A.J., Folberg, R., Hess, A., Seftor, E.A., Gardner, L.M.G., Pe'er, J., Trent, J.M., Meltzer, P.S., and Hendrix, M.J.C. (1999). Vascular Channel Formation by Human Melanoma Cells in Vivo and in Vitro: Vasculogenic Mimicry. Am. J. Pathol. *155*, 739–752.

Maris, C., Rorive, S., Sandras, F., D'Haene, N., Sadeghi, N., Bièche, I., Vidaud, M., Decaestecker, C., and Salmon, I. (2008). Tenascin-C expression relates to clinicopathological features in pilocytic and diffuse astrocytomas. Neuropathol. Appl. Neurobiol. *34*, 316–329.

Martens, L., Vandekerckhove, J., and Gevaert, K. (2005). DBToolkit: processing protein databases for peptide-centric proteomics. Bioinforma. Oxf. Engl. *21*, 3584–3585.

Martin, D., Brown-Luedi, M., and Chiquet-Ehrismann, R. (2003). Tenascin-C signaling through induction of 14-3-3 tau. J. Cell Biol. *160*, 171–175.

Martina, E., Degen, M., Rüegg, C., Merlo, A., Lino, M.M., Chiquet-Ehrismann, R., and Brellier, F. (2010). Tenascin-W is a specific marker of glioma-associated blood vessels and stimulates angiogenesis in vitro. FASEB J. *24*, 778–787.

Martino, M.M., Briquez, P.S., Ranga, A., Lutolf, M.P., and Hubbell, J.A. (2013). Heparin-binding domain of fibrin(ogen) binds growth factors and promotes tissue repair when incorporated within a synthetic matrix. Proc. Natl. Acad. Sci. U. S. A. *110*, 4563–4568.

Martino, M.M., Briquez, P.S., Güç, E., Tortelli, F., Kilarski, W.W., Metzger, S., Rice, J.J., Kuhn, G.A., Müller, R., Swartz, M.A., et al. (2014). Growth Factors Engineered for Super-Affinity to the Extracellular Matrix Enhance Tissue Healing. Science *343*, 885–888.

Masckauchán, T.N.H., and Kitajewski, J. (2006). Wnt/Frizzled Signaling in the Vasculature: New Angiogenic Factors in Sight. Physiology *21*, 181–188.

Masckauchán, T.N.H., Agalliu, D., Vorontchikhina, M., Ahn, A., Parmalee, N.L., Li, C.-M., Khoo, A., Tycko, B., Brown, A.M.C., and Kitajewski, J. (2006). Wnt5a Signaling Induces Proliferation and Survival of Endothelial Cells In Vitro and Expression of MMP-1 and Tie-2. Mol. Biol. Cell *17*, 5163–5172.

McCullough, K.D., Coleman, W.B., Ricketts, S.L., Wilson, J.W., Smith, G.J., and Grisham, J.W. (1998). Plasticity of the neoplastic phenotype in vivo is regulated by epigenetic factors. Proc. Natl. Acad. Sci. *95*, 15333–15338.

McDonald, D.M., and Choyke, P.L. (2003). Imaging of angiogenesis: from microscope to clinic. Nat. Med. *9*, 713–725.

McLendon, R.E., Wikstrand, C.J., Matthews, M.R., Al-Baradei, R., Bigner, S.H., and Bigner, D.D. (2000). Glioma-associated antigen expression in oligodendroglial neoplasms. Tenascin

and epidermal growth factor receptor. J. Histochem. Cytochem. Off. J. Histochem. Soc. *48*, 1103–1110.

Mertens, J.C., Fingas, C.D., Christensen, J.D., Smoot, R.L., Bronk, S.F., Werneburg, N.W., Gustafson, M.P., Dietz, A.B., Roberts, L.R., Sirica, A.E., et al. (2013). Therapeutic Effects of Deleting Cancer-Associated Fibroblasts in Cholangiocarcinoma. Cancer Res. *73*, 897–907.

Midgley, R., and Kerr, D. (2005). Bevacizumab—current status and future directions. Ann. Oncol. *16*, 999–1004.

Midwood, K.S., and Orend, G. (2009). The role of tenascin-C in tissue injury and tumorigenesis. J. Cell Commun. Signal. *3*, 287–310.

Midwood, K.S., and Schwarzbauer, J.E. (2002). Tenascin-C modulates matrix contraction via focal adhesion kinase- and Rho-mediated signaling pathways. Mol. Biol. Cell *13*, 3601–3613.

Midwood, K., Sacre, S., Piccinini, A.M., Inglis, J., Trebaul, A., Chan, E., Drexler, S., Sofat, N., Kashiwagi, M., Orend, G., et al. (2009). Tenascin-C is an endogenous activator of Toll-like receptor 4 that is essential for maintaining inflammation in arthritic joint disease. Nat. Med. *15*, 774–780.

Midwood, K.S., Hussenet, T., Langlois, B., and Orend, G. (2011). Advances in tenascin-C biology. Cell. Mol. Life Sci. *68*, 3175–3199.

Mitamura, Y., Takeuchi, S., Ohtsuka, K., Matsuda, A., Hiraiwa, N., and Kusakabe, M. (2002). Tenascin-C Levels in the Vitreous of Patients With Proliferative Diabetic Retinopathy. Diabetes Care *25*, 1899–1899.

Mitola, S., Ravelli, C., Moroni, E., Salvi, V., Leali, D., Ballmer-Hofer, K., Zammataro, L., and Presta, M. (2010). Gremlin is a novel agonist of the major proangiogenic receptor VEGFR2. Blood *116*, 3677–3680.

Mitselou, A., Skoufi, U., Tsimogiannis, K.E., Briasoulis, E., Vougiouklakis, T., Arvanitis, D., and Ioachim, E. (2012). Association of syndecan-1 with angiogenesis-related markers, extracellular matrix components, and clinicopathological features in colorectal carcinoma. Anticancer Res. *32*, 3977–3985.

Mongiat, M., Marastoni, S., Ligresti, G., Lorenzon, E., Schiappacassi, M., Perris, R., Frustaci, S., and Colombatti, A. (2010). The Extracellular Matrix Glycoprotein Elastin Microfibril Interface Located Protein 2: A Dual Role in the Tumor Microenvironment. Neoplasia N. Y. N *12*, 294–304.

Morellini, F., and Schachner, M. (2006). Enhanced novelty-induced activity, reduced anxiety, delayed resynchronization to daylight reversal and weaker muscle strength in tenascin-C-deficient mice. Eur. J. Neurosci. *23*, 1255–1268.

Mueller, M.M., and Fusenig, N.E. (2004). Friends or foes — bipolar effects of the tumour stroma in cancer. Nat. Rev. Cancer *4*, 839–849.

Murakami, M., Nguyen, L.T., Zhuang, Z.W., Zhang, Z.W., Moodie, K.L., Carmeliet, P., Stan, R.V., and Simons, M. (2008). The FGF system has a key role in regulating vascular integrity. J. Clin. Invest. *118*, 3355–3366.

Mustafa, D.A.M., Dekker, L.J., Stingl, C., Kremer, A., Stoop, M., Sillevis Smitt, P.A.E., Kros, J.M., and Luider, T.M. (2012). A proteome comparison between physiological angiogenesis and angiogenesis in glioblastoma. Mol. Cell. Proteomics MCP *11*, M111.008466.

Nagasaki, T., Hara, M., Nakanishi, H., Takahashi, H., Sato, M., and Takeyama, H. (2014). Interleukin-6 released by colon cancer-associated fibroblasts is critical for tumour angiogenesis: anti-interleukin-6 receptor antibody suppressed angiogenesis and inhibited tumour–stroma interaction. Br. J. Cancer *110*, 469–478.

Nakatsu, M.N., Davis, J., and Hughes, C.C.W. (2007). Optimized fibrin gel bead assay for the study of angiogenesis. J. Vis. Exp. JoVE 186.

Nash, B., Thomson, C.E., Linington, C., Arthur, A.T., McClure, J.D., McBride, M.W., and Barnett, S.C. (2011). Functional duality of astrocytes in myelination. J. Neurosci. Off. J. Soc. Neurosci. *31*, 13028–13038.

Natali, P.G., Nicotra, M.R., Bartolazzi, A., Mottolese, M., Coscia, N., Bigotti, A., and Zardi, L. (1990). Expression and production of tenascin in benign and malignant lesions of melanocyte lineage. Int. J. Cancer J. Int. Cancer *46*, 586–590.

Natali, P.G., Nicotra, M.R., Bigotti, A., Botti, C., Castellani, P., Risso, A.M., and Zardi, L. (1991). Comparative analysis of the expression of the extracellular matrix protein tenascin in normal human fetal, adult and tumor tissues. Int. J. Cancer J. Int. Cancer *47*, 811–816.

Nesvizhskii, A.I., Keller, A., Kolker, E., and Aebersold, R. (2003). A statistical model for identifying proteins by tandem mass spectrometry. Anal. Chem. *75*, 4646–4658.

Ng, E.W.M., and Adamis, A.P. (2005). Targeting angiogenesis, the underlying disorder in neovascular age-related macular degeneration. Can. J. Ophthalmol. J. Can. Ophtalmol. *40*, 352–368.

Nicholas, B.L., Skipp, P., Barton, S., Singh, D., Bagmane, D., Mould, R., Angco, G., Ward, J., Guha-Niyogi, B., Wilson, S., et al. (2010). Identification of Lipocalin and Apolipoprotein A1 as Biomarkers of Chronic Obstructive Pulmonary Disease. Am. J. Respir. Crit. Care Med. *181*, 1049–1060.

Nie, S., Gurrea, M., Zhu, J., Thakolwiboon, S., Heth, J.A., Muraszko, K.M., Fan, X., and Lubman, D.M. (2015). Tenascin-C: A Novel Candidate Marker for Cancer Stem Cells in Glioblastoma Identified by Tissue Microarrays. J. Proteome Res. *14*, 814–822.

Niewiarowska, J., Brézillon, S., Sacewicz-Hofman, I., Bednarek, R., Maquart, F.-X., Malinowski, M., Wiktorska, M., Wegrowski, Y., and Cierniewski, C.S. (2011). Lumican inhibits angiogenesis by interfering with α2β1 receptor activity and downregulating MMP-14 expression. Thromb. Res. *128*, 452–457.

Nilsson, M.B., Langley, R.R., and Fidler, I.J. (2005). Interleukin-6, Secreted by Human Ovarian Carcinoma Cells, Is a Potent Proangiogenic Cytokine. Cancer Res. *65*, 10794–10800.

Nishio, T., Kawaguchi, S., Yamamoto, M., Iseda, T., Kawasaki, T., and Hase, T. (2005). Tenascin-C regulates proliferation and migration of cultured astrocytes in a scratch wound assay. Neuroscience *132*, 87–102.

Nong, Y., Wu, D., Lin, Y., Zhang, Y., Bai, L., and Tang, H. (2015). Tenascin-C expression is associated with poor prognosis in hepatocellular carcinoma (HCC) patients and the inflammatory cytokine TNF-α-induced TNC expression promotes migration in HCC cells. Am. J. Cancer Res. *5*, 782–791.

Van Obberghen-Schilling, E., Tucker, R.P., Saupe, F., Gasser, I., Cseh, B., and Orend, G. (2011). Fibronectin and tenascin-C: accomplices in vascular morphogenesis during development and tumor growth. Int. J. Dev. Biol. *55*, 511–525.

O'Connell, J.T., Sugimoto, H., Cooke, V.G., MacDonald, B.A., Mehta, A.I., LeBleu, V.S., Dewar, R., Rocha, R.M., Brentani, R.R., Resnick, M.B., et al. (2011a). VEGF-A and Tenascin-C produced by S100A4+ stromal cells are important for metastatic colonization. Proc. Natl. Acad. Sci. *108*, 16002–16007.

O'Connell, J.T., Sugimoto, H., Cooke, V.G., MacDonald, B.A., Mehta, A.I., LeBleu, V.S., Dewar, R., Rocha, R.M., Brentani, R.R., Resnick, M.B., et al. (2011b). VEGF-A and Tenascin-C produced by S100A4+ stromal cells are important for metastatic colonization. Proc. Natl. Acad. Sci.

Öhlund, D., Lundin, C., Ardnor, B., Öman, M., Naredi, P., and Sund, M. (2009). Type IV collagen is a tumour stroma-derived biomarker for pancreas cancer. Br. J. Cancer *101*, 91–97.

Ohtsuka, M., Yamamoto, H., Oshiro, R., Takahashi, H., Masuzawa, T., Uemura, M., Haraguchi, N., Nishimura, J., Hata, T., Yamasaki, M., et al. (2013). Concurrent expression of C4.4A and Tenascin-C in tumor cells relates to poor prognosis of esophageal squamous cell carcinoma. Int. J. Oncol. *43*, 439–446.

Oliveira-Ferrer, L., Hauschild, J., Fiedler, W., Bokemeyer, C., Nippgen, J., Celik, I., and Schuch, G. (2008). Cilengitide induces cellular detachment and apoptosis in endothelial and glioma cells mediated by inhibition of FAK/src/AKT pathway. J. Exp. Clin. Cancer Res. *27*, 86.

Olumi, A.F., Dazin, P., and Tlsty, T.D. (1998). A novel coculture technique demonstrates that normal human prostatic fibroblasts contribute to tumor formation of LNCaP cells by retarding cell death. Cancer Res. *58*, 4525–4530.

Olumi, A.F., Grossfeld, G.D., Hayward, S.W., Carroll, P.R., Tlsty, T.D., and Cunha, G.R. (1999). Carcinoma-associated fibroblasts direct tumor progression of initiated human prostatic epithelium. Cancer Res. *59*, 5002–5011.

Ono, M. (2008). Molecular links between tumor angiogenesis and inflammation: inflammatory stimuli of macrophages and cancer cells as targets for therapeutic strategy. Cancer Sci. *99*, 1501–1506.

Orend, G. (2005). Potential oncogenic action of tenascin-C in tumorigenesis. Int. J. Biochem. Cell Biol. *37*, 1066–1083.

Orend, G., and Chiquet-Ehrismann, R. (2006). Tenascin-C induced signaling in cancer. Cancer Lett. *244*, 143–163.

Orend, G., Huang, W., Olayioye, M.A., Hynes, N.E., and Chiquet-Ehrismann, R. (2003). Tenascin-C blocks cell-cycle progression of anchorage-dependent fibroblasts on fibronectin through inhibition of syndecan-4. Oncogene *22*, 3917–3926.

Orend, G., Saupe, F., Schwenzer, A., and Midwood, K. (2014). The extracellular matrix and cancer: regulation of tumor cell biology by tenascin-C.

Orimo, A., Gupta, P.B., Sgroi, D.C., Arenzana-Seisdedos, F., Delaunay, T., Naeem, R., Carey, V.J., Richardson, A.L., and Weinberg, R.A. (2005). Stromal Fibroblasts Present in Invasive Human Breast Carcinomas Promote Tumor Growth and Angiogenesis through Elevated SDF-1/CXCL12 Secretion. Cell *121*, 335–348.

Oskarsson, T., Acharyya, S., Zhang, X.H.-F., Vanharanta, S., Tavazoie, S.F., Morris, P.G., Downey, R.J., Manova-Todorova, K., Brogi, E., and Massagué, J. (2011). Breast cancer cells produce tenascin C as a metastatic niche component to colonize the lungs. Nat. Med. *17*, 867–874.

Page, T.H., Charles, P.J., Piccinini, A.M., Nicolaidou, V., Taylor, P.C., and Midwood, K.S. (2012). Raised circulating tenascin-C in rheumatoid arthritis. Arthritis Res. Ther. *14*, 1–9.

Paleolog, E.M. (2009). The vasculature in rheumatoid arthritis: cause or consequence? Int. J. Exp. Pathol. *90*, 249–261.

Papadimitriou, E., Mikelis, C., Lampropoulou, E., Koutsioumpa, M., Theochari, K., Tsirmoula, S., Theodoropoulou, C., Lamprou, M., Sfaelou, E., Vourtsis, D., et al. (2009). Roles of pleiotrophin in tumor growth and angiogenesis. Eur. Cytokine Netw. *20*, 180–190.

Paszek, M.J., Zahir, N., Johnson, K.R., Lakins, J.N., Rozenberg, G.I., Gefen, A., Reinhart-King, C.A., Margulies, S.S., Dembo, M., Boettiger, D., et al. (2005). Tensional homeostasis and the malignant phenotype. Cancer Cell *8*, 241–254.

Patel, L., Sun, W., Glasson, S.S., Morris, E.A., Flannery, C.R., and Chockalingam, P.S. (2011). Tenascin-C induces inflammatory mediators and matrix degradation in osteoarthritic cartilage. BMC Musculoskelet. Disord. *12*, 164.

Pedretti, M., Rancic, Z., Soltermann, A., Herzog, B.A., Schliemann, C., Lachat, M., Neri, D., and Kaufmann, P.A. (2010a). Comparative immunohistochemical staining of atherosclerotic plaques using F16, F8 and L19: Three clinical-grade fully human antibodies. Atherosclerosis *208*, 382–389.

Pedretti, M., Verpelli, C., Mårlind, J., Bertani, G., Sala, C., Neri, D., and Bello, L. (2010b). Combination of temozolomide with immunocytokine F16-IL2 for the treatment of glioblastoma. Br. J. Cancer *103*, 827–836.

Pedrioli, P.G.A., Eng, J.K., Hubley, R., Vogelzang, M., Deutsch, E.W., Raught, B., Pratt, B., Nilsson, E., Angeletti, R.H., Apweiler, R., et al. (2004). A common open representation of mass spectrometry data and its application to proteomics research. Nat. Biotechnol. *22*, 1459–1466.

Perez-Pinera, P., Berenson, J.R., and Deuel, T.F. (2008). Pleiotrophin, a multifunctional angiogenic factor: mechanisms and pathways in normal and pathological angiogenesis. Curr. Opin. Hematol. *15*, 210–214.

Peter, N.R., Shah, R.T., Chen, J., Irintchev, A., and Schachner, M. (2012). Adhesion molecules close homolog of L1 and tenascin-C affect blood–spinal cord barrier repair: NeuroReport *23*, 479–482.

Peters, B.A., Diaz, L.A., Polyak, K., Meszler, L., Romans, K., Guinan, E.C., Antin, J.H., Myerson, D., Hamilton, S.R., Vogelstein, B., et al. (2005). Contribution of bone marrow-derived endothelial cells to human tumor vasculature. Nat. Med. *11*, 261–262.

Pezzolo, A., Parodi, F., Marimpietri, D., Raffaghello, L., Cocco, C., Pistorio, A., Mosconi, M., Gambini, C., Cilli, M., Deaglio, S., et al. (2011). Oct-4+/Tenascin C+ neuroblastoma cells serve as progenitors of tumor-derived endothelial cells. Cell Res. *21*, 1470–1486.

Pike, S.E., Yao, L., Jones, K.D., Cherney, B., Appella, E., Sakaguchi, K., Nakhasi, H., Teruya-Feldstein, J., Wirth, P., Gupta, G., et al. (1998). Vasostatin, a Calreticulin Fragment, Inhibits Angiogenesis and Suppresses Tumor Growth. J. Exp. Med. *188*, 2349–2356.

Pilarczyk, K., Sattler, K.J.E., Galili, O., Versari, D., Olson, M.L., Meyer, F.B., Zhu, X.-Y., Lerman, L.O., and Lerman, A. (2008). Placenta growth factor expression in human atherosclerotic carotid plaques is related to plaque destabilization. Atherosclerosis *196*, 333–340.

Ping, Y., Yao, X., Jiang, J., Zhao, L., Yu, S., Jiang, T., Lin, M.C., Chen, J., Wang, B., Zhang, R., et al. (2011). The chemokine CXCL12 and its receptor CXCR4 promote glioma stem cell-mediated VEGF production and tumour angiogenesis via PI3K/AKT signalling. J. Pathol. *224*, 344–354.

Pipp, F., Boehm, S., Cai, W.-J., Adili, F., Ziegler, B., Karanovic, G., Ritter, R., Balzer, J., Scheler, C., Schaper, W., et al. (2004). Elevated fluid shear stress enhances postocclusive collateral artery growth and gene expression in the pig hind limb. Arterioscler. Thromb. Vasc. Biol. *24*, 1664–1668.

Posern, G. (2002). Mutant Actins Demonstrate a Role for Unpolymerized Actin in Control of Transcription by Serum Response Factor. Mol. Biol. Cell *13*, 4167–4178.

Pugsley, M.K., and Tabrizchi, R. (2000). The vascular system: An overview of structure and function. J. Pharmacol. Toxicol. Methods *44*, 333–340.

Quail, D., and Joyce, J. (2013). Microenvironmental regulation of tumor progression and metastasis. Nat. Med. *19*, 1423–1437.

Rafii, S., and Lyden, D. (2008). A Few to Flip the Angiogenic Switch. Science *319*, 163–164.

Rafii, S., Lyden, D., Benezra, R., Hattori, K., and Heissig, B. (2002). Vascular and haematopoietic stem cells: novel targets for anti-angiogenesis therapy? Nat. Rev. Cancer *2*, 826–835.

Rascher, G., Fischmann, A., Kröger, S., Duffner, F., Grote, E.-H., and Wolburg, H. (2002). Extracellular matrix and the blood-brain barrier in glioblastoma multiforme: spatial segregation of tenascin and agrin. Acta Neuropathol. (Berl.) *104*, 85–91.

Redl, B., Wojnar, P., Ellemunter, H., and Feichtinger, H. (1998). Identification of a lipocalin in mucosal glands of the human tracheobronchial tree and its enhanced secretion in cystic fibrosis. Lab. Investig. J. Tech. Methods Pathol. *78*, 1121–1129.

Reis, M., Czupalla, C.J., Ziegler, N., Devraj, K., Zinke, J., Seidel, S., Heck, R., Thom, S., Macas, J., Bockamp, E., et al. (2012). Endothelial Wnt/β-catenin signaling inhibits glioma angiogenesis and normalizes tumor blood vessels by inducing PDGF-B expression. J. Exp. Med. *209*, 1611–1627.

Renkonen, S., Heikkilä, P., Haglund, C., Mäkitie, A.A., and Hagström, J. (2013). Tenascin-C, GLUT-1, and syndecan-2 expression in juvenile nasopharyngeal angiofibroma: correlations to vessel density and tumor stage. Head Neck *35*, 1036–1042.

Rhee, S., and Grinnell, F. (2006). P21-activated kinase 1: convergence point in PDGF- and LPA-stimulated collagen matrix contraction by human fibroblasts. J. Cell Biol. *172*, 423–432.

Rho, S.B., Dong, S.M., Kang, S., Seo, S.-S., Yoo, C.W., Lee, D.O., Woo, J.S., and Park, S.-Y. (2008). Insulin-like growth factor-binding protein-5 (IGFBP-5) acts as a tumor suppressor by inhibiting angiogenesis. Carcinogenesis *29*, 2106–2111.

Ribble, D., Goldstein, N.B., Norris, D.A., and Shellman, Y.G. (2005). A simple technique for quantifying apoptosis in 96-well plates. BMC Biotechnol. *5*, 12.

Ricci-Vitiani, L., Pallini, R., Biffoni, M., Todaro, M., Invernici, G., Cenci, T., Maira, G., Parati, E.A., Stassi, G., Larocca, L.M., et al. (2010). Tumour vascularization via endothelial differentiation of glioblastoma stem-like cells. Nature *468*, 824–828.

Ridley, A.J., Schwartz, M.A., Burridge, K., Firtel, R.A., Ginsberg, M.H., Borisy, G., Parsons, J.T., and Horwitz, A.R. (2003). Cell Migration: Integrating Signals from Front to Back. Science *302*, 1704–1709.

Rivard, A., Fabre, J.E., Silver, M., Chen, D., Murohara, T., Kearney, M., Magner, M., Asahara, T., and Isner, J.M. (1999). Age-dependent impairment of angiogenesis. Circulation *99*, 111–120.

Roduit, C., Sekatski, S., Dietler, G., Catsicas, S., Lafont, F., and Kasas, S. (2009). Stiffness Tomography by Atomic Force Microscopy. Biophys. J. *97*, 674–677.

Rolle, K., Nowak, S., Wyszko, E., Nowak, M., Zukiel, R., Piestrzeniewicz, R., Gawronska, I., Barciszewska, M.Z., and Barciszewski, J. (2010). Promising human brain tumors therapy with interference RNA intervention (iRNAi). Cancer Biol. Ther. *9*, 396–406.

Roskoski, R. (2007). Vascular endothelial growth factor (VEGF) signaling in tumor progression. Crit. Rev. Oncol. Hematol. *62*, 179–213.

Roskoski Jr., R. (2007). Sunitinib: A VEGF and PDGF receptor protein kinase and angiogenesis inhibitor. Biochem. Biophys. Res. Commun. *356*, 323–328.

Rüegg, C.R., Chiquet-Ehrismann, R., and Alkan, S.S. (1989). Tenascin, an extracellular matrix protein, exerts immunomodulatory activities. Proc. Natl. Acad. Sci. U. S. A. *86*, 7437–7441.

Ruiz, C. (2004). Differential Gene Expression Analysis Reveals Activation of Growth Promoting Signaling Pathways by Tenascin-C. Cancer Res. *64*, 7377–7385.

Sadanandam, A., Rosenbaugh, E.G., Singh, S., Varney, M., and Singh, R.K. (2010). Semaphorin 5A promotes angiogenesis by increasing endothelial cell proliferation, migration, and decreasing apoptosis. Microvasc. Res. *79*, 1–9.

Sadanandam, A., Sidhu, S.S., Wullschleger, S., Singh, S., Varney, M.L., Yang, C.-S., Ashour, A.E., Batra, S.K., and Singh, R.K. (2012). Secreted semaphorin 5A suppressed pancreatic tumour burden but increased metastasis and endothelial cell proliferation. Br. J. Cancer *107*, 501–507.

Saga, Y., Yagi, T., Ikawa, Y., Sakakura, T., and Aizawa, S. (1992). Mice develop normally without tenascin. Genes Dev. *6*, 1821–1831.

Sailer, M.H.M., Gerber, A., Tostado, C., Hutter, G., Cordier, D., Mariani, L., and Ritz, M.-F. (2013). Non-invasive neural stem cells become invasive in vitro by combined FGF2 and BMP4 signaling. J. Cell Sci. *126*, 3533–3540.

Saito, Y., Shiota, Y., Nishisaka, M., Owaki, T., Shimamura, M., and Fukai, F. (2008a). Inhibition of angiogenesis by a tenascin-c peptide which is capable of activating beta1-integrins. Biol. Pharm. Bull. *31*, 1003–1007.

Saito, Y., Shiota, Y., Nishisaka, M., Owaki, T., Shimamura, M., and Fukai, F. (2008b). Inhibition of Angiogenesis by a Tenascin-C Peptide which Is Capable of Activating Beta1-Integrins. Biol. Pharm. Bull. *31*, 1003–1007.

Salmenkivi, K., Haglund, C., Arola, J., and Heikkilä, P. (2001). Increased expression of tenascin in pheochromocytomas correlates with malignancy. Am. J. Surg. Pathol. *25*, 1419–1423.

Sarkar, S., Nuttall, R.K., Liu, S., Edwards, D.R., and Yong, V.W. (2006). Tenascin-C Stimulates Glioma Cell Invasion through Matrix Metalloproteinase-12. Cancer Res. *66*, 11771–11780.

Sarkar, S., Zemp, F.J., Senger, D., Robbins, S.M., and Yong, V.W. (2015). ADAM-9 is a novel mediator of tenascin-C-stimulated invasiveness of brain tumor-initiating cells. Neuro-Oncol. *17*, 1095–1105.

Saupe, F., Schwenzer, A., Jia, Y., Gasser, I., Spenlé, C., Langlois, B., Kammerer, M., Lefebvre, O., Hlushchuk, R., Rupp, T., et al. (2013). Tenascin-C Downregulates Wnt Inhibitor Dickkopf-1, Promoting Tumorigenesis in a Neuroendocrine Tumor Model. Cell Rep. *5*, 482–492.

Schaff, M., Receveur, N., Bourdon, C., Wurtz, V., Denis, C.V., Orend, G., Gachet, C., Lanza, F., and Mangin, P.H. (2011). Novel Function of Tenascin-C, a Matrix Protein Relevant to Atherosclerosis, in Platelet Recruitment and Activation Under Flow. Arterioscler. Thromb. Vasc. Biol. *31*, 117–124.

Scharenberg, M.A., Pippenger, B.E., Sack, R., Zingg, D., Ferralli, J., Schenk, S., Martin, I., and Chiquet-Ehrismann, R. (2014). TGF-β-induced differentiation into myofibroblasts involves specific regulation of two MKL1 isoforms. J. Cell Sci. *127*, 1079–1091.

Schenk, S., Chiquet-Ehrismann, R., and Battegay, E.J. (1999). The Fibrinogen Globe of Tenascin-C Promotes Basic Fibroblast Growth Factor-induced Endothelial Cell Elongation. Mol Biol Cell *10*, 2933–2943.

Schirmer, S.H., Nooijen, F.C. van, Piek, J.J., and Royen, N. van (2009). Stimulation of collateral artery growth: travelling further down the road to clinical application. Heart *95*, 191–197.

Schliemann, C., Gutbrodt, K.L., Kerkhoff, A., Pohlen, M., Wiebe, S., Silling, G., Angenendt, L., Kessler, T., Mesters, R.M., Giovannoni, L., et al. (2015). Targeting Interleukin-2 to the Bone Marrow Stroma for Therapy of Acute Myeloid Leukemia Relapsing after Allogeneic Hematopoietic Stem Cell Transplantation. Cancer Immunol. Res. *3*, 547–556.

Schmeichel, K.L., Weaver, V.M., and Bissell, M.J. (1998). Structural Cues from the Tissue Microenvironment Are Essential Determinants of the Human Mammary Epithelial Cell Phenotype. J. Mammary Gland Biol. Neoplasia *3*, 201–213.

Schmid, M.K., Bachmann, L.M., Fäs, L., Kessels, A.G., Job, O.M., and Thiel, M.A. (2015). Efficacy and adverse events of aflibercept, ranibizumab and bevacizumab in age-related macular degeneration: a trade-off analysis. Br. J. Ophthalmol. *99*, 141–146.

Schnapp, L.M., Hatch, N., Ramos, D.M., Klimanskaya, I.V., Sheppard, D., and Pytela, R. (1995). The human integrin alpha 8 beta 1 functions as a receptor for tenascin, fibronectin, and vitronectin. J. Biol. Chem. *270*, 23196–23202.

SCHOLZE, A., GÖTZ, B., and FAISSNER, R. (1996). GLIAL CELL INTERACTIONS WITH TENASCIN-C: ADHESION AND REPULSION TO DIFFERENT TENASCIN-C DOMAINS IS CELL TYPE RELATED. Int. J. Dev. Neurosci. *14*, 315–329.

Schoop, R.A.L., Noteborn, M.H.M., and Baatenburg de Jong, R.J. (2009). A mouse model for oral squamous cell carcinoma. J. Mol. Histol. *40*, 177–181.

Schwartz, M. (2004). Rho signalling at a glance. J. Cell Sci. *117*, 5457–5458.

Seabrook, T.J., Littlewood-Evans, A., Brinkmann, V., Pöllinger, B., Schnell, C., and Hiestand, P.C. (2010). Angiogenesis is present in experimental autoimmune encephalomyelitis and pro-angiogenic factors are increased in multiple sclerosis lesions. J. Neuroinflammation *7*, 95.

Sennino, B., Ishiguro-Oonuma, T., Wei, Y., Naylor, R.M., Williamson, C.W., Bhagwandin, V., Tabruyn, S.P., You, W.-K., Chapman, H.A., Christensen, J.G., et al. (2012). Suppression of tumor invasion and metastasis by concurrent inhibition of c-Met and VEGF signaling in pancreatic neuroendocrine tumors. Cancer Discov. *2*, 270–287.

Shahinian, H., Loessner, D., Biniossek, M.L., Kizhakkedathu, J.N., Clements, J.A., Magdolen, V., and Schilling, O. (2014). Secretome and degradome profiling shows that Kallikrein-related peptidases 4, 5, 6, and 7 induce TGFβ-1 signaling in ovarian cancer cells. Mol. Oncol. *8*, 68–82.

Sharma, B., and Albig, A.R. (2013). Matrix Gla protein reinforces angiogenic resolution. Microvasc. Res. *85*, 24–33.

Sharma, B., Ramus, M.D., Kirkwood, C.T., Sperry, E.E., Chu, P.-H., Kao, W.W., and Albig, A.R. (2013). Lumican exhibits anti-angiogenic activity in a context specific manner. Cancer Microenviron. Off. J. Int. Cancer Microenviron. Soc. *6*, 263–271.

Shellenberger, T.D., Wang, M., Gujrati, M., Jayakumar, A., Strieter, R.M., Burdick, M.D., Ioannides, C.G., Efferson, C.L., El-Naggar, A.K., Roberts, D., et al. (2004). BRAK/CXCL14 is a potent inhibitor of angiogenesis and a chemotactic factor for immature dendritic cells. Cancer Res. *64*, 8262–8270.

Shim, B.-S., Kang, B.-H., Hong, Y.-K., Kim, H.-K., Lee, I.-H., Lee, S.-Y., Lee, Y.-J., Lee, S.-K., and Joe, Y.A. (2005). The kringle domain of tissue-type plasminogen activator inhibits in vivo tumor growth. Biochem. Biophys. Res. Commun. *327*, 1155–1162.

Shimojo, N., Hashizume, R., Kanayama, K., Hara, M., Suzuki, Y., Nishioka, T., Hiroe, M., Yoshida, T., and Imanaka-Yoshida, K. (2015). Tenascin-C May Accelerate Cardiac Fibrosis by Activating Macrophages via the Integrin αVβ3/Nuclear Factor–κB/Interleukin-6 Axis. Hypertension HYPERTENSIONAHA.115.06004.

Sierko, E., Wojtukiewicz, M.Z., and Kisiel, W. (2007). The role of tissue factor pathway inhibitor-2 in cancer biology. Semin. Thromb. Hemost. *33*, 653–659.

Sieveking, D.P., Buckle, A., Celermajer, D.S., and Ng, M.K.C. (2008). Strikingly Different Angiogenic Properties of Endothelial Progenitor Cell Subpopulations: Insights From a Novel Human Angiogenesis Assay. J. Am. Coll. Cardiol. *51*, 660–668.

Silvestre, J.-S. (2012). Pro-angiogenic cell-based therapy for the treatment of ischemic cardiovascular diseases. Thromb. Res. *130 Suppl 1*, S90–S94.

Simian, M., Hirai, Y., Navre, M., Werb, Z., Lochter, A., and Bissell, M.J. (2001). The interplay of matrix metalloproteinases, morphogens and growth factors is necessary for branching of mammary epithelial cells. Development *128*, 3117–3131.

Simon-Assmann, P., Orend, G., Mammadova-Bach, E., Spenlé, C., and Lefebvre, O. (2011). Role of laminins in physiological and pathological angiogenesis. Int. J. Dev. Biol. *55*, 455–465.

Sirica, A.E. (2012). The role of cancer-associated myofibroblasts in intrahepatic cholangiocarcinoma. Nat. Rev. Gastroenterol. Hepatol. *9*, 44–54.

Sivasankaran, B., Degen, M., Ghaffari, A., Hegi, M.E., Hamou, M.-F., Ionescu, M.-C.S., Zweifel, C., Tolnay, M., Wasner, M., Mergenthaler, S., et al. (2009). Tenascin-C Is a Novel RBPJκ-Induced Target Gene for Notch Signaling in Gliomas. Cancer Res. *69*, 458–465.

Slevin, M., Krupinski, J., and Badimon, L. (2009). Controlling the angiogenic switch in developing atherosclerotic plaques: Possible targets for therapeutic intervention. Vasc. Cell *1*, 4.

Smith, G.M., and Hale, J.H. (1997). Macrophage/Microglia regulation of astrocytic tenascin: synergistic action of transforming growth factor-beta and basic fibroblast growth factor. J. Neurosci. Off. J. Soc. Neurosci. *17*, 9624–9633.

Sone, H., Sakauchi, M., Takahashi, A., Suzuki, H., Inoue, N., Iida, K., Shimano, H., Toyoshima, H., Kawakami, Y., Okuda, Y., et al. (2001). Elevated levels of vascular endothelial growth factor in the sera of patients with rheumatoid arthritis correlation with disease activity. Life Sci. *69*, 1861–1869.

Sonnenschein, C., and Soto, A.M. (2000). Somatic mutation theory of carcinogenesis: why it should be dropped and replaced. Mol. Carcinog. *29*, 205–211.

Spaeth, E.L., Dembinski, J.L., Sasser, A.K., Watson, K., Klopp, A., Hall, B., Andreeff, M., and Marini, F. (2009). Mesenchymal stem cell transition to tumor-associated fibroblasts contributes to fibrovascular network expansion and tumor progression. PloS One *4*, e4992.

Spenlé, C., Gasser, I., Saupe, F., Janssen, K.-P., Arnold, C., Klein, A., van der Heyden, M., Mutterer, J., Neuville-Méchine, A., Chenard, M.-P., et al. (2015). Spatial organization of the tenascin-C microenvironment in experimental and human cancer. Cell Adhes. Migr. *9*, 4–13.

De Spiegelaere, W., Casteleyn, C., Van den Broeck, W., Plendl, J., Bahramsoltani, M., Simoens, P., Djonov, V., and Cornillie, P. (2012). Intussusceptive angiogenesis: a biologically relevant form of angiogenesis. J. Vasc. Res. *49*, 390–404.

Sriramarao, P., Mendler, M., and Bourdon, M.A. (1993). Endothelial Cell Attachment and Spreading on Human Tenascin Is Mediated by Alpha 2 Beta 1 and Alpha V Beta 3 Integrins. J. Cell Sci. *105*, 1001–1012.

Stallcup, W.B., and Huang, F.-J. (2008). A role for the NG2 proteoglycan in glioma progression. Cell Adh Migr *2*, 192–201.

Stegemann, C., Didangelos, A., Barallobre-Barreiro, J., Langley, S.R., Mandal, K., Jahangiri, M., and Mayr, M. (2013). Proteomic identification of matrix metalloproteinase substrates in the human vasculature. Circ. Cardiovasc. Genet. *6*, 106–117.

Stewart, T.A., and Mintz, B. (1981). Successive generations of mice produced from an established culture line of euploid teratocarcinoma cells. Proc. Natl. Acad. Sci. U. S. A. *78*, 6314–6318.

Stupp, R., Hegi, M.E., Gorlia, T., Erridge, S.C., Perry, J., Hong, Y.-K., Aldape, K.D., Lhermitte, B., Pietsch, T., Grujicic, D., et al., European Organisation for Research and Treatment of Cancer (EORTC), Canadian Brain Tumor Consortium, and CENTRIC study team (2014). Cilengitide combined with standard treatment for patients with newly diagnosed glioblastoma with methylated MGMT promoter (CENTRIC EORTC 26071-22072 study): a multicentre, randomised, open-label, phase 3 trial. Lancet Oncol. *15*, 1100–1108.

Sumioka, T., Fujita, N., Kitano, A., Okada, Y., and Saika, S. (2011). Impaired angiogenic response in the cornea of mice lacking tenascin C. Invest. Ophthalmol. Vis. Sci. *52*, 2462–2467.

Swartz, D.J., and Santi, P.A. (1996). Immunofluorescent artifacts due to the pH of antifading mounting media. BioTechniques *20*, 398–400.

Swindle, C.S., Tran, K.T., Johnson, T.D., Banerjee, P., Mayes, A.M., Griffith, L., and Wells, A. (2001). Epidermal Growth Factor (EGF)-Like Repeats of Human Tenascin-C as Ligands for EGF Receptor. J. Cell Biol. *154*, 459–468.

SZEKANECZ, Z., BESENYEI, T., PARAGH, G., and KOCH, A.E. (2009). Angiogenesis in rheumatoid arthritis. Autoimmunity *42*, 563–573.

Tamaoki, M., Imanaka-Yoshida, K., Yokoyama, K., Nishioka, T., Inada, H., Hiroe, M., Sakakura, T., and Yoshida, T. (2005). Tenascin-C Regulates Recruitment of Myofibroblasts during Tissue Repair after Myocardial Injury. Am. J. Pathol. *167*, 71–80.

Tanaka, K., Hiraiwa, N., Hashimoto, H., Yamazaki, Y., and Kusakabe, M. (2003). Tenascin□C regulates angiogenesis in tumor through the regulation of vascular endothelial growth factor expression. Int. J. Cancer *108*, 31–40.

Tang, Y.-A., Chen, C.-H., Sun, H.S., Cheng, C.-P., Tseng, V.S., Hsu, H.-S., Su, W.-C., Lai, W.-W., and Wang, Y.-C. (2015). Global Oct4 target gene analysis reveals novel downstream PTEN and TNC genes required for drug-resistance and metastasis in lung cancer. Nucleic Acids Res. *43*, 1593–1608.

Taraseviciute, A., Vincent, B.T., Schedin, P., and Jones, P.L. (2010). Quantitative analysis of three-dimensional human mammary epithelial tissue architecture reveals a role for tenascin-C in regulating c-met function. Am. J. Pathol. *176*, 827–838.

Terai, Y., Abe, M., Miyamoto, K., Koike, M., Yamasaki, M., Ueda, M., Ueki, M., and Sato, Y. (2001). Vascular smooth muscle cell growth-promoting factor/F-spondin inhibits angiogenesis via the blockade of integrin alphavbeta3 on vascular endothelial cells. J. Cell. Physiol. *188*, 394–402.

Tholen, S., Biniossek, M.L., Gessler, A.-L., Müller, S., Weisser, J., Kizhakkedathu, J.N., Reinheckel, T., and Schilling, O. (2011). Contribution of cathepsin L to secretome composition and cleavage pattern of mouse embryonic fibroblasts. Biol. Chem. *392*, 961–971.

Tholen, S., Biniossek, M.L., Gansz, M., Gomez-Auli, A., Bengsch, F., Noel, A., Kizhakkedathu, J.N., Boerries, M., Busch, H., Reinheckel, T., et al. (2013). Deletion of cysteine cathepsins B or L yields differential impacts on murine skin proteome and degradome. Mol. Cell. Proteomics MCP *12*, 611–625.

Torsvik, A., Stieber, D., Enger, P.Ø., Golebiewska, A., Molven, A., Svendsen, A., Westermark, B., Niclou, S.P., Olsen, T.K., Chekenya Enger, M., et al. (2014). U-251 revisited: genetic drift and phenotypic consequences of long-term cultures of glioblastoma cells. Cancer Med. *3*, 812–824.

Trescher, K., Thometich, B., Demyanets, S., Kassal, H., Sedivy, R., Bittner, R., Holzinger, C., and Podesser, B.K. (2013). Type A dissection and chronic dilatation: tenascin-C as a key factor in destabilization of the aortic wall. Interact. Cardiovasc. Thorac. Surg. *17*, 365–370.

Tschumperlin, D.J. (2015). Matrix, mesenchyme, and mechanotransduction. Ann. Am. Thorac. Soc. *12 Suppl 1*, S24–S29.

Tschumperlin, D., Varelas, X., and Liu, F. (2014). YAP and TAZ drive matrix stiffness-dependent fibroblast activation (1180.6). FASEB J. *28*, 1180.6.

Tsujino, T., Seshimo, I., Yamamoto, H., Ngan, C.Y., Ezumi, K., Takemasa, I., Ikeda, M., Sekimoto, M., Matsuura, N., and Monden, M. (2007). Stromal Myofibroblasts Predict Disease Recurrence for Colorectal Cancer. Clin. Cancer Res. *13*, 2082–2090.

Tyan, S.-W., Kuo, W.-H., Huang, C.-K., Pan, C.-C., Shew, J.-Y., Chang, K.-J., Lee, E.Y.-H.P., and Lee, W.-H. (2011). Breast Cancer Cells Induce Cancer-Associated Fibroblasts to Secrete Hepatocyte Growth Factor to Enhance Breast Tumorigenesis. PLoS ONE *6*, e15313.

Untergasser, G., Gander, R., Lilg, C., Lepperdinger, G., Plas, E., and Berger, P. (2005). Profiling molecular targets of TGF-beta1 in prostate fibroblast-to-myofibroblast transdifferentiation. Mech. Ageing Dev. *126*, 59–69.

Urech, L., Bittermann, A.G., Hubbell, J.A., and Hall, H. (2005). Mechanical properties, proteolytic degradability and biological modifications affect angiogenic process extension into native and modified fibrin matrices in vitro. Biomaterials *26*, 1369–1379.

Vagnucci, A.H., and Li, W.W. (2003). Alzheimer's disease and angiogenesis. Lancet *361*, 605–608.

Varga, I., Hutóczki, G., Szemcsák, C., Zahuczky, G., Tóth, J., Adamecz, Z., Kenyeres, A., Bognár, L., Hanzély, Z., and Klekner, A. (2012). Brevican, Neurocan, Tenascin-C and Versican are Mainly Responsible for the Invasiveness of Low-Grade Astrocytoma. Pathol. Oncol. Res. *18*, 413–420.

Vincent, F., Bonnin, P., Clemessy, M., Contrerès, J.-O., Lamandé, N., Gasc, J.-M., Vilar, J., Hainaud, P., Tobelem, G., Corvol, P., et al. (2009). Angiotensinogen delays angiogenesis and tumor growth of hepatocarcinoma in transgenic mice. Cancer Res. *69*, 2853–2860.

Vjetrovic, J., Shankaranarayanan, P., Mendoza-Parra, M.A., and Gronemeyer, H. (2014). Senescence-secreted factors activate Myc and sensitize pretransformed cells to TRAIL-induced apoptosis. Aging Cell *13*, 487–496.

Vredenburgh, J.J., Desjardins, A., Herndon, J.E., Marcello, J., Reardon, D.A., Quinn, J.A., Rich, J.N., Sathornsumetee, S., Gururangan, S., Sampson, J., et al. (2007). Bevacizumab Plus Irinotecan in Recurrent Glioblastoma Multiforme. J. Clin. Oncol. *25*, 4722–4729.

Wallner, K., Li, C., Shah, P.K., Fishbein, M.C., Forrester, J.S., Kaul, S., and Sharifi, B.G. (1999). Tenascin-C Is Expressed in Macrophage-Rich Human Coronary Atherosclerotic Plaque. Circulation *99*, 1284–1289.

Wang, L., Wang, W., Shah, P.K., Song, L., Yang, M., and Sharifi, B.G. (2012). Deletion of tenascin-C gene exacerbates atherosclerosis and induces intraplaque hemorrhage in Apo-E-deficient mice. Cardiovasc. Pathol. Off. J. Soc. Cardiovasc. Pathol. *21*, 398–413.

Wang, L., Shah, P.K., Wang, W., Song, L., Yang, M., and Sharifi, B.G. (2013a). Tenascin-C deficiency in apo E−/− mouse increases eotaxin levels: Implications for atherosclerosis. Atherosclerosis *227*, 267–274.

Wang, X., Li, Y., Gao, S., Xia, W., Gao, K., Kong, Q., Qi, H., Wu, L., Zhang, J., Qu, J., et al. (2014). Increased serum levels of lipocalin-1 and -2 in patients with stable chronic obstructive pulmonary disease. Int. J. Chron. Obstruct. Pulmon. Dis. *9*, 543–549.

Wang, Z., Perez, M., Caja, S., Melino, G., Johnson, T.S., Lindfors, K., and Griffin, M. (2013b). A novel extracellular role for tissue transglutaminase in matrix-bound VEGF-mediated angiogenesis. Cell Death Dis. *4*, e808.

Wen, P.Y., and Kesari, S. (2008). Malignant gliomas in adults. N. Engl. J. Med. *359*, 492–507.

Wenk, M.B., Midwood, K.S., and Schwarzbauer, J.E. (2000). Tenascin-C Suppresses Rho Activation. J. Cell Biol. *150*, 913–920.

De Wever, O., Nguyen, Q.-D., Van Hoorde, L., Bracke, M., Bruyneel, E., Gespach, C., and Mareel, M. (2004). Tenascin-C and SF/HGF produced by myofibroblasts in vitro provide convergent pro-invasive signals to human colon cancer cells through RhoA and Rac. FASEB J. Off. Publ. Fed. Am. Soc. Exp. Biol. *18*, 1016–1018.

Wiese, S., Karus, M., and Faissner, A. (2012). Astrocytes as a source for extracellular matrix molecules and cytokines. Neuropharmacology *3*, 120.

Wijelath, E.S., Murray, J., Rahman, S., Patel, Y., Ishida, A., Strand, K., Aziz, S., Cardona, C., Hammond, W.P., Savidge, G.F., et al. (2002). Novel Vascular Endothelial Growth Factor Binding Domains of Fibronectin Enhance Vascular Endothelial Growth Factor Biological Activity. Circ. Res. *91*, 25–31.

Wijelath, E.S., Rahman, S., Namekata, M., Murray, J., Nishimura, T., Mostafavi-Pour, Z., Patel, Y., Suda, Y., Humphries, M.J., and Sobel, M. (2006). Heparin-II domain of fibronectin is a vascular endothelial growth factor-binding domain: enhancement of VEGF biological activity by a singular growth factor/matrix protein synergism. Circ. Res. *99*, 853–860.

Wojnar, P., van't Hof, W., Merschak, P., Lechner, M., and Redl, B. (2001). The N-terminal part of recombinant human tear lipocalin/von Ebner's gland protein confers cysteine proteinase inhibition depending on the presence of the entire cystatin-like sequence motifs. Biol. Chem. *382*, 1515–1520.

Xie, Q., Chen, J., Feng, H., Peng, S., Adams, U., Bai, Y., Huang, L., Li, J., Huang, J., Meng, S., et al. (2013). YAP/TEAD-mediated transcription controls cellular senescence. Cancer Res. *73*, 3615–3624.

Xu, S., and Venge, P. (2000). Lipocalins as biochemical markers of disease. Biochim. Biophys. Acta BBA - Protein Struct. Mol. Enzymol. *1482*, 298–307.

Yamada, S., Bu, X.-Y., Khankaldyyan, V., Gonzales-Gomez, I., McComb, J.G., and Laug, W.E. (2006). Effect of the angiogenesis inhibitor Cilengitide (EMD 121974) on glioblastoma growth in nude mice. Neurosurgery *59*, 1304–1312; discussion 1312.

Yang, J., McNeish, B., Butterfield, C., and Moses, M.A. (2013). Lipocalin 2 is a novel regulator of angiogenesis in human breast cancer. FASEB J. *27*, 45–50.

Yao, J., Liu, X., Yang, Q., Zhuang, M., Wang, F., Chen, X., Hang, H., Zhang, W., and Liu, Q. (2013). Proteomic analysis of the aqueous humor in patients with wet age-related macular degeneration. PROTEOMICS – Clin. Appl. *7*, 550–560.

Yao, Y., Jumabay, M., Wang, A., and Boström, K.I. (2011). Matrix Gla protein deficiency causes arteriovenous malformations in mice. J. Clin. Invest. *121*, 2993–3004.

Yeo, E.-J., Cassetta, L., Qian, B.-Z., Lewkowich, I., Li, J., Stefater, J.A., Smith, A.N., Wiechmann, L.S., Wang, Y., Pollard, J.W., et al. (2014). Myeloid WNT7b mediates the angiogenic switch and metastasis in breast cancer. Cancer Res. *74*, 2962–2973.

Yokosaki, Y., Palmer, E.L., Prieto, A.L., Crossin, K.L., Bourdon, M.A., Pytela, R., and Sheppard, D. (1994). The integrin alpha 9 beta 1 mediates cell attachment to a non-RGD site in the third fibronectin type III repeat of tenascin. J. Biol. Chem. *269*, 26691–26696.

Yokosaki, Y., Monis, H., Chen, J., and Sheppard, D. (1996). Differential Effects of the Integrins α9β1, αvβ3, and αvβ6 on Cell Proliferative Responses to Tenascin ROLES OF THE β SUBUNIT EXTRACELLULAR AND CYTOPLASMIC DOMAINS. J. Biol. Chem. *271*, 24144–24150.

Yoo, A.R., and Chung, S.K. (2014). Effects of subconjunctival tocilizumab versus bevacizumab in treatment of corneal neovascularization in rabbits. Cornea *33*, 1088–1094.

Yoshimura, H., Michishita, M., Ohkusu-Tsukada, K., and Takahashi, K. (2011). Increased presence of stromal myofibroblasts and tenascin-C with malignant progression in canine mammary tumors. Vet. Pathol. *48*, 313–321.

Yu, Y.-M., Cristofanilli, M., Valiveti, A., Ma, L., Yoo, M., Morellini, F., and Schachner, M. (2011). The extracellular matrix glycoprotein tenascin-C promotes locomotor recovery after spinal cord injury in adult zebrafish. Neuroscience *183*, 238–250.

Yusifov, T.N., Abduragimov, A.R., Gasymov, O.K., and Glasgow, B.J. (2000). Endonuclease activity in lipocalins. Biochem. J. *347*, 815–819.

Zagzag, D., and Capo, V. (2002). Angiogenesis in the central nervous system: a role for vascular endothelial growth factor/vascular permeability factor and tenascin-C. Common molecular effectors in cerebral neoplastic and non-neoplastic “angiogenic diseases.” Histol. Histopathol. *17*, 301–321.

Zagzag, D., Friedlander, D.R., Miller, D.C., Dosik, J., Cangiarella, J., Kostianovsky, M., Cohen, H., Grumet, M., and Alba Greco, M. (1995). Tenascin Expression in Astrocytomas Correlates with Angiogenesis. Cancer Res. *55*, 907–914.

Zagzag, D., Friedlander, D.R., Dosik, J., Chikramane, S., Chan, W., Greco, M.A., Allen, J.C., Dorovini-Zis, K., and Grumet, M. (1996). Tenascin-C Expression by Angiogenic Vessels in Human Astrocytomas and by Human Brain Endothelial Cells in Vitro. Cancer Res. *56*, 182–189.

Zagzag, D., Shiff, B., Jallo, G.I., Greco, M.A., Blanco, C., Cohen, H., Hukin, J., Allen, J.C., and Friedlander, D.R. (2002). Tenascin-C promotes microvascular cell migration and phosphorylation of focal adhesion kinase. Cancer Res. *62*, 2660–2668.

Zhang, C., Lu, L., Li, Y., Wang, X., Zhou, J., Liu, Y., Fu, P., Gallicchio, M.A., Bach, L.A., and Duan, C. (2012). IGF binding protein-6 expression in vascular endothelial cells is induced by hypoxia and plays a negative role in tumor angiogenesis. Int. J. Cancer J. Int. Cancer *130*, 2003–2012.

Zhang, Z., Kim, S.-J., Chowdhury, B., Wang, J., Lee, Y.-C., Tsai, P.-C., Choi, M., and Mukherjee, A.B. (2006). Interaction of uteroglobin with lipocalin-1 receptor suppresses cancer cell motility and invasion. Gene *369*, 66–71.

Zhao, B., Li, L., Lei, Q., and Guan, K.-L. (2010). The Hippo–YAP pathway in organ size control and tumorigenesis: an updated version. Genes Dev. *24*, 862–874.

Zukiel, R., Nowak, S., Wyszko, E., Rolle, K., Gawronska, I., Barciszewska, M.Z., and Barciszewski, J. (2006). Suppression of human brain tumor with interference RNA specific for tenascin-C. Cancer Biol. Ther. *5*, 1002–1007.

Manuscripts

Tenascin-C promotes tumor angiogenesis through pro-angiogenic and anti-angiogenic effects involving CXCR4 and YAP signaling

Tristan Rupp[1-4]+, Benoit Langlois[1-4]+, Maria M Koczorowska[5-7], Agata Radwanska[8], Thomas Hussenet[1-4], Devadarsson Murdamothoo[1-4], Olivier Lefebvre[1-4], Christiane Arnold[1-4], Annick Klein[1-4], Michael van der Heyden[1-4], Martin L Biniossek[5], Elise Naudin[1], Oliver Schilling[5-7], Ellen Van Obberghen-Schilling[8] and Gertraud Orend[1-4] *

+ equal contribution

* corresponding author

gertraud.orend@inserm.fr, Phone: 0033 (0)3 88 27 53 55

[1] INSERM U1109 - MN3T, The Microenvironmental Niche in Tumorigenesis and Targeted Therapy, 3 avenue Molière, 67200 Strasbourg, France

[2] Université de Strasbourg, Strasbourg, 67000, France

[3] LabEx Medalis, Université de Strasbourg, Strasbourg, 67000, France

[4] Fédération de Médecine Translationnelle de Strasbourg (FMTS), Strasbourg, 67000, France

[5] Institute of Molecular Medicine and Cell Research, University of Freiburg, D-79104 Freiburg, Germany

[6] BIOSS Centre for Biological Signalling Studies, University of Freiburg, D-79104 Freiburg, Germany

[7] German Cancer Consortium (DKTK), German Cancer Research Center (DKFZ), D-69120 Heidelberg, Germany

[8] University of Nice Sophia Antipolis, UFR Sciences, Inserm, U1091 CNRS, UMR7277, Nice, France.

Abstract

The extracellular matrix molecule tenascin-C (TNC), an important component of the tumor microenvironment, promotes multiple steps in cancer progression and correlates with worsened survival prognosis. TNC promotes the tumor angiogenic switch resulting in more but poorly functional blood vessels by ill defined mechanisms. We studied the impact of TNC on the behavior of vascular and tumor cells in ex vivo and in vitro assays. We showed that the number of vessel sprouts from aortic rings was increased from TNC knockout tissue and that in vitro endothelial tubulogenesis and migration was repressed by TNC. This could be due to reduced cell adhesion to a TNC substratum which promoted death of endothelial cells. We linked reduced cell adhesion by TNC to disruption of the actin cytoskeleton and subsequent cytoplasmic localization of F-actin sensing factor YAP, resulting in downregulation of YAP regulated pro-angiogenic molecules. In tumor cells and cancer associated fibroblasts, TNC regulated secretion of angio-modulatory factors that promoted endothelial cell survival and tubulogenesis in a paracrine manner. Proteomic analysis revealed that TNC induced pro-angiogenic molecules, amongst them stromal derived factor 1 (SDF1). Upon inhibition of CXCR4 signaling we confirmed SDF1 as important pro-angiogenic effector of TNC. Altogether, TNC promotes endothelial tubulogenesis through a pro-angiogenic secretome from tumor cells, and inhibits tubulogenesis by impairing endothelial cell survival. These opposing effects could explain that TNC promotes more but poorly functional tumor blood vessels. This knowledge provides for the first time opportunities to counteract TNC activities in tumor angiogenesis.

Introduction

The formation of new blood vessels is a crucial step promoting metastasis (Carmeliet and Jain, 2000). Tenascin-C (TNC) is an extracellular matrix molecule (ECM) selectively expressed during embryonic development and in pathologies including cancer. TNC is highly abundant in the tumor microenvironment and modulates tumor angiogenesis (Herold-Mende et al., 2002; Langlois et al., 2014; Martina et al., 2010; Saupe et al., 2013). High TNC levels correlated with tumor vessel density, pericyte coverage and vessel leakiness suggesting that TNC plays multiple roles in angiogenesis with potentially opposing functions (Saupe et al., 2013). How this is mechanistically accomplished is largely unknown. In the neuroendocrine Rip1Tag2 (Hanahan, 1985) model TNC downregulated the Wnt inhibitor Dickkopf-1 (DKK1) which correlated with enhanced Wnt signaling and vessel density. Moreover, TNC also plays a role at the onset of tumor angiogenesis, the angiogenic switch, as it is one of the most highly induced genes (Langlois et al., 2014). A functional link of TNC promoting the angiogenic switch is supported since in its absence more and upon ectopic overexpression less angiogenic pancreatic islets were counted (Langlois et al., 2014).

We aimed to get more insight into the roles of TNC in tumor angiogenesis by determining whether and how TNC affects normal sprouting angiogenesis and endothelial tubulogenesis. We used the ex vivo aortic ring and retinal angiogenesis assays. Whereas no differences were seen in retinal angiogenesis between TNC KO and wt mice we observed that aortic sprouting angiogenesis was negatively impacted by TNC. This unexpected result was further confirmed in in vitro endothelial tubulogenesis assays where again TNC had a negative effect. Subsequently, we determined EC adhesion, survival, proliferation and migration and saw that TNC blocked these behaviors. We concluded that a direct interaction of EC with TNC may elicit an anti-angiogenic response. We wanted to understand the underlying molecular mechanism and identified cytoplasmic localization of

YAP (Yes associated protein), due to impaired cell adhesion, as an important downstream mechanism that resulted in downregulation of pro-angiogenic factors CTGF and Cyr61 (Brigstock, 2002; Maity et al., 2014). In search for a pro-angiogenic mechanism we identified that adhesion to a TNC substratum induced a pro-angiogenic secretome in tumor cells and carcinoma associated fibroblasts (CAF). Upon analysis of the proteome we identified SDF1 (stromal cell-derived factor 1 or CXCL12) as an important molecule upregulated by TNC in tumor cells. Its associated signaling largely promoted the paracrine pro-angiogenic effect of TNC since inhibition of CXCR4 signaling significantly reduced the pro-angiogenic activity of this TNC-induced secretome.

Our study revealed cellular and molecular insight into the multiple effects of TNC on tumor angiogenesis showing that TNC exerts direct anti-angiogenic activities towards EC and paracrine pro-angiogenic activities through tumor cells and CAF. This information is of potential interest to block these TNC activities in angiogenesis driving tumor progression.

Results

Reduced vessel sprouts from aortic rings and endothelial cell tubulogenesis in coculture assays

We used tissue from TNC KO and wt mice (**Fig. S1A**), respectively in an aortic ring assay, to determine sprouting angiogenesis in dependence of TNC. The sprouts were composed of endothelial cells (EC) and mural cells as determined by staining for isolectin B4 and α-smooth muscle actin (αSMA), respectively and expressed TNC (**Fig. S1B**). Interestingly we detected TNC expression around the endothelial sprouts (**Fig. S1C**). We observed that the number and length of endothelial sprouts was higher in the absence of TNC suggesting a negative impact of TNC on vessel formation in this assay (**Fig. 1A - C**). We also used a retinal angiogenesis assay from tissue of TNC KO and wt mice (**Fig. S1D**) and determined sprouting angiogenesis in dependence of TNC. Whereas the outgrowth of the vascular network was slightly reduced (<5%), the number of branching points and endothelial filopodia density was similar in the TNC KO context suggesting that TNC does not play a major role in this angiogenic process (**Fig. S1E - G**).

Fibroblasts have been described as a major source of TNC in a breast cancer model (O'Connell et al., 2011a) and were shown to play an important role in promoting tumor angiogenesis (Kalluri and Zeisberg, 2006). Therefore, we had used CAF as provider of TNC (**Fig. 1D**) and cocultured them with EC, to create a vascular network and mimic their spatial vicinity seen in a tumor context (Ghajar et al., 2013). Upon staining with an anti-CD31 antibody we visualized tube-like structures and quantified them as read out for network complexity. We observed that HUVEC had formed tubes after 7 days (**Fig. 1E**). Since CAF expressed TNC in culture, we generated cells with reduced TNC levels by shRNA knockdown (KD) (**Fig. 1D**) and determined whether TNC secreted by these cells had an impact on tubulogenesis. We observed more tube-like structures when HUVEC were grown together with CAF

harboring a TNC KD. In comparison to CAF with TNC wt levels this number was 2.7-fold higher. This result suggests that TNC expressed by CAF represses endothelial tubulogenesis (**Fig. 1E, F**). To address whether HUVEC also expressed TNC we determined TNC expression in HUVEC by western blot. We did not detect TNC expression in HUVEC under any conditions tested that would trigger tubulogenesis such as upon plating cells on gelatin, matrigel nor upon stimulation with growth factors that had been shown to promote angiogenesis (VEGFA (Carmeliet, 2003) and TGFβ (Cunha and Pietras, 2011)) or TNC expression (TGFβ (Scharenberg et al., 2014)), respectively (**Fig. S1L, M**). Similarly, also other human EC (HUAEC, HMEC, HMVEC) (**Fig. S1N**) or bovine aortic endothelial cells (BAEC) (Radwanska et al., in preparation) did not express TNC in culture (**Fig. S1M**). Thus we conclude that TNC provided by CAF represses tubulogenesis of HUVEC in the coculture assay.

Contact with TNC represses tubulogenesis, and cell adhesion and migration

So far our results suggested that TNC negatively impacts on endothelial sprouting and tubulogenesis which could be a result of a direct interaction with TNC. Therefore, we addressed whether contact of EC with purified recombinant TNC has an impact on their tubulogenic behavior. We added TNC to HUVEC and BAEC in a matrigel tubulogenesis assay. Whereas the length and the number of closed circles of tube-like structures of HUVEC were the highest in the control conditions, both numbers were reduced in a dose-dependent manner upon addition of TNC (**Fig. 2A - C**). TNC also reduced the number of tubes formed by BAEC (**Fig. S2A, B**). This result suggests that contact of EC with TNC has a negative impact on their tubulogenic behavior. Since tubulogenesis is largely dependent on cell adhesion and migration (Carmeliet, 2003) and TNC is an adhesion modulatory ECM molecule (Chiquet-Ehrismann et al., 1988), the observed effect may be due to TNC affecting cell adhesion and/or migration of EC. We determined cell numbers upon plating HUVEC and BAEC for 1h on TNC, fibronectin (FN) and type I collagen (Col I), respectively. We saw that whereas all cells attached and

spread on FN and Col I they poorly adhered and did not spread on the TNC substratum (**Fig. 2D, E, Fig. S2C, D**).

Pericytes play an important role in maturation of blood vessels (Carmeliet, 2003) and were seen to poorly cover tumor blood vessels in tumors expressing highly abundant TNC (Saupe et al., 2013). To address whether TNC potentially had an impact on pericyte adhesion, we plated human brain vascular pericytes (HBVP) on the different substrata. We observed again that whereas all cells adhered and spread on FN and Col I, only a few cells adhered (and remained rounded) on TNC at 5h after plating (**Fig. 2F, Fig. S2E**).

We addressed cell migration by a scratch "wound healing" assay and observed that migration of HUVEC, BAEC and pericytes was reduced by TNC in a dose dependent manner down to 40% (HUVEC), 60% (BAEC) and 40% (pericytes) in comparison to control treatment, with the highest dose of TNC (10 and 20 µg/ml, respectively) (**Fig. 2G - I, Fig. S2F - H**).

By video time lapse microscopy we also addressed the role of TNC on cell migration in more detail. We observed that in comparison to a FN substratum, TNC delayed HUVEC spreading (**Fig. S2I**) and reduced cell mobility (**Fig. S2J**).

Impact of TNC on survival and proliferation of endothelial cells and pericytes

Until now we had shown that cell contact with TNC impairs cell adhesion and migration, which could explain repression of tubulogenesis by TNC. We wanted to know whether impaired cell adhesion affected survival and/or proliferation of EC. We used MTS incorporation to determine cell multiplicity

and compared cell numbers on TNC with that on FN and Col I substrata, respectively after 24h, 48h and 72h. Whereas HUVEC and BAEC expanded on FN and Col I over the 3 days time course, cell numbers only slightly increased on TNC in the same time frame suggesting an inhibitory effect of TNC on cell multiplicity (**Fig. 3A, B, Fig. S3A**). This inhibitory effect was dose dependent (**Fig. S3A**, IC50 = 3.665 +/- 0.652 µg/cm^2). In contrast to EC, despite a delayed cell adhesion on TNC, multiplicity of pericytes was unaffected by TNC and was similar to that seen on the FN and Col I substrata suggesting a cell type specific effect of TNC (**Fig. 3C**).

To mimic the three dimensional (3D) matrix environment we used cell derived matrices (CDM) with abundant and no TNC. CDM had been generated and deposited by mouse embryo fibroblasts (MEF) according to (Beacham et al., 2007) derived from TNC KO or wt mice. By immunofluorescence (IF) imaging we confirmed that both CDM presented a fibrillar network of Col I, periostin (POSTN) and FN and that CDM from TNC KO MEF indeed was devoid of TNC (**Fig. S3C, D**). Upon growth on these CDM we observed that multiplicity of both EC types (HUVEC, BAEC) was very poor on CDM that contained TNC whereas multiplicity was high when the CDM lacked the TNC protein (**Fig. 3D, E**). A similar result was also obtained when CDM was generated by CAF with abundant (shCTRL) and lowered (shTNC) TNC levels. The number of BAEC was significantly lowered when cells had grown on the control TNC containing CDM (**Fig. S3D**). This result phenocopied the result of plating cells on a substratum of purified TNC. We conclude that CDM with abundant TNC does not only recapitulate features of 2D TNC substrata but also add the 3D aspect seen in vivo and therefore are a useful tool. In contrast to EC, pericyte multiplicity was not significantly different whether TNC was present or absent from the CDM (**Fig. 3F**) suggesting that TNC had no impact on the expansion of pericytes under the tested conditions and thus corroborated a cell specific effect.

A lowered cell number by TNC could be explained by reduced survival and/or less proliferation. We investigated both possibilities by plating HUVEC on FN or TNC substrata or on CDM containing or lacking TNC. We found that both TNC containing substrata reduced survival through an increase of EC apoptosis as cleaved caspase 3 positive nuclei were more abundant in context of TNC (**Fig. 3G, H**). By measuring BrdU incorporation we assessed proliferation and observed a reduction on TNC by 45% in comparison to FN and Col I, respectively (**Fig. 3I**) which largely reflects lowered cell numbers due to apoptosis.

TNC represses YAP transcriptional activity through inhibition of actin polymerization

We wanted to understand whether and how TNC impacts on actin polymerization-dependent gene expression and cell survival. Therefore, we followed the kinetics of actin stress fiber formation in HUVEC upon adhesion on FN, Col I and TNC substrata, or upon plating of cells on CDM from TNC KO and wt MEF, respectively over 24h. Upon staining with FITC-phalloidin we observed that whereas HUVEC formed actin stress fibers on FN and Col I, they poorly did so on TNC (**Fig. 4A, Fig. S4A**). Also on CDM containing TNC no actin stress fibers were seen which was in contrast to CDM lacking TNC where actin stress fibers have formed (**Fig. S4B**). By fractionation followed by immunoblotting we quantified the relative abundance of filamentous/polymerized (F) versus globular/non-polymerized (G) actin (Posern, 2002). We found that after 5h F-actin formation is reduced by 8.5-fold on TNC in comparison to Col I and FN substrata, respectively (**Fig. 4B, C**).

The transcriptional integrator of extracellular stimuli, YAP (Yes-associated protein), is one of the molecules that senses the status of actin cytoskeleton (Halder et al., 2012). Upon actin polymerization YAP is translocated into the nucleus where it binds to the TEAD transcription factor and induces gene expression (Calvo et al., 2013b; Halder et al., 2012). By immunofluorescence

analysis we determined localization of YAP and observed that whereas 85% of HUVEC plated on FN had nuclear YAP this number was reduced to 12 % in cells plated on TNC which was in the range of FN in low serum representing a condition that prevents nuclear localization of YAP (Calvo et al., 2013b) (**Fig. 4D, E**).

Connective-tissue growth factor, CTGF (CCN2) and Cysteine rich protein 61, Cyr61 (CCN1), two pro-angiogenic molecules (Brigstock, 2002; Maity et al., 2014), have been described as YAP target genes (Calvo et al., 2013b; Xie et al., 2013). By RT-qPCR we determined their expression and observed that in HUVEC on the TNC substratum expression of CTGF and Cyr61 was downregulated by 80% and 75%, respectively in comparison to cells grown on FN (**Fig. 4F**). These results suggested that adhesion to a TNC substratum prevents actin stress fiber formation, nuclear localization of YAP and expression of pro-angiogenic factors, most likely triggering apoptosis of endothelial cells.

Induction of a pro-angiogenic secretome in glioblastoma cells and CAF by TNC

In search for a mechanism that could explain the pro-angiogenic activity of TNC in cancer tissue we considered a paracrine mechanism that potentially involves tumor and stromal cells. First, we determined whether TNC had an impact on the secretome of glioblastoma (GBM) cells. We used GBM cells since these cells highly express TNC (Herold-Mende et al., 2002; Leins et al., 2003; Martina et al., 2010) and high TNC expression correlates with worsened survival of GBM patients and high TNC abundance around tumor vessels (reviewed in (Orend et al., 2014)). Therefore, we plated U87MG on MEF-derived CDM containing or lacking TNC, collected the conditioned medium (CM) after 48h, added the CM to HUVEC and determined survival, proliferation and tubulogenesis. We observed that CM of U87MG cells grown on CDM containing TNC ("educated" by TNC) promoted HUVEC survival (**Fig. 5A)**. Also cell multiplicity was increased by 1.5-fold (48h) and 1.9-fold (72h) in

comparison to CM derived from cells educated by a CDM lacking TNC (**Fig. 5B**). Similarly, TNC-educated CM enhanced BAEC numbers by 1.5-fold (48h) and 1.7-fold (72h), respectively (**Fig. S5A**). In addition, CM from U87MG cells grown on CDM containing TNC enhanced matrigel tubulogenesis by 2.4-fold in comparison to control CM derived from tumor cells educated by a CDM lacking TNC (**Fig. 5C**). A similar TNC promoting effect on tubulogenesis was seen when CM from two other GBM cell lines (U118MG and U373MG) was added to HUVEC or when CM from U87MG cells was added to BAEC (**Fig. S5B**). To rule out that the observed effect potentially was due to a difference in abundance of growth promoting factors in the CM we performed a cell multiplicity assay. We observed that the cell numbers were identical for all tested cell lines (U87MG, U118MG, U373MG) with CM from TNC-educated and non-educated cells (**Fig. S5C**). To further address secretion of pro-angiogenic factors by TNC, we determined whether CM from U87MG with lowered TNC levels (shRNA mediated KD) (**Fig. S5D**) also had an impact on tube formation. We observed that CM from cells with wt levels of TNC triggered 40-70% more tubes in comparison to CM from cells with TNC KD levels (**Fig. 5D, E**). Again abundance of growth promoting factors in CM from cells lacking TNC was not different to that from cells expressing TNC since multiplicity of U87MG cells was equal (**Fig. S5E**).

Next we wanted to know whether TNC potentially also induced a pro-angiogenic secretome in fibroblasts. Therefore, we prepared CM from CAF that were grown on CDM derived from wt and TNC KO MEF, respectively. First we observed again no difference of CAF cell numbers in dependence of TNC in the CDM (**Fig. S5F**). We measured HUVEC cell numbers and HUVEC matrigel tubulogenesis upon addition of this CM. Whereas no effect was seen on tubulogenesis (**Fig. S5G**), we noticed 1.2-fold (24h), 1.7-fold (48h) and 2.2-fold (72h) more HUVEC when the CM was derived from TNC-educated CAF in comparison to CM from CAF grown on TNC-negative CDM (**Fig. 5F**). Finally, we used a co-culture assay in a fibrin gel where HUVEC and telomerase immortalized fibroblasts (TIF) were physically separated from TIF that served as source of TNC (**Fig. S5H**). In contrast to HUVEC that did

not express TNC (**Fig. S1L-N**) TIF expressed TNC. Therefore we lowered TNC expression in TIF by shRNA (**Fig. S5H**). We observed that whereas the number of sprouts was not different, the sprout length was significantly reduced upon coculture with shTNC TIF (**Fig. 5G, H, Fig. S5I, J**).

In summary, we had shown that TNC triggered secretion of pro-angiogenic factors in CAF and tumor cells that enhanced EC survival, multiplicity and tubulogenesis.

Proteomic analysis of the pro-angiogenic secretome induced by TNC and functional validation of candidates LCN1 and SDF1

To determine the molecular identity of the pro-angiogenic secretome, we collected CM from U87MG cells that had been grown on CDM derived from TNC KO and wt MEF, respectively. We analyzed this CM by quantitative shotgun proteomics, employing chemical stable isotope tagging as described previously (Shahinian et al., 2014). We identified a total of 1955 proteins. The ratio "proteins from U87MG cells grown on CDM from TNC wt MEF versus proteins from U87MG cells grown on CDM from TNC KO MEF" was log-transformed and followed a near normal distribution with most proteins displaying none or very little quantitative alteration. To distinguish proteins with altered abundance, we chose a cutoff of 0.58 (-0.58 for decreased abundance), representing an increase or decrease in abundance by more than 50 %. According to this cutoff, 685 proteins were differentially abundant when comparing TNC-educated and non-educated CM (**Fig. S6**). We further focused on proteins annotated as secreted or as localized at the cell surface. These criteria yielded more than 350 proteins with affected abundance in U87MG cells educated by the TNC containing CDM (**Table 1**). Such first-line criteria have been successfully applied previously (Tholen et al., 2011).

A clear pro- or anti-angiogenic fingerprint of secreted proteins with increased or decreased abundance was not noted. However, for many secreted proteins, contrasting findings are reported

with regard to their involvement in angiogenesis, leading to blurred functional profiles. Given the clear pro-angiogenic functionality of the TNC-educated CM, we specifically searched our proteomic data for proteins with increased abundance in TNC-educated CM and for which there is a clear pro-angiogenic functional profile. Several proteins are of note, including Cyr61 and CTGF (Brigstock, 2002; Leu et al., 2002; Maity et al., 2014), which are both members of the CCN family of growth factors, pleiotrophin (Papadimitriou et al., 2009; Perez-Pinera et al., 2008), lipocalin 7 (LCN7, synonym is tubulointerstitial nephritis antigen-like TINAGL1) (Brown et al., 2010; Li et al., 2007). We also noted an increased abundance of CXCL12/SDF1 (Ho et al., 2010; Kryczek et al., 2005; Orimo et al., 2005), a chemokine with important links to angiogenesis. In addition, we searched for proteins with clear anti-angiogenic functionality that present decreased abundance in the TNC-educated CM. These included angiotensinogen (Vincent et al., 2009), tissue factor pathway inhibitor 2 (Sierko et al., 2007), CXCL14 (Shellenberger et al., 2004), thrombospondin-1 (TSP1) (Lawler and Lawler, 2012) and several members of the insulin growth factor binding protein family (IGFBP3, 5, 6,7) (Chen et al., 2011; Kim et al., 2011; Rho et al., 2008; Zhang et al., 2012) and (**Table 1**).

Upon analysis of the CM by one-dimensional SDS-PAGE, we noticed a protein band at approximately 18 kDa, which was missing in TNC-educated CM and was only present in the CM of U87MG cells that were educated by a CDM lacking TNC (**Fig. 6A**). Mass spectrometric analysis of this gel band highlighted the presence of lipocalin-1 (LCN1) (**Table 2**). By RT-qPCR we confirmed transcriptional downregulation of LCN1 as well as upregulation of LCN7 by the TNC education of U87MG cells (**Fig. 6B**). Opposing regulation of related proteins has been previously observed in other systems; for example, increased kallikrein activity in ovarian cancer cells yields augmented levels of semaphorin-3A and reduced levels of semaphorin-6C (Shahinian et al., 2014). Since LCN7 is a well described angiogenesis promoting factor (Brown et al., 2010) we examined how LCN1 affects angiogenesis. We addressed this by a matrigel tubulogenesis assay. We observed that addition of purified recombinant

human LCN1 downregulated tube formation in a dose dependent manner suggesting an opposite role of LCN1 to that of LCN7 on angiogenesis (**Fig. 6C**). Thus through downregulation of LCN1 TNC may relieve its anti-angiogenic activity and promote angiogenesis. Despite binding to its cell surface receptor (Dartt, 2011) LCN1 has been described to elicit its functions through binding to not well known factors of protein or lipid origin (Dartt, 2011). By heating the CM we seeked to discriminate between these two possibilities and found that boiling completely blocked the pro-angiogenic activity of the TNC-educated CM on tube formation suggesting a proteinacious nature of responsible factors (**Fig. 6D**). Future studies need to determine through which mechanism LCN1 may affect angiogenesis.

SDF1 is an important mediator of tumor progression and angiogenesis (Ho et al., 2010; Kryczek et al., 2005; Orimo et al., 2005). We identified increased levels of SDF1 in TNC-educated CM, which was corroborated by ELISA (**Fig. 6E**). We further addressed whether the impact of TNC-education on angiogenesis is mediated by SDF1/CXCR4 signaling. We determined tube formation upon addition of CM from U87MG cells (that had been grown on TNC containing or lacking CDM) in the presence or absence of the CXCR4 inhibitor AMD3100. We observed that the inhibitor repressed tube formation in a dose dependent manner. This effect was not seen upon addition of CM from U87MG cells that were grown on CDM lacking TNC where both numbers were very low (**Fig. 6F**). Thus SDF1 is one factor of the TNC-educated secretome that is important to convey the angiogenesis-promoting activity of TNC.

Altogether this study had shown that TNC modulates the proteome composition and angiogenic properties of tumor cell secretomes. Amongst some 150 secreted angio-modulatory molecules that are regulated by TNC we identified LCN1 as a novel anti-angiogenic factor that is downregulated by TNC. On the contrary the pro-angiogenic factor SDF1 is upregulated by TNC and largely conveys the

TNC pro-angiogenic activity. These combined activities of TNC could explain the TNC pro-angiogenic function in tumors. In contrast to this paracrine effect, a direct interaction of TNC with cells triggers EC death and represses migration of pericytes which provides insight into angiogenesis counteracting activities of TNC. We had described YAP as a novel downstream target of TNC whose impaired function is linked to the anti-adhesive activity of TNC resulting in repression of autocrine pro-angiogenic signaling in EC.

DISCUSSION

There is substantial evidence for TNC promoting tumor progression which is already exploited for cancer therapy and diagnosis (reviewed in (Orend et al., 2014)) In almost all solid cancers TNC is highly expressed and these high expression levels correlate with worsened prognosis such as earlier lung metastasis in breast cancer patients and shortened survival of patients with glioma (Herold-Mende et al., 2002; Leins et al., 2003; Oskarsson et al., 2011). How TNC promotes tumor progression was recently addressed in a comprehensive approach by using a bona fide multistage immune competent tumorigenesis model with spontaneous tumorigenesis in the context of no and abundant endogenous or ectopically overexpressed TNC. This study revealed that TNC plays multiple roles in tumor progression by enhancing survival, proliferation and invasion of tumor cells. TNC also enhanced tumor angiogenesis and lung metastasis. While TNC promoted the angiogenic switch and increased blood vessel density, high TNC levels also triggered a corrupt vasculature as seen by electron microscopy, poor pericyte coverage and enhanced vessel leakiness (Langlois et al., 2014; Saupe et al., 2013).

Several studies had addressed a potential role of TNC in physiological and pathological angiogenesis by using different models including TNC KO mice (Ballard et al., 2006; Kimura et al., 2014; Kuriyama

et al., 2011; O'Connell et al., 2011a; Pezzolo et al., 2011; Sumioka et al., 2011; Tanaka et al., 2003; Wallner et al., 1999). Altogether, these studies provide convincing evidence for multiple and potentially opposing roles of TNC in blood vessel formation and function in tissue homeostasis and pathologies (reviewed in (Orend et al., 2014)). Also in vitro several contradictory observations have been made suggesting that TNC promotes pro- and anti-angiogenic behavior of EC which seems to be context dependent (reviewed in (Orend et al., 2014)). Here, we had used a plethora of state-of-the art angiogenesis models to address the multiple roles of TNC in tumor angiogenesis. In addition, we determined TNC-induced cellular effects at molecular level by a proteomic approach. By using in vivo and ex vivo models with tissue from TNC KO and wt mice, we addressed the impact of TNC loss on retinal angiogenesis and aorta sprouting. We observed no effect and an inhibitory angiogenic property of TNC, respectively. In an assay with purified TNC or with TNC provided by co-cultured CAF we showed that TNC repressed endothelial tubulogenesis. This effect could be due to impaired cell adhesion (Chiquet-Ehrismann et al., 1988). Indeed we observed that a 2D substratum of purified TNC prevented cell adhesion and spreading of EC. This had substantial consequences on EC survival and migration that was reduced by TNC. We could not detect expression of TNC in any of the EC tested even upon stimulation with factors (TGFβ) that trigger TNC expression in fibroblasts and in pericytes (data not shown). How TNC is repressed in EC is important to understand because it may open an opportunity to block TNC expression in a tumor context.

Our observation that TNC triggers death and impairs proliferation and migration of EC could be relevant in a tumor context. TNC is not expressed in non-damaged arteries or veins (Martina et al., 2010; Mustafa et al., 2012; Wallner et al., 1999) or in normal highly angiogenic tissue such as the endometrium or placenta (Mustafa et al., 2012). Although TNC is highly expressed around tumor blood vessels (Galler et al., 2011; Herold-Mende et al., 2002; Martina et al., 2010; Mustafa et al., 2012), we rarely could detect EC in close contact with TNC in human and murine insulinoma and

colon cancer tissue (Spenlé et al., 2015). Also in other studies TNC was found abundantly expressed around mural cells covering blood vessels yet not in direct vicinity to the EC (Martina et al., 2010). In cancer tissue we had described that TNC is forming ECM rich niches that seem to attract highly abundant lymphocytes and fibroblasts. Yet, EC were rarely found inside these TNC tracks (Spenlé et al., 2015). It is tempting to speculate that TNC matrix tracks are devoid of EC because a direct contact of EC with TNC would trigger their death. Along this line, since TNC is continuously expressed in a tumor and will contact EC at one point, this contact may cause EC death and potentially subsequent vessel leakage. In support of this hypothesis high TNC levels indeed increased vessel leakage in the Rip1Tag2 model (Saupe et al., 2013), seem to impair vessel regeneration in the ischemic liver (Kuriyama et al., 2011) and counteracted vessel stability in the central nervous system (Peter et al., 2012). Cancer cells have been shown to physically contribute to the formation of tumor blood vessels through a mechanism called vasculogenic mimicry (El Hallani et al., 2010). In a neuroblastoma xenograft model cancer cells seem to have transdifferentiated into EC where TNC is highly expressed suggesting a role of TNC in this process (Pezzolo et al., 2011).

We showed that adherence to TNC impairs cell adhesion signaling thus blocking actin polymerization into actin stress fibers in EC as had previously been shown also for other cell types (Huang et al., 2001b; Saupe et al., 2013). How cells interpret this particular adhesion is not completely understood. Recently, the Hippo pathway comprising YAP/TAZ has been linked to regulating survival and proliferation in response to cell adhesion (Halder et al., 2012). Importantly, YAP/TAZ is translocated into the nucleus when actin gets polymerized. In the nucleus YAP/TAZ bind to the DNA binding coreceptor TEAD triggering gene transcription (Halder et al., 2012). Here, we described that nuclear translocation of YAP is largely impaired in HUVEC upon growth on a TNC substratum. Moreover, this had an impact on gene expression of YAP target genes such as pro-angiogenic CTGF and Cyr61. Recently, we had shown that TNC downregulates DKK1 (another angio-modulatory molecule (Saupe

et al., 2013)) in an actin stress fiber dependent manner (Saupe et al., 2013) presumably through regulation of YAP by TNC since constitutive active YAP restored DKK1 expression (Zhen, Schwenzer, Rupp et al., manuscript in preparation). Thus our results suggest that TNC downregulates expression of angiogenesis modulating molecules through the YAP/TAZ pathway. Given that CTGF and Cyr61 are promoting angiogenesis and are downregulated by TNC in EC it remains to be seen whether reduced expression of these molecules has an impact on their survival.

In tumor tissue TNC acts in concert with other ECM molecules. This cannot be recapitulated by a 2D TNC substratum. To mimic the 3D context we established CDM with abundant and no or low TNC expression in CAF and MEF. We had characterized the CDM of these fibroblasts in some detail by IF analysis and proteomic approach (Koczorowska, Rupp, Radwanska, et al., in preparation) and observed that the ECM networks were fibrillar in the presence and absence of TNC. In the MEF derived CDM we did not see an obvious difference in the organization of the collagen and FN networks in the absence of TNC in comparison to its presence. Yet the molecular composition was different (Koczorowska, Rupp, Radwanska et al., in preparation) suggesting that eliminating expression of one ECM molecule from a fibroblast has a profound impact on the ECM that this cell produces. In the tumor context a TNC-dependent ECM could have a significant impact on the microenvironment affecting mechanical properties and abundance of ECM-sequestered or ECM-presented soluble factors. Most importantly, CDM from TNC KO MEF was devoid of TNC. By comparing cell behavior on CDM with abundant and no TNC we recapitulated properties of 2D substrata containing or lacking TNC such as repressed EC survival and proliferation by TNC. This result suggests that the observed biological effects seen in cells plated on CDM can be linked to the abundance of TNC and thus CDM with abundant and no TNC, respectively is a good substratum to address the functions of TNC.

Since a direct contact of EC with TNC promotes their cell death we searched for a paracrine mechanism that could explain the pro-angiogenic properties of TNC seen in cancer tissue. Here we had focused on GBM since these cells express copious amounts of TNC especially around blood vessels (Herold-Mende et al., 2002; Midwood et al., 2011). We observed that growth of three different human GBM cells triggered the secretion of soluble factors that promoted survival, proliferation and tubulogenesis of EC (HUVEC, BAEC) in a TNC context. A context with different TNC levels was either accomplished by plating cells on CDM containing or lacking TNC or by downregulating TNC expression in U87MG through shRNA. Fibroblasts have been shown to be a source of TNC in cancer models (Kalluri and Zeisberg, 2006; O'Connell et al., 2011a) and thus might also be instructed by TNC to secrete a pro-angiogenic secretome. We addressed this possibility in CAF by plating cells on CDM containing or lacking TNC and also used TIF with TNC KD. Again, we observed that TNC-instructed cells secreted factors that promoted HUVEC multiplicity (CAF) and HUVEC sprout length (TIF).

By mass spectrometric analysis we observed that the secretome of U87MG cells that had been educated by TNC was very different to that of cells not being educated by TNC. In particular, we observed that around 685 secreted molecules were different between the two conditions. Most importantly, whereas molecules with an anti-angiogenic function were predominantly found in CM from U87MG cells grown on a CDM lacking TNC, molecules with a pro-angiogenic function were mainly found in CM of cells that grew on a TNC containing CDM, suggesting that TNC is a potent inducer of a pro-angiogenic secretome in GBM cells.

In the list of molecules that are downregulated by TNC several factors are found with a well characterized anti-angiogenic property, such as angiotensinogen (Vincent et al., 2009) tissue factor pathway inhibitor 2 (Sierko et al., 2007), CXCL14 (Shellenberger et al., 2004) and several members of

the insulin growth factor binding protein family (IGFBP3, 5, 6,7) (Chen et al., 2011; Kim et al., 2011; Rho et al., 2008; Zhang et al., 2012). In addition we identified LCN1 as a novel candidate downregulated by TNC and showed for the first time that LCN1 represses EC tubulogenesis. Interestingly, LCN1 appears to play a protective role in inflammation which potentially is alleviated by TNC and thus may contribute to the pro-inflammatory effect of TNC (Dartt, 2011; Xu and Venge, 2000). On the contrary LCN1 was described to be overexpressed in situations with aberrant angiogenesis such as age-related macular degeneration (Yao et al., 2013) and cystic fibrosis (Redl et al., 1998) providing a potential link of LCN1 to angiogenesis. It is noteworthy, that TNC increased expression of another LCN family member, LCN7 that is a known promoter of angiogenesis (Brown et al., 2010). Thus TNC may alter expression of two different LCN family members thus achieving a pro-angiogenic net balance of their activities in cancer.

Amongst the TNC upregulated candidates several pro-angiogenic molecules are found such as transglutaminase-2 (TG2) (Haroon et al., 1999), pleiotrophin (Perez-Pinera et al., 2008) and Wnt family members, Wnt5a, Wnt5b and Wnt7b (Masckauchán and Kitajewski, 2006; Yeo et al., 2014). An upregulation of pro-angiogenic Wnt ligands by TNC and downregulation of the Wnt inhibitor DKK1 by TNC (Saupe et al., 2013) supports the possibility that TNC promotes angiogenesis through this pathway. Moreover, several matrisomal core-proteins (e.g. Col (COL14A1, COL15A1, COL18A1), CTGF) and matrisome-associated molecules (e.g. Loxl1) were upregulated by TNC in our study. Many of these molecules belong to the AngioMatrix, a gene expression signature that characterizes the angiogenic switch and has predictive value in glioma and colon cancer patient survival. On the contrary also TNC-downregulated molecules belong to the AngioMatrix (e.g. COL12A1, COL1A2, ECM1). Thus we speculate that an overlapping list of AngioMatrix molecules and TNC-upregulated pro-angiogenic molecules may have an even better prognostic value for negative cancer patient survival which needs to be addressed in the future.

Finally, we identified the potent pro-angiogenic factor SDF1 (Orimo et al., 2005) to be induced by TNC. By pharmacological inhibition of its receptor CXCR4 (AMD3100) we revealed that TNC largely promotes angiogenesis through this pathway. In a U87MG grafting model it was recently shown that blocking CXCR4 was highly efficient in reducing tumor angiogenesis and growth (Ping et al., 2011). In the future it will be important to determine whether targeting CXCR4 (or other identified TNC regulated pro-angiogenic molecules) is neutralizing the TNC effect on tumor angiogenesis. Importantly, targeting CXCR4 signaling with the FDA-approved SDF1 inhibitor AMD3100 or Plerixafor (Lanza et al., 2015) together with Bevacizumab (blocking VEGFA signaling) is currently applied in a clinical study for recurrent high-grade glioma (study number: NCT01339039). This approach could be superior over targeting VEGFA alone because additional targeting of CXCR4 may also counteract an important pro-angiogenic activity of TNC. Thus targeting the inherently TNC-rich TME in GBM with anti-angiogenic drugs in combination with drugs that block the TNC-related pro-angiogenic activities may lead to significantly reduced tumor angiogenesis and retarded tumor growth. Tumor vessels may also regress or normalize (Jain, 2005) when the vessel corrupting activity of TNC is blocked thus facilitating the delivery of adjuvant chemo-therapeutics such as temozolomide (Pedretti et al., 2010b). Targeting TNC activities may also have an impact on the tumor bed that remains largely unaffected by any of the currently applied therapeutic approaches.

In conclusion, our study revealed cellular and molecular insight into the multiple effects of TNC on tumor angiogenesis showing that TNC exerts direct anti-angiogenic activities towards EC and paracrine pro-angiogenic activities through tumor cells and CAF. These opposing effects could explain that TNC promotes more but poorly functional tumor blood vessels (**Fig. 7**). Identification and detailed insight into molecules responsible for the pro- and anti-angiogenic activities of TNC may provide for the first time pharmacological opportunities to counteract TNC activities in cancer.

Acknowledgements

We like to thank the following people for reagents, M. Chiquet for MEF TNC KO. The authors thank Bettina Mayer and Franz Jehle for excellent technical assistance with mass spectrometry analysis. G.O. is supported by grants from ANR (Angiomatrix), INCa, Ligue contre le Cancer. E.V.O is supported by ANR (Angiomatrix) and ARC. T.R. is supported by a fellowship from Ligue contre le Cancer. O.S. is supported by grants of the DFG (SCHI 871/2 and SCHI 871/5, SCHI 871/6, GR 1748/6, and INST 39/900-1) and the DFG SFB850 (Project B8), a starting grant of the European Research Council (Programme “Ideas” - Call identifier: ERC-2011- StG 282111-ProteaSys), and the Excellence Initiative of the German Federal and State Governments (EXC 294, BIOSS).

References

1. Carmeliet P, Jain RK. Angiogenesis in cancer and other diseases. Nature 2000; 407:249–257.

2. Herold-Mende C, Mueller MM, Bonsanto MM, Schmitt HP, Kunze S, Steiner H-H. Clinical impact and functional aspects of tenascin-C expression during glioma progression. Int J Cancer 2002; 98:362–369.

3. Martina E, Degen M, Rüegg C, et al. Tenascin-W is a specific marker of glioma-associated blood vessels and stimulates angiogenesis in vitro. FASEB J 2010; 24:778 –787.

4. Saupe F, Schwenzer A, Jia Y, et al. Tenascin-C Downregulates Wnt Inhibitor Dickkopf-1, Promoting Tumorigenesis in a Neuroendocrine Tumor Model. Cell Rep 2013; 5:482–492.

5. Langlois B, Saupe F, Rupp T, et al. AngioMatrix, a signature of the tumor angiogenic switch-specific matrisome, correlates with poor prognosis for glioma and colorectal cancer patients. Oncotarget 2014; 5:10529–10545.

6. Hanahan D. Heritable formation of pancreatic beta-cell tumours in transgenic mice expressing recombinant insulin/simian virus 40 oncogenes. Nature 1985; 315:115–122.

7. Brigstock DR. Regulation of angiogenesis and endothelial cell function by connective tissue growth factor (CTGF) and cysteine-rich 61 (CYR61). Angiogenesis 2002; 5:153–165.

8. Maity G, Mehta S, Haque I, et al. Pancreatic tumor cell secreted CCN1/Cyr61 promotes endothelial cell migration and aberrant neovascularization. Sci Rep 2014; 4:4995.

9. O'Connell JT, Sugimoto H, Cooke VG, et al. VEGF-A and Tenascin-C produced by S100A4+ stromal cells are important for metastatic colonization. Proc Natl Acad Sci 2011.

10. Kalluri R, Zeisberg M. Fibroblasts in cancer. Nat Rev Cancer 2006; 6:392–401.

11. Ghajar CM, Peinado H, Mori H, et al. The perivascular niche regulates breast tumour dormancy. Nat Cell Biol 2013; 15:807–817.

12. Carmeliet P. Angiogenesis in health and disease. Nat Med 2003; 9:653–660.

13. Cunha SI, Pietras K. ALK1 as an emerging target for antiangiogenic therapy of cancer. Blood 2011; 117:6999–7006.

14. Scharenberg MA, Pippenger BE, Sack R, et al. TGF-β-induced differentiation into myofibroblasts involves specific regulation of two MKL1 isoforms. J Cell Sci 2014; 127:1079–1091.

15. Chiquet-Ehrismann R, Kalla P, Pearson CA, Beck K, Chiquet M. Tenascin interferes with fibronectin action. Cell 1988; 53:383–390.

16. Beacham DA, Amatangelo MD, Cukierman E. Preparation of extracellular matrices produced by cultured and primary fibroblasts. Curr Protoc Cell Biol Editor Board Juan Bonifacino Al 2007; Chapter 10:Unit 10.9.

17. Posern G. Mutant Actins Demonstrate a Role for Unpolymerized Actin in Control of Transcription by Serum Response Factor. Mol Biol Cell 2002; 13:4167–4178.

18. Halder G, Dupont S, Piccolo S. Transduction of mechanical and cytoskeletal cues by YAP and TAZ. Nat Rev Mol Cell Biol 2012; 13:591–600.

19. Calvo F, Ege N, Grande-Garcia A, et al. Mechanotransduction and YAP-dependent matrix remodelling is required for the generation and maintenance of cancer-associated fibroblasts. Nat Cell Biol 2013; 15:637–646.

20. Xie Q, Chen J, Feng H, et al. YAP/TEAD-mediated transcription controls cellular senescence. Cancer Res 2013; 73:3615–3624.

21. Leins A, Riva P, Lindstedt R, Davidoff MS, Mehraein P, Weis S. Expression of tenascin-C in various human brain tumors and its relevance for survival in patients with astrocytoma. Cancer 2003; 98:2430–2439.

22. Orend G, Saupe F, Schwenzer A, Midwood K. The extracellular matrix and cancer: regulation of tumor cell biology by tenascin-C. iConcept Press.; 2014.

23. Shahinian H, Loessner D, Biniossek ML, et al. Secretome and degradome profiling shows that Kallikrein-related peptidases 4, 5, 6, and 7 induce TGFβ-1 signaling in ovarian cancer cells. Mol Oncol 2014; 8:68–82.

24. Tholen S, Biniossek ML, Gessler A-L, et al. Contribution of cathepsin L to secretome composition and cleavage pattern of mouse embryonic fibroblasts. Biol Chem 2011; 392:961–971.

25. Leu S-J, Lam SC-T, Lau LF. Pro-angiogenic Activities of CYR61 (CCN1) Mediated through Integrins αvβ3 and α6β1 in Human Umbilical Vein Endothelial Cells. J Biol Chem 2002; 277:46248–46255.

26. Papadimitriou E, Mikelis C, Lampropoulou E, et al. Roles of pleiotrophin in tumor growth and angiogenesis. Eur Cytokine Netw 2009; 20:180–190.

27. Perez-Pinera P, Berenson JR, Deuel TF. Pleiotrophin, a multifunctional angiogenic factor: mechanisms and pathways in normal and pathological angiogenesis. Curr Opin Hematol 2008; 15:210–214.

28. Li D, Mukai K, Suzuki T, et al. Adrenocortical zonation factor 1 is a novel matricellular protein promoting integrin-mediated adhesion of adrenocortical and vascular smooth muscle cells. FEBS J 2007; 274:2506–2522.

29. Brown LJ, Alawoki M, Crawford ME, et al. Lipocalin-7 Is a Matricellular Regulator of Angiogenesis. PLoS ONE 2010; 5:e13905.

30. Ho TK, Tsui J, Xu S, Leoni P, Abraham DJ, Baker DM. Angiogenic effects of stromal cell-derived factor-1 (SDF-1/CXCL12) variants in vitro and the in vivo expressions of CXCL12 variants and CXCR4 in human critical leg ischemia. J Vasc Surg 2010; 51:689–699.

31. Kryczek I, Lange A, Mottram P, et al. CXCL12 and Vascular Endothelial Growth Factor Synergistically Induce Neoangiogenesis in Human Ovarian Cancers. Cancer Res 2005; 65:465–472.

32. Orimo A, Gupta PB, Sgroi DC, et al. Stromal Fibroblasts Present in Invasive Human Breast Carcinomas Promote Tumor Growth and Angiogenesis through Elevated SDF-1/CXCL12 Secretion. Cell 2005; 121:335–348.

33. Vincent F, Bonnin P, Clemessy M, et al. Angiotensinogen delays angiogenesis and tumor growth of hepatocarcinoma in transgenic mice. Cancer Res 2009; 69:2853–2860.

34. Sierko E, Wojtukiewicz MZ, Kisiel W. The role of tissue factor pathway inhibitor-2 in cancer biology. Semin Thromb Hemost 2007; 33:653–659.

35. Shellenberger TD, Wang M, Gujrati M, et al. BRAK/CXCL14 is a potent inhibitor of angiogenesis and a chemotactic factor for immature dendritic cells. Cancer Res 2004; 64:8262–8270.

36. Lawler PR, Lawler J. Molecular Basis for the Regulation of Angiogenesis by Thrombospondin-1 and -2. Cold Spring Harb Perspect Med 2012; 2.

37. Rho SB, Dong SM, Kang S, et al. Insulin-like growth factor-binding protein-5 (IGFBP-5) acts as a tumor suppressor by inhibiting angiogenesis. Carcinogenesis 2008; 29:2106–2111.

38. Kim J-H, Choi DS, Lee O-H, Oh S-H, Lippman SM, Lee H-Y. Antiangiogenic antitumor activities of IGFBP-3 are mediated by IGF-independent suppression of Erk1/2 activation and Egr-1–mediated transcriptional events. Blood 2011; 118:2622–2631.

39. Chen D, Yoo BK, Santhekadur PK, et al. Insulin-like growth factor binding protein-7 (IGFBP7) functions as a potential tumor suppressor in hepatocellular carcinoma (HCC). Clin Cancer Res 2011:clincanres.2774.2010.

40. Zhang C, Lu L, Li Y, et al. IGF binding protein-6 expression in vascular endothelial cells is induced by hypoxia and plays a negative role in tumor angiogenesis. Int J Cancer J Int Cancer 2012; 130:2003–2012.

41. Dartt DA. Tear Lipocalin: Structure and Function. Ocul Surf 2011; 9:126–138.

42. Oskarsson T, Acharyya S, Zhang XH-F, et al. Breast cancer cells produce tenascin C as a metastatic niche component to colonize the lungs. Nat Med 2011; 17:867–874.

43. Ballard VLT, Sharma A, Duignan I, et al. Vascular tenascin-C regulates cardiac endothelial phenotype and neovascularization. FASEB J 2006; 20:717–719.

44. Kimura T, Shiraishi K, Furusho A, et al. Tenascin C protects aorta from acute dissection in mice. Sci Rep 2014; 4:4051.

45. Wallner K, Li C, Shah PK, et al. Tenascin-C Is Expressed in Macrophage-Rich Human Coronary Atherosclerotic Plaque. Circulation 1999; 99:1284–1289.

46. Sumioka T, Fujita N, Kitano A, Okada Y, Saika S. Impaired angiogenic response in the cornea of mice lacking tenascin C. Invest Ophthalmol Vis Sci 2011; 52:2462–2467.

47. Tanaka K, Hiraiwa N, Hashimoto H, Yamazaki Y, Kusakabe M. Tenascin‐C regulates angiogenesis in tumor through the regulation of vascular endothelial growth factor expression. Int J Cancer 2003; 108:31–40.

48. Pezzolo A, Parodi F, Marimpietri D, et al. Oct-4+/Tenascin C+ neuroblastoma cells serve as progenitors of tumor-derived endothelial cells. Cell Res 2011; 21:1470–1486.

49. Kuriyama N, Duarte S, Hamada T, Busuttil RW, Coito AJ. Tenascin-c: A novel mediator of hepatic ischemia and reperfusion injury. Hepatol Baltim Md 2011.

50. Mustafa DAM, Dekker LJ, Stingl C, et al. A proteome comparison between physiological angiogenesis and angiogenesis in glioblastoma. Mol Cell Proteomics MCP 2012; 11:M111.008466.

51. Galler K, Junker K, Franz M, et al. Differential vascular expression and regulation of oncofetal tenascin-C and fibronectin variants in renal cell carcinoma (RCC): implications for an individualized angiogenesis-related targeted drug delivery. Histochem Cell Biol 2011.

52. Spenlé C, Gasser I, Saupe F, et al. Spatial organization of the tenascin-C microenvironment in experimental and human cancer. Cell Adhes Migr 2015; 9:4–13.

53. Peter NR, Shah RT, Chen J, Irintchev A, Schachner M. Adhesion molecules close homolog of L1 and tenascin-C affect blood–spinal cord barrier repair: NeuroReport 2012; 23:479–482.

54. El Hallani S, Boisselier B, Peglion F, et al. A new alternative mechanism in glioblastoma vascularization: tubular vasculogenic mimicry. Brain 2010; 133:973 –982.

55. Huang W, Chiquet-Ehrismann R, Moyano JV, Garcia-Pardo A, Orend G. Interference of tenascin-C with syndecan-4 binding to fibronectin blocks cell adhesion and stimulates tumor cell proliferation. Cancer Res 2001; 61:8586–8594.

56. Midwood KS, Hussenet T, Langlois B, Orend G. Advances in tenascin-C biology. Cell Mol Life Sci 2011; 68:3175–3199.

57. Xu S, Venge P. Lipocalins as biochemical markers of disease. Biochim Biophys Acta BBA - Protein Struct Mol Enzymol 2000; 1482:298–307.

58. Yao J, Liu X, Yang Q, et al. Proteomic analysis of the aqueous humor in patients with wet age-related macular degeneration. PROTEOMICS – Clin Appl 2013; 7:550–560.

59. Redl B, Wojnar P, Ellemunter H, Feichtinger H. Identification of a lipocalin in mucosal glands of the human tracheobronchial tree and its enhanced secretion in cystic fibrosis. Lab Investig J Tech Methods Pathol 1998; 78:1121–1129.

60. Haroon ZA, Hettasch JM, Lai TS, Dewhirst MW, Greenberg CS. Tissue transglutaminase is expressed, active, and directly involved in rat dermal wound healing and angiogenesis. FASEB J Off Publ Fed Am Soc Exp Biol 1999; 13:1787–1795.

61. Masckauchán TNH, Kitajewski J. Wnt/Frizzled Signaling in the Vasculature: New Angiogenic Factors in Sight. Physiology 2006; 21:181–188.

62. Yeo E-J, Cassetta L, Qian B-Z, et al. Myeloid WNT7b mediates the angiogenic switch and metastasis in breast cancer. Cancer Res 2014; 74:2962–2973.

63. Ping Y, Yao X, Jiang J, et al. The chemokine CXCL12 and its receptor CXCR4 promote glioma stem cell-mediated VEGF production and tumour angiogenesis via PI3K/AKT signalling. J Pathol 2011; 224:344–354.

64. Lanza F, Gardellini A, Laszlo D, Martino M. Plerixafor: what we still have to learn. Expert Opin Biol Ther 2015; 15:143–147.

65. Jain RK. Normalization of Tumor Vasculature: An Emerging Concept in Antiangiogenic Therapy. Science 2005; 307:58 –62.

66. Pedretti M, Verpelli C, Mårlind J, et al. Combination of temozolomide with immunocytokine F16-IL2 for the treatment of glioblastoma. Br J Cancer 2010; 103:827–836.

67. Ribble D, Goldstein NB, Norris DA, Shellman YG. A simple technique for quantifying apoptosis in 96-well plates. BMC Biotechnol 2005; 5:12.

68. Nakatsu MN, Davis J, Hughes CCW. Optimized fibrin gel bead assay for the study of angiogenesis. J Vis Exp JoVE 2007:186.

69. Baker M, Robinson SD, Lechertier T, et al. Use of the mouse aortic ring assay to study angiogenesis. Nat Protoc 2012; 7:89–104.

70. Tholen S, Biniossek ML, Gansz M, et al. Deletion of cysteine cathepsins B or L yields differential impacts on murine skin proteome and degradome. Mol Cell Proteomics MCP 2013; 12:611–625.

71. Pedrioli PGA, Eng JK, Hubley R, et al. A common open representation of mass spectrometry data and its application to proteomics research. Nat Biotechnol 2004; 22:1459–1466.

72. Kessner D, Chambers M, Burke R, Agus D, Mallick P. ProteoWizard: open source software for rapid proteomics tools development. Bioinformatics 2008; 24:2534–2536.

73. Craig R, Beavis RC. TANDEM: matching proteins with tandem mass spectra. Bioinforma Oxf Engl 2004; 20:1466–1467.

74. Martens L, Vandekerckhove J, Gevaert K. DBToolkit: processing protein databases for peptide-centric proteomics. Bioinforma Oxf Engl 2005; 21:3584–3585.

75. Forsberg E, Hirsch E, Fröhlich L, et al. Skin wounds and severed nerves heal normally in mice lacking tenascin-C. Proc Natl Acad Sci U S A 1996; 93:6594–6599.

76. Lal A, Peters H, St Croix B, et al. Transcriptional response to hypoxia in human tumors. J Natl Cancer Inst 2001; 93:1337–1343.

77. De Wever O, Nguyen Q-D, Van Hoorde L, et al. Tenascin-C and SF/HGF produced by myofibroblasts in vitro provide convergent pro-invasive signals to human colon cancer cells through RhoA and Rac. FASEB J Off Publ Fed Am Soc Exp Biol 2004; 18:1016–1018.

78. Kääriäinen E, Nummela P, Soikkeli J, et al. Switch to an invasive growth phase in melanoma is associated with tenascin‐C, fibronectin, and procollagen‐I forming specific channel structures for invasion. J Pathol 2006; 210:181–191.

79. Midwood KS, Orend G. The role of tenascin-C in tissue injury and tumorigenesis. J Cell Commun Signal 2009; 3:287–310.

80. Casazza A, Fu X, Johansson I, et al. Systemic and targeted delivery of semaphorin 3A inhibits tumor angiogenesis and progression in mouse tumor models. Arterioscler Thromb Vasc Biol 2011; 31:741–749.

81. Maione F, Molla F, Meda C, et al. Semaphorin 3A is an endogenous angiogenesis inhibitor that blocks tumor growth and normalizes tumor vasculature in transgenic mouse models. J Clin Invest 2009; 119:3356–3372.

82. Masckauchán TNH, Agalliu D, Vorontchikhina M, et al. Wnt5a Signaling Induces Proliferation and Survival of Endothelial Cells In Vitro and Expression of MMP-1 and Tie-2. Mol Biol Cell 2006; 17:5163–5172.

83. Shim B-S, Kang B-H, Hong Y-K, et al. The kringle domain of tissue-type plasminogen activator inhibits in vivo tumor growth. Biochem Biophys Res Commun 2005; 327:1155–1162.

84. Kisker O, Onizuka S, Becker CM, et al. Vitamin D binding protein-macrophage activating factor (DBP-maf) inhibits angiogenesis and tumor growth in mice. Neoplasia N Y N 2003; 5:32–40.

85. Sadanandam A, Sidhu SS, Wullschleger S, et al. Secreted semaphorin 5A suppressed pancreatic tumour burden but increased metastasis and endothelial cell proliferation. Br J Cancer 2012; 107:501–507.

86. Goodman OB, Febbraio M, Simantov R, et al. Neprilysin inhibits angiogenesis via proteolysis of fibroblast growth factor-2. J Biol Chem 2006; 281:33597–33605.

87. Mitola S, Ravelli C, Moroni E, et al. Gremlin is a novel agonist of the major proangiogenic receptor VEGFR2. Blood 2010; 116:3677–3680.

Material and methods

Antibodies

Antibodies against the following molecules were used: mouse anti human TNC (B28.13, 0.4-1 μg/ml), rat anti mouse TNC (mTN12, 1-2 μg/), rabbit anti human and mouse FN (Sigma F3648, 1/200), rabbit anti human and mouse POSTN (gift J. Huelsken, Lausanne, 1/1000), mouse anti mouse Col I (mouse, sigma C2456, 1/1000), mouse anti human and mouse α-tubulin (mouse, Oncogene CP06, Boston, MA, USA, 1/1000), mouse anti human and mouse αSMA (clone 1A4, Sigma A2547, 1/200), mouse anti human CD31 (Invitrogen clone MEM-5, 1/400), and rabbit anti cleaved caspase 3 (Cell signaling 9661, 1/200). Secondary antibodies used were ECL horseradish peroxidase linked whole anti-rabbit (NA934V) Anti-rat (NA935) and anti-mouse (NXA931) (GE Healthcare, Buckinghamshire, UK) and donkey anti-goat IgG (sc-2020, Santa Cruz, Biotechnology) or fluorescently coupled secondary antibodies goat anti-mouse, anti-rabbit, anti-goat or anti-rat IgG (Jackson laboratory 1/2000).

Cell culture and reagents

The following media were used: pericyte medium (PM, ScienCell, 1201) for pericytes (HBVP, ScienCell, 1200), DMEM 4.5g/l glucose, and 10% FBS for all GBM cells and CAF and endothelial cell growth medium (ECGM, PromoCell, C-22010) for HUVEC (HUVEC, Promo cell, C-12203). Cells were starved in DMEM, 1% FBS (tumor cells, pericytes, CAF, BAEC) or M199, 1% FBS, 1μg/ml hydrocortisone, and 90μg/ml heparin (HUVEC). Pericytes were used at passages 2-10, and EC (HUVEC, VeraVec HUVEC and BAEC) at passages 2-6. All cell media were supplemented with 100 U/ml penicillin and 100 μg/ml streptomycin.

FN and TNC purification and coating of cell-culture dishes with FN, Col I (Corning CB-40236) and TNC was done using standard protocols as described earlier (Huang et al., 2001b). Briefly, FN, Col I and TNC were sequentially coated in PBS/0.01% Tween-20 at 1 μg/cm^2 before saturation of the non-coated surface with 10 mg/ml heat inactivated 1% BSA/PBS. Cells were seeded on the coated surfaces and analyzed using standard protocols described below.

Lentiviral transduction of cells

The silencing of TNC was done by use of short hairpin (sh) mediated gene expression knockdown (KD). For generation of shTNC cells, U87MG and CAF cells were transduced with MISSION lentiviral transduction particles (TRC2, Sigma-Aldrich, containing neomycin or puromycin box, sh1, TRCN0000230785, sequence 5'-3': CCGGGGAGTACTTTATCCGTGTATTCTCGAGAATACACGGATAAAGT ACTCCTTTTTG; and sh3, TRCN0000230788 sequence 5'-3': CCGGCCAGTGACAAC

ATCGCAATAGCTCGAGCTATTGCGATGTTGTCACTGGTTTTTG) or MISSION non-target shRNA control transduction particles (pLKO.1 vector, Sigma-Aldrich, sequence 5'-3': CCGGCAACA AGATGAAGAGCACCAACTCGAGTTGGTGCTCTTCATCTTGTTGTTTTTT) with a MOI=2, transduced cells were selected with 3 µg/ml puromycin or 1 mg/ml G418 for U87MG and CAF, respectively. Effective KD was determined at protein level after 20 passages post infection.

Adhesion assay

Ninety six well plates (BD Bioscience) were coated with 1 or 2 µg/cm^2 of purified FN, Col I or TNC (6 replicates). HUVEC, BAEC or HBVP were plated for 1h at 37°C and then washed to remove non-adherent cells. Cells were fixed with methanol (30 minutes at room temperature), washed and stained with Cristal Violet 0.1% (in H_2O). Pictures were taken at 100X magnification before cells were lysed in 50 µl DMSO and measuring the OD at 595 nm.

Production of cell derived matrix

Cell derived matrix (CDM) was prepared as previously described (Beacham et al., 2007). Briefly, 33`000 cells/cm$^2$ for MEF wt and 50`000 cells/cm^2 for MEF TNC KO and CAF control or KD for TNC were plated on chemically cross-linked gelatin on tissue culture dishes to achieve confluent dishes. Cells were maintained in confluent conditions for up to 8 days supplemented every 24 hours with 50 µg/ml fresh medium plus L-ascorbic acid (L-AA). Cells were removed with cell extraction buffer (20mM NH_4OH, 0.5% Triton-X-100 in PBS, 30 minutes at 37°C and overnight at 4°C). The cell-free CDM was treated with DNAse 100 U/ml (Invitrogen) for 1h at 37°C to remove remaining genomic DNA and was conserved at 4°C for up to one month before use.

Assessment of apoptosis by cleaved caspase 3

Serum starved HUVEC were seeded on CDM deposited by wt or TNC KO MEF or on FN and TNC precoated plastic surfaces (labtek Permanox) in full medium. After 72h cells were fixed and stained for cleaved caspase 3 and DAPI. Three independent assays were done with 4 replicates with 6 pictures taken per well at 100X magnification. The apoptotic index was determined as the percentage of cleaved caspase 3 positive cells per all DAPI positive cells.

Assessment of cell death by Ethidium Bromide / Acridine Orange (EB/AO) uptake

Following of alive, apoptotic and necrotic cells was done by the EB/AO uptake method adapted from Riddle et al., 2005 (Ribble et al., 2005) Briefly HUVEC were seeded together with CM on plastic dishes for 48h in their culture medium. After 48h EB and AO solutions in PBS at 5 µg/ml was added to the culture medium followed by precipitation (400g, 5 minutes). Up to two pictures per well were taken

with at least 100 cells per well (Zeiss AXIOZoom V16 stereoscope with 112X magnification). Totally green cells were considered as alive cells, a green and red costain as apoptotic cells (fragmented nuclei) and red cells as dead cells. Three independent experiments were done with 3 replicates per experiment.

BrdU incorporation, cell proliferation assay

Serum starved HUVEC were cultured in 96-well plates at a density of 5`000 cells/well (6 replicates) in 100 µl of complete growth media on ECM coated surfaces (Col I, FN, TNC). After 48h, cells were labeled with 100 µM BrdU (3h, 37°C). Culture medium was removed, cells fixed, and DNA was denatured in one step by adding the FixDenat solution (Cell Proliferation ELISA, BrdU Kit (Roche Applied Science) followed by addition of the anti-BrdU-POD antibody for 90 minutes at room temperature, washing and addition of pre-warmed substrate solution (10 minutes in the dark). Chemiluminescence was directly measured (TriStar2 Multimode Read LB 942 (Berthold Technology) multiplate reader). DAPI labeling was used for normalization. A minimum of 3 independent experiments was done with 6 replicates per experiment.

Cell multiplicity assay

Serum starved cells (HUVEC, BAEC and HBVP) were plated into 96-well plates (2`000 or 6`000 cells/well with 6 replicates for each time point) on ECM coated surfaces (Col I, FN or TNC) or CDM. MTS incorporation assays were done according to the manufacturer's instructions (CellTiter 96 aqueous non-radioactive cell proliferation assay, Promega) after 8h, 24h, 48h and 72h. Measured values (490nm) were normalized to the relative cell number at 8h.

Wound healing assay

Equal numbers of cells were grown to confluency in 24-well plates (24h). Confluent EC were starved for 24h, treated with mitomycin C at 2µg/ml to inhibit proliferation before application of a scratch wound with a pipet tip. Cell debris was removed by washing with PBS before adding low serum medium that contained 0.01% PBS-Tween 20 (control) or TNC (2.5, 5, 10 or 20 µg/ml in 0.01% PBS-Tween 20). Two images of the wounding area were acquired immediately after scratching and then at the same location at later time points. The relative wound closure was quantified by measuring the width of the cell-free area at the time of injury and the end point of the experiment.

Vascular co-culture assay

The protocol from Ghajar et al., 2013 (Ghajar et al., 2013) was adapted. Briefly, CAF (shCTRL, shTNC) were seeded at a density of 50`000 cells per well in 96-well culture plates together with VeraHUVEC

of a ratio 5:2. Cells were suspended in ECGM at a concentration of 70`000 cells per 100µl. During the 7 days of co-culture in ECGM the medium was replenished every 2 days. Then cells were stained with a CD31 antibody and DAPI. Tube-like structures were counted using the ZEN Blue software (Carl Zeiss). A minimum of 3 independent experiments were done with 6 replicates per experiment.

Matrigel tubulogenesis assay

Matrix was prepared by adding 10 µl of Matrigel (Corning) into 15 well dishes (µ-Slide Angiogenesis, Ibidi LLC) followed by solidification at 37°C in a humidified incubator for 1h. HUVEC (140`000 cells/ml) and BAEC (200`000 cell/ml) were trypsinized and resuspended in low FBS-containing medium (M199, 1% FBS, 1 µg/ml heparin, 200 ng/ml hydrocortisone with 10 ng/ml $VEGF_{165}$ or DMEM low glucose, 1% FBS with 10 ng/ml $VEGF_{165}$) with 0,01 % PBS-Tween (control for TNC), 2.5 µg/ml, 5 µg/ml or 10 µg/ml TNC or with CM from U87MG, U118MG or CAF. After incubation for 8h at 37°C, bright field mosaic pictures were taken (Zeiss Imager Z2 inverted microscope and AxioVision software (Carl Zeiss) at 50X magnification, a total of 9 pictures per condition) and tube-like structures or tube length were assessed by using the AxioVision or ZEN Blue software (Carl Zeiss). A minimum of 3 independent experiments were done with 5 replicates per experiment.

HUVEC spheroid sprouting assay

The fibrin gel bead assay was done according to Nakatsu et al., 2007 (Nakatsu et al., 2007). The culture media of HUVEC and fibroblasts (TIF = telomerase immortalized fibroblasts, routinely cultured in DMEM 20% FBS), were changed for EGM2 (Promocell) one day before coating on beads and embedding, respectively. HUVEC were trypsinized and coated on Cytodex beads at a ratio of 10^6 cells for 1mg of beads during 4 hours at 37°C with occasional agitation, and then cultured overnight in 6 cm dish. Next day, HUVEC-coated beads were combined at a concentration of 500 beads/ml in the 2 mg/ml fibrinogen pre-gel solution supplemented with 0.15 U/ml of aprotinin. Fibrin gel formation was initiated by adding 0.625 U/ml of thrombin and then the gels were allowed to stand for 5 minutes at room temperature, followed by 15 minutes incubation at 37°C for. Meanwhile, TIF were trypsinized and plated on top of a fibrin gels at 40,000 cells in EGM-2 medium per well in 12-well plate. The cells were cultured for up to 12 days with the media change every other day. Phase micrographs of growing tubes were captured every day using 10x objective and/or video microscopy were done (Zeiss inverted microscope Axiovert 200M with Coolsnap HQ). Quantification of number and length of sprouts was done in ImageJ software. Sprout length was calculated by measuring the distance from the bead to the end of the sprout. 10-20 beads were analyzed per well condition and each condition was done in triplicate, three independent experiments were done.

Aortic ring sprouting assay

Aortic rings were prepared upon adaption of the protocol of Baker et al., 2012 (Baker et al., 2012). Briefly, C57BL6 mice (wt or TNC KO) were euthanized with CO2 asphyxia. The thoracic aorta was cut at the posterior mediastinum and the anterior occipital parts, placed in serum-free Opti-MEM (Gibco) with antibiotics and cut in pieces of 500 µm. Fifteen to twenty rings were obtained per mouse that were starved overnight in Opti-MEM with antibiotics. The aortic rings were embedded in 1 mg/ml collagen gels (BD Bioscience rat tail collagen I), immersed in Opti-MEM 2.5% FBS 30 ng/ml $VEGF_{165}$ (Invitrogen) with antibiotics and cultured for 6 days. The growth medium was changed every 2 days. Upon fixation with 4% PFA, cultures were stained with Isolectin B4 and anti-αSMA. Immunofluorescence images were acquired (Macroscope AXIOZoom V16 (Zeiss)) using Z-stack analysis, and number and length of angiogenic sprouts was determined with the ZEN software tool (Zeiss). Aortic rings negative for αSMA positive cells were excluded from the analysis.

Retinal angiogenesis assay

Retinal sprouting angiogenesis was analyzed on tissue from wt mice and TNC KO mice (C57BL6) seven days after birth (P7). Briefly mice were euthanized using CO2 asphyxia. Eyes were fixed in 4% PFA at 4°C and retinas were dissected, permeabilized in PBS, and immersed in normal donkey serum (NDS) 5% and 0.1% Triton X-100 at 4°C (2.5) before incubation with isolectin B4 (1/50, Sigma-Aldrich) or primary antibodies against NG2, TNC or αSMA at 4°C (overnight) followed by incubation with fluorescence coupled secondary antibodies and embedding in Vectashield Antifading reagent (Invitrogen).

Immunofluorescence staining of cells and CDM

Cells or CDM were fixed in 4% PFA for 15 minutes, washed, permeabilized in 0.25% Triton/PBS for 10 minutes, incubated in blocking buffer (PBS, 10% normal donkey or goat serum), incubated with the primary antibody (4°C, overnight) and secondary antibody (1h at room temperature), DAPI or phalloidin (Sigma P1951, methanol, 20 µg/ml) and embedded with mounting medium (FluorSave™Reagent, CALBIOCHEM).

Protein silver staining

CM from U87MG was separated by PAGE in pre-casted 4-20% gradient gels (Invitrogen) and was stained with the SilverXpress Kit (Invitrogen) following the manufacturer`s instructions.

Western Blotting

Cells were lysed in lysis buffer (25 mM Tris-HCl pH 7.6, 150 mM NaCl, 1% NP-40, 1% sodium deoxycholate, 0.1% SDS), debris removed by centrigufation and stored at -20°C until use. Aortic rings were lysed in collagenase I, debris precipitated and resuspended in RIPA lysis buffer. Protein concentration was determined with Bradford Assay (500-006, Bio-Rad). Upon addition of 2x Laemmli buffer (125 mM Tris pH 6.8, 4% SDS, 20% Glycerol, 5% Mercaptoethanol and 0,01% Bromphenolblue) 40 µg protein was separated in 4-10% SDS-Polyacrylamid gels, transferred onto PVDF membranes (IPVH00010, Immobilon), blocked with 5% Blocking-Grade Blocker (170-6404, Biorad) in PBS/0.1% and incubated with the primary and secondary antibodies in 1.5% Blocking-Grade Blocker in PBS/0.1% Tween (overnight at 4°C). Signals were revealed with the Amersham ECL Plus Western Blotting Detection System (RPN2132, GE Healthcare).

G- and F-actin fractionation

Actin fractionation was done as described (Posern, 2002). Briefly, one million HUVEC (1% FCS) were seeded into 6 well plates that had been coated with Col I, FN or TNC. After 5h cells were lysed (20 mM HEPES pH 7.7, 50 mM NaCl, 1 mM EDTA and 0.5% (v/v) Triton X-100). Upon centrifugation (100`000g, 1h at 4°C) the supernatant was collected (G-actin fraction), the pellet (F-actin fraction) resuspended in the same buffer and sonicated, and both fractions were prepared for PAGE (20 µg protein).

Cell tracking assay

Cell mobility of isolated cells in 2D culture conditions was analyzed in MatLab (The MathWorks) after manual tracking of non-dividing cells. Phase contrast and video microscopy were done using Zeiss inverted microscope (Axiovert 200M) equipped with a CoolSnap HQ cooled charge-coupled-device camera (Roper Scientifique,. Image acquisition and cell tracking was done using the LSM image brower software (Zeiss).

RT-qPCR analysis

RNA isolation was done with TRIZOL according to the manufacturer's instructions (Invitrogen). Specific human primers for CTGF 5'-3' AGGAGTGGGTGTGTGACGA, 3'-5' CCAGGCAGTTGGCTCTAATC; Cyr61 5'-3' AGCCTCGCATCCTATACAACC, 3'-5' TTCTTTCACAAGGCGGCACTC; LCN1 5'-3' CAAGAACAACCTGGAAGC, 3'-5' CAAGGTGTCCCCCTAATC; LCN7 5'-3' AAACAGCAGTTGGATGTATG, 3'-5' GATGGCTTTGATCATGTCTG were used. For normalization of gene expression GAPDH 5'-3' ATCTTCTTTTGCGTCGCCAG, 3'-5'AATCCGTTGACTCCGACCTTC was used. For SYBR Green real-time RT-PCR, a total of 1 µg of RNA was reverse transcribed into cDNA using the High capacity cDNA Reverse

transcription kit (Apllied Biosystem, City) following the manufacturer's protocol. All products were from Invitrogen. Five biological replicates were analyzed.

Quantitative Secretome Profiling

U87MG cells were plated on the cell derived matrix generated by TNC KO or wt MEF and cultivated in DMEM containing 10 % FCS until 90 % confluence, washed three times with phosphate buffered saline (PBS), and incubated for 24 h (37 ° C, 5% CO2) in serum-free DMEM without phenol red. After 24 h, cell-conditioned medium (CM) was collected, supplemented with protease inhibitors (5 mM ethylenediaminetetraacetic acid (EDTA), 0.01 mM trans-epoxysuccinyl-L-leucylamido(4-guanidino)butane (E64), 1 mM phenylmethanesulfonyl fluoride (PMSF)), centrifuged (5min, 1000 x g, 4° C), and filtered using a 0.2 μm filter to remove debris. Samples were stored in -80° C until processing.

Samples for comparative proteomic analysis were prepared as described previously (Tholen et al., 2013). Briefly, proteins were precipitated with trichloracetic acid (TCA), solubilized, trypsinized, reduced, and alkylated. Samples were then labeled with 20 mM either "light" 12CH2O formaldehyde, (U87MG/CDMwt) or "heavy" 13CD2O formaldehyde (U87MG/CDM-TNCko) in the presence of 20 mM sodium cyanoborohydride. After quenching the reaction with glycine, both samples were combined in 1:1 ratio. Following desalting by C18 solid phase extraction (Sep-Pak C18 Plus Light Cartridge, Waters, Frankfurt, Germany), samples (ca. 300 μg) were fractionated by strong cation exchange chromatography as described previously (Shahinian et al., 2014; Tholen et al., 2013) and analyzed by liquid chromatography−tandem mass spectrometry (LC-MS/MS).

LC-MS/MS analysis

For nanoflow-LC-MS/MS analysis, a Q-Exactive plus (Thermo Scientific GmbH) mass spectrometer coupled to an Easy nanoLC 1000 (Thermo Scientific) with a flow rate of 300 nl / min each was used. Buffer A was 0.5 % formic acid, and buffer B was 0.5 % formic acid in 100 % acetonitrile (water and acetonitrile were at least HPLC gradient grade quality). A gradient of increasing organic proportion was used for peptide separation. As the analytical column served an Acclaim PepMap column (Thermo Scientific), 2 µm particle sizes, 100 Å pore sizes, length 150 mm, I.D. 50 μM. The mass spectrometer operated in data dependent mode with a top 10 method. LC-MS/MS data in raw format was converted to the mzXML (Pedrioli et al., 2004) format, using msconvert (Kessner et al., 2008) with centroiding of MS1 and MS2 data, and deisotoping of MS2 data. For spectrum to sequence assignment X! Tandem (Version 2013.09.01) (Craig and Beavis, 2004) was used. The proteome database consisted of human reviewed canonical uniprot sequences (without isoforms)

downloaded from UniProt on November 26, 2013. It consists of 20,240 real protein entries. It was appended with an equal number of shuffled decoy entries derived from the original human protein sequences. The decoy sequences were generated with the software DB toolkit (Martens et al., 2005). X! Tandem parameters included: pre-cursor mass error of ± 10 ppm, fragment ion mass tolerance of 20 ppm, tryptic specificity with up to one missed cleavage, static residue modifications: cysteine carboxyamidomethylation (+57.02 Da), variable modifications were isotope-labeled (+6.02 Da) arginine and lysine. X!Tandem results were further validated by PeptideProphet at a confidence level of >95 % (MPT = 0.05). Corresponding protein identifications are based on the ProteinProphet algorithm (Nesvizhskii, Keller et al. 2003) with a false discovery rate <1.0 %. The relative quantitation for each protein was calculated from the relative areas of the extracted ion chromatograms of the precursor ions and their isotopically distinct equivalents using the XPRESS algorithm (Han, Eng et al. 2001) as described previously (Shahinian, Loessner et al. 2014; Tholen, Biniossek et al. 2014).

Statistical analysis and graphical representation

Statistical analysis was done using GraphPad Prism or R. Statistical differences were analyzed by unpaired t-test or ANOVA one-way with Tukey post test (Gaussian distribution), non-parametric Mann-Whitney test or Kruskal-Wallis and Dunn post-test (no Gaussian distribution). Gaussian data sets with different variances were analyzed by Permutation ANOVA one-way and Permutation Tukey post-test. Gaussian distribution was tested with a minimum population (n = 18) by the d'Agostino-Pearson normality test, p-values < 0.05 were considered as statistically significant. All experiments were repeated at least 3 times.

Animal experiments

C57Bl6 (Charles Rivers) or TNC KO (Forsberg et al., 1996) that had been backcrossed for at least 10 generations into C57Bl6 (Saupe et al., 2013) were used. Experiments comprising animals were performed according to the guidelines of INSERM and the ethical committee of Alsace, France (CREMEAS).

Figure legends

Figure 1. TNC represses angiogenic sprouting and tubulogenesis

(A), Representative images of vessel sprouts from TNC KO and wt aortic rings upon staining with Isolectin B4 (scale bar, 150 μm). (**B**, **C**) Quantification of number (**B**) and length (**C**) of aortic sprouts. Mean with SEM (3 independent experiments, 9 mice per genotype, wt aortic rings, n = 105, TNC KO aortic rings, n = 123, $p < 0.001$). (**D**) Immunoblot of CAF shCTRL and shTNC for TNC and α-tubulin. (**E, F)** Tubulogenesis in a coculture assay of VeraHUVEC with CAFshCTRL, shTNC1 or shTNC2; representative images (scale bar, 200 μm) (**E**) and quantification of the number of tubes (**F**) of a 7 days culture, staining the vessel network with an anti-CD31 antibody (red). Nuclei are visualized upon staining with DAPI (blue). Mean with SEM (n = 9 wells, 3 independent experiments, 3 replicates, * $p < 0.05$ and ** $p < 0.01$).

Figure 2. TNC impairs EC tubulogenesis, adhesion and migration in vitro

(A-C) Tube formation in dependence of TNC. (**A**) Representative images of tubes formed by HUVEC upon plating on matrigel together with 10 μg/ml TNC or 0.01% PBS-Tween 20 as control (CTRL) followed by quantification of tube length (**B)** and tube numbers (**C**) per condition. Mean with SEM (n = 15 wells, 3 independent experiments, 5 replicates, ** $p < 0.01$, *** $p < 0.001$). (**D-F)** Quantification of adherent cells, HUVEC (**D**), BAEC (**E**) and HBVP (**F**) upon plating for 1h on wells coated with Col I, FN and TNC at 1 μg/cm^2 for HUVEC and HBVP and 2 μg/cm2 for BAEC. Mean with SEM (n = 18 wells, 3 independent experiments, 6 replicates, *** $p < 0.001$). (**G-I)** Wound closure of HUVEC (24h) (**G**), BAEC (12h) (**H**) and HBVP (18h) (**I**) was quantified upon addition of TNC (5, 10 and 20 μg/ml) or 0.01% Tween 20 (CTRL). Mean with SEM (n = 12 wells, 3 independent experiments, 4 replicates, ** $p < 0.01$, *** $p < 0.001$).

Figure 3. TNC reduces EC survival

(A-F) MTS multiplicity assay for HUVEC (**A**), BAEC (**B**) and HBVP (**C**) upon plating on the indicated ECM molecules (1 μg/cm^2) (**A-C**) or CDM derived from TNC KO (TNC -) or wt MEF (TNC +) (**D -F**) for up to 72h. (**A-C**) Mean with SEM (n = 18 wells, 3 independent experiments, 6 replicates, **** p < 0.0001, TNC vs. FN or Col I). (**D -F**) mean with SEM (n = 29 wells, 4 independent experiments, 4-6 replicates) for HUVEC, n = 9 (3 independent experiments with 3 replicates) for BAEC and n = 24 (4 independent experiments with 6 replicates) for HBVP, ** p <0.01, **** p < 0.0001). (**G-I)** Assessment of apoptotic (72h) (**G,H**) and proliferating HUVEC (48h) (**I**) upon growth on CDM containing (TNC +) or lacking TNC (TNC -) (**G**) or on ECM coated wells (**H, I**). (**G, H**) Four random fields were quantified. Mean with SEM (n = 12 wells, 3 independent experiments, 4 replicates, * p <0.05, *** p < 0.001, **** p < 0.0001). (**I)** mean with SEM (n = 18 wells, 3 independent experiments, 6 replicates, *** p <0.001, **** p < 0.0001).

Figure 4. TNC represses actin polymerization and YAP activation in EC

(A) Representative images of actin polymerization (phalloidin, white) and nuclei (DAPI, blue) of HUVEC upon growth on FN or TNC for 5h (scale bar, 5 μm). (**B, C**) Analysis of G and F actin in HUVEC by immunoblotting upon plating on the indicated substrata for 5h. (**C**) Quantification of the immunoblotting signal represented as ratio of F/G actin (n = 3 wells). (**D**) Representative images of YAP (red), polymerized actin (phalloidin, green) and nuclei (DAPI, blue) of HUVEC upon growth on FN or TNC for 5h (scale bar, 5 μm). (**E**) Quantification of YAP positive nuclei normalized to DAPI positive nuclei. 30-40 cells were counted in the triplicates (3 experiments) of 4-6 randomly chosen fields per condition. Mean with SEM, described as a percentage of nuclei positive for YAP (n = 9 wells, 3 independent experiments, 3 replicates, * p < 0.05, ** p < 0.01, *** p < 0.001). (**F**) RT-qPCR analysis of YAP target genes CTGF and Cyr61 in HUVEC upon growth on FN or TNC for 24 hours (n = 5, ** p < 0.01).

Figure 5. TNC-educated CM from GBM cells or transformed fibroblasts promotes angiogenesis in vitro

(A), Assessment of HUVEC viability by EB/AO staining upon addition of CM derived from U87MG cells that had been grown on CDM laid down by TNC KO (TNC -) and wt MEF (TNC +). Bars represent the percentage of viable, apoptotic and dead cells with SEM (n = 9 wells, 3 independent experiments, 3 replicates). (**B)** Assessment of HUVEC multiplicity (MTS assay) upon treatment with CM derived from TNC educated U87MG cells. Mean with SEM (n = 18 wells, 3 independent experiments, 6 replicates, * $p < 0.05$, **** $p < 0.0001$). (**C**) Number of tubes upon growth of HUVEC (7h) on matrigel and treatment with CM from TNC educated U87MG cells (grown on CDM from MEF expressing or lacking TNC). Mean with SEM (wt, n = 13 wells, TNC KO, n = 15 wells, 3 independent experiments with at least 4 replicates, *** $p < 0.001$). (**D, E)** Tube formation with CM of TNC educated U87MG cells. (**D**) Representative phase contrast images of HUVEC upon growth on matrigel for 7h with CM derived from U87MG shCTRL, shTNC1 and shTNC2 cells. (**E**) Quantification of tubes. Mean with SEM (n = 15 wells, 3 independent experiments, 5 replicates, ** $p < 0.01$, *** $p < 0.001$). (**F)** Cell multiplicity (MTS assay) for HUVEC treated with CM derived from TNC educated U87MG cells. Mean with SEM (n = 18 wells, 3 experiments, 6 replicates, ** $p < 0.01$, **** $p < 0.0001$). (**G**, **H**) Sprouting upon coculture with TIF. (**G**) Representative images of HUVEC sprouting from cytodex beads in coculture with TIFshCTRL and TIFshTNC after 3 days of embedding into fibrin gels (scale bar, 200 µm). (**H**) Quantification of sprout length. Mean with SEM (TIF shCTRL, n = 47 beads, 3 independent experiments, 3 replicates, TIFshTNC, n = 46 beads, 3 independent experiments, 3 replicates, *** $p < 0.001$).

Figure 6. Proteomic analysis of the U87MG-derived CM

(A) Representative image of a silver stained polyacrilamide gel. CM from U87MG grown on CDM laid down by TNC KO or wt MEF was separated by PAGE before staining. The experiment was repeated four times with four independent batches of CM. Arrow points at the LCN1 containing band. (**B**) Heat

map representing selected secreted molecules from U87MG-educated cells involved in angiogenesis and regulated by TNC. Yellow and blue showed respectively upregulated and downregulated proteins (Log2 values). (**C**) Validation of differential expression of lipocalin-1 (LCN1) and lipocalin-7 (LCN7) in TNC educated CM of U87MG cells that had been grown on CDM laid down by MEF expressing or lacking TNC. (**D**) Number of tubes upon growth of HUVEC (7h) on matrigel together with recombinant LCN1. Normalization towards CTRL (no LCN1). Mean with SEM (n = 15-20 wells, 3 independent experiments, at least 5 replicates, * $p < 0.05$, ** $p < 0.01$). (**E**) Number of tubes upon growth of HUVEC (7h) on matrigel together with boiled CM of TNC educated U87MG cells. Mean with SEM (n = 15 wells, 3 experiments, 5 replicates, **** $p < 0.0001$). (**F**) Quantification (ELISA) of the human SDF1 (CXCL12) in TNC educated CM from U87MG cultivated for 48h on CDM of MEF expressing or lacking TNC. Mean with SEM (n = 2-5). (**G**) Assessment of tubes (7h) upon growth of HUVEC on matrigel together with TNC-educated CM derived from U87MG cells and AMD3100 (10 - 1000 ng/ml). Mean with SEM (n = 15 wells, 3 independent experiments, 5 replicates, * $p < 0.05$, ** $p < 0.01$, *** $p < 0.001$).

Figure 7. Hypothesis of TNC's role in driving and shaping tumor angiogenesis

Tumor cells divide and generate a tumor mass that when reaching a diameter bigger than 1 mm^2 gets hypoxic. Hypoxia is one of the triggers known to induce TNC (Lal et al., 2001). Hypoxia as well as TNC may promote recruitment of fibroblasts that convert into CAF (De Wever et al., 2004). Upon contact with TNC tumor cells (TC) and CAF express an angio-modulatory secretome (AMS) where SDF1 is an important factor (this study). This secretome promotes EC survival and tubulogenesis thus potentially counteracting cell death upon adhesion to TNC (this study). The AMS is partially overlapping with the AngioMatrix, a gene expression signature with poor survival prognosis, that drives the angiogenic switch (this study, (Langlois et al., 2014)). In the AngioMatrix, TNC is one of the most highly induced matrisomal molecules promoting the angiogenic switch (Langlois et al., 2014). In addition to CAF, TNC also attracts other cells such as bone-marrow derived cells (Ballard et al., 2006) and EC (Spenlé et al., 2015), that promote and facilitate angiogenesis. Newly formed vessels either mature or prune. TNC appears to promote pruning (+) and to counteract maturation (-) by a mechanism that involves

functional impairment of YAP (this study). Finally contact of tumor cells with TNC may contribute to their transdifferentiation into cells that integrate into the tumor vasculature, a phenotype known as vasculogenic mimicry, where TNC seems to play a promoting role (Kääriäinen et al., 2006; Midwood and Orend, 2009; Pezzolo et al., 2011; Spenlé et al., 2015). Altogether these events may culminate in destabilized poorly functional vessels that would offer a poor barrier for cancer cells, thus facilitating dissemination and metastasis. Indeed TNC promoted increased vessel leakage and enhanced lung micrometastasis in the Rip1Tag2 model (Saupe et al., 2013). Events where TNC is involved are marked in red. Positive or negative effects of TNC are marked with a "+" or "-" sign.

Figure S1. TNC is expressed in wt aorta, but not in retina nor in cultured endothelial cells

(A) Expression of TNC in aorta of TNC KO and wt mice upon growth for 6 days in Col I gels assessed by immunoblotting for TNC with α-tubulin as control. (**B, C**) Co-staining of endothelial cell spouts for EC (isolectin B4, green), perivascular cells (αSMA, red) (**B**) or TNC (red) (**C**) and nuclei (DAPI) (scale bar, 10 µm). **D**, Immunofluorescence staining of P7 wt mouse retina for EC (Isolectin B4, green), pericytes (NG2, red) and TNC (blue). Note no expression of TNC in the retinal tissue (scale bar, 10 µm). (**E**, **F**) representative pictures of vessel outgrowth in culture upon labeling with isolectin B4 (green) (scale bar, 500 µm). (**G**) Quantification of the migration front of the vascular network. Bars represent mean with SEM (wt, n = 33 retinas and TNC KO, n = 27 retina, $p < 0.05$). (**H**, **I**) Representative picture of vessel branching in retinas from wt and TNC KO mice. Mean with SEM (wt, n = 38 retinas, TNC KO, n = 42 retinas, no statistical difference). (**J**, **K**) Representative images of retinal filopodia at the migration front upon staining with isolectin B4. Mean with SEM (wt, n = 38 retinas, TNC KO, n = 48, no statistical difference). (**L-N**) Assessment of TNC expression in EC (VeraHUVEC, VeraHUAEC, HMEC-SV40 and HMVEC-hTERT) by immunoblotting for TNC (α-tubulin as control) upon growth of cells on different substrata (24h) (**L**), or upon stimulation with VEGF or TGFβ (24h) (**M**).

Figure S2. TNC disturbs EC tubulogenesis, adhesion and migration in vitro

(**A, B**) Tube formation of BAEC in dependence of TNC. Representative images of tubes formed by BAEC upon plating on matrigel together with 5 or 20 µg/ml TNC or 0.01% PBS-Tween 20 as control (CTRL) with quantification of number of tubes per condition. Mean with SEM (n = 15 wells, 3 experiments, 5 replicates, $p < 0.001$). (**C-E**) Phase contrast images of HUVEC (**C**), BAEC (**D**) and HBVP (**E**) upon adhesion on the indicated substrata for 1h. (**F-H)** Wound closure assay**.** Representative phase contrast images of confluent monolayers of HUVEC (**F**), BAEC (**G**) and HBVP (**H**) are shown for the indicated time points and upon addition of TNC (5 and 20 µg/ml). (**I**, **J**), Representative phase contrast images (**I**) of HUVEC on FN or TNC substratum (lime lapse acquisition) after 1h and 11h and manual cell tracking labelling mobility of six cells on FN and three cells on TNC over the 11h period (**J**).

Figure S3. TNC impacts on cell multiplicity in a dose dependent manner when offered as 2D substratum and in CDM

(A) Assessment of cell numbers with a MTS assay in HUVEC that were grown for 24h on substrata with different amounts of TNC. The IC50 was extrapolated upon non-linear curve fit (red) as 3.665 +/- 0.652 µg/cm^2. Mean with SEM (n = 9 wells, 3 experiments, 3 replicates). (**B**) Schematic showing the protocol to obtain CDM. (**C**, **D**) Representative immunofluorescence images of CDM laid down by TNC KO or wt MEF for Col I (**B**) and TNC, POSTN and FN (**C**). Pictures of (**B)** have been merged to show partial overlap of the ECM networks (scale bar, 40 µm). (**E**) Cell multiplicity assessed by a MTS assay of BAEC plated on CDM laid down by CAF shCTRL, shTNC1 and shTNC2. Mean with SEM (n = 20-24 wells, 4 independent experiments, at least 5 replicates, shCTRL vs. shTNC1, $p < 0.05$ and shCTRL vs. shTN2, $p < 0.001$). (**F**) Representative images of immunofluorescence staining for cleaved caspase 3 in HUVEC upon growth (72h) on CDM laid down by MEF containing or lacking TNC (scale bar, 100 µm).

Figure S4. TNC represses cell spreading and actin stress fiber formation

(**A, B**) Representative images of HUVEC grown for 2h, 5h and 24h on the indicated 2D substrata (**A**) or upon growth (24h) on CDM laid down by MEF expressing or lacking TNC (**B**) upon staining for polymerized actin with phalloidin. Note that TNC inhibited actin stress fiber formation. (scale bar, 5 μm).

Figure S5. TNC-educated CM from GBM cells and from transformed fibroblasts promotes multiplicity and EC sprouting

(A) Cell numbers of BAEC assessed by a MTS assay upon growth on CDM laid down by MEF expressing (TNC +) or lacking TNC (TNC -). Mean with SEM (n = 18 wells, 3 experiments, 6 replicates, * $p < 0.05$, ** $p < 0.01$). (**B**) Number of tubes of HUVEC grown on matrigel (7h) upon treatment with CM from TNC-educated U118MG or U373MG that had been grown on CDM laid down by MEF expressing (TNC +) or lacking TNC (TNC -). Mean with SEM (n = 15 wells, 3 experiments, 5 replicates, * $p < 0.05$, **** $p < 0.001$). (**C**) Comparison of cell numbers of U87MG, U118MG and U373MG upon growth (24h) and treatment with TNC-educated CM (described in (**B**)). Mean with SEM (n = 18 wells, 3 experiments, 6 replicates, no statistical difference). (**D**) Expression of TNC in U87MG shCTRL and shTNC by immunoblotting with α-tubulin as control 48h after plating. (**E**) Assessment of HUVEC cell numbers by MTS assay (48h) upon addition of CM from U87MG shCTRL, shTNC1 and shTNC2 cells. Mean with SEM (n = 18 wells, 3 experiments, 6 replicates, ns = not significant). (**F, G**) Assessment of cell numbers (**F**) and number of tubes on matrigel (**G**) in HUVEC upon treatment with CM from CAF that had been grown on CDM of MEF expressing (TNC +) or lacking TNC (TNC -). (**F**) Mean with SEM (n = 12 wells, 3 experiments, 4 replicates, no statistical difference). (**G**) Mean with SEM (n = 15 wells, 3 experiments, 5 replicates, no statistical difference). (**H**) Schematic representation of the HUVEC sprouting assay in fibrin gel coculture with TIF control or KD for TNC. (**I**) Expression of TNC in 24h cultures of TIF shCTRL and TIF shTNC as determined by immunoblotting for TNC and ERK1/2 as

control. (**F**) Quantification of the number of HUVEC sprouts per bead. Mean with SEM (TIFshCTRL, n = 47 beads, TIF shTNC, n = 46 beads, 3 independent experiments, 3 replicates per condition, no statistical difference).

Figure S6. Proteomic analysis of the U87MG-derived CM

(A) Pie chart representing all proteins deregulated in U87MG educated by CDM laid down by MEF expressing or lacking TNC. (**B**) Quantification of the human VEGFA concentration in CM from U87MG grown for 48h on CDM laid down by MEF expressing or lacking TNC. Mean with SEM (n = 2-3).

Figure 1.

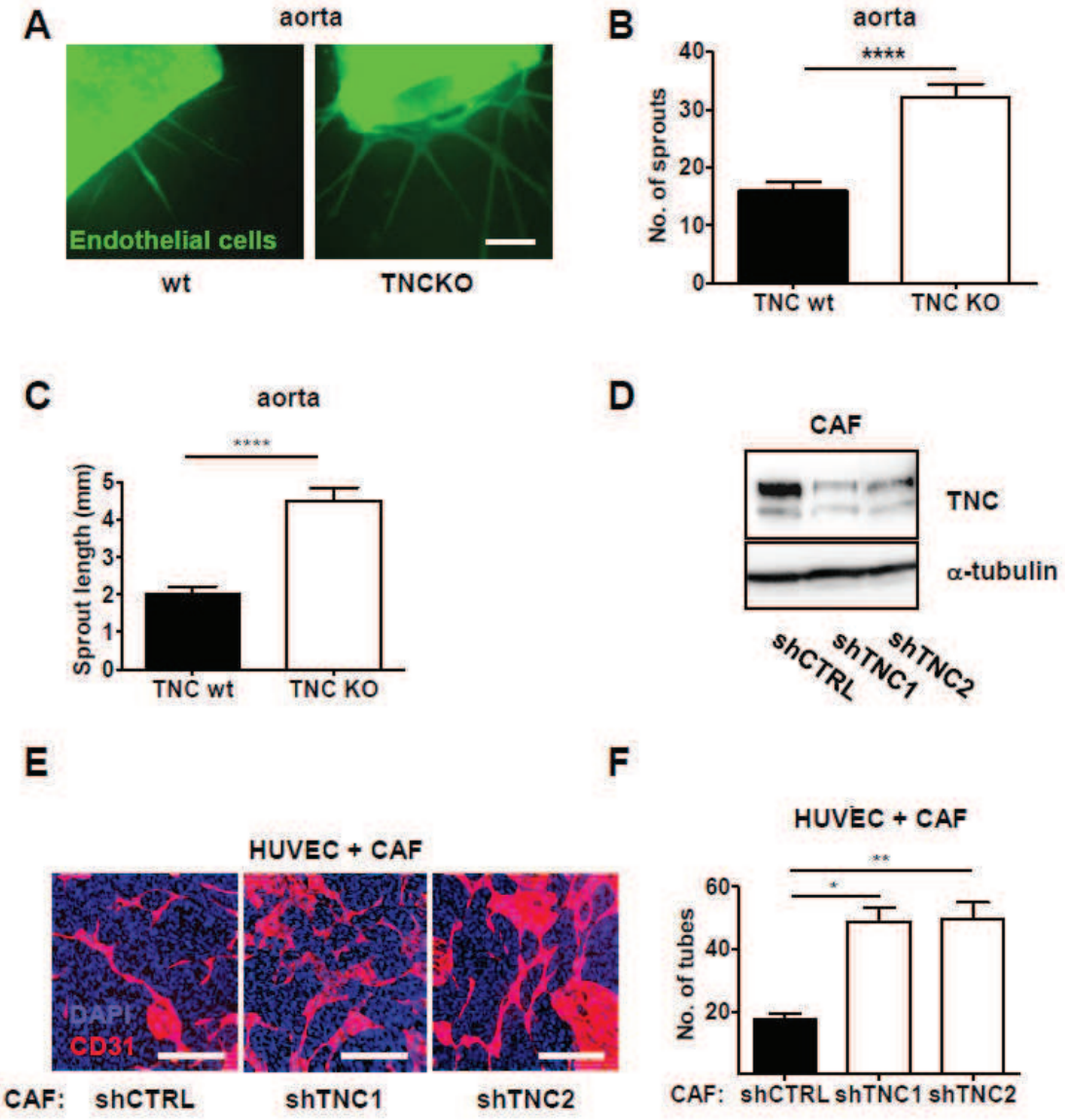
A
aorta
Endothelial cells
wt
TNCKO
B
aorta
****
No. of sprouts
40
30
20
10
0
TNC wt
TNC KO
C
aorta
****
Sprout length (mm)
5
4
3
2
1
0
TNC wt
TNC KO
D
CAF
TNC
α-tubulin
shCTRL
shTNC1
shTNC2
E
HUVEC + CAF
DAPI
CD31
CAF: shCTRL
shTNC1
shTNC2
F
HUVEC + CAF
**
*
No. of tubes
60
40
20
CAF: shCTRL shTNC1 shTNC2

Figure 2.

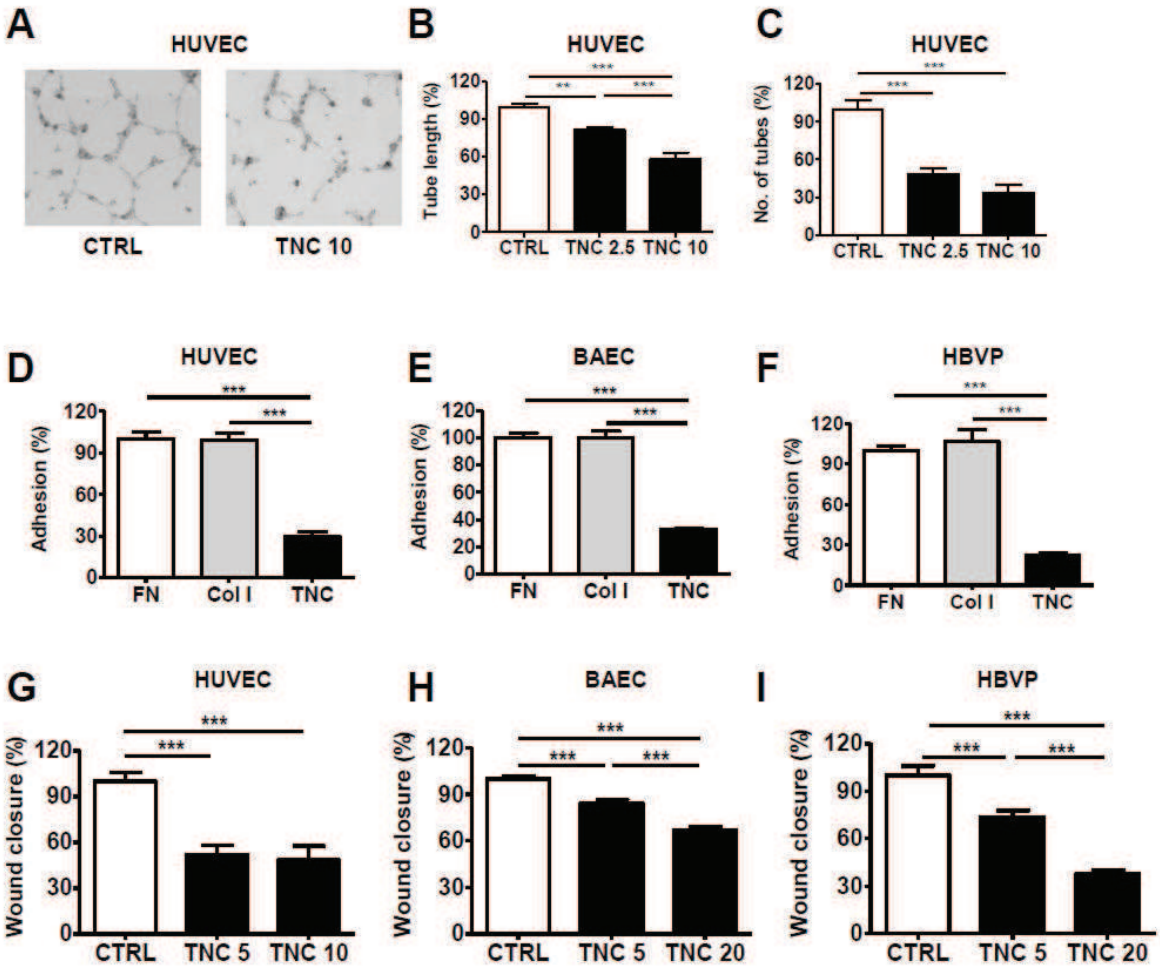
A
HUVEC
CTRL
TNC 10
B
HUVEC
Tube length (%)
CTRL
TNC 2.5
TNC 10
C
HUVEC
No. of tubes (%)
CTRL
TNC 2.5
TNC 10
D
HUVEC
Adhesion (%)
FN
Col I
TNC
E
BAEC
Adhesion (%)
FN
Col I
TNC
F
HBVP
Adhesion (%)
FN
Col I
TNC
G
HUVEC
Wound closure (%)
CTRL
TNC 5
TNC 10
H
BAEC
Wound closure (%)
CTRL
TNC 5
TNC 20
I
HBVP
Wound closure (%)
CTRL
TNC 5
TNC 20

Figure 3.

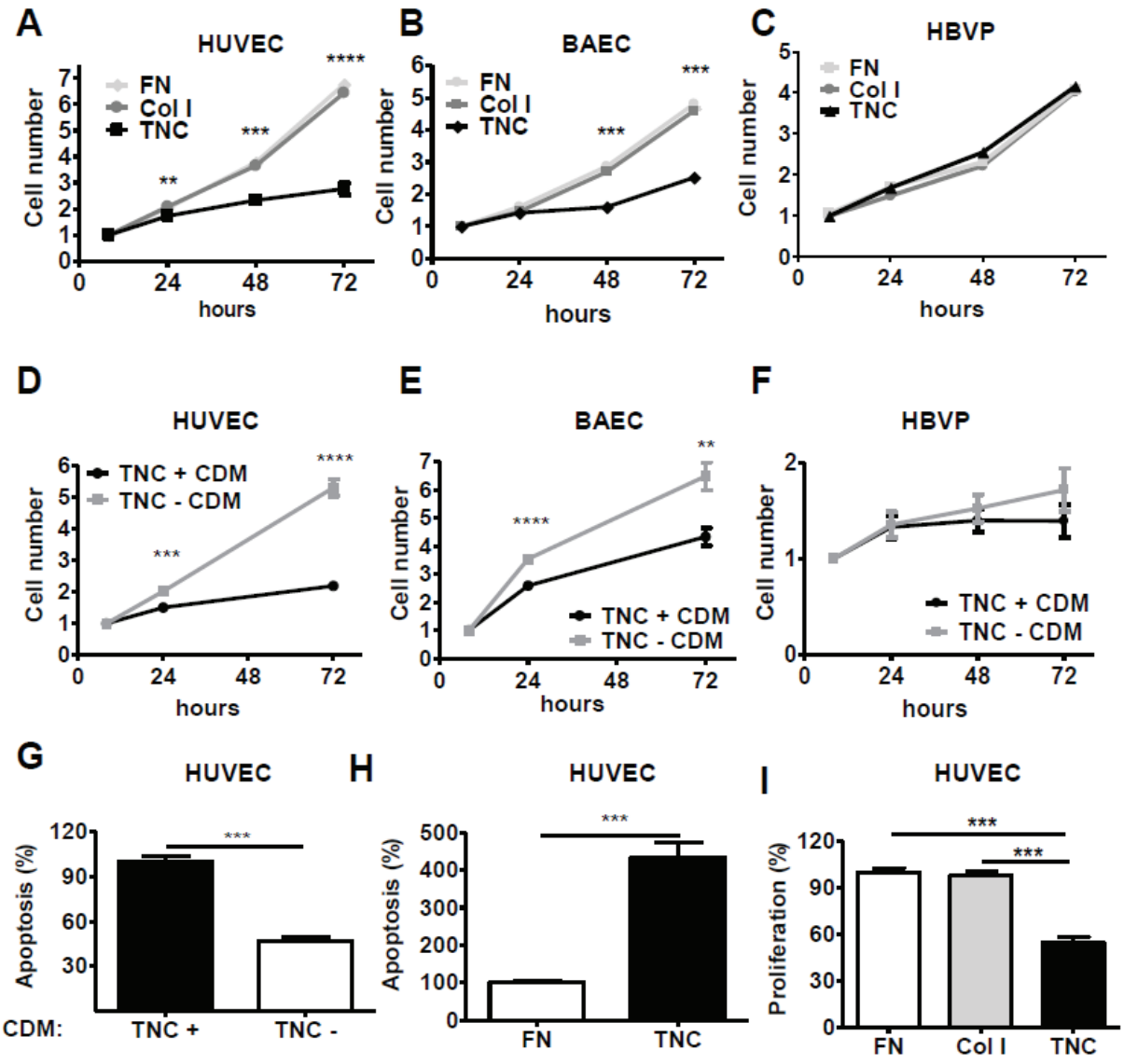
A
HUVEC
FN
Col I
TNC
Cell number
hours
B
BAEC
C
HBVP
D
HUVEC
TNC + CDM
TNC - CDM
E
BAEC
F
HBVP
G
HUVEC
Apoptosis (%)
CDM:
TNC +
TNC -
H
HUVEC
I
HUVEC
Proliferation (%)

Figure 4.

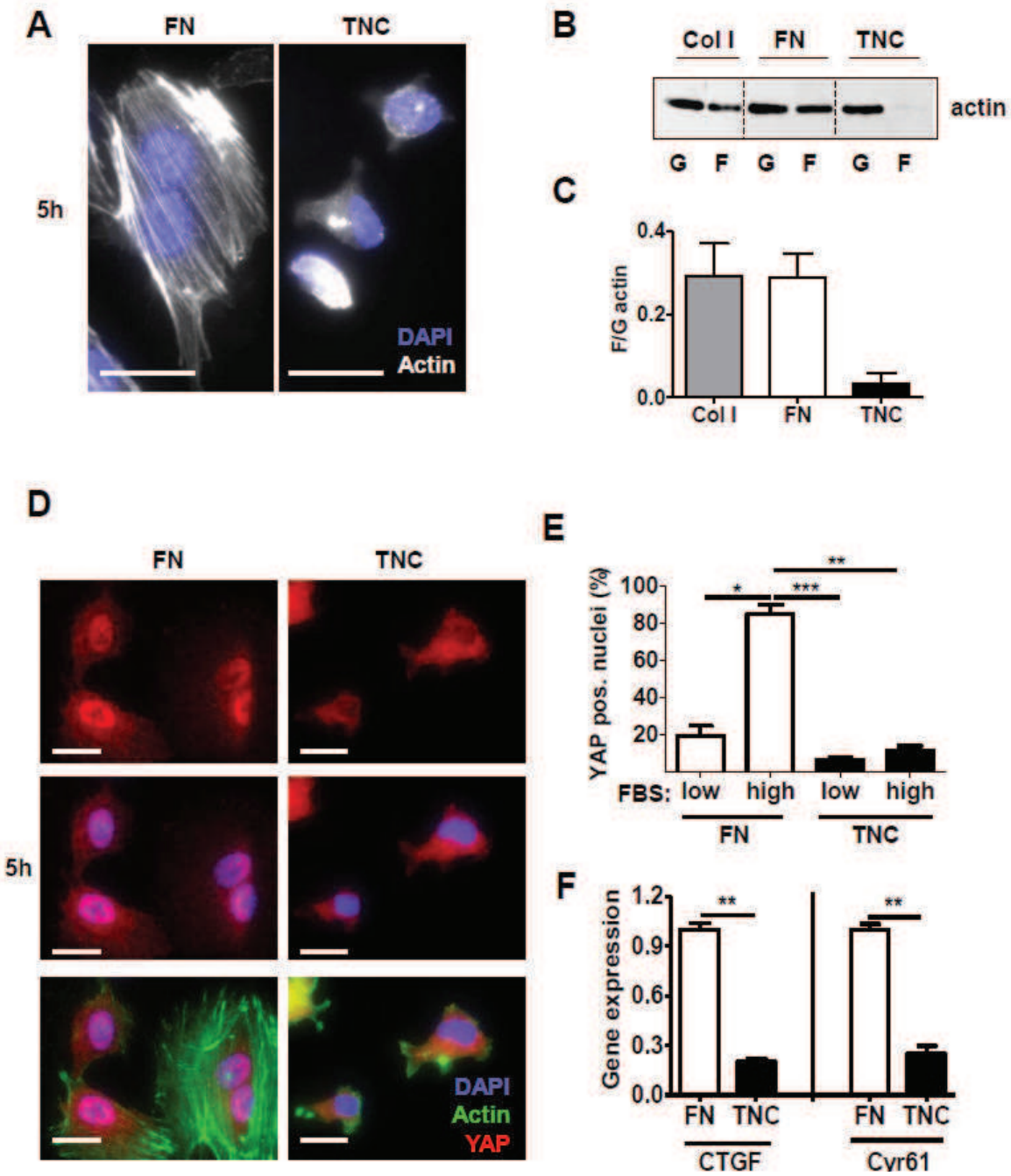
A
FN
TNC
5h
DAPI
Actin
B
Col I
FN
TNC
actin
G F G F G F
C
F/G actin
0.4
0.2
0.0
Col I
FN
TNC
D
FN
TNC
5h
DAPI
Actin
YAP
E
YAP pos. nuclei (%)
100
80
60
40
20
*
**
***
FBS: low high low high
FN
TNC
F
Gene expression
1.2
0.9
0.6
0.3
0.0
**
**
FN TNC FN TNC
CTGF
Cyr61

Figure 5.

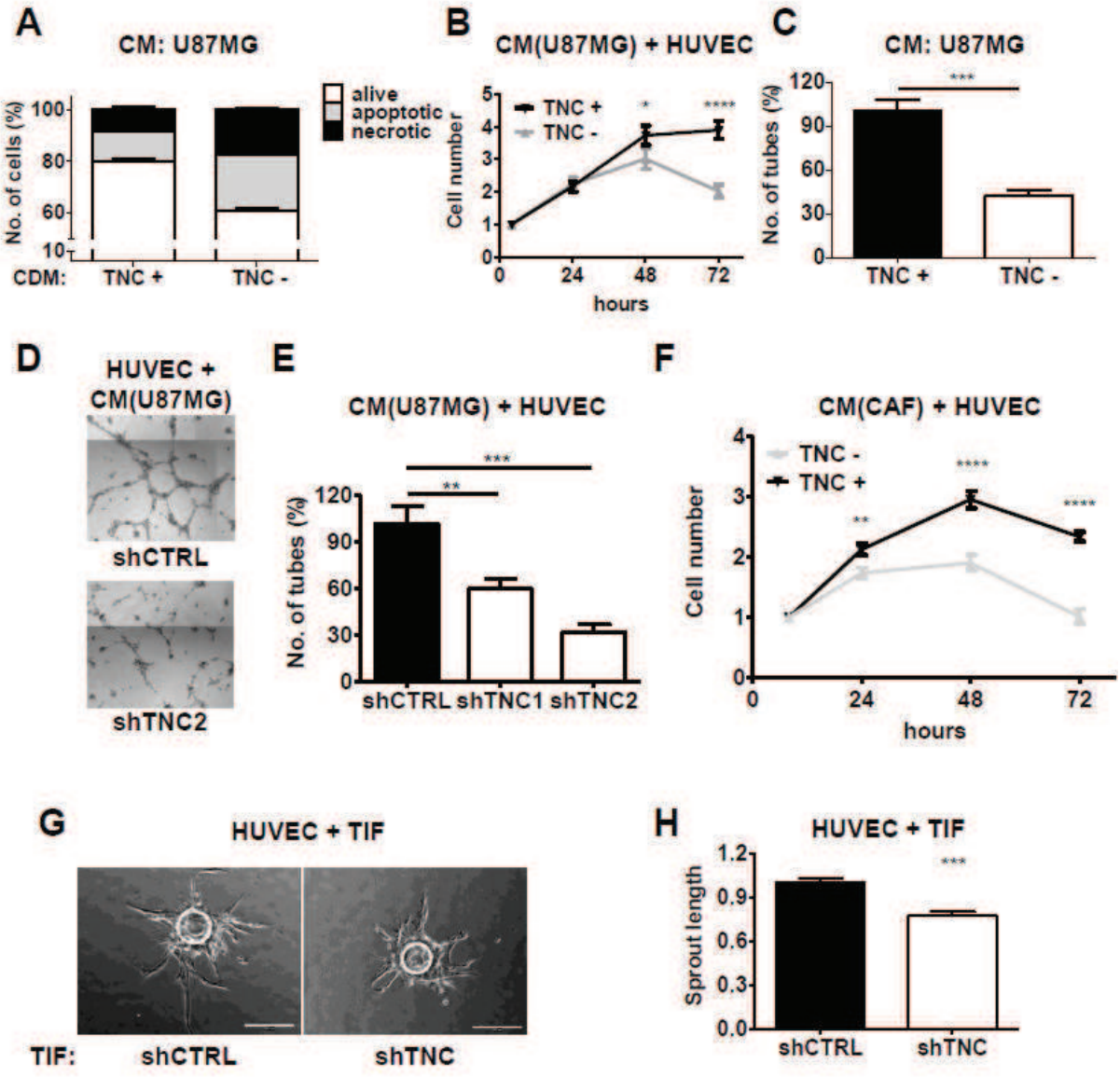
A
CM: U87MG
No. of cells (%)
100
80
60
10
alive
apoptotic
necrotic
CDM:
TNC +
TNC -
B
CM(U87MG) + HUVEC
Cell number
TNC +
TNC -
*
****
0
24
48
72
hours
C
CM: U87MG
No. of tubes (%)
***
120
90
60
30
0
TNC +
TNC -
D
HUVEC +
CM(U87MG)
shCTRL
shTNC2
E
CM(U87MG) + HUVEC
***
**
No. of tubes (%)
120
90
60
30
0
shCTRL
shTNC1
shTNC2
F
CM(CAF) + HUVEC
TNC -
TNC +
Cell number
**
****
****
0
24
48
72
hours
G
HUVEC + TIF
TIF:
shCTRL
shTNC
H
HUVEC + TIF
Sprout length
***
1.2
0.9
0.6
0.3
0.0
shCTRL
shTNC

Figure 6.

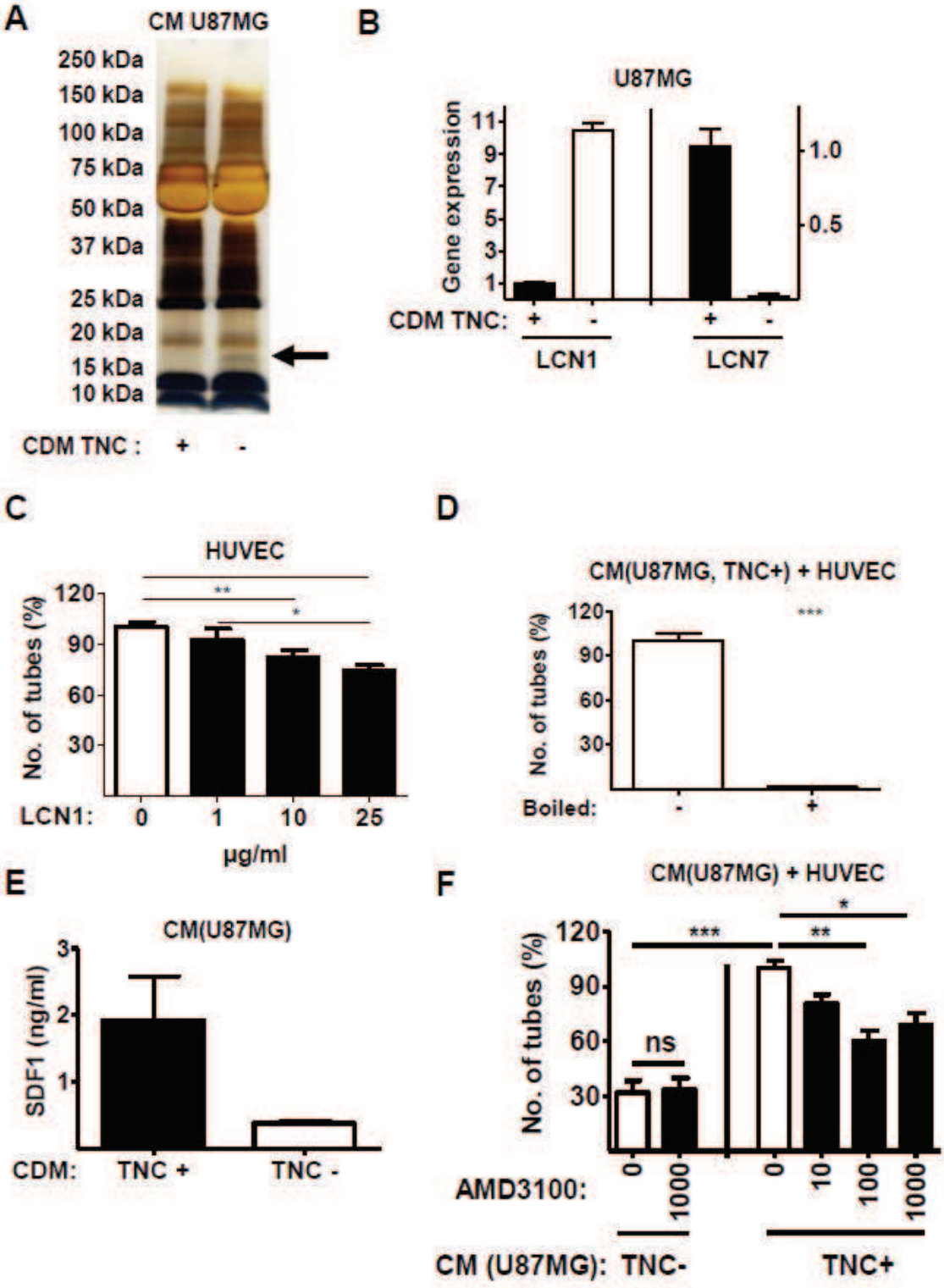
A
CM U87MG
250 kDa
150 kDa
100 kDa
75 kDa
50 kDa
37 kDa
25 kDa
20 kDa
15 kDa
10 kDa
CDM TNC : + -
B
U87MG
Gene expression
11
9
7
5
3
1
1.0
0.5
CDM TNC: + - + -
LCN1
LCN7
C
HUVEC
No. of tubes (%)
120
90
60
30
**
*
LCN1: 0 1 10 25
µg/ml
D
CM(U87MG, TNC+) + HUVEC
No. of tubes (%)
120
90
60
30
***
Boiled: - +
E
CM(U87MG)
SDF1 (ng/ml)
3
2
1
CDM: TNC + TNC -
F
CM(U87MG) + HUVEC
No. of tubes (%)
120
90
60
30
***
**
*
ns
AMD3100: 0 1000 0 10 100 1000
CM (U87MG): TNC- TNC+

Figure 7.

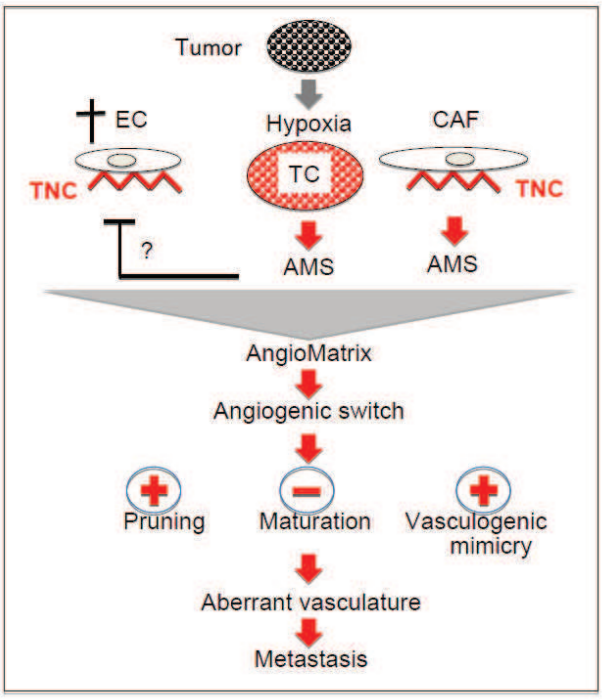
Tumor
EC
Hypoxia
CAF
TNC
TC
TNC
?
AMS
AMS
AngioMatrix
Angiogenic switch
Pruning
Maturation
Vasculogenic mimicry
Aberrant vasculature
Metastasis

Figure S1.

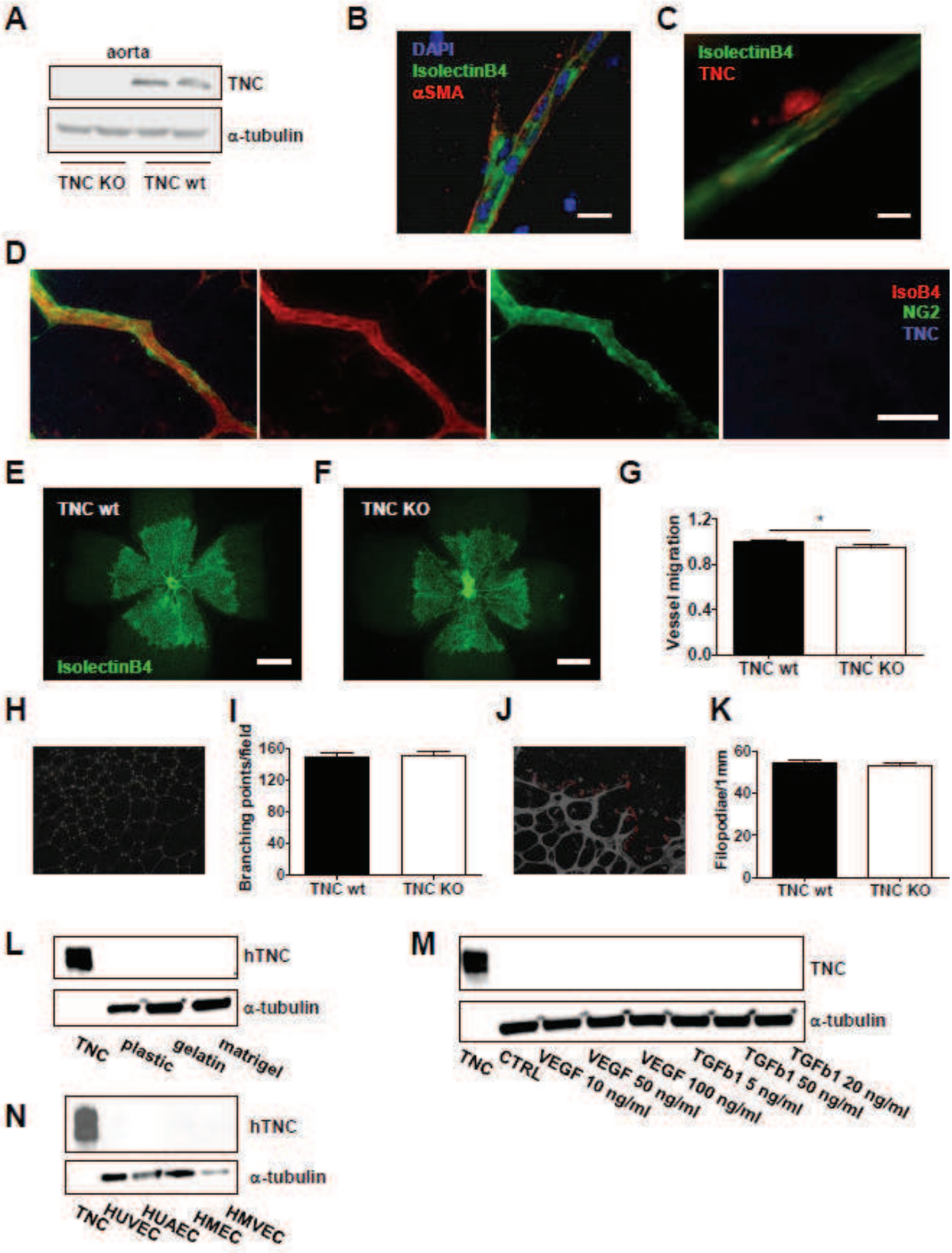
A
aorta
TNC
α-tubulin
TNC KO
TNC wt
B
DAPI
IsolectinB4
αSMA
C
IsolectinB4
TNC
D
IsoB4
NG2
TNC
E
TNC wt
IsolectinB4
F
TNC KO
G
Vessel migration
1.2
0.8
0.4
0.0
*
TNC wt
TNC KO
H
I
Branching points/field
160
120
80
40
0
TNC wt
TNC KO
J
K
Filopodiae/1 mm
60
40
20
0
TNC wt
TNC KO
L
hTNC
α-tubulin
TNC
plastic
gelatin
matrigel
M
TNC
α-tubulin
TNC
CTRL
VEGF 10 ng/ml
VEGF 50 ng/ml
VEGF 100 ng/ml
TGFb1 5 ng/ml
TGFb1 50 ng/ml
TGFb1 20 ng/ml
N
hTNC
α-tubulin
TNC
HUVEC
HUAEC
HMEC
HMVEC

Figure S2.

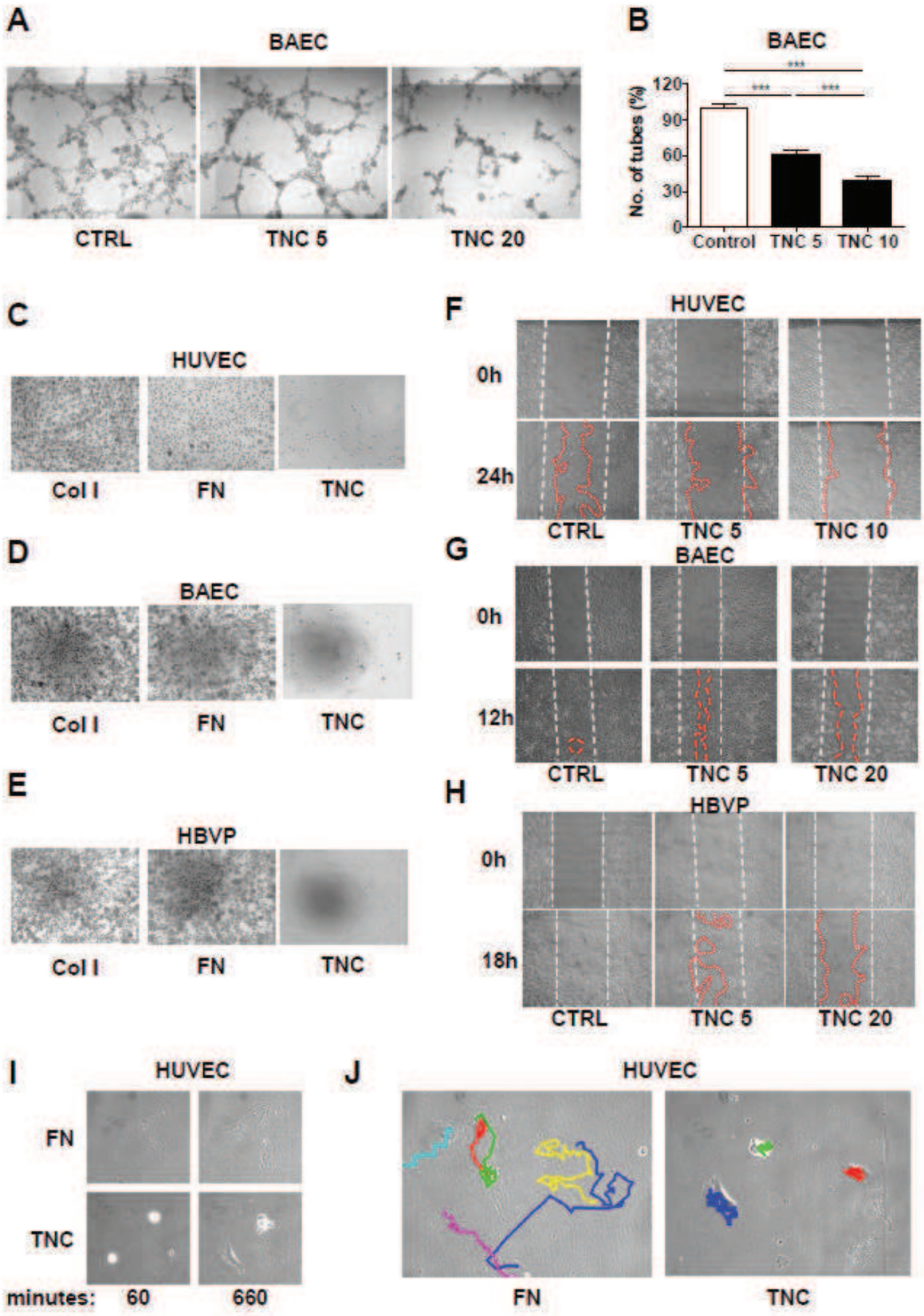
A
BAEC
CTRL
TNC 5
TNC 20
B
BAEC
No. of tubes (%)
120
90
60
30
0
***
***
***
Control
TNC 5
TNC 10
C
HUVEC
Col I
FN
TNC
D
BAEC
Col I
FN
TNC
E
HBVP
Col I
FN
TNC
F
HUVEC
0h
24h
CTRL
TNC 5
TNC 10
G
BAEC
0h
12h
CTRL
TNC 5
TNC 20
H
HBVP
0h
18h
CTRL
TNC 5
TNC 20
I
HUVEC
FN
TNC
minutes:
60
660
J
HUVEC
FN
TNC

Figure S3.

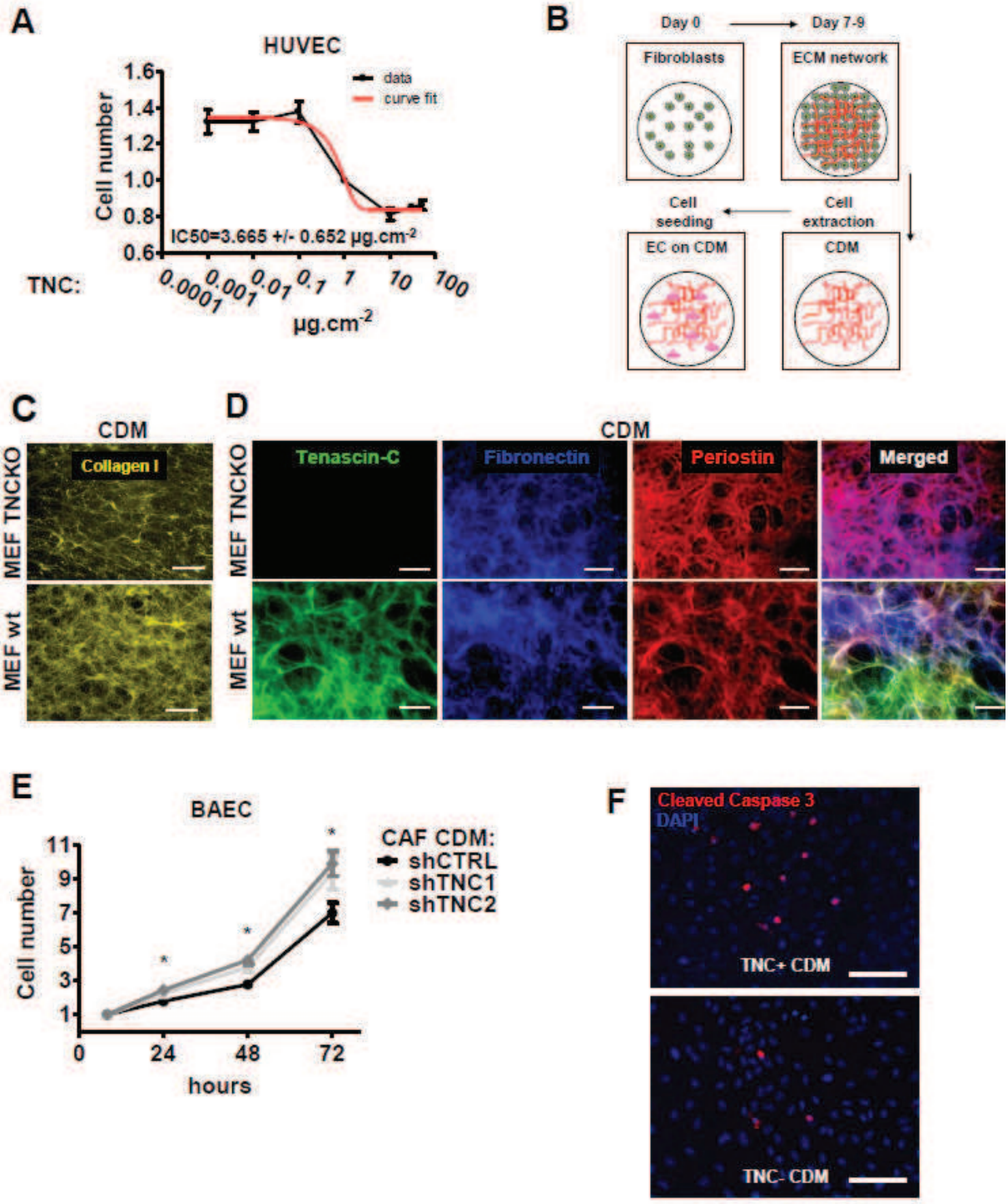
A
HUVEC
data
curve fit
Cell number
1.6
1.4
1.2
1.0
0.8
0.6
IC50=3.665 +/- 0.652 µg.cm-2
TNC:
0.0001
0.001
0.01
0.1
1
10
100
µg.cm-2
B
Day 0
Day 7-9
Fibroblasts
ECM network
Cell seeding
Cell extraction
EC on CDM
CDM
C
CDM
Collagen I
MEF TNCKO
MEF wt
D
CDM
Tenascin-C
Fibronectin
Periostin
Merged
MEF TNCKO
MEF wt
E
BAEC
CAF CDM:
shCTRL
shTNC1
shTNC2
Cell number
11
9
7
5
3
1
0
24
48
72
hours
F
Cleaved Caspase 3
DAPI
TNC+ CDM
TNC- CDM

Figure S4.

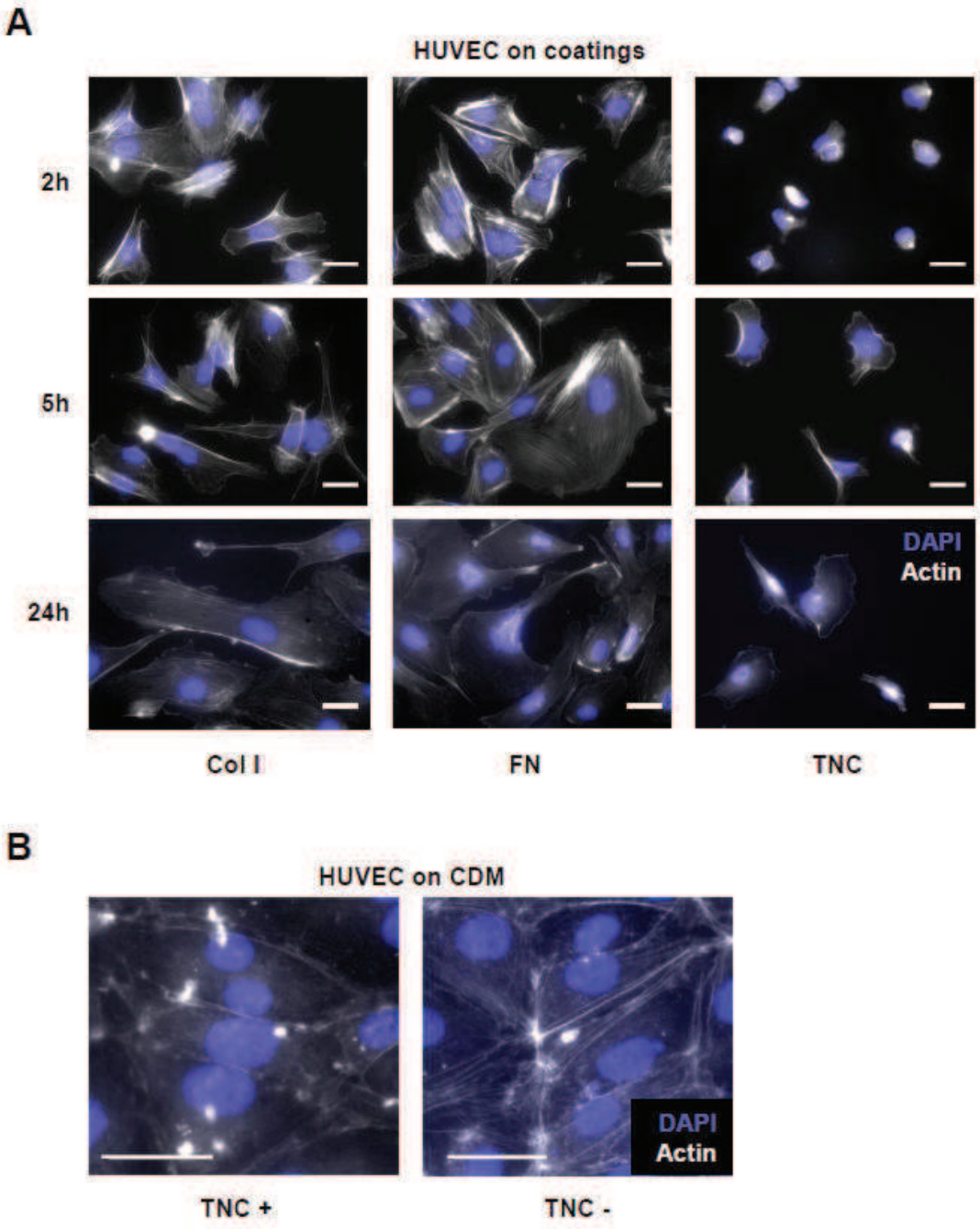
A
HUVEC on coatings
2h
5h
24h
DAPI
Actin
Col I
FN
TNC
B
HUVEC on CDM
DAPI
Actin
TNC +
TNC -

Figure S5.

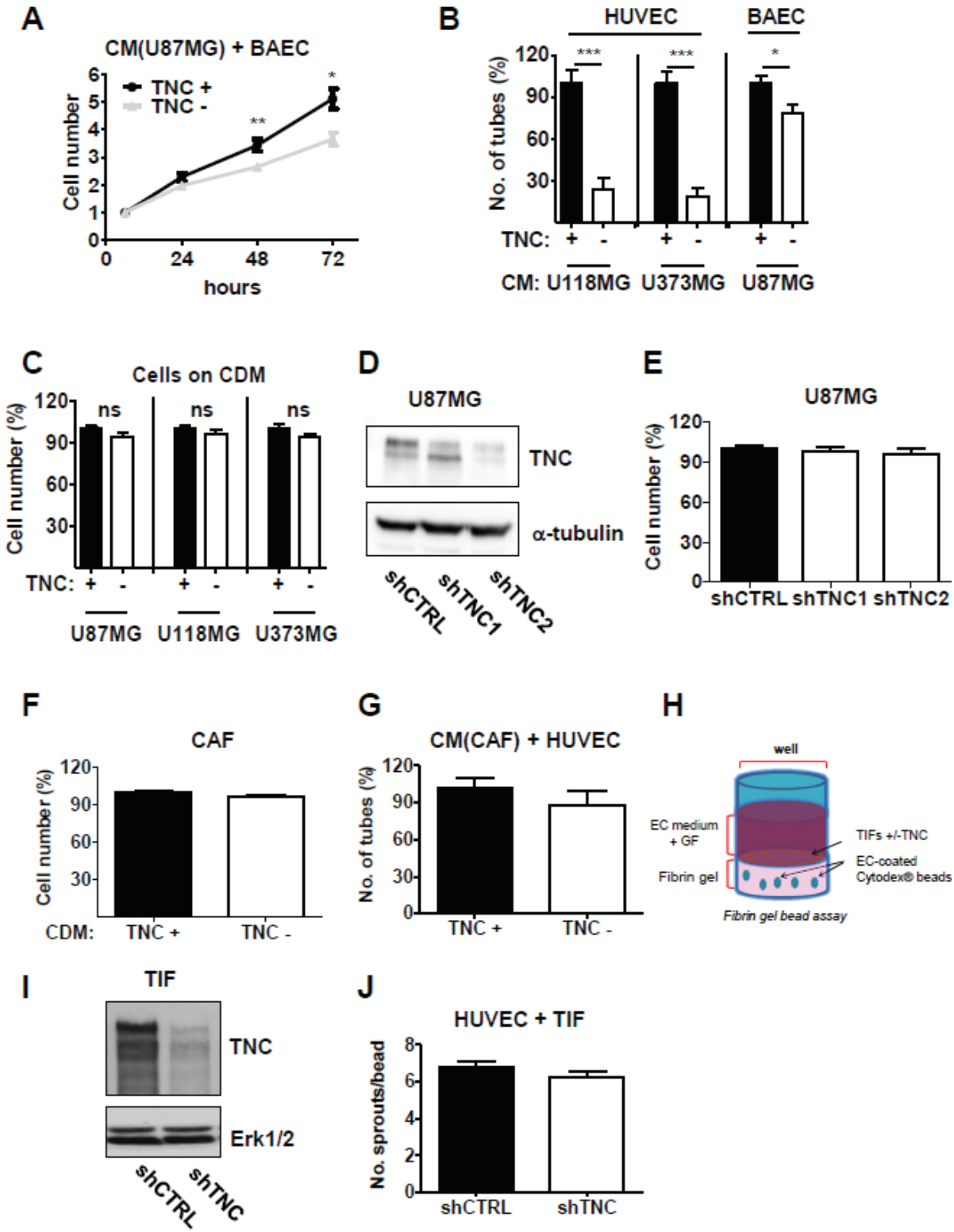
A
CM(U87MG) + BAEC
TNC +
TNC -
Cell number
hours
B
HUVEC
BAEC
No. of tubes (%)
TNC:
CM: U118MG U373MG U87MG
C
Cells on CDM
Cell number (%)
ns
TNC:
U87MG U118MG U373MG
D
U87MG
TNC
α-tubulin
shCTRL shTNC1 shTNC2
E
U87MG
Cell number (%)
shCTRL shTNC1 shTNC2
F
CAF
Cell number (%)
CDM: TNC + TNC -
G
CM(CAF) + HUVEC
No. of tubes (%)
TNC + TNC -
H
well
EC medium + GF
Fibrin gel
TIFs +/-TNC
EC-coated Cytodex® beads
Fibrin gel bead assay
I
TIF
TNC
Erk1/2
shCTRL shTNC
J
HUVEC + TIF
No. sprouts/bead
shCTRL shTNC

Figure S6.

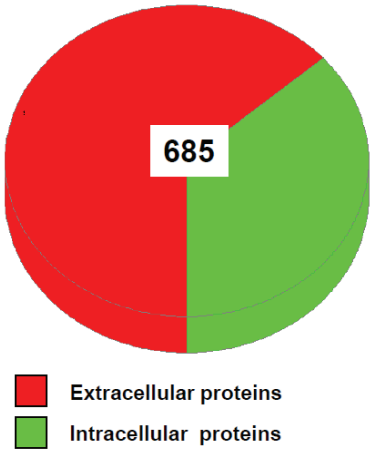

Table 1. Expression of selected TNC-regulated angio-modulatory factors

	Molecule	Fc (Log2)	Function in angiogenesis	Reference
Up	LCN7 (TINAGL1)	5.158	promote angiogenesis in vivo, ex vivo and in vitro	(Brown et al., 2010)
	TG2	3.308	promote angiogenesis through VEGF signaling and ECM remodeling	(Haroon et al., 1999)
	Pleiotrophin	2	stimulate normal and pathological angiogenesis	(Perez-Pinera et al., 2008)
	Wnt 7b	1.434	promote the angiogenic switch	(Yeo et al., 2014)
	CXCL12 (SDF1)	1.336	promote angiogenesis in vitro and tumor angiogenesis	(Orimo et al., 2005)
	Cyr61	1.279	promote angiogenesis in vitro and tumor angiogenesis	(Maity et al., 2014)
	Semaphorin-3A	1.111	repress tumor angiogenesis	(Casazza et al., 2011; Maione et al., 2009)
	Wnt 5a/b	0.548 / 0.798	induce tumor angiogenesis	(Masckauchán et al., 2006)
	CTGF	0.644	promote angiogenesis in vitro and tumor angiogenesis	(Brigstock, 2002)
Down	LCN1	na	no described role	(Dartt, 2011)
	Angiotensinogen	3.737	inhibit tumor angiogenesis and growth	(Vincent et al., 2009)
	tPA	2.077	decrease VEGFA expression and angiogenesis	(Shim et al., 2005)
	Vitamin D-binding protein	1.932	impair angiogenesis in vitro and in vivo	(Kisker et al., 2003)
	Semaphorin-5A	1.932	promote tumor vessel density and metastasis formation	(Sadanandam et al., 2012)
	Neprilysin	1.515	inhibit angiogenesis via proteolysis of FGF2	(Goodman et al., 2006)

	IGFBP5	1.37	act as tumor suppressor by inhibiting angiogenesis	(Rho et al., 2008)
	CXCL14	1.235	inhibit angiogenesis	(Shellenberger et al., 2004)
	Gremlin-1	1.235	act as agonist of VEGFR2	(Mitola et al., 2010)
	IGFBP6	1.114	reduce angiogenesis in vitro, in zebrafish and in tumors	(Zhang et al., 2012)
	IGFBP3	0.966	repress tumor angiogenesis and progression	(Kim et al., 2011)
	IGFBP7	0.737	inhibit tumor angiogenesis	(Chen et al., 2011)
	TSP1	0.678	inhibits angiogenesis	(Lawler and Lawler, 2012)

Candidate list of angio-modulatory molecules identified by LC-MS/MS that were differentially abundant in CM of U87MG cells that had been grown on CDM laid down by MEF TNC KO or wt. Expression in presence of TNC is compared to its absence. Fc, fold change, na, not applicable.

Abbreviations: Cysteine-rich angiogenic protein 61 (Cyr61), Connective tissue growth factor (CTGF), Chemokine (C-X-C motif) ligand 14 (CXCL14), Chemokine (C-X-C motif) ligand 12 (CXCL12) or Stromal cell-derived factor 1 (SDF1), Insulin-like growth factor-binding protein (IGFBP), Tubulointerstitial nephritis antigen-like 1 (TINAGL1)/Lipocalin-7 (LCN7), Thrombospondin-1 (TSP1), Tissue plasminogen activator (tPA), Transglutaminase-2 (TG2).

Table 2. Identification of protein expression of the gel band, related to Fig. 6A

Name	MW (Da)	gene name	GO compartment	Uniprot localization
Proline-rich protein 4	15097	PRR4	extracellular space	Secreted
Lipocalin-1	19250	LCN1	extracellular region; extracellular space; extracellular vesicular exosome	Secreted

Candidate list of secreted (Uniprot localization) protein identified by LC-MS/MS that were identified from the gel band (15-20 kDa) in CM of U87MG cells that had been grown on CDM laid down by MEF TNC KO or TNC wt. Note that no secreted molecules have been detected in CM from U87MG educated by TNC.

Laminin α1 orchestrates VEGFA signaling in the tumor ecosystem to promote colon cancer

E. Mammadova-Bach[1-5], T.Rupp[1-4], I. Jivkov[1-4] S. Pattabhiraman[1-4], M. Edwards[6], A. Klein[1-4], L. Pisarsky[1-4,7], A. Méchine-Neuville[8], G. Cremel[1-4], M. Kedinger[1-4], O. De Wever[9], N. Ambartsumian[10], S. Robine[11], E. Pencreach[12], D. Guenot[12], J. Goetz[1-4], P. Simon-Assmann[1-4], G. Orend[1-4] and O. Lefebvre[1-4,*]

[1]Inserm U1109, MN3T, Strasbourg, F-67200, France.

[2]Université de Strasbourg, Strasbourg, F-67000, France.

[3]LabEx Medalis, Université de Strasbourg, Strasbourg, F-67000, France.

[4]Fédération de Médecine Translationnelle de Strasbourg (FMTS), Strasbourg, F-67000, France.

[5]present address, Inserm UMR-S 949, Etablissement Français du Sang-Alsace, Strasbourg, F-67065, France.

[6]Wilmer Ophthalmological Institute, Johns Hopkins Hospital, Baltimore, MD 21287, USA.

[7]present address, Department of Biomedicine, University of Basel, Basel, 4058, Switzerland.

[8]Department of Anatomy and Pathology, CHRU Hautepierre, Strasbourg, F-67200, France.

[9]Laboratory of Experimental Cancer Research, Department of Radiotherapy and Nuclear Medicine, Ghent University Hospital, Ghent, 9000, Belgium.

[10]Institut for Cancer Biology, Copenhagen, DK-2100, Denmark.

[11]Institut Curie, Paris, F-75248, France.

[12]EA 3412, Université de Strasbourg, Strasbourg, F-67000, France.

Running title: Laminin α1 promotes colon tumorigenesis

Key words: Laminin α1, colorectal cancer, tumor angiogenesis, VEGFA,

Abbreviations

BM, basement membrane; ECM, extracellular matrix; LM, laminin; vLMα1, villin-LMα1 transgenic mice; FN, fibronectin; CAF, cancer-associated fibroblasts; IF, immunofluorescence; VEGF, vascular endothelial growth factor.

***Correspondence**

Olivier Lefebvre

Inserm U1109 - The Microenvironmental Niche in Tumorigenesis and Targeted Therapy (MN3T).

3, avenue Molière, 67200 Strasbourg, France

E-mail: olivier.lefebvre@inserm.fr

Phone: (33) 3 67 15 11 90 - Fax: (33) 3 88 26 35 38

Abstract

In human colorectal tumors LMα1 is the most highly expressed laminin isoform suggestive of a role of LMα1 in tumorigenesis. We describe the laminin α1 chain (LMα1) as driver of cross talk between tumor and stromal cells promoting tumorigenesis. LMα1 overexpression leads to increased colon tumor incidence, growth and angiogenesis. LMα1 attracts carcinoma-associated-fibroblasts (CAF) and promotes CXCR4-dependent VEGFA secretion, which in turn stimulates tumor cell survival, proliferation and angiogenesis.

Significance

Tumor stroma remodeling is a key feature of malignant tumors and an important promoter of cancer progression. We describe that a basement membrane molecule, the laminin alpha1 chain (LMα1), is overexpressed in human colon tumors. In mice, its overexpression leads to increased incidence, growth and angiogenesis of colon tumors. We also identified VEGFA and CXCR4 as key players. We provide a novel mechanism comprising tumor / stromal crosstalk with the LMα1-rich ECM to promote cancer cell survival, proliferation, endothelial cell expansion and pericyte coverage of new blood vessels. Overexpression of LMα1 in human colon cancer does not correlate with tumor stage and thus may represent an early event in tumorigenesis potentially useful for colon cancer diagnosis.

Highlights

- In human colon tumors laminin α1 (LMα1) is the most highly overexpressed isoform
- In mice LMα1 increases tumor incidence, angiogenesis and growth of colon tumors
- LMα1 exerts its effect on the tumor ecosystem through CXCR4 and VEGFA signaling
- Binding of VEGFA to LMα1 stimulates proliferation and survival of cancer cells

Introduction

Cancer progression is considered as a multistep process, where tumor cells acquire properties that enable their survival, proliferation and invasion, finally leading to dissemination and establishment of metastasis. Some steps are cell autonomous while others need the interactions with other cell types and the extracellular matrix (ECM) within the tumor stroma (Hanahan and Weinberg, 2011). Tumor cells and tumor associated cells such as endothelial cells, immune cells and carcinoma associated fibroblasts (CAF) secrete soluble factors as well as specific ECM that usually is very different from that of normal tissue and altogether provides a particular presumably tumor type specific tumor microenvironment (TME) (Bissell and Hines, 2011; Hynes, 2009).

Laminins (LMs) are heterotrimeric glycoproteins that together with other ECM molecules form a highly organized basement membrane (BM), which serves as barrier between epithelial and mesenchymal cells (Hohenester and Yurchenco, 2013). The LM family comprises at least 15 isoforms. The LM trimers are composed of an α, β and γ chain (Simon-Assmann et al., 2011). In particular LMα1 is present in LM111 and LM121. Importantly, LM111 is highly expressed in most BMs during embryonic development but its expression in the adult is restricted to a few sites (Falk et al., 1999). The function of LMα1 containing LMs in physiology and diseases is poorly understood. We and others have shown that mice with a complete LMα1 knockout die *in utero* due to the lack of the extra embryonic Reichert's BM (Alpy et al., 2005; Miner et al., 2004). Recently, we have demonstrated that mice with a point mutation in the LN domain (Y265C) of LMα1 or with a Sox2-driven conditional knockout of LMα1 in embryonic tissues ($LM\alpha1^{cko}$) are viable (Edwards et al., 2010). However, they exhibit several defects in the retina and the central nervous system. In particular, these mice suffer from vision defects which may be due to the observed profoundly disorganized vasculature in the cerebellum and the retina and an aberrant localisation of Muller glial cells in the inner limiting retinal BM (Edwards et al., 2010, 2011, Heng et al., 2011; Ichikawa-Tomikawa et al., 2012). A high abundance of LMs has been noted in several cancers including

gastrointestinal, ovary and breast cancer (Aghcheli et al., 2012; Chu et al., 2002; Sidhom and Imam, 1999) and correlates with poor prognosis in particular in colorectal cancer (Saito and Kameoka, 2005) suggesting a role of aberrantly expressed LMs in colon cancer progression. However, which LM isoform(s) would be involved was unknown until recently, when we had discovered that LMα1 promotes tumorigenesis in an immune compromized colon cancer model (De Arcangelis et al., 2001). Nevertheless, the underlying molecular mechanisms remained elusive.

To address how LMα1 promotes colon tumorigenesis here, we have established novel transgenic mouse models with ectopic expression of LMα1 in the intestinal epithelium. Using chemical (De Robertis et al., 2011) and genetic (Fodde et al., 1994) induction of colon tumorigenesis, we determined the impact of ectopically expressed LMα1 on stochastically arising tumors in immune competent mice. We observed that LMα1 promotes tumor formation and angiogenesis by triggering an intimate crosstalk between tumor and stromal cells and their LMα1 matrix. Notably, CAF are key players as they are attracted by LMα1. They respond to LMα1 by expression of VEGFA in a CXCL12/CXCR4 dependent manner. We demonstrate that in turn the matrix-bound form of VEGFA enhances tumor cell proliferation and survival. Thus, our data provide evidence for a causal link between high LMα1 abundance and enhanced angiogenesis and tumor growth, employing CXCR4 and VEGFA signaling. This link could be relevant for diagnosis and targeting of human colon cancer where LMα1 is highly expressed.

Results

LMα1 is overexpressed in colon cancer

Elevated LM levels in serum had been correlated with worsened prognosis of colon cancer patients (Saito and Kameoka, 2005). To identify the LM isoforms involved we determined expression levels of the eleven LM chains in 42 primary human colorectal cancer specimens (**Supplemental Table S1**) in comparison to matched adjacent apparently normal colonic tissue by quantitative reverse transcription PCR (qRTPCR). LMα1 was highly overexpressed (on average more than 10-fold) in cancer tissue compared to non-affected adjacent tissue and is the most abundantly expressed LM chain amongst all subunits tested (**Fig. 1A**). Notably, two other LM chains were also significantly but less abundantly overexpressed in tumor tissue, LMβ1 (3-fold) and LMα5 (1.9-fold). In contrast, three other LM chains showed a decreased expression in tumors, LMα3 (3.6-fold), LMβ3 (2.7-fold) and LMγ3 (6-fold). Tissue staining revealed that LMα1 is expressed in the stroma and at the interface between cancer cells and the tumor stroma (**Fig. 1B**).

LMα1 promotes survival and proliferation and increases colon cancer incidence and growth in transgenic murine models with intestine specific overexpression of LMα1

To investigate the role of LMα1 in colon cancer we have generated transgenic mice where the LMα1 cDNA is expressed under the control of the villin promoter (vLMα1, **Supplemental Fig. S1 A**). The villin promoter drives specific and high expression of the transgene in the epithelium of the gut and along the entire intestinal crypt–villus axis (Pinto et al., 1999). By qRTPCR we confirmed that indeed LMα1 was strongly overexpressed at mRNA and protein level in colon of transgenic vLMα1 mice compared to wildtype littermates as determined by qRTPCR and Western blot, respectively (**Supplemental Fig. S1D, E**). Moreover, immunofluorescence (IF) analysis revealed that transgenic LMα1 was expressed in the BM

of the crypt region whereas endogenous LMα1 was only poorly expressed in control colon tissue (**Supplemental Fig. S1B, C**). However, LMα1 overexpression did not lead to abnormalities in gut morphology and homeostasis (data not shown).

To investigate the consequences of LMα1 overexpression on colon cancer, we used the carcinogen azoxymethan (AOM) or a combination of AOM and dextran sulfate sodium (DSS) to induce colon carcinogenesis and observed intraepithelial carcinomas up to colon adenocarcinomas pT2 resembling the human pathology (Papanikolaou et al., 1998; De Robertis et al., 2011) (**Supplemental Fig. S1I-J**). To determine how LMα1 promotes colon tumorigenesis, we compared the tumor incidence in wildtype and vLMα1 transgenic mice (**Fig. 2A**). We observed that 100% of carcinogen (AOM, AOM/DSS) treated transgenic vLMα1 mice developed at least one tumor in the colon whereas control wildtype littermates only showed a tumor incidence of 36% (AOM) and 50% (AOM/DSS), respectively. When vLMα1 expressing mice were crossed with $APC^{+/1638N}$ mice lacking an allele of the APC tumor suppressor gene (Fodde et al., 1994) we observed a 75% tumor incidence in compound vLMα1/$APC^{+/1638N}$ mice in comparison to 17% tumor incidence in control littermates (**Fig. 2A**). Thus, gut specific overexpression of LMα1 significantly promotes tumorigenesis in both chemically and genetically induced carcinogenesis models.

Since increased tumorigenesis was seen in all three models overexpressing LMα1, we focused our studies on the AOM/DSS tumor model. We first observed an increase in tumor size (**Fig. 2B**) and in tumor number (**Supplemental Fig. S1K**) in AOM/DSS treated vLMα1 mice compared to wildtype control littermates. This was indeed correlated with an increased expression of LMα1 at mRNA (**Supplemental Fig. S1F**) and protein level as seen upon tissue staining (**Supplemental Fig. S1G, H**). In particular we observed high levels of LMα1 at the interface between cancer cells and the stroma both in control and transgenic tumors and within the stroma of vLMα1 tumors (**Supplemental Fig. S1G, H**).

To address whether the observed increased tumorigenesis is indeed linked to the abundance of LMα1, we analyzed tumorigenesis under conditions with lowered LMα1 expression. Therefore, we established a HCT116 xenograft model with reduced LMα1 expression upon knock down (HCT116shLMα1, **Supplemental Fig. S1L)**. Upon subcutaneous injection into immunompromized mice, we observed that HCT116shLMα1 cells induced significantly smaller (2.5-fold) tumors than HCT116 control cells (with a scrambled shRNA) (**Fig. 2B).** Altogether our results showed that tumor incidence and growth correlated with LMα1 abundance suggesting that LMα1 promotes tumorigenesis.

We considered the possibility that LMα1 impacts on survival and/or proliferation which we addressed by signal quantification upon immunostaining for the apoptosis marker cleaved caspase 3 and the proliferation marker Ki67. We observed that colon tumors from AOM/DSS treated vLMα1 mice exhibited 1.4-fold more proliferating cells (**Fig. 2C**) and 1.3-fold less apoptotic cells (**Fig. 2D**) than tumors from control littermates. Although each effect is rather mild a synergism in survival and proliferation could explain enhanced tumor growth by LMα1.

LMα1 promotes tumor angiogenesis and vessel maturation

We had previously shown that overexpression of LMα1 in the HT29 human colon carcinoma xenograft model leads to increased tumor growth with strong vascularization (De Arcangelis et al., 2001). Now we quantified tumor angiogenesis upon CD31 staining and observed that increased LMα1 levels in HT29 tumors correlates with 2.5-fold enhanced angiogenesis (**Fig. 3A, Supplemental Fig. S2C-D**). This result suggests that elevated LMα1 expression promotes tumor angiogenesis. To address this possibility further we quantified the CD31 staining signal in our novel LMα1 tumor model and indeed observed a 2.5-fold increased

expression in AOM/DSS induced vLMα1 colon tumors in comparison to control tumors (**Fig. 3A, Supplemental Fig. S2A-B**). We further confirmed a link of LMα1 abundance to the extent of tumor angiogenesis in another tumor grafting model with lowered LMα1 levels. In particular, we observed a 2.5-fold lowered CD31 signal in HCT116shLMα1 tumors in comparison to control tumors (**Fig. 3A, Supplemental Fig. S2E-F**).

Mature vessels are characterized by pericyte coverage. Thus next we assessed whether LMα1 had an impact on tumor vessel maturation by tissue staining for the pericyte marker NG2. We observed that whereas pericyte covered blood vessels (NG2/CD31 ratio) were significantly increased in vLMα1 (1.8-fold) and HT29LMα1 xenograft (1.5-fold) tumors they were 1.5-fold reduced in HCT116shLMα1 xenograft tumors (**Fig. 3B, Supplemental Fig.S2G-L)**.

Together our data demonstrate that LMα1 expressed by tumor cells drives tumor angiogenesis characterized by a stronger pericyte coverage.

CAF are attracted by LMα1 which are abundant in tumors with high LMα1 expression

Carcinoma associated fibroblasts (CAF) play an important role in tumor progression by several mechanisms including promotion of angiogenesis. Therefore, we determined their abundance by immunostaining for αSMA. In LMα1 overexpressing tumors we observed a significant enrichment of these cells, as evidenced by a 1.7- and 1.6-fold increased signal in AOM/DSS induced vLMα1 and HT29LMα1 tumors, respectively (**Fig. 3C, Supplemental Fig. S2A-D)**. In addition the αSMA positive signal was 2.2-fold decreased in HCT116shLMα1 tumors (**Fig. 3C, Supplemental Fig. S2A-F**). A similar trend was observed for another CAF marker, S100A4/Mts1 (Grum-Schwensen et al., 2005) showing an 1.9-fold increase in the vLMα1 tumors in comparison to controls (**Supplemental Fig. S2G-H, I**). The enrichment of

CAF and endothelial cells (**Fig. 3**) led us to explore the possibility that LMα1 deposited by tumor cells attracted these cells to the TME. We tested this hypothesis by assessing transmigration of fibroblasts and endothelial cells in a Boyden chamber assay towards LMα1 provided as condition medium (CM) derived from HT29LMα1 (or control cells), or towards purified LM111. We observed that purified LM111 (2.5-fold) and CM from HT29LMα1 cells (1.7-fold) enhanced CAF recruitment (**Fig. 3D-E**). In contrast LMα1 did not stimulate transmigration of HMEC, HUVEC or pericytes (**Fig. 3D-E**). We conclude that LM111 attracts CAF but not endothelial cells nor pericytes.

Expression of LMα1 is linked with an angiogenic signature in the tumor stroma

In order to understand what mechanism underlies the increase of tumor blood vessels by LMα1, we performed a comparative RNAseq analysis of HT29LMα1 and HT29 control xenograft tumors. This approach allows to discriminate between the contributions from the human tumor cells and the murine stroma. By using the newly described Xenome tool (Conway et al., 2012) we analyzed and stratified the results according to human and murine origin. We identified 393 and 834 genes that are significantly up- or downregulated, respectively, in the stromal compartment of HT29LMα1 tumors, as well as 1741 and 2149 genes that are significantly up- or downregulated, respectively in the tumor cells (Supplemental Table S4 (Excel file)). We focused our attention on genes that were upregulated in the stromal compartment, using the AMIGO on-line tool to assign gene functions by gene ontology annotation (**Supplemental Fig. S4**). This analysis revealed a set of 62 genes to be upregulated in HT29LMα1 tumors with a majority annotated for having an angiogenesis promoting activity (**Supplemental Table S2**).

CAF are stimulated to express VEGFA by LMα1

The RNAseq analysis identified VEGFA as a molecule that is highly expressed by stromal cells of HT29LMα1 tumors. VEGFA is a key factor driving tumor angiogenesis and promoting tumor cell survival (Chung et al., 2010; Goel and Mercurio, 2013). We confirmed increased expression of VEGFA in the stromal compartment by LMα1 at mRNA (2.4-fold) and protein level (1.5-fold) in HT29LMα1 tumors compared to control tumors by using species specific primers (**Fig. 4A, Supplemental Fig. S5A**). In contrast, VEGFA mRNA and protein levels of tumor cells were independent of LMα1 abundance and not altered. This result suggests that LMα1 expressed by tumor cells induces VEGFA expression in stromal but not in the tumor cells. We confirmed these data in the tumor models with abundant and poor LMα1

expression. We observed that both VEGFA mRNA (1.6-fold) and protein (1.4-fold) levels were significantly increased in AOM/DSS-induced vLMα1 tumors in comparison to control tumors (**Fig. 4A, Supplemental Fig. S5A**). Consistently, VEGFA expression levels were significantly reduced in HCT116shLMα1 xenograft tumors in comparison to control tumors (**Fig. 4A)** suggesting that in these tumors VEGFA expression correlates with LMα1 expression levels**.**

Next we addressed which stromal cells were stimulated by LMα1 to express VEGFA. Therefore VEGFA expression was determined upon growth of endothelial cells, pericytes and cancer associated fibroblast (CAF) on a LM111 substratum. We observed that VEGFA expression levels were indeed significantly increased at mRNA (2.5-fold) and protein level (2-fold) in CAF grown on LM111. Yet, VEGFA levels did not increase in normal fibroblasts, pericytes nor endothelial cells under the same conditions (**Fig. 4B, Supplemental Fig. S5B)**. We next investigated which of the two major LM111 binding integrins α2β1 or α6β1 triggered VEGFA expression. Therefore, these integrins were inhibited in CAF grown on a LM111 substratum with blocking antibodies against integrin α2, α6 or β1. We observed that these α2 and β1 blocking antibodies caused a decrease in VEGFA expression at mRNA (1.9-fold) and protein level (1.9-fold) which was not the case with a blocking antibody against integrin α6 (**Fig. 4C, Supplemental Fig. S5C)**. This result points to an important role of CAF in the LMα1 rich TME and suggests that in these cells VEGFA is induced by cell binding to LMα1 through integrin α2β1 (but not α6β1).

Binding to LMα1 stimulates CXCL12/CXCR4 signaling in CAF to induce VEGFA in an integrin α2β1 dependent manner

We further addressed the mechanism of VEGFA induction by a LM111 substratum through integrin α2β1 in CAF. Data from our RNAseq analysis (Table S5) supported published results

suggesting that LM111 promotes expression of CXCR4 through an integrin mediated mechanism (Grzesiak et al., 2007). Moreover, it has been reported that CXCL12/CXCR4 signaling enhances VEGFA expression (Ping et al., 2011; Yang et al., 2005). To see whether LMα1 triggers CXCL12/CXCR4 signaling to promote VEGFA induction we determined SDF1/CXCL12 and CXCR4 expression in CAF and other stromal cells. We found that CAF were the only cell type that exhibited a detectable expression of SDF1/CXCL12 at protein and mRNA level, respectively which was in contrast to IMR-90, MEF, HMEC and pericytes that only poorly expressed these molecules (**Supplemental Fig. S5D**). To provide a potential link to VEGFA we used the specific CXCL12/CXCR4 pathway inhibitor AMD3100 and determined VEGFA expression in cells grown on LM111. We noticed that AMD3100 blocked VEGFA expression induced by a LM111 substratum in CAF (**Fig. 4D, Supplemental Fig. S5E**). Next we wanted to know whether this effect was mediated by integrin α2β1. Therefore, we determined SDF1/CXCL12 and CXCR4 expression in CAF upon growth on LM111. We observed that whereas SDF1/CXCL12 levels were not affected (not shown) CXCR4 mRNA (2.2-fold) and protein levels (1.9-fold) were significantly decreased with the integrin α2 blocking antibody. This was specific since it did not occur with an integrin α6 blocking antibody (**Fig. 4E, Supplemental Fig. S5F**). Finally, to provide evidence for a mechanistic link of α2β1 specific signaling induced by LM111 to VEGFA induction through CXCL12/CXCR4, we determined VEGFA expression upon stimulation with SDF1/CXCL12 and upon addition of an integrin α2 or β1 integrin blocking antibody. We observed that recombinant SDF1/CXCL12 triggered VEGFA expression at mRNA (2.2-fold) and protein level (1.4-fold) in CAF on a LM111 substratum. Moreover, CXCR4 and VEGFA expression was downregulated with the function blocking antibodies against integrins α2 and β1 (**Fig. 4F, Supplemental Fig. S5G).** Thus, LMα1 triggers VEGFA expression only in CAF that were the only cells expressing CXCR4. Inhibition of CXCR4 signaling blocked VEGFA expression in CAF which occurred in an integrin α2β1 dependent manner.

Finally we tested whether CAF-derived VEGFA is able to trigger angiogenesis. Therefore, we used the classical HUVEC tubulogenesis assay. The CM was prepared from CAF that were grown on a LM111 substratum. This CM was tested whether it impacted on the proliferation of HUVEC which was not the case (**Fig. 4G**). In contrast to proliferation, CM of LM111 instructed CAF increased HUVEC tubulogenesis by 25% in comparison to CM from CAF grown on plastic (**Fig. 4H, Supplemental Fig. S6A-B**). Moreover, this effect was VEGFA dependent since a treatment with the VEGFA blocking antibody Bevacizumab largely reduced the tubulogenesis promoting effect of the LM111 instructed CM (**Fig. 4I, Supplemental Fig. S6A-C**)

Altogether, these results suggest that LMα1 expressed by tumor cells triggers VEGFA expression especially in CAF by a mechanism that involves integrin α2β1 and CXCL12/CXCR4.

CAF derived VEGFA promotes cell proliferation and survival of tumor cells

We asked whether increased VEGFA levels have also an impact on tumor cell survival and/or proliferation in our tumor models, as had been described in other tumor models (Chung et al., 2010). However, whether VEGFA expressed by CAF mediates these effects and whether this is regulated by LMα1 was unknown. Therefore we first investigated whether CM from CAF grown on LM111 impacted on tumor cell proliferation. We observed that this CM indeed increased the proliferation of LMα1 overexpressing tumor cells as more cells entered S and G2/M phases which was accompanied by a decrease of cells in the G0/G1-phase (43% compared to 66% for control cells) in comparison to control CM (**Fig. 5A**). To investigate a potential effect of LMα1 on tumor cell survival, we induced apoptosis with staurosporine (Qiao et al., 1996). We observed that LMα1 promoted survival as only 9.5% HT29LMα1 were arrested in the subG1 fraction compared to 12.2% of control cells (**Fig. 5B**).

Notably, this LMα1 associated survival effect was further potentiated (16%) upon pre-stimulation of cells with CM derived from CAF previously grown on LM111 (**Fig. 5B**).

Next we asked whether LM111 associated enhanced survival/proliferation is linked to VEGFA binding to the ECM. We analyzed survival and proliferation by FACS analysis upon addition of VEGFA165, the major active and heparin binding isoform (Miralem et al., 2001), and observed that VEGFA165 enhanced entry in S and G2/M phases concomitant with a reduced number of cells in the G0/G1-phase (39% compared to 66% of control cells) (**Fig. 5C**). In survival assays, we observed that in comparison to control cells HT29LMα1 cells were less prone to staurosporine-induced cell death (9.3% subG1 fraction versus 14.3% of control cells) (**Fig. 5D**). This effect was further potentiated by pre-stimulation of HT29LMα1 cells with VEGFA165 resulting in an additional reduction of dying cells to 5.8%. This effect was not observed in the parental cells lacking LMα1 (**Fig. 6D**). These results suggest that LM111 and VEGFA165 collaboratively exert the pro-survival and proliferation stimulating effects.

We wanted to know whether this collaboration potentially involves a physical interaction of both molecules. This possibility is supported by published work showing that growth factors such as VEGFA bind heparan sulfates and ECM molecules (Wu et al., 2009). Whether this also applies to LMα1 was unknown. Since LMα1 contains a heparin binding site in the G domain (Harrison et al., 2007) we addressed whether VEGFA165 binds to LM111 by Biacore. Indeed we observed a strong binding of VEGFA165 to LM111. This was not the case for VEGFA121, a non-ECM-binding VEGFA isoform (**Fig. 5E**). We showed that VEGFA 165 binds LM111 in a dose dependent manner with a Kd of 4,7 10^{-8} M which is in a similar range as the previously reported binding of VEGFA165 to glycosaminogycans (2.4 x 10^{-8} M, Wu et al., 2009). To confirm that the observed VEGFA effect is dependent on binding to

LMα1 we compared survival and proliferation of HT29LMα1 cells with that of control cells upon stimulation with VEGFA121 and found no differences in the distribution between subG1 and G0/G1, S and G2/M phases amongst the two cell types upon staurosporin treatment (**Fig. 5F-G**). Altogether our results indicate that VEGFA, whose expression is triggered by LMα1 in CAF, enhances tumor cell survival and proliferation involving binding of VEGFA to LMα1.

Discussion

The molecular mechanisms underlying colon cancer have been intensively investigated for decades and important insights into the genetic alterations leading to malignant transformation of the intestinal epithelium have been discovered (Fearon and Vogelstein, 1990). Recently, the formation of new blood vessels has been recognized as a key step in colon cancer progression (Rmali et al., 2007) prompting targeting of VEGFA as a second line treatment in colon cancer therapy. Unfortunatley, the success of this treatment is rather moderate (Saif, 2013). Thus an improved understanding of the roles of VEGFA and the TME in colon cancer progression is needed.

LMs are components of BMs and deletion of some LMs leads to organ defect or death consistent with their crucial role in tissue homeostasis (Simon-Assmann et al., 2011). BMs are believed to serve as physical and chemical barrier. Therefore, one would anticipate high LM expression to strengthen BM barrier function and thus reducing tumorigenesis and cancer progression. But the situation seems more complicated. Increased levels of LMα5 have been observed in progressed stages of human breast tumors and melanomas (Pouliot and Kusuma, 2013) and forced expression of LMα1 promoted tumor growth in a colon cancer model (De Arcangelis et al., 2001). Altogether these findings suggested that LMs expressed out of their normal context may acquire other than barrier functions (Spenle et al., 2014). Despite an earlier publicati*o*n, describing the presence of LMα1 only in one out of six human colon cancer specimens examined (Maatta et al., 2001), here we showed that in the majority of the analyzed 42 human colorectal cancer specimens, LMα1 is highly abundant in comparison to adjacent non-tumorigenic tissue and that LMα1 is the only LM chain with a high about 10-fold induction in the colon tumors. Differences in experimental approaches may explain this discrepancy. According to our results abundant LM isoforms are presumably representing LM111 and/or LM511, since LMα1, LMα5 and LMβ1 are the only LM chains that

are more expressed in colon cancer tissue compared to healthy tissue. We observed that high LMα1 levels did not correlate with any genetic alterations in colon cancer (data not shown) which may argue for an induction of LMα1 before the appearance of gross genetic divergence. Thus LMα1 expression is potentially useful as marker of colon tumor onset. Yet high LM levels in serum of colon cancer patients were seen to correlate with poor prognosis (Saito and Kameoka, 2005). Since we had identified LMα1 as the most abundant LM isoform in colon cancer it needs to be seen in the future whether blood screening of colon cancer patients for LMα1 has diagnostic value.

To mimic the effects of high LMα1 expression in human cancer, we developed three novel immune competent murine cancer models with ectopic expression of LMα1 where AOM, AOM/DSS (De Robertis et al., 2011) or $APC^{1638N/+}$ (Fodde et al., 1994) drive stochastic intestinal tumorigenesis. In all three tumor mice we observed an enhanced tumor incidence, tumor growth and most importantly increased angiogenesis upon elevation of LMα1. We provide a molecular mechanism that can explain how LMα1 is promoting tumor growth. We demonstrated that abundant LMα1 promotes survival, proliferation and angiogenesis. Angiogenesis has been shown to promote tumor growth (Folkman, 1974) and thus may contribute to tumor growth by LMα1. We showed that LMα1 overexpressing tumors display elevated expression of several pro-angiogenic factors among them VEGFA. Now our in vivo tumor models and in vitro data (including CAF and endothelial cells) elucidate an intricate crosstalk of stromal cells with LMα1 expressing tumor cells that could explain the LMα1 promoting effect on tumor angiogenesis and tumor growth. By using the xenograft model with human colon cancer cells we identified the cellular source and biological targets of LMα1. We revealed a signaling network of stromal cells with LMα1 overexpressing tumor cells leading to VEGFA stimulation in CAF that in turn promotes tumor cell survival, proliferation and angiogenesis (**Figure 6**). That VEGFA promotes survival also in colon tumors is novel and resembles observations made in skin tumors (Lichtenberger et al., 2010).

Upon adhesion to LM111, VEGFA was induced in CAF through integrin α2β1. This effect was specific for CAF as neither normal fibroblasts and endothelial cells nor tumor cells expressed VEGFA on a LM111 substratum. We further demonstrated that colon cancer cell survival and proliferation is enhanced on a LM111 substratum upon stimulation with VEGFA. This could be relevant in a LMα1 rich TME, a hypothesis that is supported by our observation of LM111 binding to VEGFA165 but not to VEGFA121. We showed that VEGFA165 binds LM111 with a Kd in the range described for binding of VEGFA to glycosaminoglycans (Wu et al., 2009), an interaction that presumably also applies here involving the heparin binding site in the LMα1 G domain (Harrison et al., 2007). Our result suggests that LMα1 containing LMs potentially sequester VEGFA in the TME and this binding may be necessary to achieve the biological effects of VEGFA. Indeed ECM bound VEGFA was shown to be active (Park et al., 1993) and to induce proliferation of breast tumor cells (Miralem et al., 2001). In contrast VEGFA121 which is not ECM bound had no effect on colon tumor cell proliferation and survival.

Tumor and stromal cells adhere to LM111 but which adhesion receptor mediates the interaction of cells with LM111 and LM121 in vivo was unknown. Candidates for this interaction are integrins α2β1 and α6β1 as they were shown to mediate cell adhesion of HUVEC (Estrach et al., 2011) and CAF on a LM111 substratum (our data). Our results support a crucial role of integrin α2β1 (and not α6β1) in CAF binding to a LM substratum containing LMα1. This induces VEGFA expression through CXCL12/CXCR4 thus presumably creating an autocrine loop (as had been reported in breast cancer (Kojima et al., 2010)) and potentially accounting for an increase in CAF numbers in colon tumors with abundant LMα1.

In summary, here we have shown that ectopically expressed LMα1 promotes colon cancer incidence, tumor growth and tumor angiogenesis by triggering an intricate crosstalk between cells and the LMα1 matrix. LMα1 expressed by colon cancer cells attracts fibroblasts that secrete VEGFA in response to adhesion to the LM111 substratum. In turn a LMα1 matrix binds VEGFA that promotes tumor cell survival and proliferation. VEGFA signaling also promotes angiogenesis leading to more vessels that are well covered by pericytes in the presence of LMα1 (**Fig. 6**). Altogether in response to abundantly expressed LMα1 a tumor vasculature arises that may be functional thus supporting tumor growth. Such a vasculature may not support tumor cell dissemination and metastasis. This is in agreement with the absence of liver and lung metastasis in the three murine tumor models with ectopic LMα1 expression. Our study provides important novel insights into signaling within the tumor ecosystem that offers anti-cancer treatment opportunities as e.g. interference with CXCR4 and integrin α2β1 to block VEGFA expression by CAF. Targeting CAF as major stromal players might also present an opportunity. In addition, our novel murine tumor models may further our understanding of vascular BM assembly to develop strategies for improved anti cancer drug delivery and, for testing drugs targeting the LMα1 specific tumor ecosystem.

Experimental procedures

Cloning of the villin-LMα1 vector

The plasmid pBS-villin-promoter containing 3.5 Kb of the murine villin promoter, the first non coding exon, 5.5 kb of the first intron and 15 nucleotides of the second villin exon, was kindly provided by Sylvie Robine (Institute Curie, Paris, France). The EcoRI site in the multi cloning site was destroyed by fill in ligation with T4 polymerase according to the manufacturer`s instructions (NEB, OZYME, Saint Quentin Yvelines, France). Site directed mutagenesis (GeneEditor in vitro Site-Directed Mutagenesis system, Promega, Charbonnières-les-Bains**,** France) was then used to introduce a BsiWI site before the start codon of the villin coding sequence using the 5' phosphorylated primer: 5'CCTTCTCCTCTAGGCTC GCGTACGATGACGTCGGACTTGCGG3'. A double strand annealed oligonucleotide, 5'GGCCGGACGCGTGAATTCGTCGACGC3' and 5'GGCCGCGTCGACGAATTCACGC GTCC3' containing restriction sites for MluI, EcoRI and SalI were inserted in the NotI site (present in the multi cloning site), generating the plasmid pBS-villin-promoter-MES. The SV40 polyA region of the pEGFP plasmid (Clontech, OZYME, Saint Quentin Yvelines, France) was amplified by PCR using primers 5'GGCGCCTCTAGATCATAATCAGCCATA3' and 5'GGCGCCCTTAAGATACATTGATGAGTT3' before subcloning into the pGEMTeasy vector (Promega, Charbonnières-les-Bains**,** France). After EcoRI digestion, the SV40 polyA fragment was purified with NucleoSpin Extract II kit (Machery-Nagel, Hoerdt, France) and then subcloned into the EcoRI site of the plasmid pBS-villin-promoter-MES. Site directed mutagenesis was used to introduce a BsiWI site (5' phosphorylated AGCGCAGGGAGCGGCGGCCGTACGATGCGCGGCAGCGGCACG3') before the initiation codon and a MluI site (5' phosphorylated CCCGGGCCTGAGCCCTAAACGCGTGCC AGCCTCTGCCCTTGG3') after the stop codon in the full length cDNA coding for the mouse LMα1 in the pCIS vector (kindly provided by Peter Yurchenco, Piscataway, USA). The BsiWI-MluI fragment containing the LMα1 cDNA was gel purified and subcloned into the BsiWI-MluI

sites of the pBS-villin-promoter-MES-SV40-polyA vector giving rise to plasmid pBS-villin-LMα1.

Generation of vLMα1 transgenic mice

From the pBS vLMα1 plasmid a SalI fragment containing the 9 kb villin promoter region followed by the mouse LMα1 cDNA and the SV40 polyA was obtained, purified and used for injection into pronuclei of fertilized oocytes (F1 hybrid C57Bl/6 x DBA/2, transgenic facility of the IGBMC, Strasbourg, France). Germline transmission was determined by PCR analysis of tail DNA, using the villin1 primer present in the villin promoter (5'ATAGGAAGCCAGTTTCCCTTC3') and the LM17 primer present in the 5' region of the LMα1 cDNA (5'TGACCCAGAGCACCGAGGCCA3') generating a fragment of 152 bp. For confirmation a second PCR was done obtaining a 166 bp product with primer LM116 present in the 3' region of the Lama1 cDNA (5'GCCTCATTCCGGGGCTGTGTG3') and primer SV40 3' (5'AATGTGGTATGGCTGATTATG3') encompassing the SV40 polyA sequence. Two founders villin-LMα1 (vLMα1) out of 68 showed stable integration and expression and were further used in parallel for all experiments. Heterozygous vLMα1 mice were kept in a CD1 background (Charles River, L'Arbresle Cedex, France).

Azoxymethan (AOM) and AOM/ Dextran Sulfate Sodium (DSS) treatment

Eight week old wildtype (WT) mice and vLMα1 littermates were injected intra-peritoneally (i.p.) with AOM (10 mg/kg, Sigma Aldrich, Lyon, France) once a week for 5 weeks. Animals were sacrificed 9 months after the last AOM injection. For a combined AOM/DSS treatment eight week old WT and vLMα1 littermates were injected i.p. with a single dose of AOM. The day after, 3 % DSS (molecular weight 36000-50000, MP Biomedicals, Illkirch, France) was provided in the drinking water for 5 days. Afterwards mice obtained regular water for 2 months before sacrifice. Tumor size was measured with a caliper and tumor volume was determined using the following calculation $V= (width)^2 \times length/2$.

Colon tumor tissue were prepared, immediately snap frozen for RNA or protein extraction in liquid nitrogen or was embedded into OCT (Labonord, Templemars, France) for tissue and immunofluorescence analysis. Samples were stored at -80°C.

Generation of vLMα1/APC$^{+/1638N}$ mice

vLMα1 mice were crossed with APC$^{+/1638N}$ mice (Fodde et al., 1994). Double transgenic mice were kept on a CD1 background.

Cell culture

HT29 control and HT29LMα1 cells were cultured as previously described (De Arcangelis et al., 2001). A primary cancer associated fibroblast (CAF) culture (Wever et al., 2004) was infected with a pBABE retroviral vector expressing the hTERT open reading frame, and a pool was selected. The replicative life span of hTERT transduced pool was examined and compared with that of mock-transduced pool. Growth in control CAF populations typically plateaued by population doubling 15, whereas hTERT populations continued to divide far beyond the senescence point of control cells. These CAF hTERT immortalized fibroblasts, Mouse Embryonic Fibroblasts (kindly provided by Pr. Ruth Chiquet-Ehrissman, Basel, Switzerland) and IMR90, a human normal lung fibroblasts (CCL-186, ATCC, France) were cultured in DMEM supplemented with 10% fetal calf serum, penicillin-streptomycin 1% (Gibco, USA). Human immortalized dermal microvascular endothelial cells (HMEC, a gift from Dr E. Van Obberghen-Schilling, Nice, France) were maintained in MCDB 131 medium (Invitrogen) supplemented with 12.5% fetal calf serum, glutamin (10 mM; Invitrogen, Life Technologies, Saint Aubin, France), EGF (10 ng/mL), bFGF (10 ng/mL), heparin (10 µg/mL) and hydrocortisone (1 µg/mL), all compounds from Sigma Aldrich, Lyon, France. The Human Umbilical Vein Endothelial Cells (HUVEC) were purchased at Promocell (Promocell,

Heidelberg, Germany) and grown according to the manufactory instructions. Human Brain Vascular Pericytes (ScienCell, CliniSciences, France) were maintained in pericyte medium (CliniSciences, France), containing basal medium, fetal bovine serum 2%, penicillin-streptomycin 1% and pericyte growth supplement 1%.

For surface coating, cell culture dishes were coated with LM111 (L2020, Sigma Aldrich, Lyon, France) or fibronectin (FN), purified from horse serum as previously described (Huang et al., 2001). Both ECM molecules were used at a concentration of 10µg/cm^2.

CAF, HMEC and pericytes were plated onto uncoated, LM111 or FN coated plastic dishes for up to 24 hours in their appropriate medium. After 24 hours, CAF plated onto uncoated and LM111 plastic dishes were incubated for 4 hours with AMD3001 (Merck, Darmstadt, Germany) and mouse monoclonal function-blocking antibodies against human integrins α2 (10µg/mL, BHA2.1, Millipore), integrin β1 (10µg/mL, 4B4, Beckman Coulter, Fullerton, CA) and rat monoclonal function-blocking antibody against human integrin α6 (10µg/mL,GoH3, Santa Cruz Biotechnology) in absence and presence of recombinant human CXCL12/SDF1α (100 nM, R&D system), then RNA and protein were extracted.

For Boyden chamber chemo-attraction assays, the conditioned media from HT29 control and HT29LMα1 cells were collected, centrifuged to remove cell debris and stored at -20^o C for up to 2 months before use.

Generation of LMα1 knock-down cells

HEK293T cells were transfected with pGFP-sh LMα1 Lenti Vector (TL311806D: 5'-GAGATGTGCAGATGGTTACTATGGAAACC-3') or pGFP-sh control Lenti Vector (TR30021) containing non-effective 29-mer scrambled shRNA cassette (OriGene, Cliniscience, Nanterre, France)) together with the vectors of pLP1, pLP2, and pLP/VSVG vectors (Invitrogen, Life Technologies, Saint Aubin, France) to obtain lentiviral particules. After 48h,

conditioned media from HEK293T were collected, filtrated through a 0.22 µm filter to remove cell debris and used to transduce HCT116 cells in the presence of 5µg/mL polybrene (Sigma Aldrich, Lyon, France), followed by selection with puromycin (1.6 µg/mL, Sigma Aldrich, Lyon, France) in DMEM supplemented with 10% fetal calf serum, penicillin-streptomycin 1% (Gibco, USA). Expression of LMα1 was determined by qRTPCR and ELISA.

Protein extraction, immunoblotting and ELISA

Proteins were extracted from cells and tissue using lysis buffer (50mM Tris pH 7, 150 mM NaCl, 1 % NP-40, and 1% protease inhibitors, Roche, Meylan, France). 50 µg of protein lysate (quantified by Bradford assay) was separated by SDS PAGE (6%) and transferred onto nitrocellulose membrane (Millipore, Molsheim, France). Membranes were incubated (see **Supplemental Table S3**) with primary and secondary antibodies and bound HRP-coupled secondary antibodies were detected with ECL (Amersham, GE Healthcare, Velizy-Villacoublay, France).

Murine or human specific ELISA kits were used to determine the amount of VEGFA 165, CXCL12/SDF1α from R&D systems (R&D systems Minneapolis, USA), CXCR4 (reference CSB-E12825h) from Cusabio company (Cusabio, CliniSciences, Nanterre, France) using total protein lysates of tumors or conditioned medium from CAF, MEF, IMR90, HMEC and pericytes, following the manufacturer's instructions and measuring absorbance at 450 nm (Biotek plate reader E800, Biotek, Colmar, France).

Boyden chamber chemo-attraction assay

Chemo-attraction assays were performed in 24 well Boyden Chambers with a polycarbonate filter of 8 µm pore size (Falcon, Dutcher, Brumath, France). Conditioned media from HT29 control or HT29LMα1 cells were put in the lower chamber or LM111 (10µg/cm^2) was coated

on the lower surface of the insert. CAF, HMEC, HUVEC, IMR90, MEF or Pericytes were cultured in the upper chamber ($3x10^3$ cells) and incubated for 6 hours at 37°C in 5% CO_2. Transmigrated cells were fixed, stained with DAPI and quantified using the ImageJ software and the analyze particles modules (National Institutes of Health, USA). Three independent experiments with triplicates were done.

Matrigel tubulogenesis assay

Matrix was prepared by adding 10 µl of Matrigel (Corning, New York, USA) into 15 well dishes (IBIDI µ-Slide Angiogenesis, Biovalley, Nanterre, France) followed by solidification at 37°C in a humidified incubator for 1 houre. HUVEC (140`000 cells/ml) were trypsinized and resuspended in condition medium from CAF grown on plastic or LM111 (Sigma, Lyon, France). After incubation for 7h at 37°C, bright field mosaic pictures were taken (Zeiss Imager Z2 inverted microscope and AxioVision software, Carl Zeiss, Le Pecq, France) at 40X magnification (with a total of 9 pictures per condition) and tube-like structures (defined as closed loop) were assessed by using the AxioVision or ZEN Blue software (Carl Zeiss, Le Pecq, France). A minimum of three independent experiments were done with five replicates per experiment.

Cell cycle and apoptosis analysis

HT29 control and HT29LMα1 cells were plated in 24-well plates (10.000 cells per well) during 3 days and then treated for 24 hours with recombinant VEGFA 165 (10ng/µL, R&D systems, Minneapolis, USA) or VEGFA 121 (10ng/µL, Prospecbio, East Brunswick, USA). For apoptosis quantification, HT29 and HT29LMα1 cells were treated for 4 hours with the apoptosis inducing agent staurosporine as previously described (Qiao et al., 1996), and then treated for 24 hours with VEGFA. After collection, cells were resuspended in 300 µL

hypotonic fluorochrome solution (5 µg propidium iodide, 3.4 mmol/L sodium citrate, and 0.1% Triton X-100 in PBS). DNA content was analyzed by a fluorescence activated cell sorter (FACS, Becton Dickinson, San Diego, USA). Ten thousand events per sample were acquired, and cell cycle repartition was determined using the ModFit software. The subG1 apoptotic cell population was quantified by the CellQuest computer software.

Apoptosis were measured using protein lysates from tumors and the Apoptag apoptosis detection kit following the manufacturer's instructions (Millipore, Molsheim, France).

Surface Plasmon Resonance

Surface Plasmon Resonance—Binding experiments were performed by surface plasmon resonance measurements on a Biacore 2000 instrument (Biacore Inc., GE Healthcare, Velizy-Villacoublay, France) at 25 °C. VEGFA165 (Millipore, Molsheim, France) or VEGFA 121 (Prospecbio, USA) was immobilized at high surface density (5.000 response units) on an activated CM5 chip using standard amine-coupling procedures, as described by the manufacturer. LM111 was injected at a concentration of 10 µg/mL in 10 mM sodium acetate, pH 5.0, and at a flow rate of 5 µL/min during 20 min. Unreacted groups were blocked by injecting 1M ethanolamine. To perform binding assays, LM111 at different concentrations (from 5 to 20µg in 200µL) was injected in 10 mM MES, pH 6.0, 150 mM NaCl, 0.005% (v/v) surfactant P20, at a flow rate of 10 µL/min. Blank surfaces were used for background corrections. Injections of 10 mM glycine, pH 2.0, at 100 µL/min for 1 min were used to regenerate surfaces between two binding experiments. Steady state analysis was used to estimate the affinity of VEGF165 to LM111. Dissociation constants (Kd) were estimated using 1:1 Langmuir association model as described by the manufacturer.

Tumor xenograft experiments

10 million cells of each cell line HT29 control, HT29LMα1 or 4 million cells of HCT116 control sh and HCT116 shLMα1 were injected subcutaneously into eight week old nude MRF1 female mice (Janvier, La plaine Saint Denis, France). Mice were sacrificed 4 weeks after injection. Tumor tissue was fixed overnight in 4% PFA and embedded in paraffin or directly frozen in OCT or frozen on dry ice or liquid nitrogen for RNA or protein extraction. All material was preserved at - 80° C.

Colorectal cancer specimens

Primary human colorectal tumors and matched adjacent tissue with no signs of tumorigenesis (considered as normal) were obtained from 42 patients with a written consent according to conventional ethic standards. All surgical specimens were evaluated and histologically analyzed by an experienced pathologist. MIN (microsatellite instability) and CIN (chromosomal instability) signature of all surgical specimens was determined and provided by the Centre de Ressources Biologiques, (Hôpitaux Universitaires de Strasbourg, Hôpital de Hautepierre, Strasbourg, France). Patient information is listed in Supplementary Table S1. Tumor material and healthy tissue were isolated, immediately snap frozen for RNA and protein extraction or were embedded into OCT (Labonord, Templemars, France) for tissue and immunofluorescence analysis.

Gene expression analysis

RNA was extracted with the TriReagent according to manufacturer instructions (Molecular Research Center Inc., Euromedex, Souffelweyersheim, France). For RNAseq, the RNA extracted from the tumors were sequenced on Illumina HiSeq2000. The separation of RNA sequencing reads coming from the human tumor and the mouse host was performed in silico using the Xenome software (Conway et al., 2012), that is designed to discriminate species

specific sequences in a xenograft environment. Each Fastq file was separated into mouse specific and human specific sequencing reads. These were subsequently aligned using Tophat2 (Kim et al., 2013) and processed using the Cufflinks (Roberts et al., 2011) pipeline to generate the final expression files.

For qRTPCR, RNA was treated with DNaseI and reverse transcribed using the High Capacity cDNA RT Kit. qRTPCR was performed using the Power SYBR Green PCR Master Mix or TaqMan Gene Expression Master Mix. All compounds were from Life Technologies (St Aubin, France). Primer sequences or probes are listed in **Supplemental Table S4**. Two sets of primers/probes were used for determination of expression of LMα1 in human tumors, one located in the 5' and the other in the 3' region of the gene, giving similar results. All data were normalized to the reference gene GAPDH (Glyceraldehyde 3-phosphate dehydrogenase) for colon tumors. Relative expression level $2^{-\Delta\Delta ct}$ was calculated for each individual sample. A primer design approach was used to obtain species specific real-time qRTPCR primers. The coding regions of the mouse and human homologous cDNA sequences were aligned (www.ensembl.org). Regions of low homology were chosen for selection of species specific primers that always were spanning an intron. Primer specificity was confirmed by using cDNA from human or mouse tissues. Only primers giving an efficiency value between 93 to 108% were used. When calculating murine or human gene expression in the xenograft tumors, primers for mouse or human PBDG (porphobilinogen deaminase) were used for normalization respectively.

Immunohistochemistry and immunofluorescence analysis

For histological analysis 7 µm paraffin sections were deparaffinized with toluene and stained with periodic acid-Schiff reagent and hematoxylin. The list of primary antibodies used is listed in the **Supplemental Table S3.** For immunohistochemistry, tissue sections were

deparaffinized with toluene, then boiled with the antigen retrieval sodium citrate buffer (pH 6) for 10 minutes. Sections were incubated with primary antibodies overnight at 4°C. Slides were thereafter incubated with biotinylated secondary antibodies (Vector Laboratories, Eurobio/Abcys, Les Ulis, France), amplified with the ABC Elite Vectorstain kit and developed with the DAB kit from Vector Laboratories. Slides were examined using Zeiss Axio Imager A1 microscope equipped with an A-Plan x5/0.12, an A-Plan x20/0.45 objective and a Zeiss Axiocam Icc3 color camera (Carl Zeiss, Le Pecq, France). For immunofluorescence staining, 7 µm cryosections were incubated overnight with primary antibodies, washed three times in PBS and incubated for 1 hour with Alexa 488- or cyanine3-conjugated secondary antibodies (Jackson ImmunoResearch Laboratories, West Grove, PA). After washing, nuclei were stained with DAPI (1/30000) and mounted using the FluorSave reagent (Calbiochem-Merck, Lyon France). Slides were examined using an epifluorescence Zeiss axio imager 2 microscope equipped with a Plan Apochromat x20/0.8, a Plan Apochromat x40/0.95 objectives and an apotome module. Pictures were taken with a Zeiss Axiocam MRm black and white digital camera. Control sections were processed as above with omission of the primary antibodies. All images were acquired using the Zeiss Axiovision software. Quantification of immunofluorescence and immunohistochemistry surface signals was done using the ImageJ software and the analyze particles module (National Institutes of Health, USA). Several images per tumor were taken using a 20x objective to cover most of the tumor surface. Data are presented as average area fraction per tumor in all defined groups. The following calculation was used to quantify pericyte coverage of vessels: area fraction of NG2/area fraction of CD31 = area fraction of pericyte positive vessels.

Statistical analysis

Statistical significance of results was analysed by using the GraphPad Prism program version 5.0 and the R open source software version 3.0. The Shapiro-Wilk normality test was used to confirm the normality of the data, the difference in variance was analyzed using the F-test and the statistical difference of the mean was analyzed using the Student unpaired two-tailed t test, with Welch's correction in case of unequal variances. The one way ANOVA test followed by a Tukey's multiple comparison post-test was used for multiple data comparison. For data not following a Gaussian distribution, the non-parametric permutation test was used. The one way ANOVA test followed by the permutation multiple comparisons post-test was used for multiple data comparison. Illustrations of these statistical analyses are displayed as the mean +/- standard deviation (SD) using columns. Contingency was analysed using the chi-square test. p-values smaller than 0.05 were considered as significant. *, $p<0.05$, **, $p < 0.01$, ***, $p < 0.001$, ****, $p < 0.0001$.

Acknowledgments

We thank Ruth Chiquet-Ehrissman (Friedrich Miescher Institute for Biomedical Research, Basel, Switzerland) for the gift of Mouse Embryonic Fibroblasts and E. Van Obberghen-Schilling (University of Nice-Sophia Antipolis, Nice, France) for the gift of HMEC and HUVEC cell lines, P. Yurchenco (Robert Wood Johnson Medical School, Piscataway, USA) for the mouse LMα1 cDNA, Dr L. Sorokin (Institute for Physiological Chemistry and Pathobiochemistry, University of Muenster, Muenster, Germany), H. Kleinman (National Institute of Dental Research/NIH, Bethesda, Maryland, USA), T. Sasaki (Department of Molecular Medicine, Max Planck Institute of Biochemistry, Martinsried, Germany) and D. Gullberg (Department of Biomedicine, University of Bergen, Bergen, Norway) for the gift of antibodies, R. Fodde (Department of Human Genetics, Leiden University Medical Center, The Netherlands) for $APC^{+/1638N}$ mice and the Mouse Clinical Institute (Illkirch, France) for the generation of transgenic mice. We thank the Centre de Ressources Biologiques, (Hôpitaux Universitaires de Strasbourg, Hôpital de Hautepierre, Strasbourg, France) for the human tissue biopsies. This work was supported by Inserm, the Ligue contre le Cancer (OL), Institut National du Cancer (PSA, GO), the Association pour La Recherche sur le Cancer and Hautepierre Hospital, Strasbourg (GO) and the Knights Templar Eye Foundation (ME). EMB and IJ were recipients of a fellowship from the Ligue contre le Cancer and the Fondation pour la Recherche Médicale, respectively. We thank D. Bagnard for critical reading of the manuscript.

Author contribution

EMB, GO and OL designed the experiments. EMB, TR, IJ, SP, LP, GC and OL performed the experiments. AK and AMN provided technical assistance. EMB, IJ, GC, and OL analyzed

the data. ME, ODW, NA, SR, EP and DG contributed to material acquisition. JG, GO, EMB and OL wrote the paper with support from PSA and MK.

Conflicts of interest

The authors declare no conflicts of interest

References

Aghcheli, K., Parsian, H., Qujeq, D., Talebi, M., Mosapour, A., Khalilipour, E., Islami, F., Semnani, S., and Malekzadeh, R. (2012). Serum hyaluronic acid and laminin as potential tumor markers for upper gastrointestinal cancers. Eur. J. Intern. Med. *23*, 58–64.

Alpy, F., Jivkov, I., Sorokin, L., Klein, A., Arnold, C., Huss, Y., Kedinger, M., Simon-Assmann, P., and Lefebvre, O. (2005). Generation of a conditionally null allele of the laminin alpha1 gene. Genesis *43*, 59–70.

De Arcangelis, A., Lefebvre, O., Mechine-Neuville, A., Arnold, C., Klein, A., Remy, L., Kedinger, M., and Simon-Assmann, P. (2001). Overexpression of laminin alpha1 chain in colonic cancer cells induces an increase in tumor growth. Int.J.Cancer *94*, 44–53.

Bissell, M.J., and Hines, W.C. (2011). Why don't we get more cancer? A proposed role of the microenvironment in restraining cancer progression. Nat. Med. *17*, 320–329.

Chu, Y., Yang, Y., Lin, M., and Wang, Z. (2002). Detection of laminin in serum and ascites from patients with epithelial ovarian tumor. JHuazhongUniv SciTechnologMedSci *22*, 58–59, 68.

Chung, A.S., Lee, J., and Ferrara, N. (2010). Targeting the tumour vasculature: insights from physiological angiogenesis. Nat. Rev. Cancer *10*, 505–514.

Conway, T., Wazny, J., Bromage, A., Tymms, M., Sooraj, D., Williams, E.D., and Beresford-Smith, B. (2012). Xenome—a tool for classifying reads from xenograft samples. Bioinformatics *28*, i172–i178.

Edwards, M.M., Mammadova-Bach, E., Alpy, F., Klein, A., Hicks, W.L., Roux, M., Simon-Assmann, P., Smith, R.S., Orend, G., Wu, J., et al. (2010). Mutations in lama1 disrupt retinal vascular development and inner limiting membrane formation. J.Biol.Chem. *285*, 7697–7711.

Estrach, S., Cailleteau, L., Franco, C.A., Gerhardt, H., Stefani, C., Lemichez, E., Gagnoux-Palacios, L., Meneguzzi, G., and Mettouchi, A. (2011). Laminin-binding integrins induce Dll4 expression and Notch signaling in endothelial cells. Circ. Res. *109*, 172–182.

Falk, M., Ferletta, M., Forsberg, E., and Ekblom, P. (1999). Restricted distribution of laminin alpha1 chain in normal adult mouse tissues. Matrix Biol *18*, 557–568.

Fearon, E.R., and Vogelstein, B. (1990). A genetic model for colorectal tumorigenesis. Cell *61*, 759–767.

Fodde, R., Edelmann, W., Yang, K., van Leeuwen, C., Carlson, C., Renault, B., Breukel, C., Alt, E., Lipkin, M., Khan, P.M., et al. (1994). A targeted chain-termination mutation in the mouse Apc gene results in multiple intestinal tumors. Proc.Natl.Acad.Sci.U.S.A *91*, 8969–8973.

Folkman, J. (1974). Proceedings: Tumor angiogenesis factor. Cancer Res. *34*, 2109–2113.

Goel, H.L., and Mercurio, A.M. (2013). VEGF targets the tumour cell. Nat. Rev. Cancer *13*, 871–882.

Grum-Schwensen, B., Klingelhofer, J., Berg, C.H., El-Naaman, C., Grigorian, M., Lukanidin, E., and Ambartsumian, N. (2005). Suppression of Tumor Development and Metastasis Formation in Mice Lacking the S100A4(mts1) Gene. Cancer Res. *65*, 3772–3780.

Grzesiak, J.J., Smith, K.C., Burton, D.W., Deftos, L.J., and Bouvet, M. (2007). Integrin-mediated laminin-1 adhesion upregulates CXCR4 and IL-8 expression in pancreatic cancer cells. Surgery *141*, 804–814.

Hanahan, D., and Weinberg, R.A. (2011). Hallmarks of Cancer: The Next Generation. Cell *144*, 646–674.

Harrison, D., Hussain, S.A., Combs, A.C., Ervasti, J.M., Yurchenco, P.D., and Hohenester, E. (2007). Crystal Structure and Cell Surface Anchorage Sites of Laminin {alpha}1LG4-5. J.Biol.Chem. *282*, 11573–11581.

Heng, C., Lefebvre, O., Klein, A., Edwards, M., Simon-Assmann, P., Orend, G., and Bagnard, D. (2011). Functional role of laminin α1 chain during cerebellum development. Cell Adhes. Migr. *5*, 480–489.

Hohenester, E., and Yurchenco, P.D. (2013). Laminins in basement membrane assembly. Cell Adhes. Migr. *7*, 56–63.

Huang, W., Chiquet-Ehrismann, R., Moyano, J.V., Garcia-Pardo, A., and Orend, G. (2001). Interference of Tenascin-C with Syndecan-4 Binding to Fibronectin Blocks Cell Adhesion and Stimulates Tumor Cell Proliferation. Cancer Res. *61*, 8586–8594.

Hynes, R.O. (2009). The extracellular matrix: not just pretty fibrils. Science *326*, 1216–1219.

Ichikawa-Tomikawa, N., Ogawa, J., Douet, V., Xu, Z., Kamikubo, Y., Sakurai, T., Kohsaka, S., Chiba, H., Hattori, N., Yamada, Y., et al. (2012). Laminin α1 is essential for mouse cerebellar development. Matrix Biol. *31*, 17–28.

Kim, D., Pertea, G., Trapnell, C., Pimentel, H., Kelley, R., and Salzberg, S.L. (2013). TopHat2: accurate alignment of transcriptomes in the presence of insertions, deletions and gene fusions. Genome Biol. *14*, R36.

Kojima, Y., Acar, A., Eaton, E.N., Mellody, K.T., Scheel, C., Ben-Porath, I., Onder, T.T., Wang, Z.C., Richardson, A.L., Weinberg, R.A., et al. (2010). Autocrine TGF-β and stromal cell-derived factor-1 (SDF-1) signaling drives the evolution of tumor-promoting mammary stromal myofibroblasts. Proc. Natl. Acad. Sci. *107*, 20009–20014.

Lichtenberger, B.M., Tan, P.K., Niederleithner, H., Ferrara, N., Petzelbauer, P., and Sibilia, M. (2010). Autocrine VEGF signaling synergizes with EGFR in tumor cells to promote epithelial cancer development. Cell *140*, 268–279.

Maatta, M., Virtanen, I., Burgeson, R., and Autio-Harmainen, H. (2001). Comparative analysis of the distribution of laminin chains in the basement membranes in some malignant epithelial tumors: the alpha1 chain of laminin shows a selected expression pattern in human carcinomas. J.Histochem.Cytochem. *49*, 711–726.

Miner, J.H., Li, C., Mudd, J.L., Go, G., and Sutherland, A.E. (2004). Compositional and structural requirements for laminin and basement membranes during mouse embryo implantation and gastrulation. Development *131*, 2247–2256.

Miralem, T., Steinberg, R., Price, D., and Avraham, H. (2001). VEGF(165) requires extracellular matrix components to induce mitogenic effects and migratory response in breast cancer cells. Oncogene *20*, 5511–5524.

Papanikolaou, A., Wang, Q.S., Delker, D.A., and Rosenberg, D.W. (1998). Azoxymethane-induced colon tumors and aberrant crypt foci in mice of different genetic susceptibility. Cancer Lett *130*, 29–34.

Park, J.E., Keller, G.A., and Ferrara, N. (1993). The vascular endothelial growth factor (VEGF) isoforms: differential deposition into the subepithelial extracellular matrix and bioactivity of extracellular matrix-bound VEGF. Mol. Biol. Cell *4*, 1317–1326.

Ping, Y., Yao, X., Jiang, J., Zhao, L., Yu, S., Jiang, T., Lin, M.C.M., Chen, J., Wang, B., Zhang, R., et al. (2011). The chemokine CXCL12 and its receptor CXCR4 promote glioma stem cell-mediated VEGF production and tumour angiogenesis via PI3K/AKT signalling. J. Pathol. *224*, 344–354.

Pinto, D., Robine, S., Jaisser, F., Marjou, F.E. El, and Louvard, D. (1999). Regulatory sequences of the mouse villin gene that efficiently drive transgenic expression in immature and differentiated epithelial cells of small and large intestines. J.Biol.Chem. *274*, 6476–6482.

Pouliot, N., and Kusuma, N. (2013). Laminin-511: A multi-functional adhesion protein regulating cell migration, tumor invasion and metastasis. Cell Adhes. Migr. *7*, 142–149.

Qiao, L., Koutsos, M., Tsai, L.L., Kozoni, V., Guzman, J., Shiff, S.J., and Rigas, B. (1996). Staurosporine inhibits the proliferation, alters the cell cycle distribution and induces apoptosis in HT-29 human colon adenocarcinoma cells. Cancer Lett. *107*, 83–89.

Rmali, K.A., Puntis, M.C.A., and Jiang, W.G. (2007). Tumour-associated angiogenesis in human colorectal cancer. Colorectal Dis. Off. J. Assoc. Coloproctology G. B. Irel. *9*, 3–14.

De Robertis, M., Massi, E., Poeta, M.L., Carotti, S., Morini, S., Cecchetelli, L., Signori, E., and Fazio, V.M. (2011). The AOM/DSS murine model for the study of colon carcinogenesis: From pathways to diagnosis and therapy studies. J. Carcinog. *10*, 9.

Roberts, A., Pimentel, H., Trapnell, C., and Pachter, L. (2011). Identification of novel transcripts in annotated genomes using RNA-Seq. Bioinformatics *27*, 2325–2329.

Saif, M.W. (2013). Is there a Benefit from Addiction to Anti-VEGF Therapy in Patients with Colorectal Cancer? Anticancer Res. *33*, 2377–2380.

Saito, N., and Kameoka, S. (2005). Serum laminin is an independent prognostic factor in colorectal cancer. IntJColorectal Dis *20*, 238–244.

Sidhom, G., and Imam, M. (1999). Evaluation of serum laminin as a tumor marker in breast cancer. Int. J. Clin. Lab. Res. *29*, 26–29.

Simon-Assmann, P., Orend, G., Mammadova-Bach, E., Spenle, C., and Lefebvre, O. (2011). Role of laminins in physiological and pathological angiogenesis. Int. J. Dev. Biol. *55*, 455–465.

Wever, O.D., Nguyen, Q.-D., Hoorde, L.V., Bracke, M., Bruyneel, E., Gespach, C., and Mareel, M. (2004). Tenascin-C and SF/HGF produced by myofibroblasts in vitro provide convergent proinvasive signals to human colon cancer cells through RhoA and Rac. FASEB J.

Wu, F.T.H., Stefanini, M.O., Mac Gabhann, F., and Popel, A.S. (2009). A Compartment Model of VEGF Distribution in Humans in the Presence of Soluble VEGF Receptor-1 Acting as a Ligand Trap. PLoS ONE *4*, e5108.

Yang, S., Chen, J., Jiang, X., Wang, Q., Chen, Z., Zhao, W., Feng, Y., Xin, R., Shi, J., and Bian, X. (2005). Activation of chemokine receptor CXCR4 in malignant glioma cells promotes the production of vascular endothelial growth factor. Biochem. Biophys. Res. Commun. *335*, 523–528.

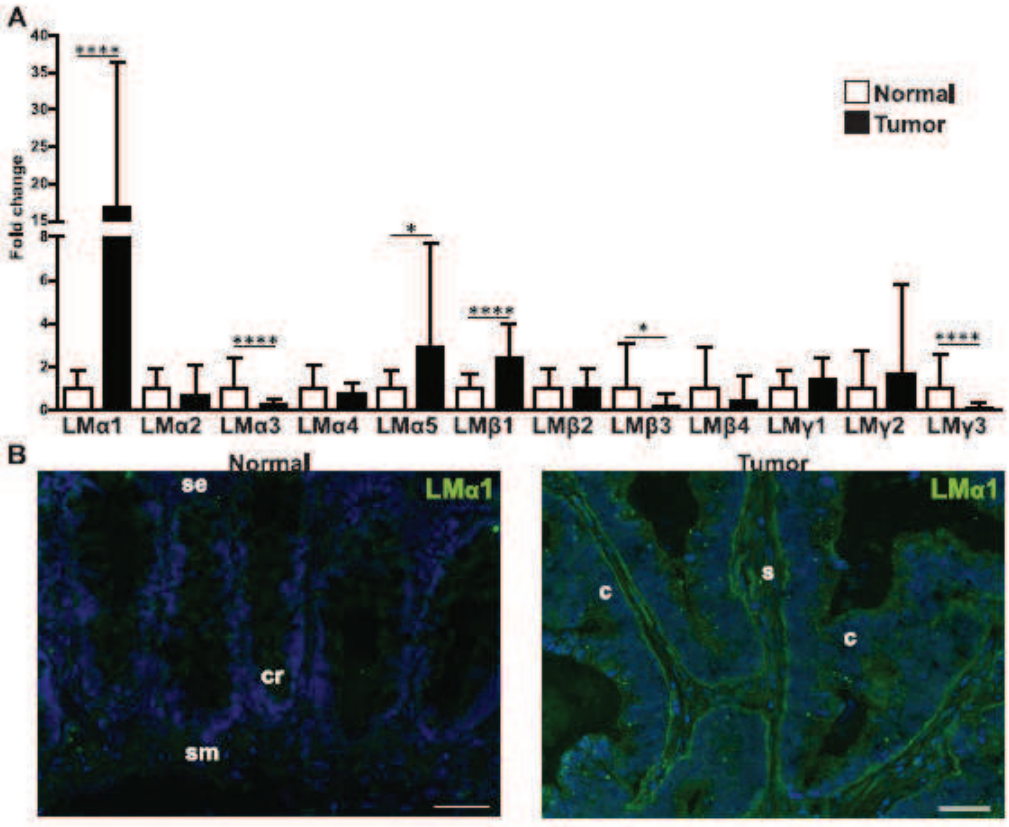
A
Normal
Tumor
Fold change
40
35
30
25
20
15
8
6
4
2
0
****
*
****
*
****
LMα1
LMα2
LMα3
LMα4
LMα5
LMβ1
LMβ2
LMβ3
LMβ4
LMγ1
LMγ2
LMγ3
B
Normal
Tumor
se
LMα1
cr
sm
c
s
c
LMα1

Figure 1

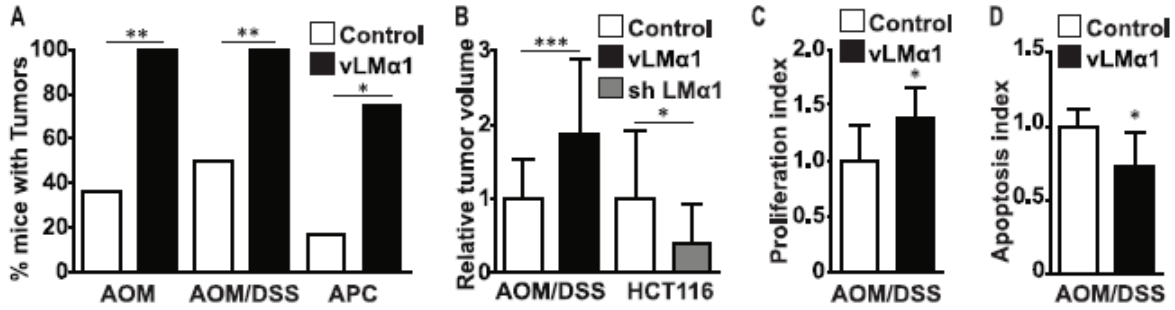

Figure 2

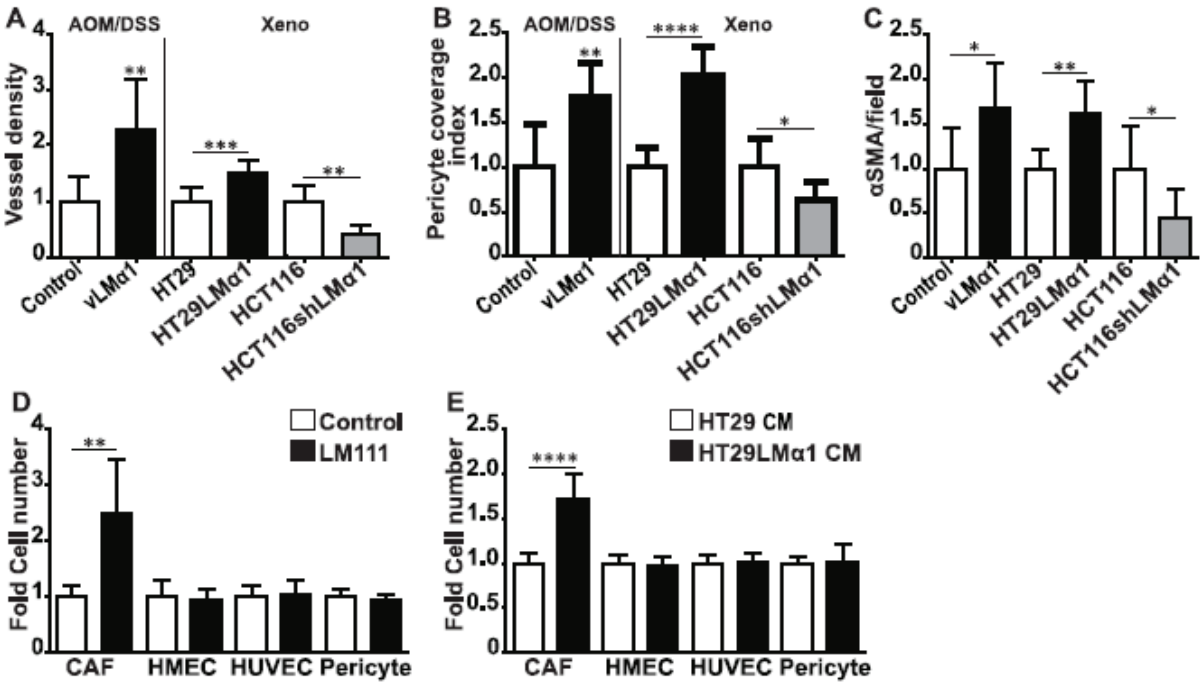

Figure 3

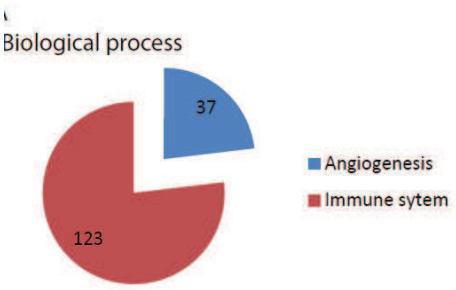

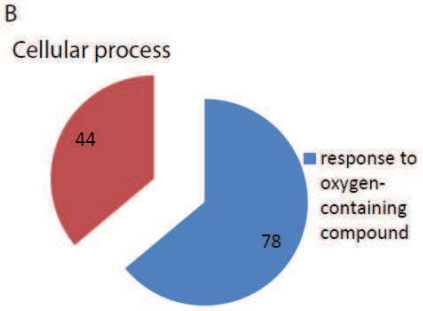

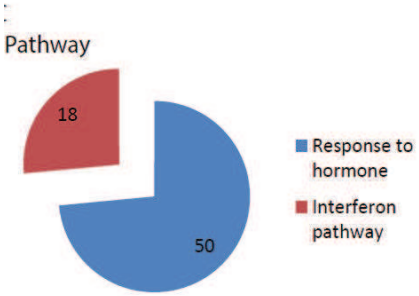

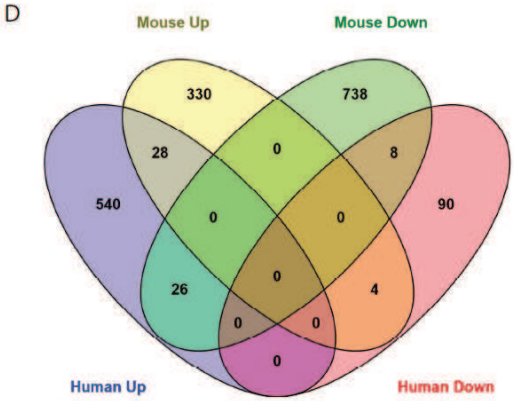

Gene ID	log2 (fold_change)	p_value	Name	Function
ADAMTS6	1.62714	5.0E-5	A disintegrin and metalloproteinase with thrombospondin motifs 6	metalloprotease
AKAP12	1.16757	5.0E-5	A-kinase anchor protein 12	
CX3CL1	2.13119	5.0E-5	Fractalkine	chemokine
CYR61	1.07273	5.0E-5	Protein CYR61	growth factor
FGF9	2.20118	5.0E-5	Fibroblast growth factor 9	growth factor
IFI44	1.46027	5.0E-5	Interferon-induced protein 44	
IFIT1	1.64127	1.0E-4	Interferon-induced protein with tetratricopeptide repeats 1	
IFIT2	1.31391	0.0074	Interferon-induced protein with tetratricopeptide repeats 2	
IFIT3	1.27047	1.50E-04	Interferon-induced protein with tetratricopeptide repeats 3	
IL33	1.06558	1.0E-4	Interleukin-33	
KIF21B	1.76116	5.0E-5	Kinesin-like protein KIF21B	microtubule binding motor protein
KIF26B	1.67643	5.0E-5	Kinesin-like protein KIF26B	microtubule binding motor protein
LEPREL2	1.28989	5.0E-5	Prolyl 3-hydroxylase 3	extracellular matrix glycoprotein
NDUFA4L2	1.19085	4.90E-03	NADH dehydrogenase [ubiquinone] 1 alpha subcomplex subunit 4-like 2	oxidoreductase
NES	1.76287	8.50E-04	Nestin	structural protein;intermediate filament
NKD2	1.63171	5.0E-5	Protein naked cuticle homolog 2	
P4HA2	1.58041	5.0E-5	Prolyl 4-hydroxylase subunit alpha-2	hydroxylase;oxygenase
PGF	1.41734	8.0E-4	Placenta growth factor	growth factor
PTK7	1.36373	5.0E-5	Inactive tyrosine-protein kinase 7	non-receptor tyrosine protein kinase
RASL11A	1.50233	5.0E-5	Ras-like protein family member 11A	small GTPase
RGS16	1.14213	5.0E-5	Regulator of G-protein signaling 16	G-protein modulator
RGS4	1.63177	8.10E-04	Regulator of G-protein signaling 4	G-protein modulator
RSAD2	1.99574	5.0E-5	Radical S-adenosyl methionine domain-containing protein 2	
RTP4	2.52079	5.0E-5	Receptor-transporting protein 4	
STARD13	1.14733	5.0E-5	StAR-related lipid transfer protein 13	
STRA6	3.53705	5.0E-5	Stimulated by retinoic acid gene 6 protein homolog	
TNFAIP3	1.01738	5.0E-5	Tumor necrosis factor alpha-induced protein 3	DNA binding protein;hydrolase
WNT11	1.50025	5.0E-5	Protein Wnt-11	signaling molecule

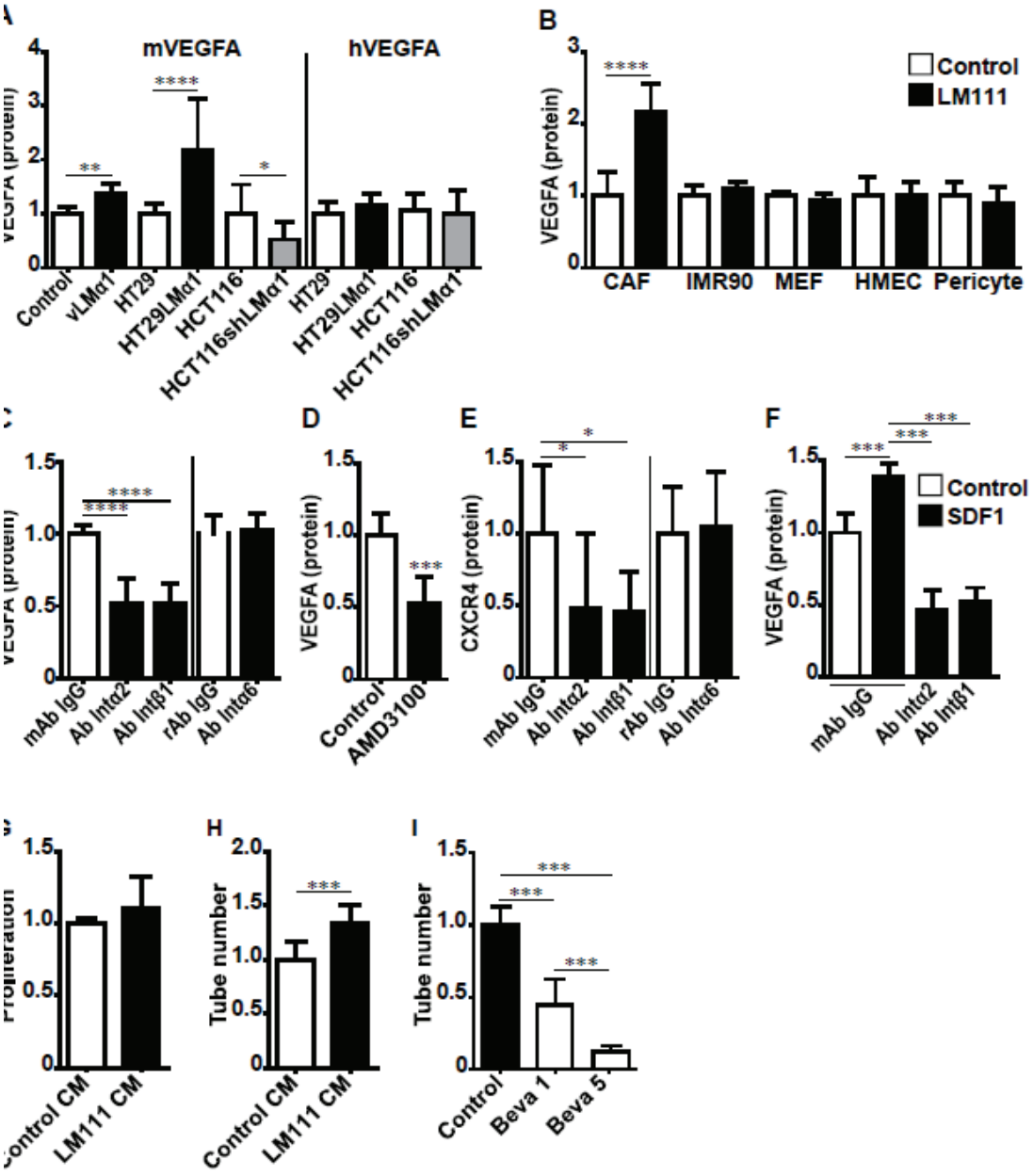
A
mVEGFA
hVEGFA
VEGFA (protein)
Control
vLMα1
HT29
HT29LMα1
HCT116
HCT116shLMα1
HT29
HT29LMα1
HCT116
HCT116shLMα1
B
Control
LM111
VEGFA (protein)
CAF
IMR90
MEF
HMEC
Pericyte
C
VEGFA (protein)
mAb IgG
Ab Intα2
Ab Intβ1
rAb IgG
Ab Intα6
D
VEGFA (protein)
Control
AMD3100
E
CXCR4 (protein)
mAb IgG
Ab Intα2
Ab Intβ1
rAb IgG
Ab Intα6
F
Control
SDF1
VEGFA (protein)
mAb IgG
Ab Intα2
Ab Intβ1
G
Proliferation
Control CM
LM111 CM
H
Tube number
Control CM
LM111 CM
I
Tube number
Control
Beva 1
Beva 5

Figure 4

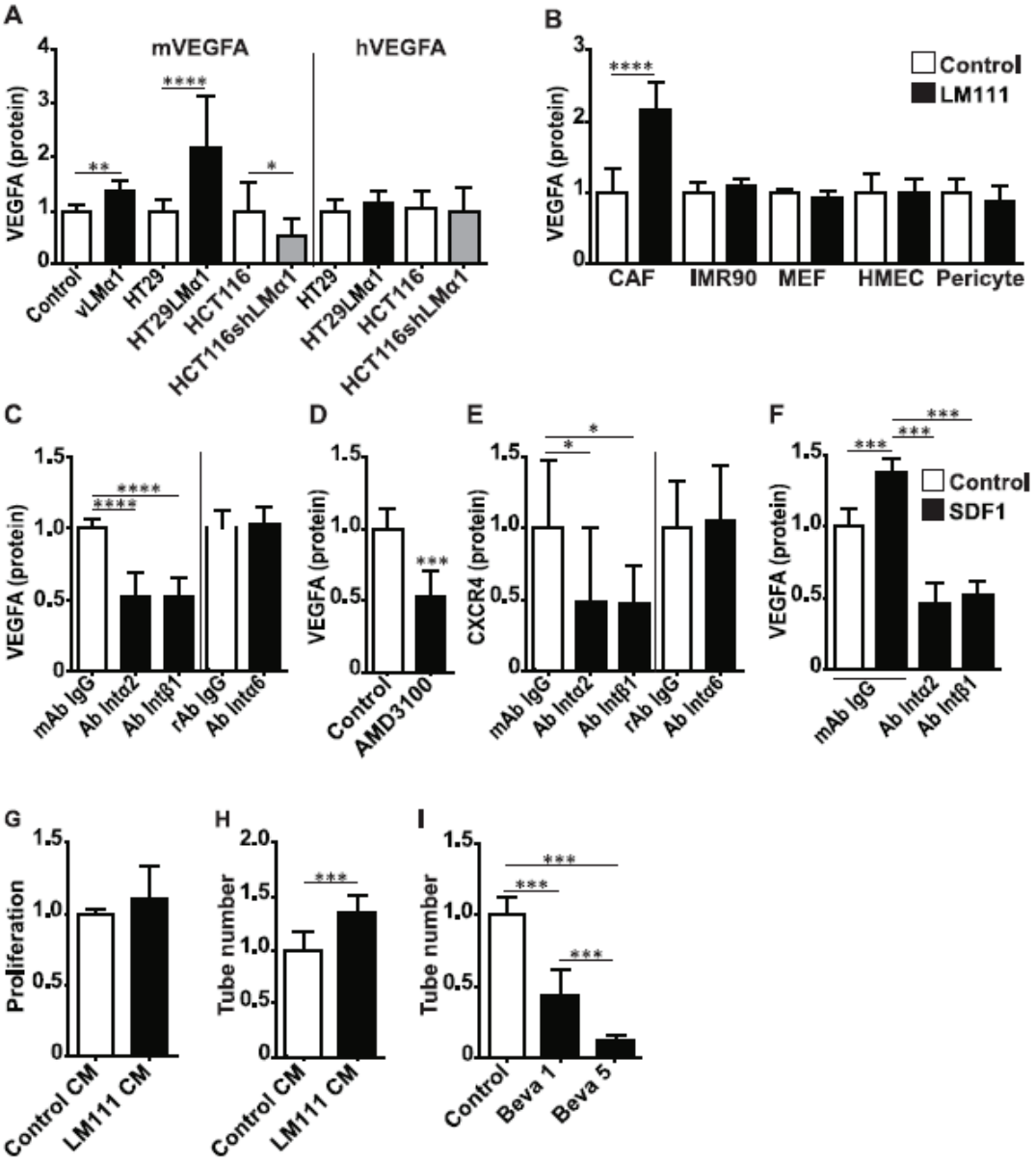
A
mVEGFA
hVEGFA
VEGFA (protein)
Control
vLMα1
HT29
HT29LMα1
HCT116
HCT116shLMα1
B
Control
LM111
CAF
IMR90
MEF
HMEC
Pericyte
C
mAb IgG
Ab Intα2
Ab Intβ1
rAb IgG
Ab Intα6
D
Control
AMD3100
E
CXCR4 (protein)
F
SDF1
G
Proliferation
Control CM
LM111 CM
H
Tube number
I
Beva 1
Beva 5

Figure 5

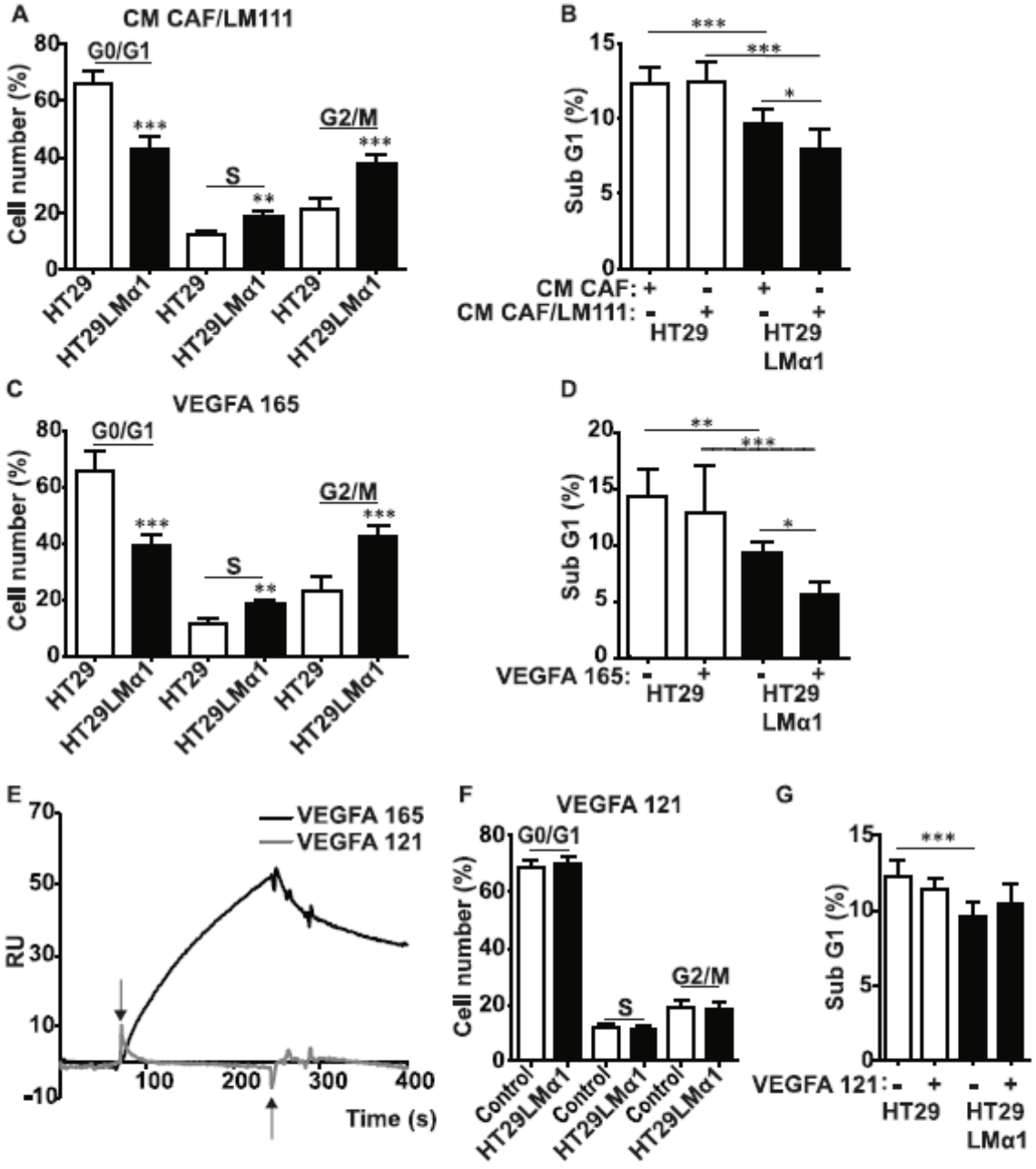
A
CM CAF/LM111
Cell number (%)
G0/G1
S
G2/M
HT29
HT29LMα1
B
Sub G1 (%)
CM CAF:
CM CAF/LM111:
HT29
HT29 LMα1
C
VEGFA 165
D
VEGFA 165:
E
VEGFA 165
VEGFA 121
RU
Time (s)
F
VEGFA 121
Control
G
VEGFA 121:

Figure 6

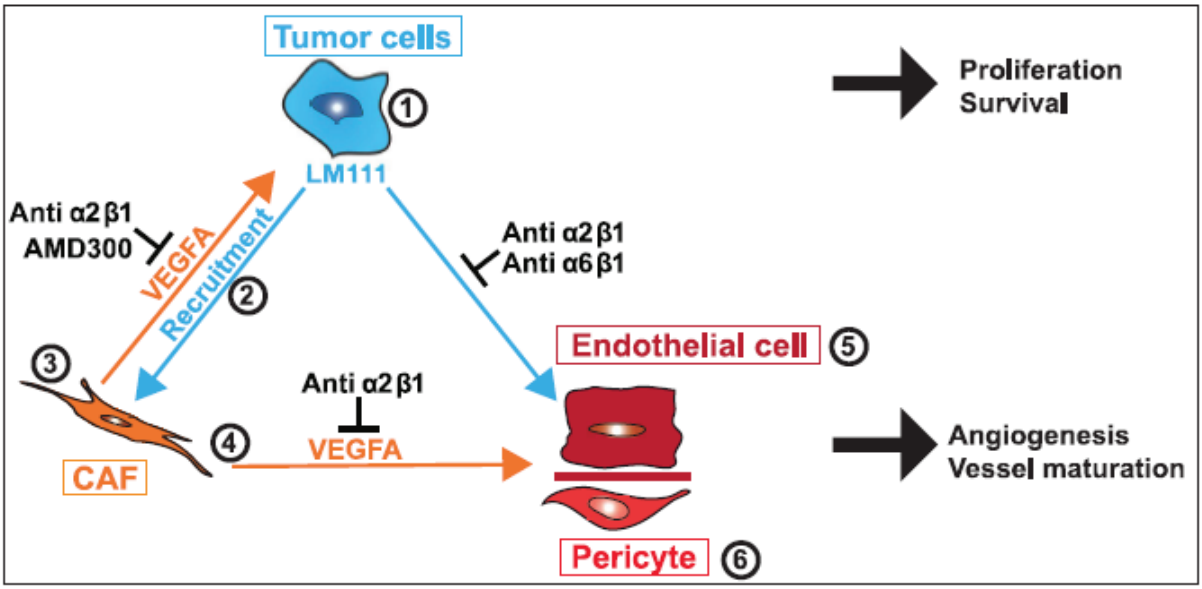
Tumor cells
1
LM111
Proliferation
Survival
Anti α2β1
AMD300
VEGFA
Recruitment
2
Anti α2β1
Anti α6β1
Endothelial cell
5
3
Anti α2β1
4
VEGFA
CAF
Angiogenesis
Vessel maturation
Pericyte
6

Figure 7

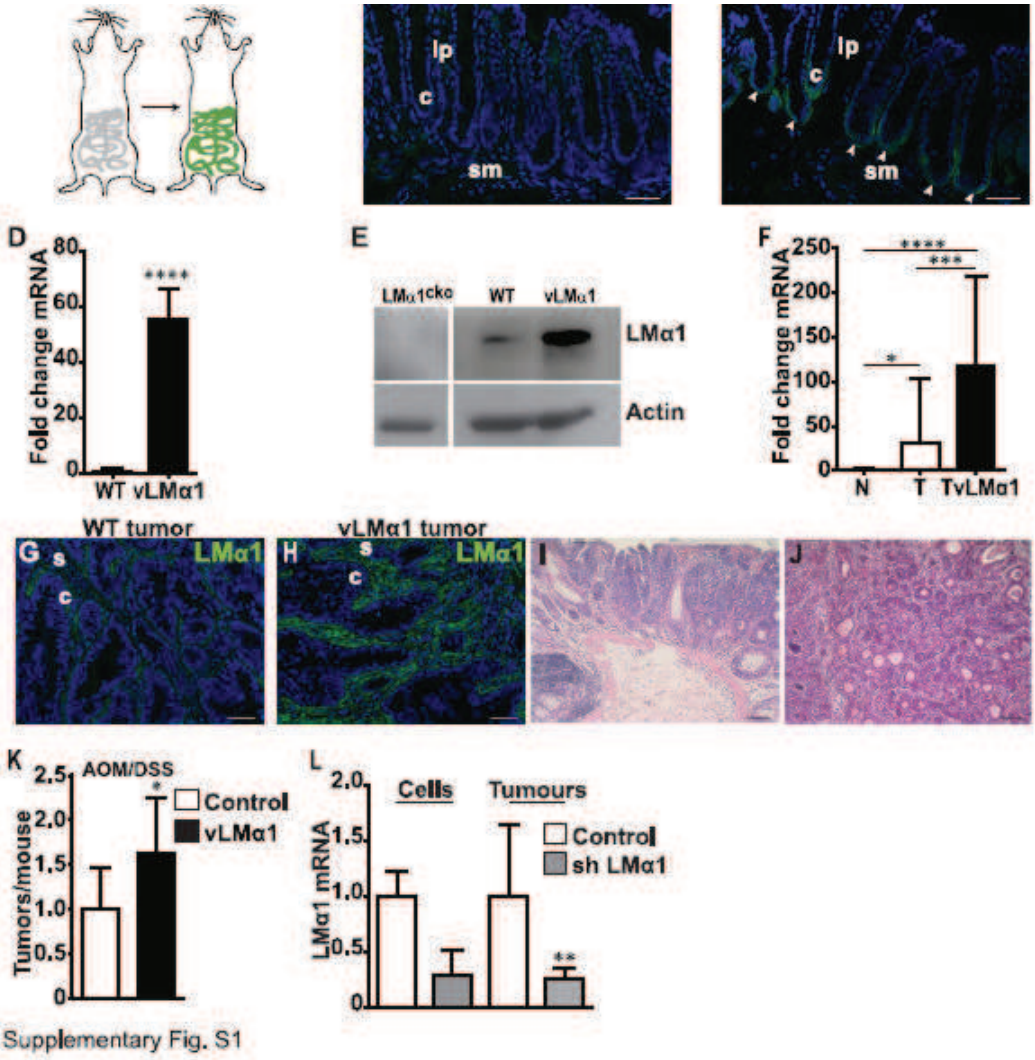

Supplementary Fig. S1

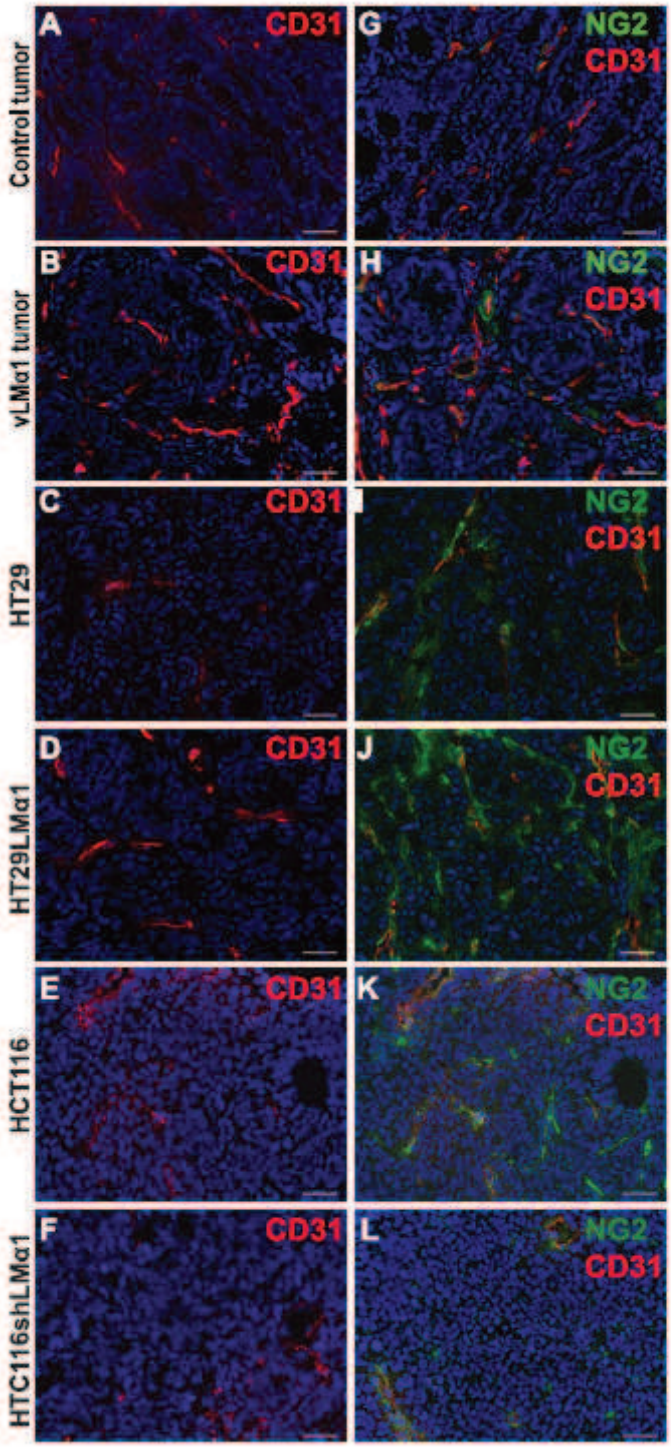

Supplementary Fig. S2

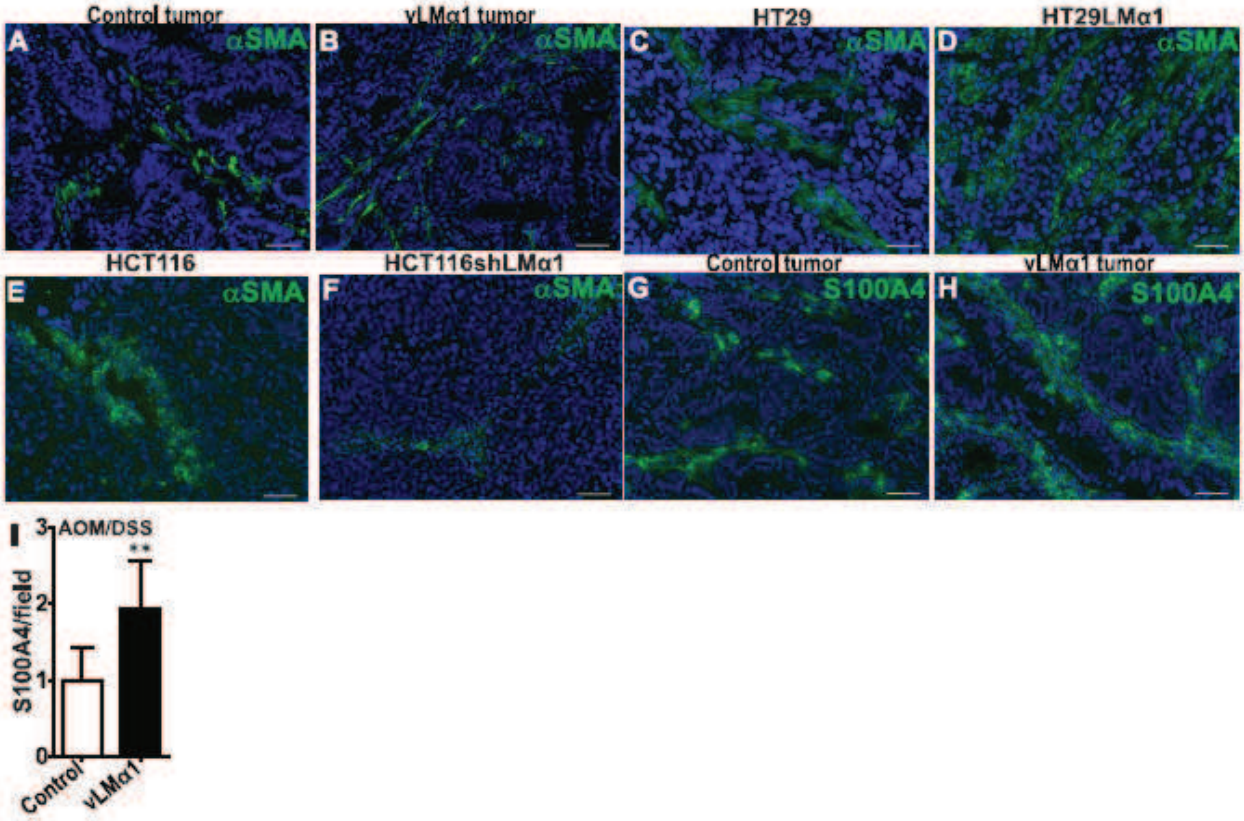

Supplementary Fig. S3

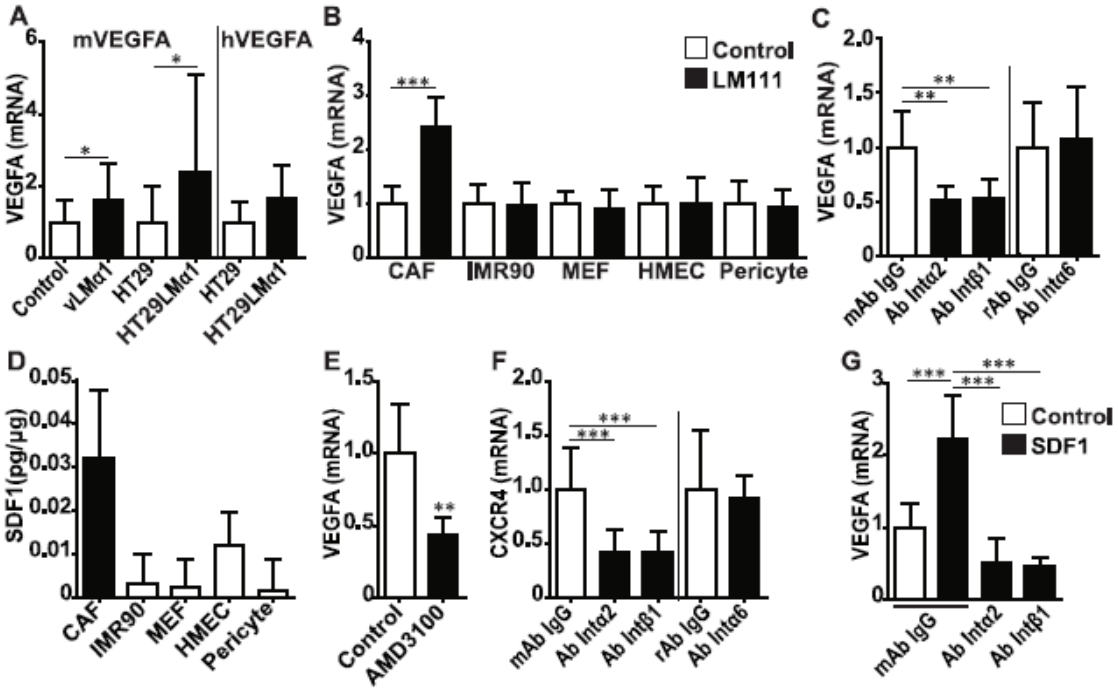

Supplementary Fig. S4

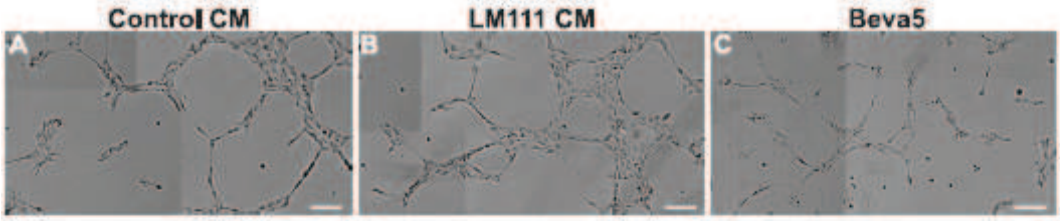

Supplemental Figure S5

Sample	Sexe	Age	Localisation	Tumoral Stage	CIN or MIN
1	F	81	colon	ADK pT3N1	CIN
2	M	74	rectum	ADK T3N0	CIN
3	M	73	colon	ADK T3N2M1	CIN
4	M	57	colon	ADK T2N0	CIN
5	M	85	colon	ADK pT3N1	CIN
6	M	88	colon	ADK PT3N1	CIN
7	M	74	rectum	ADK pT2N0	CIN
8	M	57	colon	ADK pT2N0	CIN
9	M	67	rectum	ADK pT3N0	CIN
10	M	56	rectum	ADK pTisN0	CIN
11	M	66	colon	ADK pT2N0	MIN
12	M	69	colon	ADK pT4N2M1	CIN
13	F	59	rectum	ADK pT1N0	CIN
14	M	67	colon	ADK pT3N0	CIN
15	F	81	caecum	ADK pT3N1	MIN
16	M	60	colon	polype pTis	CIN
17	M	79	colon	ADK pT3N1	CIN
18	M	71	colon	ADK pT3N2	CIN
19	F	57	colon	ADK pT2N1	CIN
20	F	71	colon	ADK pT3N0	CIN
21	F	71	colon	polype pTis	CIN
22	M	77	colon	ADK pT4N2M1	MIN
23	F	83	colon	ADK pT3N1	CIN
24	M	71	colon	ADK pT2N0	CIN
25	F	55	colon	ADK pT1N0	CIN
26	M	67	colon	ADK pT3N0	CIN
27	F	83	colon	ADK pT3N0	MIN
28	M	58	colon	ADK pT3N2	CIN
29	M	82	colon	ADK pT3N1	MIN
30	M	54	colon	ADK pT4N2M1	CIN
31	M	72	colon	ADK pT3N1	MIN
32	M	54	colon	ADK pT3N0	MIN
33	M	65	colon	ADK pT4N0	CIN
34	M	56	rectum	polype pTis	CIN
35	F	62	caecum	ADK pT1N0M0	CIN
36	M	57	rectum	ADK pT2N0M0	CIN
37	F	57	rectum	ADK pT4N0M1	CIN
38	F	91	caecum	ADK pT3N1M1	CIN
39	F	57	colon	ADK pT3N1M1	CIN
40	F	50	colon	ADK pT4N1M1	CIN
41	M	65	rectum	polype pTis	CIN
42	M	70	colon	ADK pT2N0M0	MIN
43	M	71	colon	ADK pT2N0M0	CIN
44	M	75	colon	ADK pT1N0M0	CIN

CIN: chromosome instability
MIN: microsatellite instabilty

Supplementary Table S2

Antigen recognized	Antibody	Species recognized	Type	Dilution	Use	Source/reference
Actin	C4	mouse, human	mouse mAB	1/15000	WB	Chemicon Millipore
αSMA	1A4	mouse	mouse mAB	1/200	IF	Sigma Aldrich
αSMA	E184	mouse	rabbit mAB	1/500	IF	Chemicon Millipore
CD31	73117	mouse	rat mAB	1/500	IF	Pharmingen
Integrin α2	BHA2.1	human	mouse mAB	10µg/mL	Blocking	Millipore
Integrin α6	GoH3	human	rat mAB	10µg/mL	Blocking	Santa Cruz Biotechnology
Integrin β1	4B4	human	mouse mAB	10µg/mL	Blocking	Beckman Coulter
Ki67	RM-9106	mouse	rabbit pAB	1/200	IHC	Thermo Scientific
LMα1 VI/V domain	1057	mouse	rabbit pAB	1/500	IF	Sasaki et al., 2002
LMα1	Tiger II	human	rabbit pAB	1/200	IF	Tiger et al.,1997
LMα1	200	mouse	rat mAB	1/200	IF	Sorokin et al.,1992
LMα1	YY4	mouse	rabbit pAB	1/500	WB	gift from Yinda Kleinman
Mts1 Fsp S100A4+	8828	mouse	rabbit pAB	1/500	IF	gift from Nona Ambartsumian
NG2	AB5320	mouse, human	rabbit pAB	1/200	IF	Chemicon Millipore
mAB: monoclonal antibody						
pAB: polyclonal antibody						

Supplementary Table S2

Name	Sequence 5'-3' Forward	Sequence 5'-3' Reverse
h VEGFA sp	AAGGAGGAGGGCAGAATCAT	CCAGGCCCTCGTCATTG
h LMα1	HS00300550_M1 (TAQMAN PROBE, APPLIED)	
h LMα1	GACAGCCCGGTGTCTGCCTTCACG	GTGGCGGTTTTGGGCTCATATGCA
h LMα2	ATGCAATGCGTTTGTTGGT	CACGTACAGCATCAGCCTTC
h LMα3	TGCCCATGTCCTCACACTAA	CACGTCTCCCCCATTCAC
h LMα4	ACCTCCTCAATCAAGCCAGA	TCAGCCACTGCTTCATCACT
h LMα5	TCCCCTACTGCGAAGCTG	CCTCAGGAAGGGCAGGAT
h LMβ1	CCACTGAAAAACATTGGGAATC	TGAGCCATCATCATTTCTGTAACATC
h LMβ2	GAGGCTGAGCAGCTGCTACGCGGT	CCCGTCCAACTGGGCTGCCTTACT
h LMβ3	GAAGATGTCAGACGCACACG	GCATCAGTGTCGGGGTCT
h LMβ4	GATCAGCCCTCAATCAGACC	GGACACTCCATGGGACTCAC
h LMγ1	CACAGAGGCCAAGAACAAGG	CTTGGTGCTGGTGGCATT
h LMγ2	GATGCACAGAGGGCAAAGAATGGG	GGAAAGCTTCTGCTCCAGTAAGAC
h LMγ3	AGACGAGGAGGAGCTCACAG	TATGAGGGGCTGCCCATAG
h GAPDH	HS99999905_M1 (TAQMAN PROBE, APPLIED)	
h Pbgd sp	QT00014462 (QUIAGEN)	
m VEGFA sp	GTACCTCCACCATGCCAAGT	TGGGACTTCTGCTCTCCTTC
m LMα1	CCGACAACCTCCTCTTCTACC	TCTCCACTGCGAGAAAGTCA
m GAPDH	MM99999915_G1 (TAQMAN PROBE, APPLIED)	
m Pbgd sp	QT00494130 (QUIAGEN)	

sp: species specific

Supplementary Table S3

AngioMatrix, a signature of the tumor angiogenic switch-specific matrisome, correlates with poor prognosis for glioma and colorectal cancer patients

Benoit Langlois[1,2,3,4,*], Falk Saupe[1,2,3,4,*], Tristan Rupp[1,2,3,4], Christiane Arnold[1,2,3,4], Michaël van der Heyden[1,2,3,4], Gertraud Orend[1,2,3,4], Thomas Hussenet[1,2,3,4]

[1]Inserm U1109, MN3T team, Molière, Strasbourg, 67200, France

[2]Université de Strasbourg, Strasbourg, 67000, France

[3]LabEx Medalis, Université de Strasbourg, Strasbourg, 67000, France

[4]Fédération de Médecine Translationnelle de Strasbourg (FMTS), Strasbourg, 67000, France

[*]These authors contributed equally to this work

Correspondence to:
Gertraud Orend, **e-mail:** gertraud.orend@inserm.fr
Thomas Hussenet, **e-mail:** hussenetthomas@gmail.com

Keywords: Tumor angiogenesis, angiogenic switch, extracellular matrix, matrisome

Received: July 23, 2014 ***Accepted:*** September 06, 2014 ***Published:*** October 07, 2014

ABSTRACT

Angiogenesis represents a rate-limiting step during tumor progression. Targeting angiogenesis is already applied in cancer treatment, yet limits of anti-angiogenic therapies have emerged, notably because tumors adapt and recur after treatment. Therefore, there is a strong need to better understand the molecular and cellular mechanisms underlying tumor angiogenesis. Using the RIP1-Tag2 transgenic murine model, we identified 298 genes that are deregulated during the angiogenic switch, revealing an ingression/expansion of specific stromal cell types including endothelial cells and pericytes, but also macrophages and perivascular mesenchymal cells. Canonical TGF-β signaling is up-regulated during the angiogenic switch, especially in tumor-associated macrophages and fibroblasts. The matrisome, comprising extracellular matrix (ECM) and ECM-associated molecules, is significantly enriched, which allowed us to define the AngioMatrix signature as the 110 matrisomal genes induced during the RIP1-Tag2 angiogenic switch. Several AngioMatrix molecules were validated at expression level. Ablation of tenascin-C, one of the most highly induced ECM molecules during the switch, resulted in reduced angiogenesis confirming its important role. In human glioma and colorectal samples, the AngioMatrix signature correlates with the expression of endothelial cell markers, is increased with tumor progression and finally correlates with poor prognosis demonstrating its diagnostic and therapeutic potential.

INTRODUCTION

Angiogenesis, a fundamental biological process by which novel blood vessels are formed from pre-existing ones [1], represents a rate-limiting step during tumor progression [2]. Studies from murine models have indicated that angiogenesis occurs relatively early along tumor formation and progression [2]. In particular, the murine RIP1-Tag2 model of pancreatic neuroendocrine tumorigenesis (PNET; ref. [3]) has recurrently allowed to gain novel insights into the molecular and cellular mechanisms governing tumor angiogenesis and progression. In this model of multistep tumorigenesis, pancreatic beta cells of the Langerhans islets over-express the SV40 T antigen oncogene which stochastically drives the sequential transformation of a fraction of normal islets into hyperplastic, angiogenic and macroscopic tumor islets [2]. This *in vivo* PNET model was key to provide evidences demonstrating that a fraction of islets undergoes an angiogenic switch early during tumor progression [4].

Several molecular and cellular mechanisms were described to promote the RIP1-Tag2 angiogenic switch. These include the crucial role of VEGFA and its signaling [5] and in particular, the matrix metalloprotease MMP-9-mediated regulation of VEGF bioavailability [6]. Neutrophils appear to be a source of MMP-9 hereby promoting the angiogenic switch [7, 8].

The RIP1-Tag2 model is widely used in a pre-clinical setting to evaluate anti-tumor therapeutic strategies, including angiogenesis inhibitors [9–15]. Importantly, several key conceptual advances in our understanding of how tumors adapt and become resistant to anti-angiogenic therapies, a major clinical challenge that has emerged [16, 17], were also obtained using this model [18, 19].

Here we used a genome-wide gene expression profiling strategy to uncover potential novel mechanisms underlying the angiogenic switch during RIP1-Tag2 tumor progression. We show that the angiogenic switch is associated with the deregulation of a limited number of genes, some of which reflect the expansion and ingression of stromal cells and the activation of canonical TGF-β signaling in tumor-associated macrophages and fibroblasts. Furthermore, a significant part of these genes encodes ECM and ECM-associated molecules, together defining the AngioMatrix signature. We show that this signature correlates with endothelial cell (EC) markers and tumor progression in human colorectal cancer (CRC) and glioma. Finally, its high expression correlates with poor prognosis for CRC, low grade glioma and glioblastoma (GBM) patients.

RESULTS

Gene expression profiling of the tumor angiogenic switch in a murine PNET model

We used the RIP1-Tag2 mouse model as a prototypical *in vivo* model of the tumor angiogenic switch [2, 20] to comprehensively address the underlying mechanisms. We chose an early time point (8 weeks) when a subset of pancreatic islets has undergone the angiogenic switch (Fig. 1A and Supplementary Fig. S1A) but had not yet progressed into macroscopic tumors. Islets were isolated from RIP1-Tag2 mice and classified as angiogenic or non angiogenic based on their appearance. RNA was extracted from the isolated islets to determine genome-wide gene expression levels using microarrays (Fig. 1B). The comparison of the transcriptome of non angiogenic *versus* angiogenic islets yielded a restricted list of 298 significantly deregulated genes, the "AngioSwitch signature". We first noted that this signature included several markers of stromal cells (Fig. 1C). Characteristic markers of EC (e.g. *Pecam1* and *Cdh5* encoding CD31 and VE-cadherin, respectively), perivascular cells (*Acta2* encoding alpha-smooth muscle actin or αSMA, *Cspg4* encoding NG2, *Pdgfrb*) and monocytes/macrophages (*Emr1* encoding F4/80, *Csf1r*) were found up-regulated in angiogenic islets, which was confirmed by RT-qPCR (Fig. 1D) and tissue staining (Fig. 1, E-G and Supplementary Fig.S1, B-D).

Stromal-specific activation of canonical TGF-β signaling during the RIP1-Tag2 angiogenic switch

Several TGF-β pathway members and target genes were found up-regulated, including ligands and extracellular regulators, *Cd105* (encoding endoglin, a TGF-β co-receptor) and known target genes (Fig. 2A). The up-regulation of genes encoding TGF-β ligands (*Tgfb1* and *Tgfb3*) and prototypical SMAD2/3 target genes (*Tgfbi*, *Serpine1* and *Plat* encoding PAI-1 and t-PA, respectively) was confirmed by RT-qPCR (Fig. 2B). We hypothesized that TGF-β signaling may occur preferentially within stromal cells, as a previous study revealed the presence of ALK5 (Tgf-β receptor 1)-positive cells of presumably stromal origin within RIP1-Tag2 angiogenic islets [21], which suggested that these unidentified stromal cell type(s) could undergo canonical TGF-β signaling. We used Gene Set Enrichment Analysis (GSEA) to determine the enrichment of stromal cell-specific TGF-β response signatures (TBRS; ref [22]) and found that the fibroblast- and the macrophage-specific TBRS were significantly enriched in angiogenic islets (Fig. 2C), suggesting that these stromal cell types may undergo canonical TGF-β signaling. To test this hypothesis, we analyzed the expression and sub-cellular localization of SMAD3 phosphorylated on S423/S425 (pSMAD3), as readout for TGF-β signaling activation, in RIP1-Tag2 tissue sections co-stained with stromal markers. While in non angiogenic islets an exclusively cytoplasmic staining was observed in some cells, within angiogenic islets pSMAD3 expression and nuclear localization was recurrently detected in some tumor cells but also more strikingly in both αSMA-positive fibroblasts and F4/80-positive macrophages (Fig. 2, D and E), demonstrating that these stromal cells undergo canonical TGF-β signaling in the angiogenic islets.

Up-regulation of ECM and ECM-associated genes during the RIP1-Tag2 angiogenic switch: identification of the AngioMatrix signature

We then addressed whether groups of functionally-related genes are over-represented in the AngioSwitch signature using GeneOntologies (GO). This revealed significant enrichment of angiogenesis-related GO categories, supporting the biological relevance of the profiling data, but also of several GO categories related to

ECM and secreted molecules (Fig. 3A). By RT-qPCR we validated the up-regulation of 12 of these genes (Fig. 3B), leading to a total of 25 validated genes with a significant correlation between array and RT-qPCR data (Fig. 3C).

As GO analysis revealed enrichment of several ECM-related categories, we examined the overlap of the AngioSwitch signature with the matrisome [23, 24], a comprehensive list of genes coding for ECM molecules and regulators. Of note, 37% of the genes composing the AngioSwitch signature encode matrisomal proteins (Fig. 3D), and core matrisomal genes are particularly over-represented (Supplementary Fig. S2). Moreover, GSEA revealed significant enrichment of the whole matrisome and its subclasses the core matrisome and matrisome-associated divisions (Fig. 3, E and F). We further defined the AngioMatrix signature as the 110 matrisomal genes induced during the RIP1-Tag2 angiogenic switch (Table 1). The expression of several AngioMatrix molecules, including vascular basement membrane components (collagen IV, laminin α4) and ECM glycoproteins (fibronectin, periostin, tenascin-C and sparc), was confirmed by tissue staining, which revealed their strong and stromal perivascular expression in angiogenic islets (Fig. 4 and Supplementary Fig. S3). Furthermore, we generated RIP1-Tag2 mice knocked-out for tenascin-C (TNC; ref. [25]), an ECM glycoprotein that was among the most highly up-regulated

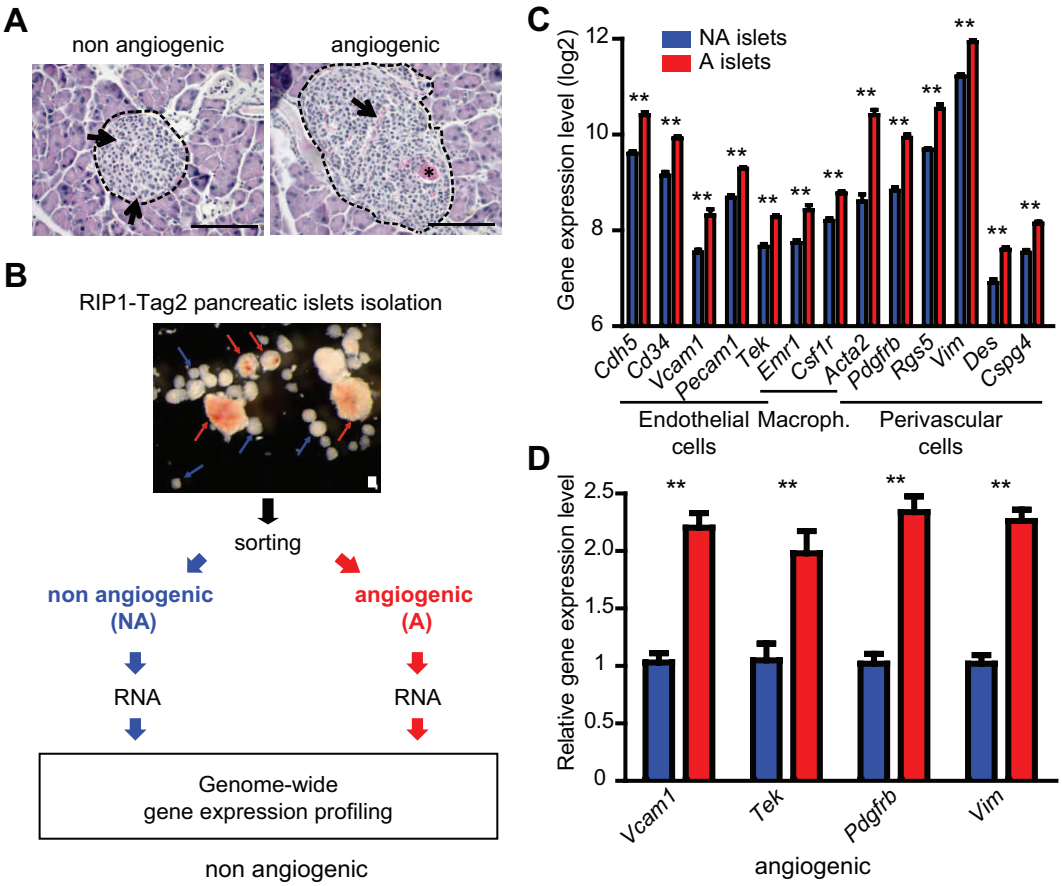

Figure 1: Transcriptomic profiling of the RIP1-Tag2 angiogenic switch reveals the up-regulation of stromal cell markers. (A) patterns of non-angiogenic (left) and angiogenic (right) islets in H&E stained tissue sections from RIP1-Tag2 pancreata. Examples of normal capillaries in a non angiogenic islet (arrows) and of a dilated vessel (arrow) and micro-hemorrhaging (asterisk) in the angiogenic islet. **(B)** strategy used to compare angiogenic and non angiogenic pancreatic tumor islets by gene expression profiling upon their differential isolation, sorting and RNA extraction. **(C)** up-regulation of specific stromal cell markers in the transcriptome of RIP1-Tag2 angiogenic (red) compared to non angiogenic (blue) islets: markers for EC (*Cdh5*, *Cd34*, *Vcam1*, *Pecam1*, *Tek* or Tie2, also expressed by macrophages), macrophages/monocytes (*Emr1*, *Tek* and *Csf1r*) perivascular and smooth muscle cells (*Acta2*, *Pdgfrb*, *Rgs5*, *Vim*, *Des* and *Cspg4* encoding NG2). Measures represent the mean expression level from two independent profiling experiments, error bars the SEM. ** $p < 5x10^{-3}$. **(D)** RT-qPCR confirmation of the up-regulation of stromal cell markers (*Vcam1*, EC; *Tek*: ECs and macrophages/monocytes; *Pdgfrb*: pericytes; *Vim*: perivascular SMC) in angiogenic (red) compared to non angiogenic (blue) islets. Measures represent the mean expression level from two independent experiments, error bars the SEM. ** $p < 5x10^{-3}$.

(*Continued*)

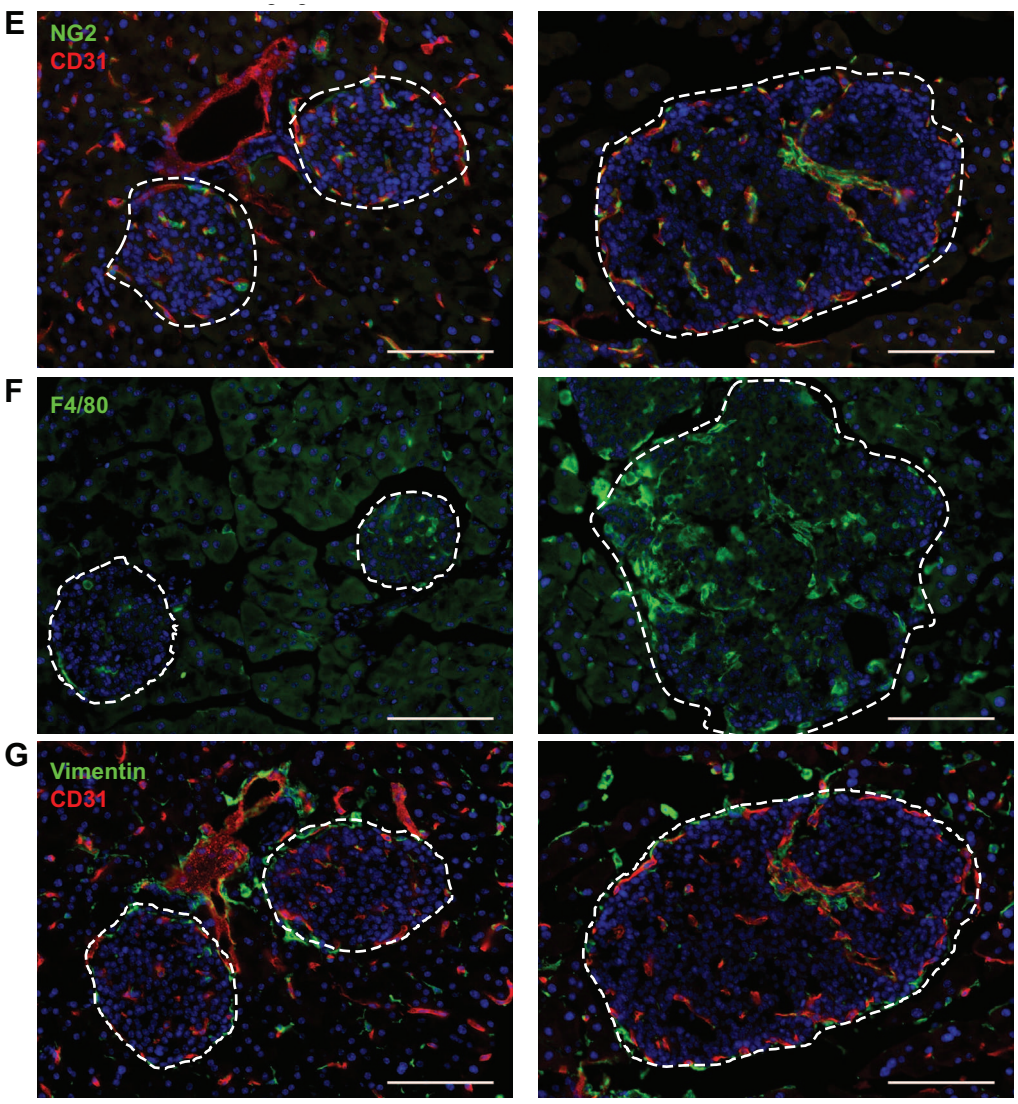

Figure 1: (E-G) expression (immunofluorescence) of stromal cell markers in non angiogenic and angiogenic islets, CD31 and NG2 (E), F4/80 (F) and Vimentin and CD31 (G). Nuclei are stained with Dapi (blue). In A and E-G dashed lines encircle islets. Scale bars, 100 μm.

AngioMatrix genes (Fig. 3B and Table 1). We compared the number of angiogenic islets and the relative proportion of non-angiogenic and angiogenic islets from control and TNC-depleted RIP1-Tag2 mice on tissue sections, which revealed a significant decrease in the absence of TNC (Fig. 4, F and G).

Expression of the AngioMatrix signature correlates with angiogenesis markers, tumor progression and poor prognosis for CRC, low grade glioma and GBM patients

To address the potential relevance of the AngioMatrix signature for cancer patients, we analyzed transcriptomic datasets, as this strategy enables investigating large and independent patient cohorts. Since insulinoma is rare and mostly benign (and no dataset could be retrieved), we focused on colorectal cancer and glioma, as their incidence is higher, angiogenesis is known to drive their progression and several independent datasets could be retrieved for CRC [26–30] and glioma [31–33].

We addressed whether expression of the AngioMatrix signature correlates with surrogate markers of blood vessels and angiogenesis in CRC. We determined for each sample the AngioMatrix signature expression level by averaging the expression levels of the 110 genes forming the signature, thereafter referred to as "AngioMatrix expression", and observed significant correlations with the expression of the EC markers *PECAM1* (Fig. 5A) and *CDH5* (Fig. 5B). We next analyzed the pattern of AngioMatrix expression along CRC formation and progression. This revealed higher expression in normal

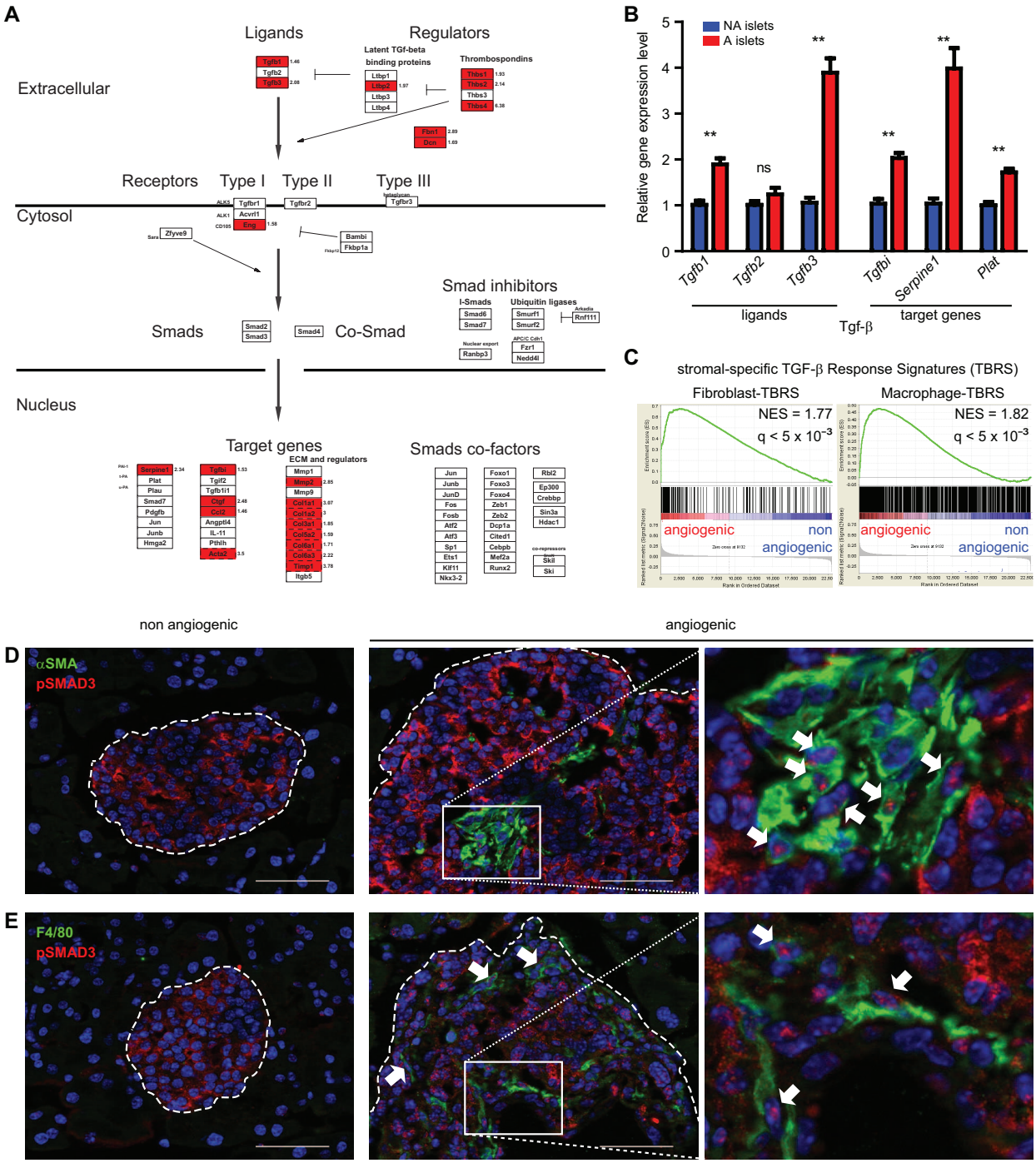

Figure 2: TGF-β signaling activation during the RIP1-Tag2 angiogenic switch. (A) schematic depiction of gene expression profiling data on a TGF-β signaling GenMapp. Genes (represented by boxes) in red indicate genes significantly up-regulated in angiogenic islets. No gene in this pathway was down-regulated. Several TGF-β ligands, extracellular regulators, the *Endoglin* co-receptor (*Eng*, encoding CD105), together with target genes are up-regulated in angiogenic islets. **(B)** RT-qPCR analysis of TGF-β ligands and target gene expression in non angiogenic (blue) and angiogenic (red) islets. The *Tgfb1* and *Tgfb3* genes are significantly up-regulated in angiogenic islets together with the prototypical Smad2/3 target genes *Tgfbi*, *Serpine1* and *Plat*. Measures represent the mean of two independent experiments, error bars the SEM, ** $p < 5x10^{-3}$, ns not significant. **(C)** GSEA demonstrates significant enrichment of fibroblast- and macrophage- specific TGF-β response signatures in the transcriptome of angiogenic islets. The Normalized Enrichment Score (NES) and the FDR q-value assessing the significance of enrichment are indicated. **(D-E)** co-staining of phosphorylated SMAD3 (pSMAD3) with αSMA (D) or F4/80 (E) in RIP1-Tag2 islets. Nuclear localization of pSMAD3 is observed in angiogenic islets, predominantly in tumor-associated αSMA+ fibroblasts (D) and F4/80+ macrophages (E) (arrows). Nuclei are stained in blue (DAPI). Dashed lines encircle islets; non angiogenic: left column, angiogenic: middle column and higher magnification pictures corresponding to the boxed areas within angiogenic islets are presented (right column). Scale bars, 50 μm.

A

Gene Set Name	p-value	FDR q-value
EXTRACELLULAR_MATRIX	0.00E+00	0.00E+00
EXTRACELLULAR_MATRIX_PART	0.00E+00	0.00E+00
PROTEINACEOUS_EXTRACELLULAR_MATRIX	0.00E+00	0.00E+00
COLLAGEN	0.00E+00	0.00E+00
EXTRACELLULAR_REGION	0.00E+00	0.00E+00
EXTRACELLULAR_REGION_PART	0.00E+00	0.00E+00
EXTRACELLULAR_MATRIX_STRUCTURAL_CONSTITUENT	2.92E-14	1.93E-12
BASEMENT_MEMBRANE	1.88E-09	8.28E-08
COLLAGEN_BINDING	1.08E-06	3.21E-05
ANGIOGENESIS	9.06E-06	2.22E-04
REGULATION_OF_ANGIOGENESIS	1.53E-05	3.37E-04

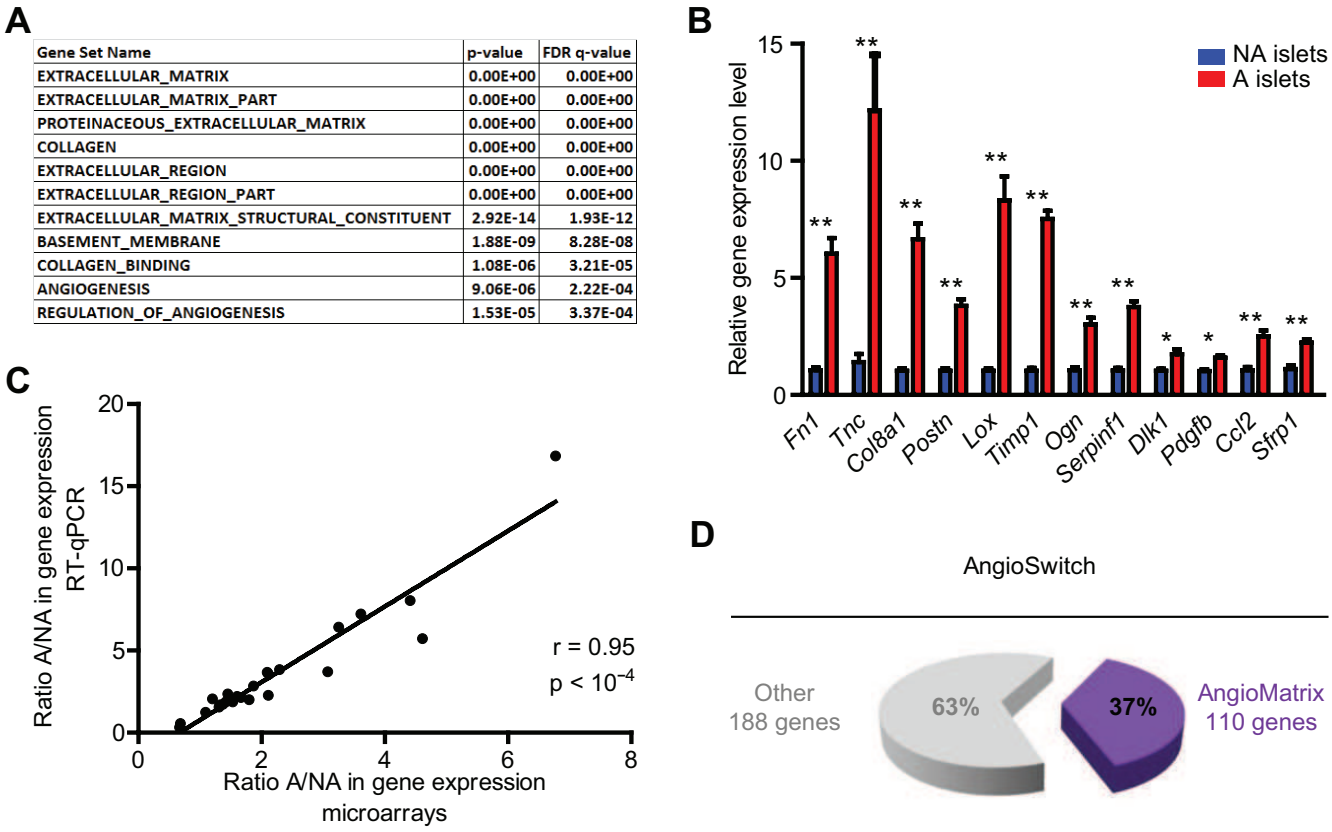

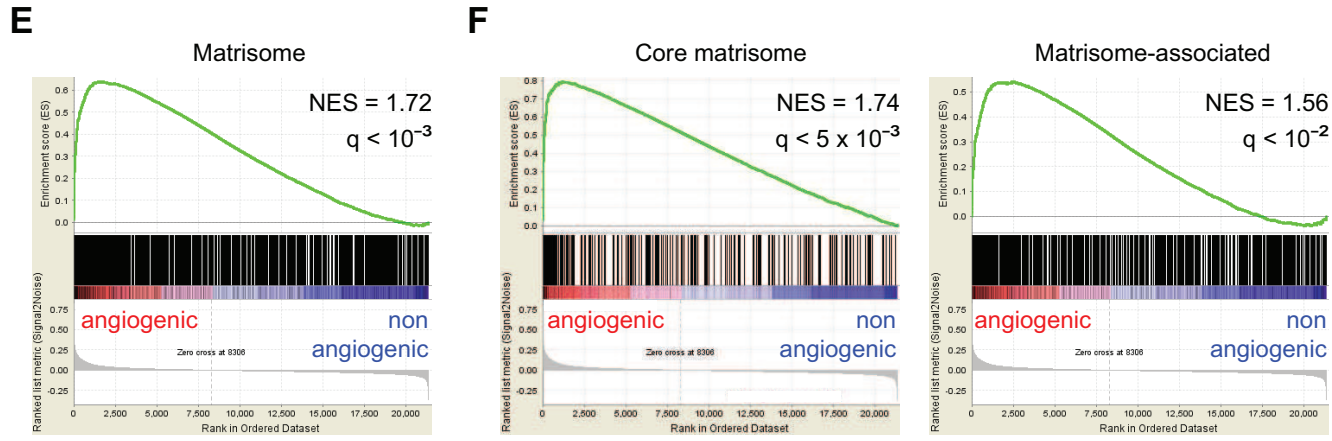

Figure 3: Genes encoding the extracellular matrix and regulators, or matrisome, are up-regulated during the RIP1-Tag2 angiogenic switch. **(A)** significantly enriched GO categories in the AngioSwitch signature. The p- and FDR q-values indicate the significance of enrichment. **(B)** RT-qPCR validation of increased expression for 12 candidate genes up-regulated in angiogenic islets. Data (blue, non-angiogenic; red, angiogenic islets) represent mean and error bars the SEM from two independent experiments. **, $p < 5x10^{-3}$; *, $p < 10^{-2}$. **(C)** comparison of the gene expression ratio determined by array profiling and RT-qPCR for 25 validated genes (22 up-regulated, 1 unchanged and 2 down-regulated). The Pearson correlation coefficient and the p-value are indicated. **(D)** overlap between the AngioSwitch signature and the matrisome: 37% of genes induced during the angiogenic switch belong to the matrisome, defining the AngioMatrix signature (110 genes). **(E-F)** GSEA demonstrate significant enrichment of the matrisome (E) and its divisions (F) in the transcriptome of angiogenic islets. The Normalized Enrichment Score (NES) and the FDR q-value assessing the significance of enrichment are indicated.

Table 1: Composition of the AngioMatrix signature. Gene symbol, expression ratio during the RIP1-Tag2 angiogenic switch and matrisome classification are indicated. Genes are grouped by matrisome division and categories, and ranked in descending order of expression ratio.

			Matrisome	
Gene symbol	Ratio A / NA	p-value	Division	Category
Col8a1	3.25	1.1869E-07	Core matrisome	Collagens
Col10a1	3.11	9.3207E-04		
Col1a1	2.95	1.5235E-08		
Col1a2	2.77	1.0141E-09		
Col6a3	2.26	5.9958E-08		
Col12a1	2.22	4.7032E-08		
Col14a1	2.01	5.4409E-06		
Col3a1	1.91	1.4790E-07		
Col15a1	1.87	6.7506E-08		
Col4a2	1.74	4.5137E-06		
Col6a1	1.71	8.8071E-07		
Col5a2	1.68	6.1916E-07		
Col6a2	1.67	3.2904E-06		
Col4a1	1.57	5.2897E-07		
Col18a1	1.40	1.9590E-03		
Thbs4	6.77	3.9919E-09		ECM Glycoproteins
Fn1	4.61	6.5803E-08		
Tnc	3.71	1.2366E-08		
Postn	3.07	7.7478E-08		
Mfap5	2.87	3.2983E-09		
Fbn1	2.74	7.9111E-08		
Ctgf	2.34	7.4667E-07		
Srpx2	2.28	7.0478E-07		
Cilp	2.22	3.0748E-06		
Svep1	2.21	1.0975E-07		
Mgp	2.21	3.7883E-05		
Thbs2	2.12	8.1086E-07		
Spon1	2.04	5.5033E-06		
Nid1	1.98	1.4637E-07		
Ltbp2	1.95	1.9311E-05		
Pcolce	1.92	1.9741E-08		
Mfap4	1.91	2.4071E-07		
Thbs1	1.90	3.1110E-04		
Lama4	1.86	4.4791E-07		
Sparc	1.83	1.0330E-07		
Aebp1	1.71	1.4840E-05		
Lama2	1.71	8.5452E-06		
Dpt	1.70	1.5983E-03		
Gas6	1.69	1.7581E-04		
Sparcl1	1.64	1.3306E-04		
Slit2	1.63	2.5898E-07		
Lamc1	1.58	9.9984E-08		
Eln	1.58	8.1302E-05		
Igfbp4	1.57	5.5755E-04		
Fbln5	1.56	1.5923E-04		
Fbln2	1.49	1.3614E-06		
Tgfbi	1.48	2.0248E-05		
Mmrn2	1.48	3.4566E-05		
Wisp1	1.46	1.5947E-03		
Igfbp5	1.44	3.2103E-03		
Nid2	1.44	1.3026E-05		
Slit3	1.43	4.6296E-05		
Pxdn	1.41	8.0373E-06		

(*Continued*)

			Matrisome	
Gene symbol	Ratio A / NA	p-value	Division	Category
Lum	2.60	2.9885E-05		Proteoglycans
Fmod	2.53	3.8582E-05		
Bgn	2.36	5.6766E-08		
Aspn	1.91	1.0662E-06		
Ogn	1.87	1.0220E-02		
Prelp	1.77	2.5035E-04		
Dcn	1.66	1.9182E-02		
Vcan	1.62	7.8882E-05		
Hspg2	1.45	1.0067E-04		
Lox	4.41	1.0907E-07	Matrisome-associated	ECM Regulators
Timp1	3.61	1.0843E-06		
Mmp2	2.70	6.4945E-05		
Serpine1	2.29	8.7933E-07		
Adamts2	2.17	9.2591E-07		
Serpinf1	2.10	1.9858E-06		
Serpine2	2.03	2.6508E-05		
Loxl1	1.97	3.9437E-07		
Mmp14	1.94	9.5446E-07		
Ctsc	1.70	1.5301E-05		
Ctsh	1.69	3.0313E-02		
Serpinh1	1.65	1.5995E-05		
Adamts12	1.61	2.0488E-06		
Adamts5	1.59	1.0358E-05		
Adam12	1.57	4.4749E-07		
Adamts1	1.52	5.9751E-06		
Adamtsl3	1.49	3.8709E-05		
Mmp13	1.48	4.2445E-04		
Cd109	1.47	1.1918E-04		
Serpina3n	1.47	6.5008E-03		
Sulf2	1.43	1.1640E-04		
Loxl3	1.40	3.8243E-05		
Adamts9	1.40	1.9618E-04		
Anxa1	2.20	1.9866E-05		ECM-affiliated Proteins
Clec4n	2.11	7.5384E-04		
Plxdc2	1.81	5.2764E-08		
Frem1	1.78	4.3323E-06		
Anxa3	1.77	4.4351E-03		
Lgals1	1.73	1.0923E-06		
Plxnd1	1.73	1.2998E-04		
Anxa2	1.72	2.6193E-05		
Colec12	1.57	6.4004E-04		
Cspg4	1.48	3.5828E-05		
Clec7a	1.45	9.1353E-05		
C1qb	1.42	2.8805E-04		
Sema6a	1.41	3.1453E-06		
Gpc6	1.41	9.0537E-07		
Fstl1	2.92	1.0280E-05		Secreted Factors
Tgfb3	2.09	5.2714E-07		
Igf1	1.93	5.8883E-07		
Sfrp1	1.80	4.0155E-03		
Cxcl9	1.63	8.7549E-03		
Ccl3	1.57	2.1757E-03		
S100a6	1.54	1.7308E-04		
Angptl2	1.45	1.2141E-04		
Ccl2	1.45	1.7686E-04		
Pdgfc	1.42	9.5455E-04		
Tgfb1	1.42	1.8128E-03		

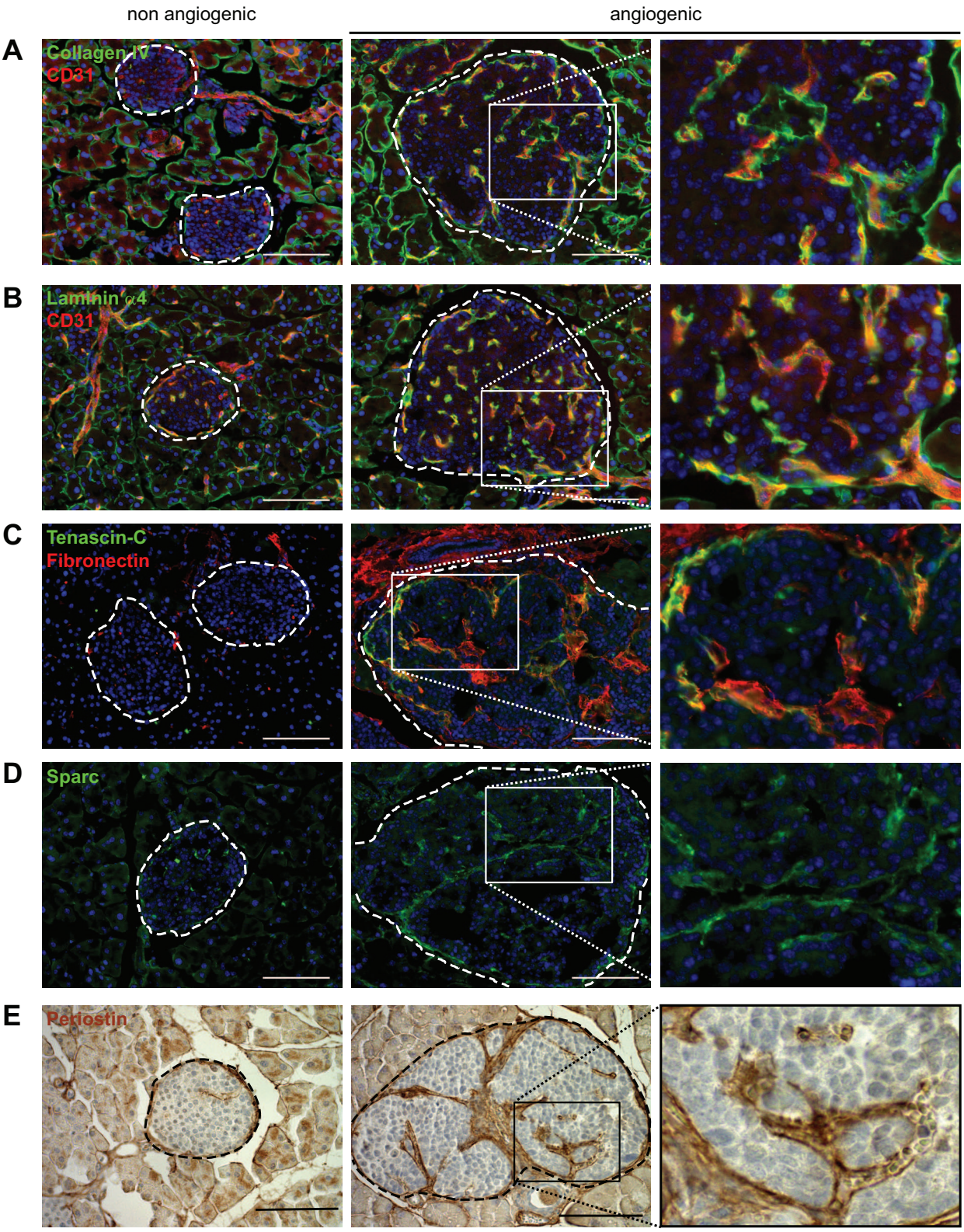

Figure 4: Analysis of AngioMatrix protein expression and functional validation of tenascin-C role in the RIP1-Tag2 angiogenic switch. (A-E) expression pattern of the vascular basement membrane components collagen IV (A) and laminin α4 (B), and of the ECM glycoproteins fibronectin and tenascin-C (C), sparc (D) and periostin (E)**.** Dashed lines encircle islets; non angiogenic: left column, angiogenic: middle column and higher magnification pictures corresponding to the boxed areas within angiogenic islets are presented (right column). Scale bars, 100 μm.

(*Continued*)

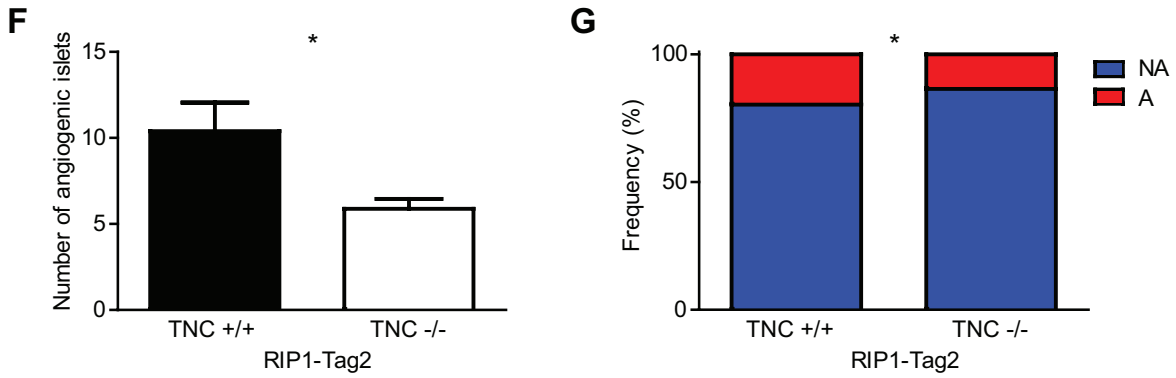

Figure 4: (F-G) functional validation of tenascin-C contribution to the angiogenic switch. The number (F) and relative proportion (G) of angiogenic islets are significantly decreased in RIP1-Tag2 TNC -/- mice (n = 8 mice) as compared to TNC +/+ controls (n = 5 mice). A: angiogenic islets, NA: non angiogenic islets. * $p < 5x10^{-2}$.

tissue compared to adenoma and up-regulation during the adenoma-carcinoma transition (Fig. 5C), which was confirmed in an independent cohort (Supplementary Fig. S4A). We observed significantly higher AngioMatrix expression in primary CRC classified as Duke B or Duke C (*versus* A; Supplementary Fig. S4B), and higher expression in advanced primary CRC in an independent cohort (stage 3 or 4 *versus* 0, TNM; Supplementary Fig. S4C). We next asked if AngioMatrix expression could vary according to CRC molecular subtypes [29, 34] and found a significantly higher AngioMatrix expression in the Inflammatory subtype (compared to the Goblet-like or the Transit-amplifying subtypes) and in the Stem-like subtype compared to any other subtype (Fig. 5D). Furthermore, AngioMatrix expression was significantly lower in the C3 and the C1 subtypes and higher in the C4 subtype (Fig. 5E). We then wondered if AngioMatrix expression may vary during the ultimate steps of CRC progression. We found slightly increased AngioMatrix expression in metastatic (compared to non-metastatic) primary CRC (Supplementary Fig. S4D). In CRC metastasis, while no difference is observed in the lung (Supplementary Fig. S4E), AngioMatrix expression is significantly up-regulated in liver metastasis compared to normal tissue (Fig. 5F). The recurrent link between increased AngioMatrix expression and CRC progression prompted us to test a potential correlation with CRC patient survival. We used datasets from two independent cohorts of patients [28, 29], which were stratified using cut-off values into AngioMatrix low or high groups and survival analysis was performed to compare the outcome of these groups. A high expression of the AngioMatrix signature significantly correlated with a shorter relapse-free survival in the two CRC cohorts (Fig. 5, G and H, and Supplementary Figure S4, F and G).

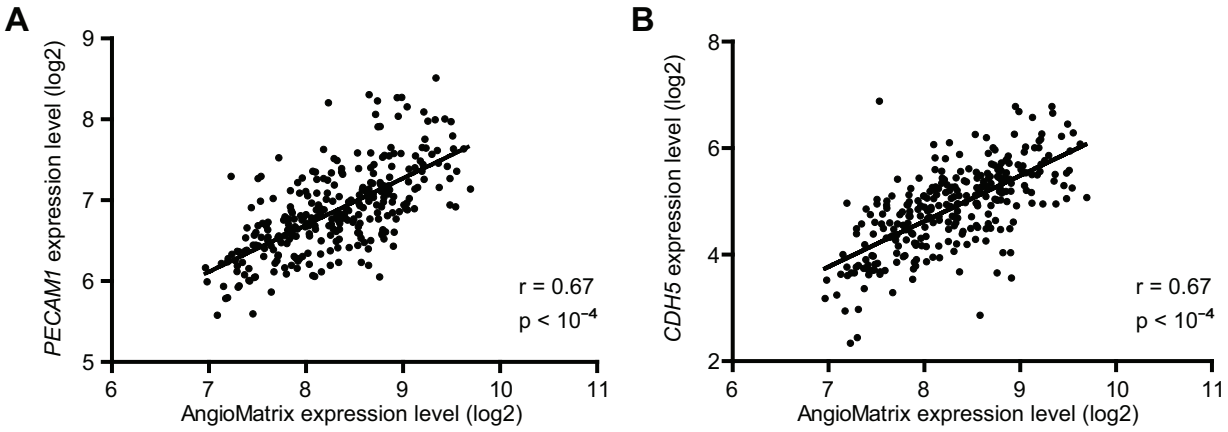

Figure 5: Correlation between AngioMatrix signature expression and EC markers, tumor progression and poor prognosis in human CRC. (A-B) correlation between AngioMatrix expression level and *PECAM1* (A) or *CDH5* (B) expression in normal, adenoma and primary CRC samples. The Pearson correlation coefficient and the p-value are indicated.

(*Continued*)

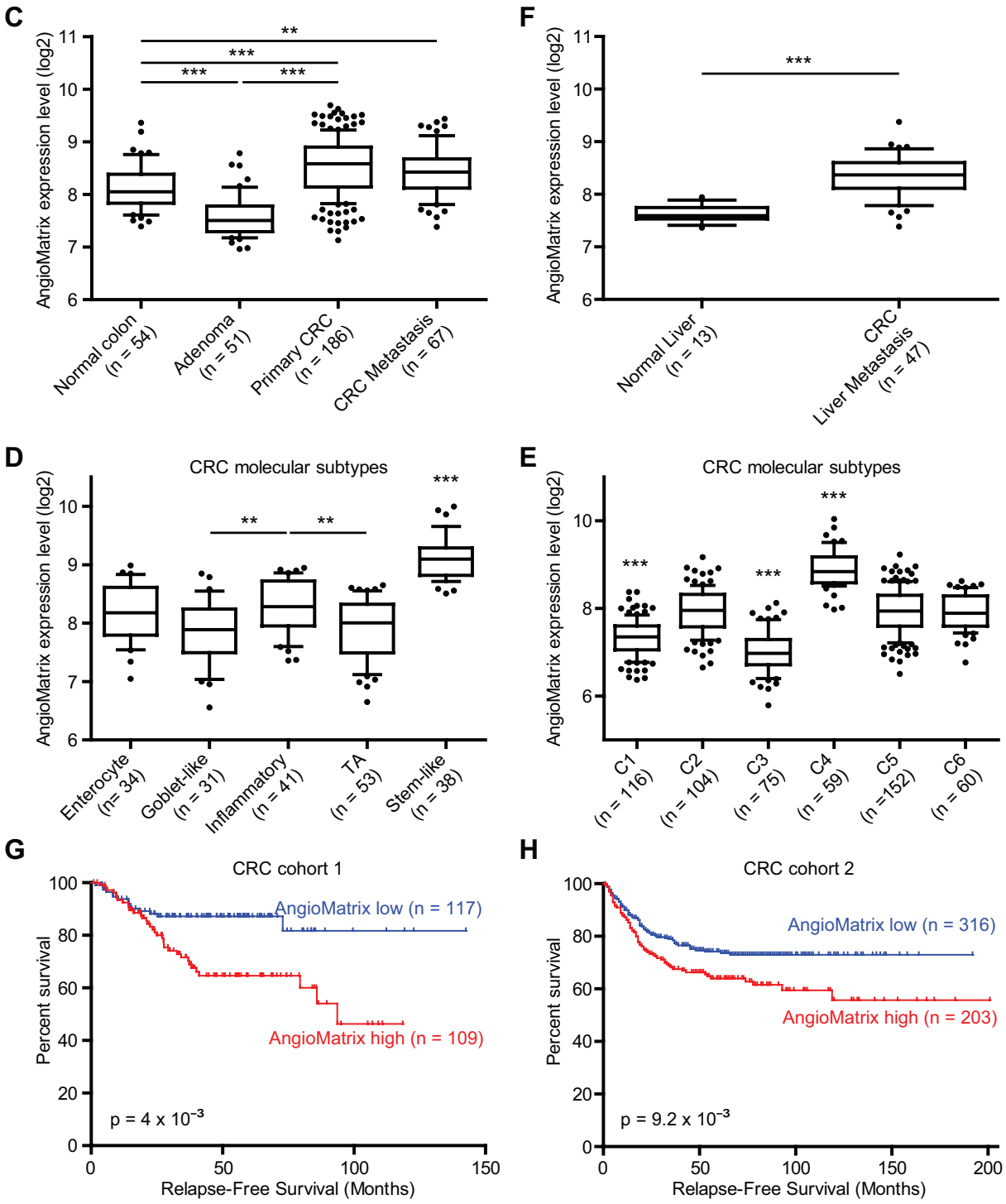

Figure 5: **(C, F)** analysis of AngioMatrix expression during CRC progression. Comparison of normal colon, adenoma, primary CRC and CRC metastasis (C) and CRC metastasis *versus* normal liver (F). **(D-E)** analysis of AngioMatrix expression in the different primary CRC molecular subytpes. Note the significant higher levels of AngioMatrix in the Stem-like (D) and C4 (E) subtypes. In C-F, ***and ** indicate p-values < 10^{-3} and 10^{-2}, respectively. **(G-H)** Kaplan-Meier survival analysis of CRC patients. Patients were stratified according to the average expression of the AngioMatrix signature as AngioMatrix high or low using a cutoff value. In each cohort, high AngioMatrix expression significantly correlates with poor prognosis for patients. P-values indicate the significance of survival difference between the groups of individuals. In C-H, n indicates the number of samples per group.

We analyzed AngioMatrix expression in independent glioma datasets and observed again a significant correlation between AngioMatrix expression and the EC markers *PECAM1* (Fig. 6A) and *CDH5* (Supplementary Fig. S5A). Comparing glioma histological subtypes revealed higher AngioMatrix expression in GBM compared to astrocytoma or oligodendroglioma (Fig. 6B), which was confirmed in an independent cohort (Supplementary Fig. S5B). Also, AngioMatrix expression increased with grade (Fig. 6C). Differences in AngioMatrix expression were observed between the GBM molecular subtypes [35], of which the highest expression in the mesenchymal subtype was the most significant (Fig. 6D). The recurrent correlation between AngioMatrix expression and glioma progression led us to test the potential use of the signature to stratify glioma patients and analyze their survival. High AngioMatrix expression significantly correlated with poor prognosis for all glioma patients (Supplementary Fig. S5C) and for subgroups of low-grade glioma: astrocytoma, oligodendroglioma, grade II, grade III or combined grade II and III glioma (Supplementary Fig. S5D-H). Finally, we analyzed GBM from two independent cohorts and found that high AngioMatrix expression significantly correlated with shortened patient survival (Fig. 6, E and F, and Supplementary Figure S5, I and J).

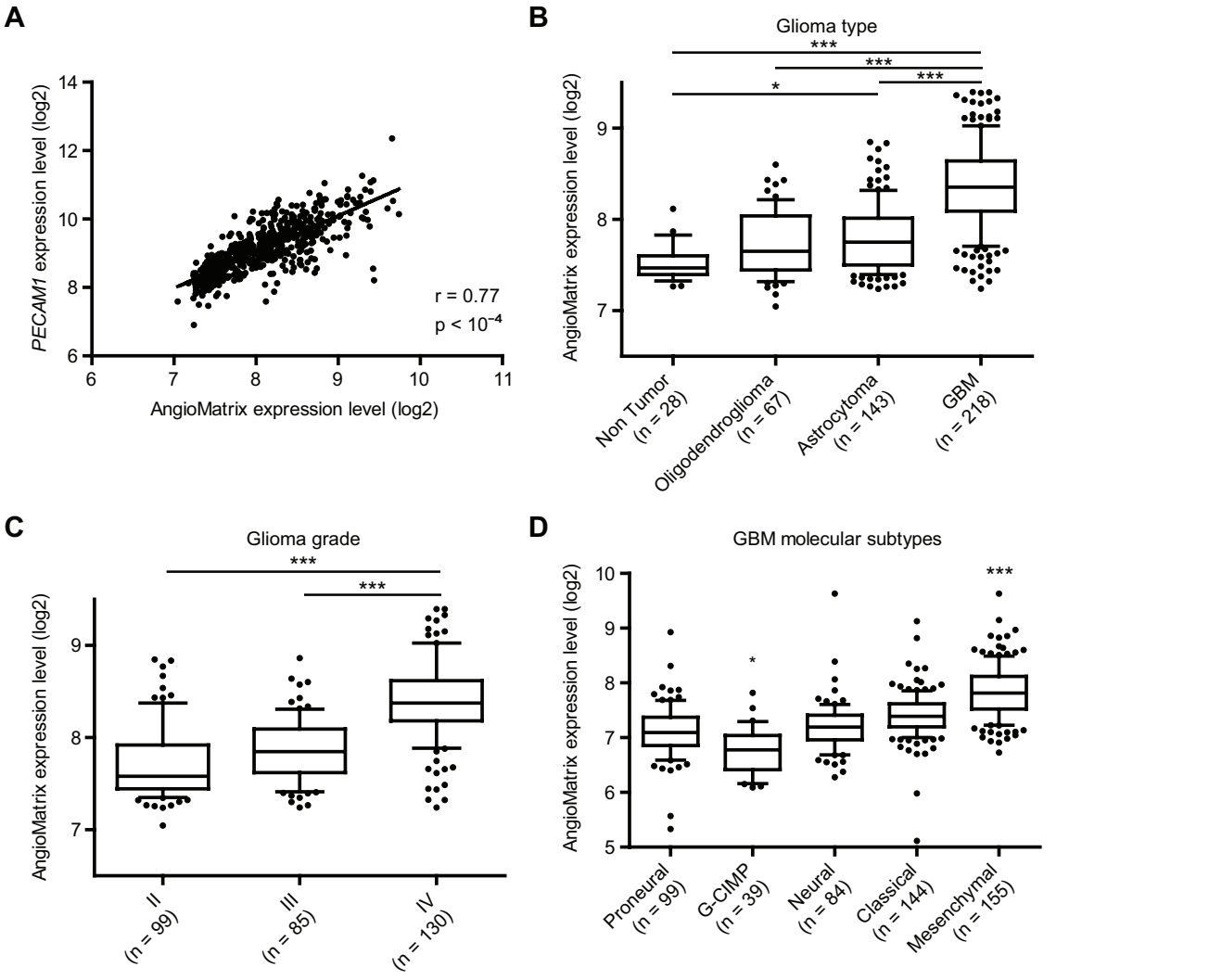

Figure 6: Correlation between AngioMatrix signature expression and EC marker, tumor progression and poor prognosis in human glioma. **(A)** correlation between AngioMatrix expression and *PECAM1* in glioma samples. The Pearson correlation coefficient (r) and the p-value are indicated. **(B)** comparison of AngioMatrix expression between non tumor brain samples and glioma histological subtypes. Note the higher levels of AngioMatrix expression in GBM compared to normal brain tissue, oligodendroglioma or astrocytoma. **(C-D)** analysis of AngioMatrix expression according to glioma grade (C) and the different GBM molecular subtypes (D). Note the significantly higher levels in grade IV glioma (C) and in the GBM mesenchymal subtype (D). In B-D, * and *** indicate p-values $< 5x10^{-2}$ and 10^{-3}, respectively.

(*Continued*)

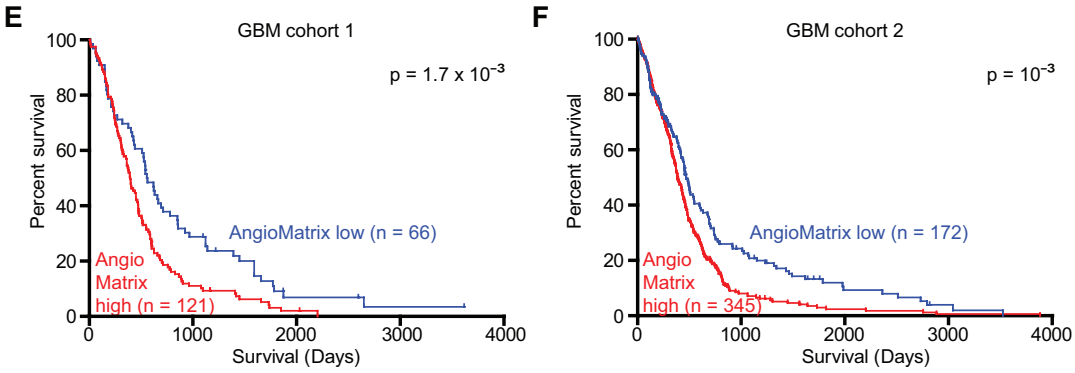

Figure 6: (E-F) Kaplan-Meier survival analysis of GBM patients. Patients were stratified according to the average expression of the AngioMatrix signature as AngioMatrix high or low using a cutoff value. In each cohort, high AngioMatrix expression significantly correlates with poor prognosis for patients. P-values indicate the significance of survival difference between the groups of individuals. In B-F, n indicates the number of samples per group.

DISCUSSION

We have used a strategy based on gene expression profiling to comprehensively describe the angiogenic switch in a prototypical murine cancer model [2, 4]. Our microarray analysis first revealed the up-regulation of cell type specific markers in the angiogenic islets, suggesting an expansion of stromal cells. This was confirmed at tissue level using specific markers for endothelial cells, pericytes and macrophages. Of note, no neutrophil marker was retrieved, although neutrophils have been functionally implicated in the RIP1-Tag2 angiogenic switch [7, 8]. Since we have extracted RNA from whole islets for gene expression profiling, we may have missed the low abundant neutrophils (0.4% of RIP1-Tag2 islet cells; ref. [7]). At the molecular level, we noted a recurrent overlap between the AngioSwitch signature and several cellular signaling pathways that have been functionally implicated in RIP1-Tag2 tumor progression, including the PDGF receptor β and its ligand PDGF-BB [36] or endoglin [37]. We also observed and confirmed up-regulation of several genes encoding canonical TGF-β signaling pathway members, suggesting that TGF-β signaling is activated during the RIP1-Tag2 angiogenic switch. This is in line with a previous report showing the up-regulation of *Tgfb1* and the presence of ALK5-positive cells, (expressing TGF-β receptor 1 and therefore susceptible of undergoing canonical TGF-β signaling in the presence of ligand) within RIP1-Tag2 angiogenic islets, and presumably representing stromal cells [21]. We found significant enrichment of fibroblast- and macrophage-specific TBRS, which suggested that these tumor-associated stromal cells may undergo signaling. Accordingly, we demonstrated their presence and that they undergo canonical TGF-β signaling as revealed by the nuclear localization of phosphorylated SMAD3 within these stromal cells in angiogenic but not in non angiogenic RIP1-Tag2 islets. Altogether, these observations strongly support the notion that the AngioSwitch signature is biologically and functionally meaningful, and that the activation of canonical TGF-β signaling within stromal cells may represent a key event driving this transition. Mechanistically it remains to be determined which specific signals trigger TGF-β signaling during the RIP1-Tag2 angiogenic switch and how specific AngioMatrix molecules are implicated. MMP-9 and MMP-2 represent candidate drivers of the transition since both are induced during the RIP1-Tag2 angiogenic switch and MMP9 in particular exerts a crucial role [6] and both MMPs are able to activate latent TGF-β [38]. Furthermore we uncovered that the RIP1-Tag2 angiogenic switch is associated with the up-regulation of genes encoding ECM and ECM-associated molecules. This is in line with our and others findings, as canonical TGF-β signaling regulates the production of ECM and regulators in the microenvironment of tissue under various physio-pathological conditions including cancer [39, 40]. Although beyond the current scope, it will be important to evaluate in the future whether blocking TGF-β signaling potentially impinges on the angiogenic switch affecting the expression of AngioMatrix molecules.

Using an elegant approach combining *in silico* and proteomic analysis, Naba and co-workers defined the matrisome, a comprehensive list of ECM and ECM-associated molecules [23, 24]. Using this resource we assessed the overlap with the AngioSwitch signature to define the AngioMatrix signature and validated the induction of expression for several AngioMatrix proteins during the angiogenic switch, including the ECM glycoproteins fibronectin, tenascin-C, sparc and periostin. Functionally, we demonstrated that *TNC* ablation impairs the RIP1-Tag2 angiogenic switch, in line with our macroscopical characterization of the two islet classes [25]. These data again support the notion that components of the AngioMatrix signature promote the RIP1-Tag2 angiogenic switch.

To evaluate the potential translational relevance of the AngioMatrix signature for cancer patients, we showed that AngioMatrix expression significantly correlated with EC markers in human CRC and glioma, supporting the notion that this signature also correlates with the angiogenesis status within human tumors. During CRC progression, AngioMatrix expression is increased at the adenoma-carcinoma transition, in partial agreement with previous studies showing that the angiogenic switch occurs early along the adenoma-carcinoma sequence [41, 42]. In glioma, AngioMatrix expression is significantly up-regulated in GBM compared to lower grade glioma. This may reflect vascular co-option in low-grade glioma in contrast to angiogenesis that is more important for GBM vascularization [20]. AngioMatrix expression varies according to primary CRC molecular subtypes [29, 34]. Although these studies have followed different approaches to define CRC subtypes, we found significantly higher levels of AngioMatrix expression in the stem-like [34] and the C4 [29] subtypes, the latter being also enriched in stem cell-like signatures [29]. We speculate that higher AngioMatrix expression in stem-like CRC reflects a potential role of some AngioMatrix molecules not only in angiogenesis but also in the regulation of cell fate within (cancer) stem cell niches. Moreover, tenascin-C and periostin are both expressed in the hair follicle stem cell niche in murine skin and are crucial for metastatic breast cancer stem cells colonizing the lung [43–45]. It will be interesting to determine if other AngioMatrix molecules represent normal and cancer stem cell niches components. We found lower AngioMatrix expression levels in the C1 and C3 subtypes, and higher level in the C4 subtype, which correlates with the respective enrichment of the GO sprouting angiogenesis category within these subtypes [29], reinforcing the notion that this signature correlates with angiogenesis in human CRC. Also, higher AngioMatrix expression levels are found in the GBM mesenchymal subtype, described as enriched in EC and angiogenesis markers [35]. Finally, the AngioMatrix signature allows to identify CRC, low-grade glioma and GBM patients with a poorer prognosis. It will be important to determine whether this can be extended to other tumor types and if specific AngioMatrix subsets may improve stratification of patients at higher risk of tumor relapse.

ECM molecules and regulators exert key functions during vascular remodeling in tumors and play instrumental roles in promoting tumor progression by multiple mechanisms as e.g. providing pro-angiogenic niches and favoring tumor cell survival and dissemination. Importantly, ECM molecules represent potential therapeutic targets as functional studies have underlined their importance in the process of blood vessel regrowth after anti-angiogenic therapy [12]. Whether AngioMatrix molecules are potentially relevant in tumor vessel regrowth is unknown and important to be addressed in the future. It is interesting to note that the ECM glycoproteins fibronectin, tenascin-C and periostin, that were found here among the most highly up-regulated genes during the angiogenic switch, have also been identified as crucial for metastatic colonization in other cancer models *in vivo* [44–46]. Further studies are warranted to assess if additional AngioMatrix molecules also contribute to the generation of metastatic niches. Finally, AngioMatrix expression is significantly higher in hepatic metastases, the most common metastatic site for CRC. It will be interesting to determine if some AngioMatrix molecules represent metastasis-specific components as these could represent novel opportunities to develop targeted therapies.

In summary, we have shown that the angiogenic switch, a rate-limiting and early step during PNET progression in a murine model, is associated with a specific transcriptome, which allowed us to define the AngioMatrix signature and show that it correlates with tumor progression and poor prognosis for CRC, low-grade glioma and GBM patients. Our study paves the way for the identification of novel molecular and cellular mechanisms that are key to tumor angiogenesis and might unravel novel opportunities for diagnosis and therapeutic targeting.

METHODS

A detailed description is available from the Supplementary methods.

RIP1-Tag2 mice

Experiments involving RIP1-Tag2 animals [3] were done at 8 weeks and in accordance with the guidelines from INSERM (National Institute for Health and Medical Research), as described [25].

Genome-wide gene expression profiling and data mining

Pools of angiogenic and non angiogenic pancreatic islets were sorted as described [25] and RNA was extracted for labeling and hybridization (Affymetrix arrays). Data are deposited in the Gene Expression Omnibus (NCBI, GSE51637). Significantly deregulated genes were selected using the BRB-ArrayTools software (NCI, USA). The matrisome [23, 24] was used to compare the overlap with the AngioSwitch signature and define the AngioMatrix signature. Enrichments of TBRS from specific stromal cell types [22], the matrisome and its divisions [23] in the profiling dataset of RIP1-Tag2

angiogenic and non angiogenic islets we generated (GSE51637) were analyzed using GSEA [47]. Correlations between AngioMatrix expression and various parameters were analyzed in independent cohorts of CRC [26–30] and glioma [31–33]. Molecular subtypes of CRC [29, 34] and GBM [35] were previously defined. Kaplan-Meier survival analysis was performed by analyzing transcriptomic datasets from independent cohorts of human CRC [28, 29], glioma and subtypes [31] and glioblastoma [31, 33].

Statistical analysis and graphical representation

Analysis was performed using GraphPad Prism (GraphPad Software, Inc. USA), Epi Info (Centers for Disease Control and Prevention, USA), BRB-ArrayTools (NCI, USA) and GSEA [47]. Histograms represent data expressed as mean +/- SEM. When comparing two groups, data were analyzed using two-tailed Mann Whitney U or unpaired Student t tests. When comparing three groups or more, data were analyzed using one-way ANOVA (with Tukey's post-test) or Kruskal-Wallis (with Dunn's post-test) tests. In box plots, whiskers represent the 10^{th} and 90^{th} centiles, and data points outside this interval are represented. The false discovery rate (FDR) q-value and the log-rank test were used to assess the significance of GSEA enrichments and of survival differences, respectively. P-values and q-values < 0.05 were considered as significant.

AUTHORS' CONTRIBUTIONS

Conception and design: G. Orend, T. Hussenet

Development of methodology: B. Langlois, F. Saupe, T. Rupp, C. Arnold, M. van der Heyden, G. Orend, T. Hussenet

Acquisition of data: B. Langlois, F. Saupe, T. Rupp, C. Arnold, M. van der Heyden, T. Hussenet

Analysis and interpretation of data: B. Langlois, F. Saupe, G. Orend, T. Hussenet

Writing, review, and/or revision of the manuscript: B. Langlois, F. Saupe, G. Orend, T. Hussenet

Administrative, technical, or material support: B. Langlois, F. Saupe, T. Rupp, C. Arnold, M. van der Heyden, G. Orend, T. Hussenet

Study supervision: G. Orend, T. Hussenet

ACKNOWLEDGEMENTS

We are grateful to Gerhard Christofori, Joerg Huelsken, Lydia Sorokin and Patricia Simon-Assman and the MN3T team for sharing material and comments on the manuscript. We acknowledge animal caretakers and the IGBMC Microarray Facility (Christelle Thibault).

GRANT SUPPORT

This work was supported by grants to G.O. from the Institut National du Cancer (INCa), Association pour la Recherche sur le Cancer (ARC), Oncosuisse, the Agence Nationale de la Recherche (ANR) and Ligue Régionale Grand-Est Contre le Cancer. F.S. was supported by the Fondation des Treilles.

Conflicts of interest

The authors disclose no potential conflicts of interest.

REFERENCES

1. Potente M, Gerhardt H, Carmeliet P. Basic and therapeutic aspects of angiogenesis. Cell. 2011; 146: 873–887.
2. Hanahan D, Folkman J. Patterns and emerging mechanisms of the angiogenic switch during tumorigenesis. Cell. 1996; 86:353–364.
3. Hanahan D. Heritable formation of pancreatic beta-cell tumours in transgenic mice expressing recombinant insulin/simian virus 40 oncogenes. Nature. 1985; 315:115–122.
4. Folkman J, Watson K, Ingber D, Hanahan D. Induction of angiogenesis during the transition from hyperplasia to neoplasia. Nature. 1989; 339:58–61.
5. Inoue M, Hager JH, Ferrara N, Gerber H-P, Hanahan D. VEGF-A has a critical, nonredundant role in angiogenic switching and pancreatic beta cell carcinogenesis. Cancer Cell. 2002; 1:193–202.
6. Bergers G, Brekken R, McMahon G, Vu TH, Itoh T, Tamaki K, Tanzawa K, Thorpe P, Itohara S, Werb Z, Hanahan D. Matrix metalloproteinase-9 triggers the angiogenic switch during carcinogenesis. Nat Cell Biol. 2000; 2:737–744.
7. Nozawa H, Chiu C, Hanahan D. Infiltrating neutrophils mediate the initial angiogenic switch in a mouse model of multistage carcinogenesis. Proc Natl Acad Sci U S A. 2006; 103:12493–12498.
8. Shojaei F, Singh M, Thompson JD, Ferrara N. Role of Bv8 in neutrophil-dependent angiogenesis in a transgenic model of cancer progression. Proc Natl Acad Sci U S A. 2008; 105:2640–2645.
9. Parangi S, O'Reilly M, Christofori G, Holmgren L, Grosfeld J, Folkman J, Hanahan D. Antiangiogenic therapy of transgenic mice impairs de novo tumor growth. Proc Natl Acad Sci U S A. 1996; 93:2002–2007.
10. Bergers G, Javaherian K, Lo KM, Folkman J, Hanahan D. Effects of angiogenesis inhibitors on multistage carcinogenesis in mice. Science. 1999; 284:808–812.

11. Bergers G, Song S, Meyer-Morse N, Bergsland E, Hanahan D. Benefits of targeting both pericytes and endothelial cells in the tumor vasculature with kinase inhibitors. J Clin Invest. 2003; 111:1287–1295.
12. Mancuso MR, Davis R, Norberg SM, O'Brien S, Sennino B, Nakahara T, Yao VJ, Inai T, Brooks P, Freimark B, Shalinsky DR, Hu-Lowe DD, McDonald DM. Rapid vascular regrowth in tumors after reversal of VEGF inhibition. J Clin Invest. 2006; 116:2610–2621.
13. Xie L, Duncan MB, Pahler J, Sugimoto H, Martino M, Lively J, Mundel T, Soubasakos M, Rubin K, Takeda T, Inoue M, Lawler J, Hynes RO, Hanahan D, Kalluri R. Counterbalancing angiogenic regulatory factors control the rate of cancer progression and survival in a stage-specific manner. Proc Natl Acad Sci U S A. 2011; 108:9939–9944.
14. You W-K, Sennino B, Williamson CW, Falcón B, Hashizume H, Yao L-C, Aftab DT, McDonald DM. VEGF and c-Met blockade amplify angiogenesis inhibition in pancreatic islet cancer. Cancer Res. 2011; 71:4758–4768.
15. Sennino B, Ishiguro-Oonuma T, Wei Y, Naylor RM, Williamson CW, Bhagwandin V, Tabruyn SP, You W-K, Chapman HA, Christensen JG, Aftab DT, McDonald DM. Suppression of tumor invasion and metastasis by concurrent inhibition of c-Met and VEGF signaling in pancreatic neuroendocrine tumors. Cancer Discov. 2012; 2:270–287.
16. Jain RK, Duda DG, Clark JW, Loeffler JS. Lessons from phase III clinical trials on anti-VEGF therapy for cancer. Nat Clin Pract Oncol. 2006; 3:24–40.
17. Bergers G, Hanahan D. Modes of resistance to anti-angiogenic therapy. Nat Rev Cancer. 2008; 8:592–603.
18. Casanovas O, Hicklin DJ, Bergers G, Hanahan D. Drug resistance by evasion of antiangiogenic targeting of VEGF signaling in late-stage pancreatic islet tumors. Cancer Cell. 2005; 8:299–309.
19. Pàez-Ribes M, Allen E, Hudock J, Takeda T, Okuyama H, Viñals F, Inoue M, Bergers G, Hanahan D, Casanovas O. Antiangiogenic therapy elicits malignant progression of tumors to increased local invasion and distant metastasis. Cancer Cell. 2009; 15:220–231.
20. Bergers G, Benjamin LE. Tumorigenesis and the angiogenic switch. Nat Rev Cancer. 2003; 3:401–410.
21. Cunha SI, Pardali E, Thorikay M, Anderberg C, Hawinkels L, Goumans M-J, Seehra J, Heldin C-H, ten Dijke P, Pietras K. Genetic and pharmacological targeting of activin receptor-like kinase 1 impairs tumor growth and angiogenesis. J Exp Med. 2010; 207:85–100.
22. Calon A, Espinet E, Palomo-Ponce S, Tauriello DVF, Iglesias M, Céspedes MV, Sevillano M, Nadal C, Jung P, Zhang XH-F, Byrom D, Riera A, Rossell D, Mangues R, Massagué J, Sancho E, Batlle E. Dependency of colorectal cancer on a TGF-β-driven program in stromal cells for metastasis initiation. Cancer Cell. 2012; 22: 571–584.
23. Naba A, Clauser KR, Hoersch S, Liu H, Carr SA, Hynes RO. The matrisome: in silico definition and in vivo characterization by proteomics of normal and tumor extracellular matrices. Mol Cell Proteomics. 2012; 11:M111.014647.
24. Hynes RO, Naba A. Overview of the matrisome–an inventory of extracellular matrix constituents and functions. Cold Spring Harb Perspect Biol. 2012; 4:a004903.
25. Saupe F, Schwenzer A, Jia Y, Gasser I, Spenlé C, Langlois B, Kammerer M, Lefebvre O, Hlushchuk R, Rupp T, Marko M, van der Heyden M, Cremel G, Arnold C, Klein A, Simon-Assmann P, Djonov V, Neuville-Méchine A, Esposito I, Slotta-Huspenina J, Janssen K-P, de Wever O, Christofori G, Hussenet T, Orend G. Tenascin-C downregulates wnt inhibitor dickkopf-1, promoting tumorigenesis in a neuroendocrine tumor model. Cell Rep. 2013; 5:482–492.
26. Sheffer M, Bacolod MD, Zuk O, Giardina SF, Pincas H, Barany F, Paty PB, Gerald WL, Notterman DA, Domany E. Association of survival and disease progression with chromosomal instability: a genomic exploration of colorectal cancer. Proc Natl Acad Sci U S A. 2009; 106:7131–7136.
27. Galamb O, Wichmann B, Sipos F, Spisák S, Krenács T, Tóth K, Leiszter K, Kalmár A, Tulassay Z, Molnár B. Dysplasia-carcinoma transition specific transcripts in colonic biopsy samples. PloS One. 2012; 7:e48547.
28. Jorissen RN, Gibbs P, Christie M, Prakash S, Lipton L, Desai J, Kerr D, Aaltonen LA, Arango D, Kruhøffer M, Orntoft TF, Andersen CL, Gruidl M, Kamath VP, Eschrich S, Yeatman TJ, Sieber OM. Metastasis-Associated Gene Expression Changes Predict Poor Outcomes in Patients with Dukes Stage B and C Colorectal Cancer. Clin Cancer Res Off J Am Assoc Cancer Res. 2009; 15:7642–7651.
29. Marisa L, de Reyniès A, Duval A, Selves J, Gaub MP, Vescovo L, Etienne-Grimaldi M-C, Schiappa R, Guenot D, Ayadi M, Kirzin S, Chazal M, Fléjou J-F, et al. Gene expression classification of colon cancer into molecular subtypes: characterization, validation, and prognostic value. PLoS Med. 2013; 10:e1001453.
30. Watanabe T, Kobunai T, Yamamoto Y, Matsuda K, Ishihara S, Nozawa K, Iinuma H, Konishi T, Horie H, Ikeuchi H, Eshima K, Muto T. Gene expression signature and response to the use of leucovorin, fluorouracil and oxaliplatin in colorectal cancer patients. Clin Transl Oncol Off Publ Fed Span Oncol Soc Natl Cancer Inst Mex. 2011; 13:419–425.
31. Madhavan S, Zenklusen J-C, Kotliarov Y, Sahni H, Fine HA, Buetow K. Rembrandt: helping personalized medicine become a reality through integrative translational research. Mol Cancer Res. 2009; 7:157–167.
32. Bredel M, Bredel C, Juric D, Harsh GR, Vogel H, Recht LD, Sikic BI. Functional network analysis reveals

extended gliomagenesis pathway maps and three novel MYC-interacting genes in human gliomas. Cancer Res. 2005; 65:8679–8689.

33. Cancer Genome Atlas Research Network: Comprehensive genomic characterization defines human glioblastoma genes and core pathways. Nature. 2008; 455:1061–1068.
34. Sadanandam A, Lyssiotis CA, Homicsko K, Collisson EA, Gibb WJ, Wullschleger S, Ostos LCG, Lannon WA, Grotzinger C, Del Rio M, Lhermitte B, Olshen AB, Wiedenmann B, et al. A colorectal cancer classification system that associates cellular phenotype and responses to therapy. Nat Med. 2013; 19:619–625.
35. Brennan CW, Verhaak RGW, McKenna A, Campos B, Noushmehr H, Salama SR, Zheng S, Chakravarty D, Sanborn JZ, Berman SH, Beroukhim R, Bernard B, Wu C-J, et al. The somatic genomic landscape of glioblastoma. Cell. 2013; 155:462–477.
36. Joyce JA, Laakkonen P, Bernasconi M, Bergers G, Ruoslahti E, Hanahan D. Stage-specific vascular markers revealed by phage display in a mouse model of pancreatic islet tumorigenesis. Cancer Cell. 2003; 4: 393–403.
37. Anderberg C, Cunha SI, Zhai Z, Cortez E, Pardali E, Johnson JR, Franco M, Páez-Ribes M, Cordiner R, Fuxe J, Johansson BR, Goumans M-J, Casanovas, et al. Deficiency for endoglin in tumor vasculature weakens the endothelial barrier to metastatic dissemination. J Exp Med. 2013; 210:563–579.
38. Yu Q, Stamenkovic I. Cell surface-localized matrix metalloproteinase-9 proteolytically activates TGF-beta and promotes tumor invasion and angiogenesis. Genes Dev. 2000; 14:163–176.
39. Roberts AB, Heine UI, Flanders KC, Sporn MB. Transforming growth factor-beta. Major role in regulation of extracellular matrix. Ann N Y Acad Sci. 1990; 580: 225–232.
40. Verrecchia F, Mauviel A. Transforming growth factor-beta signaling through the Smad pathway: role in extracellular matrix gene expression and regulation. J Invest Dermatol. 2002; 118:211–215.
41. Takahashi Y, Ellis LM, Mai M. The angiogenic switch of human colon cancer occurs simultaneous to initiation of invasion. Oncol Rep. 2003; 10:9–13.
42. Staton CA, Chetwood ASA, Cameron IC, Cross SS, Brown NJ, Reed MWR. The angiogenic switch occurs at the adenoma stage of the adenoma carcinoma sequence in colorectal cancer. Gut. 2007; 56:1426–1432.
43. Tucker RP, Ferralli J, Schittny JC, Chiquet-Ehrismann R. Tenascin-C and tenascin-W in whisker follicle stem cell niches: possible roles in regulating stem cell proliferation and migration. J Cell Sci. 2013; 126: 5111–5115.
44. Oskarsson T, Acharyya S, Zhang XH-F, Vanharanta S, Tavazoie SF, Morris PG, Downey RJ, Manova-Todorova K, Brogi E, Massagué J. Breast cancer cells produce tenascin C as a metastatic niche component to colonize the lungs. Nat Med. 2011; 17:867–874.
45. Malanchi I, Santamaria-Martínez A, Susanto E, Peng H, Lehr H-A, Delaloye J-F, Huelsken J. Interactions between cancer stem cells and their niche govern metastatic colonization. Nature. 2012; 481:85–89.
46. Kaplan RN, Riba RD, Zacharoulis S, Bramley AH, Vincent L, Costa C, MacDonald DD, Jin DK, Shido K, Kerns SA, Zhu Z, Hicklin D, Wu Y, et al. VEGFR1-positive haematopoietic bone marrow progenitors initiate the pre-metastatic niche. Nature. 2005; 438:820–827.
47. Subramanian A, Tamayo P, Mootha VK, Mukherjee S, Ebert BL, Gillette MA, Paulovich A, Pomeroy SL, Golub TR, Lander ES, Mesirov JP. Gene set enrichment analysis: a knowledge-based approach for interpreting genome-wide expression profiles. Proc Natl Acad Sci U S A. 2005; 102:15545–15550.

SUPPLEMENTARY METHODS, FIGURES AND TABLE

RIP1-Tag2 mice

C57BL/6 RIP1-Tag2 mice, obtained from G. Christofori (Basel University, Switzerland), were bred and housed according to standard protocols and were given food and water *ad libidum*. Genotyping was performed by PCR on DNA extracted from mouse tail. The presence of the RIP1-Tag2 transgene was identified using primers "Tag1": 5′-GGA CAA ACC ACA ACT AGA ATG CAG-3′ and "Tag2": 5′-CAG AGC AGA ATT GTG GAG TGG-3′. TNC-deficient mice [1] were backcrossed for ten generations into the C57BL/6 mouse strain. These mice were bred with wild-type TNC expressing (TNC+/+) mice or mice lacking (TNC-/-). The presence or deletion of TNC was determined using primers "TNCKO_TNCup": 5′-CTG CCA GGC ATC TTT CTA GC-3′, "TNCKO_TNCdown": 5′-TTC TGC AGG TTG GAG GCA AC-3′ and "TNCKO_TNCNeoPA": 5′-CTG CTC TTT ACT GAA GGC TC-3′.

Isolation of pancreatic islets

Langerhans islets were isolated from 8 (7.9–8.4) week-old RIP1-Tag2 mice using Liberase (RI or TL, Roche), dissolved in DMEM (1 g/l glucose) and diluted to 0.82–1.0 Wünsch units/ml. Mice were sacrificed by cervical dislocation and pancreata were perfused via the bile duct with 2 ml Liberase solution, removed and digested at 37°C for 17–24 min. Digestion was stopped by addition of DMEM/15% FCS and strong shaking. The digested tissue was washed with DMEM, filtered through a mesh (with 380 µm pores), mixed with 10 ml Histopaque 1077 (Sigma) and covered with 10 ml of DMEM to create a gradient. Islets were separated by centrifugation (30 minutes, 1500 g at room temperature), recovered from the gradient interphase, washed with DMEM and transferred into islet culture medium (RPMI 1640 containing 11.1 mM glucose, 15% FCS, 1% penicillin/streptomycin, 7.5% NaHCO3, 66 µM β-mercaptoethanol). Intact islets were observed under a stereomicroscope (Leica), classified into non-angiogenic (completely white appearance) or angiogenic (few reddish spots up to completely reddish) and, were hand-picked and isolated. For each mouse, non-angiogenic and angiogenic islet pools were collected separately in sterile microcentrifuge tubes. Samples were shortly centrifuged, medium removed, washed with PBS, snap frozen in liquid nitrogen and kept at -80°C.

Gene expression profiling of isolated RIP1-Tag2 islets

Pools of non-angiogenic and of angiogenic islets isolated from 8 week-old RIP1-Tag2 mice were prepared and total RNA was extracted (NucleoSpin RNA XS kit, Macherey-Nagel, Düren, Germany). Isolated islets from 1 to 4 mice were pooled to obtain 63 to 211 non-angiogenic islets or 23 to 93 angiogenic islets for each sample profiled on a microarray. Quality of extracted RNA was assessed using the Agilent 2100 Bioanalyzer (RNA 6000 Nano Kit). All microarray experiments were performed by the IGBMC Microarray facility (Illkirch, France) following manufacturer (Affymetrix) instructions. Briefly, for each sample, 200 ng RNA was used to prepare labeled cRNA probes hybridized to Mo-Gene 1.0 ST arrays. For each experiment, three biological replicates (3 pools of non-angiogenic islets and 3 pools of angiogenic islets) were profiled. The experiment (from islets isolation to RNA profiling using microarrays) was repeated twice independently, giving rise to 6 microarrays for each condition (NA or A) in total, that were normalized and analyzed together. Raw data were normalized by the RMA method using the Expression Console software (Affymetrix, build 1.2.1.20). Data are deposited in the NCBI Gene Expression Omnibus repository (GSE51637). The BRB-ArrayTools software (NCI, USA) was used to select significantly deregulated genes (ratio angiogenic/non-angiogenic > 1.4 - fold, p-value < 0.05). The Molecular Signature database [2] was used to analyze the Gene Ontologies significantly enriched in the AngioSwitch signature. The matrisome [3,4], a list of genes known and inferred to encode ECM molecules was used to compute overlaps with the AngioSwitch signature, in order to generate the AngioMatrix signature (110 murine genes induced during the RIP1-Tag2 angiogenic switch and belonging to the matrisome division). GSEA [2,5] (version 2.0.13) was used to analyze enrichment of the matrisome and its divisions in the angiogenic versus non-angiogenic islets microarray dataset we generated. Mapping of TGF- β signaling associated genes in the AngioSwitch signature was performed using a custom-built map in GenMAPP 2 [6].

RT-qPCR analysis

Expression validation of genes found deregulated from the microarray analysis were done on 3 islets pools that were used for the microarray profiling together with 3 islets pools that were independently prepared, comparing in total 6 pools of non-angiogenic islets to 6 pools of angiogenic islets. Reverse Transcription reactions were performed on 200 ng of RNA using MultiScribe reverse transcriptase (Applied Biosystems) and following the manufacturer's instructions. Primer sequences (Table S1) were designed using Roche Probefinder (v2.45 or later). Primer pairs were initially tested and validated for specificity and efficiency using cDNA dilutions prepared from RIP1-Tag2 tumor derived RNA. Quantitative PCR were performed using a 7500 Real Time PCR System (Applied Biosystems) using SYBR green reagent (Applied Biosystems) and results analyzed using the $2^{\Delta\Delta Ct}$ method [7]. The *Rpl19* gene was used as reference gene as it was found to be the gene with the most stable expression (compared to the other reference genes tested, *Hmbs* and *Tbp*) in RIP1-Tag2 pools of angiogenic and non angiogenic islets. Relative expression levels ($2^{-\Delta\Delta ct}$) were calculated for each individual sample, and compared between non-angiogenic and angiogenic islet pools. All RT-qPCR experiments were performed twice independently and measures subsequently were averaged.

Tissue analysis

Pancreata were fixed for 2h at room temperature in 4% paraformaldehyde in PBS 1X, immersed in 20% sucrose for 12h at 4°C and embedded in Tissue-Tek OCT (Sakura Fine Tek). Alternatively, pancreata were fixed for 2h at 4°C in 4% paraformaldehyde in PBS 1X, dehydrated and embedded in paraffin. Tissue was cut and sections were routinely stained with hematoxylin and eosin (H&E), or used for immuno-staining analysis. Quantification of non-angiogenic and angiogenic islets was performed using a histological analysis of H&E stained tissue sections from paraffin embedded pancreata, comparing tissue from 5 TNC+/+ and 8 RIP1-Tag2 TNC-/- mice. Islets were considered as angiogenic when their biggest diameter was above 350 µm. This cutoff was chosen as it was enabling to correctly classify all angiogenic islets and with a minimal number of false positive (non angiogenic islets misclassified as angiogenic; < 2%) from a setup analysis comparing a previously described set of criteria [8] to the measure of islet biggest diameter in a series of tissue sections from five 8-week old RIP1-Tag2 mice. For immunostainings, primary antibodies used were: rat monoclonal anti-CD31 (BD Pharmingen 550274, 1/50), rabbit monoclonal anti-vimentin (Epitomics 2707-1, 1/500), rabbit polyclonal anti-NG2 (Millipore AB5320, 1/200), rat monoclonal anti F4/80 (AbD serotec MCA497G, 1/200), Cy3-conjugated monoclonal anti-α-Smooth Muscle Actin (αSMA, Sigma C6198, 1/400), rabbit polyclonal anti-phospho-S423/S425 SMAD3 (Rockland, 600-401-919, 1/100), rabbit polyclonal anti-Fibronectin (Sigma F3648, 1/200), goat polyclonal anti-SPARC (R&D systems, 1/200), rat monoclonal anti-Tenascin-C [9] (MTn 12, purified from hybridoma culture supernatants; 20µg/mL), rabbit polyclonal anti-Collagen IV 2a [10] (1/200), rabbit polyclonal anti-Laminin-α4 [11] (1/500), mouse monoclonal anti-Periostin [12] used for IHC (1/500). For immunofluorescent detection primary antibodies were incubated overnight at 4°C, Cy3-conjugated anti-αSMA and secondary antibodies (Interchim Dylight488-anti-rabbit, Cy3-anti-rat, Cy3-anti-goat, Cy5-anti-rabbit 1/2000) were incubated for 1h at room temperature and cell nuclei were stained with DAPI. Immunohistochemistry for detection of periostin was performed on paraffin-embedded sections using Vectastain developing system (Vector Laboratories) followed by tissue staining with hematoxylin. For analysis of nuclear localization of phosphorylated SMAD3, Z-series acquisitions (seven Z-plans with a step of 0.34µm) were performed with an Axio Imager.Z2 microscope (Zeiss) equipped with 40x objective and an ApoTome module. Pictures presented correspond to one Z-section with nuclear focus in αSMA or F4/80 positive cells.

Analysis of AngioMatrix signature expression in publicly-available gene expression datasets of human samples, stratification of patients and survival analysis

The murine AngioMatrix signature was first converted to human homologs using the Homologene database (release 67; NCBI, USA). AngioMatrix expression level was calculated by averaging the expression level of the 110 genes forming the signature in a given sample.

To analyze AngioMatrix expression along CRC progression a first dataset comprising colorectal adenoma, primary CRC of different Duke stage, liver and lung metastases, and corresponding normal tissue samples was used [13]. In addition, independent datasets comprising normal, adenoma and primary CRC [14], and metastatic *versus* non metastatic primary CRC [15] were also analyzed. Correlation between AngioMatrix expression levels and *PECAM1* or *CDH5* expression was determined in normal intestinal mucosa, adenoma and primary CRC samples [13]. The primary CRC cohort 1 [16] was used to analyze AngioMatrix expression levels in the five

different CRC molecular subtypes identified and defined by Sadanandam et al. [17]. The primary CRC cohort 2 [18] was used to analyze AngioMatrix expression levels in the six different CRC molecular subtypes identified and defined by these authors [18].

Correlations between AngioMatrix expression level and *PECAM1* or *CDH5* expression, and AngioMatrix expression levels in different glioma subtypes were analyzed in the glioma cohort 1 [19]. In addition, AngioMatrix expression level in different glioma histologic types was determined in an independent cohort [20]. Analysis of AngioMatrix expression level in the different GBM molecular subtypes [21] was performed using the GBM cohort 2 [22].

Kaplan-Meier analysis of cancer patient survival was performed as previously described [23], using Epi Info (version 3.5.4; Centers for Disease Control and Prevention, USA) and GraphPad (GraphPad Software, Inc. USA) to analyze genome-wide gene expression datasets from human colorectal cancers (cohort 1, ref. [16]; cohort 2, ref. [18]), all glioma or glioma subgroups [19] and glioblastoma (cohort 1, ref. [19]; cohort 2, ref. [22]). For each cohort, a cutoff was used to assign a tumor/patient to the AngioMatrix high group if the average expression of the 110 genes defining the human AngioMatrix signature was above the cutoff, and conversely to the AngioMatrix low group if this value was below the cutoff. The cutoff values were either empirically determined as to provide the best possible stratification between AngioMatrix high and low groups for each cohort (Figure 5 and 6) or the median as a cutoff based on data distribution in the cohorts (Supplementary Figure 4 and 5). Note that both stratification methods gave similar results: in either case a poorer prognosis was observed for the AngioMatrix high patient group. The log-rank test was used to assess the significance of survival differences between patient groups.

REFERENCES

1. Forsberg E, Hirsch E, Fröhlich L, Meyer M, Ekblom P, Aszodi A, Werner S, Fässler R. Skin wounds and severed nerves heal normally in mice lacking tenascin-C. Proc Natl Acad Sci U S A. 1996; 93:6594–6599.
2. Subramanian A, Tamayo P, Mootha VK, Mukherjee S, Ebert BL, Gillette MA, Paulovich A, Pomeroy SL, Golub TR, Lander ES, Mesirov JP. Gene set enrichment analysis: a knowledge-based approach for interpreting genome-wide expression profiles. Proc Natl Acad Sci U S A. 2005; 102:15545–15550.
3. Hynes RO,, Naba A. Overview of the matrisome—an inventory of extracellular matrix constituents and functions. Cold Spring Harb Perspect Biol. 2012; 4:a004903.
4. Naba A, Clauser KR, Hoersch S, Liu H, Carr SA, Hynes RO. The matrisome: in silico definition and in vivo characterization by proteomics of normal and tumor extracellular matrices. Mol Cell Proteomics. 2012; 11 M111.014647.
5. Mootha VK, Lindgren CM, Eriksson K-F, Subramanian A, Sihag S, Lehar J, Puigserver P, Carlsson E, Ridderstråle M, Laurila E, Houstis N, Daly MJ, Patterson N, et al. PGC-1alpha-responsive genes involved in oxidative phosphorylation are coordinately downregulated in human diabetes. Nat Genet. 2003; 34:267–273.
6. Dahlquist KD, Salomonis N, Vranizan K, Lawlor SC, Conklin BR. GenMAPP, a new tool for viewing and analyzing microarray data on biological pathways. Nat Genet. 2002; 31:19–20.
7. Pfaffl MW. A new mathematical model for relative quantification in real-time RT-PCR. Nucleic Acids Res. 2001; 29:e45.
8. Lopez T, Hanahan D. Elevated levels of IGF-1 receptor convey invasive and metastatic capability in a mouse model of pancreatic islet tumorigenesis. Cancer Cell. 2002; 1: 339–353.
9. Aufderheide E, Ekblom P. Tenascin during gut development: appearance in the mesenchyme, shift in molecular forms, and dependence on epithelial-mesenchymal interactions. J Cell Biol. 1988; 107:2341–2349.
10. De Arcangelis A, Neuville P, Boukamel R, Lefebvre O, Kedinger M, Simon-Assmann P. Inhibition of laminin alpha 1-chain expression leads to alteration of basement membrane assembly and cell differentiation. J Cell Biol. 1996; 133:417–430.
11. Sixt M, Engelhardt B, Pausch F, Hallmann R, Wendler O, Sorokin LM. Endothelial cell laminin isoforms, laminins 8 and 10, play decisive roles in T cell recruitment across the blood-brain barrier in experimental autoimmune encephalomyelitis. J Cell Biol. 2001; 153:933–946.
12. Malanchi I, Santamaria-Martínez A, Susanto E, Peng H, Lehr H-A, Delaloye J-F, Huelsken J. Interactions between cancer stem cells and their niche govern metastatic colonization. Nature. 2012; 481:85–89.
13. Sheffer M, Bacolod MD, Zuk O, Giardina SF, Pincas H, Barany F, Paty PB, Gerald WL, Notterman DA, Domany E. Association of survival and disease progression with chromosomal instability: a genomic exploration of colorectal cancer. Proc Natl Acad Sci U S A. 2009; 106:7131–7136.
14. Galamb O, Wichmann B, Sipos F, Spisák S, Krenács T, Tóth K, Leiszter K, Kalmár A, Tulassay Z, Molnár B. Dysplasia-carcinoma transition specific transcripts in colonic biopsy samples. PloS One. 2012; 7:e48547.
15. Watanabe T, Kobunai T, Yamamoto Y, Matsuda K, Ishihara S, Nozawa K, Iinuma H, Konishi T, Horie H,

Ikeuchi H, Eshima K, Muto T. Gene expression signature and response to the use of leucovorin, fluorouracil and oxaliplatin in colorectal cancer patients. Clin Transl Oncol Off Publ Fed Span Oncol Soc Natl Cancer Inst Mex. 2011; 13:419–425.

16. Jorissen RN, Gibbs P, Christie M, Prakash S, Lipton L, Desai J, Kerr D, Aaltonen LA, Arango D, Kruhøffer M, Orntoft TF, Andersen CL, Gruidl M et al. Metastasis-Associated Gene Expression Changes Predict Poor Outcomes in Patients with Dukes Stage B and C Colorectal Cancer. Clin Cancer Res Off J Am Assoc Cancer Res. 2009; 15:7642–7651.
17. Sadanandam A, Lyssiotis CA, Homicsko K, Collisson EA, Gibb WJ, Wullschleger S, Ostos LCG, Lannon WA, Grotzinger C, Del Rio M, Lhermitte B, Olshen AB, Wiedenmann B, et al. A colorectal cancer classification system that associates cellular phenotype and responses to therapy. Nat Med. 2013; 19:619–625.
18. Marisa L, de Reyniès A, Duval A, Selves J, Gaub MP, Vescovo L, Etienne-Grimaldi M-C, Schiappa R, Guenot D, Ayadi M, Kirzin S, Chazal M, Fléjou J-F, et al. Gene expression classification of colon cancer into molecular subtypes: characterization, validation, and prognostic value. PLoS Med. 2013; 10:e1001453.
19. Madhavan S, Zenklusen J-C, Kotliarov Y, Sahni H, Fine HA, Buetow K. Rembrandt: helping personalized medicine become a reality through integrative translational research. Mol Cancer Res. 2009; 7:157–167.
20. Bredel M, Bredel C, Juric D, Harsh GR, Vogel H, Recht LD, Sikic BI. Functional network analysis reveals extended gliomagenesis pathway maps and three novel MYC-interacting genes in human gliomas. Cancer Res. 2005; 65:8679–8689.
21. Brennan CW, Verhaak RGW, McKenna A, Campos B, Noushmehr H, Salama SR, Zheng S, Chakravarty D, Sanborn JZ, Berman SH, Beroukhim R, Bernard B, Wu C-J, et al. The somatic genomic landscape of glioblastoma. Cell. 2013; 155:462–477.
22. Cancer Genome Atlas Research Network: Comprehensive genomic characterization defines human glioblastoma genes and core pathways. Nature. 2008; 455:1061–1068.
23. Hussenet T, Dembélé D, Martinet N, Vignaud J-M, du Manoir S. An adult tissue-specific stem cell molecular phenotype is activated in epithelial cancer stem cells and correlated to patient outcome. Cell Cycle Georget Tex. 2010; 9:321–327.

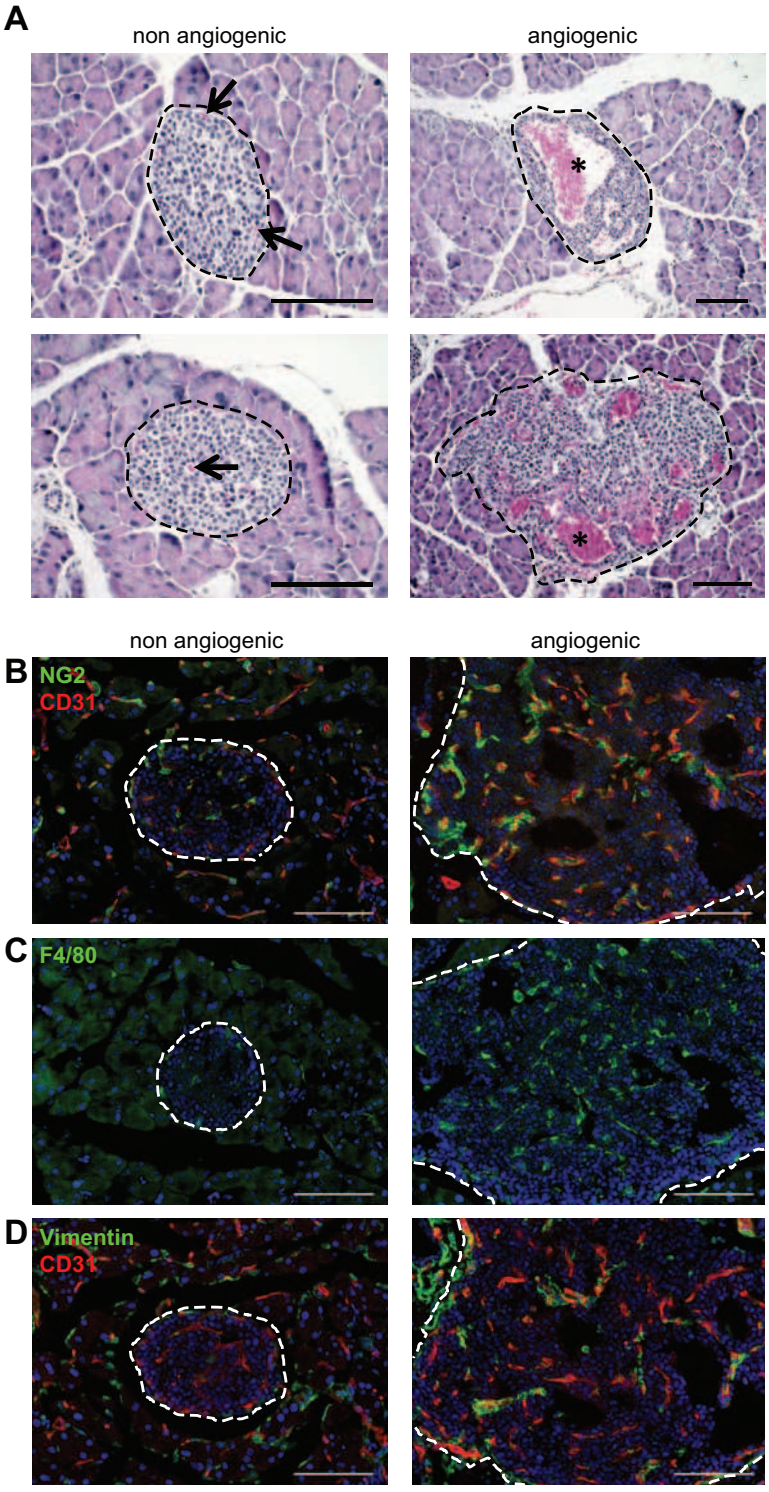

Supplementary Figure S1: Histological patterns of RIP1-Tag2 angiogenesis and increased expression of stromal cell markers during the angiogenic switch. **(A)** patterns of non-angiogenic (left) and angiogenic (right) islets in H&E stained pancreata tissue sections from 8 week old RIP1-Tag2 mice. Examples of normal capillaries in non angiogenic islets (arrows) and of hemorrhaging/blood lakes (asterisks) in angiogenic islets are highlighted. **(B-D)** immunofluorescence analysis of stromal cell markers in non angiogenic and angiogenic RIP1-Tag2 islets. Representative composite images obtained after CD31 (EC) and NG2 (pericyte) co-staining (D), F4/80 (macrophages) (E), and vimentin (perivascular smooth muscle cells) and CD31 (EC) (F) are shown. Nuclei were counterstained with Dapi (blue). RIP1-Tag2 pancreatic islets are encircled by dashed lines. Scale bars, 100 μm.

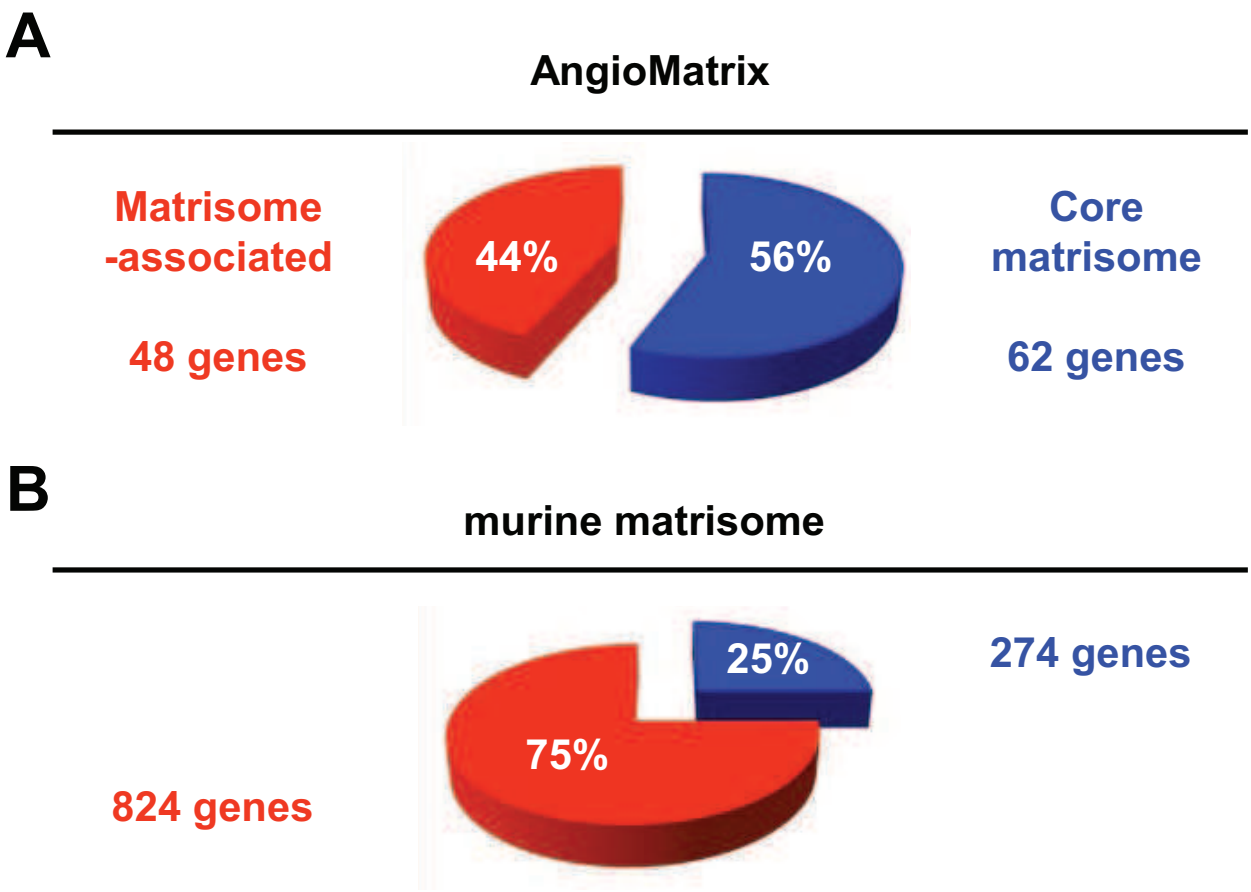

Supplementary Figure S2: Composition of the AngioMatrix signature according to divisions of the matrisome. **(A)** a majority of genes forming the AngioMatrix signature belong to the core matrisome division (56%, 62 genes), and a minority to the matrisome-associated division (44%, 48 genes). **(B)** the relative proportion of core matrisome (25%, 274 genes) and matrisome-associated (75%, 824 genes) components in the entire murine matrisome are shown for comparison.

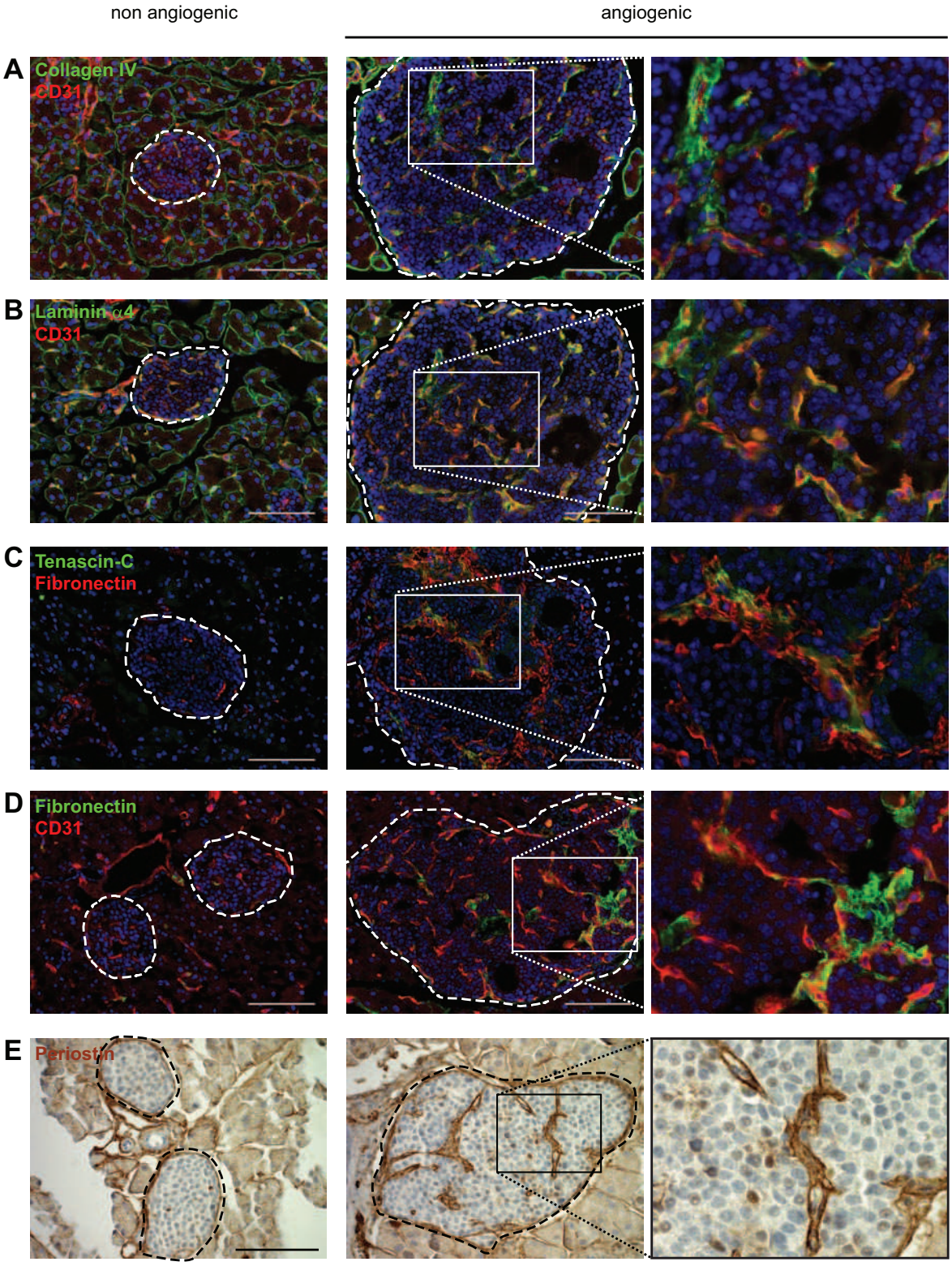

Supplementary Figure S3: Analysis of AngioMatrix protein expression patterns in the RIP1-Tag2 angiogenic switch. **(A-B)** Expression pattern of the vascular basement membrane molecules Collagen IV (A) and Laminin α4 (B) together with the EC marker CD31 in non angiogenic and angiogenic islets. **(C-E)** Expression pattern of the ECM glycoproteins fibronectin and tenascin-C (C), fibronectin and CD31 (D) and periostin (E) in non angiogenic and angiogenic islets. RIP1-Tag2 pancreatic islets are encircled by dashed lines, and the right column present higher magnification pictures of the corresponding boxed areas in the pictures from angiogenic islets (middle column). Scale bars, 100 μm.

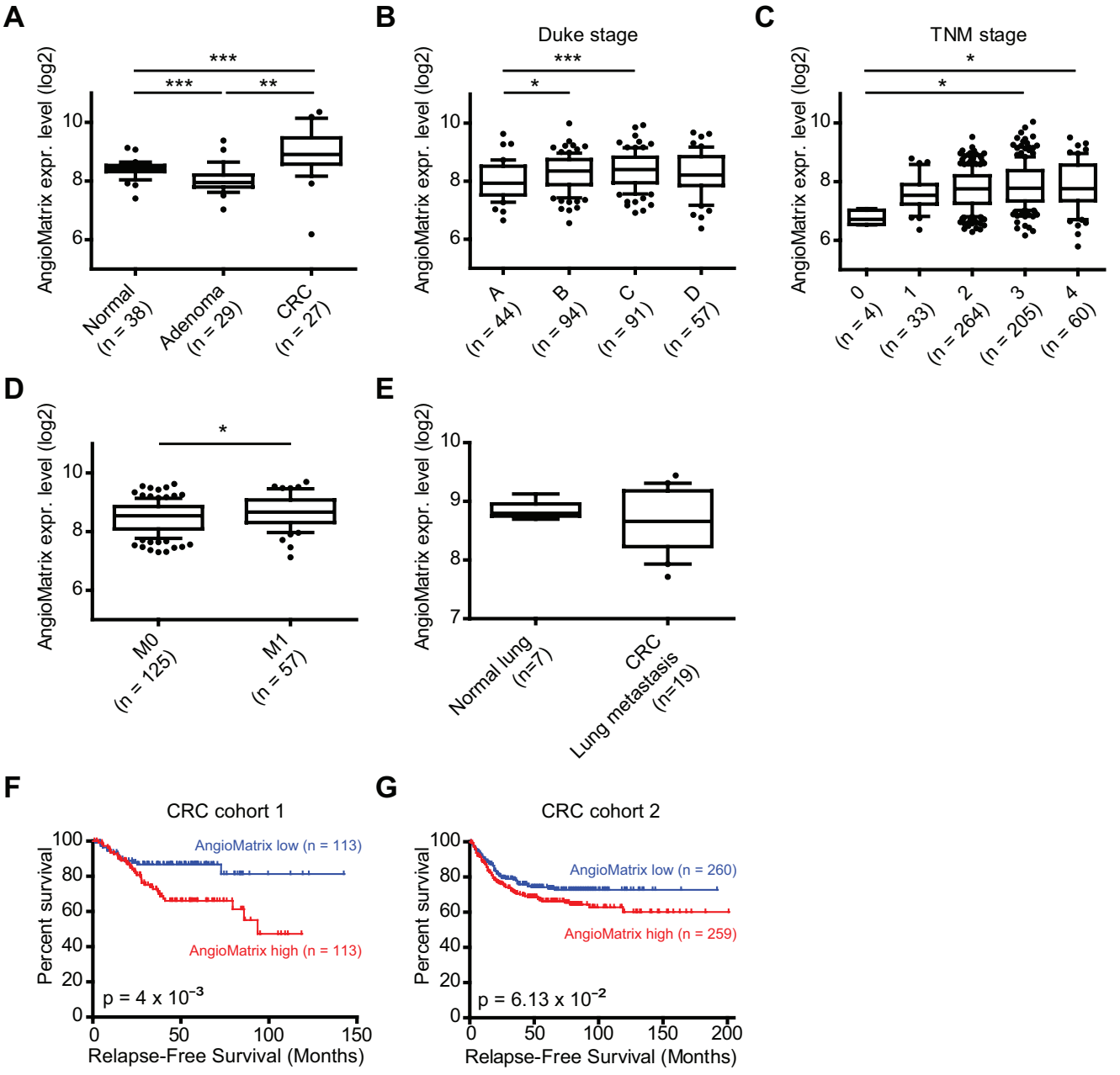

Supplementary Figure S4: Analysis of AngioMatrix expression levels along CRC progression and correlation to clinical parameters. **(A)** AngioMatrix expression level along primary CRC establishment: comparison of normal colonic samples, colorectal adenoma and primary CRC. AngioMatrix expression levels are decreased in adenoma compared to normal samples and increased in primary CRC. *** and ** denote p-values < 10^{-3} and 10^{-2}, respectively, Kruskal-Wallis test with Dunn's post test. **(B-C)** AngioMatrix expression level according to primary CRC stage (B: CRC cohort 1, Duke classification; C: CRC cohort 2, TNM classification). Note the significantly higher levels of AngioMatrix expression in Duke B or C compared to Duke A tumors (B) and in TNM stage 3 or 4 compared to stage 0 (CIS) tumors. *** and * denote p-values < 10^{-3} and 5.10^{-2}, respectively, Kruskal-Wallis test with Dunn's post test. **(D)** comparison of AngioMatrix expression level between non metastatic (M0) and metastatic (M1) primary CRC. A sligt increase of AngioMatrix expression level is observed for metastatic primary CRC. * indicates $p < 0.05$, unpaired Student t-test. **(E)** comparison of AngioMatrix expression level between normal lung and CRC lung metastasis samples. No significant difference is observed. **(F-G)** Kaplan-Meier survival analysis upon stratification of human CRC patients from two independent cohorts using the median expression of the AngioMatrix signature as a cut-off. A significant stratification is observed in the first cohort (F) and a trend in the second cohort (G). Numbers between brackets indicate the number of patients in each group. P-values were calculated with the log-rank test to assess the significance of the observed survival differences between the groups.

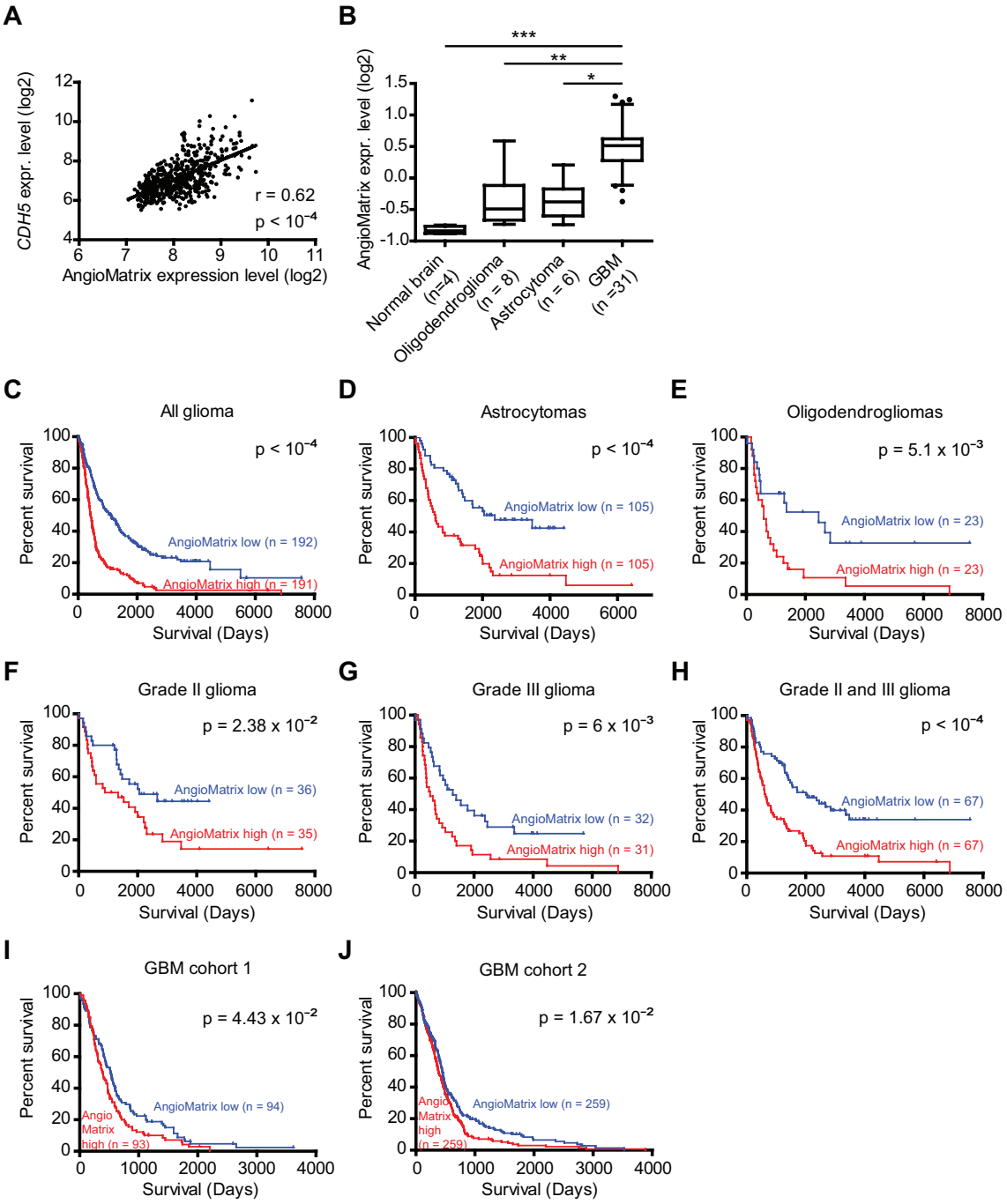

Supplementary Figure S5: Analysis of AngioMatrix expression levels in human glioma and correlation to clinical parameters. **(A)** correlation between AngioMatrix and *CDH5* (encoding vascular endothelial-cadherin) expression levels in glioma. The value of the pearson correlation coefficient (r) and the p-value are indicated. **(B)** AngioMatrix expression level according to glioma histological subtype. Note the significantly higher levels of AngioMatrix expression in GBM compared to any other type. ***, ** and * denote p-values < 10^{-3}, 10^{-2} and 5.10^{-2}, respectively, Kruskal-Wallis test with Dunn's post test. **(C-J)** Kaplan-Meier survival analysis upon stratification of human glioma patients from two independent cohorts using the median expression of the AngioMatrix signature as a cut-off. The glioma cohort 1, composed of different glioma histological types and both lower and higher grade glioma was exhaustively analyzed: glioma patients were stratified by analyzing all glioma samples together (C), or according to subtypes (D-I), defined at histological level (D, E and I) or according to grade for low grade glioma (F-H). In each case, high AngioMatrix expression significantly correlates with poor prognosis for glioma patients. The cohort 2 is composed of high grade glioma (GBM) only (J). Note that for GBM, a significant stratification is observed in both the first (I) and the second (J) cohorts. Numbers between brackets indicate the number of patients in each group. P-values were calculated with the log-rank test to assess the significance of the observed survival differences between the groups.

Supplementary Table S1. Sequences of primer pairs used for qPCR analyses.

Gene	Forward primer (5′ – 3′)	Reverse primer (5′ – 3′)
Ccl2	ggctggagagctacaagagg	ctcttgagcttggtgacaaaaa
Col8a1	gccagccaagcctaaatgt	tgatgaacagtattcccagca
Dlk1	cgggaaattctgcgaaatag	tgtgcaggagcattcgtact
Fn1	gatgccgatcagaagtttgg	ggttgtgcagatctcctcgt
Frzb	caccgtcaatctttataccacct	tcagctatagagccttctaccaaga
Lox	tactcctgggagtggcaca	gacgtgtcctccagacagaag
Ogn	aggaattaaagcaaacacattcaa	tttctggtaaattaggaggcaca
Pdgfb	cggcctgtgactagaagtcc	gagcttgaggcgtcttgg
Pdgfrb	tcaagctgcaggtcaatgtc	ccattggcagggtgactc
Plat	gctacggcaagcatgagg	ggacgggtacagtctgacg
Postn	aatgctgccctggctatatg	gtatgacccttttccttcaa
Rpl19	accctggcccgacgg	taccttcctcttccctatgcc
Serpine1	ggcacctttgaatactcagga	tttcccagagaccagaacca
Serpinf1	cagagtgcaggctgtgagag	ggctccagtccagaggagtag
Sfrp1	acgagttgaagtcagaggccatc	acagtcggcaccgttcttcag
Sfrp5	gatctgtgcccagtgtgaga	ttaatgcgcatcttgaccac
Tek	gtatggactctttagccggctt	ttcgcccattctctggtcac
Tnc	gcgcagacacacaccctagc	tttccaggtcgggaaaagca
Tgfb1	tgacgtcactggagttgtacgg	ggttcatgtcatggatggtgc
Tgfb2	tcctacagactggagtcacaaca	gcagcaattatcctgcacatt
Tgfb3	gcagacacaacccatagcac	gggttctgcccacatagtaca
Tgfbi	aggaagatctgcggcaagt	tctctcctgggacctttcat
Thbs4	cagacaactgcaggctcgt	gatatctcctaccccgtcattg
Timp1	gcaaagagctttctcaaagacc	agggatagataaacagggaaacact
Vcam1	ggaagctggaacgaagtatcc	tccagcctgtaaactgggtaa
Vim	ccaacctttttcttccctgaac	ttgagtgggtgtcaaccaga

Please cite this article in press as: Saupe et al., Tenascin-C Downregulates Wnt Inhibitor Dickkopf-1, Promoting Tumorigenesis in a Neuroendocrine Tumor Model, Cell Reports (2013), http://dx.doi.org/10.1016/j.celrep.2013.09.014

Cell Reports
Article

Tenascin-C Downregulates Wnt Inhibitor Dickkopf-1, Promoting Tumorigenesis in a Neuroendocrine Tumor Model

Falk Saupe,[1,2,3,4,12] Anja Schwenzer,[1,2,3,4,12] Yundan Jia,[1,2,3,4,5,12] Isabelle Gasser,[1,2,3,4] Caroline Spenlé,[1,2,3,4] Benoit Langlois,[1,2,3,4] Martial Kammerer,[1,2,3,4] Olivier Lefebvre,[1,2,3,4] Ruslan Hlushchuk,[6] Tristan Rupp,[1,2,3,4] Marija Marko,[1,2,3,4] Michael van der Heyden,[1,2,3,4] Gérard Cremel,[1,2,3,4] Christiane Arnold,[1,2,3,4] Annick Klein,[1,2,3,4] Patricia Simon-Assmann,[1,2,3,4] Valentin Djonov,[6] Agnès Neuville-Méchine,[7] Irene Esposito,[8] Julia Slotta-Huspenina,[8] Klaus-Peter Janssen,[9] Olivier de Wever,[10] Gerhard Christofori,[11] Thomas Hussenet,[1,2,3,4,*] and Gertraud Orend[1,2,3,4,5,*]

[1]Inserm U1109, MN3T Team, The Microenvironmental Niche in Tumorigenesis and Targeted Therapy, 3 Avenue Molière, 67200 Strasbourg, France

[2]Université de Strasbourg, 67000 Strasbourg, France

[3]LabEx Medalis, Université de Strasbourg, 67000 Strasbourg, France

[4]Fédération de Médecine Translationnelle de Strasbourg (FMTS), 67000 Strasbourg, France

[5]Institute of Biochemistry and Genetics, Department of Biomedicine, University of Basel, Extracellular Matrix Adhesion Team, Mattenstraße 28, 4058 Basel, Switzerland

[6]Institute of Anatomy, University of Bern, Baltzerstrasse 2, 3000 Bern, Switzerland

[7]Hospital Hautepierre, Department of Anatomy and Pathology, 1 Avenue Molière, 67200 Strasbourg, France

[8]Institute of Pathology and Anatomy, Technical University Munich, Trogerstrasse 18, 81675 München, Germany

[9]Department of Surgery Technical University Munich, Ismaningerstrasse 22, 81675 München, Germany

[10]Laboratory of Experimental Cancer Research, Department of Radiation Oncology and Experimental Cancer Research, Ghent University Hospital, De Pintelaan 185, 9000 Ghent, Belgium

[11]Institute of Biochemistry and Genetics, Department of Biomedicine, University of Basel, Switzerland, Tumor Biology Team, Mattenstraße 28, 4058 Basel, Switzerland

[12]These authors contributed equally to this work

*Correspondence: hussenetthomas@gmail.com (T.H.), gertraud.orend@inserm.fr (G.O.)

http://dx.doi.org/10.1016/j.celrep.2013.09.014

SUMMARY

The extracellular matrix molecule tenascin-C (TNC) is a major component of the cancer-specific matrix, and high TNC expression is linked to poor prognosis in several cancers. To provide a comprehensive understanding of TNC's functions in cancer, we established an immune-competent transgenic mouse model of pancreatic β-cell carcinogenesis with varying levels of TNC expression and compared stochastic neuroendocrine tumor formation in abundance or absence of TNC. We show that TNC promotes tumor cell survival, the angiogenic switch, more and leaky vessels, carcinoma progression, and lung micrometastasis. TNC downregulates Dickkopf-1 (*DKK1*) promoter activity through the blocking of actin stress fiber formation, activates Wnt signaling, and induces Wnt target genes in tumor and endothelial cells. Our results implicate DKK1 downregulation as an important mechanism underlying TNC-enhanced tumor progression through the provision of a proangiogenic tumor microenvironment.

INTRODUCTION

Manifestation of cancer requires many steps in which the microenvironment plays an essential role (Bissell and Labarge, 2005). A group of tumor cells with oncogenic mutations does not readily cause cancer, a phenomenon known as tumor dormancy (Aguirre-Ghiso, 2007). Angiogenesis presents an important step in awakening quiescent tumors and in driving their development into metastatic cancer (Almog, 2010). Tumor cells secrete soluble factors that attract endothelial cells (Kerbel, 2008). In addition, the extracellular matrix (ECM) constitutes a major fraction of cancer tissue and contributes to tumor angiogenesis and metastasis (Lu et al., 2012). An important component of the tumor-specific ECM is tenascin-C (TNC). TNC is known to promote malignant tumor progression and lung metastasis; yet, the underlying mechanisms are poorly understood (Midwood et al., 2011).

Because no stochastic and immune-competent in vivo model existed that would recapitulate the roles of TNC in tumor progression, we generated mouse lines with different expression levels of TNC (overexpression, wild-type, knockout) in the Rip1-Tag2 (RT2) model of pancreatic β-cell carcinogenesis (Hanahan, 1985). This model recapitulates multistage tumorigenesis as observed in most human cancers (Nevins, 2001; Pipas and Levine, 2001).

Here, we demonstrate that TNC promotes several steps in RT2 tumorigenesis including the angiogenic switch and lung micrometastasis. We provide a mechanistic basis showing that TNC downregulates expression of the soluble Wnt inhibitor Dickkopf-1 (DKK1) (Glinka et al., 1998) by blocking actin stress fiber formation and induces canonical Wnt signaling in tumor and endothelial cells. Our data suggest that DKK1 downregulation by TNC in tumor and stromal cells may provide a tumorigenesis signaling promoting microenvironment. Given that Wnt signaling is a crucial pathway driving angiogenesis and is activated by TNC, this pathway may play an important role in promoting tumor angiogenesis and metastasis by TNC. Thus, targeting TNC or its associated signaling pathways may represent a strategy to counteract tumor progression.

RESULTS

Tenascin-C Promotes Tumor Cell Survival, Proliferation, and Invasiveness

To address whether TNC potentially plays a role in the RT2 model (Hanahan, 1985), we determined TNC expression during RT2 tumorigenesis by immunofluorescence microscopy analysis (immunofluorescence [IF]). In normal pancreatic islets, TNC expression was undetectable, whereas a large fraction of hyperplastic and almost all angiogenic and tumorigenic islets expressed TNC (Figure S1A), suggesting a potential role of TNC during RT2 tumor progression. Therefore, we generated RT2 mice with overexpression of TNC (RT2/TNC) and a lack of TNC (RT2/TNCKO) (Figures S1B–S1G).

We performed tissue analysis to address whether ectopically expressed TNC had an effect on cell proliferation. We quantified the proportion of cells positive for phosphohistone-H3 by IF (Figure S2A) and observed that tumors of RT2/TNC mice exhibited 1.4-fold more proliferating cells than those from RT2 mice (Figure 1A) with a significant difference in hyperplastic islets (Figure S2C). Surprisingly, a similar difference was also seen in RT2/TNCKO tumors (Figures 1B and S2D). We also investigated a potential impact of ectopically expressed TNC on apoptosis by staining for cleaved caspase-3 (Figure S2B). RT2/TNC tumors exhibited 2.8-fold less apoptotic cells than RT2 wild-type tumors (Figures 1C and S2E). In contrast, apoptosis was unchanged in RT2/TNCKO tumors in comparison to RT2 controls (Figures 1D and S2F). However, no difference was seen in tumor multiplicity or tumor volume between genotypes (Figures S2G and S2H). Interestingly, upon tumor grading we observed that the frequency of carcinomas and the ratio of carcinomas over adenomas were higher in RT2/TNC mice (1.8) than in RT2 controls (0.8) (Figure 1E; Table S1). We conclude that transgenic TNC increases proliferation and survival in RT2/TNC mice and more importantly promotes tumor progression.

Tenascin-C Promotes the Angiogenic Switch and the Formation of Leaky and Abnormal Tumor Vessels

To address whether TNC has an effect on RT2 tumor angiogenesis, we isolated islets at the age of 8 weeks when the angiogenic switch takes place in a subset of neoplastic islets (Hanahan et al., 1996; Parangi et al., 1996) (Figure S2I). We noticed that the number of angiogenic islets was 2.4-fold higher in RT2/TNC and 2.9-fold lower in RT2/TNCKO mice in comparison to RT2 littermates (Figures 1F and 1G; Table S2). By quantification of CD31-positive endothelial cells (Figure S2J) in tumor sections of 12-week-old RT2 mice, we observed that the abundance of blood vessels was 2.6-fold higher and 1.6-fold lower in tumors of RT2/TNC and RT2/TNCKO mice, respectively, than in RT2 controls (Figures 1H and 1I).

We next addressed the question of a potential impact of TNC on vessel anatomy by scanning electron microscopy in Mercox corrosion casts of the tumor vasculature of multiple tumors of RT2 and RT2/TNC mice. Using this descriptive approach, we observed a highly aberrant vessel phenotype in some RT2/TNC tumors that has not been seen in RT2 tumors. These vessels were irregularly shaped, wider, discontinued, and bifurcated (see arrows), reminiscent of high vessel branching and/or leakage (Figures 1J and S2K). Because this approach is not suitable for quantitative determinations, we then studied vessel lining by pericytes using NG2 staining as readout for vessel functionality and maturation (Figure S2L). Despite more abundant pericytes in RT2/TNC tumors (Figure S2M), quantification of combined NG2 and CD31 staining signals revealed a 23.7% reduced ratio of NG2 over CD31 in RT2/TNC tumors (Figure 1K), which is indicative of a reduced pericyte coverage of vessels (Song et al., 2005). Finally, we assessed vessel functionality by analyzing fibrinogen (FBG) leakage in tumors upon PBS perfusion of tumor vessels followed by FBG staining (Huijbers et al., 2010) (Figure S2N). Whereas FBG leakage was slightly increased (close to significance, $p = 0.064$) in RT2/TNC over control tumors (Figures 1L and S2O), this analysis revealed a 1.7-fold significantly reduced FBG staining in RT2/TNCKO tumors over RT2 wild-type tumors (Figures 1M and S2P).

Altogether, our results suggest that, whereas TNC promotes the angiogenic switch and increases tumor blood vessel density, it decreases vessel coverage by pericytes and increases leakage, thus perturbing tumor vessel functionality.

Tenascin-C Increases Lung Micrometastasis

In a C57Bl/6 background, RT2 mice do not exhibit macroscopically visible metastasis. To address whether TNC had an effect on micrometastasis formation, we determined expression of insulin (as tumor cell-specific marker) in liver and lung tissue of tumor-bearing mice. Upon tissue staining, we detected cohorts of insulinoma cells within liver and lung tissue confirming their metastatic nature (Figures 2A and S3A). Hematoxylin and eosin (H&E) staining revealed their parenchymal localization. In a subset of mice, we compared quantification of insulin by immunostaining and quantitative RT-PCR (qRT-PCR). This showed a good correlation between both methods and indicates that quantification by qRT-PCR reflects parenchymal localization of micrometastasis rather than circulating tumor cells. We then analyzed a larger sample size of liver and lung tissue by qRT-PCR. Although we did not observe differences in liver tissue between genotypes (Figures S3B and S3C), *insulin* mRNA levels in lungs of RT2/TNC mice were 5.4-fold higher in comparison to lungs of RT2 controls (Figure 2B). Moreover, we observed 28.3-fold lower *insulin* mRNA levels in lungs of mice lacking TNC in comparison to control littermates carrying one TNC allele

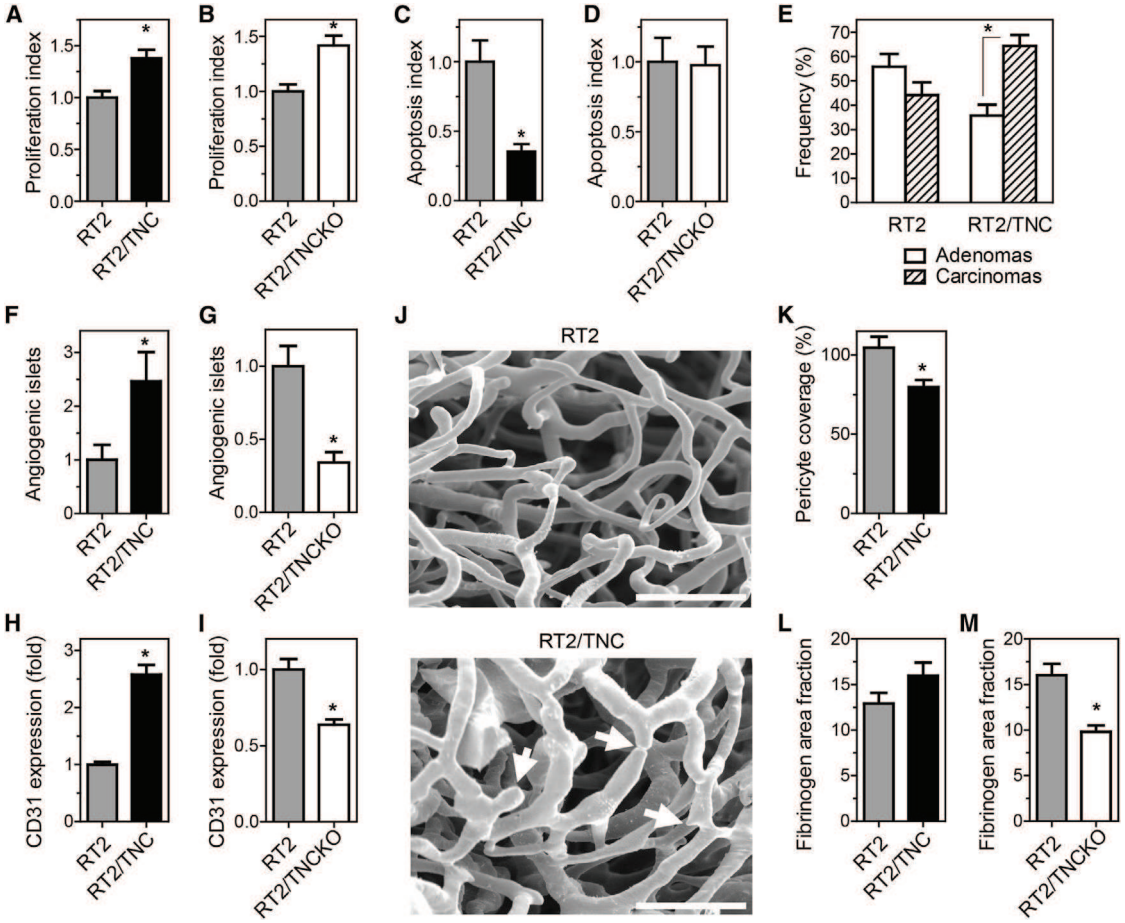

Figure 1. TNC Enhances Proliferation, Survival, and Tumor Progression in RT2 Tumors

(A and B) Quantification of proliferating cells in tumor sections as PH3-positive nuclei in 12-week-old mice. (A) RT2 (n = 9 mice, n = 150 islets), RT2/TNC (n = 8, n = 140). (B) RT2 (n = 6, n = 131) and RT2/TNCKO (n = 6, n = 137).

(C and D) Quantification of apoptotic cells as cleaved caspase-3-positive cells in tumor sections of 12-week-old mice. (C) RT2 (n = 6 mice, n = 84 islets), RT2/TNC (n = 8, n = 123). (D) RT2 (n = 4, n = 95) and RT2/TNCKO (n = 4, n = 83).

(E) Tumor grading into adenoma or invasive carcinoma (H&E-stained tumor sections) of RT2 tumors (n = 26 mice, 78 adenomas, 79 carcinomas) and RT2/TNC (n = 22, 44 adenomas, 76 carcinomas). See Table S1.

(F and G) Number of angiogenic islets per mouse normalized to RT2 controls. See Table S2.

(H and I) Tumor blood vessel quantification upon CD31 staining of tumor sections from 12-week-old mice as CD31-positive area fraction per tumor normalized to RT2 controls. (H) RT2 (n = 6 mice, n = 34 tumors, 203 images) and RT2/TNC (n = 4, n = 17, 106 images). (I) RT2 (n = 3, n = 71) and RT2/TNCKO (n = 3, n = 111).

(J) Morphology of the tumor vasculature in Mercox perfusion casts from 12-week-old RT2 and RT2/TNC mice. Arrows point at break point, branching, and constriction. Scale bars, 50 μm.

(K) Pericyte coverage of tumor blood vessels upon quantification of the ratio of NG2 over CD31 staining signals. RT2 (n = 6 mice, n = 155 tumors) and RT2/TNC (n = 8, n = 204).

(L and M) Quantification of tumor blood vessel leakage upon fibrinogen staining of tumor sections from 12-week-old mice as fibrinogen-positive area fraction per tumor. (L) RT2 (n = 5 mice, n = 62 tumors) and RT2/TNC (n = 3, n = 50). (M) RT2 (n = 4, n = 60) and RT2/TNCKO (n = 5, n = 125). Error bars represent SEM. *$p < 0.05$. See also Figures S1 and S2 and Tables S1 and S2.

(Figure 2C). Our results suggest that in the RT2 model TNC does not affect liver metastasis but increases lung micrometastasis formation.

TNC Expression Correlates with Low Dkk1 Levels and Increases Wnt Target Gene Expression

Because we had noticed downregulation of the Wnt pathway inhibitor DKK1 in T98G glioblastoma cells cultivated on a TNC-containing substratum (Ruiz et al., 2004), we assessed a potential impact of TNC on Dkk1 expression in tumors of the different RT2 genotypes. By qRT-PCR, we noticed that 12 times more RT2/TNC tumors (46.1%) lacked *Dkk1* expression as compared to RT2 controls (3.7%) (Figure 3A). In RT2/TNC tumors with detectable *Dkk1* expression, the levels were 16.1-fold reduced in comparison to RT2 controls (Figure 3B). In contrast, *Dkk1* levels were 2.6-fold higher in tumors lacking TNC as compared to control tumors with one TNC allele (Figure 3C). These observations demonstrate an inverse correlation between TNC and

Please cite this article in press as: Saupe et al., Tenascin-C Downregulates Wnt Inhibitor Dickkopf-1, Promoting Tumorigenesis in a Neuroendocrine Tumor Model, Cell Reports (2013), http://dx.doi.org/10.1016/j.celrep.2013.09.014

Cell PRESS
Open ACCESS

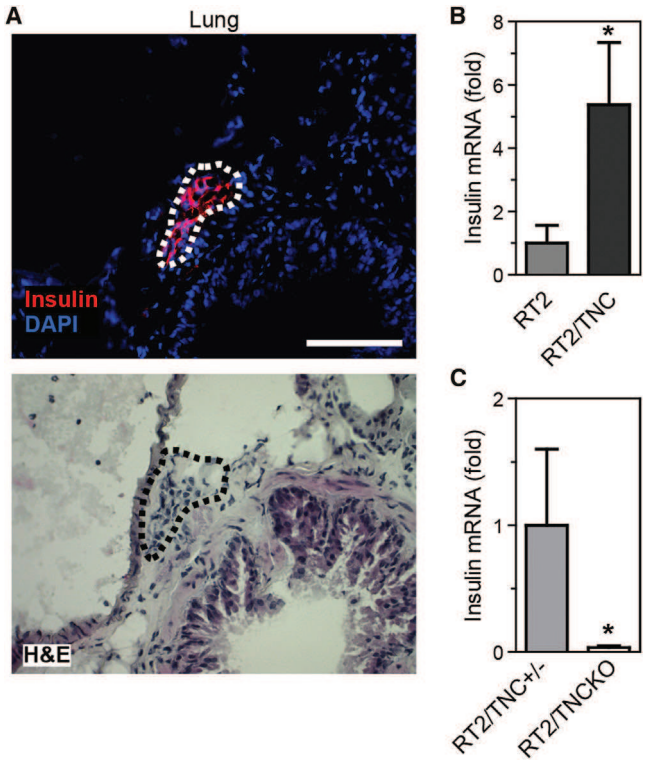

Figure 2. Lung Micrometastasis in RT2 Mice

Insulin expression in a lung RT2 micrometastasis (A) and quantification by qRT-PCR (B and C). (A) Detection of metastasized insulin-positive tumor cells in lung parenchyma (RT2 mouse) by immunostaining (upper panel) and H&E staining (adjacent section, lower panel). Scale bar 50 μm. Detection of insulin expression in RT2 (9/24) and RT2/TNC mice (11/24) (B) and in RT2/TNC$^{+/-}$ (8/13) and RT2/TNCKO littermates (4/13) (C). Error bars represent SEM. *p < 0.05. See also Figure S3.

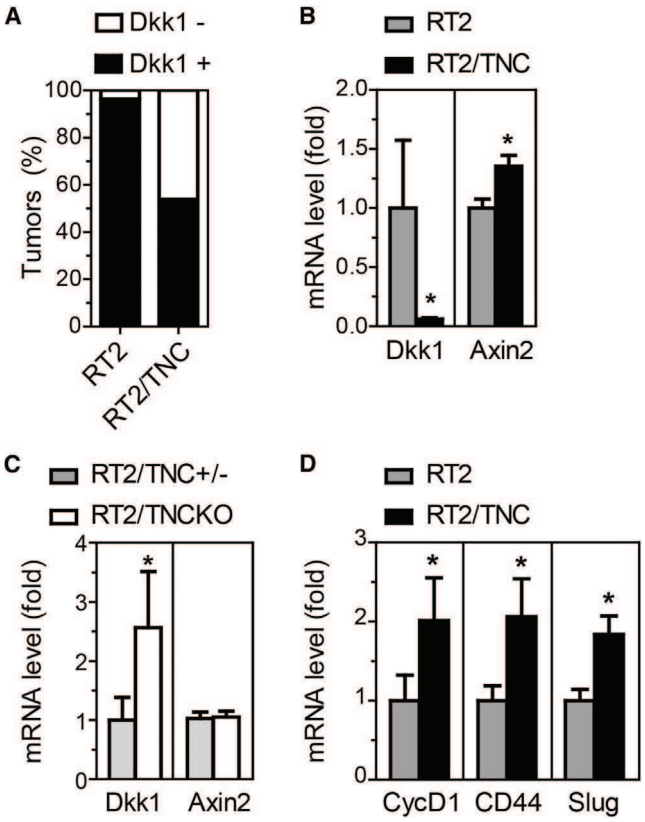

Figure 3. Dkk1 Expression in RT2 Tumors

(A) Tumors were stratified according to *Dkk1* levels, as Dkk1 expressing (Dkk1^{+}) or not expressing (Dkk1^{-}). *Dkk1* was found to be expressed in 26 of 27 RT2 tumors and in 7 of 13 RT2/TNC tumors. Difference between genotypes, $p < 0.05$.

(B) Dkk1 expression was largely reduced in those RT2/TNC tumors with detectable *Dkk1* expression. *Axin2* expression was enhanced in RT2/TNC tumors.

(C) In RT2/TNCKO tumors (15 of 24 tumors were Dkk1 positive) Dkk1 expression was higher compared to RT2/TNC$^{+/-}$ tumors (16 of 23 tumors were Dkk1 positive). Axin2 expression was not changed.

(A–C) *Dkk1* and *Axin2* expression was analyzed by qRT-PCR.

(A–D) Wnt target gene expression in all RT2/TNC and RT2/TNCKO tumors (A–C) or in small differentiated tumors (D), see Table S3. Error bars represent SEM. *p < 0.05.

Dkk1 expression and suggest that TNC may activate Wnt signaling through *Dkk1* repression. To address this possibility, we determined the expression of Wnt target genes by qRT-PCR. We observed an increased expression of the bona fide Wnt signaling target *Axin2* (1.4-fold) in RT2/TNC tumors (Figure 3B), whereas its expression was unchanged in RT2/TNCKO tumors (Figure 3C). This result suggested that ectopic TNC expression induced Wnt signaling, prompting us to analyze expression of other Wnt target genes. Indeed, other Wnt targets such as *Cyclin D1* (2.0-fold), *CD44* (2.0-fold), and *Slug* (1.8-fold) were upregulated in small differentiated tumors of RT2/TNC mice (Figure 3D; Table S3). These results suggest that TNC may contribute to Wnt signaling activation in RT2/TNC tumors through downregulation of the inhibitor Dkk1.

Wnt Activation and DKK1 Inhibition by TNC in Cultured Tumor and Stromal Cells

We then designed in vitro experiments to evaluate a potential Wnt activation by TNC involving DKK1. We used a Wnt reporter (TOPFlash) assay where the expression of the *luciferase* gene is driven by a promoter containing TCF/LEF binding sites. Upon growth of Wnt-3A-stimulated osteosarcoma KRIB cells on a TNC-containing substratum, we observed a 3.5-fold increased Wnt reporter activity (Figure 4A) and a 2.0-fold increased expression of *AXIN2* (Figure 4B), demonstrating that TNC activates the Wnt pathway.

Next, we determined whether TNC affects secretion of soluble factors regulating Wnt signaling in KRIB cells. Therefore, we measured Wnt reporter activity of Wnt-3A-stimulated KRIB cells upon incubation with conditioned medium (CM) from the same cells previously grown on fibronectin (FN) or FN/TNC and observed that, indeed, Wnt activity was higher with CM from cells cultured in the presence of TNC (Figure 4C). These results suggest that TNC activates Wnt signaling through modulating the secretion of activators or inhibitors of the Wnt pathway.

To address whether Wnt inhibitors are regulated by TNC, we investigated their expression by qRT-PCR in cells grown on FN/TNC and FN. Although some inhibitors (*DKK4* and *SFRP2*)

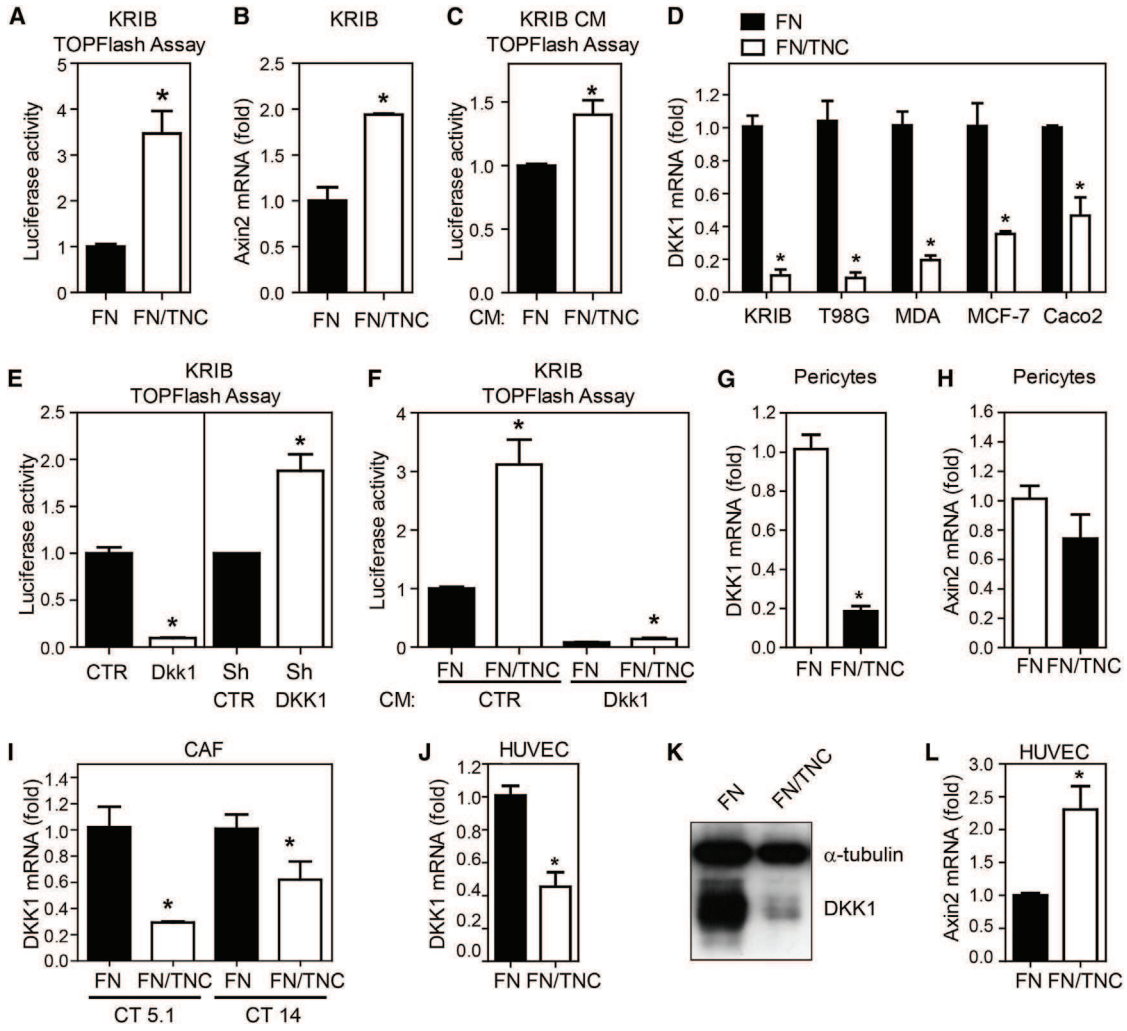

Figure 4. TNC Leads to DKK1 Downregulation and Wnt Signaling Activation in Tumor Cells and Endothelial Cells

(A–C) Enhanced Wnt signaling in Wnt-3A-treated KRIB cells by TNC. TOPFlash activity of cells grown on FN or FN/TNC for 48 hr (A) or treated for 48 hr with Wnt-3A CM and CM of cells grown on FN or FN/TNC (C). (B) *AXIN2* mRNA levels (qRT-PCR, 5 hr).

(D) *DKK1* expression (qRT-PCR, 24 hr) in the indicated tumor cell lines (KRIB, T98G, MDA-MB-435 [MDA], MCF-7, and Caco2) on FN/TNC is represented relative to its expression on FN.

(E) Cell autonomous impact of low (knockdown) and high (overexpression) DKK1 on Wnt signaling as analyzed by TOPFlash activity after 48 hr.

(F) Repression of TNC-mediated Wnt signaling activation by Dkk1. TOPFlash luciferase activity was performed as in (A) except the addition of CM from KRIB control or Dkk1-overexpressing cells after 5 hr of cell seeding on the indicated substrata. Note that the TNC-containing substratum still induced Wnt signaling activity in presence of Dkk1-containing CM, but to a lesser extent (1.8-fold) than in the control conditions (3.1-fold).

(G–I) *DKK1* and *Axin2* mRNA levels in pericytes (G and H) and two human colorectal-cancer-derived CAF primary lines (I) seeded on FN or FN/TNC (5 hr). TNC leads to downregulation of *DKK1* in pericytes and CAFs (G and I), but *AXIN2* expression remains unchanged in pericytes (H).

(J–L) Enhanced Wnt signaling by TNC in HUVECs. qRT-PCR for DKK1 and AXIN2 (5 hr) (J and L) and DKK1 immunoblotting (24 hr) (K). Data from three independent experiments (except D: MCF-7 and Caco2 cell lines, one and two experiments, respectively; and I: two experiments) are shown as mean ± SEM. *$p < 0.05$. See also Figure S4.

were not expressed, no consistent effect of TNC was observed on the expression of other analyzed Wnt inhibitors (*DKK2*, *DKK3*, *SFRP1*, *SFRP3*, *SFRP4*) in KRIB, T98G, and MDA-MB435 cells (Figure S4A). In contrast, we observed a robust downregulation of *DKK1* in all five analyzed tumor cell lines of different origin after 24 hr on the TNC-containing substratum (Figures 4D and S4A). DKK1 downregulation was observed at both RNA and protein levels, with a fast (5 hr) and long-lasting (up to 12 days) effect in T98G cells (Figures S4B and S4C).

To determine whether modulation of DKK1 expression contributes to TNC-dependent Wnt signaling in KRIB cells, TOPFlash activity was measured upon overexpression and knockdown of DKK1, respectively (Figures S4D–S4G). Indeed, activity of the Wnt signaling reporter was DKK1 dependent because it was increased upon DKK1 knockdown and decreased upon Dkk1 overexpression (Figure 4E) and was repressed by Dkk1-containing CM in a dose-dependent manner (Figure S4H). When KRIB cells were incubated with Dkk1 CM on

Please cite this article in press as: Saupe et al., Tenascin-C Downregulates Wnt Inhibitor Dickkopf-1, Promoting Tumorigenesis in a Neuroendocrine Tumor Model, Cell Reports (2013), http://dx.doi.org/10.1016/j.celrep.2013.09.014

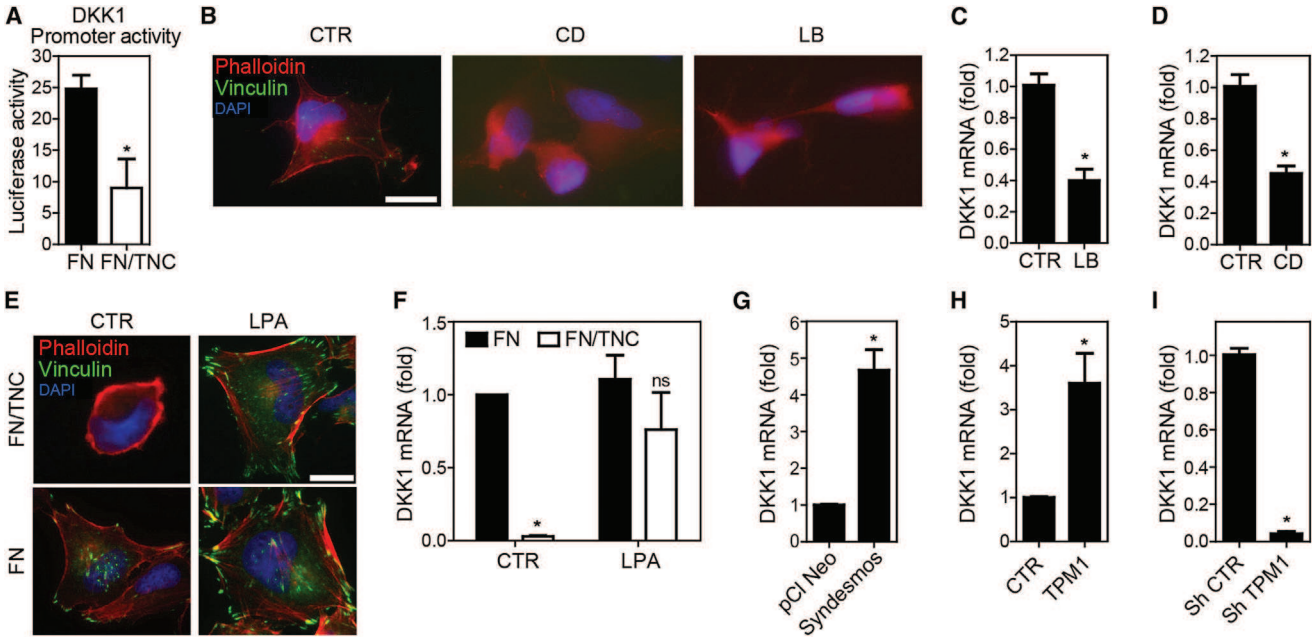

Figure 5. Mechanism of DKK1 Downregulation

(A) Reduced *DKK1* promoter activity by TNC. *DKK1* promoter driven luciferase activity in T98G cells is shown upon growth for 48 hr on the indicated substrata.

(B and E) Phalloidin (red) and vinculin (green) stainings of serum-starved T98G cells upon CTR, CD (2 μM), or LB (5 μM) treatment for 3 hr (B). Nuclei are stained in blue (DAPI). Scale bar 20 μm.

(C and D) *DKK1* mRNA levels in serum-starved T98G upon LB (5 μM, 3 hr) (C) or CD (2 μM, 3 hr) (D) treatment.

(E) IF staining of T98G cells upon control or LPA (30 μM) treatment. Serum-starved T98G were plated on fibronectin (FN) or fibronectin/tenascin-C (FN/TNC), and after 1 hr LPA was added for 4 hr. Although cells are poorly spread under control conditions on FN/TNC (no actin stress fibers, few focal adhesions), LPA treatment restored cell spreading associated with the formation of focal adhesions and actin stress fibers. Scale bar, 20 μm.

(F) *DKK1* mRNA expression determined by qRT-PCR upon treatment with 30 μM LPA. LPA restores *DKK1* expression on FN/TNC.

(G–I) *DKK1* mRNA expression determined by qRT-PCR upon ectopic expression of chicken syndesmos (G) and mouse TPM1 (H) or upon knockdown of TPM1 (I). Syndesmos or TPM1 overexpression induces *DKK1* mRNA expression, whereas TPM1 knockdown leads to *DKK1* downregulation.

Data are shown as mean ± SEM. *$p < 0.05$. See also Figure S5.

FN/TNC and FN, Wnt reporter activity was largely reduced (Figure 4F), suggesting that TNC-induced repression of DKK1 facilitates Wnt pathway activation.

Next, we determined whether stromal cells also downregulated DKK1 on a TNC substratum. Therefore, *DKK1* expression was determined in two monocytic/macrophage cell lines, primary human brain pericytes, two colorectal cancer derived carcinoma associated fibroblasts (CT5.1, CT14), and human umbilical vein endothelial cells (HUVECs) upon growth on FN/TNC and FN. We noticed that in contrast to the two macrophage lines that did not at all express *DKK1*, pericytes (5-fold), CAFs (3.0- and 1.6-fold), and HUVECs (2.2-fold) significantly downregulated DKK1 mRNA (Figures 4G, 4I, and 4J) and protein (Figure 4K) on a TNC substratum. Whereas *Axin2* expression was not affected in pericytes (Figure 4H), *Axin2* mRNA was 2.3-fold increased in HUVECs on FN/TNC in comparison to FN (Figure 4L). Altogether, our results show that TNC induces downregulation of DKK1 in tumor and stromal cells and activates Wnt signaling in tumor and endothelial cells.

Mechanism of DKK1 Downregulation by TNC

First, we determined whether *DKK1* mRNA stability is substratum dependent. Therefore, T98G cells were treated with the RNA polymerase II inhibitor Actinomycin D, but DKK1 mRNA levels were equally low in cells on FN and FN/TNC, suggesting that *DKK1* is not regulated by mRNA stabilization (Figure S5A). Next, we addressed whether TNC downregulates DKK1 at transcriptional level. Therefore, we performed reporter assays by measuring luciferase activity under control of a 3.2 kb *DKK1* promoter sequence. Indeed, we observed a 2.5-fold reduced *DKK1* promoter activity in cells grown for 48 hr on a TNC-containing substratum (Figure 5A).

Because TNC blocks actin stress fiber formation (Huang et al., 2001; Midwood et al., 2004; Murphy-Ullrich et al., 1991; Orend et al., 2003), we investigated whether disruption of the actin cytoskeleton has an impact on *DKK1* mRNA levels. Treatment with Latrunculin B (LB) and Cytochalasin D (CD) disrupted actin stress fibers and focal adhesions and, importantly, reduced *DKK1* expression (Figures 5B–5D). To address the converse whether more actin stress fibers stimulate *DKK1* expression, we treated KRIB and T98G cells with lysophosphatidic acid (LPA) and observed an increased and dose-dependent *DKK1* mRNA expression similar to serum response factor (SRF), a known actin stress fiber-regulated gene (Gineitis and Treisman, 2001; Spencer and Misra, 1999) (Figures S5B–S5F). Moreover, LPA (30 μM) restored cell spreading, actin stress fibers, and focal

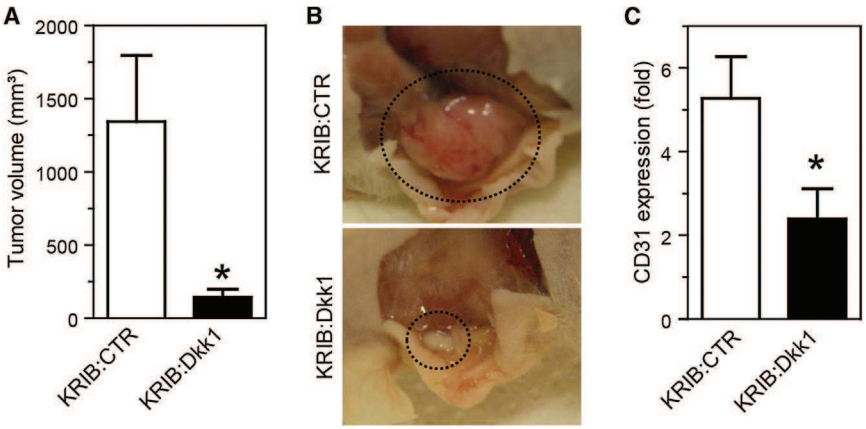

Figure 6. Dkk1 Overexpression Inhibits Osteosarcoma Growth and Angiogenesis

(A) Mean tumor volume of control (CTR, n = 10) and Dkk1-overexpressing (n = 9) KRIB tumors upon subcutaneous injection of the corresponding cells into nude mice.

(B) Representative tumor images.

(C) Tumor microvessel density, as determined by CD31 staining and quantification, was 2.2-fold reduced in KRIB:Dkk1 tumors (n = 8) as compared to control KRIB tumors (n = 10).

Error bars represent SEM. *p < 0.05. See also Figure S6.

adhesions in T98G cells on a FN/TNC substratum and most importantly largely restored *DKK1* levels on this substratum to that on FN (Figures 5E and 5F). Because LPA can trigger RhoA signaling (Mills and Moolenaar, 2003), and RhoA expression (Lange et al., 2007) and function (Wenk et al., 2000) are impaired by TNC, we determined whether overexpression of a constitutively active (CA) RhoA molecule impacts on *DKK1* expression. Whereas, CA-RhoA increased SRF target gene expression (Figures S5G–S5J), it did not alter *DKK1* expression (Figures S5K and S5L), suggesting that LPA triggers *DKK1* expression by a RhoA-independent pathway.

Because tropomyosin-1 (TPM1) and syndesmos overexpression bypass the cell adhesion blocking and actin stress-fiber-disrupting effect of TNC on a FN/TNC substratum (Lange et al., 2008), we determined whether ectopic expression of syndesmos and TPM1 have an impact on *DKK1* expression. Whereas shTPM1 blocked *DKK1* expression, overexpression of syndesmos and TPM1 increased *DKK1* mRNA levels to 4.7- and 3.6-fold, respectively (Figures 5G–5I and S5M–S5P).

Altogether, these results demonstrated that *DKK1* expression is regulated at the promoter level and that actin stress fibers and focal adhesion signaling drive *DKK1* transcription independently of RhoA. We conclude that TNC downregulates *DKK1* transcription by blocking focal adhesion and actin stress fiber formation.

Repression of Tumor Angiogenesis by DKK1

As we observed that TNC promotes tumor angiogenesis and downregulates *DKK1* expression, we addressed whether DKK1 impacts on tumor angiogenesis in xenografted tumors of KRIB cells with different DKK1 levels. We found that upon Dkk1 overexpression (Figure S6A) tumors were significantly smaller (Figure 6A) and pale (Figure 6B). Quantification of microvessel density upon CD31 staining revealed that Dkk1-overexpressing tumors were less vascularized (Figure 6C), suggesting that Dkk1 overexpression impaired tumor angiogenesis. In addition, conditioned medium from KRIB cells overexpressing Dkk1 inhibited HUVEC tubulogenesis on Matrigel in vitro (Figure S6D). We addressed whether Dkk1 potentially had an impact on tumor growth through inhibiting tumor cell proliferation and found no statistically significant difference in proliferation in cultured cells or in the tumors with elevated Dkk1 levels (Figures S6B and S6C).

Because Dkk1 influenced proliferation of tumor cells neither in vitro nor in vivo, our data suggest that Dkk1 overexpression impairs angiogenesis and thereby inhibits KRIB tumor growth. Because DKK1 blocks angiogenesis in a VEGFA context (Min et al., 2011), we investigated whether full-length TNC binds VEGFA. Indeed, by surface plasmon resonance we observed a dose-dependent binding of VEGFA to TNC (Figure S7), extending data on binding of VEGFA to the fifth FNIII domain in TNC (De Laporte et al., 2013) by providing a K_d of 2.7×10^{-7} M, which is in the range of a VEGFA/glycosaminoglycan interaction (2.4×10^{-8} M) (Wu et al., 2009).

TNC Expression in Human Insulinomas

As we demonstrated a tumor-promoting effect of TNC in the murine RT2 insulinoma model, we assessed a potential clinical relevance by determining TNC expression in human insulinomas using qRT-PCR and immunohistochemical staining of patient tumor tissue. Of note, insulinomas are rare and most are benign, yet a few (10%–15%) metastasize to lymph nodes and liver (Metz and Jensen, 2008). At RNA level, we found that *TNC* expression was detectable in all analyzed human insulinomas (Figure 7A). Most importantly, we observed the highest *TNC* expression levels (3/14) in tumors from patients with metastasis to liver or lymph nodes (Figures 7A and 7B), suggesting that a high TNC expression correlates with metastasis formation in human insulinomas.

DISCUSSION

We have used the RT2 model of multistage pancreatic β-cell tumorigenesis with abundant and no TNC expression to obtain a better understanding of TNC contribution to tumor progression and we have observed multiple effects. Enhanced TNC levels in TNC transgenic RT2 mice correlate with an increase in tumor cell proliferation and survival, carcinoma formation, angiogenesis, and lung micrometastasis. On the contrary, the absence of TNC results in reduced angiogenesis and lung micrometastasis. These results confirm a crucial role of TNC in tumor progression as has been suspected in human cancer.

There is much evidence for an important role of TNC in promoting tumor angiogenesis (Midwood et al., 2011). However, despite the fact that TNC has been extensively investigated for almost three decades (Chiquet-Ehrismann et al., 1986), it is not

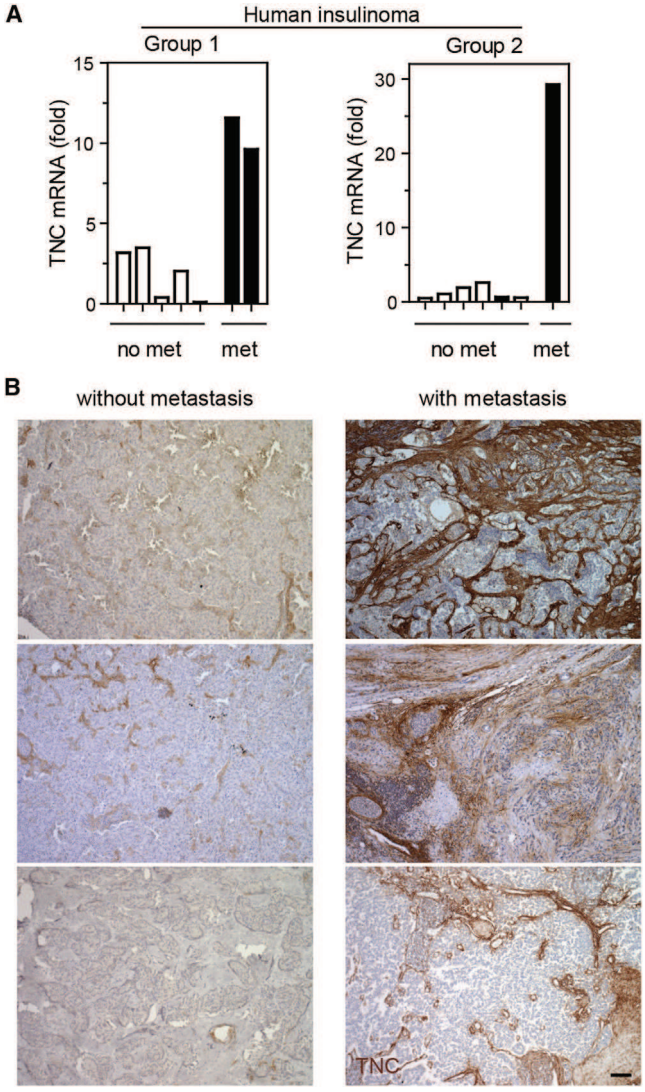

Figure 7. TNC Expression Correlates with Metastasis Formation in Human Insulinomas

(A) *TNC* mRNA expression was determined by qRT-PCR in two patient groups (group 1, Munich cohort; group 2, Strasbourg cohort) and is displayed as relative expression upon normalization to *GAPDH*. Upon combining data of the two groups, *TNC* expression in patients with metastasis is increased over that in patients without metastasis ($p < 0.05$).

(B) TNC expression was determined by IHC in all tumors of the two groups of insulinomas. Representative pictures of the three metastatic and three non-metastatic insulinomas are shown. Scale bar, 100 μm.

resolved how TNC impacts tumor angiogenesis at the molecular level. Whereas TNC can have stimulatory effects on endothelial cell migration, conflicting reports exist concerning its impact on tubulogenesis. A proangiogenic effect of TNC linked to VEGFA expression was seen in human melanoma xenografts implanted into immune-compromised mice lacking TNC (Tanaka et al., 2004). Of note, in the RT2/TNC tumors we did not observe an increased *VEGFA* expression (M.K., F.S., G.O., unpublished data). Our study addresses the role of TNC on tumor angiogenesis systematically by using a stochastic genetic tumor model with an intact immune system. Here, we investigated the angiogenic switch, tumor blood vessels, and their functionality. Most importantly, our study shows that TNC promotes the angiogenic switch, a rate-limiting step along tumor progression (Hanahan and Folkman, 1996), and the abundance of endothelial cells. However, TNC seems to impair vessel functionality because tumor vessels of RT2/TNC mice are morphologically aberrant and less covered by pericytes. Moreover, vessels in RT2 tumors lacking TNC are less leaky than those with TNC, suggesting a role of TNC in the formation of more but less functional tumor vessels.

We have identified DKK1 as an important TNC target in RT2 tumors. Our in vivo and in vitro results suggest that TNC promotes tumor progression involving DKK1 downregulation and activation of Wnt signaling. First, the *TNC* copy number inversely correlates with *DKK1* expression in RT2 tumors, and a TNC substratum downregulates *DKK1* expression in tumor and several stromal cell types (CAFs, pericytes, and endothelial cells). Second, Wnt signaling is increased by TNC in the RT2 model and in cultured endothelial and tumor cells. Third, TNC-induced Wnt activation is reduced in tumor cells by DKK1. Finally, downregulation of *DKK1* by TNC may be a key event because no other major Wnt inhibitor is consistently regulated by a TNC-containing substratum (our data; Ruiz et al., 2004).

Several transcriptional regulators, epigenetic silencing, and tissue tension were shown to regulate DKK1 expression (Aguilera et al., 2006; Barbolina et al., 2013; Liao et al., 2008; Menezes et al., 2012; Pendás-Franco et al., 2008; Zhou et al., 2012). Here, we demonstrate that TNC downregulates *DKK1* expression by promoter inhibition. Because TNC blocks actin stress fiber formation (Huang et al., 2001; Midwood et al., 2004; Murphy-Ullrich et al., 1991; van Obberghen-Schilling et al., 2011), we investigated whether *DKK1* expression is regulated by the actin polymerization state and demonstrated that TPM1 antisense and drug-induced disruption of the actin cytoskeleton reduced *DKK1* mRNA levels. On the contrary, enforcing actin polymerization and stress fiber formation by overexpression of syndesmos, bridging integrin $\alpha5\beta1$ and syndecan-4 in focal adhesions (Bass and Humphries, 2002), largely increased *DKK1* expression. We further showed that LPA rescued focal adhesion and actin stress fiber formation and cell spreading on FN/TNC, which we linked to restored *DKK1* expression in a RhoA-independent manner. How TNC downregulates *DKK1* expression at promoter level is currently unknown and requires further investigation, but it does not appear to be exclusively dependent on the SRF cotranscription factor MKL1 that is regulated by actin polymerization (Miralles et al., 2003) (A.S. and G.O., unpublished data). Previously, it was shown that a stiffened collagen substratum, implicating integrin adhesion signaling (Levental et al., 2009), induces *DKK1* downregulation in several cell types including endothelial cells (Barbolina et al., 2013). Here, we report a mechanism whereby TNC blocks *DKK1* transcription through disruption of actin stress fibers.

The role of DKK1 in developmental and tumor angiogenesis appears to be context dependent, because DKK1 can produce pro- and antiangiogenic effects (Aicher et al., 2008; De Langhe et al., 2005; Min et al., 2011; Oh et al., 2012; Reis

et al., 2012; Smadja et al., 2010). Interestingly, the growth factor context seems to be particularly critical for the outcome, because, for example, DKK1 promotes basic fibroblast-growth-factor-induced angiogenesis (Aicher et al., 2008; Reis et al., 2012; Smadja et al., 2010) but blocks VEGFA-induced (Min et al., 2011) angiogenesis in Matrigel plug assays in vivo. We here confirm that DKK1 inhibits HUVEC tubulogenesis in vitro (Min et al., 2011) and tumor angiogenesis in an osteosarcoma xenograft model in vivo.

Employing the RT2 model, we show that TNC promotes metastasis formation to the lung but not to the liver. This is reminiscent of breast cancer where TNC is part of a gene expression signature specifically associated with lung but not bone metastasis (Minn et al., 2005), an initial observation that has been subsequently confirmed and functionally validated using xenograft models (Oskarsson et al., 2011; Tavazoie et al., 2008). Mechanistically, TNC expression was linked to an increased tumor cell survival and activation of Wnt and Notch signaling, as revealed by increased expression of Lgr5 and Msi1, respectively (Oskarsson et al., 2011). Although we have shown that Wnt signaling is activated in TNC-overexpressing RT2 tumors and in cellular models comprising tumor and endothelial cells in vitro, the expression of Lgr5 and of several Notch pathway members are unaffected in the in vivo and in vitro models we used (Table S3; F.S. and G.O., unpublished data). Multiple explanations for these differences may exist, such as difference in model systems and in organ and tissue context. We have shown that the ectopic expression of TNC leads to *DKK1* downregulation and Wnt signaling activation in RT2/TNC tumors as revealed by the upregulation of other Wnt target genes, including the prototypical Wnt target *Axin2*. Conversely, in RT2/TNCKO tumors DKK1 levels were increased, but *Axin2* expression was unchanged. This result is in line with a previous report showing that the Wnt pathway has minimal basal activity in pancreatic beta tumor cells and is dispensable for RT2 tumor progression (Herzig et al., 2007). In addition to canonical Wnt signaling, the DKK1 receptor LRP6 was shown to promote PDGF-BB, TGF-β and CTGF signaling in pericytes and fibroblasts. Importantly, these signaling activities were blocked by DKK1 through binding to LRP6 (Ren et al., 2013). We suggest that a TNC-rich matrix induces a microenvironment with low DKK1 levels that is susceptible to angiogenic signaling from Wnt and other pathways regulated by DKK1. This possibility is supported by our results that have shown an inverse correlation of TNC and DKK1 expression, promotion of the angiogenic switch by TNC, and a strong downregulation of DKK1 by TNC in tumor and several stromal cell types.

In the TNC transgenic RT2 model, we observed that TNC promotes multiple early events such as proliferation and survival in hyperplastic islets, Wnt target upregulation in small, differentiated tumors, and the angiogenic switch. A major role of TNC early in tumorigenesis combined with a less functional vasculature may explain why macroscopically visible RT2 tumors of the different genotypes did not differ in size. A potential early role of TNC in tumorigenesis has not received much attention because cancer patient data with a correlation of high TNC expression and malignancy (Midwood and Orend, 2009; Oskarsson et al., 2011) rather suggested a major role of TNC in late events. In human cancer tissue, early events cannot be easily addressed, which might explain why we did not see a correlation of *TNC* and *DKK1* mRNA expression levels in human cancer tissues. TNC promotes metastasis (Minn et al., 2005; Oskarsson et al., 2011; Tavazoie et al., 2008), which has also been recapitulated here in the RT2 model and in human insulinomas where the highest TNC expression levels were observed in the few available metastatic insulinomas.

In summary, we have shown that DKK1 expression is dependent on actin stress fibers that are disrupted by TNC. We have established a transgenic immune-competent tumor mouse model that mimics the high expression of TNC observed in human cancer. Our results prove that TNC plays crucial roles along tumor progression by promoting early and late events. We demonstrate that TNC levels determine the extent of tumor cell survival, invasion, tumor angiogenesis, and metastasis. These phenotypes appear to be linked to DKK1 downregulation creating a proangiogenic tumor microenvironment. Finally, our human TNC-expressing transgenic tumor mice offer a model for human insulinoma progression and for the preclinical evaluation of drugs that target human TNC.

EXPERIMENTAL PROCEDURES

Mice

Generation of transgenic RipTNC mice, breeding, genotyping, xenograft experiments, and analysis of tumor material are specified in the Supplemental Information. RT2 mice developing pancreatic neuroendocrine tumors (Hanahan, 1985) were crossed with RipTNC (this study) or TNCKO (Forsberg et al., 1996) mice to generate double-transgenic mice with forced expression of TNC (RT2/TNC) or lacking TNC expression (RT2/TNCKO). Experiments comprising animals were performed according to the guidelines of INSERM and the Swiss Federal Veterinary Office.

Histopathological Analysis of Mouse and Human Tissue

Tumor incidence per mouse was determined as the number of all visible tumors with a minimal diameter of 1 mm. Tumor volume was calculated assuming a spherical shape with formula $V = 1/6 \times \pi \times d^3$ (d = tumor diameter). Pancreata, liver, and lung tissue were isolated, fixed in 4% paraformaldehyde (PFA) overnight followed by embedding in paraffin, fixed for 2 hr in 4% PFA, immersed in 20% sucrose overnight, and embedded in Tissue-Tek O.C.T. (Sakura Finetek) or freshly embedded in O.C.T. and frozen on dry ice.

Histological analysis was performed on 5 μm (paraffin embedded) and 7 μm (cryopreserved) tissue sections by staining with H&E or immunostaining. Primary antibodies were incubated overnight at 4°C. Immunohistochemical (IHC) detection was performed on paraffin-embedded tissue using Vectastain developing system (Vector Laboratories), followed by staining with hematoxilin. Detection by IF was performed on fixed or fresh-frozen tissue using fluorescein-isothiocyanate- or Cy3-coupled secondary antibodies (Jackson ImmunoResearch Laboratories); cell nuclei were stained with DAPI. Primary antibodies detecting the following molecules were used: phosphohistone H3 (PH3, 1:200, Upstate 06-570), cleaved caspase-3 (1:50, Cell Signaling Technology 9661), CD31 (1:50, BD Pharmingen 550274, Acris BM4086), NG2 (1:200, Millipore AB5320), insulin (1:200, Dako Cytomation A0564), glucagon (1:1000, Sigma G2654), KI67 (1:200, clone SP6, Thermo Scientific, RM-9106-S1), human TNC (BC-24, 1:3000, Sigma T2551), and fibrinogen (1:500, Dako A0080). Anti-mouse TNC MTn12 (Aufderheide and Ekblom, 1988) and anti-human TNC B28.13 antibodies (Schenk et al., 1995) were purified from hybridoma culture supernatants.

Quantification of IF microscopic pictures was done using ImageJ (National Institutes of Health) software. Staining protocols (fixation, blocking, antibody dilution) and image acquisition setting (microscope, magnification, light intensity, exposure time) were kept constant per experiment. Data were quantified

as counted events over analyzed tumor area (PH3), as area fraction over analyzed DAPI-positive cell area (cleaved caspase-3, PH3, and KI67) or as area fraction over analyzed tumor area (CD31, NG2, and fibrinogen).

Cell-Culture Experiments

Coating of cell-culture dishes with FN and TNC was performed as described earlier (Huang et al., 2001; Lange et al., 2007). Cells were seeded on the coated surfaces and analyzed using standard protocols as described. mRNA was extracted from paraffin-embedded tissue and analyzed by qRT-PCR.

Human Insulinomas

Tumor material was obtained from the Klinikum rechts der Isar (Munich, Germany) or the Hôpital de Hautepierre (Strasbourg, France). Analysis of the human insulinomas had been approved by the respective ethics committees. All samples were obtained after prior patient informed written consent. Tumor tissue was obtained from 14 patients (group 1, Munich, and group 2, Strasbourg) with endocrine pancreatic cancer and was histopathologically confirmed as insulinoma by an experienced pathologist. Presence of metastasis was diagnosed in three patients (liver or lymph node n = 2, group 1; liver and lymph node n = 1, group 2).

SUPPLEMENTAL INFORMATION

Supplemental Information includes Supplemental Experimental Procedures, seven figures, and three tables and can be found with this article online at http://dx.doi.org/10.1016/j.celrep.2013.09.014.

ACKNOWLEDGMENTS

We thank W. Huang, A.-C. Feutz, K. Strittmatter, H. Antoniadis, P. Lorentz, M.-F. Hamou, B. Scolari, R. Buergy, E. Domany, J. Huelsken, R. Fässler, M. Kedinger, I. Gross, G. Posern, R. Moon, and R. Chiquet-Ehrismann for technical assistance, reagents, mice, discussion, and help with the generation of the transgenic mice. Support was generously provided by the University Strasbourg and the Association pour la Recherche sur le cancer (to A.S.); the Fondation des Treilles (to F.S.); INSERM/Region Alsace (to I.G.); the Ligue contre le Cancer (to O.L., P.S.-A., and G.O.); and INSERM, University Strasbourg, Agence National de la Recherche, Krebsliga Beider Basel, the Association for International Cancer Research, the Swiss National Science Foundation, Oncosuisse, the Novartis Foundation for Biological and Medical Sciences, the Hôpital de Hautepierre, the Association pour la Recherche contre le Cancer, and the Institut National du Cancer (to G.O.).

Received: March 20, 2013
Revised: August 7, 2013
Accepted: September 10, 2013
Published: October 17, 2013

REFERENCES

Aguilera, O., Fraga, M.F., Ballestar, E., Paz, M.F., Herranz, M., Espada, J., García, J.M., Muñoz, A., Esteller, M., and González-Sancho, J.M. (2006). Epigenetic inactivation of the Wnt antagonist DICKKOPF-1 (DKK-1) gene in human colorectal cancer. Oncogene *25*, 4116–4121.

Aguirre-Ghiso, J.A. (2007). Models, mechanisms and clinical evidence for cancer dormancy. Nat. Rev. *7*, 834–846.

Aicher, A., Kollet, O., Heeschen, C., Liebner, S., Urbich, C., Ihling, C., Orlandi, A., Lapidot, T., Zeiher, A.M., and Dimmeler, S. (2008). The Wnt antagonist Dickkopf-1 mobilizes vasculogenic progenitor cells via activation of the bone marrow endosteal stem cell niche. Circ. Res. *103*, 796–803.

Almog, N. (2010). Molecular mechanisms underlying tumor dormancy. Cancer Lett. *294*, 139–146.

Aufderheide, E., and Ekblom, P. (1988). Tenascin during gut development: appearance in the mesenchyme, shift in molecular forms, and dependence on epithelial-mesenchymal interactions. J. Cell Biol. *107*, 2341–2349.

Barbolina, M.V., Liu, Y., Gurler, H., Kim, M., Kajdacsy-Balla, A.A., Rooper, L., Shepard, J., Weiss, M., Shea, L.D., Penzes, P., et al. (2013). Matrix rigidity activates Wnt signaling through down-regulation of Dickkopf-1 protein. J. Biol. Chem. *288*, 141–151.

Bass, M.D., and Humphries, M.J. (2002). Cytoplasmic interactions of syndecan-4 orchestrate adhesion receptor and growth factor receptor signalling. Biochem. J. *368*, 1–15.

Bissell, M.J., and Labarge, M.A. (2005). Context, tissue plasticity, and cancer: are tumor stem cells also regulated by the microenvironment? Cancer Cell *7*, 17–23.

Chiquet-Ehrismann, R., Mackie, E.J., Pearson, C.A., and Sakakura, T. (1986). Tenascin: an extracellular matrix protein involved in tissue interactions during fetal development and oncogenesis. Cell *47*, 131–139.

De Langhe, S.P., Sala, F.G., Del Moral, P.M., Fairbanks, T.J., Yamada, K.M., Warburton, D., Burns, R.C., and Bellusci, S. (2005). Dickkopf-1 (DKK1) reveals that fibronectin is a major target of Wnt signaling in branching morphogenesis of the mouse embryonic lung. Dev. Biol. *277*, 316–331.

De Laporte, L., Rice, J.J., Tortelli, F., and Hubbell, J.A. (2013). Tenascin C promiscuously binds growth factors via its fifth fibronectin type III-like domain. PLoS ONE *8*, e62076.

Forsberg, E., Hirsch, E., Fröhlich, L., Meyer, M., Ekblom, P., Aszodi, A., Werner, S., and Fässler, R. (1996). Skin wounds and severed nerves heal normally in mice lacking tenascin-C. Proc. Natl. Acad. Sci. USA *93*, 6594–6599.

Gineitis, D., and Treisman, R. (2001). Differential usage of signal transduction pathways defines two types of serum response factor target gene. J. Biol. Chem. *276*, 24531–24539.

Glinka, A., Wu, W., Delius, H., Monaghan, A.P., Blumenstock, C., and Niehrs, C. (1998). Dickkopf-1 is a member of a new family of secreted proteins and functions in head induction. Nature *391*, 357–362.

Hanahan, D. (1985). Heritable formation of pancreatic beta-cell tumours in transgenic mice expressing recombinant insulin/simian virus 40 oncogenes. Nature *315*, 115–122.

Hanahan, D., and Folkman, J. (1996). Patterns and emerging mechanisms of the angiogenic switch during tumorigenesis. Cell *86*, 353–364.

Hanahan, D., Christofori, G., Naik, P., and Arbeit, J. (1996). Transgenic mouse models of tumour angiogenesis: the angiogenic switch, its molecular controls, and prospects for preclinical therapeutic models. Eur. J. Cancer *32A*, 2386–2393.

Herzig, M., Savarese, F., Novatchkova, M., Semb, H., and Christofori, G. (2007). Tumor progression induced by the loss of E-cadherin independent of beta-catenin/Tcf-mediated Wnt signaling. Oncogene *26*, 2290–2298.

Huang, W., Chiquet-Ehrismann, R., Moyano, J.V., Garcia-Pardo, A., and Orend, G. (2001). Interference of tenascin-C with syndecan-4 binding to fibronectin blocks cell adhesion and stimulates tumor cell proliferation. Cancer Res. *61*, 8586–8594.

Huijbers, E.J., Ringvall, M., Femel, J., Kalamajski, S., Lukinius, A., Abrink, M., Hellman, L., and Olsson, A.K. (2010). Vaccination against the extra domain-B of fibronectin as a novel tumor therapy. FASEB J. *24*, 4535–4544.

Kerbel, R.S. (2008). Tumor angiogenesis. N. Engl. J. Med. *358*, 2039–2049.

Lange, K., Kammerer, M., Hegi, M.E., Grotegut, S., Dittmann, A., Huang, W., Fluri, E., Yip, G.W., Götte, M., Ruiz, C., and Orend, G. (2007). Endothelin receptor type B counteracts tenascin-C-induced endothelin receptor type A-dependent focal adhesion and actin stress fiber disorganization. Cancer Res. *67*, 6163–6173.

Lange, K., Kammerer, M., Saupe, F., Hegi, M.E., Grotegut, S., Fluri, E., and Orend, G. (2008). Combined lysophosphatidic acid/platelet-derived growth factor signaling triggers glioma cell migration in a tenascin-C microenvironment. Cancer Res. *68*, 6942–6952.

Levental, K.R., Yu, H., Kass, L., Lakins, J.N., Egeblad, M., Erler, J.T., Fong, S.F., Csiszar, K., Giaccia, A., Weninger, W., et al. (2009). Matrix crosslinking forces tumor progression by enhancing integrin signaling. Cell *139*, 891–906.

Liao, Y.L., Sun, Y.M., Chau, G.Y., Chau, Y.P., Lai, T.C., Wang, J.L., Horng, J.T., Hsiao, M., and Tsou, A.P. (2008). Identification of SOX4 target genes using phylogenetic footprinting-based prediction from expression microarrays suggests that overexpression of SOX4 potentiates metastasis in hepatocellular carcinoma. Oncogene *27*, 5578–5589.

Lu, P., Weaver, V.M., and Werb, Z. (2012). The extracellular matrix: a dynamic niche in cancer progression. J. Cell Biol. *196*, 395–406.

Menezes, M.E., Mitra, A., Shevde, L.A., and Samant, R.S. (2012). DNAJB6 governs a novel regulatory loop determining Wnt/β-catenin signalling activity. Biochem. J. *444*, 573–580.

Metz, D.C., and Jensen, R.T. (2008). Gastrointestinal neuroendocrine tumors: pancreatic endocrine tumors. Gastroenterology *135*, 1469–1492.

Midwood, K.S., Valenick, L.V., Hsia, H.C., and Schwarzbauer, J.E. (2004). Coregulation of fibronectin signaling and matrix contraction by tenascin-C and syndecan-4. Mol. Biol. Cell *15*, 5670–5677.

Midwood, K.S., and Orend, G. (2009). The role of tenascin-C in tissue injury and tumorigenesis. J. Cell Commun. Signal *3*, 287–310.

Midwood, K.S., Hussenet, T., Langlois, B., and Orend, G. (2011). Advances in tenascin-C biology. Cell. Mol. Life Sci. *68*, 3175–3199.

Mills, G.B., and Moolenaar, W.H. (2003). The emerging role of lysophosphatidic acid in cancer. Nat. Rev. *3*, 582–591.

Min, J.K., Park, H., Choi, H.J., Kim, Y., Pyun, B.J., Agrawal, V., Song, B.W., Jeon, J., Maeng, Y.S., Rho, S.S., et al. (2011). The WNT antagonist Dickkopf2 promotes angiogenesis in rodent and human endothelial cells. J. Clin. Invest. *121*, 1882–1893.

Minn, A.J., Kang, Y., Serganova, I., Gupta, G.P., Giri, D.D., Doubrovin, M., Ponomarev, V., Gerald, W.L., Blasberg, R., and Massagué, J. (2005). Distinct organ-specific metastatic potential of individual breast cancer cells and primary tumors. J. Clin. Invest. *115*, 44–55.

Miralles, F., Posern, G., Zaromytidou, A.I., and Treisman, R. (2003). Actin dynamics control SRF activity by regulation of its coactivator MAL. Cell *113*, 329–342.

Murphy-Ullrich, J.E., Lightner, V.A., Aukhil, I., Yan, Y.Z., Erickson, H.P., and Höök, M. (1991). Focal adhesion integrity is downregulated by the alternatively spliced domain of human tenascin. J. Cell Biol. *115*, 1127–1136.

Nevins, J.R. (2001). The Rb/E2F pathway and cancer. Hum. Mol. Genet. *10*, 699–703.

Oh, H., Ryu, J.H., Jeon, J., Yang, S., Chun, C.H., Park, H., Kim, H.J., Kim, W.S., Kim, H.H., Kwon, Y.G., and Chun, J.S. (2012). Misexpression of Dickkopf-1 in endothelial cells, but not in chondrocytes or hypertrophic chondrocytes, causes defects in endochondral ossification. J. Bone Miner. Res. *27*, 1335–1344.

Orend, G., Huang, W., Olayioye, M.A., Hynes, N.E., and Chiquet-Ehrismann, R. (2003). Tenascin-C blocks cell-cycle progression of anchorage-dependent fibroblasts on fibronectin through inhibition of syndecan-4. Oncogene *22*, 3917–3926.

Oskarsson, T., Acharyya, S., Zhang, X.H., Vanharanta, S., Tavazoie, S.F., Morris, P.G., Downey, R.J., Manova-Todorova, K., Brogi, E., and Massagué, J. (2011). Breast cancer cells produce tenascin C as a metastatic niche component to colonize the lungs. Nat. Med. *17*, 867–874.

Parangi, S., O'Reilly, M., Christofori, G., Holmgren, L., Grosfeld, J., Folkman, J., and Hanahan, D. (1996). Antiangiogenic therapy of transgenic mice impairs de novo tumor growth. Proc. Natl. Acad. Sci. USA *93*, 2002–2007.

Pendás-Franco, N., Aguilera, O., Pereira, F., González-Sancho, J.M., and Muñoz, A. (2008). Vitamin D and Wnt/beta-catenin pathway in colon cancer: role and regulation of DICKKOPF genes. Anticancer Res. *28*(5A), 2613–2623.

Pipas, J.M., and Levine, A.J. (2001). Role of T antigen interactions with p53 in tumorigenesis. Semin. Cancer Biol. *11*, 23–30.

Reis, M., Czupalla, C.J., Ziegler, N., Devraj, K., Zinke, J., Seidel, S., Heck, R., Thom, S., Macas, J., Bockamp, E., et al. (2012). Endothelial Wnt/β-catenin signaling inhibits glioma angiogenesis and normalizes tumor blood vessels by inducing PDGF-B expression. J. Exp. Med. *209*, 1611–1627.

Ren, S., Johnson, B.G., Kida, Y., Ip, C., Davidson, K.C., Lin, S.L., Kobayashi, A., Lang, R.A., Hadjantonakis, A.K., Moon, R.T., and Duffield, J.S. (2013). LRP-6 is a coreceptor for multiple fibrogenic signaling pathways in pericytes and myofibroblasts that are inhibited by DKK-1. Proc. Natl. Acad. Sci. USA *110*, 1440–1445.

Ruiz, C., Huang, W., Hegi, M.E., Lange, K., Hamou, M.F., Fluri, E., Oakeley, E.J., Chiquet-Ehrismann, R., and Orend, G. (2004). Growth promoting signaling by tenascin-C [corrected]. Cancer Res. *64*, 7377–7385.

Schenk, S., Muser, J., Vollmer, G., and Chiquet-Ehrismann, R. (1995). Tenascin-C in serum: a questionable tumor marker. Int. J. Cancer *61*, 443–449.

Smadja, D.M., d'Audigier, C., Weiswald, L.B., Badoual, C., Dangles-Marie, V., Mauge, L., Evrard, S., Laurendeau, I., Lallemand, F., Germain, S., et al. (2010). The Wnt antagonist Dickkopf-1 increases endothelial progenitor cell angiogenic potential. Arterioscler. Thromb. Vasc. Biol. *30*, 2544–2552.

Song, S., Ewald, A.J., Stallcup, W., Werb, Z., and Bergers, G. (2005). PDGFRbeta+ perivascular progenitor cells in tumours regulate pericyte differentiation and vascular survival. Nat. Cell Biol. *7*, 870–879.

Spencer, J.A., and Misra, R.P. (1999). Expression of the SRF gene occurs through a Ras/Sp/SRF-mediated-mechanism in response to serum growth signals. Oncogene *18*, 7319–7327.

Tanaka, K., Hiraiwa, N., Hashimoto, H., Yamazaki, Y., and Kusakabe, M. (2004). Tenascin-C regulates angiogenesis in tumor through the regulation of vascular endothelial growth factor expression. Int. J. Cancer *108*, 31–40.

Tavazoie, S.F., Alarcón, C., Oskarsson, T., Padua, D., Wang, Q., Bos, P.D., Gerald, W.L., and Massagué, J. (2008). Endogenous human microRNAs that suppress breast cancer metastasis. Nature *451*, 147–152.

van Obberghen-Schilling, E., Tucker, R.T., Saupe, F., Gasser, I., Cseh, B., and Orend, G. (2011). Fibronectin and tenascin-C: accomplices in vascular morphogenesis during development and tumor growth. Int. J. Dev. Biol. *55*, 511–525.

Wenk, M.B., Midwood, K.S., and Schwarzbauer, J.E. (2000). Tenascin-C suppresses Rho activation. J. Cell Biol. *150*, 913–920.

Wu, F.T., Stefanini, M.O., Mac Gabhann, F., and Popel, A.S. (2009). A compartment model of VEGF distribution in humans in the presence of soluble VEGF receptor-1 acting as a ligand trap. PLoS ONE *4*, e5108.

Zhou, A.D., Diao, L.T., Xu, H., Xiao, Z.D., Li, J.H., Zhou, H., and Qu, L.H. (2012). β-Catenin/LEF1 transactivates the microRNA-371-373 cluster that modulates the Wnt/β-catenin-signaling pathway. Oncogene *31*, 2968–2978.

Cell Reports, Volume *5*
Supplemental Information

Tenascin-C Downregulates Wnt Inhibitor Dickkopf-1, Promoting Tumorigenesis in a Neuroendocrine Tumor Model

Falk Saupe, Anja Schwenzer, Yundan Jia, Isabelle Gasser, Caroline Spenle, Benoit Langlois, Martial Kammerer, Olivier Lefebvre, Ruslan Hlushchuk, Tristan Rupp, Marija Marko, Michael van der Heyden, Gerard Cremel, Christiane Arnold, Annick Klein, Patricia Simon-Assmann, Valentin Djonov, Agnes Neuville-Mechine, Irene Esposito, Julia Slotta-Huspenina, Klaus-Peter Janssen, Olivier de Wever, Gerhard Christofori, Thomas Hussenet, and Gertraud Orend

Extended Experimental Procedures

Generation of transgenic RipTNC mice

The human TNC cDNA sequence (GenBank X78565.1) comprising all but AD1 and AD2 extra domains was removed from the HxBL.pBS plasmid (Aukhil et al., 1993) and cloned into the Rip1 expression vector (Hanahan, 1985) for insulin promoter driven expression by using the intermediate pcDNA3.1/Hygro(-) vector (**Figure S1B**). Successful cloning was confirmed by restriction enzyme analysis and partial sequencing. Expression and secretion of TNC was determined in a RT2 cell line by immunostaining and sandwich ELISA. The TNC expression vector was injected into the pronucleus of fertilized oocytes giving rise to transgenic RipTNC mice with stable transmission and expression of the transgene. Transgenic mice were healthy and fertile and did not exhibit any detectable alterations in tissue morphology (**Figure S1F**) nor blood glucose homeostasis (**Figure S1G**). All experimental procedures involving mice were done according to the guidelines of INSERM and the Swiss Federal Veterinary Office.

Generation of tumor mice with different TNC expression levels

RT2 mice (Hanahan, 1985) were bred with RipTNC mice (three lines) or TNCKO mice (Forsberg et al., 1996) to generate RT2/TNC or RT2/TNCKO mice respectively, with different TNC expression levels (**Figure S1D, E**). TNC expression analysis confirmed that tumors of RT2/TNC mice expressed transgenic human TNC (**Figure S1D**), whereas those from RT2/TNCKO mice lacked the TNC protein (**Figure S1E).** Starting at the age of 10

weeks the drinking water was supplemented with 5% (w/v) glucose (FLUKA). Most data were obtained from mice in a C57Bl6 background except results in **Figure 2C, Figure 3C** and **Figure S3C** that were derived from RT2/TNCKO mice and littermates with one TNC copy (RT2/TNC+/-) in a mixed 129/Sv-C57Bl6 background. For genotyping by PCR the following primers were used, RipTNC (Fwd: 5'-TAA TGG GAC AAA CAG CAA AG-3', Rev: 5'-GAA AGA CAC CTG CCA ACA GC-3'), SV40 Tag (Fwd: 5'-GGA CAA ACC ACA ACT AGA ATG CAG-3', Rev: 5'-CAG AGC AGA ATT GTG GAG TGG-3') and TNCKO (Fwd wt: 5'-CTG CCA GGC ATC TTT CTA GC-3', Fwd TNCKO: 5'-CTG CTC TTT ACT GAA GGC TC-3', Rev: 5'-TTC TGC AGG TTG GAG GCA AC-3').

Tumor grading

Tumor grading was performed on H&E stained paraffin sections and classified into adenomas (differentiated tumor cells, encapsulated tumors) and Grade 1 carcinomas (differentiated tumor cells, one invasive tumor front), Grade 2 carcinomas (partially dedifferentiated tumor cells, more than one invasive tumor front) and Grade 3 carcinomas (heterogeneous appearance and loss of differentiated tumor cells, many invasion sites).

Human insulinomas

Tumor material was obtained from the Klinikum rechts der Isar (Munich, Germany) or the Hôpital de Hautepierre (Strasbourg, France) with prior patient informed written consent. Patients underwent surgical resection at the Department of Surgery, Klinikum rechts der Isar, Munich, Germany (between 1991 and 2011) (Group 1) and at the Hôpital de Hautepierre, Strasbourg (between 1994 and 2007) (Group 2). Tissue specimens were transferred into liquid nitrogen and stored until further processing for mRNA extraction, embedded in Tissue-Tek (Sakura, Labonord) and stored at -80°C, or fixed in formalin and embedded in paraffin. The median age of patients from Group 1 was 52 years (35 to 82 years, 5 male and 2 female patients) and of patients from Group 2 was 46 years (13 to 69 years, 2 male and 5 female patients). Presence of metastasis was diagnosed in three

patients (liver or lymph node n = 2, Group 1; liver and lymph node n = 1, Group 2). Analysis by qRTPCR, IF and IHC was performed as described.

Oral glucose tolerance test

12 week old mice (14 RipTNC and 15 wildtype) were starved overnight in clean cages with free access to water. Tail vein blood glucose concentration was measured at time = 0 using Glucofix sensor for Glucofix mio (A. Menarini Diagnostics). 2 mg glucose per g body weight was orally administered by gavage and blood glucose levels (mg/dl) were measured every 15 minutes for 1.5h.

Perfusion, fibrinogen staining and quantification of tumor vessel leakiness

Twelve week old mice were anesthesized by i.p. injection of pentobarbital (5%, 4µl/g body weight). The chest was opened and the right atrium was cut. The left heart ventricle was perfused with 10 ml of 4% paraformaldehyde (PFA) followed by 10 ml of PBS through a 23G syringe connected to a peristaltic pump at constant pressure. The pancreas was dissected, incubated overnight in 20% sucrose at 4°C and frozen in O.C.T. Seven µm sections were processed for fibrinogen and CD31 immunofluorescent staining as described. Fibrinogen immunoreactive areas were measured by using the ImageJ software and were expressed as percentage of tumor/islet total area (area fraction).

Gene expression analysis of mouse tissue and human insulinomas

Tissue from isolated tumors, liver and lung was snap frozen in liquid nitrogen. Total RNA extracted with NucleoSpin RNA II kit (Macherey-Nagel) from liver, KRIB tumors (1 µg), RT2 tumors or lung tissue (2 µg) was treated with DNase I (Invitrogen) and reverse transcribed (MultiScribe reverse transcriptase, Applied Biosystems). qRTPCR was done on cDNA diluted 1:5 (liver, lung) or 1:10 (tumors) with specific primers (Roche Probefinder v2.45, see primer list) on a 7500 Real Time PCR machine (Applied Biosystems) using SYBR green or Taqman reaction mixtures (Applied Biosystems). Data were normalized versus TBP (liver, lung), HMBS (KRIB tumors), GAPDH (human insulinoma) or a combined

value of RPL19, TBP and GAPDH (RT2 tumors). Relative expression levels ($2^{-\Delta\Delta ct}$) were calculated for each individual sample.

Isolation of pancreatic islets

Langerhans islets were isolated from 8 week old RT2 mice by using Liberase RI (Roche) (RT2/TNC and RT2) and Liberase TL (Roche) (RT2/TNCKO and RT2). The pancreas was perfused via the bile duct with 2 ml Liberase solution (0.82 (RI), 1 (TL) Wünsch units/ml), collected and digested at 37°C (24 minutes (Liberase RI), 17 minutes (Liberase TL)). Upon recovery from the interphase of a Histopaque 1077 (Sigma)/DMEM centrifugation gradient (30 minutes, 1500 x g) intact islets were handpicked under a stereomicroscope and quantified as non-angiogenic (white) or angiogenic (red).

Methylmethacrylate (Mercox) casting and SEM analysis

Anaesthetized mice were perfused through the thoracic aorta with a 0.9% sodium chloride/1% heparin/1% procaine solution followed by a freshly prepared Mercox solution (Vilene Japan Hospital Co. Ltd.) containing 0.1 ml accelerator per 5 ml resin. After solidification pancreata were excised and kept for 3 weeks in 7.5% KOH for tissue dissolution. Casts were dehydrated in ethanol and vacuum dried. Samples were mounted on aluminum stubs, sputtered with gold and examined in a Philips XL-30 SFEG scan electron microscope.

Cell culture, gene expression and immunoblotting

Human brain vasculature pericytes (ScienCell 1200), tumor cell lines, monocyte/macrophage cell lines (J774.A1 and RAW264.7) and L cells (fibroblasts, control and overexpression of Wnt-3A) (American Type Culture Collection, Rockville, MD, (ATCC)) were maintained in DMEM/4.5g/l glucose/10% FCS. Cancer associated fibroblasts (CAF) CT5.1 and CT14 were cultured in DMEM/1g/l glucose/10% FCS. BOSC cells (ATCC) were maintained in DMEM/10% FCS supplemented with 1 mM sodium pyruvate/10 mM Hepes and, HUVEC (Promo cell, C-12203) were maintained in

Endothelial cell growth medium (PromoCell, C-22010). T98G:TPM1, T98G:Syndesmos and T98G:shTPM1 cells (Lange et al., 2008; Ruiz et al., 2004) were cultured in DMEM/10%FCS with 400 µg/ml G418.

Human CAFs were isolated from colorectal adenocarcinoma resection specimens from 2 patients that were obtained in accordance with the local ethics committee (Ghent University Hospital) (De Boeck et al., 2013; De Wever et al., 2004). Tissue fragments were cut in 1-2 mm^3 pieces and transferred into a pre-scratched 6-well plate with 100 µl FCS supplemented antibiotica DMEM. Cultures were incubated at 37°C with 10% CO2 in air for 24h. DMEM containing 10% FCS was added into each well. Cell outgrowth was observed after 3-6 days. After 15 days, adherent cells were transferred to 25 cm^2 tissue culture flasks.

Conditioned medium containing Wnt-3A or mDKK1 was collected from L cells overexpressing Wnt-3A and from KRIB cells overexpressing mDKK1, respectively after 3 to 4 days of culture. Medium was filter-sterilized and stored at -20°C. Cells starved in DMEM/1% FCS (tumor cells, pericytes, CAF) or M199/1% FCS/1µg/ml hydrocortison/10 ng/ml heparin/10 ng/ml mEGF/10 ng/ml bFGF (HUVEC) were seeded onto matrix coated dishes as published (Huang et al., 2001; Lange et al., 2007). Briefly, FN and TNC were sequentially coated in PBS/0.01% Tween-20 at 1 µg/cm^2 before saturation of the non-coated surface with 10 mg/ml BSA/PBS.

Cells were starved overnight before treatment with 1, 10 or 30 µM LPA for 3-4h on FN or FN/TNC substrata (Santa Cruz, H_2O), 5 µg/ml Actinomycin D for 30, 60 or 90 minutes (Sigma-Aldrich, DMSO), 5 µg/ml Latrunculin B for 3h (Calbiochem, DMSO) and 2 µg/ml Cytochalasin D four 3h (Calbiochem, DMSO).

Gene expression analysis of cultured cells

RNA was isolated (NucleoSpin RNA extraction kit, Macherey-Nagel or Trizol, Life Technologies) according to the manufacturer's instructions. RNA was reverse transribed (MultiScribe reverse transcriptase, Applied Biosystems) and qRTPCR was done on cDNA diluted 1:2.5 in water with specific primers (see primer list) on a 7500 Real Time PCR

machine (Applied Biosystems) using SYBR green reaction mixture (Applied Biosystems). Data were normalized versus ß2-microglobulin expression and relative expression levels was calculated ($2^{-\Delta\Delta ct}$).

Immunoblotting

For immunoblotting cells were lysed in Laemmli buffer (Laemmli, 1970). Antibodies against the following molecules were used: DKK1 (n-terminal, Sigma-Aldrich, D3195, 1:1500), DKK1 (R&D, AF1096, 1:500), 6x His-tag (Abcam, ab18184, 1:1000), RhoA (Santa-Cruz, sc-418, 1:5000), α-tubulin (CP06, Oncogene, Boston, MA, USA, 1:2000). Secondary antibodies were ECL horseradish peroxidase linked whole anti-rabbit (NA934V) and anti-mouse (NXA931) (GE Healthcare, Buckinghamshire, UK) and donkey anti-goat IgG (sc-2020, Santa Cruz, Biotechnology). Amersham ECL (RPN2106) or Amersham ECL-Plus Western blotting detection system (RPN2132) (GE Healthcare, Buckinghamshire, UK) was used.

Immunofluorescence staining of cultured cells

Cells were fixed in 1% PFA for 10 minutes and permeabilized in PBS-Triton 0.1% for 10 minutes. Cells were stained with anti-vinculin (Abcam; 1/50; 2h) and anti-mouse Alexa-488 (Jackson ImmunoResearch; 1/800; 1h). For phalloidin staining cells were incubated for 20 minutes with phalloidin-tetramethylrhodamine B isothiocyanate (Sigma P1951; 1/200). Nuclei were stained with DAPI (Sigma D9542).

Retrovirus construction and infection, plasmid transfection and reporter assays

For generating mDKK1 cDNA with a V5-His-tag the mDKK1 cDNA (Ruiz et al., 2004) was cloned into the pcDNA3.1-V5-His-TOPO vector (Invitrogen) according to the manufacturer's guidelines. For generating the pQCXIP-mDKK1-V5-His vector a BamHI and an EcoRI site were added in pcDNA3.1-mDKK1-V5-His-TOPO plasmid before the ATG or the stop codon of the mouse DKK1 cDNA respectively, using the GeneEditor™ in vitro

site-directed mutagenesis system, with the primers 5'-GGT GGA ATT GCC CTT GGA TCC ACA TGA TGG TTG TGT-3' and 5'-P-ACC ATC ACC ATT GAG AAT TCA CCC GCT GAT CAG CC-3'. Upon BamHI-EcoRI cleavage, the mDKK1-V5-His fragment was gel purified (NucleoSpin® Extract II, Machery-Nagel, France) and cloned in the BamHI-EcoRI site of the pQCXIP retroviral vector (Clontech, Ozyme, France) generating the pQCXIP-mDKK1-V5-His vector. BOSC cells were transfected with the pQCXIP-mDKK1-V5-His vector or empty control (CTR) vector to obtain retroviruses for transduction of KRIB cells followed by selection with puromycin (2.5 µg/ml). Expression of mDKK1 was determined by qRTPCR and immunoblotting.

T98G were transiently transfected (JetPEI, Polyplus, Strasbourg, France) with plasmids encoding RhoA wt (Addgene Plasmid 12962: pRK5-myc-RhoA-wt), RhoA-Q63L (Addgene Plasmid 12964: pRK5-myc-RhoA-Q63L) and RhoA-T19N (Addgene Plasmid 12963: pRK5-myc-RhoA-T19N). Empty pCB6 plasmid was used for control transfection.

Luciferase reporter assays

For the β-catenin luciferase reporter assay, cells were transiently transfected (JetPEI, Polyplus, Strasbourg, France) with the Super-8xTOPFlash or control Super-8xFOPFlash plasmids (mutant TCF/LEF binding sites) (Veeman et al., 2003) (obtained from Addgene, plasmids 12456 and 12457). Upon seeding for 5h on matrix coated dishes, CM containing Wnt-3A, mDKK1 or CTR medium was added for a total of 48h. TOPFlash luciferase activity was calculated after normalization to Renilla and FOPFlash activity (Dual-luciferase reporter assay system, Promega, Madison, WI, USA).

For SRF luciferase reporter assays T98G cells were transfected with the 3DA.Luc plasmid (provided by Guido Posern, University Halle-Wittenberg, Halle, Germany) encoding c-fos derived SRF binding sites and a pRL-TK plasmid for normalization of the luciferase signal.

A 3177 bp human DKK1 promoter sequence was cloned from HCT116 genomic DNA into

the multiple cloning site of the pGL3-basic luciferase reporter vector (Promega). Cells were transiently transfected with the pGL3-DKK1 promoter construct or empty pGL3-basic vector for 40h. Luciferase activity normalized to Renilla activity is presented as the ratio of pGL3-DKK1 to pGL3-basic.

Generation of KRIB shDKK1 cells

For generation of KRIB shDKK1 cells, KRIB cells were infected with MISSION lentiviral transduction particles (SHCLNV, clone ID TRCN0000033386, Sigmal-Aldrich) or MISSION non-target shRNA control transduction particles (SHC002V, Sigma-Aldrich) with a MOI = 10 and, transduced cells were selected with 10 µg/ml puromycin.

Cell proliferation assay

To determine cell proliferation, cells were plated into 96-well plates (5 x 10^3 cells/well in quadruplicate for each time point). A MTS assay was performed following manufacturer's instructions (CellTiter 96® aqueous non-radioactive cell proliferation assay, Promega) after 24h (day 1), 48h (day 2) and 72h (day 3). Measures were normalized to the relative cell number on day 1.

HUVEC tubulogenesis assay

Tubulogenesis assessment was done in 15 well dishes (µ-Slide Angiogenesis, Ibidi LLC), using growth factor reduced Matrigel (BD Bioscience). The matrix was prepared by loading 10 µl of Matrigel in each well followed by solidification for 45-60 minutes at 37°C in a humidified incubator. HUVEC (Promocell) were trypsinized and resuspended at 100,000 cell/ml in conditioned medium (CM) obtained from KRIB cells overexpressing mouse DKK1 or its respective control (CM was collected after 2 days in confluent layers of both KRIB cell types). 5 X 10^3 cells/well (50 µl) were loaded on top of the solidified Matrigel and was incubated for 6h at 37°C in a humidified incubator in a 5% CO2 atmosphere. Bright field mosaic pictures were taken using a Zeiss Imager Z2 inverted microscope and AxioVision software (Carl Zeiss) at 5X magnification, which allowed

imaging of the whole well in 9 pictures. Tube-like structures (defined by the numbers of closed loops) were counted using the ZEN Blue software (Carl Zeiss). 3 independent experiments were performed with 3-5 replicates per experiment, and measures subsequently were averaged.

Tumor xenograft experiments

4 x 10^6 KRIB CTR or mDKK1 overexpressing cells were injected subcutaneously in the left upper back of nude mice (Charles River). After 3.5 weeks, mice were sacrificed, the tumor size was measured with a caliper and the tumor volume was calculated using formula $V=(a^2*b)/2$, where b is the longest axis and a is the perpendicular axis to b. Tumor tissue was snap frozen in liquid nitrogen or directly embedded in O.C.T. and further analyzed by qRTPCR and immunostaining as described.

VEGFA/TNC binding study

Surface plasmon resonance binding experiments were performed on a Biacore 2000 instrument (Biacore Inc.) at 25°C. VEGFA165 (Millipore) or TNC (Huang et al., 2001) were immobilized at high surface density (around 7000 resonance units) on an activated CM5 chip (Biacore Inc.) using a standard amine-coupling procedure according to the manufacturer's instruction. Soluble molecules were added at a concentration of 10 µg/ml in 10 mm sodium acetate, pH 5.0, and at a flow rate of 5 µl/min for 20 min before addition of 1 M ethanolamine. Soluble TNC (5 - 20µg in 200µl) or VEGFA165 was added to the chip in 10 mm MES, pH 6.0, 150 mm sodium chloride, 0.005% (v/v) surfactant P20, at a flow rate of 10 µl/min. A blank CM5 chip was used for background correction. 10 mm glycine, pH 2.0, at 100 µl/min for 1 min was used to regenerate the chip surface between two binding experiments. A steady state condition was used to determine the affinity of VEGFA165 for TNC and the affinity of TNC for VEGFA165. The Dissociation constant (Kd) was determined using the 1:1 Langmuir association model as described by the manufacturer.

Statistical analysis and graphical representation

Statistical analysis was performed using GraphPad Prism. For significance of an association (contingency) Fisher's exact test was applied (tumor staging, gene expression, metastasis incidence). Statistical differences were analyzed by unpaired t-test (Gaussian distribution) or nonparametric Mann-Whitney test (no Gaussian distribution). Gaussian data sets with different variances were analyzed by unpaired t-test with Welch's correction. Gaussian distribution was tested by the Shapiro-Wilk normality test. p-values < 0.05 were considered as statistically significant.

Primer list for qRTPCR on tumor, liver and lung tissue

Gene	Species	Forward primer	Reverse primer
Axin2	mouse	CTGCTGGTCAGGCAGGAG	TGCCAGTTTCTTTGGCTCTT
CD44	mouse	GTCTGCATCGCGGTCAATAG	GGTCTCTGATGGTTCCTTGTTC
CyclinD1	mouse	CGCACTTTCTTTCCAGAGTCA	AAGGGCTTCAATCTGTTCCTG
DKK1	mouse	Taqman (ABI) Mm00438422_m1	
DKK1	mouse	CCGGGAACTACTGCAAAAAT	CCAAGGTTTTCAATGATGCTT
DKK2	mouse	GCCAAACTCAACTCCATCAAG	TCACTGCTGCAAGGGTAGG
Dll4	mouse	AGGTGCCACTTCGGTTACAC	GGGAGAGCAAATGGCTGATA
E-Cadherin	mouse	CAGCCTTCTTTTCGGAAGACT	GGTAGACAGCTCCCTATGACTG
GAPDH	mouse	Taqman (ABI) Mm99999915_g1	
GAPDH	human	ATCTTCTTTTGCGTCGCCAG	AATCCGTTGACTCCGACCTTC
Hey-1	mouse	CATGAAGAGAGCTCACCCAGA	TTGGGGACATGGAACACAG
HMBS	human	Qiagen QT00494130 (for Sybr green)	
Insulin	mouse	TGGCTTCTTCTACACACCCAAG	ACAATGCCACGCTTCTGCC
Insulin	mouse	Taqman mIns1 Mm01259683_g1	
Lgr5	mouse	GGAAAGAAATGCTTTGATGGAC	AGTGGGGAATTCATCAAGGTT
RPL19	mouse	ACCCTGGCCCGACGG	TACCCTTCCTCTTCCCTATGCC
Slug	mouse	GAAAAGCACATTGCATCTTTTCT	TGTTCCTTTGGTTGAAATGGT
TBP	mouse	CCCCACAACTCTTCCATTCT	GCAGGAGTGATAGGGGTCAT
TNC	human	GTCACCGTGTCAACCTGATG	GTTAACGCCCTGACTGTGGT

Primer list for qRTPCR on cultured cells

Gene	Forward primer	Reverse primer
Axin2	CCACACCCTTCTCCAATCC	TGCCAGTTTCTTTGGCTCTT
DKK-1	GACCATTGACAACTACCAGCCG	TACTCATCAGTGCCGCACTCCT
DKK-2	GGCAGTAAGAAGGGCAAAAA	CCTCCCAACTTCACACTCCT

DKK-3	GAGGACACGCAGCACAAA	TGCCAGGTTCACTTCTGATG
DKK-4	AGGAGGTGCCAGCGAGAT	CATCTTCCATCGTAGTACAAACATC
SFRP1	GCTGGAGCACGAGACCAT	TGGCAGTTCTTGTTGAGCA
SFRP2	GCTTGAGTGCGACCGTTT	CAGGCTTCACATACCTTTGGA
SFRP3/FRZB	GGGCTATGAAGATGAGGAACG	CTGAGTCCAAGATGACGAAGC
SFRP4	CGATCGGTGCAAGTGTAAAA	ACCACCGTTGTGACCTCATT
SRF	AGACGGGCATCATGAAGAAG	TGATCATGGGCTGCAGTTT
TPM1	CCCGTAAGCTGGTCATCATC	CTTGTGTGCTCATCATTCCGA
RhoA [1](Sauzeau et al., 2003)	GCAGGTAGAGTTGGCTTTATGG	CTTGTGTGCTCATCATTCCGA
β2-Microglobulin	GTGGGATCGAGACATGTAAGCA	AATGCGGCATCTTCAAACCT

[1], Sauzeau et al., 2003

Table S1 Carcinoma progression by TNC - Related to Figure 1

Genotype	Adenomas (%)	Carcinomas (%)				
		Grade 1	Grade 2	Grade 3	Grade 1 - 3	Ca/Ad
RT2	55.8	32.7	10.5	0.9	44.2	0.8
RT2/TNC	35.7	39.9	21.3	3.2	64.3	1.8

Numbers of adenomas and carcinomas Grade 1 to 3 in 12 week old mice. Average frequency of each tumor grade per mouse is displayed; 26 RT2 mice (78 adenomas, 79 carcinomas) and 22 RT2/TNC mice (44 adenomas, 76 carcinomas). p = 0.038, Fisher's exact test. RT2/TNC mice developed 1.8-fold more carcinomas than adenomas (p = 0.001, Student's t-test) compared to RT2 mice (0.8-fold, p = 0.945, Student's t-test).

Table S2 TNC dependent angiogenic switch - Related to Figure 1

Genotype	All islets			Islets per mouse	
	A plus NA	A	NA	A	NA
RT2 (n = 9)	826	71	755	7.9 (±2.2)	83.9 (±7.4)
RT2/TNC (n = 7)	810	136	674	19.4 (±4.3)	96.3 (±10.0)
RT2/TNC versus RT2 (fold)				2.46	1.15
p-value		< 0.0001 [a]		0.0226 [b]	0.3248 [b]
RT2 (n = 7)	809	255	554	36.4 (±5.0)	79.1 (±8.6)
RT2/TNCKO (n = 7)	840	87	753	12.4 (±2.6)	107.6 (±11.8)
RT2/TNCKO versus RT2 (fold)				- 2.94	1.36
p-value		< 0.0001 [a]		0.0011 [c]	0.2008 [b]

Angiogenic (A) and non-angiogenic (NA) islets were isolated from 8 week old RT2 mice with the indicated genotypes and were quantified (average number including SEM per mouse). Islets from RT2 littermates were prepared independently in both series of experiments. (a) Fisher's exact test, (b) Student's t-test, (c) Mann Whitney test. Note that differences between RT2 controls originate from inherent experimental conditions (e.g. efficiency of collagenase treatment).

Table S3 Gene expression analysis of RT2 and RT2/TNC tumors - Related to Figure 3

Gene	Tumor class	Relative expression	p-value	Gene	Tumor class	Relative expression	p-value
Axin2	All	**1.35**	0.008	**Dll4**	All	1.66	0.153
	Small	**1.30**	0.034		Small	1.55	0.186
	Small+Diff	1.27	0.055		Small+Diff	1.43	0.258
	Big	1.49	0.194		Big	1.93	0.376
	Big+Diff	1.18	0.571		Big+Diff	1.61	0.786
	Diff	**1.25**	0.037		Diff	1.45	0.194
CD44	All	1.64	0.225	**Hey-1**	All	-1.27	0.134
	Small	1.72	0.077		Small	-1.02	0.911
	Small+Diff	**2.06**	0.029		Small+Diff	1.03	0.843
	Big	-1.63	0.133		Big	**-3.08**	0.019
	Big+Diff	-1.58	0.143		Big+Diff	**-2.67**	0.036
	Diff	1.85	0.157		Diff	-1.16	0.343
CyclinD1	All	1.45	0.166	**Lgr5**	All	-6.81	0.931
	Small	1.45	0.113		Small	-1.72	0.477
	Small+Diff	**2.01**	0.037		Small+Diff	-1.73	0.340
	Big	1.17	0.776		Big	-23.06	0.279
	Big+Diff	-1.02	0.571		Big+Diff	-6.74	0.786
	Diff	1.78	0.112		Diff	-2.65	0.528
DKK1	All	**-16.07**	0.035	**Slug**	All	1.28	0.220
	Small	-16.34	0.062		Small	**1.67**	0.010
	Small+Diff	**-4.13**	0.043		Small+Diff	**1.84**	0.004
	Big	-15.49	n.a.		Big	-2.56	0.081
	Big+Diff	-3.19	n.a.		Big+Diff	-2.20	0.294
	Diff	**-3.90**	0.044		Diff	1.46	0.063
DKK2	All	-1.85	0.204				
	Small	-1.46	0.551				
	Small+Diff	-1.35	0.841				
	Big	**-3.69**	0.032				
	Big+Diff	**-4.67**	0.036				
	Diff	-1.85	0.366				

Relative gene expression in RT2/TNC versus RT2 tumors as determined by qRTPCR. RNA was isolated from tumors of 14 week old RT2 (N = 11 mice, n = 27 tumors) and RT2/TNC mice (N = 3, n = 13). Data are presented for all tumors (All) and subgroups : small tumors (Small : 1 – 3 mm in diameter, RT2 (n = 19), RT2/TNC (n = 10)), big

tumors (Big : > 3 mm, RT2 (n = 8), RT2/TNC (n = 3)), differentiated tumors (Diff. : high expression of insulin and E-cadherin, RT2 (n = 22), RT2/TNC (n = 13)), small and differentiated tumors (Small + Diff : RT2 (n = 17), RT2/TNC (n = 10)) and big and differentiated tumors (Big + Diff, RT2 (n = 5), RT2/TNC (n = 3)). Bold numbers represent statistically significant changes in relative expression, n.a., not applicable due to low sample number.

Fig. S1

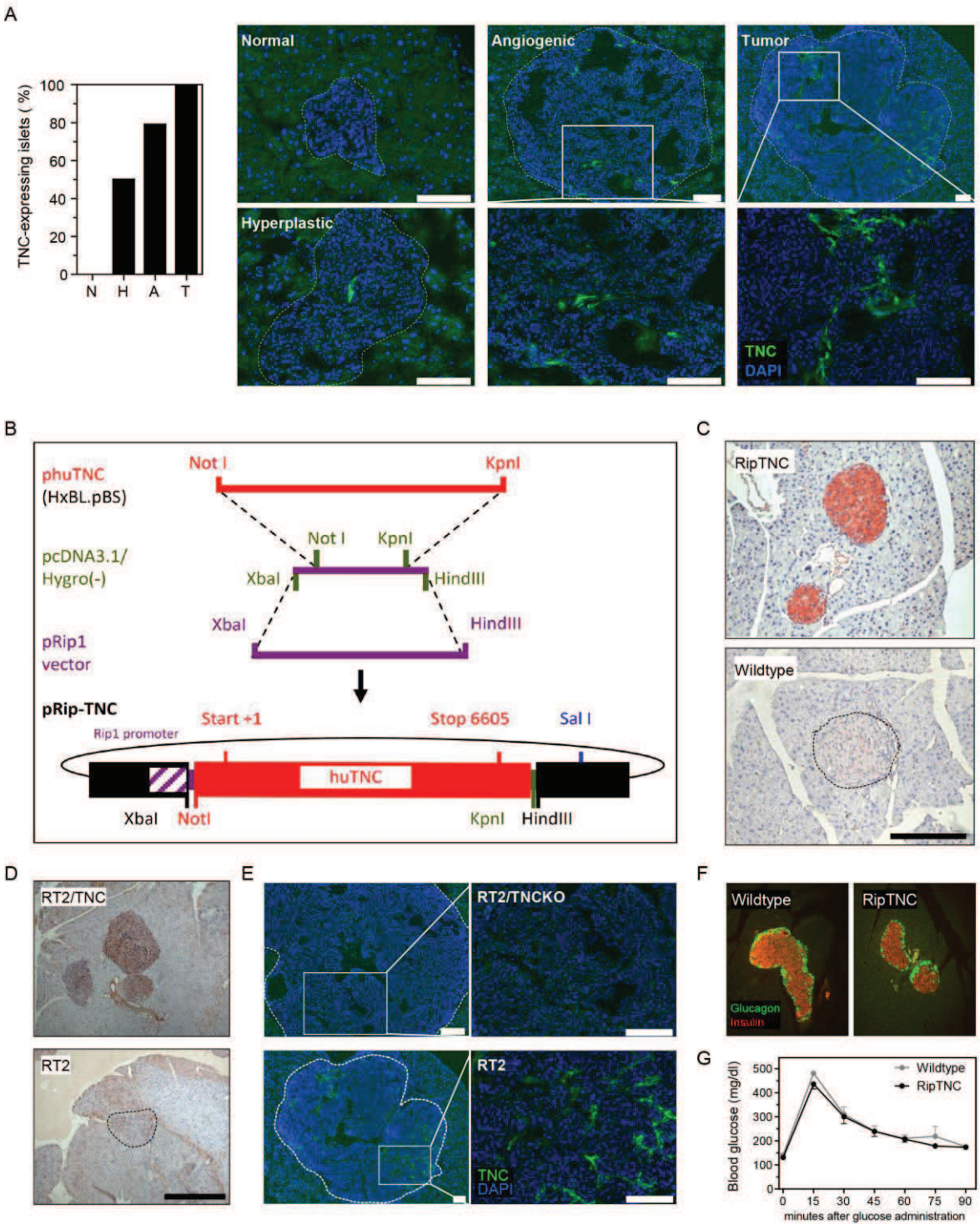

Figure S1 TNC expression in RT2 mice, TNC expression vector and impact of transgenic TNC on pancreatic tissue function. Related to Figure 1

(A) TNC expression in RT2 islets determined by IF analysis (MTn12 antibody) in tissue sections of 12 week old RT2 mice. In contrast to the absence of TNC from normal islets (N < 0.2 mm diameter), TNC is expressed in 50%, 80% and 100% of hyperplastic (H, 0.2 – 0.5 mm diameter), angiogenic (A, > 0.5 – 1 mm diameter) and tumorigenic islets

(T, diameter above 1 mm), respectively. Right panels, dotted lines delineate the islet circumferences. 82 islets (N = 26, H = 34, A = 14, T = 8) of 3 RT2 mice were analyzed. Scale bar, 100 μm. **(B)** Strategy for the generation of the TNC expression vector. The human cDNA (Gherzi et al., 1995) was removed from the HxBL-pBS plasmid (Aukhil et al., 1993) and cloned into the Rip1 expression vector (Hanahan, 1985) for insulin-promoter driven expression of the transgene by using the pcDNA3.1./Hygro(-) plasmid as intermediate vector. The inserted human cDNA sequence comprises 45 nucleotides upstream of the start site and 639 nucleotides downstream of the stop signal. **(C-E)** TNC expression analysis in RipTNC **(C),** RT2/TNC **(D)** and RT2/TNCKO pancreatic tissue **(E)** by IHC **(C, D)**, IF **(E)**. Scale bar 100 μm. **(F)** No sorting difference of α-glucagon and insulin positive α- and β-cells in pancreatic tissue of wildtype and RipTNC mice was observed as determined by IF. **(G)** Determination of blood glucose levels after an oral glucose tolerance test in 14 RipTNC and 15 wildtype mice. Average ±SEM is presented for each time point.

Fig. S2

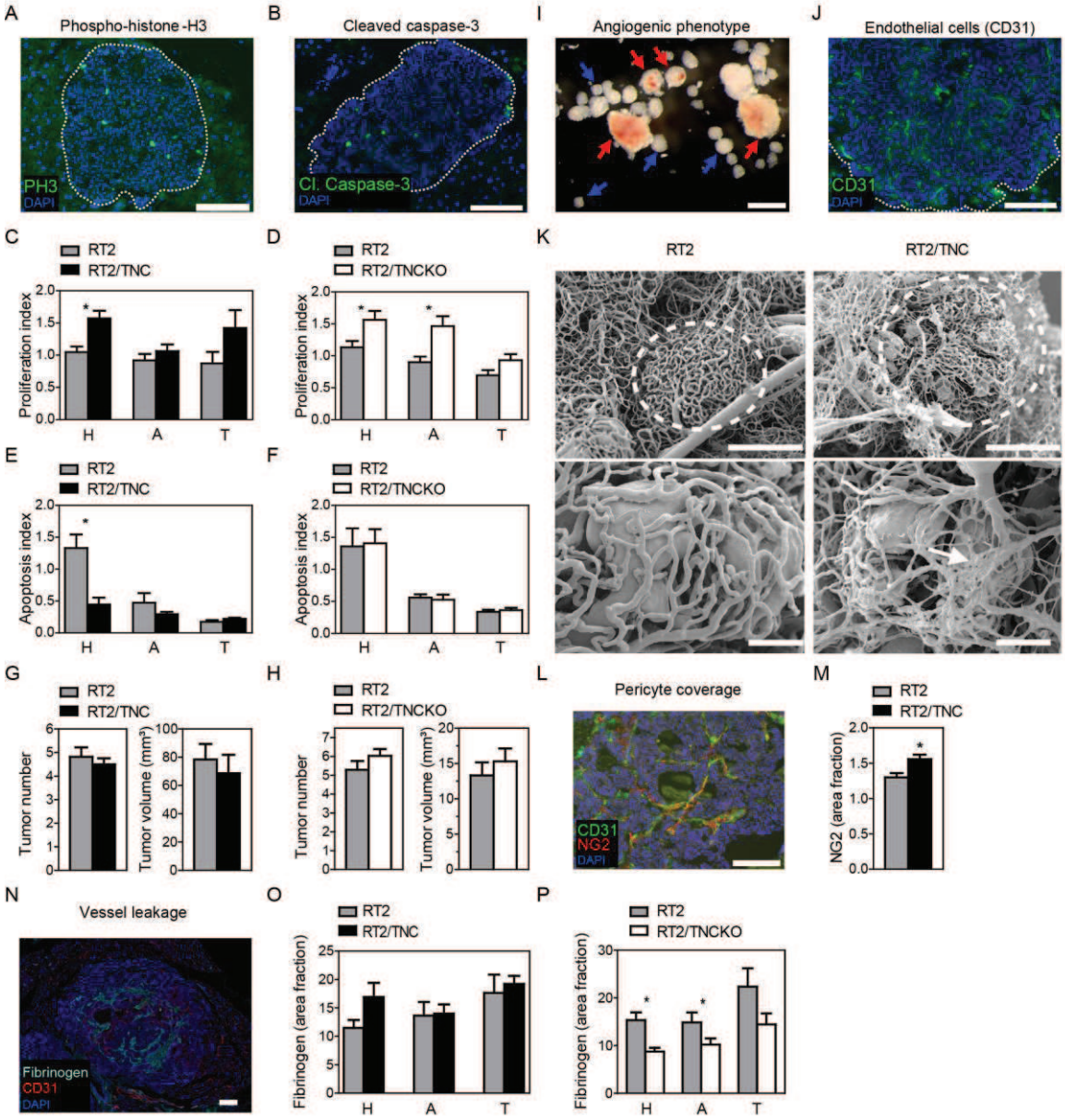

Figure S2. Expression analysis, islet quantification, tumor incidence and burden, Related to Figure 1

(A, B, J, L, N) Expression of the indicated molecules in RT2 tumor tissue upon IF analysis. Scale bar 100 µm. **(C, D)** Quantification of proliferation according to tumor stage in 12 week old mice, **(C)** RT2, 9 mice, 99 hyperplastic (H), 37 angiogenic (A) and 14 tumorigenic (T) islets; RT2/TNC, 8 mice, H = 71, A = 47, T = 22, **(D)** RT2, 6 mice, H = 73, A = 38, T = 20; RT2/TNCKO, 6 mice, H = 72, A = 40, T = 25. **(C)** In RT2/TNC mice a significant 1.5 - fold increase in proliferation in hyperplastic islets is observed. **(D)** a signifcant increase in proliferation in hyperplastic (1.4-fold) and angiogenic (1.6-fold) islets from RT2/TNCKO mice is observed. **(E, F)** Quantification of apoptosis in 12 week

old mice, **(E)** RT2, 6 mice, H = 55, A = 19, T = 10; RT2/TNC, 8 mice, H = 59, A = 43, T = 21, **(F)** RT2, 4 mice, H = 56, A = 26, T = 13; RT2/TNCKO, 4 mice, H = 72, A = 40, T = 25. In hyperplastic islets of RT2/TNC mice a significant 2.9-fold decrease in apoptosis is observed, while no significant difference was seen in RT2/TNCKO mice. **(G, H)** Tumor incidence and burden, **(G)** RT2, N = 33 mice, RT2/TNC, N = 26, **(H)** RT2, N = 28, RT2/TNCKO, N = 31. Differences were not statistically significant. **(I)** Image of isolated angiogenic and non-angiogenic islets of an 8 week old RT2 mouse. Scale bar 500 µm. Red arrows: angiogenic islets, blue arrows: non-angiogenic islets. **(K)** Representative SEM pictures from RT2 (N = 5 mice) and RT2/TNC tumors (N = 3). Arrow points at small aggregated vessels. Scale bars: top panels 200 µm, bottom panels 100 µm. **(M)** Quantification of NG2, a marker for pericytes, area fraction in 12 week old RT2 (N = 6 mice, n = 155 islets) and RT2/TNC (N = 8 mice, n = 204 islets) mice. A significant 1.2-fold increase of NG2 area fraction is observed in RT2/TNC islets. **(O, P)** Quantification of fibrinogen, a marker of vessel leakiness; area fraction according to tumor stage in 12 week old mice, **(O)** RT2, 5 mice, H = 36, A = 18, T = 8; RT2/TNC, 3 mice, H = 26, A = 20, T = 4; **(P)** RT2, 4 mice, H = 35, A = 18, T = 7; RT2/TNCKO, 5 mice, H = 59, A = 47, T = 9. **(O)** In hyperplastic islets of RT2/TNC mice an increased fibrinogen leakiness is observed (1.5-fold, p = 0.06). **(P)** In hyperplastic (1.8-fold) and angiogenic islets (1.5-fold) of RT2/TNCKO mice, a significant decrease of fibrinogen area fraction is observed. Error bars represent SEM and asterisks (*) indicate p values < 0.05.

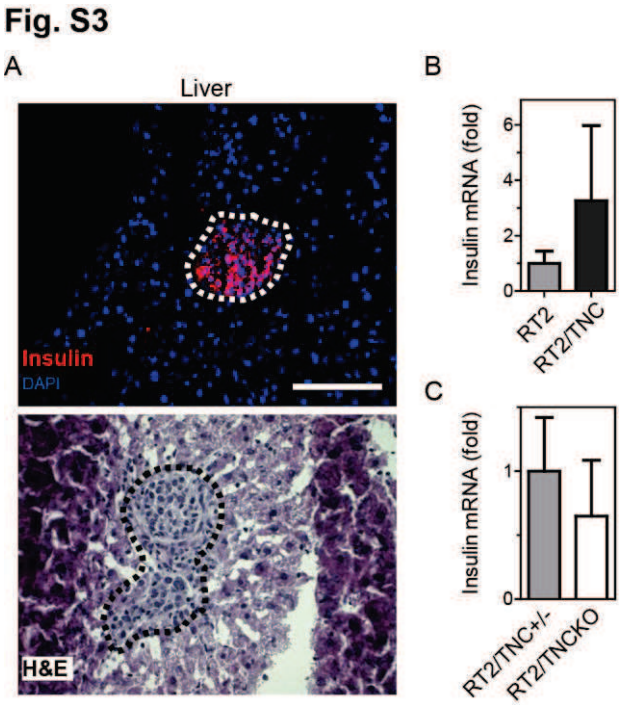

Figure S3. Liver micrometastasis in RT2 mice, Related to Figure 2

(A) Detection of insulin expressing tumor cells in liver tissue of a RT2 mouse by IF (upper panel) and H&E of a neighboring section (lower panel). Scale bar, 50 μm. **(B, C)** Quantification of insulin expression in liver tissue of RT2 mice. Insulin expression was detected in RT2/TNC (7/24) and RT2 (6/24) **(B)** and RT2/TNCKO (5/10) and RT2/TNC+/- littermates (6/8) **(C)**. Differences were not statistically significant. Error bars represent SEM.

Fig. S4

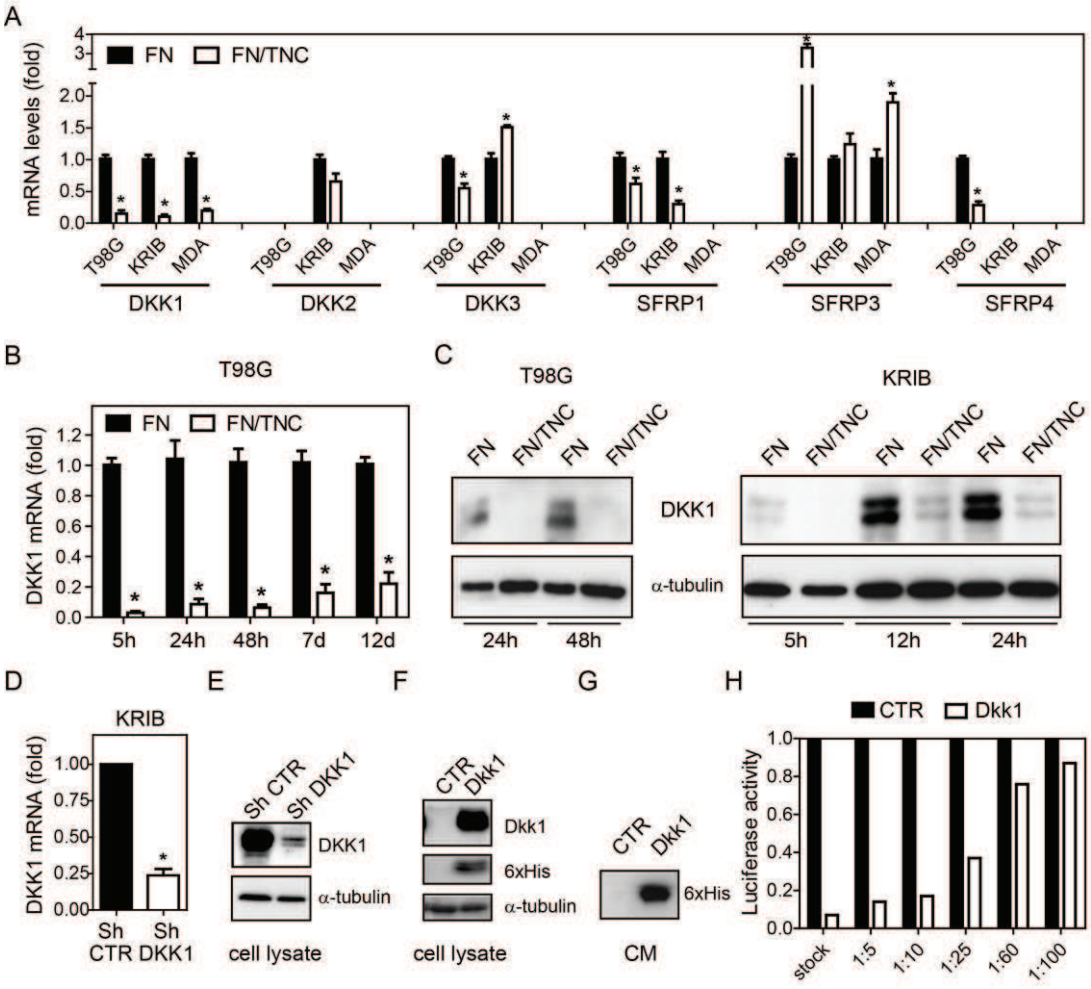

Figure S4. Impact of TNC on the expression of Wnt inhibitors, DKK1 downregulation and activation of Wnt signaling in tumor cells, Related to Figure 4

(A) Expression of Wnt inhibitors in T98G, KRIB and MDAMB-435 (MDA) cells as determined by qRTPCR upon plating on the indicated substrata for 24h (KRIB, MDAMB-435) or 48h (T98G). There was no expression of SFRP2 nor DKK4 detectable in any of the cell lines and conditions tested. **(B)** DKK1 expression (qRTPCR) upon plating T98G cells on FN/TNC and FN for the indicated time. DKK1 expression on FN/TNC is represented relative to its expression on FN. **(C)** Reduced DKK1 protein levels by TNC in T98G or KRIB cells upon plating for the indicated time as determined by immunoblotting. **(D, E)** Reduced DKK1 expression upon shRNA mediated DKK1 knockdown as determined by qRTPCR **(D)** and immunoblotting **(E)** in KRIB Sh-DKK1 cells in comparison to KRIB Sh-control (CTR) cells. **(F)** Expression of murine DKK1 in control (CTR) and mDKK1

overexpressing KRIB cells. Overexpression of murine DKK1 in KRIB:mDKK1 cells. Lysates of KRIB cells expressing His-tagged mDKK1 or empty vector control were analyzed by immunoblotting with antibodies against DKK1 or the His-tag. **(G)** Expression of murine DKK1 in the conditioned media (CM) from control (CTR) and mDKK1 overexpressing KRIB cells. Supernatants from the KRIB cells expressing His-tagged mDKK1 or empty vector control were analyzed by immunoblotting. **(H)** Addition of DKK1 containing CM assessed by immunoblotting inhibits TOPFlash activity in KRIB cells in a dose dependent manner. KRIB cells were plated for 48h and treated with increasing dilutions of CM from KRIB:mDKK1 cells. Data are derived from at least 3 independent experiments, except for (**H**). Error bars represent SEM and asterisks (*) indicate p values < 0.05.

Fig. S5

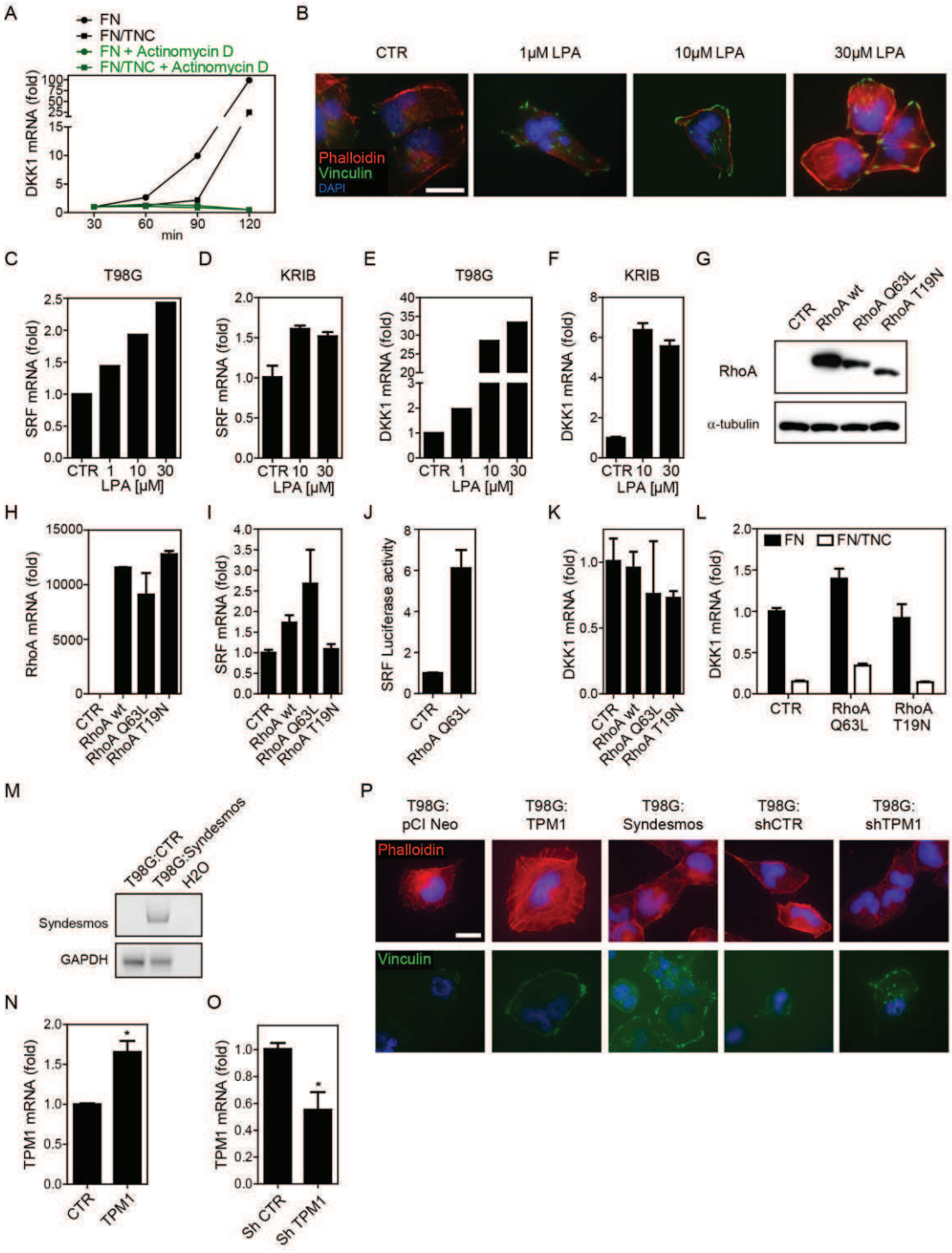

Figure S5. Mechansim of DKK1 downregulation, Related to Figure 5

(A) Serum starved T98G cells were seeded on FN or FN/TNC. After 30 minutes 5 μg/ml Actinomycin D was added and cells were lysed after an additional 30, 60 or 90 minutes for analysis of DKK1 mRNA expression. **(B)** Serum starved T98G cells were treated with the indicated concentrations of LPA. IF staining of vinculin (green) and phalloidin (red). **(C, D)** SRF and **(E, F)** DKK1 mRNA expression of serum starved T98G and KRIB cells

treated with the indicated concentrations of LPA. **(G-L)** T98G cells were transfected with RhoA wt, RhoA Q63L (CA) or RhoA T19N (DN). **(G, H)** Overexpression of RhoA was validated by immunoblotting **(G)** and qRTPCR **(H). (I, J)** SRF mRNA expression **(I)** and SRF luciferase activity of T98G cells **(J). (K, L)** DKK1 mRNA expression analysed by qRTPCR of cells seeded on uncoated **(K)** or FN and FN/TNC coated dishes **(L). (M)** RTPCR for chicken syndesmos of T98G CTR and T98G:syndesmos cells. **(N, O)** TPM1 mRNA levels analyzed by qRTPCR in T98G:TPM1 **(N),** T98G:shTPM1 **(O)** and control cells. **(P)** IF of vinculin (green) and phalloidin (red) in T98G control, T98G:TPM1, T98G:syndesmos and T98G:shTPM1 cells. Nuclei are stained with DAPI (blue). Error bars represent SEM and asterisks (*) indicate p values < 0.05.

Fig. S6

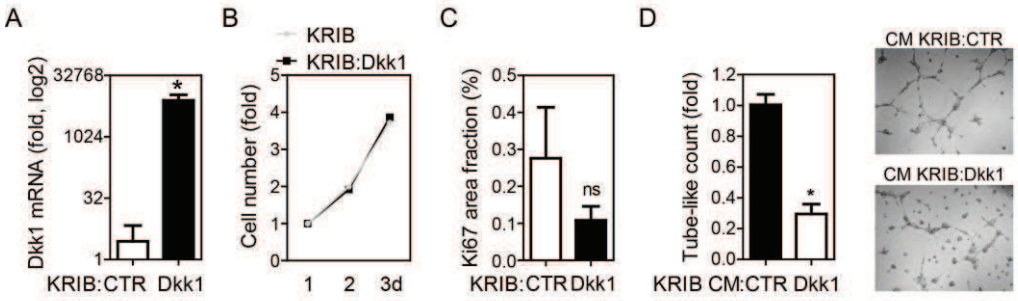

Figure S6. DKK1 expression in KRIB:mDKK1 tumors and impact of DKK1 overexpression on tumor cell proliferation and migration, Related to Figure 6

(A) Quantification of murine *Dkk1* gene expression by qRTPCR in control or Dkk1 overexpressing KRIB derived tumors. **(B)** Dkk1 does not change tumor cell proliferation *in vitro*. Proliferation of KRIB (parental) and KRIB:Dkk1 cells was analyzed with a MTS assay. Data are normalized in each group to values of day 1. **(C)** Dkk1 does not change tumor cell proliferation *in vivo*. Proliferating cells were quantified in tumors derived from KRIB control or KRIB:Dkk1 cells. Ki67-positive areas were determined using ImageJ software upon staining for Ki67 and reported to the DAPI positive areas per tumor. No significant (ns) difference was observed (n = 5 per group). **(D)** HUVEC tubulogenesis on Matrigel upon addition of CM derived from KRIB control or Dkk1 overexpressing cells. Quantification of three independent experiments (left) and representative phase contrast pictures (right) are shown. Error bars represent SEM and asterisks (*) indicate p values < 0.05.

Fig. S7

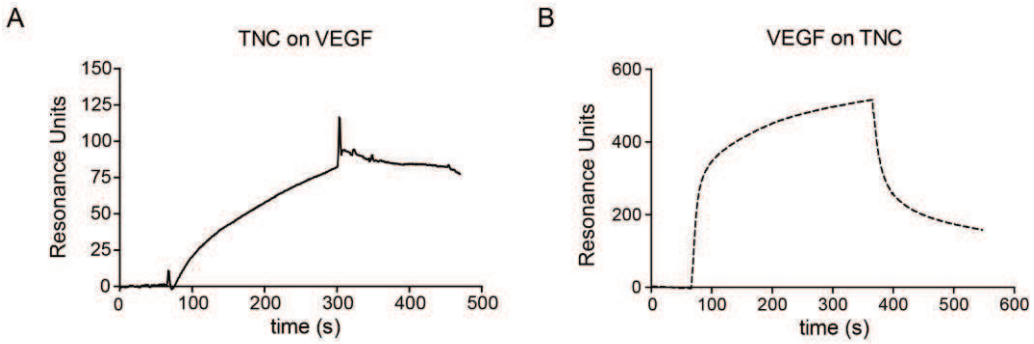

Figure S7. Binding of TNC to VEGFA

Binding of VEGFA to TNC was determined by Biacore including normalization to a blank surface. Binding of TNC and VEGFA to a sensorchip adsorbed with VEGFA **(A)** and TNC **(B)**, respectively is shown. We observed that VEGFA and TNC bind to each other in a dose dependent manner with a Kd of 2.7 x 10^{-7} M (TNC binding to VEGFA) and 1.5 x 10^{-9} M (VEGFA binding to TNC) which is lower than VEGFA binding to its receptor (3.3 x 10^{-11} M) but is in the range of a VEGFA/glycosaminogycan interaction (2.4 x 10^{-8} M) (Wu et al., 2009).

References to SI Material

Aukhil, I., Joshi, P., Yan, Y., and Erickson, H.P. (1993). Cell- and heparin-binding domains of the hexabrachion arm identified by tenascin expression proteins. J Biol Chem *268*, 2542-2553.

De Boeck, A., Hendrix, A., Maynard, D., Van Bockstal, M., Daniels, A., Pauwels, P., Gespach, C., Bracke, M., and De Wever, O. (2013). Differential secretome analysis of cancer-associated fibroblasts and bone marrow-derived precursors to identify microenvironmental regulators of colon cancer progression. Proteomics *13*, 379-388.

De Wever, O., Nguyen, Q.D., Van Hoorde, L., Bracke, M., Bruyneel, E., Gespach, C., and Mareel, M. (2004). Tenascin-C and SF/HGF produced by myofibroblasts in vitro provide convergent pro-invasive signals to human colon cancer cells through RhoA and Rac. Faseb J *18*, 1016-1018.

Forsberg, E., Hirsch, E., Frohlich, L., Meyer, M., Ekblom, P., Aszodi, A., Werner, S., and Fassler, R. (1996). Skin wounds and severed nerves heal normally in mice lacking tenascin-C. Proceedings of the National Academy of Sciences of the United States of America *93*, 6594-6599.

Gherzi, R., Ponassi, M., Gaggero, B., and Zardi, L. (1995). The first untranslated exon of the human tenascin-C gene plays a regulatory role in gene transcription. FEBS letters *369*, 335-339.

Hanahan, D. (1985). Heritable formation of pancreatic beta-cell tumours in transgenic mice expressing recombinant insulin/simian virus 40 oncogenes. Nature *315*, 115-122.

Huang, W., Chiquet-Ehrismann, R., Moyano, J.V., Garcia-Pardo, A., and Orend, G. (2001). Interference of tenascin-C with syndecan-4 binding to fibronectin blocks cell adhesion and stimulates tumor cell proliferation. Cancer research *61*, 8586-8594.

Laemmli, U.K. (1970). Cleavage of structural proteins during the assembly of the head of bacteriophage T4. Nature *227*, 680-685.

Lange, K., Kammerer, M., Hegi, M.E., Grotegut, S., Dittmann, A., Huang, W., Fluri, E., Yip, G.W., Gotte, M., Ruiz, C.*, et al.* (2007). Endothelin receptor type B counteracts tenascin-C-induced endothelin receptor type A-dependent focal adhesion and actin stress fiber disorganization. Cancer research *67*, 6163-6173.

Lange, K., Kammerer, M., Saupe, F., Hegi, M.E., Grotegut, S., Fluri, E., and Orend, G. (2008). Combined lysophosphatidic acid/platelet-derived growth factor signaling triggers glioma cell migration in a tenascin-C microenvironment. Cancer research *68*, 6942-6952.

Ruiz, C., Huang, W., Hegi, M.E., Lange, K., Hamou, M.F., Fluri, E., Oakeley, E.J., Chiquet-Ehrismann, R., and Orend, G. (2004). Growth promoting signaling by tenascin-C Cancer research *64*, 7377-7385.

Sauzeau, V., Rolli-Derkinderen, M., Marionneau, C., Loirand, G., and Pacaud, P. (2003). RhoA expression is controlled by nitric oxide through cGMP-dependent protein kinase activation. J Biol Chem *278*, 9472-9480.

Veeman, M.T., Slusarski, D.C., Kaykas, A., Louie, S.H., and Moon, R.T. (2003). Zebrafish prickle, a modulator of noncanonical Wnt/Fz signaling, regulates gastrulation movements. Curr Biol *13*, 680-685.

Wu, F.T., Stefanini, M.O., Mac Gabhann, F., and Popel, A.S. (2009). A compartment model of VEGF distribution in humans in the presence of soluble VEGF receptor-1 acting as a ligand trap. PloS one *4*, e5108.

Tristan Rupp

Mechanisms of Tenascin-C dependent tumor angiogenesis

Résumé

Une expression élevée de la protéine de la matrice extracellulaire ténascine-C (TNC) favorise la progression du cancer et est corrélée à une réduction de la survie des patients. Dans cette thèse, j'ai étudié comment la TNC affecte l'angiogenèse tumorale. J'ai montré que la TNC altère le les protrusions angiogéniques, la tubulogenèse, la migration et la prolifération des cellules endothéliales. J'ai lié ces effets à la perturbation du cytosquelette d'actine et la réduction de la signalisation YAP par la TNC. Chez les cellules tumorales et les fibroblastes associés au cancer, la TNC favorise la sécrétion de facteurs angio-modulateurs qui stimulent la survie et la tubulogenèse des cellules endothéliales de façon paracrine. Cet effet implique la régulation de l'expression de SDF1 (CXCL12) et de deux membres de la famille des lipocalines. Ainsi, la TNC favorise l'angiogenèse en activant chez les cellules tumorales un sécrétome pro-angiogénique, et inhibe la tubulogenèse en altérant la survie des cellules endothéliales. Ces effets opposés pourraient expliquer pourquoi nous avons observé dans un modèle de tumeur spontanée chez la souris que la TNC favorise le switch angiogénique résultant en la formation d'une forte vascularisation tumorale, mais qui reste peu fonctionnelle associée à la formation de plus de métastases. Ce travail fournit pour la première fois la possibilité de contrer l'action de la TNC dans l'angiogenèse tumorale.

Résumé en anglais

A high expression of the extracellular matrix molecule tenascin-C (TNC) enhances multiple steps in cancer progression and correlates with worsened survival prognosis. In this thesis I studied how TNC affects tumor angiogenesis. I showed that TNC impairs endothelial sprouting, tubulogenesis, migration and proliferation. I linked this effect to disruption of the actin cytoskeleton and reduced YAP signaling activity by TNC. In tumor cells and cancer associated fibroblasts, TNC regulated secretion of angio-modulatory factors that promoted endothelial cell survival and tubulogenesis in a paracrine manner involving regulation of SDF1 (CXCL12) and two lipocalin family members. Altogether, TNC promotes endothelial tubulogenesis through a pro-angiogenic secretome from tumor cells, and inhibits by direct contact tubulogenesis by impairing endothelial cell survival. These opposing effects could explain why we observed that TNC promotes the tumor angiogenic switch resulting in more but poorly functional blood vessels associated with more metastasis in a spontaneous tumor mouse model. This knowledge provides for the first time opportunities to counteract TNC activities in tumor angiogenesis.

Keywords: tumor microenvironment, extracellular matrix, tenascin-C, angiogenesis, cancer